

A Performance Comparison Between A Novel Tapered Piezoprobe And The Piezocone In Boston Blue Clay

by

Amy Jeanne Varney

Bachelor of Science in Civil and Environmental Engineering
Massachusetts Institute of Technology, Cambridge, Massachusetts
(1996)

Submitted to the
Department of Civil and Environmental Engineering
in partial fulfillment of the requirements for the degree of
Master of Science in Civil and Environmental Engineering
at the

MASSACHUSETTS INSTITUTE OF TECHNOLOGY
February 1998

© Massachusetts Institute of Technology, 1998
All rights reserved.

Signature of Author _____
Department of Civil and Environmental Engineering, February 9, 1998

Certified by _____
Professor Andrew J. Whittle, Thesis Co-Supervisor

Certified by _____
Professor Harold F. Hemond, Thesis Co-Supervisor

Accepted by _____
Joseph M. Sussman
Chairman, Departmental Committee on Graduate Studies

MASSACHUSETTS INSTITUTE OF TECHNOLOGY

FEB 13 1998

LIBRARIES

V.I

ETD

A Performance Comparison Between A Novel Tapered Piezoprobe And The Piezocone In Boston Blue Clay

by

Amy Jeanne Varney

Submitted to the Department of Civil and Environmental Engineering on February 9,
1998

in partial fulfillment of the requirements for the degree of
Master of Science in Civil and Environmental Engineering

ABSTRACT

A 45 day field program was conducted at MIT's I-95 test site in Saugus, Massachusetts (Station 246) in order to compare the performance and results of a novel tapered piezoprobe in clay to that of a standard piezocone. The site investigation was designed with the intention of performing dissipation tests in a deep deposit of Boston Blue Clay, a low plasticity marine illitic clay. A minimum of 6 dissipation tests were performed concurrently at 10 ft intervals in five boreholes using two tapered piezoprobes, two standard piezocones (with base pore pressure measurement) and one MIT Research piezocone (tip pore pressure measurement). Twenty-four hour operation of the data acquisition system allowed complete dissipation records to be obtained. Long term dissipation measurements from both piezoprobe and piezocone devices are within 2-3% of the in situ pore pressures measured by the standpipe piezometer. A supporting laboratory investigation was performed utilizing undisturbed samples collected during this field program.

The main purpose of the tapered piezoprobe is to reduce the dissipation times in offshore site investigations, such that in situ pore pressures, u_o , can be measured reliably within a practical time frame of 1-2 hours. The field data show that the tapered piezoprobes do accelerate the initial phase of dissipation, reaching 50% of the installation excess pore pressure ($u_i - u_o$) approximately 17 times faster than a conventional piezocone. However, there is a marked retardation in dissipation response for excess pore pressure ratios $[(u - u_o)/(u_i - u_o)] < 20\%$. This brake in the dissipation response confirms prior theoretical predictions, and shows the need for caution in estimating u_o from incomplete dissipation records. The in situ pore pressure can be estimated within 5% by i) inverse time extrapolation within $t = 0.3$ hrs; and ii) two point matching method (Sutabutr, PhD 1998) within $t = 1$ hour.

Hydraulic conductivity can be interpreted by comparing experimental data with theoretical dissipation curves, using a variety of time matching methods (T_{50} , Goodness of Fit, Concurrent Matching). This thesis uses theoretical predictions based on non-linear finite element analysis incorporating the MIT-E3 effective stress soil model, and the Stress Path Method to model initial undrained penetration.

The dissipation data consistently show that k is almost uniform within the BBC at depths below El. -22 m ($OCR < 1.2$). However, values of k derived from conventional piezocones are approximately 20% lower than those from the tapered piezoprobe and these, in turn, are a factor of 2.1 less than independent laboratory measurements in CRSC tests. Further research is necessary to establish if these small differences in k are related to penetrometer dimension and hence, can affect the scaling of dissipation properties for prototype offshore piles.

Thesis Co-Supervisor: Associate Professor Andrew J. Whittle
Title: Professor of Civil and Environmental Engineering

Thesis Co-Supervisor: Professor Harold F. Hemond
Title: Professor of Civil and Environmental Engineering

DEDICATION

To my parents.

ACKNOWLEDGMENTS

The author wants to extend her deepest appreciation to:

Professors Andrew Whittle and Harold Hemond for unexpectedly taking on supervision of my thesis.

Mr. John Sutabutr who performed the analyses for this project, who was willing to assist on a moment's notice, and who wrote the sections describing the analyses.

Dr. Douglas Cauble and Ms. Stacy Sonnenberg for their friendship and for introducing me to the geotechnical engineering laboratory at MIT.

The geotechnical laboratory group for the interaction, understanding, and their assistance in the major sample tube cutting event in preparation for index testing; Mr. Kurt Sjoblom, Mr. Laurent Levy, and Mr. Greg DaRe, for their vital assistance in preparing the Phase I Report for this project; Ms. Ann Chen for support and cut and paste assistance; Ms. Catalina Marulanda who donated the use of her laptop in my time of need; Mr. Kurt Sjoblom for additional assistance whenever necessary, Ms. Marika Santagata and Mr. Joe Sinfield for understanding, and Ms. Erin Force who, among many other things, assisted and performed many of the Constant Rate of Strain Tests.

Mr. Michael Kashambuzi who spent endless hours and many sleepless nights preparing the data acquisition and power equipment for the field program, and who spent numerous early, uncomfortable, cold rainy days and hot afternoons out in the field while being attacked by green head insects; Mr. Pete Fuentes who performed many of the Atterberg Limits; Ms. Amy Kukla who was on call for finding data and articles, performing Atterberg Limits, trimming and preparing for the Constant Rate of Strain Consolidation tests, battling the computers, redrawing the equipment figures that appear in this thesis, in addition to helping in many of the other things that needed to be done.

Dr. John T. Germaine whose technical assistance was vital to the project and whose relationship and patience I treasure.

My parents, sister, brother-in-law, grandparents, aunts, uncles, cousins, Ms. Heather Durrell, Mr. William Holden, and friends who tolerated the dedication necessary to complete this thesis, and for their understanding during this time of our lives.

Table of Contents

Abstract	3
Dedication	5
Acknowledgments	7
Table of Contents	9
List of Tables	13
List of Figures	15
1 Introduction	23
1.1 Purpose of this Project	24
1.2 Organization of Thesis	25
2 Background	27
2.1 Site	27
2.2 Previous Site Work at MIT's I-95 Test Site	29
2.2.1 Research Programs	29
2.2.2 Summary of Soil Deposit from Previous Investigations	31
2.3 Scope of Phase I, 1996 Field Program	33
2.3.1 Piezometers	34
2.3.2 Continuous Profile	35
2.3.3 Penetrations	35
2.3.4 Dissipations	35
2.3.5 Sampling	36
2.3.6 Survey of Site	36
2.4 Theoretical Framework for Predictions	37
3 Equipment	69
3.1 Penetrometers	69
3.1.1 Piezocone	69
3.1.2 Piezoprobe	69
3.1.3 MIT Piezocone	70
3.2 Depth Locator Box	70
3.3 Porous Element Saturation System	70
3.4 Response Chamber	71
3.5 Sampling Equipment and Piezometers	72
3.5.1 Fixed Piston Sampler	72
3.5.2 Hydraulic Sampler	72
3.5.3 Sample Tubes and Packers	73
3.5.4 Geonor Standpipe Piezometers	73
3.6 Data Acquisition and Power Supply	74
3.6.1 Power Supply and Protection	76
3.7 Field Logistics	77
3.7.1 Cables and Plastic Tubing	77
3.7.2 Housings and Watertight Connections	78
3.7.3 Support Equipment	78
3.7.4 Site Security System	79
4 Test Procedures	95

4.1	Piezometers	95
4.1.1	Installation	95
4.1.2	Water Level Measurements	96
4.2	Undisturbed Soil Samples	97
4.2.1	Borehole Advancement and Sampling Procedure	97
4.2.2	Tube Processing	98
4.3	Piezocone Profiling	98
4.4	Dissipation Experiments	99
4.5	Equipment Evaluation	102
4.5.1	Stability and Resolution	102
4.5.2	Calibrations	107
4.5.3	Response Evaluation	109
4.5.4	Penetration Rate	110
4.6	Saturation of Pore Pressure Elements	111
4.7	Site Cleanup	111
5	Field Data	123
5.1	Piezometers	123
5.1.1	Determination of Equilibrium Pore Pressures	123
5.2	Penetration Results	125
5.2.1	Continuous Piezocone Profile	125
5.2.2	Piecewise Penetration	127
5.3	Dissipation Results	128
5.3.1	Time for 50% Dissipation (t_{50})	131
6	Supporting Laboratory Investigation Data	159
6.1	Radiography	159
6.2	Bedding Layer Thickness	160
6.3	Atterberg Limits	161
6.4	Stress Profile	161
6.5	Constant Rate of Strain Consolidation (CRSC) Testing	162
6.5.1	Preconsolidation Pressure	163
6.5.2	Hydraulic Conductivity	163
7	Interpretation	187
7.1	Notation	187
7.2	Determination of In Situ Pore Pressure (u_0)	188
7.2.1	Full Dissipation	188
7.2.2	Inverse Time ($1/t$) Extrapolation	190
7.2.3	Two Point Intersection Method	192
7.2.4	Comparison of Methods for Estimating u_0	193
7.3	Determination of Hydraulic Conductivity (k)	195
7.3.1	T_{50} Matching Method	195
7.3.2	R^2 Goodness of Fit Matching Method	197
7.3.3	Concurrent Matching Method	198
7.3.4	Comparison of Field Hydraulic Conductivity Interpretation Methods	199
7.3.5	Comparison of Laboratory and Field Determined Hydraulic Conductivity	200

7.4 Rate Sensitivity	203
7.5 Uncertainty in Installation Pore Pressure Value (u_i)	204
7.6 Uncertainty in Dissipated Pore Pressure Value (u_{diss})	205
7.7 Initial Dissipation Point Sensitivity	206
8 Summary, Conclusions, and Recommendations	257
8.1 Summary and Conclusions	257
8.1.1 Relative Performance Between the Three Types of Devices	259
8.2 Recommendations	260
8.2.1 Procedures	260
8.2.2 Equipment	261
8.2.3 Further Investigations	262
References	265
Appendix A	269
Appendix B	328
Appendix C	331
Appendix D	370

LIST OF TABLES

Table 2.1	Geologic Profile (After Morrison, 1984).	46
Table 2.2	Elevations of the Various Borings Installed for the 1996 Field Program at Saugus (Station 246). Elevations are Referenced to the 1929 National Geodetic Vertical Datum (NGVD).	47
Table 2.3	Input Parameters used by MIT-E3 Soil Model (After Whittle et al., 1997).	48
Table 3.1	Gain Values for Each Transducer.	80
Table 4.1	Summary of Installation Details.	113
Table 4.2	Summary of Measurement Resolutions.	114
Table 4.3	Summary of Selection of Zero Voltage Values for Piezoprobe 63.	115
Table 4.4	Summary of Selection of Zero Voltage Values for Piezoprobe 62.	116
Table 4.5	Summary of Selection of Zero Voltage Values for Piezocone 790.	117
Table 4.6	Summary of Selection of Zero Voltage Values for Piezocone 881.	118
Table 4.7	Summary of Selection of Zero Voltage Values for the MIT Piezocone.	119
Table 4.8	Summary of Device Calibration Factors.	120
Table 5.1	Manual Piezometer Readings for M206A, M206B, and M206C.	133
Table 5.2	Calculated Time for 50% Dissipation (t_{50}).	134
Table 6.1	Summary of Atterberg Limits.	165
Table 6.2	Summary Table of CRSC Tests.	166
Table 7.1	Summary of Dissipated Pore Pressures.	210
Table 7.2	Values of In Situ Pore Pressure Determined by the Two Point Intersection Method.	211
Table 7.3	Comparison of u_0 Methods.	212
Table 7.4	Hydraulic Conductivity (k) Determined by the T_{50} Matching Method.	213
Table 7.5	Hydraulic Conductivity (k) Determined by the Goodness of Fit Method and Profile 1 (from Sutabutr, 1998).	214

Table 7.6	Hydraulic Conductivity (k) Determined by the Concurrent Matching Method (from Sutabutr, 1998).	215
Table 7.7	Ratio of Hydraulic Conductivity from a Method to the Value Determined by the Lower Bound of the Concurrent Matching Method.	216
Table 7.8	Hydraulic Conductivity Comparison between Interpretation Methods and Laboratory Data.	217
Table 7.9	Summary of Penetration Pore Pressures.	219
Table 7.10	Summary of Installation Rate and Subsequent Value of $(u_i - u_o) / \sigma'_{vo}$ for the Piezoprobes.	220
Table 7.11	Summary of Installation Rate and Subsequent Value of $(u_i - u_o) / \sigma'_{vo}$ for the Piezocones.	221
Table 7.12	Summary of Installation Rate and Subsequent Value of $(u_i - u_o) / \sigma'_{vo}$ for the MIT Piezocone.	222
Table 7.13	Summary of Sensitivity of Hydraulic Conductivity to Variation in the Installation Pore Pressure Value.	223
Table 7.14	Summary of Sensitivity of Hydraulic Conductivity to Variation in the Dissipated Pore Pressure Value.	224
Table 7.15	Summary of Sensitivity of Hydraulic Conductivity to Variation of the Initial Dissipation Point.	225

LIST OF FIGURES

Figure 2.1	Site Map of the I-95 Embankment (Station 246).	49
Figure 2.2	Index Properties and Stress History (After Baligh and Vivatrat, 1979).	50
Figure 2.3	Plasticity Chart (After Germaine, 1980).	51
Figure 2.4	Field Vane Strength (After Baligh et al., 1980, After Baligh & Vivatrat, 1979).	52
Figure 2.5	Typical Piezocone Profile for Station 246 (After Morrison, 1984).	53
Figure 2.6	Laboratory Measurements of Hydraulic Conductivity (After Morrison, 1984).	54
Figure 2.7	Dissipation Measurement Locations within Soil Profile (After Varney et al., 1997).	55
Figure 2.8	Overview of the Method of Analysis used to Compute Stress, Strain and Pore Pressure During Penetration and Dissipation of Probes (After Whittle et al., 1997).	56
Figure 2.9	Comparison of the Actual FMMG Piezoprobe and Strain Path Model (After Whittle et al., 1997).	57
Figure 2.10	Comparison of Simple Pile Solution to 18° Cone Solution (After Aubeny, 1992 and Whittle et al., 1997).	58
Figure 2.11	Soil Deformations during Penetration of FMMG Piezoprobe (After Whittle et al., 1997).	59
Figure 2.12	Predicted Deformation Pattern around FMMG Piezoprobe (After Whittle et al., 1997).	60
Figure 2.13	Strain Contours around FMMG Piezoprobe (After Whittle et al., 1997).	61
Figure 2.14	Effective Stress Contours around FMMG Piezoprobe (After Whittle et al., 1997).	63
Figure 2.15	Pore Pressure Contours around FMMG Piezoprobe (After Whittle et al., 1997).	65
Figure 2.16	Comparison of Installation Pore Pressure Computed by Poisson's Equation vs. Radial Integration (After Whittle et al., 1997).	66
Figure 2.17	Typical Finite Element Mesh for Coupled Consolidation Analysis (After Whittle et al., 1997).	67
Figure 2.18	Typical Results of Dissipation Pore Pressure for FMMG Piezoprobe (After Whittle et al., 1997).	68

Figure 3.1	Illustration of the “Standard” (FMMG) Piezocone with Porous Plastic Ring at the Base of the Shaft, above the 60° Tip.	81
Figure 3.2	Illustration of the FMMG Tapered Piezoprobe with a Fine Sintered Stainless Steel Porous Element at the Base of the Shaft.	82
Figure 3.3	Schematic of the MIT Piezocone with a Cylindrical Fine Stainless Steel Porous Element at the Tip of the 60° Taper (After Zeeb, 1996).	83
Figure 3.4	Schematic of the Depth Locator Box.	84
Figure 3.5	Schematic of the Evacuation System used to Evacuate the Chamber in Preparation for Saturation of Porous Elements (After Jordan, 1979).	85
Figure 3.6	Schematic of the Deaired Water System used to Saturate Porous Elements (After Jordan, 1979).	86
Figure 3.7	Schematic of Response Chamber used to Calibrate and Perform Equipment Evaluation of Piezocones and Piezoprobes (After Varney et al., 1997).	87
Figure 3.8	Illustration from Acker Catalog of the Acker Mechanical Fixed Piston Sampler used to Obtain 3.5” Undisturbed Soil Samples.	88
Figure 3.9	Illustration from Acker Catalog of Gus Hydraulic Fixed Piston Sampler used to Obtain 3” Undisturbed Soil Samples.	89
Figure 3.10	Schematic of Geonor Casagrande Type M-206 Field Piezometer.	90
Figure 3.11	Schematic of Data Acquisition and Power System used for Field Operation (After Varney et al., 1997).	91
Figure 3.12	Schematic of Housings used to Couple Piezocones and Piezoprobes to Standard AW Drill Rod (After Varney et al., 1997).	92
Figure 3.13	Schematic of Housings used to Couple the MIT Piezocone to Standard AW Drill Rod.	93
Figure 4.1	Summary of Electrical Noise Components for Pore Pressure Measurements of Each Device (After Varney et al., 1997).	121
Figure 4.2	Example of a.) a Poor Response after Cavitation of the Porous Element and b.) of a Satisfactory Response with a Porous Element Saturated with Water (After Varney et al., 1997).	122
Figure 5.1	Manual Piezometer Readings for M206A, M206B, and M206C over the Duration of the 1996 Field Program at Saugus (Station 246).	135
Figure 5.2	Response Curve for Piezometers: a.) M206A; b.) M206B; and c.) M206C.	136

Figure 5.3	Equilibrium Pore Pressure Profile at Saugus (Station 246) Determined from Piezometers.	137
Figure 5.4	Pore Pressure, Corrected Tip Resistance and Sleeve Friction during Continuous Penetration with Piezocone 790 at Saugus (Station 246).	138
Figure 5.5	Uncorrected Tip Resistance Profile using 60° Piezocone with Pore Pressure Measured at the Tip during 1982 Field Program (After Morrison, 1984).	139
Figure 5.6	Pore Pressure and Uncorrected Tip Resistance Profile using 60° Piezocone with Pore Pressure Measured at the Base of the Shaft during 1996 Field Program.	139
Figure 5.7	Pore Pressure Profile using 60° Piezocone with Pore Pressure Measured at the Tip during 1982 Field Program (After Morrison, 1984).	139
Figure 5.8	Comparison of Piecewise Penetration Pore Pressure with Standard Piezocones to Continuous Penetration Pore Pressure with Piezocone 790.	140
Figure 5.9	Comparison of Piecewise Penetration Pore Pressure with Tapered Piezoprobes to Continuous Penetration Pore Pressure with Piezocone 790.	141
Figure 5.10	Comparison of Piecewise Penetration Pore Pressure with the MIT Piezocone to Continuous Penetration Pore Pressure with Piezocone 790.	142
Figure 5.11	Dissipation Results for Piezocone 790 and Piezocone 881 at El. -12 m (45 ft. Depth).	143
Figure 5.12	Dissipation Results for Piezocone 790 and Piezoprobe 63 at El. -13 m (50 ft. Depth).	144
Figure 5.13	Dissipation Results for Piezocone 790 and Piezoprobe 63 at El. -15 m (55 ft. Depth).	145
Figure 5.14	Dissipation Results for Piezocone 881 at El. -16 m (60 ft. Depth).	146
Figure 5.15	Dissipation Results for Piezocone 790, Piezocone 881, Piezoprobe 62, Piezoprobe 63, and the MIT Piezocone at El. -18 m (65 ft. Depth).	147
Figure 5.16	Dissipation Results for Piezocone 790, Piezocone 881, Piezoprobe 62, Piezoprobe 63, and the MIT Piezocone at El. -21 m (75 ft. Depth).	148
Figure 5.17	Dissipation Results for Piezocone 790, Piezocone 881, Piezoprobe 62, Piezoprobe 63, and the MIT Piezocone at El. -24 m (85 ft. Depth).	149

Figure 5.18	Dissipation Results for Piezocone 790, Piezocone 881, Piezoprobe 62, Piezoprobe 63, and the MIT Piezocone at El. -27 m (95 ft. Depth).	150
Figure 5.19	Dissipation Results for Piezocone 790, Piezocone 881, Piezoprobe 62, Piezoprobe 63, and the MIT Piezocone at El. -30 m (105 ft. Depth).	151
Figure 5.20	Dissipation Results for Piezocone 790, Piezocone 881, Piezoprobe 62, Piezoprobe 63, and the MIT Piezocone at El. -33 m (115 ft. Depth).	152
Figure 5.21	Normalized Pore Pressure vs. Time for Piezocone 790 Dissipations.	153
Figure 5.22	Normalized Pore Pressure vs. Time for Piezocone 881 Dissipations.	154
Figure 5.23	Normalized Pore Pressure vs. Time for Piezoprobe 62 Dissipations.	155
Figure 5.24	Normalized Pore Pressure vs. Time for Piezoprobe 63 Dissipations.	156
Figure 5.25	Normalized Pore Pressure vs. Time for the MIT Piezocone Dissipations.	157
Figure 5.26	Calculated Time for 50% Dissipation (t_{50}) for: a.) Piezoprobe 62; b.) Piezoprobe 63; c.) Piezocone 790; d.) Piezocone 881; and e.) MIT Piezocone.	158
Figure 6.1	Location of Undisturbed Soil Samples obtained at Saugus (Station 246) during the 1996 Field Program.	170
Figure 6.2	Schematic of Setup used to Perform Radiography on Undisturbed Soil Samples (After Ladd et al., 1980).	171
Figure 6.3	Layer Interface Distribution over the Deposit of Boston Blue Clay at Station 246, as Determined by the Number of Interfaces (per 1.5 Inches) seen on the Radiographs.	172
Figure 6.4	Plastic Limit, Liquid Limit, and Natural Water Content of Undisturbed Soil Samples obtained during the 1996 Field Program.	173
Figure 6.5	Casagrande Plasticity Chart for Undisturbed Soil Samples obtained during the 1996 Field Program.	174
Figure 6.6	Water Content Profile for Undisturbed Soil Samples obtained during the 1996 Field Program at Saugus (Station 246).	175
Figure 6.7	Total Unit Weight Profile and Interpreted Values of Total Unit Weight from Undisturbed Soil Samples obtained during the 1996 Field Program at Saugus (Station 246).	176
Figure 6.8	In Situ Stress Profile.	177

Figure 6.9	Schematic of Constant Rate of Strain Consolidation (CRSC) Device (After Wissa, 1971).	178
Figure 6.10	Example Construction of Casagrande Technique for Preconsolidation Pressure Performed on Data from Test Number CRS210.	179
Figure 6.11	Example Construction of Strain Energy Technique for Preconsolidation Pressure Performed on Data from Test Number CRS210.	180
Figure 6.12	Preconsolidation Profile Determined from CRSC Tests Performed on Undisturbed Soil Samples obtained during the 1996 Field Program.	181
Figure 6.13	Overconsolidation Ratio (OCR) Profile.	182
Figure 6.14	Example Construction of Determination of In Situ Hydraulic Conductivity Performed on Data from Test Number CRS210.	183
Figure 6.15	Summary of In Situ Hydraulic Conductivity Values for Undisturbed Samples at Saugus (Station 246) from the 1984 and the 1986 Field Programs.	184
Figure 6.16	Void Ratio Versus Hydraulic Conductivity Measured from CRSC Tests Performed on Undisturbed Soil Samples at Station 246 (Varney, Germaine, & Ladd, 1998).	185
Figure 7.1	Example of Dissipated Pore Pressure Value Determination.	226
Figure 7.2	Dissipated Pore Pressure Ratio (u_{diss}/u_o) for: a.) Piezoprobe 62 and Piezoprobe 63; b.) Piezocone 790 and Piezocone 881; and c.) the MIT Piezocone.	227
Figure 7.3	Example of Inverse Time Construction on Measured Data: Piezoprobe 63 at El. -30 m (105 ft Depth).	228
Figure 7.4	Example of Inverse Time Plot for Model Prediction: Piezoprobe at El. -33 m (Depth 115 ft).	229
Figure 7.5	Convergence of the Pore Pressure Predicted by the Inverse Time Extrapolation Method to the Equilibrium Pore Pressure for the Piezoprobes.	230
Figure 7.6	Convergence of the Pore Pressure Predicted by the Inverse Time Extrapolation Method to the Equilibrium Pore Pressure for the Piezocones.	231
Figure 7.7	Convergence of the Pore Pressure Predicted by the Inverse Time Extrapolation Method to the Equilibrium Pore Pressure for the MIT Piezocone.	232

Figure 7.8	Probe Geometry and Brake Point (After Whittle et al., 1997).	233
Figure 7.9	Two Point Intersection Method for u_0 (After Whittle et al., 1997).	234
Figure 7.10	Two Point Intersection Construction for Determining u_0 : El. -18 m (Depth 65 ft).	235
Figure 7.11	Two Point Intersection Construction for Determining u_0 : El. -21 m (Depth 75 ft).	236
Figure 7.12	Two Point Intersection Construction for Determining u_0 : El. -24 m (Depth 85 ft).	237
Figure 7.13	Two Point Intersection Construction for Determining u_0 : El. -27 m (Depth 95 ft).	238
Figure 7.14	Two Point Intersection Construction for Determining u_0 : El. -30 m (Depth 105 ft).	239
Figure 7.15	Two Point Intersection Construction for Determining u_0 : El. -33 m (Depth 115 ft).	240
Figure 7.16	Stress History Profiles 1 & 2 (After Ladd et al., 1994).	241
Figure 7.17	Summary of Interpretation of Hydraulic Conductivity from the T_{50} Interpretation Method with Data Measured by the Piezoprobes.	242
Figure 7.18	Summary of Interpretation of Hydraulic Conductivity from the T_{50} Interpretation Method with Data Measured by the Piezocones.	243
Figure 7.19	Summary of Interpretation of Hydraulic Conductivity from the T_{50} Interpretation Method with Data Measured by the MIT Piezocone.	244
Figure 7.20	Summary of Interpretation of Hydraulic Conductivity from the T_{50} Interpretation Method with Data Measured by the Piezoprobes, Piezocones, and MIT Piezocone.	245
Figure 7.21	Example of the Goodness of Fit Matching Method.	246
Figure 7.22	Summary of Interpretation of Hydraulic Conductivity from the Goodness of Fit Matching Method with Data Measured by the Piezoprobes (After Sutabutr, 1998).	247
Figure 7.23	Summary of Interpretation of Hydraulic Conductivity from the Goodness of Fit Matching Method with Data Measured by the Piezocones (After Sutabutr, 1998).	248
Figure 7.24	Summary of Interpretation of Hydraulic Conductivity from the Goodness of Fit Matching Method with Data Measured by the MIT Piezocone (After Sutabutr, 1998).	249
Figure 7.25	Summary of Interpretation of Hydraulic Conductivity from the Goodness of Fit Matching Method with Data Measured by the Piezoprobes, Piezocones, and the MIT Piezocone (After Sutabutr, 1998).	250

Figure 7.26	Summary of Interpretation of Hydraulic Conductivity from the Concurrent Matching Method with Data Measured by the Piezoprobes and Piezocones (After Sutabutr, 1998).	251
Figure 7.27	Summary of the Ratio k_{lab}/k_{150} for the Piezoprobes and the Piezocones.	252
Figure 7.28	Penetration Pore Pressure Ratio $[(u_i - u_o)/\sigma'_{vo}]$ versus Penetration Rate for the Piezoprobes and the Piezocones.	253
Figure 7.29	Initial Dissipation Point Variation on Measured Data for Piezoprobe 62 at El. -33 m (Depth 115 ft.): a.) Penetration; b.) Dissipation, Absolute Pore Pressure; c.) Dissipation, Normalized Pore Pressure.	254
Figure 7.30	Slope of the Dissipation Curve of Absolute Pressure Versus Time using Measured Data for Piezoprobe 62 at El. -33 m (Depth 115 ft).	255
Figure 7.31	Initial Dissipation Point Variation on Theoretical Data for the Piezoprobe at El. -33 m (Depth 115 ft.): a.) Penetration; b.) Dissipation, Absolute Pore Pressure; c.) Dissipation, Normalized Pore Pressure Ratio.	256

1. INTRODUCTION

There is a long history of the use of penetrometers in clays as an in situ measuring device for geotechnical engineering. Their current widespread use reflects advances in instrumentation and methods of interpretation. The main application of penetration data is to define the vertical stratigraphic profile, while many authors report correlations between cone resistance and undrained shear strength. Undrained penetration in clays generates large excess pore pressures. The dissipation of these pore pressures, when penetration is halted, has been used to interpret either consolidation properties (linear methods, after Baligh and Levadoux, 1980) or hydraulic conductivity (nonlinear method, after Aubeny, 1992).

Modern history of the piezocone starts with the electrical cone (deRuiter, 1970). The electrical cone has an axial load cell to measure tip resistance and a friction sleeve to determine the soil/steel interface resistance. This was intended to provide a continuous measurement of in situ strength and to determine variations in soil properties, thus serving as a continuous soil profiling tool. Today, the piezocone provides the fastest and most sensitive device for determining soil profiles in sedimentary deposits. There are several methods of interpretation for the in situ strength of clay, but values are difficult to determine reliably due to the large strains and complex deformations around the device during penetration. As a result, interpretation depends on site specific correlations.

Janbu and Senneset (1974) and Schmertmann (1974) first used the electrical cone concurrently with a piezometer probe (Torstensson, 1975; Wissa, 1975) in a separate borehole to record pore pressures over the profile. The measurement of pore pressure contributed information concerning the relative hydraulic conductivity of the penetrated soil layers, thus increasing the profiling capabilities of the device. Senneset (1974) then developed the piezocone by including a pressure transducer in the design of the electrical cone, and was able to concurrently measure the tip resistance, friction resistance, and pore pressure in the same borehole.

Torstensson (1975) first explored the determination of the coefficient of consolidation, c_v , from the pore pressure decay measured by his device, using cavity

expansion to model the penetration process and uncoupled consolidation theory to model the dissipation behavior. Levadoux (1980) extended this work by developing an approximate analysis of undrained penetration in two dimensions, referred to as the Strain Path Method (Baligh, 1985) and radial uncoupled consolidation.

Hydraulic conductivity, k , can be extracted from pore pressure dissipation by using soil models that predict effective stresses during consolidation. This approach was first used by Whittle (1987) using the MIT-E3 soil model and analyzing radial dissipation around the shaft of long offshore piles. Aubeny (1992) extended this work (using improved estimation of installation pore pressures) to consider coupled two dimensional consolidation around penetrometer tips.

The oil industry uses the piezocone extensively for profiling, however, dissipation data are rarely used because complete dissipation of installation pore pressure around a conventional piezocone requires several days in typical Gulf of Mexico sediments. Constrained by the cost of offshore drilling, dissipation measurements are limited to a few hours at each location. Incomplete dissipation records are very difficult to interpret, especially when in situ pore pressures are expected to be non-hydrostatic. As a result, current prediction of pile set-up are based on laboratory measurements of k and theoretical models (cf. Whittle, 1992).

Fugro-McClelland Marine Geosciences, Inc. (FMMG), have recently designed a tapered piezoprobe device in order to measure reliably the in situ pore pressure at deepwater sites. The design assumes that by altering the geometry of the tip almost complete dissipation of installation pore pressure can be achieved during the two hour measurement period.

1.1 Purpose Of This Project

This thesis is part of a larger research program funded by the Joint Oil Industry Consortium, consisting of Amoco Worldwide Engineering & Construction, BP International Ltd., Chevron Petroleum Technology Company, Conoco Inc., Mobil Oil Corporation, Shell E&P Technology, and Texaco Inc.

The tapered piezoprobe has been used in several offshore site investigations. However, this is the first project to measure the complete dissipation response of the

tapered piezoprobe and to compare the results from this device with those obtained by a standard (FMMG) piezocone with identical installation methods and soil properties.

The project consists of three Phases with the following purposes: I) to conduct a field program, providing detailed field measurements with the tapered piezoprobe and the piezocone; II) to perform analytical predictions of piezoprobe performance and interpretation of data obtained in Phase I; and III) to develop a design manual for the application of piezoprobe data in practical calculations of pile set-up. This thesis presents the results of Phases I and II. Complete details of the laboratory investigation are to be included in a forthcoming report (Varney, Germaine, and Ladd, 1998) while further details of the parametric studies and discussion concerning the analytical predictions are presented in the Phase II research report (Whittle et al., 1997) and in a forthcoming thesis (Sutabutr, 1998).

1.2 Organization Of Thesis

The thesis presents the data, analysis and interpretation of pore pressure dissipation results obtained in Boston Blue Clay at the MIT test section in Saugus, Massachusetts.

Chapter 2 provides a background of research performed at the Saugus test site and details the scope of the 1996 field program at Station 246. Chapter 2 also provides a review of the Strain Path Method (Baligh, 1985) and the MIT-E3 soil model (Whittle, 1987), and the methods used to interpret the measured dissipation curves obtained during this field program.

Chapter 3 describes the equipment used to perform the various measurements performed at the site. Chapter 4 includes field details followed to make measurements as well as procedures adapted to evaluate the performance of the equipment.

Chapter 5 presents the results of the field program including the equilibrium pore pressure distribution and the dissipation curves. The dissipation curves are used in Chapter 7 in conjunction with the theoretical framework to interpret in situ pore pressure and hydraulic conductivity.

Chapter 6 briefly summarizes the supporting laboratory investigation data, which consists of Atterberg Limits, index properties, and Constant Rate of Strain Consolidation

(CRSC) tests. The data obtained from the laboratory investigation are used along with previous data obtained at the site to establish the site stratigraphy, stress history and reference hydraulic conductivity.

Chapter 7 provides the data interpretation methods and presents values for in situ equilibrium pore pressures and hydraulic conductivity as determined by the various methods. The chapter also investigates the sensitivity to various interpretation and field installation effects on the determined values.

Finally, Chapter 8 summarizes the results and conclusions of the research, suggests future research needs, and provides recommendations for efficient conduct of field programs.

2. BACKGROUND

This chapter provides a background of the site used to perform the field program, a description of the objectives of the 1996 field program, and an overview of the theoretical framework used to interpret the dissipation curves.

2.1 Site

The field program was conducted at a site which has been used by MIT to conduct various test programs since the mid-1960's. The site is approximately 10 miles from MIT, located in the Rumney Marsh at the southern town line in Saugus, Massachusetts. The MIT geotechnical group originally became involved with the site during the design phase for extending Interstate I-95 through Metropolitan Boston. Construction of a 10.7 m (35 ft) high embankment through the marsh was performed from 1967-1969 with two instrumented sections at Station 246 and 263 to monitor deformation during the construction process. The embankment design involved the use of preloading to control post construction deformations. The initial plans called for completion of construction of the embankment in 1973. However, a moratorium was placed on highway construction which ultimately caused termination of the highway project. To characterize the deposit for subsequent analysis, MIT conducted field vane tests and laboratory programs involving Boston Blue Clay. Due to the problems associated with construction of embankments on soft clay deposits, the Federal Highway Administration sponsored a research project to conduct field scale loading (Station 263) and unloading (Station 246) tests using the abandoned sand and gravel fill embankment. In 1974, MIT in cooperation with Massachusetts Department of Public Works (MDPW) removed the fill from Station 246 and added it to the embankment at Station 263 in order to cause collapse. A prediction symposium was held at MIT in 1974 (MIT, 1975) in order to determine the profession's ability to predict embankment failures.

In the Mid 1970's, MIT used the fill material to place 18 to 24 inch thick sand mats over the marsh peat deposits to the East of the embankment at Station 246 and to the West of the embankment at Station 263. These mats have served as working platforms

for a number of field investigations over the past 20 years, that focus on properties of the deep deposit (37 m) of underlying Boston Blue Clay. In the early 1980s, the mat at Station 246 was extended to the North, increasing the area available for field testing.

In 1994, the embankment was lowered to approximately ten feet above the marsh. The remaining fill is essentially flat providing easy access by car. There are two entries to the embankment at opposite ends of the marsh. Both are gated and locked at all times. The site is owned by the Commonwealth of Massachusetts. It was operated by the Massachusetts Highway Department until 1995, when authority was transferred to Metropolitan District Commission (MDC). Since the site is in the middle of a protected wetland marsh, permission to proceed with the project was required by the Saugus Conservation Commission.

A detailed plan of the site is presented in Figure 2.1. The plan includes locations of the boreholes installed for this project and the identifiable instrumentation from previous research projects. The plan also includes the two manholes which connected to the original instrumentation tunnel. These serve as the reference markers for the site. The current program was conducted on the northern end of the extended mat at Station 246 and essentially used the last available space for installing borings in virgin ground. It is therefore the last program to be conducted on the existing sand mat at this station. The plan also shows the locations of the van, which was used to house the instrumentation, and the silt fence, which was installed to prevent contamination of the drainage ditch. The ditch (actually part of an extensive network) was installed during the embankment construction as part of an effort to control mosquitoes.

The site has been desirable because of its proximity to the MIT campus, the isolation from general traffic, and the ability to perform the field tests under relatively well controlled (and supervised) testing conditions, allowing long term tests. The previous field programs were conducted using one or many of the following tools: Field Vane, CAMKOMETER, Push-in Lateral Stress Cells, Self-Boring Pressuremeters (PAFSOR), Dutch Cone Penetrometer, Piezometer Probe, Piezocone, and the evaluation of the ability of these field devices to predict soil conditions. Undisturbed samples were

also obtained during a number of the studies, which were used to conduct UUC, drained and undrained triaxial tests, constant rate of strain, oedometer, direct simple shear tests.

2.2 Previous Site Work at MIT's I-95 Test Site

MIT's I-95 site has served as the platform for a number of field programs and analysis studies. These research programs, along with a short description of the prediction symposium, are summarized in order to provide the reader with a general idea of the objectives of the studies and to determine the closeness of which the properties have been examined and evaluated. The site is well documented, both for soil properties, deposit characteristics, and general site behavior, such as pore water pressures for Stations 246 and 263. A partial listing of the theses originating from data collected at the Saugus test site follows.

2.2.1 Research Programs

2.2.1.1 "Proceedings of the Foundation Deformation Prediction Symposium," MIT (1975)

The symposium was conducted in order to evaluate the profession's ability to predict the performance of a soft clay foundation subjected to an embankment load. Fill was removed from Station 246 and placed on Station 263 to load the embankment to failure. An extensive site investigation was performed as part of this prediction symposium, and included installation of piezometers, settlement points, inclinometers, field vane tests, undisturbed sampling, Atterberg Limits, oedometer tests, Constant Rate of Strain Consolidation tests, Unconfined Compression tests, Unconfined Unconsolidated Compression tests, Drained Triaxial Compression Loading tests, CK_0U Triaxial Compression tests, and CK_0U Triaxial Extension tests.

2.2.1.2 Marr (1974)

Marr evaluates methods to measure in situ horizontal stress in Boston Blue Clay. The objective of the research is to verify the method of hydraulic fracturing of Geonor M206 piezometers. Fifteen hydraulic fracturing tests and thirteen tests with the

Cambridge self boring pressiometer are performed at Saugus Station 263. The results are compared to values of stress predicted by laboratory measurements.

2.2.1.3 “Cone Penetration in Clays,” Vivatrat (1978)

Vivatrat develops a method for estimating strains and strain-rates due to cone penetration based on incompressible flow analogies. He proposes an approach which combines the strain-path of soil elements with appropriate constitutive laws or laboratory testing of soil samples to analyze the penetration process. Extensive penetration testing was performed at Saugus Station 246, with companion undisturbed sampling. The penetration testing (26 profiles) was performed with electrical and mechanical Fugro cones, and with pore pressure probes, all with varying tip geometries and pore pressure element locations.

2.2.1.4 “Pore Pressure Dissipation After Cone Penetration,” Levadoux (1980)

Levadoux explores the determination of the coefficient of consolidation from pore pressure dissipation records. He obtains the initial pore pressure distribution due to undrained penetration by the Strain Path Method. Strain fields are computed by the method of sources and sinks. The stresses are computed with a modified total stress soil model which captures the strain softening and anisotropy of normally consolidated clay. Pore pressures are computed separately from strain fields. The results of undrained penetration are used in a two dimensional uncoupled consolidation model to compute the coefficient of consolidation. Predictions are compared to dissipation measurements made with piezometer probes of various geometries at Station 246. This is the same field program which was conducted by Vivatrat. He concludes that the Strain Path Method provides accurate initial pore pressure distributions.

2.2.1.5 “Evaluation of Self-Boring Pressuremeter Tests In Soft Cohesive Soils,” Germaine (1982)

Germaine evaluates the use of self-boring pressuremeters at Stations 246 and 263 at Saugus to obtain the in situ horizontal stress, the limit pressure, the undrained shear strength, and the undrained modulus of Boston Blue Clay. Measurements were made

with the French PAFSOR self-boring pressuremeter device. Results were compared to measurements made with the English CAMKOMETER device (Marr). A number of Constant Rate of Strain tests were performed to refine the stress history profile.

2.2.1.6 “Predictions of In Situ Consolidation Parameters of Boston Blue Clay,” Ghantous, (1982)

Ghantous evaluates the consolidation and hydraulic conductivity characteristics of Boston Blue Clay at Saugus Station 246. He compares values determined from conventional oedometer, Constant Rate of Strain Consolidation, and constant head tests performed on undisturbed soil samples at Station 246 (Boring M2) to those determined by Baligh and Levadoux (1980) from dissipation records at the same location.

2.2.1.7 “In Situ Measurements on a Model Pile in Clay,” Morrison, (1984)

Morrison investigates the development of a rational method for the prediction of the shaft capacity of axial loaded piles driven in clays. His research was based on an instrumented model pile shaft referred to as the Piezo-Lateral Stress Cell (PLS) which measures simultaneously, and at the same location, the pore pressure and total radial stress acting on the shaft. This thesis analyzed the results from the PLS used at Saugus during June, 1980, October 1981, and September/October 1982 and from piezocone profiles (Baligh et al, 1981). Cone penetration data was also measured with a Fugro 60° cone while the penetration pore pressure was measured with 18° conical piezometer used in three different holes. Pore pressure on the 18° cone was measured at different locations along the tip.

2.2.2 Summary of Soil Deposit from Previous Investigations

The following description of the deposit has been abstracted from Morrison (1984) and is based on a number of the field and sampling programs described above. Figure 2.2 illustrates the major layers of the deposit. The geological profile (Table 2.1) consists of 4 to 6 ft of peat overlying a thick layer of sand. Boston Blue Clay first appears at a depth of about 18 ft. The upper 13 ft of the clay (Zone A) is stiff and strongly interbedded with sand. Below a depth of 30 ft, the clay becomes dominant and is

divided into four sublayers according to piezocone characteristics. The top ten feet (Upper Clay Zone B) is stiff with frequent sand layers with large variations in penetration resistance due to desiccation. The next 20 ft (Upper Clay Zone C) is stiff and has thicker layers with large variations in penetration resistance. A transition layer (Middle Clay Zone D) shows a constant to decreasing resistance with depth and is much more uniform. The rest of the clay deposit is (Lower Clay Zone E) softer and more uniform with a few sand layers. The clay is underlain by a dense glacial till at about 140 ft.

The index properties and stress history for the clay as determined from previous studies at the site is presented in Figure 2.2 (After Baligh & Vivatrat, 1979). According to Germaine (1980), the natural water content increases gradually from approximately 30% in the top crust to approximately 45% in the soft clay, and is constant through the rest of the deposit. The plasticity index varies between 15 and 30% and is lower and more variable in the upper 50 ft. Figure 2.3 is a plasticity chart indicating the location of Boston Blue Clay (after Germaine, 1980). Boston Blue Clay is designated in the USCS as CL, a low plasticity clay, and plots above the A-Line.

The preconsolidation pressure (Figure 2.2) is a maximum at the top of the clay, decreases to a minimum within the upper 50 ft (bottom of Zone D) and then gradually increases with depth. The scatter is larger in the upper layers. Combining the preconsolidation pressure with the in situ effective stress indicates that the deposit has an overconsolidation ratio of 6 at the top, which decreases to about 1.2 within the upper 50 ft and then remains constant with depth.

Figure 2.4 presents the undrained strength profile as measured with a Geonor field vane. This profile is very similar in trend to the preconsolidation pressure profile. It clearly shows the higher strength and increased scatter in the upper 50 ft followed by a consistent increase with depth in the lower material. Figure 2.5 shows a typical piezocone profile for Station 246. Pore pressure is measured at the tip of the cone with a cylindrical stone (similar to the MIT piezocone used for this study). The uncorrected tip resistance clearly shows the variability and increased resistance in the upper material. The cone also identifies two major sand layers in the deep deposit which are between 100 and 120 ft.

Figure 2.6 presents the data from laboratory measurements of hydraulic conductivity. The data are sparse in the upper material. However, the trend is to decrease with depth for the upper 40 ft followed by a slight increase. There is almost one order of magnitude variation in the lower deposit.

2.3 Scope Of Phase I, 1996 Field Program

The intention of the field program is to compare detailed measurements of pore pressure dissipation rates and in situ pore pressures as determined by five devices. These devices are two recently developed Fugro McClelland Marine Geosciences (FMMG) tapered piezoprobes, two “standard” piezocone FMMG penetrometers, and one MIT designed piezocone. The field program included three separate tasks: collecting penetration and dissipation measurements with both the piezoprobes and piezocones as a function of depth, establishing the equilibrium pore pressure using standard hydraulic piezometers, and collecting undisturbed samples. The measurements were performed at the I-95 site in Saugus, Massachusetts for 45 days starting July 18, 1996.

Two boreholes (790PUSH and 881PUSH) were installed to perform continuous penetration soundings. Five penetration holes were installed to make long term dissipation measurements: one for each piezocone (PC790 and PC881), one for each tapered probe (PP62 and PP63), and one for the MIT piezocone (MIT). One borehole (B96) was installed to collect undisturbed samples. Three boreholes (M206A, M206B, and M206C) were used to install piezometers.

The boreholes were placed in a rough rectangular grid pattern with ten foot spacing. (refer to Figure 2.1). Hole locations were controlled by the geometry of the existing sand mat, boreholes from prior studies, and the need to move the drill rig from hole to hole.

A cargo van was used to provide field support and to house the data acquisition system which operated on a 24 hour basis. The van was protected by a remotely monitored security system whenever the site was not manned. Electrical power was provided by a gas generator during the day and batteries at night.

Equipment and technical support for the field program came from three sources; Fugro-McClelland Marine Geosciences Inc. (FMMG), MIT, and Con-Tec, Inc. Their contributions were as follows:

FMMG supplied the tapered probes with pressure transducers, replacement shafts, seal fittings, stones, and the original cables. They also supplied a replacement Kulite pressure transducer when the first one was damaged by a water leak. FMMG also supplied the piezocones with replacement porous Teflon rings, seal fittings, and the original cables. FMMG designed and fabricated the housings to connect the electrical cables to the devices and maintain a water tight seal. They also provided technical assistance as needed in preparing for the program and troubleshooting the field problems.

MIT supplied the data acquisition hardware and software, MIT piezocone with replacement transducers, stones, cables, and seal fittings, M206 piezometers, plastic tubing for the eight devices, night time and day time power supply, rental van and security system, and manpower. MIT designed and fabricated the housing to connect the penetrometers to the drill rod and acquired the replacement cables and tubing for all devices.

Con-Tec, Inc was subcontracted by FMMG to supply the drill rig, driller, driller's apprentice, some of the drill rod, water, bentonite and barite, sampling equipment and tubes, and standard drilling equipment.

GZA Drilling Inc. donated the use of several hundred feet of AW drill rod that was necessary to install the five devices at the deeper depths at the same time.

2.3.1 Piezometers

Equilibrium pore pressures were measured with Geonor M206 standpipe piezometers installed at the beginning of the field program and monitored throughout its duration. A piezometer was located in the upper, middle, and lower clay zones (as determined by Morrison) to establish the equilibrium pore pressure distribution throughout the deposit. The piezometers were also used to examine the pore pressure response to the tidal cycle.

2.3.2 Continuous Profile

A continuous profile was measured with a Fugro 60° tip piezocone with pore pressure measured at the base of the shaft¹. This was performed in order to establish the soil profile, compare results with Morrison as measured in the previous field program, and to establish that the penetrometers and data acquisition system were in working order. The continuous profile also served as a reference for the piecewise penetrations for the pore pressure, tip stress, and friction sleeve stress.

2.3.3 Penetrations

Measurements were collected during the installation procedure to ensure that the device stopped in a low permeability layer (with high excess) pore pressure to prevent difficulties in subsequent interpretation of dissipation data. This allowed the field observer to determine the general characteristics of the deposit during the five foot push and at the dissipation depth. The main focus of this research is the dissipation response. However, reliable penetration data are important as they provide insight into layering and undrained shear strength of the clay, as well as controlling initial conditions for dissipation.

2.3.4 Dissipations

The core goal of the field program was to make full dissipation measurements with the devices. Dissipation measurements were made with all five devices at nine depths between depths of 13.7 m and 35.1 m (45 to 115 ft) in a deposit of Boston Blue Clay, a low plasticity (CL) marine illitic clay with low to moderate overconsolidation ratio (OCR). Sufficient data was collected to establish reproducibility and to investigate the effects of OCR on the dissipation rates. The locations of dissipation were chosen to have at least one dissipation measurement in each of the zones of the soil deposit as established by Morrison (1984). The devices were left at their locations until installation pore pressures had fully dissipated, the duration of which lasted from 2 to 5 days.

¹ Performed with Piezocone 790. A profile was also measured with Piezocone 881, but was discarded as the unshielded electrical cable was deemed unsatisfactory.

Figure 2.7 shows the location within the profile for each of these measurements. The open symbols are locations where measurements were attempted but failed due to various reasons such as faulty electrical connections, water leaks, computer failures, etc. The resulting database of dissipation experiments used to analyze for in situ hydraulic conductivity and in situ pore pressure consists of 6 elevations at which all five devices were working. In addition, one set of dissipation experiments exist for the piezocones, one for one piezocone alone, and two elevations at which one piezoprobe and one piezocone were working. These partially successful installations all occur within the upper installations, from El. -11.5 to -16 m (45 to 60 Ft depth).

2.3.5 Sampling

Undisturbed samples were obtained to perform a supporting laboratory investigation, with the main goal of increasing the database of laboratory measurements of hydraulic conductivity. Samples were obtained from each of the soil zones previously described by Morrison (1984) to provide soil to further verify soil model parameters for natural Boston Blue Clay. Sample locations were also selected to provide soil at the dissipation test elevations in addition to providing a distribution across the clay deposit. Nineteen 3" samples and four 3.5" samples were collected. Sampling was performed as a secondary priority to the penetration and dissipation measurements.

2.3.6 Survey of Site

The site was surveyed to establish the elevations of the various borings. The plan view is included as Figure 2.1, while the listing of elevations for the various boreholes installed for this project are listed in Table 2.2. All elevations in this report are referenced to the 1929 NGVD (National Geodetic Vertical Datum) datum. The elevation of the surface of the marsh is approximately 1.55 m. The surface of the mat slopes downward to the East. Near the sampling hole (B96) the elevation is 2.20 m (6.62 ft). At the location of M206a, the elevation is 1.78 m (5.85 ft). It should be noted that the maximum tide elevation is above the elevation of the majority of the mat, leading to flood conditions of the mat during several high tides each month.

2.4 Theoretical Framework For Predictions

The following presents a description of the analyses used to predict the dissipation of penetration induced pore pressures in clay. This discussion has been extracted from the Phase II report (Whittle et al., 1997), where further details of the analysis can be found.

The flow chart in Figure 2.8 summarizes the analyses that are used to predict the dissipation of penetration induced pore pressures in clay. The calculations are subdivided into two phases:

I) Simulation of undrained probe penetration using the Strain Path Method (SPM, Baligh, 1985), and

II) Finite element calculations of pore pressure dissipation.

The SPM is an approximate analytical framework which models the disturbance caused by deep, quasi-static penetration of a pile or probe in a saturated, homogeneous clay. The key assumption of the analysis is that the deep penetration problem is heavily kinematically constrained, such that deformations and strains induced in the soil are effectively independent of its shearing resistance. In the simplest application of the strain path method for steady penetration, soil velocities are equated with the irrotational flow of an incompressible, inviscid fluid moving around the stationary penetrometer. In this case, the velocity field satisfies the conservation of volume requirement for undrained penetration, while different penetrometer shapes can be developed using well established methods from potential theory. (Baligh, 1986a; Chin, 1986; Baligh et al., 1987; Whittle et al., 1991).

More realistic penetrometer geometries can also be developed from the basic solutions using methods of superposition. For example, the “method of sources and sinks” (Weinstein, 1948; Rouse, 1959) can be used to model the geometry of axisymmetric penetrometers using a series of line sources and sinks distributed along the centerline of the body (known as a ‘Rankine body’). This technique was originally used by Levadoux and Baligh (1980) for 18° and 60° cone penetrometers. In this study, the FMMG piezoprobe geometry is modeled using a combination of a single point source and

a series of line sources and sinks as shown in Figure 2.9. The model geometry has the following properties:

1.) The extension piece has a round tip geometry modeled by a single point source similar to a simple pile, and has a radius, R_1 , that matches the actual probe geometry (i.e., $R_1/R_2 = 0.179$). The porous filter is assumed to be located at $z = 0.59R_2$ behind the base of the probe. The actual piezoprobe has a sharp conical tip which is not simulated in the strain path model. However, previous studies (Aubeny, 1992) have shown that this approximation has minimal influence on prediction of pore pressures at the location of the porous filter. For example, Figure 2.10 compares pore pressure prediction at the penetrometer surface for a rounded tip geometry ('simple pile') and an 18° conical tip. By setting the elevation of the rounded tip at the same level as the base of the cone, the two analyses generate almost identical pore pressure distribution at all point above the tip ($z/R_2 > 0$).

2.) The tapered sections of the FMMG probe are modeled using a distribution of approximately 180 source-sink combinations. One important limitation of the method of sources and sinks is that there are an infinite number of possible source configurations which can match a prescribed surface geometry. Numerous trials are necessary to establish reliable and accurate solutions which describe a smooth surface geometry and smooth strain paths for soil elements close to the surface of the penetrometer.

Figure 2.11 shows the displacement paths of five soil elements initially located at radial distances, $r_0/R_2 = 0.1 - 4.0$, from the centerline of the probe. Each of the elements is displaced vertically downwards and radially outwards to accommodate the volume displaced by the approaching probe tip. As the tip passes the elevation of the elements there is a reversal in the vertical displacement component. The net vertical displacement far above the tip is very small ($w/R_2 < 0.07$, at $r/R_2 = 1.1$, element B). Figure 2.12 shows strain path predictions of deformations for an initially square grid ($\Delta r/R_2 = \Delta z/R_2 = 0.25$) of points in the soil around the FMMG tapered probe. These results confirm the very small vertical deformations and consequent shear distortions associated with the tapered probe geometry in the (r,z) plane.

Following Baligh (1985), the shear strains caused by undrained simple pile penetration can be conveniently characterized by three components: , $E_2 = \frac{1}{\sqrt{3(\epsilon_{rr} - \epsilon_{\theta\theta})}}$, and $E_3 = \frac{2}{\sqrt{3\epsilon_{rz}}}$, which correspond to triaxial, pressuremeter (cylindrical cavity expansion) and direct simple shear modes, respectively. Each of these components contributes equally to the overall magnitude of the shear strain described by the second invariant of deviatoric strains, $E = \frac{1}{\sqrt{2(E_1^2 + E_2^2 + E_3^2)}}$. Figures 2.6a-d compare contours of octahedral shear strain, E, cavity shear strain, E₂, axial strain, E₁, and shear strain, E₃. The results show the following:

1.) The octahedral shear strain gives a general measure of shear strain intensity. Figure 2.13c shows that the zone of high shear strains, $E > 10\%$, is confined to a thin annular zone of radius, $r \approx R_1$. The contour $E = 0.1\%$ corresponds to the typical shear level necessary to induce significant non-linearity in the shear stress-strain properties of a typical soft clay. The region defined by $E = 0.1\%$ extends laterally to $r/R_2 \approx 20$ around the probe shaft, and approximately $z/R_2 = 5$ ahead of the tip.

2.) The cavity shear strain, E₂, (Figure 2.13a) is very similar in magnitude to the octahedral shear strain, E, at all points above the tip of the extension piece. This result shows that the one-dimensional radial cavity expansion is the dominant mode of shearing for the tapered piezoprobe. This result is further confirmed by contours of the other shear components: The vertical strains E₁ (Figure 2.13c) are very small except in a local region around the tip of the probe, while the third component is significant around the taper section where there is a zone $E_3 > 5\%$ (Figure 2.6d).

Two types of analysis are then possible for the dissipation phase: Total stress soil models and Uncoupled consolidation (T-U analyses) or Effective stress soil models and Coupled consolidation (E-C analyses). The current research uses E-C analyses using the MIT-E3 soil model (Whittle, 1987) in order to relate piezoprobe dissipation behavior to pile shaft set-up.

According to the framework of the E-C analyses in Figure 2.8, effective stress fields around the penetrometer can be computed directly from the strain paths using an effective stress soil model. The current analyses use the MIT-E3 soil model for this purpose: MIT-E3 (Whittle, 1987) is a rate independent, elasto-plastic model which describes many aspects of the observed behavior of K_0 -normally and lightly overconsolidated clays including: a) small-strain non-linearity, b) anisotropic stress-strain-strength; and c) hysteretic and inelastic behavior due to cyclic loading. Table 2.3 lists the model input parameters and the laboratory tests from which they are obtained. Full details of the procedures used in parameter selection have been presented elsewhere (e.g., Whittle & Kavvas, 1994). Table 2.3 also lists the model input parameters (Whittle, 1987; Whittle et al., 1994) corresponding to Resedimented Boston Blue Clay [BBC(R)] that is used as the reference material for the predictions in this thesis.

Figures 2.7a-d show predictions of the effective stress components for undrained penetration of the tapered piezoprobe in K_0 -normally consolidated BBC(R):

1.) The radial effective stress is a key component in the prediction and interpretation of pile set-up in clays. Figure 2.14a shows that probe penetration causes a large reduction in σ'_r/σ'_{vo} from the $K_0=0.48$ condition (in the far field) to minimum values, $\sigma'_r/\sigma'_{vo} < 0.2$ close to the surface of the probe. This behavior is similar to previous predictions for piezocone/simple pile geometries and reflects the strain softening behavior of BBC(R) when sheared to large strains.

2.) Contours of the mean effective stress, σ'/σ'_{vo} (Figure 2.14b) are a measure of the shear induced pore pressure cause by probe penetration ($-\Delta\sigma'/\sigma'_{vo} = \Delta u_s/\sigma'_{vo}$). In the far field $\sigma'/\sigma'_{vo} = 0.65$, while most of the region around the penetrometer, $\sigma'/\sigma'_{vo} < 0.2$ (corresponding to shearing close to critical state conditions). Hence, significant positive shear induced pore pressures are caused by the penetration process.

3. The cavity shear stress $q_h/\sigma'_{vo} = (\sigma'_r - \sigma'_{tt})/(2s'_{vo})$ (Figure 2.14c) corresponds to the shear component computed in one-dimensional radial cavity expansion models. The results confirm a characteristic feature of strain path models, that $q_h/\sigma'_{vo} \approx 0$ close to the surface of the penetrometer, while maximum cavity shear resistance is mobilized within

the soil at $r/R_2 = 1.5 - 2.0$ ($r/R_1 = 8 - 11$) around the extension piece; and at $r/R_2 = 8 - 11$ around the shaft.

4. The strain path model predicts very small values of the shear stress τ_{rz}/σ'_{vo} (Figure 2.14d) except in the region close to the base of the taper section.

In principle, the excess pore pressures can be estimated from the effective stress fields by invoking the equilibrium condition, i.e., by solving the following equations:

$$-\frac{\partial u}{\partial r} = -g_r = \frac{\partial \sigma'_{rr}}{\partial r} + \frac{\partial \sigma'_{rz}}{\partial z} + \frac{\sigma'_{rr} - \sigma'_{\theta\theta}}{r} \quad \text{Equation 2.1a}$$

$$-\frac{\partial u}{\partial z} = -g_z = \frac{\partial \sigma'_{zz}}{\partial z} + \frac{\partial \sigma'_{rz}}{\partial r} + \frac{\sigma'_{rz}}{r} \quad \text{Equation 2.1b}$$

If the effective stress fields are exact solutions, then the pore pressures can be obtained by integrating in either the radial or vertical direction (using the known distribution, g_r , g_z , respectively) i.e., the predicted pore pressures are independent of the path of integration and the stress gradients satisfy the relation:

$$\frac{\partial g_r}{\partial z} = \frac{\partial g_z}{\partial r} \quad \text{Equation 2.1c}$$

This condition is only satisfied if the strain paths are compatible with the model used to determine the stresses. However, the Strain Path Method uses an approximate strain field which is not fully compatible with the soil model. Non-uniqueness of the pore pressure (or octahedral stress) field was first observed by Levadoux and Baligh (1980) and has been studied extensively in previous work on piezocone penetrometers by Chin (1986) and Aubeny (1992). These studies have shown that:

1.) In the region ahead of the cone, the soil is subject to triaxial compression modes of shearing only. Vertical equilibrium can reliably be used to estimate pore pressures at the tip of a piezocone (Baligh, 1986b; and Elghaib, 1989).

2.) Far behind the penetrometer tip, predictions of excess pore pressures can be obtained from radial equilibrium. Predicted stresses in this region are very susceptible to inelastic effects (Baligh, 1986a) due to reversal of individual strain components. Consequently, predicted pore pressures will be strongly influenced by complex aspects of soil behavior including anisotropy, strain softening, and rate dependence.

3. Errors due to the non-uniqueness are most significant in the region immediately above the tip of the piezocone penetrometer and can affect the interpretation of pore pressures measured in this region.

The last result is of particular importance for the FMMG tapered probe. It should be noted that the preliminary analyses of the tapered piezoprobe (Whittle, 1995) used radial integration to estimate penetration pore pressures.

Aubeny (1992) has shown that one successful method for ameliorating the difficulties associated with path dependent pore pressures, is to solve both equilibrium equations by taking the divergence of Equations 2.1:

$$\nabla^2 u = \nabla \cdot g = -q \quad \text{Equation 2.2}$$

In this case the scalar pore pressure field, u , is determined as the solution of a Poisson equation using standard finite element techniques. In general, Poisson pore pressure fields will not satisfy either equilibrium equation exactly. However, the Poisson solution does not rely upon an arbitrary selection of an integration path; it therefore provides a flexible method for extending SPM solutions to penetrometers of general shape.

Aubeny (1992) obtained accurate numerical solutions of Equation 2.2 by: 1) computing the first derivatives of the effective stresses (g_r , g_z) numerically (using an isoparametric interpolation scheme); and 2) using the divergence theorem to compute the average flux, q , within individual finite elements. This same procedure has been adopted in this research.

Figure 2.15 shows the comparison of pore pressure at the end-of-installation of the FMMG piezoprobe, calculated by Poisson's equation and Radial Integration. At the shaft location where the behavior in the radial direction dominates, the normalized pore pressure calculated by both Poisson's Equation and Radial Integration are in close agreement. At the location of the porous filter, however, the normalized pore pressure by Poisson's equation is approximately 20% greater than that calculated by the radial integration.

Figure 2.15 and Figure 2.16 compare predictions of excess pore pressures around the tapered piezoprobe using the methods of radial integration (equation 2.1a) and

Poisson's Equation (equation 2.2). Both methods predict similar radial distributions of excess pore pressures around the shaft (far above the tapered tip), extending more than 30 radii from the penetrometer (Figure 2.16). The excess pore pressures predicted at the pile shaft $\Delta u_i/\sigma'_{vo} = 1.2$ to 1.3, are comparable to previous strain path predictions for the simple pile (Whittle, 1992). There are large differences in the distribution of pore pressure ahead of the penetrometer tip, where the Poisson equation solutions are considered more reliable than radial integration (i.e., they take into account the vertical equilibrium in this region). The Poisson solution also generates higher excess pore pressures at the tip of the probe and along the surface of the main taper section ($z/R_2 = 10 - 16$, Figure 2.16).

This section illustrates typical results of coupled consolidation analyses that predict changes in both the pore water pressures and effective stresses which occur after probe installation. The analyses are carried out by non-linear finite element methods (using the ABACUS™ finite element code) which solve concurrently the equations of equilibrium and continuity of fluid flow. These analyses are complex and involve the following assumptions and procedures:

1. The installation effective stresses and excess pore pressures are used as initial conditions in the finite element analysis. However, some corrections are necessary in order to account for a) lack of equilibrium in the strain path fields; and b) incompatibility in the boundary conditions of the strain path penetration and finite element dissipation analyses. These connection problems were resolved by Aubeny (1992) by applying a field of corrective nodal forces, which remain constant throughout consolidation.

2. Figure 2.10 shows the boundary conditions used in the coupled consolidation model. Drainage and deformation conditions on the top, bottom, centerline and far field boundaries are well defined. However, boundary conditions along the surface of the penetrometer are not well defined (or controlled in the field situation). The current analyses assume there is no flow normal to the surface ($\partial u/\partial n = 0$) and no vertical displacement of the penetrometer tip itself (i.e., $-0.18 \leq z/R_2 \leq 15$). However, the drill shaft is assumed to be rigid and smooth, with no constraint on the vertical deformations for $z/R_2 > 15$.

3. The finite element analysis uses mixed elements with eight displacement nodes and four pore pressure corner nodes, which enable quadratic interpolation of displacements and linear interpolation of pore pressures. Figure 2.17 illustrates the high resolution of the finite element mesh which is required in the tip region in order to achieve reliable numerical solutions of pore pressure dissipation. This typical mesh used for the FMMG piezoprobe geometry, consists of 1344 elements and 4047 nodes.

4. Non-linear stress-strain properties of the soil are modeled using the MITE-3 effective stress soil (with input parameters for BBC(R) listed in Table 2.3). The typical analyses assume that the movement of pore fluid is controlled by D'Arcy's law, with a constant, isotropic hydraulic conductivity, k . Detailed analyses which investigate the effects of anisotropy and density dependent hydraulic conductivity properties on dissipation predictions in Whittle et al. (1997).

Figure 2.18 shows typical predictions of pore pressure dissipation for penetration in K_0 -normally consolidated BBC(R). The results compare excess pore pressure ratios, $\Delta u/\Delta u_i$, for the tapered piezoprobe with the response predicted for a porous filter located at the base of a conventional piezocone (simulated using the Strain Path Method with simple pile geometry and radius, $R = R_2$) and a hypothetical miniature cone with $R = R_1$. The figure shows predictions based on initial excess pore pressures computed by both Radial integration and Poisson equation (i.e. from Figure 2.8). The results show the following:

1. The initial dissipation of the tapered piezoprobe follows very closely the behavior of the miniature piezocone (simple pile). However, as consolidation proceeds there is a marked retardation as the response of the piezoprobe is influenced by the pore pressure field around the drill shaft. The onset of this transition is termed a "brake point" in Figure 2.18. Ultimately, the response of the probe approaches the behavior expected for the piezocone, and there is no benefit of the tapered section. In this example, the brake point occurs at $\Delta u/\Delta u_i \approx 0.4$, the main transition corresponds to a 'residual pore pressure ratio', $\Delta u/\Delta u_i = 0.2 - 0.1$, and the response only converges towards the piezocone for $\Delta u/\Delta u_i < 0.05$.

2. The method of obtaining installation pore pressures has a significant effect on the predicted dissipation response of the tapered piezoprobe. The most notable differences are in the shape of the dissipation curves during the initial and transition phases. These account for a 60% difference in the consolidation time T_{50} at $\Delta u/\Delta u_i = 0.5$. The results can be related directly to the predicted distributions of pore pressures around the penetrometer tip in Figure 2.15. The calculations presented in this thesis use the more reliable Poisson equation method to obtain installation pore pressures.

Description	depth (ft)	Characteristics
a layer of <u>peat</u> exists over this depth	4 - 8	q_c is low with small variability (Fig 4.11).
<u>sand</u> layer	8 - 17	sharp increase in q_c (Fig. 4.11)
transition zone starting with clean sand changing to sandy clay with interstitial sand lenses (referred to as upper clay- <u>Zone A</u>).	17 - 30	very clear decrease in mean value of q_c with high variability. u is very low at $d=20$ ft and increases thereafter with large variability in magnitude.
Upper clay- <u>Zone B</u>	30 - 40	u and q_c are essentially constant with some variability.
Upper clay- <u>Zone C</u>	40 - 60	Both u and q_c increase at approximately the same rate.
Middle clay- <u>Zone D</u>	60 - 75	Smaller rate of increase in both u and q_c compared to above.
Lower clay- <u>Zone E</u>	75 - 140	Both u and q_c increase at the same rate with small variability.
<u>Glacial Till</u>	140	Sharp increase in q_c and decrease in u .

Table 2.1 Geologic Profile (After Morrison, 1984).

Description	Abbreviation	Ground Surface Elevation (NGVD)	
		(ft)	(m)
Continuous Push, Piezocone 790	790PUSH	6.35	1.94
Continuous Push, Piezocone 881	881PUSH	6.47	1.97
Piezometer A	M206A	5.85	1.78
Piezometer B	M206B	5.95	1.81
Piezometer C	M206C	6.03	1.84
Sampling Hole	B96	6.55	2.00
Installation Hole, Piezoprobe 62	PP62	6.47	1.97
Installation Hole, Piezoprobe 63	PP63	6.36	1.94
Installation Hole, Piezocone 790	PC790	6.87	2.09
Installation Hole, Piezocone 881	PC881	6.18	1.88
Installation Hole, MIT Piezocone	MIT	6.62	2.02

Table 2.2 Elevations of the Various Borings Installed for the 1996 Field Program at Saugus (Station 246). Elevations are Referenced to the 1929 National Geodetic Vertical Datum (NGVD).

Test Type	Parameter /Symbol	Physical Contribution/meaning	BBC(R)
Oedometer or CRS	e_0	Void ratio at reference stress	1.12
	λ	Compressibility of NC clay	0.184
	C	Non-linear volumetric swelling behaviour	22
	n		1.6
	h	Irrecoverable plastic strain	0.2
K_0 -oedometer or K_0 -triaxial	K_{0nc}	K_0 for virgin normally consolidated clay	0.48
	$2G/K$	Ratio of elastic shear to bulk modulus	1.05
Undrained Triaxial Shear Test : OCR=1 : CK_0UC OCR=1 : CK_0UE OCR=2 : CK_0UC	ϕ'_{TC}	Critical state friction angles in triaxial compression and extension	33.4°
	ϕ'_{TE}		45.9°
	c	Size of bounding surface	0.86
	s_t	Strain softening factor	4.5
	ω	Small strain non-linearity	0.07
	γ	Shear induced pore pressure for OC clay	0.5
Resonant Column	κ_0	Small strain compressibility at load reversal	0.001
Drained Triaxial	ψ_0	Rate of evolution of anisotropy	100.0

Table 2.3 Input Parameters used by MIT-E3 Soil Model (After Whittle et al., 1997).

Saugus Site Plan

Scale
1" = 20'

- Probe location
- ⊕ Boring
- Piezometer
- ⊖ Inclinator
- ⊙ Manhole

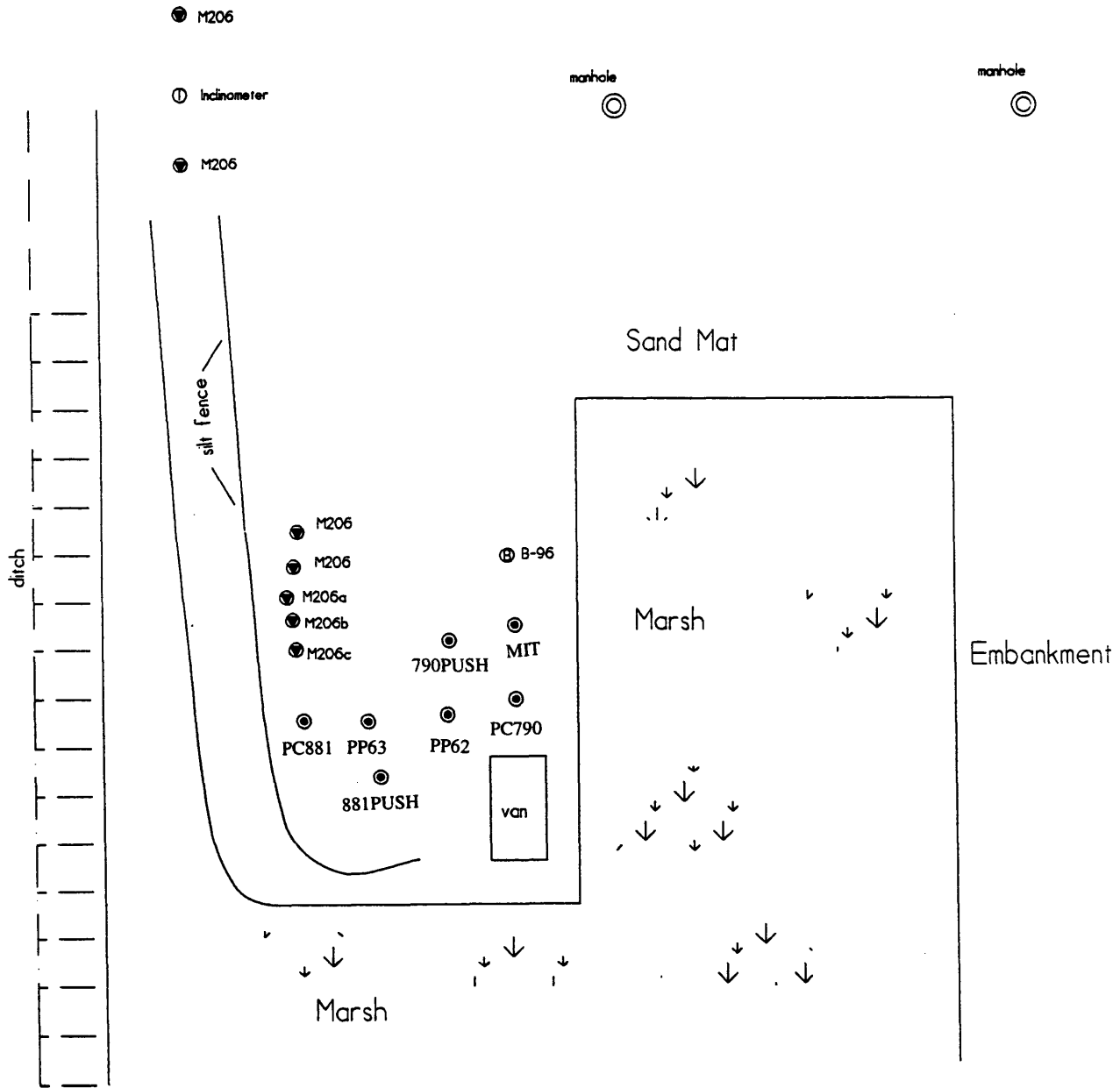


Figure 2.1 Site Map of the I-95 Embankment (Station 246).

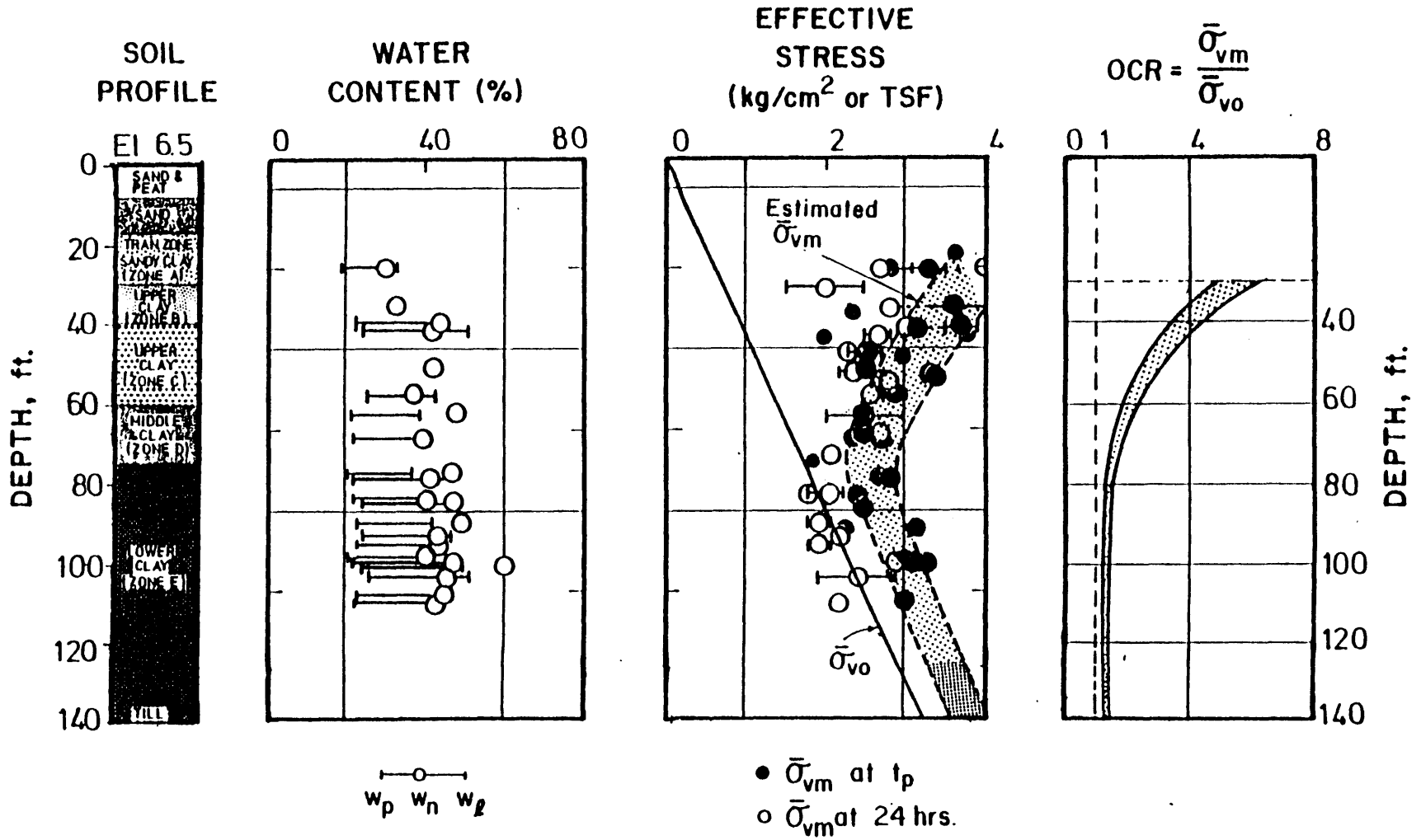


Figure 2.2 Index Properties and Stress History (After Baligh and Vivatrat, 1979).

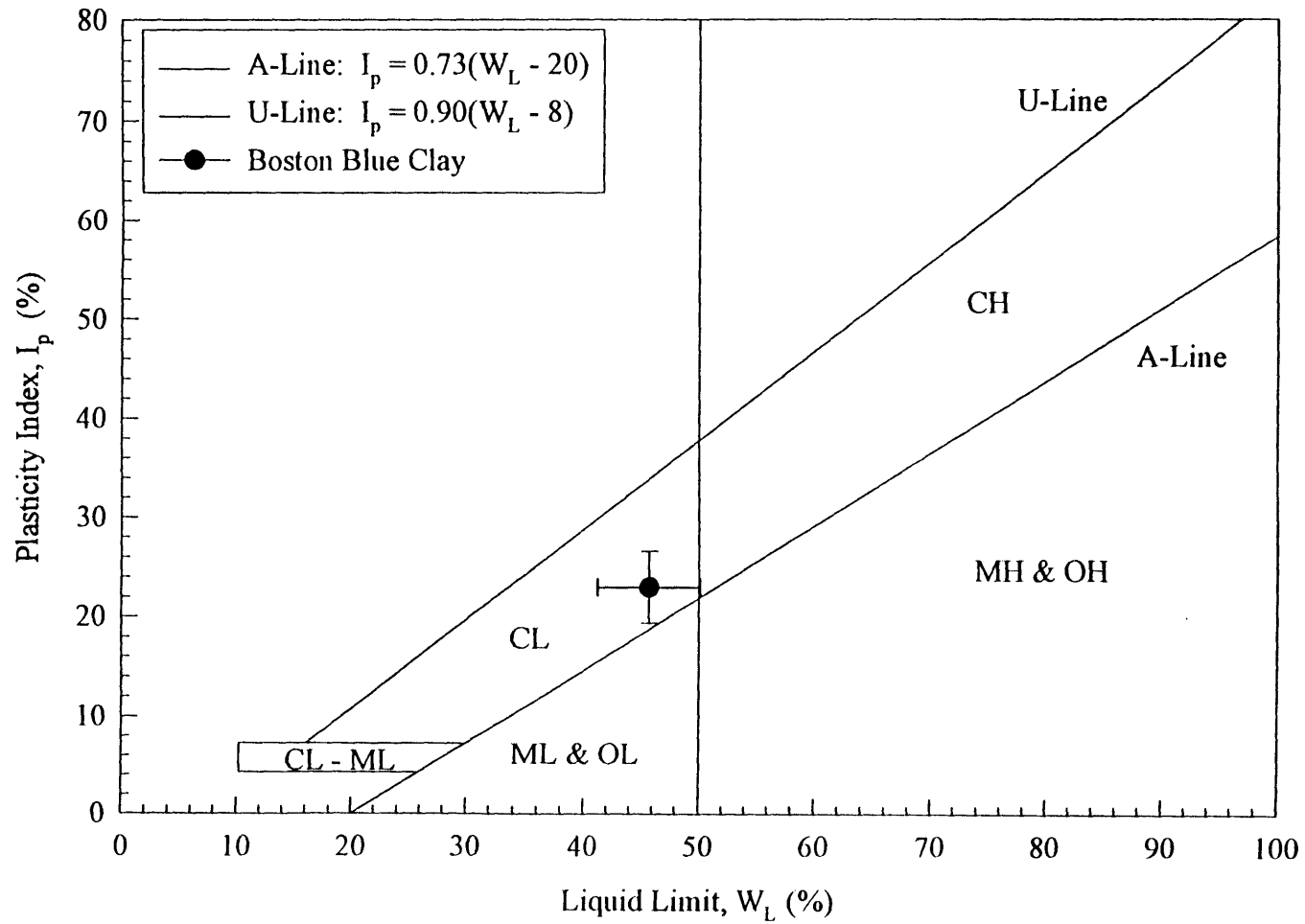


Figure 2.3 Plasticity Chart (After Germaine, 1980).

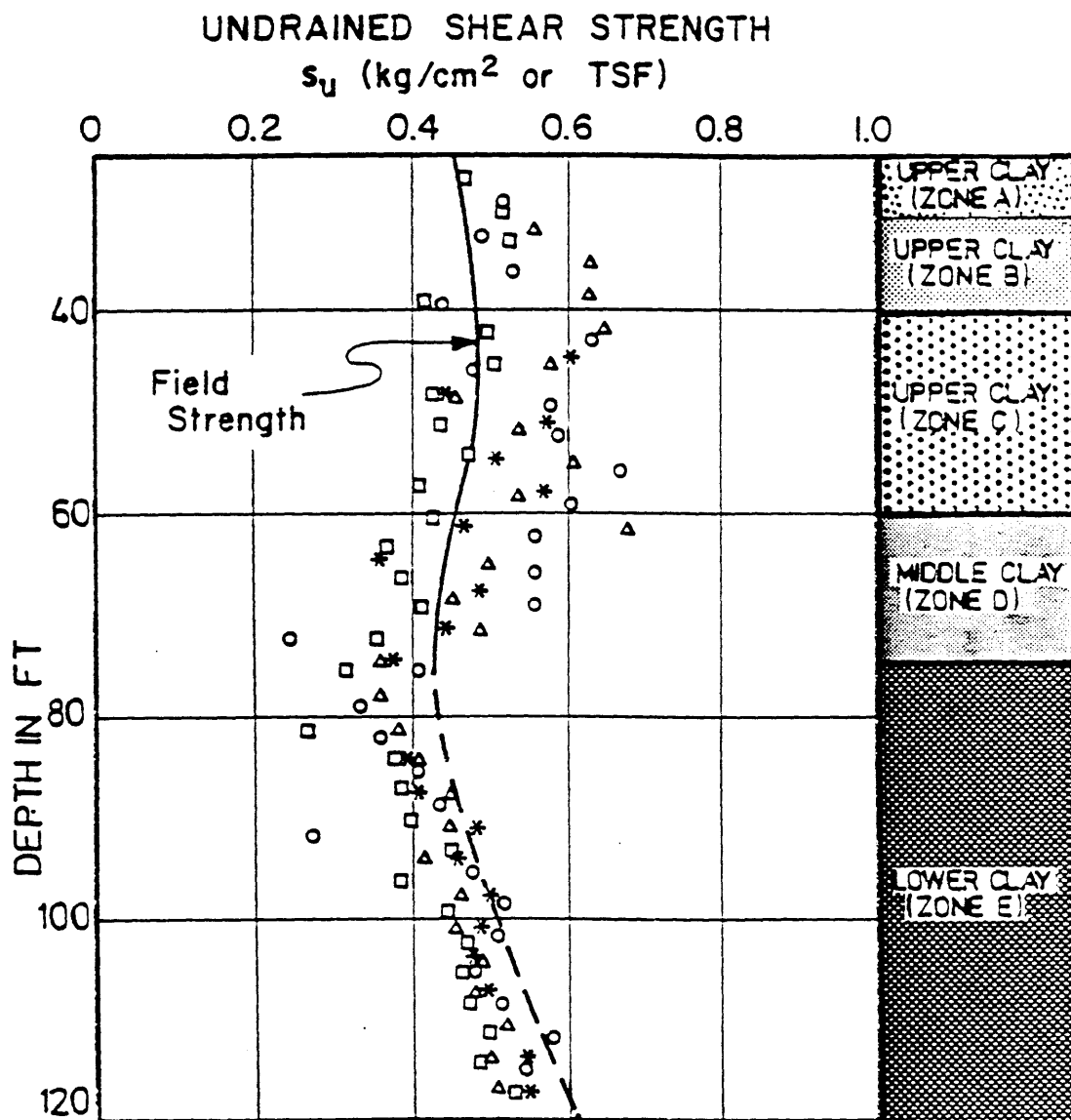


Figure 2.4 Field Vane Strength (After Baligh et al., 1980, After Baligh & Vivatrat, 1979).

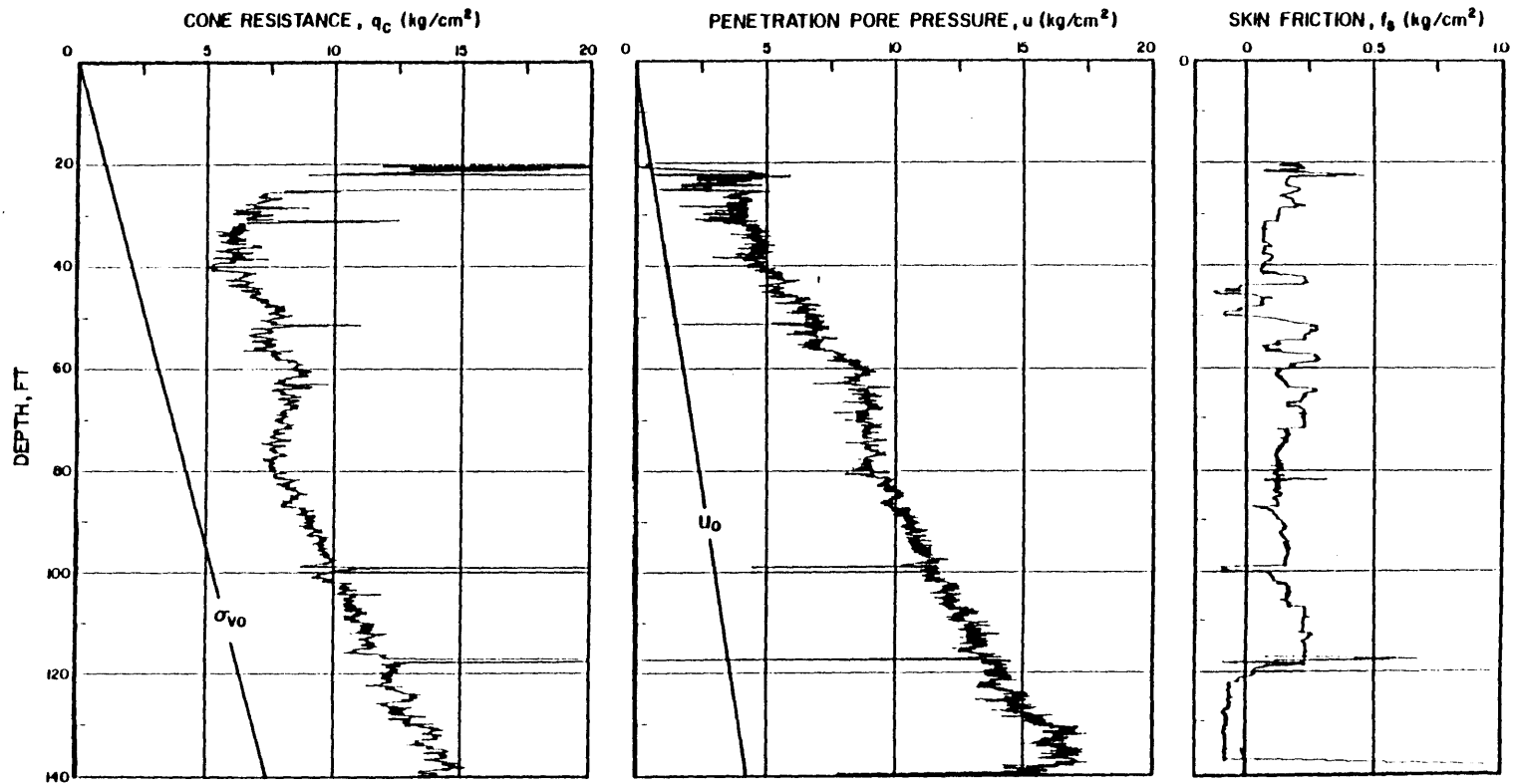


Figure 2.5 Typical Piezocone Profile for Station 246 (After Morrison, 1984).

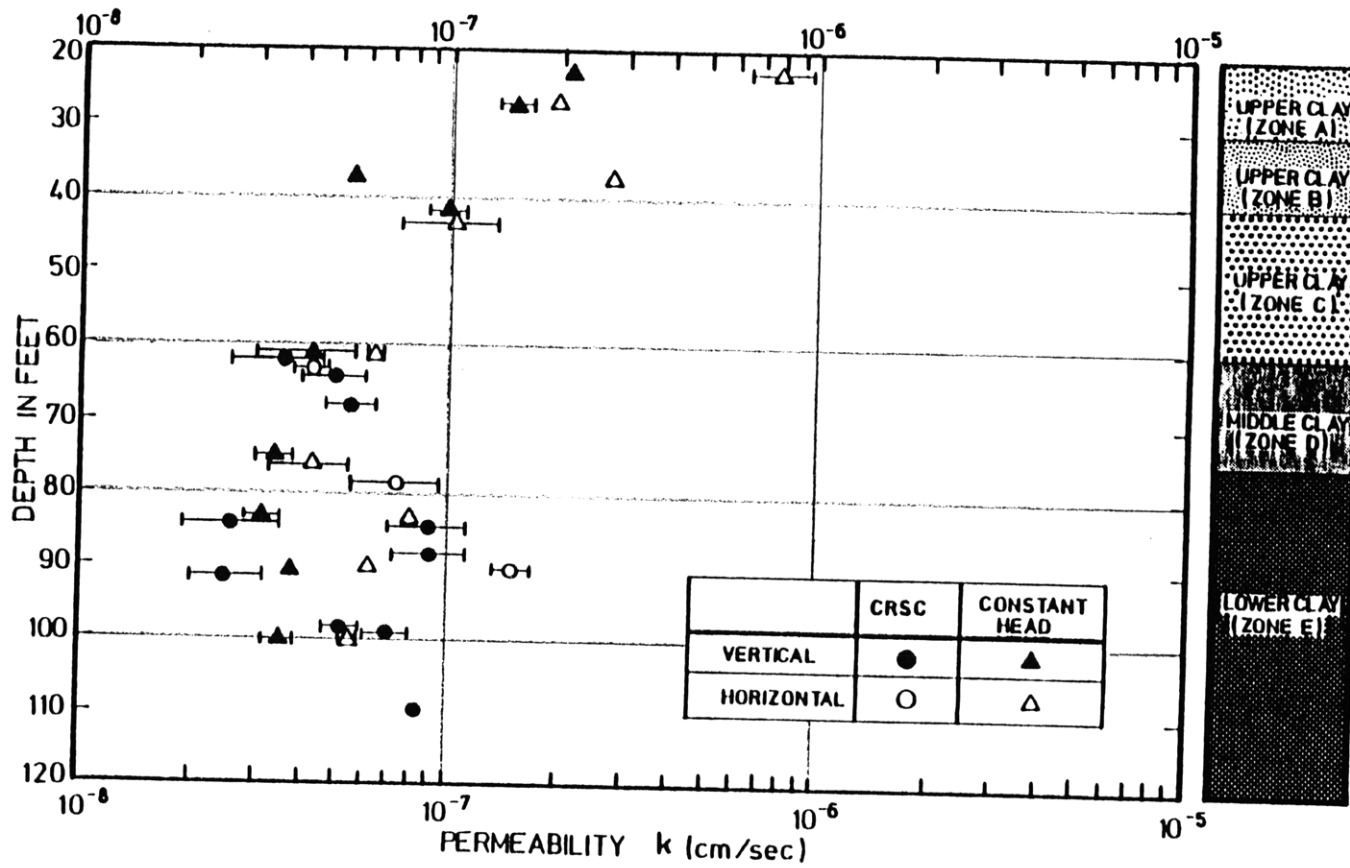


Figure 2.6 Laboratory Measurements of Hydraulic Conductivity (After Morrison, 1984).

Measurement Profile
 I-95 Embankment Station 246
 Saugus, Massachusetts

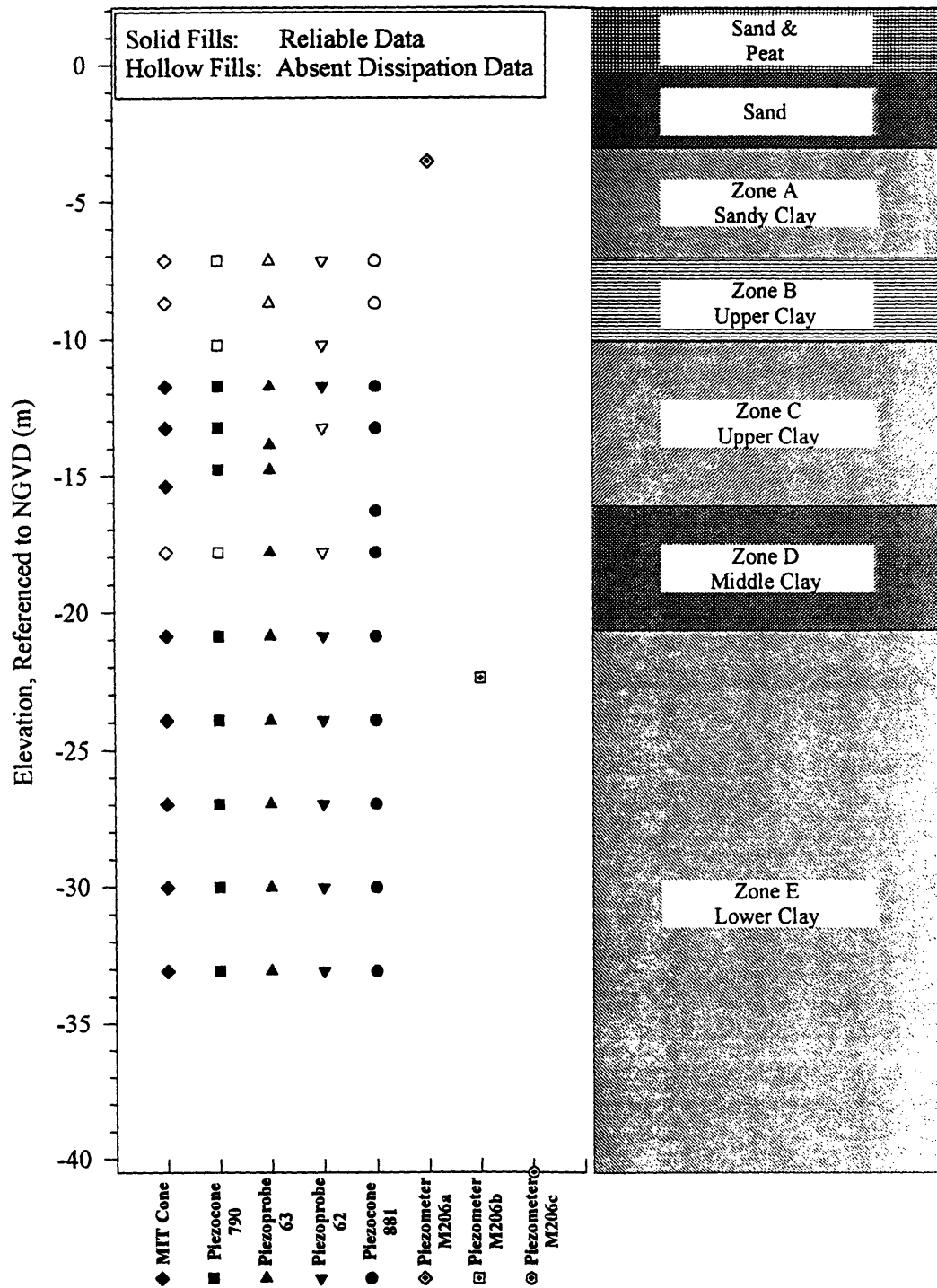


Figure 2.7 Dissipation Measurement Locations within Soil Profile (After Varney et al., 1997).

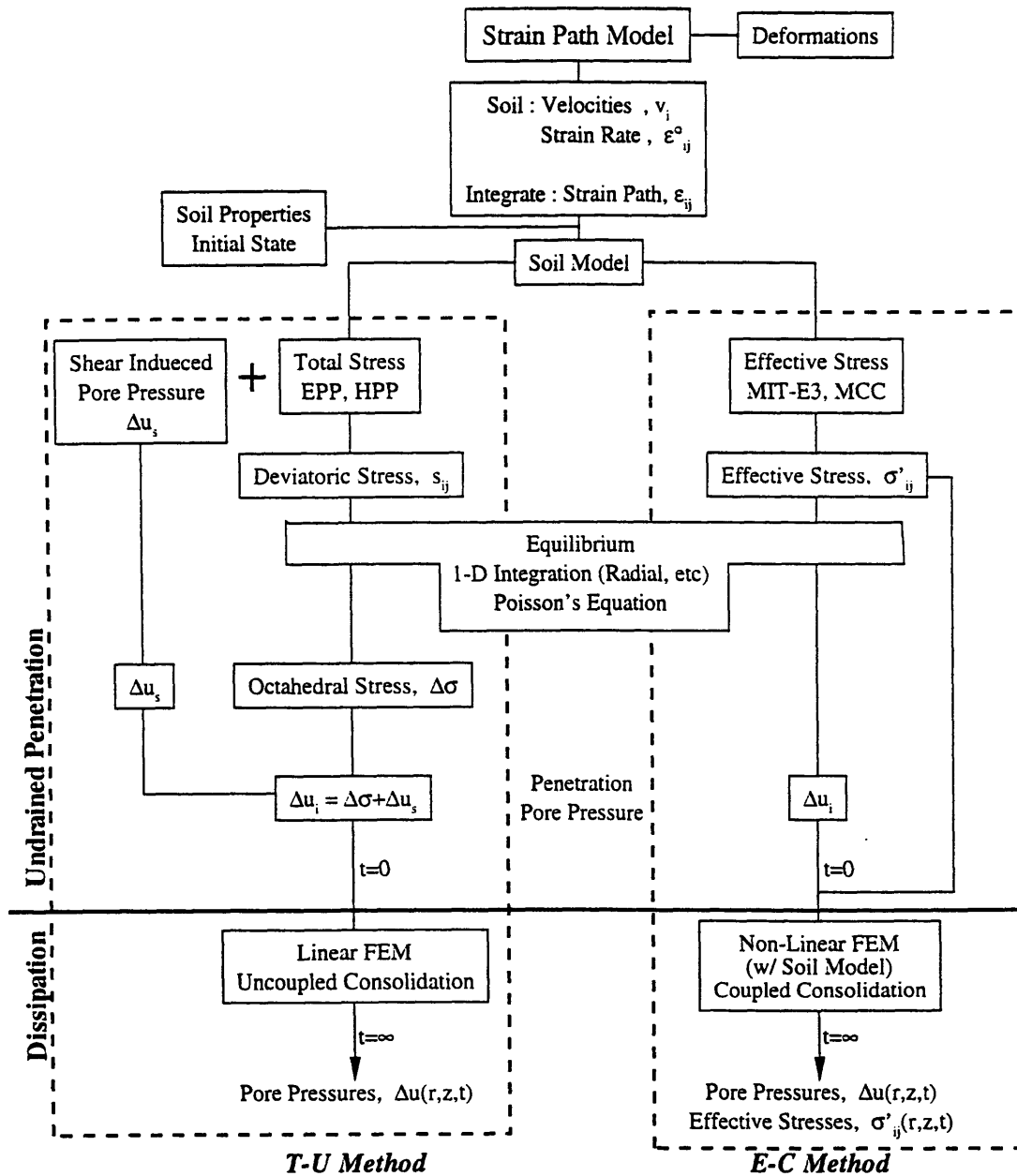


Figure 2.8 Overview of the Method of Analysis used to Compute Stress, Strain and Pore Pressure During Penetration and Dissipation of Probes (After Whittle et al., 1997).

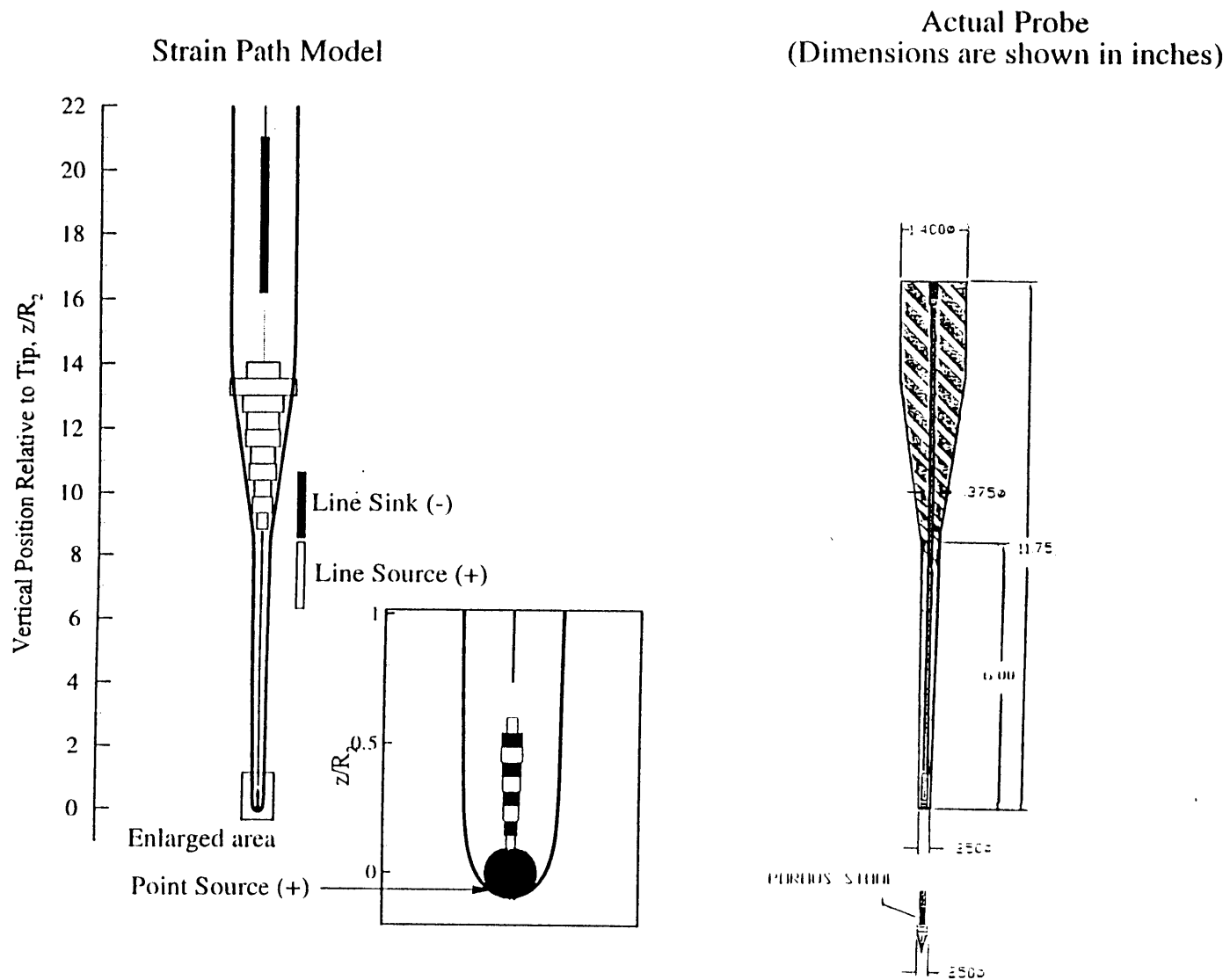


Figure 2.9 Comparison of the Actual FMMG Piezoprobe and Strain Path Model (After Whittle et al., 1997).

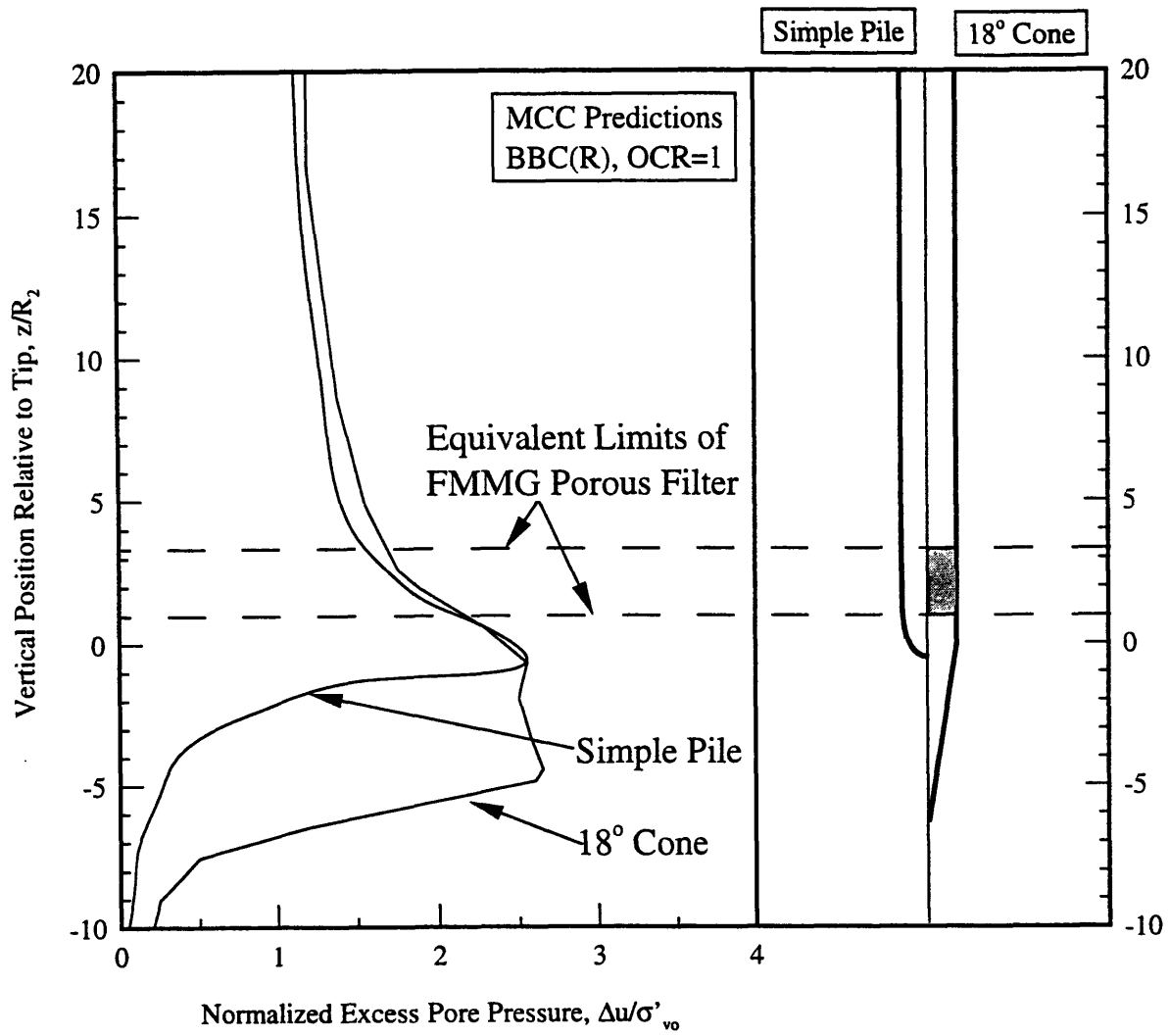


Figure 2.10 Comparison of Simple Pile Solution to 18° Cone Solution (After Aubeny, 1992 and Whittle et al., 1997).

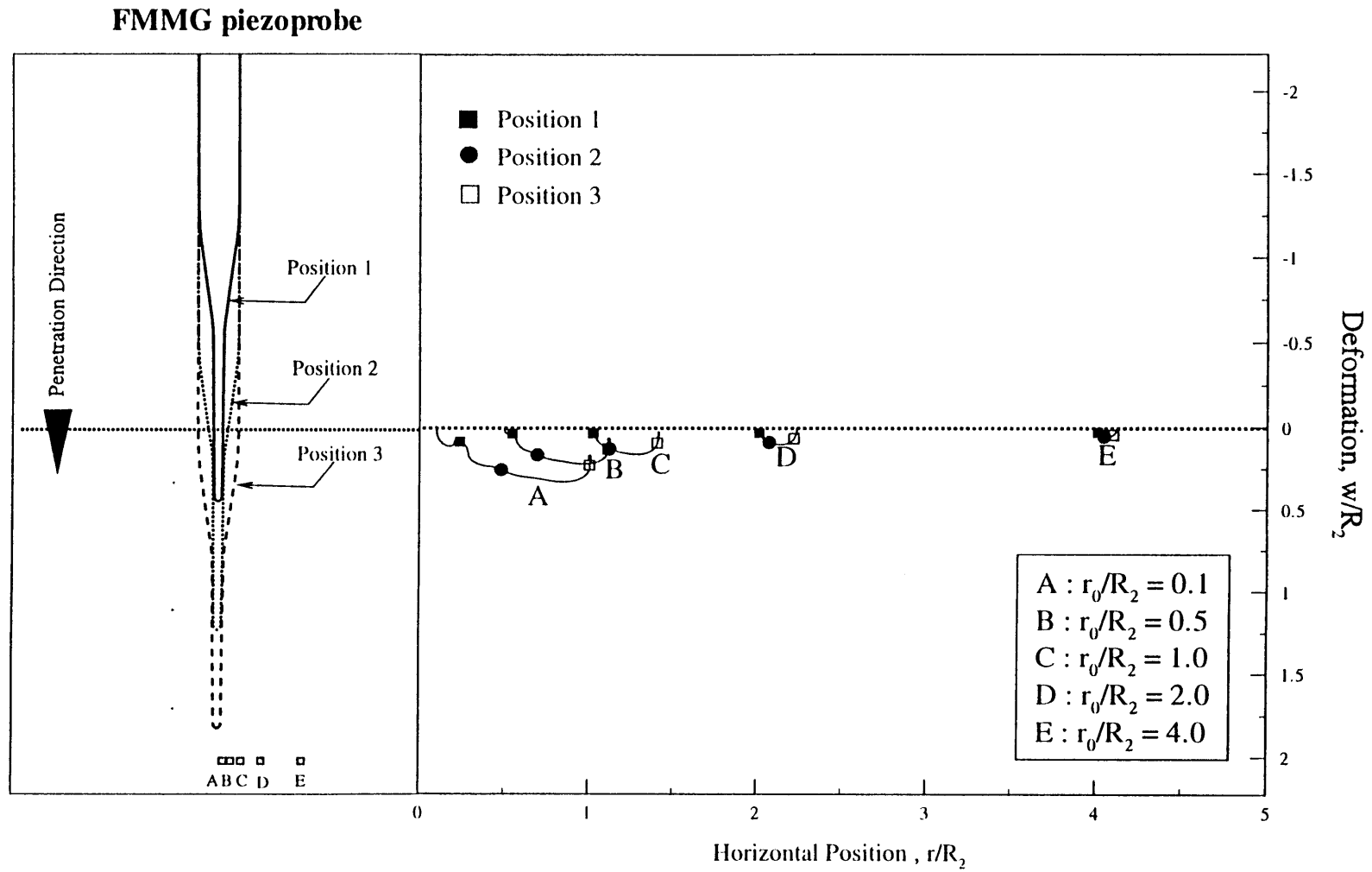


Figure 2.11 Soil Deformations during Penetration of FMMG Piezoprobe (After Whittle et al., 1997).

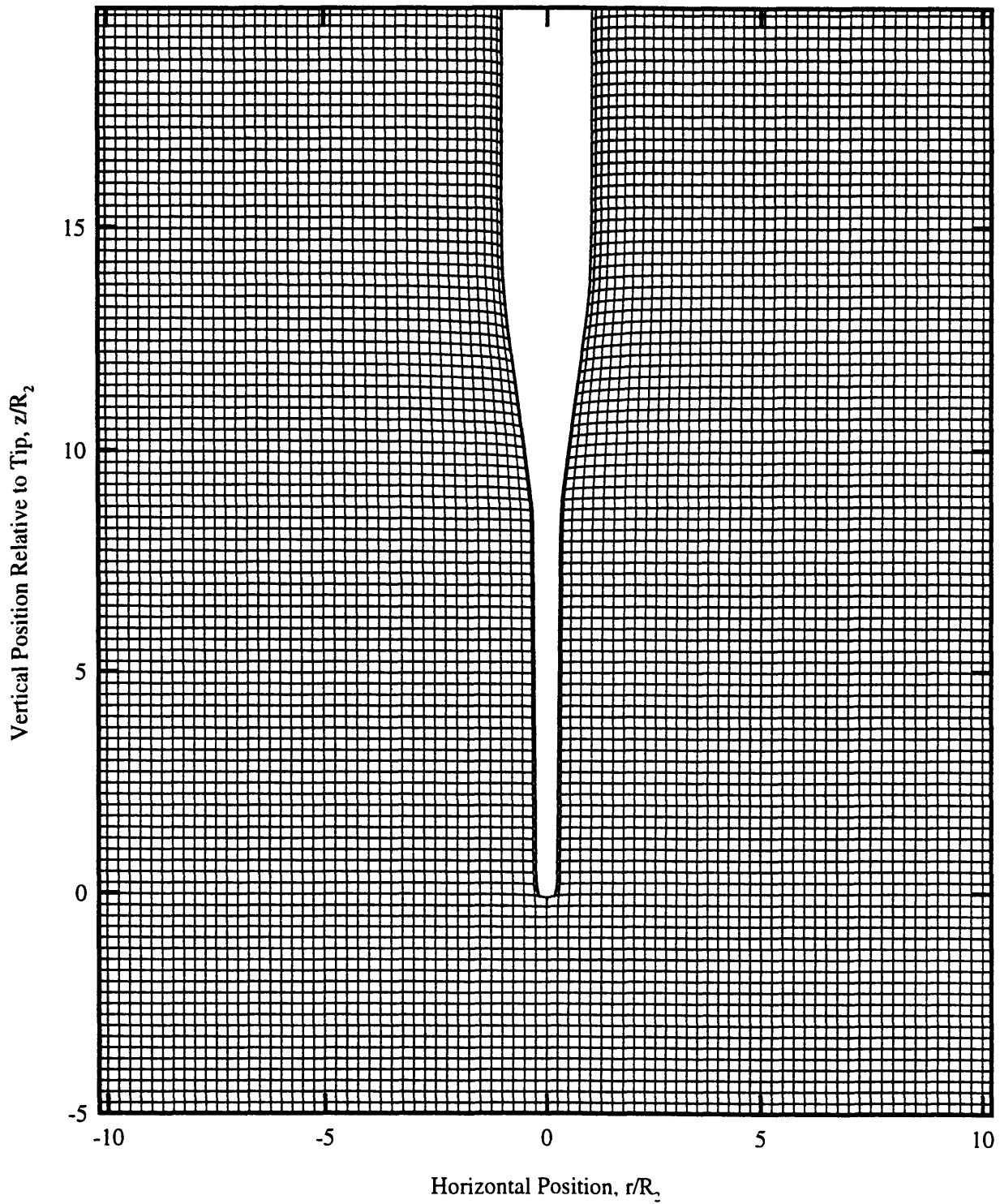
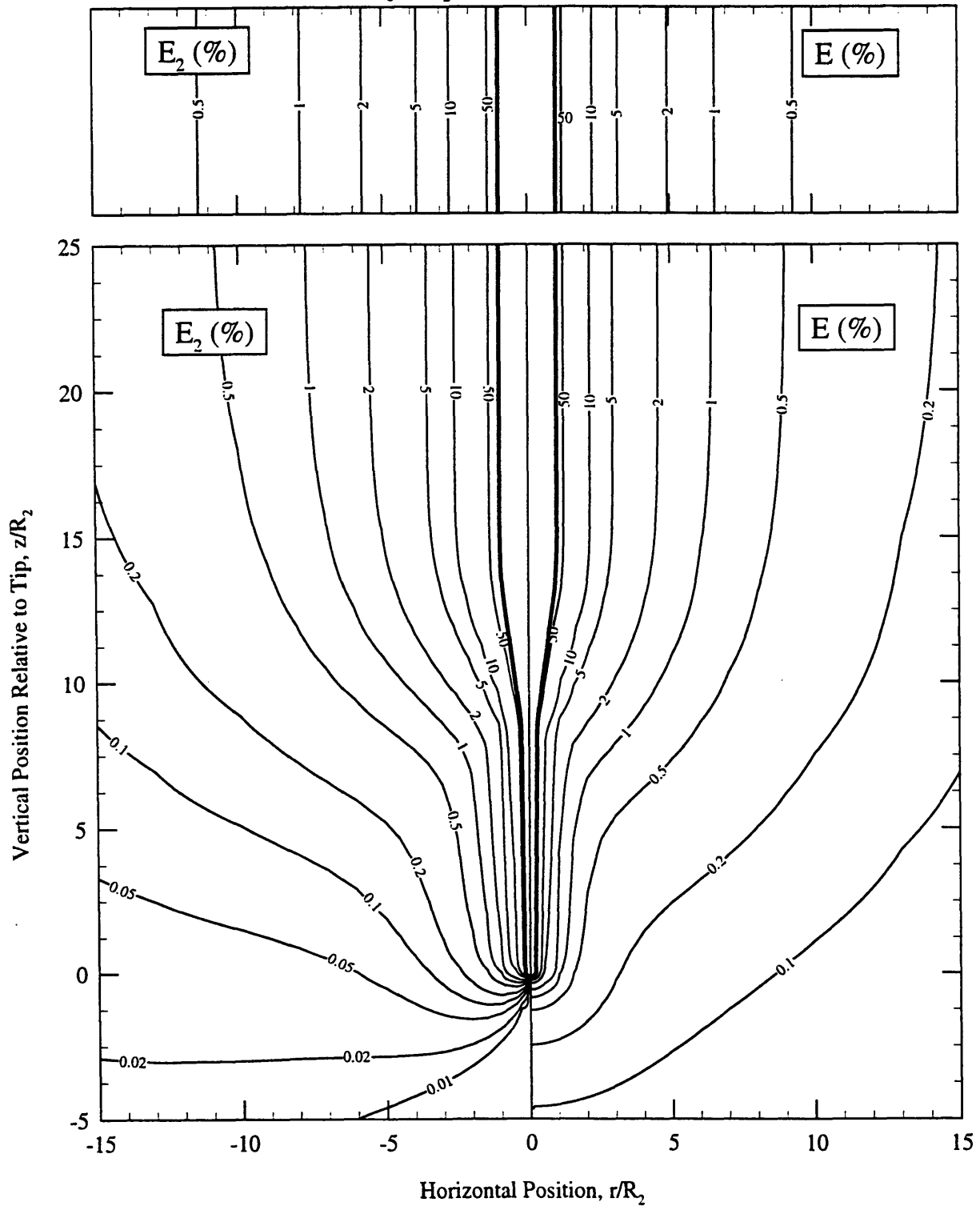


Figure 2.12 Predicted Deformation Pattern around FMMG Piezoprobe (After Whittle et al., 1997).

Cavity Expansion Method (CEM)



(a) Cavity Expansion Shear Strain

(b) Octahedral Strain

Figure 2.13 Strain Contours around FMMG Piezoprobe (After Whittle et al., 1997).

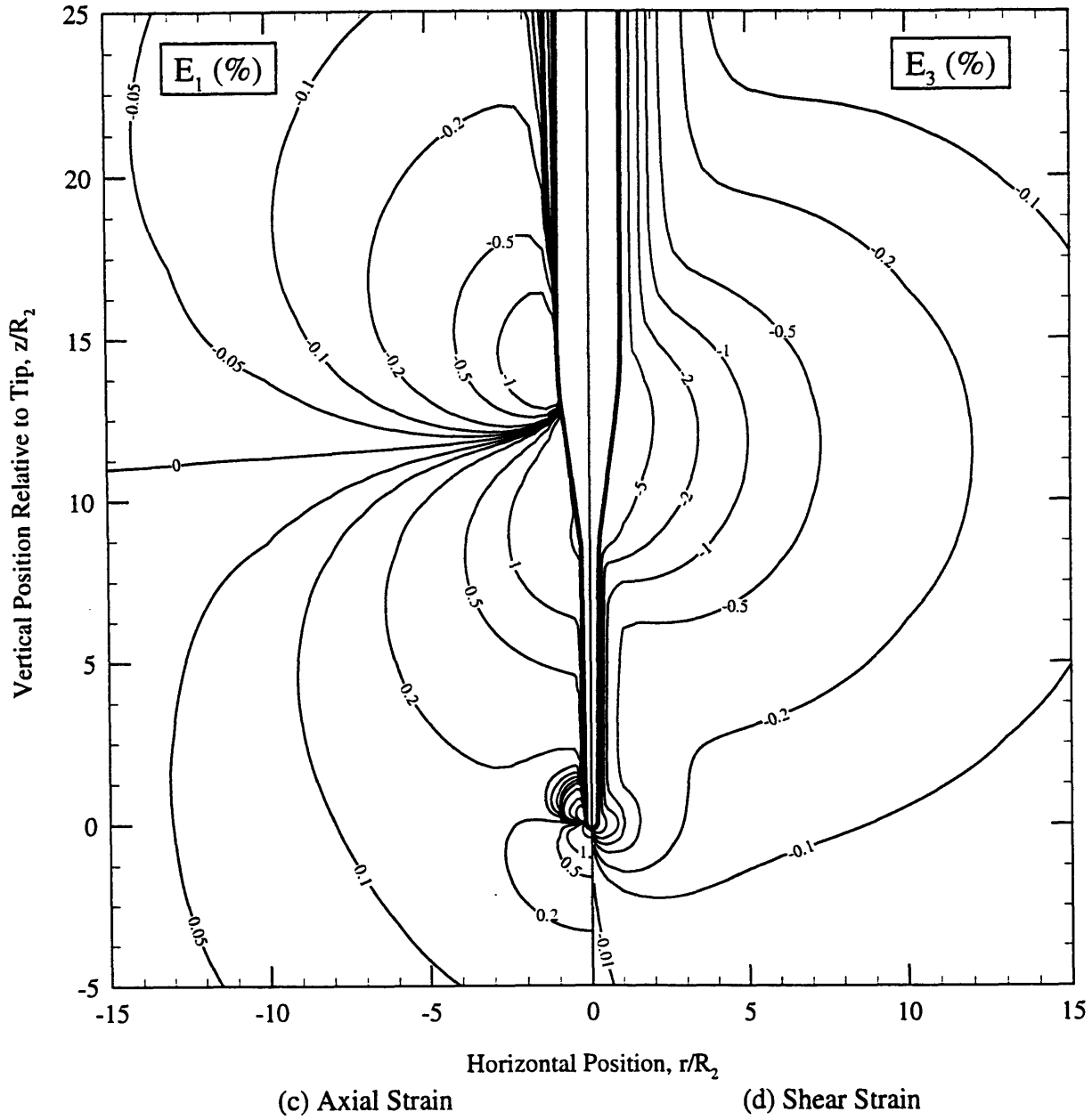


Figure 2.13 (cont.) Strain Contours around FMMG Piezoprobe (After Whittle et al., 1997).

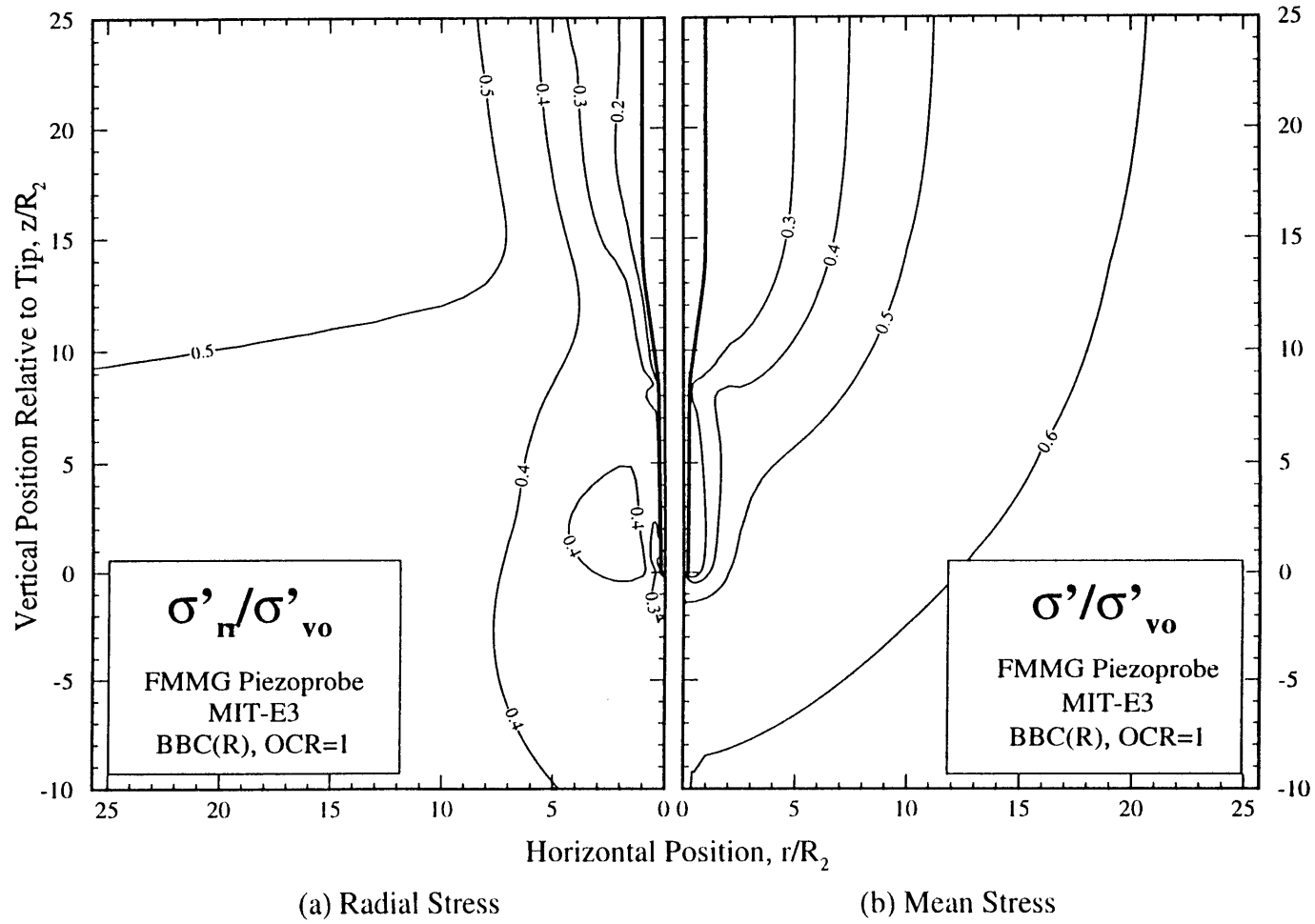


Figure 2.14 Effective Stress Contours around FMMG Piezoprobe (After Whittle et al., 1997).

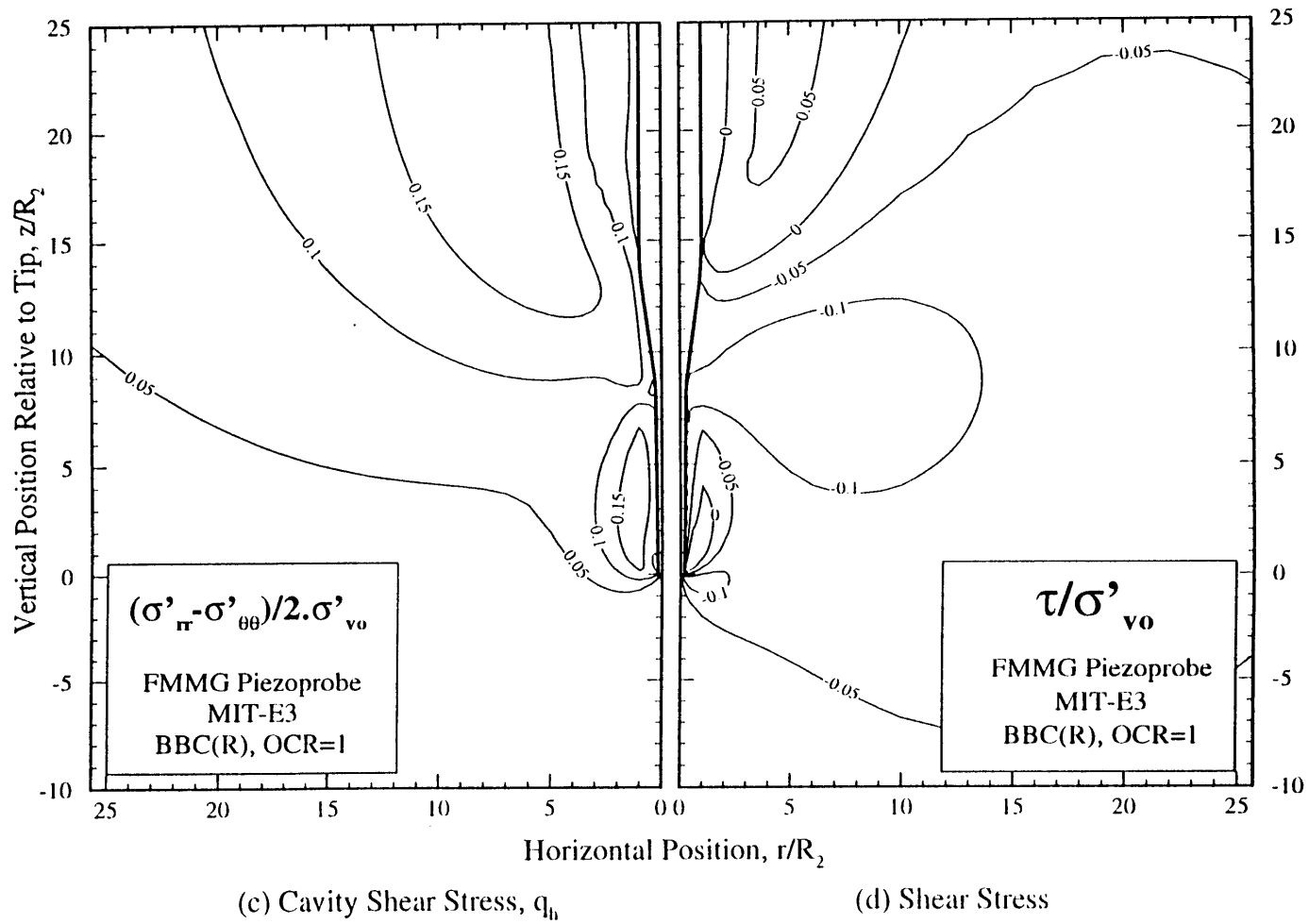


Figure 2.14 (cont.) Effective Stress Contours around FMMG Piezoprobe (After Whittle et al., 1997).

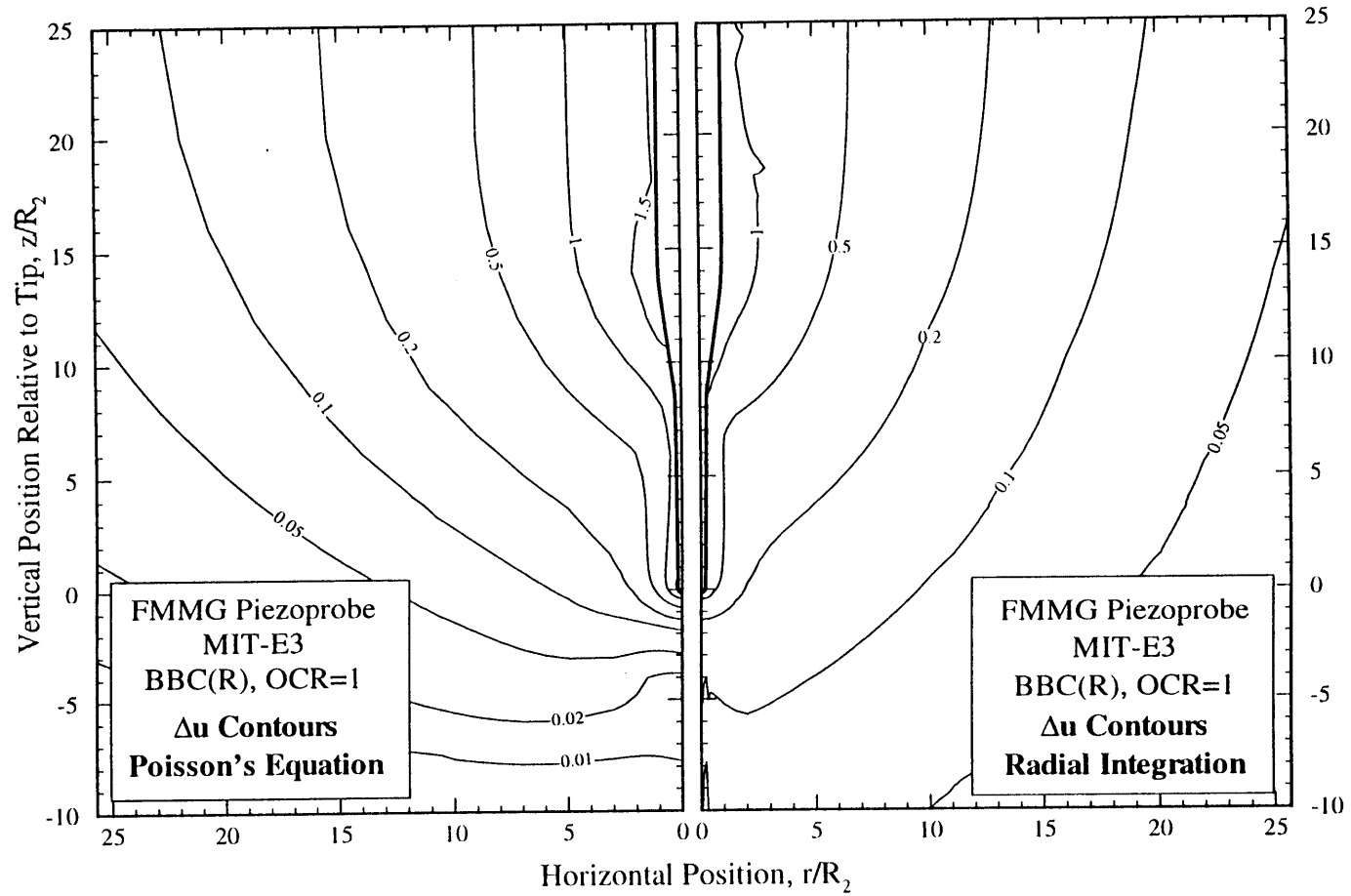


Figure 2.15 Pore Pressure Contours around FMMG Piezoprobe (After Whittle et al., 1997).

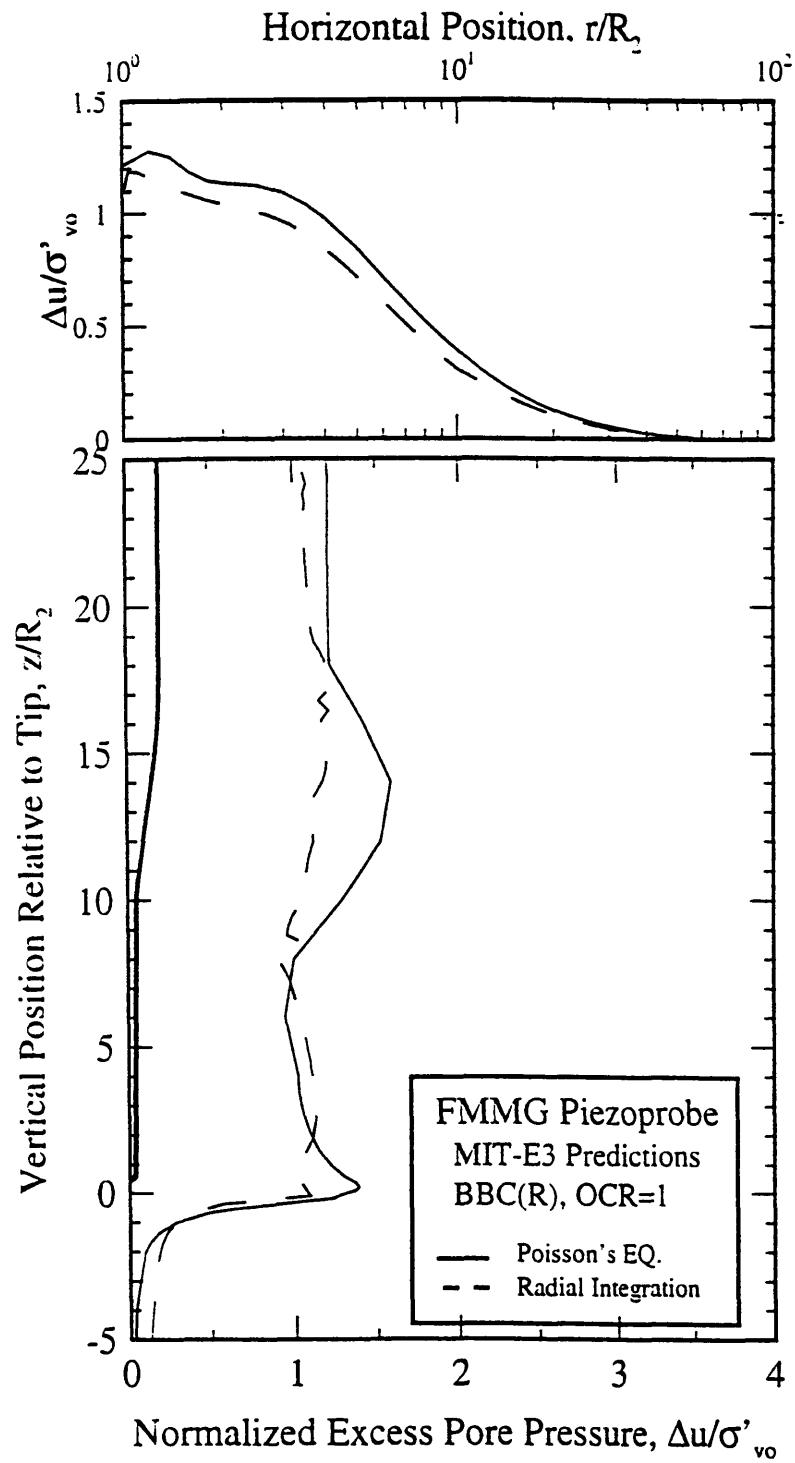


Figure 2.16 Comparison of Installation Pore Pressure Computed by Poisson's Equation vs. Radial Integration (After Whittle et al., 1997).

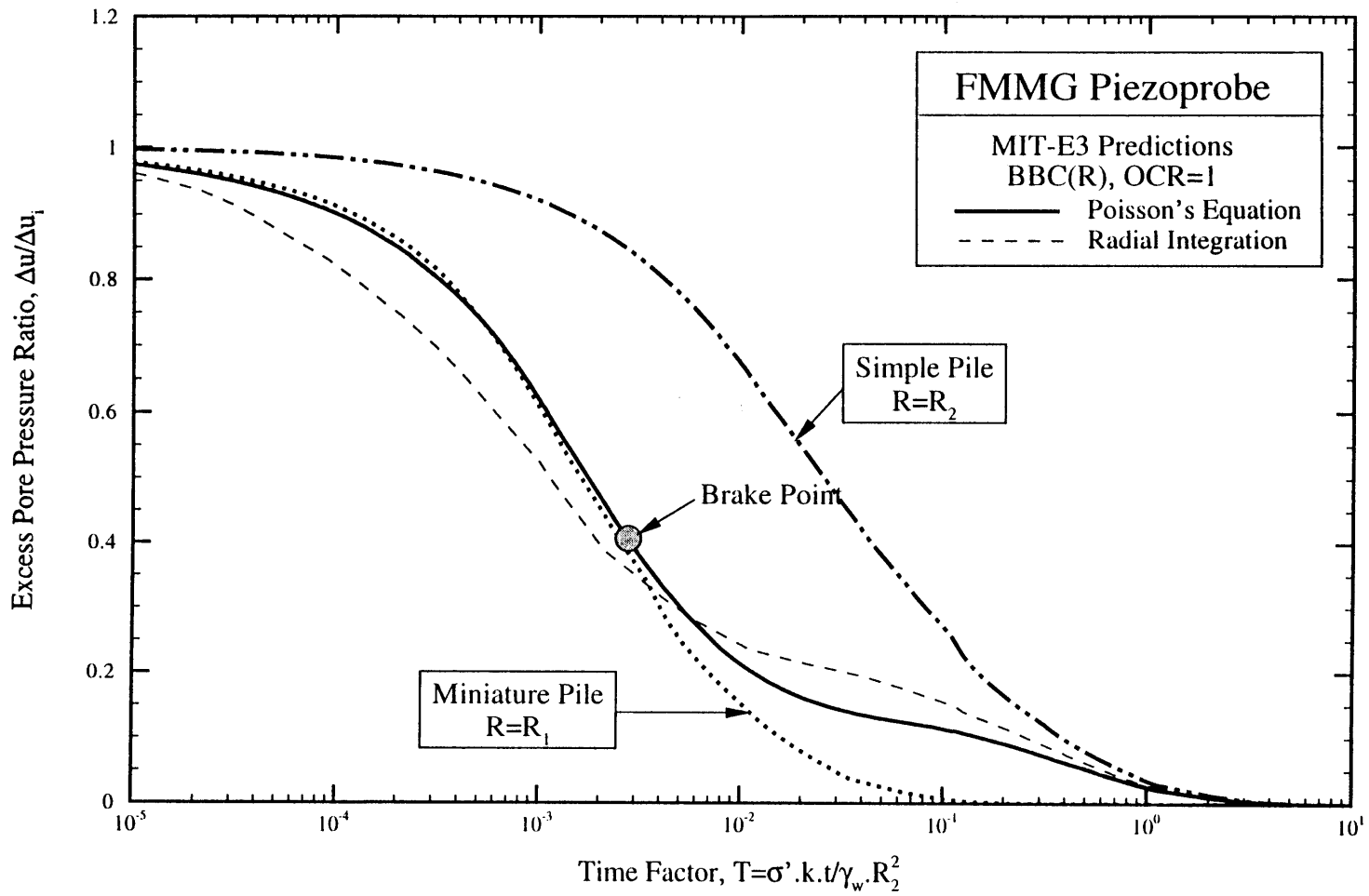


Figure 2.18 Typical Results of Dissipation Pore Pressure for FMMG Piezoprobe (After Whittle et al., 1997).

3. EQUIPMENT

3.1 Penetrometers

Five penetration devices (three different configurations) were used in the field program to measure pore pressure dissipation rates. These included two Fugro-McClelland Marine Geosciences (FMMG) designed “standard” Piezocones, two FMMG designed tapered Piezoprobes, and a research piezocone designed at MIT (Zeeb, 1996), referred to as the MIT Piezocone. This section describes the basic design features of each type of device.

3.1.1 Piezocone

The two piezocones, supplied for the project by FMMG, have 1.4” diameter shafts with a 60° tip and a porous element located above the tip (Figure 3.1). The pore pressure element is an annular coarse (large pore size) plastic filter which fits loosely in the groove on the end of the shaft section. The cone has a sealed instrumentation section which houses the point load cell, friction sleeve load cell and pore pressure transducer. The cone has a force capacity of 5000 kg at a maximum voltage output of 10 mV at ± 10 volts excitation. The pore pressure transducer is manufactured by Keller and has a capacity of 35 ksc. Manufacturer specifications give the maximum output of the transducer as 500 mV for ± 10 volts input. However, laboratory calibrations give a maximum output of only 4 mV, suggesting that the electrical circuit has been modified to match the output with that of the load cells. The piezocones are referred to as Piezocone 790 and Piezocone 881, after their serial numbers, to distinguish between the two devices.

3.1.2 Piezoprobe

The two piezoprobes, also supplied by FMMG, have 1.4” diameter base shafts which taper to a ¼” diameter at the tip. The shaft has a two step taper as shown in Figure 3.2. The removable tip holds a fine sintered stainless steel porous element tightly in place, at its base. The element is hydraulically connected to a pressure transducer located 12” above the tip, in the housing. The piezoprobes were supplied with Kulite pressure transducers that have a capacity of 35 ksc and a maximum output voltage of 75 mV at

± 10 volts input. The piezoprobes are referred to as Piezoprobe 62 and Piezoprobe 63, after the serial numbers of the original pore pressure transducers.

3.1.3 MIT Piezocone

The MIT Piezocone (Figure 3.3, Zeeb, 1996) also has a 1.4" diameter shaft with a 60° conical tip. Pore pressure is measured at the tip of the cone through a cylindrical ¼" diameter by ½" long stainless steel fine porous tip. At ± 5.5 volts input, the MIT Piezocone has a 14 ksc capacity Data Instruments pressure transducer at the tip, a 450 kg capacity axial load cell, a 450 kg capacity friction sleeve load cell, and two 14 ksc Cooper side pressure transducers. For this program, the side port transducers were not used due to failure of their seals during the laboratory pressure tests.

3.2 Depth Locator Box

A "depth locator box" (Figure 3.4) was constructed in order to coordinate the output of the cone instrumentation with the cone displacement from the known depth of the bottom of the borehole. This was done by means of a Claristat potentiometer which indicated the rotational displacement of a spindle.

The depth box was outfitted with a case to protect it from the elements and with a hole for the string to pass through. One end of the string was attached to the depth locator box clamped to the drill string while the other end was referenced to the borehole casing. The string is wrapped around a spring loaded spindle, which recoils as the string slackens when the drill rod is pushed into the ground. The spindle is referenced to the potentiometer so that as the spindle rotates, the potentiometer turns. The outside circumference of the spindle was sized to allow five feet of displacement for the 10 turns of the potentiometer.

3.3 Porous Element Saturation System

Two laboratory methods were used with equal success to saturate the porous elements for all three types of devices with water. The first method has been used at MIT since the early 1970's to saturate both ceramic and porous steel elements of laboratory

and field devices. It consists of a two step system as shown schematically in Figure 3.5 and Figure 3.6.

1. Evacuation: The porous elements are placed in a 70° C oven for at least eight hours to remove moisture. They are immediately transferred to a bell jar which is attached to a vacuum pump and deaired water supply (Figure 3.5). The bell jar is sealed and evacuated to about 200 mTorr. At this point, the liquid nitrogen trap located between the vacuum pump and the bell jar is filled to create an ion collector. This continues to increase the vacuum and stops the migration of oil vapor from the pump to the chamber. The vacuum is applied for 24 hours.

2. Saturation: Once the stones are free of moisture and air, distilled and deaired water is introduced to the stones. The line from the sealed bell jar to the deaired water is evacuated, then the three way valve is opened to connect the deaired water to the sealed bell jar, thus saturating the stones. The vacuum is then released and the porous elements transferred to containers which are completely filled (i.e., there is no air in the head space) with deaired water for transport to the field.

An alternative saturation method consists of boiling the porous elements for 20 minutes. They are then sealed in a container and placed in an ultrasound bath for 45 minutes. Detailed evaluations have shown that this much simpler and shorter method also achieves satisfactory response times for the porous elements, and hence provides adequate saturation.

3.4 Response Chamber

A small hydraulic pressure chamber was constructed in order to calibrate the pressure transducers in the piezocones, perform leak checks on the transducers and connections, determine appropriate pore pressure correction factors for the cones, and evaluate the responsiveness of the pore pressure system in the field. This pressure chamber is shown schematically with the witness pressure transducer in Figure 3.7. The procedures for the various uses of the pressure chamber will be described in Chapter 4.

The chamber has a 2” inside diameter and is 11.5” long. The witness pressure transducer is connected near the base to be as close as possible to the porous element. The top plate is fitted with an o-ring seal designed to fit all five devices. The piezocone or

piezoprobe devices, which are always stored in a tube filled with water, can be transferred into the water filled chamber with the witness pressure transducer detached. Once the piezocone is in place with clearance between the tip of the cone and the bottom of the chamber, the witness pressure transducer is tightened in place with a nut, thus sealing the chamber.

3.5 Sampling Equipment and Piezometers

Undisturbed samples were taken using two devices: 1) a 3.5” diameter, Acker mechanical fixed piston sampler, and 2) a 3” diameter Gus hydraulic fixed piston sampler.

3.5.1 Fixed Piston Sampler

The Acker mechanical fixed piston sampler uses a double rod system to independently connect the sample tube and the piston assembly to the drill rig at the ground surface. This is shown in Figure 3.8. The internal rods provide positive control of the piston which prevents loose cuttings from entering the tube and provides the driller with a measure of the bottom of the hole. The piston locks in place after the sample is collected which applies suction to the top of the sample during extraction. The two rod system makes the sampling process more cumbersome but does not significantly increase sampling time.

3.5.2 Hydraulic Sampler

The Gus hydraulic sampler is also a fixed piston design. This is shown in Figure 3.9. With this device, the piston is connected to the surface through the drill string. The sample tube is pushed into the soil by means of hydraulic pressure. In soft soils, it is not possible to tell the relative location of the piston and the bottom of the hole which makes it hard to correct problems associated with partial recovery. The hydraulic pressure advances the tube until it reaches the full stroke. In the fully extended position, the hydraulic pressure is vented back into the boring. The sample has been taken once the driller observes that the wash water is returning to the surface. The tube must be in the

fully extended position in order to rotate the tube to shear the soil at the base. It is only in this position that the latch on the piston rod will engage the roll pin on the tube adapter.

3.5.3 Sample Tubes and Packers

The 3" sample tubes were made of brass¹, while the 3.5" tubes were stainless steel. Brass and stainless steel are used for long term storage of samples because experience indicates that the soil undergoes considerable oxidation within six months when stored in steel tubes. The geometry of the sample tubes conform to ASTM D1587 (ASTM, 1995) specifications for thin walled tube samplers. The 3" diameter tubes have an area ratio (area of steel based on wall thickness/total area), $A_1=8.6\%$, a projected area ratio (area of steel based on cutting diameter/total area), $A_2=11.6\%$ and an inside clearance ratio, $IC=1.7\%$ ². In comparison, the 3.5" diameter tubes have an $A_1=6.2\%$, an $A_2=10.5\%$ and an $IC=2.4\%$. The inside of the tubes were coated with a thin spray coat of acrylic lacquer prior to sampling to reduce the friction between the soil and the Shelby tube, which prevents bending of soil layers during the sampling process.

3.5.4 Geonor Standpipe Piezometers

Equilibrium water pressures at the site were measured by means of Casagrande type Geonor M206 single tube open standpipe brass piezometers. Figure 3.10 provides a general schematic of this device. A hollow center shaft has perforations to provide drainage between the plastic standpipe and the outer porous sleeves. The permeable collection section in contact with the soil is approximately 12" long and 1.4" in diameter. This collection section is made up of three porous sleeves that are approximately 3" in length. The drive point is a 60° conical solid brass tip. The piezometer is hydraulically connected to the ground surface by means of 3/8" outside diameter plastic tubing with a 1/4" inside diameter. The tube is threaded into the shaft of the piezometer, and sealed with a compression nut and an o-ring. The piezometer was mechanically coupled to one 10 ft section of EW rod. Thick walled black pipe with standard couplings were used for the rest of the drill string.

¹ The first 3" sample was taken with a galvanized steel tube because the brass tubes were not yet available.

² Symbols used to describe the area and clearance ratios are used here for convenience and are not used by ASTM.

3.6 Data Acquisition and Power Supply

The field data acquisition system was based on the system used for test automation and data acquisition in the MIT geotechnical laboratories. (after Sheahan, 1992)

The hardware for the data acquisition system consists of the DC power supply, transducers, a junction box, a computer, and three analog to digital converters which plug into the computer. A schematic of the hardware system setup is shown in Figure 3.11. Analog to digital (A/D) conversion is performed by cards designed at MIT by Sheahan, (1992), using an Analog Devices semiconductor AD1170 chip, which is a programmable dual slope integrating A/D converter. The converter has a ± 5 volt capacity. Both the integration time and bit precision can be input. Each card has seven differential input channels and each channel is isolated from ground using an isolation instrumentation quality amplifier. The gains on each channel can be set at nominal values of 1, 10, 100, or 1000 using jumper wires. Three cards were installed in one computer to provide the 21 channel capacity required for this project.

Having three separate cards proved very useful. Since each card has one A/D converter, channels must be read sequentially and separated by the integration time period. This makes it difficult to synchronize data in time and space. The three cards made it possible to record data from three separate channels concurrently. This was accomplished by wiring the three transducers (pore pressure, tip load, and sleeve friction) of a particular device to the same channel position on each card. In this way, the three transducer readings for each piezocone were coincident in time, while the depth measurement was separated by one integration time increment.

The output of the transducers was matched to the range of the A/D converter by setting a separate gain on each channel. The piezocone and the piezoprobe transducers have capacities which are much greater than the values expected at the Saugus site. Therefore, a gain was chosen for each transducer based on the expected field value, the calibration of the transducer, and the range of the A/D converter. The maximum expected values were 15 ksc for the pore pressure, 150 kg for the axial load, and 75 kg for the skin friction. Table 3.1 lists each of the gain values as established by the system

calibrations. Basically, the nominal gains were 1000 for the MIT Piezocone load cells and for all transducers in the FMMG cones, 100 for the probes, and 10 for the remaining pressure transducers.

Two configurations were used for the A/D converter. During penetration and dissipation measurements, the cards were set for an integration time of 166.7 milliseconds and a 22 bit resolution. This means that the transducer signal was averaged over a period of 10 cycles of the AC input voltage. The signal voltage is then discretized to 0.0000024 volts. With this configuration, the system takes about three sets of readings per second during penetration. During the initial stages of dissipation three readings were taken every second, then the time interval between readings was increased in stages to five minutes. During the evaluation of the response of the pore pressure system, the cards were reconfigured for an integration time of 16.7 milliseconds and an 18 bit resolution. This results in slightly more noise and a coarser resolution (0.000038 volts). However, it increases the reading rate to 20 sets of readings per second which is necessary to evaluate the response.

The software used to control the data acquisition system is a modified version of a code written in BASIC by Dr. J. T. Germaine and used in the MIT geotechnical laboratory. The BASIC programs record the data while allowing interactive graphing of the data from any channel and interactive alteration of the reading rate. Rather than rely on one general code, 12 separate programs were written to limit the number of inputs during field operation. Copies of the code for the twelve programs are included as Appendix A.

Five *Penetration* programs were used to collect data for penetration measurements, one for each device. Each program was configured to measure the proper channels for the device and the depth box at the appropriate reading rate and A/D specifications. Since only one program could be run at one time, readings were suspended on all other devices while one device was being pushed. The same was true for the five *Response* programs, written to perform response evaluation.

At all other times, data were collected on all transducers using the *Dissipation* program or the *Night* program. The *Dissipation* program read all device transducers at a

specified interval. The data were written to the hard disk when the file was closed. The *Night* program recorded the same channels, but saved data under a different file name every thirty minutes to prevent the loss of data due to electrical power loss.

3.6.1 Power Supply and Protection

The entire field system operated on 120 volt AC power. The site was so remote that it was impossible to connect to the local power grid. Therefore, power had to be generated on site. To avoid the need for 24 hour supervision, two separate systems were used: a gas generator during the day and a DC to AC inverter at night. The power demand on the system was minimized during the night in order to extend the life of the batteries. The complete power system is described in the following paragraphs and shown schematically in Figure 3.11.

The power system is divided into two sections: equipment central to the data acquisition function and support equipment. The data acquisition equipment include the DC power supply, which energizes the transducers, and the computer, which contains the analog to digital converters and controls the data collection function. Both of these devices are connected to an APC smart Uninterruptable Power Source (UPS) which is independently grounded to the marsh with a five foot metal rod. This equipment along with the security system required about 300 W of power. The support equipment included the computer used for data reduction, the two monitors, voltmeter, two battery chargers, telephone, soldering equipment, etc. The total power requirement during the day was about 3500 W.

During the daylight hours, electrical power was provided by a gas generator. The original unit was a 5000 W Coleman generator. However, this unit failed at the end of July and was replaced by a 4200 W Sears Craftsman generator. This power system was independently grounded through the generator to the marsh using a five foot metal rod. This provided the common ground for all the support equipment.

The night time power supply consisted of three deep cycling, 12 volt, 50 amp hour marine batteries. These were connected to an Analytic Systems 600 W DC to AC true sine wave inverter. The batteries and inverter were grounded to the same post as the generator. Switching between the inverter and generator was done manually. Power

during the short disconnect period was supplied by the UPS. The three marine batteries supplied enough power to operate the system for about 6 hours. Late in the program three car batteries were added to the system. This increased the operation time by one or two hours, depending on the day, but these batteries could not be charged quickly enough to supply the required daily power. The batteries were recharged during the day with two 20 ampere chargers operating off the generator.

3.7 Field Logistics

3.7.1 Cables and Plastic Tubing

Cables were initially provided by Fugro. These were vinyl encased cables which were unshielded. They were approximately ¼" in diameter with at least 10 individual wires. The vinyl covering was able to resist most surface abrasions and, when equipped with an o-ring compression fitting, provided a watertight seal for the cone. However, the cables were not sufficient for the current purposes as they were influenced by electrical noise that surpassed the range of the measurements being made. Therefore, shielded cables were procured.

The transducers in the piezocone were connected to the junction box at the surface by means of a 200 ft cable protected by ½" diameter plastic tubing. The electrical cable (Carol #2426) consisted of eight #22 AWG copper wire conductors with an aluminum shield and a single external drain wire. This cable was not ideal as the pairs of conductors were not individually shielded, but had the aluminum shield around the group of wires, making them more suitable than the vinyl encased cables.

The single transducer in the piezoprobe was connected to the junction box at the surface by means of a 200 ft cable protected by 3/8" or ½" (one of each) diameter plastic tubing. The electrical cable (Belden #8723) consisted of 2 pairs of twisted #22 AWG copper wire conductors with individual aluminum shields and one common drain wire. The two different sizes of plastic tubing were used due to the availability of the plastic tubing in 200 ft. lengths.

The transducers in the MIT Piezocone were connected to the junction box at the surface by means of a 200 ft cable protected by ½" diameter plastic tubing. The electrical

cable (Belden #9991) consisted of 6 pairs of twisted #24 AWG copper wire conductors with individual aluminum shields and individual drain wires inside the shields.

3.7.2 Housings and Watertight Connections

The piezocones and piezoprobes were supplied with male M24x1.5 straight threads for the mechanical connection and a standard 3/8" Swagelok connector to seal the electrical cable. This seal was designed with the assumption that the cables originally supplied would be adequate. Stainless steel housings were fabricated to couple the piezocones and piezoprobes to the AW drill rod. The housings are identical for all four devices and a detailed drawing is shown in Figure 3.12. The female end has o-ring seals to couple to the cones and probes and the male end, originally without seals, couples with the AW box thread. Once the problem of electrical noise was identified, and the cables replaced, a 3/4 x 16 female thread and a 1/2" Swagelok o-ring connector were added to the top of the housing to provide the electrical cable seal.

The MIT piezocone was also designed with a straight thread connection. Therefore, a similar geometry stainless steel housing was designed to connect the 1 x 14 male straight thread to the AW box thread. This is depicted in Figure 3.13. The housing was made to enclose the electrical connections. The connection to the MIT Piezocone has an o-ring seal and the end connecting to the AW rod has a female thread to attach the Swagelok o-ring connector.

3.7.3 Support Equipment

Support equipment refers to the various tools and devices necessary to make the field operation self supporting. The major item was a second computer for data reduction as the data acquisition computer was not able to be used for any other purpose. The data reduction computer was a 386sx computer with Lotus 1-2-3, Microsoft Office, and Sigma Plot software installed. A voltmeter, battery charger, soldering iron, and all the required tools were also included.

3.7.4 Site Security System

Security was a real concern at the site as it is in a relatively remote location with two access points at opposite ends of the abandoned embankment. Although the area was used during the day by a local model airplane club, in the evenings and after dark it was frequented by an assortment of less responsible individuals. During the first weekend (Sunday night) of the program, the drill rig was stoned, breaking every piece of glass on the truck. However, once the field van was in place, the site was protected by a remote security system, installed and monitored by Lexington Alarm Systems of Lexington, Ma. This system was activated and deactivated on site with a password and was used for night time security (or whenever the site was unattended). The system was in constant communication with the central office through short wave radio signals to eliminate the possibility of disconnecting the power to disarm the system. The system consisted of four security loops: one for motion in the van, one for broken cables to the devices in the ground, one for broken windows, and one for radio communications. Fortunately, there was only one false alarm during the remainder of the program, when a window screen fell and triggered the motion sensor. Otherwise the security signs and the regular occupation of the site during all daylight hours were sufficient to deter vandalism. Expensive and valuable items, such as the personal computer and data disks, were removed from the site at the end of each day.

CH #	Device Specifications				
	Device **	Measurement	Make	Range	Gain
5	P62	Pore Pressure	Kulite	35 ksc	98
11	P63	Pore Pressure	Kulite	35 ksc	98
7	P790	Pore Pressure	Keller	35 ksc	948
8	P790	Tip Load	Fugro	5000 kg	949
9	P790	Friction Sleeve	Fugro	5000 kg	960
1	P881	Pore Pressure	Keller	35 ksc	977
2	P881	Tip Load	Fugro	5000 kg	955
3	P881	Friction Sleeve	Fugro	5000 kg	951
13	MITC	Pore Pressure	DI	14 ksc	10
14	MITC	Tip Load	MIT	450 kg	965
15	MITC	Friction Sleeve	MIT	450 kg	964
16	MITC	Sleeve PP1	Cooper	14 ksc	
17	MITC	Sleeve PP2	Cooper	14 ksc	
19	Depth			150 cm	1
19	Water			1 ksc	1
21	Witness		DI	14 ksc	10

- * Calibration Factors at the conclusion of the Field Program, 1
- **
- P62 Piezoprobe with Kulite Pressure Transducer Ser
 - P63 Piezoprobe with Kulite Pressure Transducer Ser
 - P790 Standard Piezocone #790
 - P881 Standard Piezocone, #881
 - MIT MIT Piezocone

Table 3.1 Gain Values for Each Transducer.

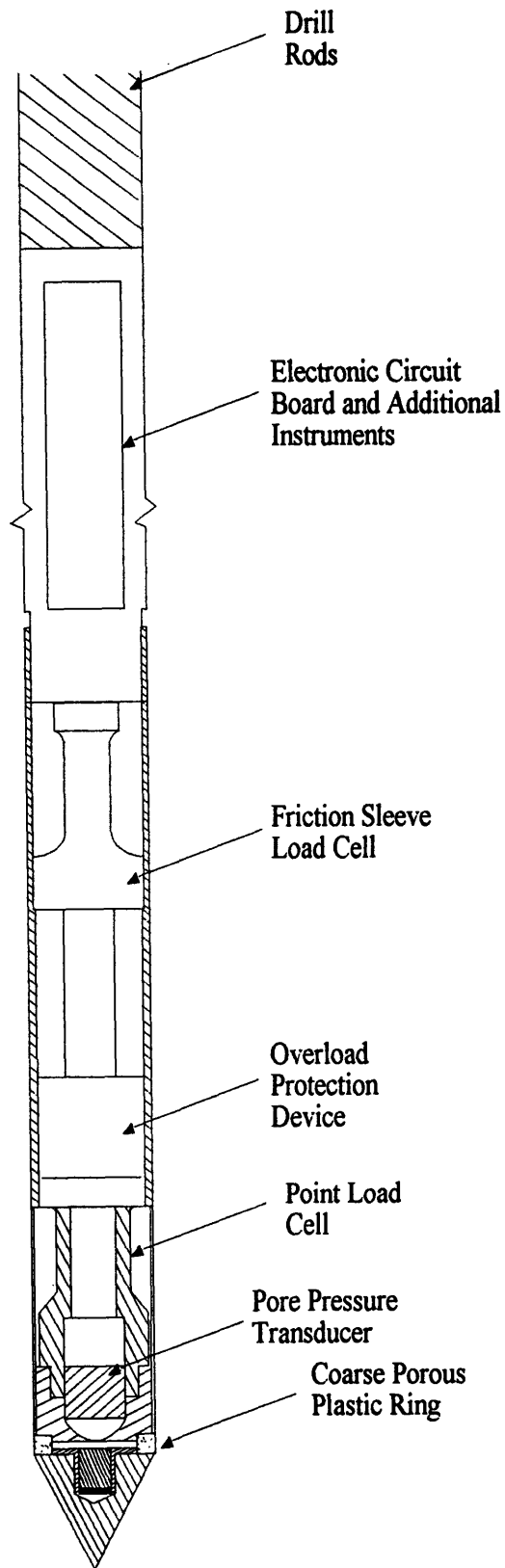


Figure 3.1 Illustration of the "Standard" (FMMG) Piezocone with Porous Plastic Ring at the Base of the Shaft, above the 60° Tip.

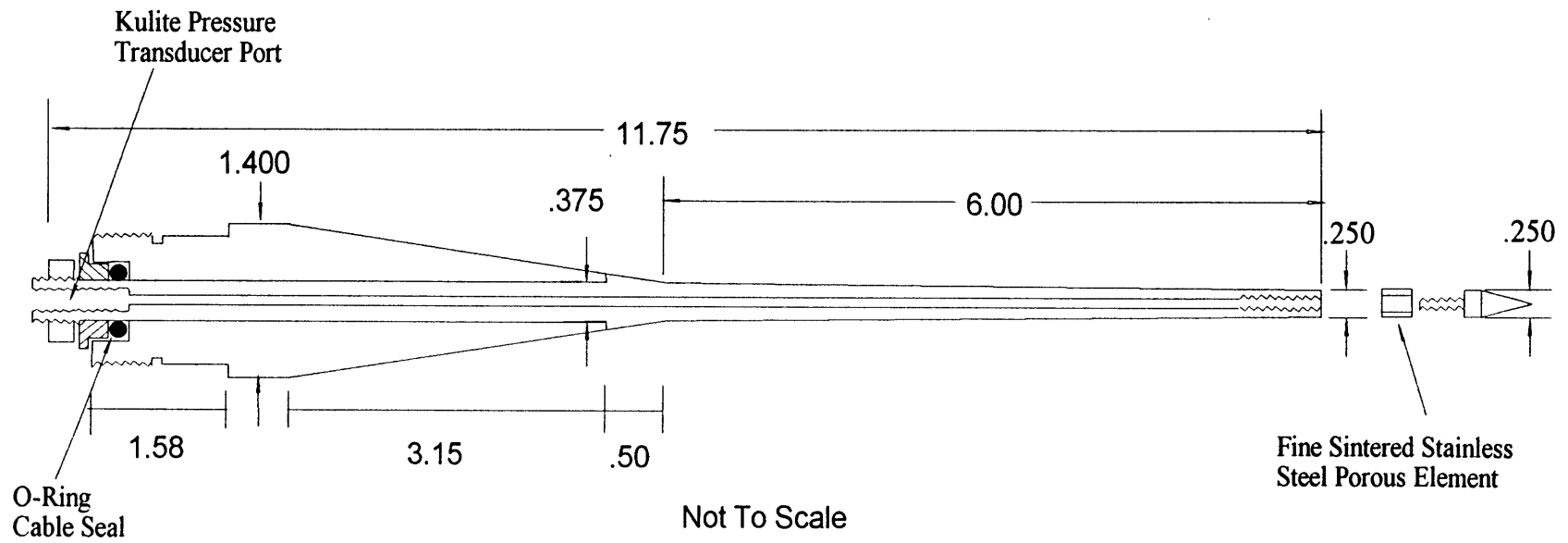


Figure 3.2 Illustration of the FMMG Tapered Piezoprobe with a Fine Sintered Stainless Steel Porous Element at the Base of the Shaft.

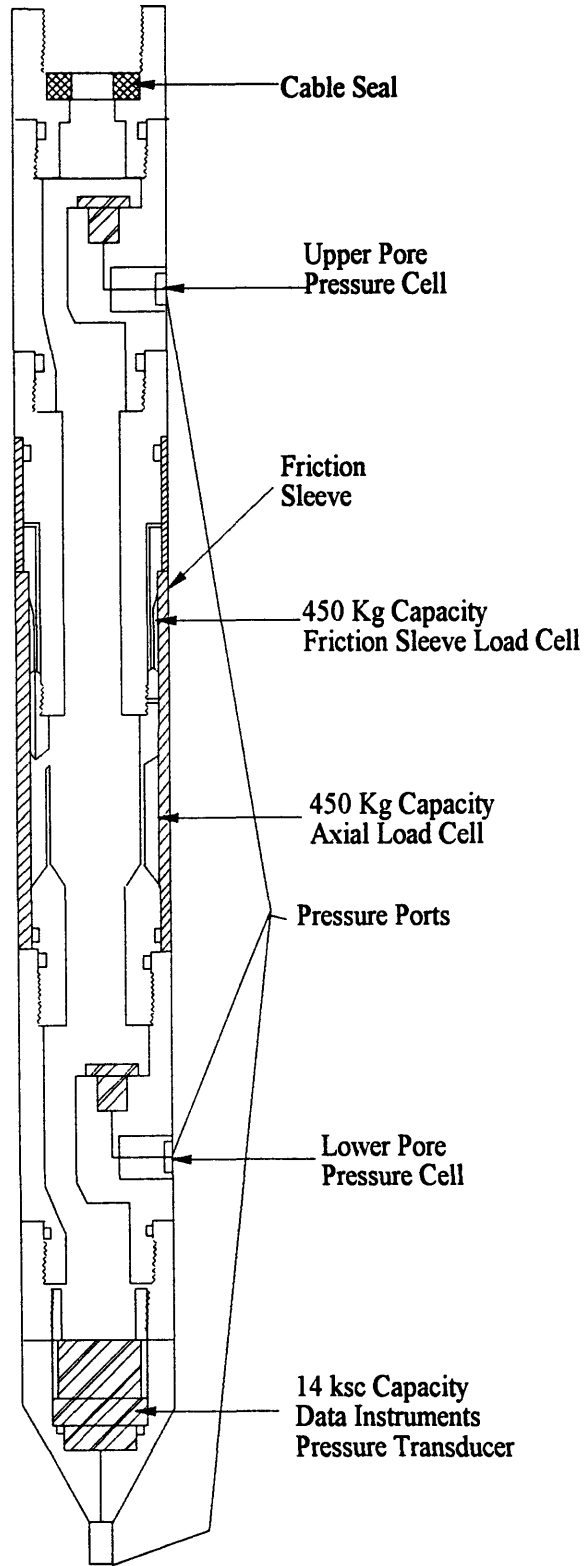


Figure 3.3 Schematic of the MIT Piezocone with a Cylindrical Fine Stainless Steel Porous Element at the Tip of the 60° Taper (After Zeeb, 1996).

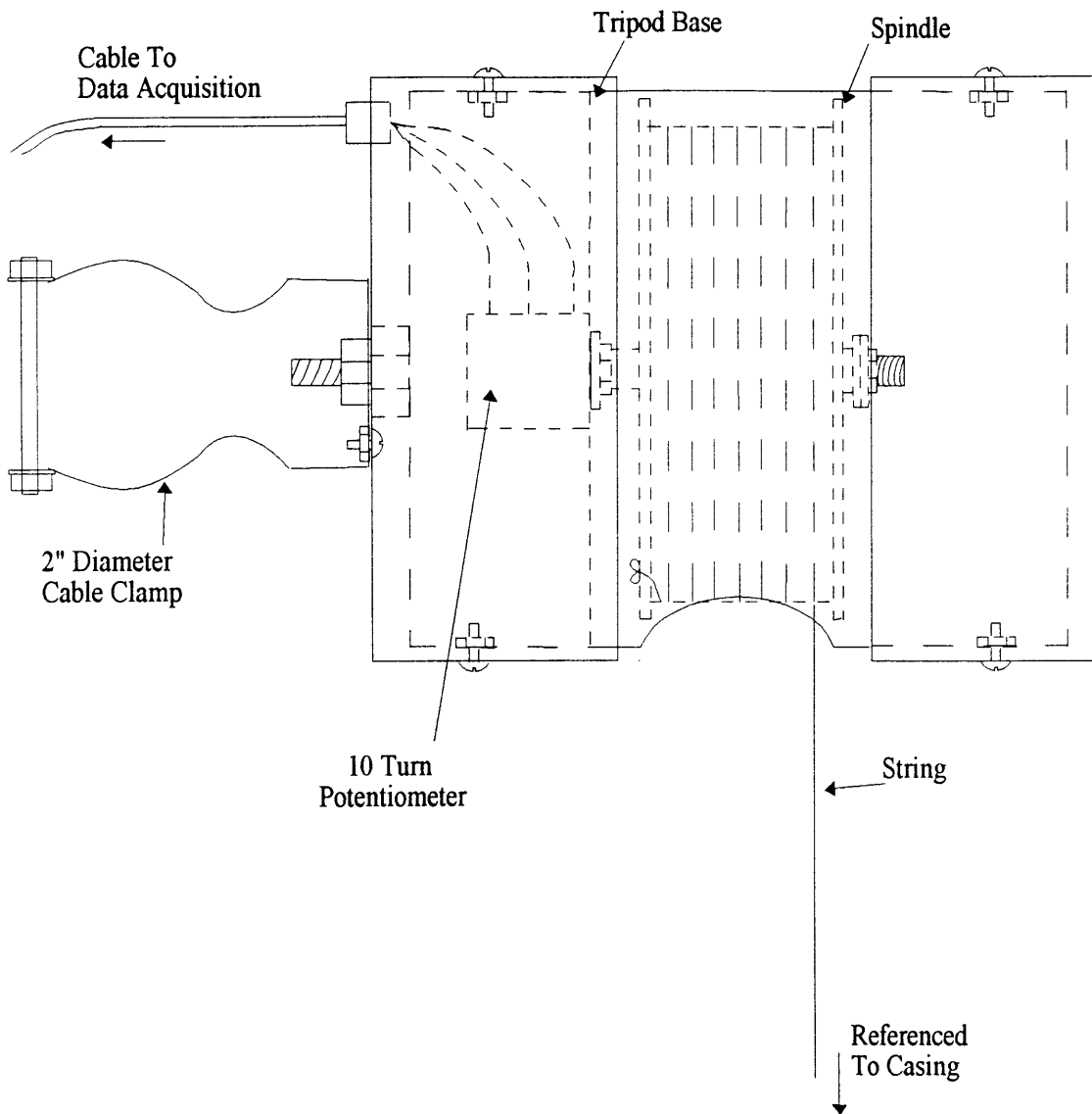


Figure 3.4 Schematic of the Depth Locator Box.

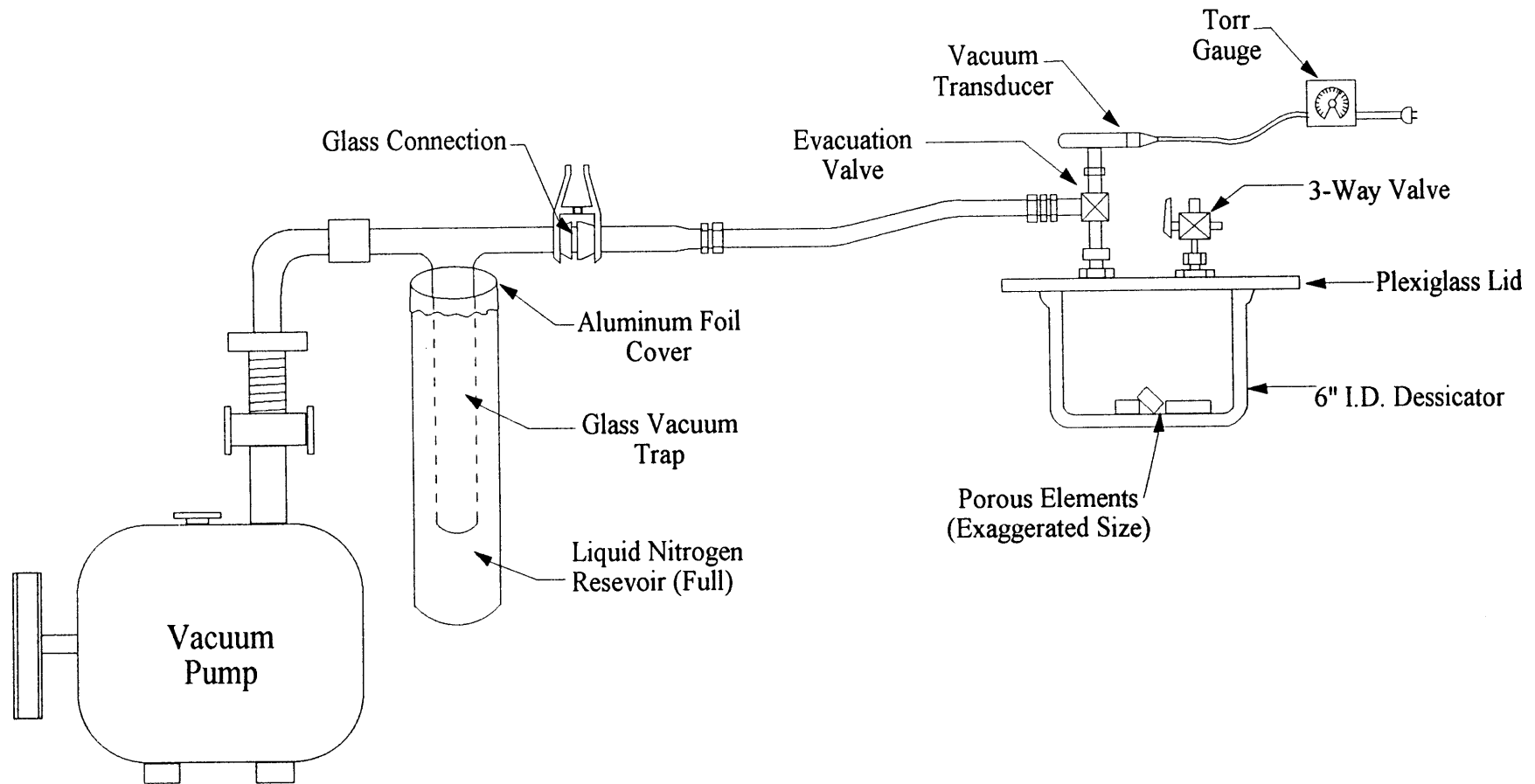


Figure 3.5 Schematic of the Evacuation System used to Evacuate the Chamber in Preparation for Saturation of Porous Elements (After Jordan, 1979).

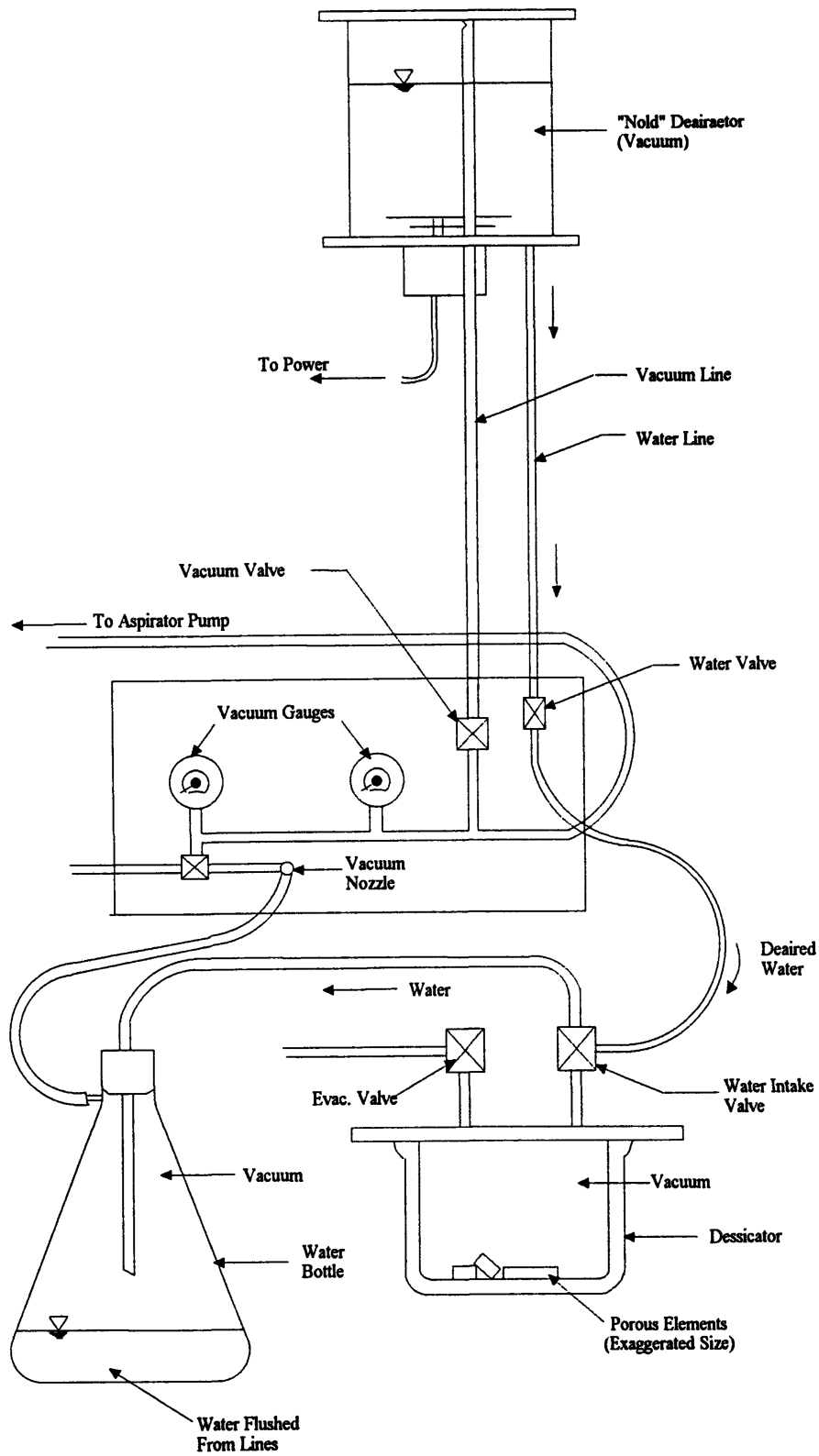


Figure 3.6 Schematic of the Deaired Water System used to Saturate Porous Elements (After Jordan, 1979).

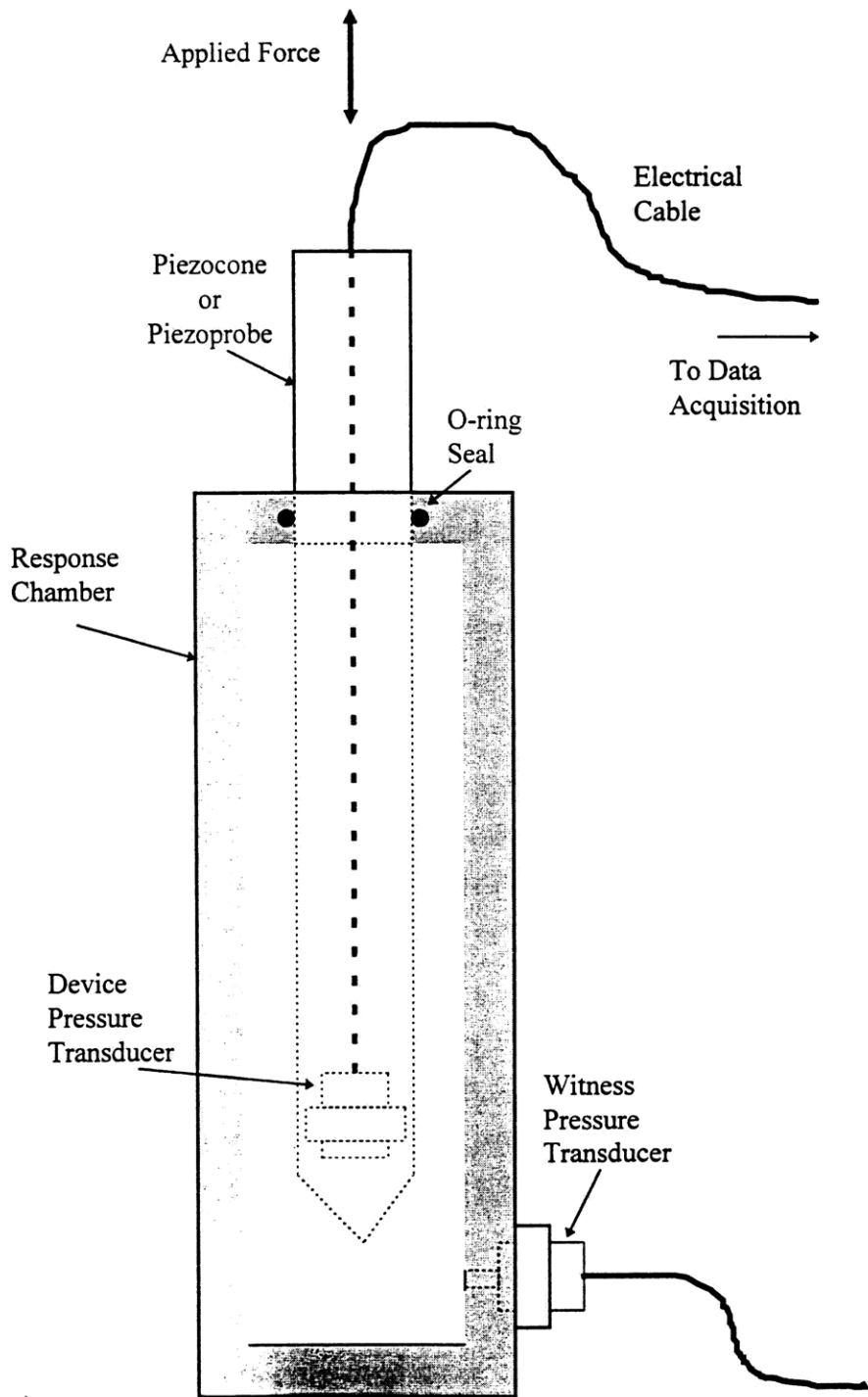


Figure 3.7 Schematic of Response Chamber used to Calibrate and Perform Equipment Evaluation of Piezocones and Piezoprobes (After Varney et al., 1997).

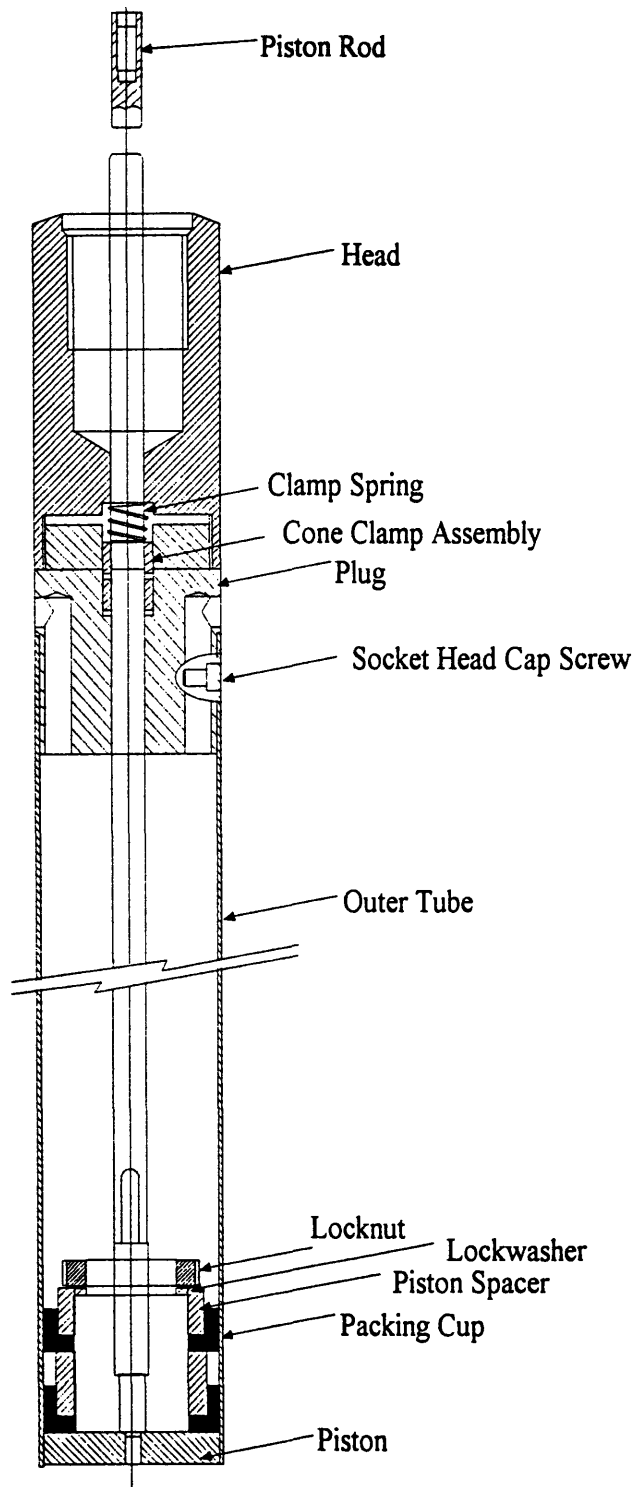


Figure 3.8 Illustration from Acker Catalog of the Acker Mechanical Fixed Piston Sampler used to Obtain 3.5" Undisturbed Soil Samples.

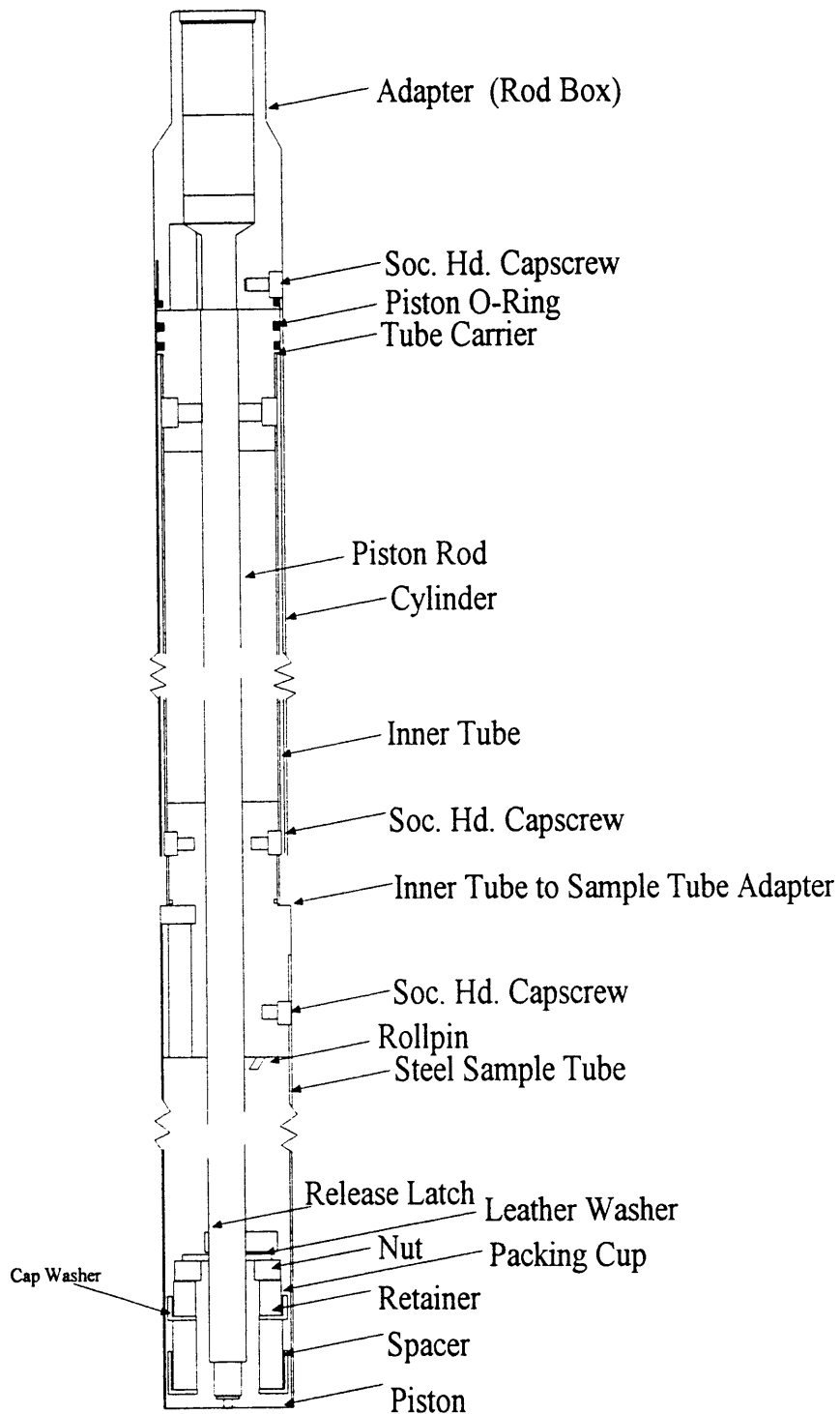


Figure 3.9 Illustration from Acker Catalog of Gus Hydraulic Fixed Piston Sampler used to Obtain 3" Undisturbed Soil Samples.

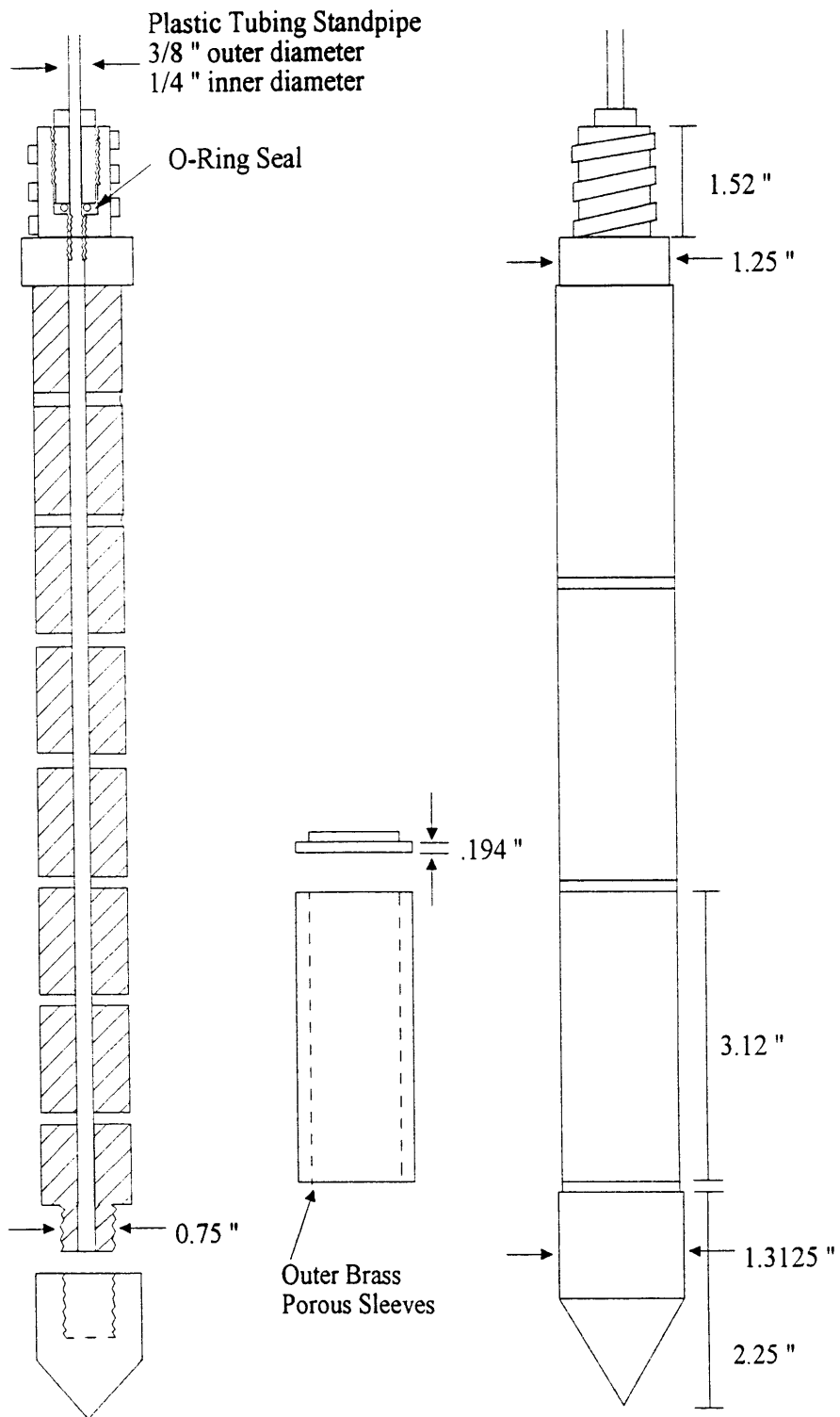


Figure 3.10 Schematic of Geonor Casagrande Type M-206 Field Piezometer.

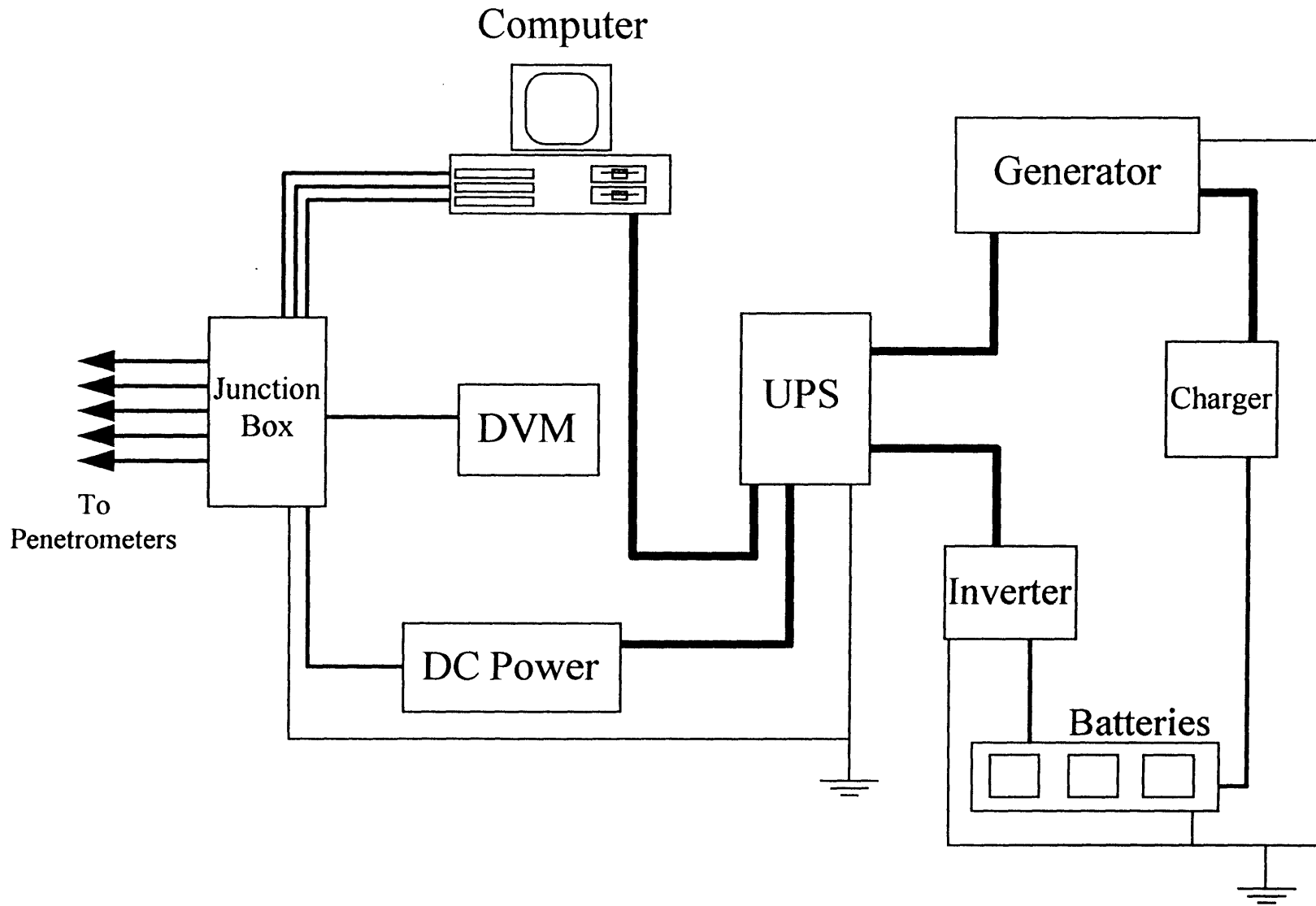


Figure 3.11 Schematic of Data Acquisition and Power System used for Field Operation (After Varney et al., 1997).

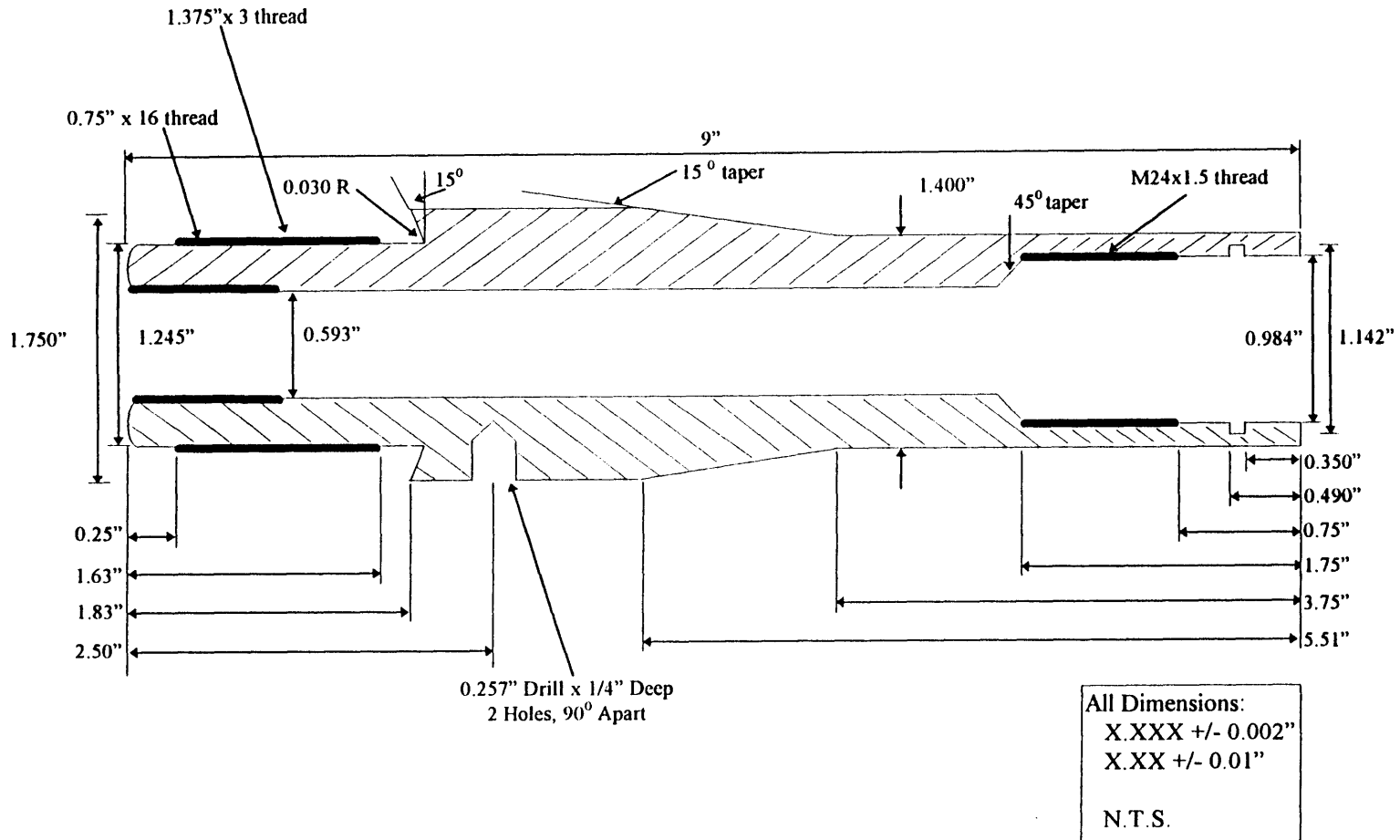


Figure 3.12 Schematic of Housings used to Couple Piezocones and Piezoprobes to Standard AW Drill Rod (After Varney et al., 1997).

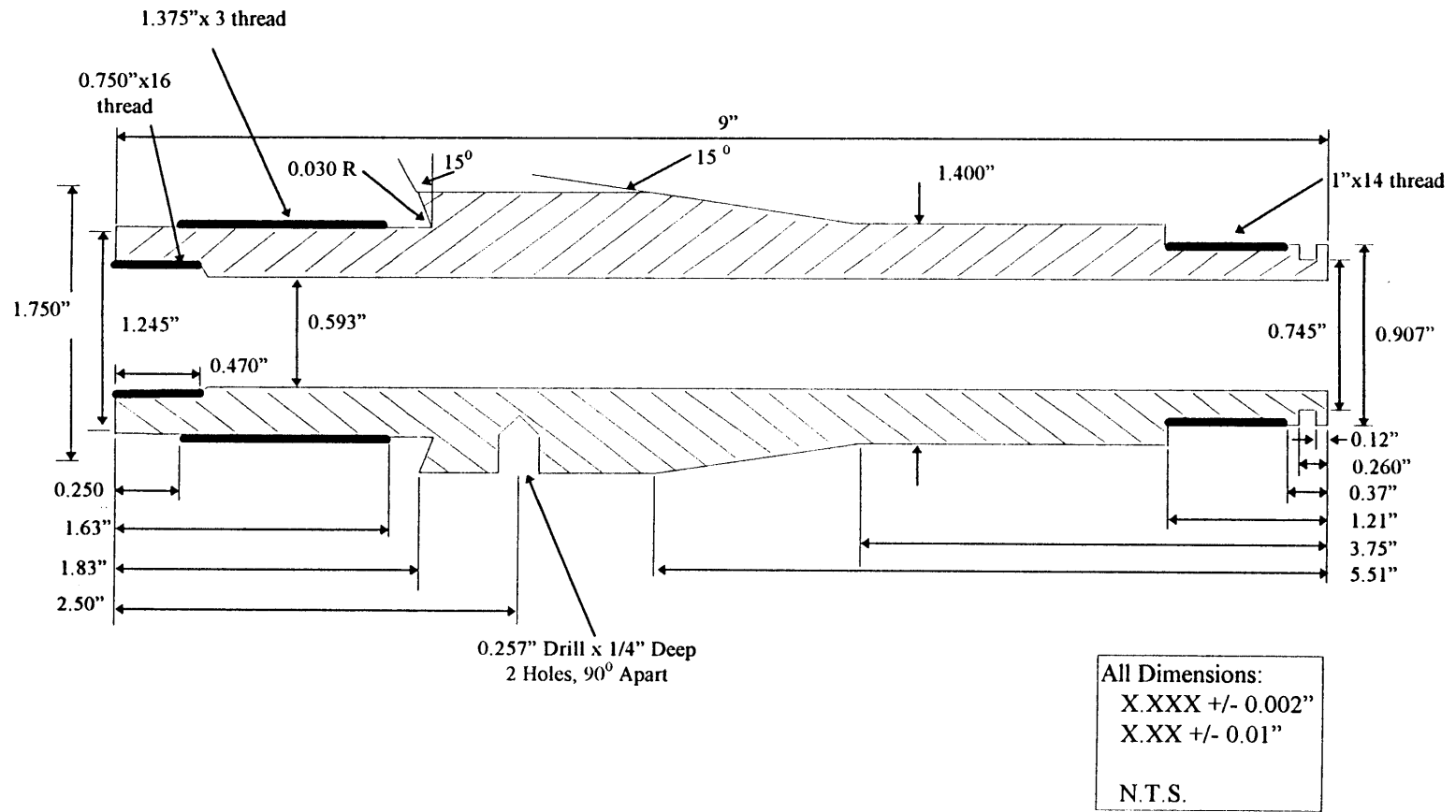


Figure 3.13 Schematic of Housings used to Couple the MIT Piezocone to Standard AW Drill Rod.

4. TEST PROCEDURES

This chapter will describe in detail the procedures used to conduct the field program. The intention is to provide an understanding of the measures used to insure quality, repeatable data.

4.1 Piezometers

The reference values for the equilibrium pore pressures were obtained from water elevations measured in Casagrande type M206 single tube hydraulic piezometers.

4.1.1 Installation

These devices were installed at three elevations: one at -3.70 meters (18.0 ft. depth) at the base of the sand layer, one at -24.09 meters (85.0 ft. depth) in the middle of the clay and at -40.68 meters (139.5 ft. depth) at the clay/till interface.

The piezometers were installed using the following procedures. A three inch casing was set to the top of the clay (elevation -4.28 meters, depth 20 ft.) and the hole was advanced by rotary cutting with wash water through the clay to 3.05 meters (10 ft.) above the intended measurement location with a 2" diameter open-ended clay bit. One attempt was made to clean the cuttings from the hole. The brass filters for the piezometers were deaired in the laboratory and transported to the field under water. The devices were assembled under water and the hydraulic tubing sealed in place. The first length of EW drill pipe was attached to the piezometer and the probe quickly lowered 3 meters into the water filled casing. This was done to be sure the tubing would fill without trapping air pockets. The piezometer was lowered into the hole in 3.05 meter increments as each section of thick walled black pipe was added.

The deepest piezometer was pushed two feet below the wash depth where it met refusal. It was driven a few more inches with a 63.6 kg (140 lb.) hammer; however, it was unable to penetrate into the till. The middle piezometer was pushed with moderate pressure 3.05 meters below the bottom of the hole, while the upper piezometer was simply lowered to the bottom of the hole within the casing. The casing for the upper piezometer was removed to allow the sand to collapse against the steel pipes. The upper

3 meters of all three holes were packed with bentonite pellets to seal the device from the surface water ingress.

4.1.2 Water Level Measurements

Measurements of water level in the piezometer standpipes were made both automatically with continuous readings on the data acquisition system and manually in order to evaluate the short term water level fluctuations and to determine the long term equilibrium water level, respectively.

Continuous electronic readings of the water level inside the plastic tubing were taken on each of the three piezometers, one at a time. These measurements were made with a Data Instruments pressure transducer having a range of one atmosphere. The transducer block was connected to a 3/16" OD plastic tube with a 1/16" inside diameter. The tubing and block were saturated with water and the tube inserted into the M206 tubing to a distance which was well below the expected lowest water level. The transducer was then rigidly attached to a wooden stake at a height of 0.46 meters (1.5 ft.) above the ground surface. Readings were taken on the data acquisition system over time. The transducer was then monitored with the data acquisition system to measure fluctuations in the water level with time. This method was used to estimate the response time of the piezometers and to evaluate the tidal fluctuations in the upper sand layer.

Manual readings of the water level inside the plastic tubing were made using coaxial cable and a bench model digital resistance meter. The end of the cable was stripped for a distance of 1/4" to provide good contact between the conductors when submerged in water. The wire was lowered into the tube until the resistance changed from infinity to several thousand ohms, indicating that the tip of the wire was in water. The wire was removed and the length of wire extended into the tube was measured with a tape measure to the nearest 0.1 foot. These manual readings were obtained intermittently throughout the field program at various times of the day.

4.2 Undisturbed Soil Samples

4.2.1 Borehole Advancement and Sampling Procedure

The same general procedures were used to collect undisturbed samples with both the 3" diameter Gus hydraulic sampler and the 3½" diameter Acker fixed piston sampler. The hole was cased with four inch diameter flush connection casing to a depth of 7.6 meters (25 ft.), at the top of the clay. The casing was washed with a tricone rotary bit to the first sampling location using fresh water. After taking the first sample, a recirculation system was established to allow the use of drilling mud. The next three samples were taken with mud consisting of recirculated clay cuttings from the hole because the soil has a high overconsolidation ratio (OCR) and the stress relief at the base of the hole is relatively small due to the shallow depth.

Weighted mud was used starting with sample B96-U4. The mud was mixed using a combination of bentonite clay to develop the necessary viscosity, soda ash to prevent flocculation, and barite to add weight. The average mud weight for the entire sampling program was $1.30 \pm 0.06 \text{ g/cm}^3$ ($81.1 \pm 3.7 \text{ lbs/ft}^3$). As the hole was advanced, the additional mass due to the clay cuttings was sufficient to maintain the mud weight and hence it was not necessary to add bentonite or barite.

The hole was advanced to the sample location using the tricone rotary bit at a relatively slow rate of 0.3 m (1 ft) per minute. The bit was then cycled up and down to clean the sides of the hole. Circulation was continued until the return fluid was free of clay cuttings. The cutting tool was removed slowly while the water level was maintained at the top of the hole, and the sampler was lowered to the bottom of the hole.

With the Acker double rod mechanical sampler, it is possible to observe the point at which the sampler touches the bottom of the hole because the inner rod is connected to the piston and moves relative to the outer rod. This provides a means for checking the drilling operation. Once the rod indicates that the sampler is at the bottom of the hole, the piston rod is locked to the drill rig and the outside rod is attached to the drive head. The sample tube is then pushed into the soil at a fast rate of approximately 1.5 m (5 ft) per minute while the piston rod is held in place.

With the Gus hydraulic sampler it is not possible to tell when the sampler is at the bottom of the hole. This sampler is lowered to the calculated bottom of the hole. The drill rod is connected to the swivel and is locked in place. Fresh water is pumped into the drill string at about 500 psi, which advances the sample tube into the soil, while the piston is locked in place by the drill string. Pressure is applied until drill fluid recirculation occurs.

Once the sample tubes are advanced into the soil, the soil is given 5 to 10 minutes to expand radially into the gap created by the inside clearance ratios. This waiting period is essential to develop some adhesion along the inside of the tube which holds the sample in place while the tube is extracted from the ground. After the waiting period, the tube is turned several revolutions to shear the soil at the base of the tube and along the outside of the side walls. The tube is then extracted at a slow, steady rate until the suction is broken at the base (i.e. the sampler is within the washed section of the borehole). The sample is finally retracted to the ground surface and the driller removes the sample tube from the drill string.

4.2.2 Tube Processing

Field processing of the samples consisted of measuring the soil recovery, the total sample mass (tube and soil; used to compute average density) and the torvane strengths on the bottom of the tube. The ends were then sealed with mechanical o-ring packers and stored in the shade under the van. Samples were taken to the laboratory, the bottom seals removed and soil removed to determine the natural water content. The seals were replaced and the samples were stored in the humid room to await further testing.

4.3 Piezocone Profiling

Piezocone measurements were performed in boreholes which were prepared by installing two inch diameter BX casings were driven from the surface to the top of the clay layer. These casings were driven to a depth of 6.7 meters (22 ft.). After setting the casings, the holes were washed with a 1.85" diameter open ended clay bit on the end of 1.75" diameter AW drill rod. Two continuous penetration soundings were performed in the following manner. The drill rods were laid out in ten foot sections and strung with the

electrical cable encased by the plastic tubing. The cable was connected to the junction box and piezocone and given 30 minutes to warm-up. The first drill rod was connected and the cone suspended over the hole with the pore pressure element in water. The zero readings were recorded and the device lowered to the bottom the hole. A slotted AW coupling was used to connect the drill rod to the cross head of the drill rig while providing a space for the cable. The depth box was connected to the drill rod and referenced to the casing. The cone was then pushed into the ground at approximately 2 cm/sec. while recording time, penetration, pore pressure, tip load and sleeve friction at approximately 2 readings/second. At the end of each 1.5 meter push, which is the maximum stroke of the drill rig, penetration was stopped while the cross head was reset. Data were not collected during this period. This process was continued to the full depth of penetration. The cone was immediately extracted after the final rod was pushed to minimize consolidation and setup. The cone was extracted in 1.5 m (five ft) lengths without recording any data. A final set of zeros was recorded with the cone at the surface and completely cleaned.

4.4 Dissipation Experiments

For the five dissipation boreholes, the casings were also originally driven and washed to a depth of 6.7 meters. However, as the holes were advanced between dissipation measurements, wash water was not returning to the surface, suggesting that the casings were not sealed into the top of the clay layer. In fact, while advancing the hole for one device, wash water expelled from the adjacent casing 3 meters away. Therefore, an additional length of casing was added to increase the casing depth to 9.1 to 10.7 meters (30 to 35 ft.). This attempt to develop a better seal in the clay layer was only partially successful. Throughout the program most of the water used to advance the holes was lost into the sand layer. As all boreholes were cross connected, the influence can not be determined.

Prior to a dissipation measurement, the hole was advanced to within 0.9 to 1.5 meters (3 to 5 ft.) of the measurement elevation using the clay bit. Fresh water was used to wash the cuttings from the hole. In general, the holes remained sufficiently open so that the tools could be lowered to the bottom of the hole under the weight of the drill rod.

The only exception to this was a 3 meter section in the 19.8 to 22.9 meter depth (65 to 75 ft. depth) range which tended to partially close during the process of washing the hole prior to each installation. While penetrating this zone, it was necessary to apply several hundred pounds of force to the rods. Once the tip passed this zone, the rods would again advance due to self weight penetration.

Dissipation measurements were made using the same basic measurement sequence as the continuous profile with a few modifications made necessary by the fact that the five devices were being operated at one time. The following text presents an overview of the procedures.

During the day prior to moving the cones to a new depth, the required length of drill rod was added to each device. During this operation, dissipation on all devices was being collected at relatively long time intervals (>10 min). Adding a length of drill rod was done by disconnecting the electrical cable from the junction box, stringing the cable with plastic tubing through the additional drill rod, and rehooking the cable to the junction box. This allowed the transducers time to return to equilibrium after the loss of electrical power, minimized disruption to the dissipation measurements during the day of penetration and saved a considerable amount of time for the following day.

For each installation, the device was removed from the ground and the drill rod, still strung with the electrical cable, was arranged on a stand. While the driller washed the hole to within 0.9 to 1.5 meters of the next dissipation depth, the device was cleaned, inspected for damage, and evaluated in preparation for the next set of measurements. The response of the pore pressure system was measured using the response chamber. The porous element was changed if the response was not sufficient, and the response evaluation repeated. This was continued until an acceptable response was established¹.

Upon satisfactory response, zero values for each transducer were recorded with the cone attached to the drill rod and suspended in a tube of water. The cone was then lowered to 6.1 meters (20 ft.) below the top of the casing which was filled with water, and another set of transducer readings were recorded with the data acquisition system to provide a second calibration point for the pore pressure. The device was lowered into the

¹ See Section 4.5.3: Response Evaluation for a definition of an acceptable response.

hole to the wash depth and allowed to penetrate under its own weight. The magnitude of penetration depended on the type of device and the depth. It generally ranged between 0.03 and 0.73 meters (0.1 and 2.4 ft). A summary table listing the details of the installation is presented as Table 4.1².

The depth locator box was attached to the drill rod and the data acquisition system initialized. The device was then pushed with constant rate of displacement to the desired measurement location. Pore pressure, tip load, skin friction, and penetration were measured during penetration. The pore pressure was observed on the computer screen and a target penetration depth was selected with a contingency to penetrate deeper if the pore pressure dropped while the penetration rate remained constant. This procedure was adopted in order to insure that the device stopped in a clay layer with the highest pore pressure and therefore did not undergo partial drainage.

At the dissipation depth, the cross head was stopped but left in contact with the drill rod for several minutes in order to prevent a change in pore pressure due to the sudden removal of total stress. During this early time period, the axial load slowly relaxed as observed on the tip load measurement, and hence the early pore pressure changes are due to a combination of total stress changes and consolidation around the device. However, holding the cross head stationary eliminated dramatic changes in the pore pressure at the time load was removed from the top of the drill rod. After several minutes the cross head was retracted and the drill rig moved to the next hole.

The cone remained at each depth while recording pore pressure, tip load and skin friction until full dissipation. This duration varied with depth, and increased from two days for the shallower tests, to five days at the deepest installations. At the end of the dissipation, the drill rig was used to remove the cone from the ground. The drill rod and cones were always covered with a one half inch layer of clay, which was scraped from the tool using a piece of jute rope. A final set of zeroes was obtained, pore pressure response evaluated, the stone changed if necessary, and the process was repeated at the next elevation.

² Settlement depth is given as "Initial Penetration" in this Table.

4.5 Equipment Evaluation

Measurements were made to evaluate the overall electrical performance characteristics of the equipment components and the integrated field system. Individual transducers were first calibrated against physical references in the laboratory using the central data acquisition system to determine calibration factors, and to establish linearity and stability. Next, the entire electronic system was assembled and tested against physical references in the laboratory to establish the field calibration factors which include the influence of cabling and the field data acquisition system.

This system was also evaluated for electronic noise. However, these pre-field calibrations turned out to be unimportant as the unshielded cables were found to be inadequate during the first day of field operation and were replaced during the first week in the field. As a result, the final calibrations were obtained in the laboratory after the field program was completed. While this is not a preferred practice, it was the only option which allowed the program to be completed before the start of the fall semester. Electronic noise was evaluated in the field for the final system configuration.

4.5.1 Stability and Resolution

In general, the practical resolution of electronic systems is determined by the long term stability rather than the transducer nonlinearities. Instability of the measurements can be caused by the transducer, power system or measurement system. This instability can be inherent to the system or be induced by external sources. The field system was evaluated both in the laboratory and in the field to determine the various sources of instability. These results were then used to establish the performance characteristics of each measurement.

Table 4.2 presents a summary of the available data on individual measurement resolutions. The first column presents the theoretical system resolution, which is the value in physical units represented by one bit of the analog to digital converter. These values are extremely small (2×10^{-5} ksc, 0.001 kg, and 0.04 cm) and will not have any practical value. The second and third column present the expected transducer variation due to a 20° C change in temperature and the manufacturer's quoted value for drift,

respectively. These data are not available for the force transducers because they are not commercial devices. The thermal drift is relatively small (0.044 ksc) for the piezocone transducers but rather substantial (0.252 ksc) for the tapered piezoprobe transducers. Long term stability is twice the value of the thermal drift for the piezocones and far less than the thermal drift for the piezoprobes (0.07 ksc). These values are approximately one third of the transducer nonlinearity; however, the comparison is transducer specific. The next two columns present the system noise which was measured in the laboratory and field, respectively. These numbers were obtained by collecting a short duration data set (about 100 readings) and computing the standard deviation of what should be a constant value. These values are not available for all the transducers. The field and laboratory noise are basically the same for any particular transducer. For the piezoprobe transducers, the noise is 10 times the system resolution and much less than the stability or drift. This suggests that the system is inherently quiet. For the other transducers, the noise is comparable to the nonlinearity. Based on all these evaluations it is clear that the resolution of the measurements should be very good.

About half way into the field program it became apparent that the measurements were being influenced by random long term instability. The long term dissipation data (second and third day readings), contained instantaneous voltage shifts which lasted various lengths of time and appeared to be reversible³. In order to assess this problem, a series of manual readings were collected on each of the channels with the input to the data acquisition system shunted. A “shunt” is obtained by connecting the positive output voltage directly to the negative output and is performed in order to determine the voltage value of a ground shift. “Shunt” data were collected between August 15th and 31st. These data confirmed that the voltage shifts observed on the transducers were consistent with a shift in the reference (ground) of the data acquisition system. The magnitude of the shift was different for each channel and was particularly severe for one analog to digital card on August 22nd. These data are presented in Appendix A for completeness and are summarized in Table 4.2 as the standard deviation (SD, without data from August 22nd) and the difference between the maximum and minimum values (including August 22nd

³ For an example, see Dissipation plots in Appendix A, Piezocone 881 at El. -21 m.

data) converted to physical units. The columns are labeled S.D. Shunts and Max-Min Shunts. The impact of these jumps is largest for the pore pressure measurements of the two piezocones and the MIT cone. All of these transducers are connected to the same analog to digital card. For the pore pressure measurements, the standard deviation of this error is more than 10 times any other error source. In terms of the max-min, the error is even larger. Unfortunately, the cause of the reference changes could not be identified during the field program nor could it be eliminated. The problem only occurs in the field and hence it is assumed to be caused by induced electrical currents in the ground system by external transmissions, such as the nearby radio tower.

Figure 4.1 summarizes the level of electrical noise in terms of pressure in a bar chart for the pore pressure measurement. The level of electrical noise was determined by the transducer resolution and the system calibration factor. The dominant source of noise for the piezocones is due to changes in ground reference as characterized by the Max - Min Shunts. For the piezoprobes, the greatest influence is due to the thermal drift over the maximum expected temperature variation: 20⁰C. These are identical for the two probes because it is based on the manufacturer's specifications. The greatest electrical influence for the MIT cone is also the thermal drift, although the level of influence is approximately 20% of the level for the probes. The piezocones are influenced more severely by electrical noise in all cases except thermal drift.

Voltage values corresponding to zero force and pressure in the calculations were selected based on a review of the entire data base from the field program in order to obtain a consistent and representative value. Since the various sources of error discussed above will influence individual readings, an attempt was made to combine data and select best estimates for each transducer and each depth. This approach should yield the best possible average dissipation values. The choice of zeros has no impact on the shape of the dissipation curve and little impact on the penetration values. For each dissipation measurement, four pressure values provide useful data: a zero reading taken just prior to putting the instrument in the hole, a reading with the tool located 6.1 meters (20 ft.) in the water filled casing ($\gamma_w = 1.05 \text{ gm/cm}^3$ due to residual particles from washing the hole), the final dissipation reading (with an estimate of the variability) and a final zero reading

when the tool is returned to the surface (generally equal to the zero reading of the next push). These data are presented in Table 4.3 through Table 4.7 (one per device). In general, the zero values were selected using the zero and 6.1 meter readings and then evaluated using the dissipation readings. The following presents a review for each device.

Piezoprobe P63 (Table 4.3) was the most consistent of the probes. A single zero was used for all the depths which represented an average of all the zero readings except August 5th. The variation in the final value is generally less than 0.3 m (1 ft) of water which is consistent with the noise associated with the ground variation. The importance of selecting an average over the individual zeros is tested by comparing the final dissipation values with the equilibrium values measured with the piezometers. The average values for the two sets of calculations are slightly different -0.0015 and 0.06 ksc (-0.05 and 1.99 ft) while the standard deviation is higher when using the individual zero readings.

Piezoprobe P62 (Table 4.4) was a more problematic device. This tool experienced twenty feet of free fall when dropped down the hole by the driller which stretched the cable. Piezoprobe P62 also had several electrical connection problems and had a cracked connector, which caused several water leaks that destroyed the first transducer. Data are only good for depths below 19.8 meters (65 ft.) and with the new transducer. The zero value for this transducer appears to steadily decrease with time. This is also reflected in the 6.1 meter readings. In addition, the readings taken on August 19th are completely unreasonable. The probe was rewired again after the measurements at 95 feet due to a loose connection in the housing. Therefore, three zero values were used for the final calculations as shown in the table. One for El. -17.8 m, a lesser value for the next three locations and a third value for the final two locations. Using these three zeros results in very reasonable values for the 6.1 meter check point readings. Comparing the final dissipation and the equilibrium values shows that the average values are closer and have less variation than the individual zeros. However, the average is almost 0.15 ksc (5 ft) greater than the P63 measurements which suggests a zero offset between the two

devices. The variation in values is larger than for P63 which is also consistent with the resolution evaluation.

Piezocone P790 (Table 4.5) performed rather well. A partial short was found in the down hole connection and repaired on August 9th. This short was caused by a thin film of soldering paste at the base of the connector. The dissipation measurements at -17.7 m (Depth 65 ft) contained a large jump in the middle of the curve. As seen in Table 4.5 the zero and 6.1 m (20 ft) readings for this push are very different. During this period there were intense thunder storms in the area which seem to have affected all the readings on data acquisition card number one. Therefore, two average zeros, separated at the start of the test at El. -17.7 m (65 ft), were used to compute the dissipation data. In addition, a third zero was used for the early portion of the 65 foot push to compensate for the jump in the middle of the dissipation record. The observed variation in the pressure at the end of dissipation is larger than for the probes, slightly larger than the standard deviation of the shunts but much less than the maximum shunt variation. The final dissipation values are on average in good agreement with the equilibrium values, however the range is larger than for the probes. The calculations using the selected zeros are slightly more consistent and 0.3 m (1 ft) closer to the equilibrium values. Average values were used for both the point and sleeve load zeros. As shown in the table, the standard deviation of the load transducer zero readings are consistent with the field noise in the system, which justifies the use of average zero values.

Piezocone P881 (Table 4.6) generally suffered from higher noise levels than P790. The cause of this is unknown. As with P790 the dissipation measurements at El. -17.9 m (65 ft) contained a large jump and the zero and 6.1 m readings are unusual. The data were reduced using two average zero values separated at the start of the test at El. -17.9 m. A third zero was used only for the start of the El. -17.9 m push. This is the same procedure as used for P790. Using these selected zero values results in measurements at the 6.1 m (20 ft) reference point which are relatively high. The final dissipation values are also high compared to the equilibrium measurements for both sets of zeros. The difference between these values and P790 is consistent for both the 6.1 m and equilibrium values, which again suggests an average offset in the zeros. The selected zeros give much

less variability than the individual zeros. The force measurements were computed using average values (except the zero taken for the test at El. -33 m is not used) for both the sleeve and the point. The zero readings are very erratic for both transducers even when compared to the noise measurements. Unfortunately, there is no independent method to check these values. These errors can be as large as one ksc for the point but is only 0.15 ksc for the sleeve.

The MIT piezocone (Table 4.7) had relatively stable readings throughout the program. However, it did experience the same problem as the two cones during the dissipation at El. -17.8 m on August 9th. The data were reduced using an average of all the zero readings except the tests at El. -13.2 m and El -17.8 m. A second zero value was used for the start of the El. -17.8 m dissipation. The 6.1 m reference point measurement is very reasonable when using the selected zero values. The variation in the final dissipation values is consistent with the shunt observations, which show generally low noise with occasional periods of increased instability. The final dissipation values are on average in excellent agreement with the equilibrium measurements and the variability is reasonably low.

4.5.2 Calibrations

Calibrations were performed by putting the response chamber (Section 3.3.1) in a load frame and pushing the cone into the chamber to create a controlled pressure. Since the chamber was stiff and tightly sealed, the displacement control of the load frame provided excellent pressure control for calibrations and leak checks. The pore pressure and witness transducers were monitored on either the central laboratory or field data acquisition systems.

Individual transducers were calibrated in the laboratory using the central data acquisition system which has a one microvolt resolution. The transducers were energized using a constant voltage supply. Each calibration consisted of two complete load and unload cycles in which approximately 20 measurements were taken in each direction. Transducers were evaluated based on the goodness of fit (R^2) of a linear regression line.

Removable pressure transducers were calibrated using a dead weight pressure calibrator which generates a constant pressure through application of a known mass on a

piston which penetrates into an oil filled chamber. The pressure transducers of the piezocones are integral to the device and therefore were calibrated against a witness transducer. The witness transducer was initially calibrated using the dead weight pressure calibrator. The cone was inserted into the response chamber which was in turn mounted into a screw driven load frame. Pressures were applied to the pressure vessel by manually driving the cone into the chamber while readings were taken on the two transducers.

The force transducers are all integral to the cone assemblies. Therefore, these devices were calibrated against a witness force transducer using a screw driven load frame to apply forces. The witness transducer was calibrated up to 2000 lbs in a dead weight calibrator with a 10 to 1 lever advantage. The cones were mounted in the load frame with a ball joint above and below the cone section to be sure the forces were applied concentrically. The cones were loaded manually while the two transducers were monitored by the data acquisition system.

Table 4.8 presents a summary of the instruments used for the field program. The columns under the Transducer Calibration heading provide the results of the individual calibrations. The Ave. Error column presents the average difference between the linear regression line and the calibration data. This represents a composite error expected due to both transducer nonlinearity and data acquisition noise. In general, all the transducers are considered to be in good working order and sufficiently linear. The error in the force measurements is dominated by the system noise rather than the nonlinearity of the transducer. This is due to the high capacity of the device and low voltage output. The pore pressure transducers all have errors on the order of 0.1 ksc, which is within the manufacturers' specifications.

Upon completion of the field program, the field system was set up in the laboratory with the field configuration. Electrical power was provided by the laboratory but the ground wires were removed and the field system grounded to the building water pipes. The transducers were once again calibrated using the field cables and the field data acquisition system with gain amplifiers to enhance the signals. These calibration factors are the values which were used to reduce all the field data. In general, the degree of linearity is maintained using the field system (compare the two sets of R^2 values in Table

4.8). The gain value is the ratio of the transducer calibration factor to that of the system calibration factor. This gain combines the effects of the power transmission loss in the long cables and the analog signal amplification applied before the analog to digital converter. Gains were selected such that the transducer output would make use of the maximum possible range of the analog to digital converter. A gain of approximately 1000 was used with the cone because the devices have inherently low output (full scale output equals 4 and 10 millivolts for the pore pressure and force, respectively) and only a small fraction of the capacity would be used (about 30% of the pressure and 3% of the force). A gain of 100 was selected for the piezoprobes which have higher full scale outputs (75 millivolts) but only 25% of the range will be used. The MIT cone has a higher output and lower capacity pressure transducer and hence the gain was set at 10.

4.5.3 Response Evaluation

As discussed in Section 4.4, the rate of pore pressure response was measured before and after each dissipation measurement to be sure the stones were completely saturated. The measurement was obtained using the following procedure. The device was assembled in the chamber. The data acquisition system was started and pressure pulses were generated by manually pushing on the shaft of the device. This method was sufficient to generate pulses of 2 to 3 ksc with a duration of 1 to 2 seconds. The readings were immediately viewed on the screen to determine if the system was operating and sufficiently responsive.

Whenever poor or questionable response was measured, the stone was replaced and the system reevaluated. Figure 4.2a shows an unacceptable pore pressure response for piezoprobe P63 after penetration, and an excellent response following the replacement of the cavitated stone with a laboratory saturated stone. The figure plots pressure versus time for both the piezoprobe transducer and the witness transducer, which measures the chamber pressure. After the probe was removed from the ground the response was so slow that it was unable to detect the three pressure pulses of one to two second duration. These pulses were measured as a very broad pulse with about 20% of the peak magnitude. Changing the stone returned the response to adequate as seen in Figure 4.2b. In this case the probe faithfully follows the one second applied pulses.

No device was inserted into the ground unless the pore pressure response was determined by visual inspection to be adequate. In all cases, replacement with a laboratory saturated stone converted poor response to good response. This leads to the conclusion that de-saturation of the pore pressure measurement system only occurs along the surface of the stone.

The last column of Table 4.1 shows when the response was unsatisfactory after removal of the device. The stones were replaced any time the final response was determined to be unsatisfactory⁴. In addition, the stones were replaced several times on the piezocones to provide a clean interface. However, poor response was never measured on the piezocones. This is either because the stones fit loosely in the cone allowing water to flow around the stone or the very coarse grained nature of the stones makes them free draining. Both situations raise concerns about the possibility of having undesirable pressure sensitivity to changes in total stress.

In an attempt to reduce the negative pore pressure developed during extraction, the penetrometers were pushed several inches before extracting. This seemed to have no effect on the piezoprobes. Inadequate response was measured 15 out of 18 times for the piezoprobes.

4.5.4 Penetration Rate

The use of the depth locator box and the time synchronization allowed the accurate measurement of penetration rate. The penetrometers were pushed into the ground at a nominal rate of 2 cm/sec. However, the rate was increased to a nominal rate of 8 cm/second in cases where two of the same type of device were inserted to the same depth. For example, both piezocones were working at El. -27 m, so Piezocone 881 was installed with a penetration rate of 2 cm/sec and Piezocone 790 was installed at a rate of 8 cm/sec. This was performed in order to assess the effects of penetration rate on the measurements of load, skin friction, and pore pressure during penetration and dissipation. A summary of penetration rate for each working device at each depth is given in the summary table of installation details (Table 4.1).

⁴ A satisfactory response is indicated by "OK" while an unsatisfactory response is indicated by "NG".

4.6 Saturation of Pore Pressure Elements

At the end of each day when the penetrometers were installed at a new depth, the cavitated porous elements were taken to the laboratory at MIT and re-saturated. Following drying, evacuation, and saturation, the elements were placed in deaired water in sealable containers and kept on site until needed.

Upon an unsatisfactory pore pressure response, the penetrometer and the pressure response chamber were transferred to a 1.2 m tall bucket filled with water. Once under water, the penetrometer was removed from the chamber, taking care to keep the porous element under the water surface. This was done assuming that cavitation occurred on the surface of the porous element and air had not entered the pore pressure port.

The replacement element was then transferred. Careful attention was given to ensure that air bubbles were not trapped in the small threads on the piezoprobe tip. The piezoprobe tip screws into the end of the piezoprobe shaft, which also serves as the hydraulic connection to the pressure transducer. Any air bubbles in this small diameter tube would cause a very poor pore pressure response.

After the porous element was changed, the device was transferred to the pressure chamber and another response evaluation carried out.

4.7 Site Cleanup

The agreement with the site owner and the Saugus Conservation Commission included returning the site to its original condition upon completion of the project. On the last day of the field program, all tools were removed from the ground including the piezometers. The casings were removed and at least the upper 3 m of all the holes was packed with bentonite pellets. Most of the drilling mud for the sampling hole, which at this point comprised a mixture of bentonite and Boston Blue Clay, was injected into the hole after the casing was removed. This mud presumably penetrates into the sand layer until it forms a plug. The rest of the mud was put in shallow holes and mixed with the sand from the mat. This stabilized the mixture to the extent that it would support a person. The top several inches of the work area was tilled to combine any slippery Boston Blue Clay on the surface with the coarse sand mat material. The site was raked

level and covered with a layer of salt marsh hay to give the grass protection as it reestablished in the area. All materials used for the project were removed from the site.

Nominal Tip Depth (feet)	Pen. Date	Device	Wash Elev (m)	Initial Pen. (m)	Push Pen. (m)	Total Pen. (m)	Nominal Tip Depth (m)	Tip Elevation (m)	Pen. Speed (cm/s)	Final Response
45	8/2/96	P790	-10.10	0.49	1.04	1.52	13.72	-11.62	2.3	OK
		P881	-10.31	0.15	1.37	1.52	13.72	-11.83	1.7	OK
50	8/5/96	P63	-11.93	0.46	0.91	1.37	15.24	-13.30	8.8	NG
		P790	-12.29	0.21	1.16	1.37	15.54	-13.66	1.6	OK
55	8/7/96	P63	-13.61	0.37	0.91	1.28	16.82	-14.89	1.6	OK
		P790	-13.66	0.30	0.91	1.22	16.76	-14.88	1.7	OK
65	8/9/96	P62	-16.93	0.43	1.10	1.52	20.42	-18.45	1.8	OK
		P63	-17.57	0.46	0.46	0.91	20.42	-18.48	1.1	NG
		P790	-16.80	0.15	0.76	0.91	19.81	-17.72	1.7	OK
		P881	-17.01	0.03	0.88	0.91	19.81	-17.93	1.4	OK
		MIT	-16.88	0.37	0.96	1.33	20.22	-18.21	1.4	OK
75	8/12/96	P62	-19.67	0.52	0.70	1.22	22.86	-20.89	1.5	NG
		P63	-19.70	0.43	0.79	1.22	22.86	-20.92	1.3	NG
		P790	-19.55	0.09	1.13	1.22	22.86	-20.77	1.4	OK
		P881	-19.76	0.24	0.98	1.22	22.86	-20.98	1.6	OK
		MIT	-19.62	0.24	0.98	1.22	22.86	-20.84	1.6	OK
85	8/16/96	P62	-22.72	0.43	0.79	1.22	25.91	-23.94	1.3	NG
		P63	-22.75	0.61	0.61	1.22	25.91	-23.97	1.7	OK
		P790	-22.59	0.18	1.04	1.22	25.91	-23.81	1.7	OK
		P881	-22.81	0.52	0.70	1.22	25.91	-24.02	1.2	OK
		MIT	-22.67	0.49	0.73	1.22	25.91	-23.89	1.8	OK
95	8/19/96	P62	-25.76	0.03	1.19	1.22	28.96	-26.98	8.6	NG
		P63	-25.80	0.43	0.79	1.22	28.96	-27.02	2.0	NG
		P790	-25.64	0.21	1.01	1.22	28.96	-26.86	8.8	OK
		P881	-25.85	0.06	1.16	1.22	28.96	-27.07	1.6	OK
		MIT	-25.72	0.18	1.04	1.22	28.96	-26.94	1.5	OK
105	8/24/96	P62	-28.51	1.04	0.79	1.83	32.31	-30.34	16.0	NG
		P63	-28.54	0.52	1.01	1.52	32.00	-30.07	1.6/3.2/5.2	NG
		P790	-25.34	3.05	1.52	4.57	32.00	-29.91	11.8	OK
		P881	-28.60	0.40	1.13	1.52	32.00	-30.12	1.3	OK
		MIT	-28.46	0.55	0.98	1.52	32.00	-29.99	2.9	OK
115	8/27/96	P62	-31.56	0.73	0.79	1.52	35.05	-33.08	9.9	NG
		P63	-31.59	0.70	0.82	1.52	35.05	-33.11	2.3	NG
		P790	-31.43	0.24	1.28	1.52	35.05	-32.96	13.0	OK
		P881	-31.64	0.00	1.52	1.52	35.05	-33.17	2.0	OK
		MIT	-31.51	0.70	0.82	1.52	35.05	-33.03	1.7	OK

Table 4.1 Summary of Installation Details.

CH #	Device Specifications				System Resolution (ksc,kg,cm)	Thermal Drift (ksc,kg,cm)	Long Term Stability (ksc,kg,cm)	Lab Noise (ksc,kg,cm)	Field Noise (ksc,kg,cm)	S.D. Shunts (ksc,kg,cm)	Max-Min Shunts (ksc,kg,cm)
	Device **	Measurement	Make	Units							
5	P62	Pore Pressure	Kulite	ksc/v/v	0.00001	0.2520	0.0700	0.0005	0.0004	0.0199	0.0751
11	P63	Pore Pressure	Kulite	ksc/v/v	0.00001	0.2520	0.0700	0.0003	0.0004	0.0094	0.0293
7	P790	Pore Pressure	Keller	ksc/v/v	0.00002	0.0440	0.0880	0.0021	0.0081	0.0795	0.2979
8	P790	Tip Load	Fugro	kg/v/v	0.00102	N/A	N/A	0.3130	0.2938	0.7419	2.3518
9	P790	Friction Sleeve	Fugro	kg/v/v	0.00102	N/A	N/A	0.1154	0.4442	0.0329	0.1070
1	P881	Pore Pressure	Keller	ksc/v/v	0.00002	0.0440	0.0880	N/A	0.0138	0.1241	0.3696
2	P881	Tip Load	Fugro	kg/v/v	0.00106	N/A	N/A	N/A	0.6753	0.8363	3.1748
3	P881	Friction Sleeve	Fugro	kg/v/v	0.00105	N/A	N/A	N/A	0.3182	0.0236	0.0886
13	MITC	Pore Pressure	DI	ksc/v/v	0.00003	0.0540	0.0300	N/A	0.0313	0.0064	0.0191
14	MITC	Tip Load	MIT	kg/v/v	0.00052	N/A	N/A	N/A	0.6356	0.2964	0.9928
15	MITC	Friction Sleeve	MIT	kg/v/v	0.00036	N/A	N/A	N/A	0.3363	0.0777	0.3499
19	Depth			cm/v/v	0.00008	N/A	N/A	N/A	N/A	0.0159	2.5510
19	Water	Water Level	DI	cm/v/v	0.04059	7.3220	4.0680	N/A	N/A	8.5070	1366.3600
21	Witness		DI	ksc/v/v	0.00003	0.0460	0.0260	N/A	N/A	0.0333	0.1383

- ** P62 Piezoprobe with Kulite Pressure Transducer Serial # X2862; on 8/9/96 changed - Serial# D3289
P63 Piezoprobe with Kulite Pressure Transducer Serial # X2863
P790 Standard Piezocone #790
P881 Standard Piezocone, #881
MIT MIT Piezocone

Table 4.2 Summary of Measurement Resolutions.

Piezoprobe 63														
Pen. Date	Measured U _o (volts)	Selected U _o (volts)	U ₂₀ (volts)	Measured U ₂₀ (feet)	Selected U ₂₀ (feet)	U _{diss} (volts)	+/- U _{diss} (volts)	+/- U _{diss} (feet)	U _{equil} (feet)	Measured		Selected		Nom. Depth
										U _{diss} (feet)	Δ U _{equil} (feet)	U _{diss} (feet)	Δ U _{equil} (feet)	
8/5/96	-0.1910	-0.1000	-0.2000	1.31	14.54									50
						-0.4000	0.0010	0.15	46.29	31.90	-14.39	45.79	-0.50	
8/7/96	-0.0919	-0.1000	-0.2283	19.83	18.65									55
8/9/96						-0.4580	0.0030	0.46	51.41	55.88	4.47	54.64	3.23	
	-0.1401	-0.1000	-0.2295	12.99	18.82									65
8/12/96						-0.5450	0.0030	0.46	61.64	61.80	0.15	67.92	6.27	
	-0.0911	-0.1000	-0.2201	18.75	17.46									75
8/16/96						-0.5930	0.0020	0.31	71.88	76.60	4.72	75.24	3.36	
	-0.0870	-0.1000	-0.2158	18.72	16.83									85
8/19/96						-0.6280	0.0060	0.92	82.11	82.57	0.45	80.58	-1.53	
	-0.0934	-0.1000	-0.2270	19.42	18.46									95
8/24/96						-0.7103	0.0150	2.29	92.35	94.15	1.80	93.15	0.80	
	-0.1010	-0.1000	-0.2374	19.82	19.96									105
8/27/96						-0.7850	0.0040	0.61	102.59	104.39	1.81	104.55	1.96	
	-0.1115	-0.1000	-0.2237	16.31	17.98									115
8/30/96						-0.8545	0.0018	0.27	112.82	113.40	0.57	115.15	2.33	
AVE:					15.89	17.84					-0.05		1.99	
S.D.					6.33	1.63					6.05		2.45	

* "Measured" refers to values obtained using the measured zero.

"Selected" refers to values obtained using the average selected zero.

** ΔU_{equil} refers to the deviation of the value from the equilibrium pore pressure determined by the piezometers.


 Note: Shaded values not included in average and standard deviation calculations.

Table 4.3 Summary of Selection of Zero Voltage Values for Piezoprobe 63.

Piezoprobe 62														
Pen. Date	Measured U_o (volts)	Selected U_o (volts)	U_{20} (volts)	Measured U_{20} (feet)	Selected U_{20} (feet)	U_{diss} (volts)	+/- U_{diss} (volts)	+/- U_{diss} (feet)	U_{equil} (feet)	Measured		Selected		Nom. Depth
										U_{diss} (feet)	ΔU_{equil} (feet)	U_{diss} (feet)	ΔU_{equil} (feet)	
8/9/96	-0.1627	-0.1627	-0.2598	14.42	14.42									65
8/12/96						-0.5630	0.0040	0.62	61.64	62.38	0.74	62.38	0.74	
	-0.0548	-0.0560	-0.1880	19.77	19.59									75
8/16/96						-0.6020	0.0020	0.31	71.88	85.28	13.40	85.09	13.21	
	-0.0568	-0.0560	-0.2280	25.41	25.53									85
8/19/96						-0.6295	0.0070	1.09	82.11	89.25	7.14	89.37	7.26	
	0.0165	-0.0560	0.0890	10.76	21.52									95
8/24/96						-0.6818	0.0025	0.39	92.35	108.82	16.47	97.53	5.17	
	-0.0306	-0.0190	-0.1555	18.54	20.25									105
8/27/96						-0.7170	0.0090	1.40	102.59	106.97	4.39	108.78	6.19	
	-0.0079	-0.0190	-0.1511	21.25	19.60									115
8/30/96						-0.7950	0.0100	1.56	112.82	122.67	9.85	120.93	8.11	
AVE:				19.88	19.88						8.66		6.78	
S.D.				4.00	3.94						5.80		4.07	

* "Measured" refers to values obtained using the measured zero.

"Selected" refers to values obtained using the average selected zero.

** ΔU_{equil} refers to the deviation of the value from the equilibrium pore pressure determined by the piezometers.


 Note: Shaded values not included in average and standard deviation calculations.

Table 4.4 Summary of Selection of Zero Voltage Values for Piezoprobe 62.

Piezocone 790														
Pen. Date	Measured U_o (volts)	Selected U_o (volts)	U_{20} (volts)	Meas. U_{20} (feet)	Selected U_{20} (feet)	U_{diss} (volts)	+/- U_{diss} (volts)	+/- U_{diss} (feet)	U_{equil} (feet)	Measured		Selected		Nom. Depth
										U_{diss} (feet)	ΔU_{equil} (feet)	U_{diss} (feet)	ΔU_{equil} (feet)	
8/2/96	-0.7308	-0.7356	-0.6651	16.44	17.64									45
8/5/96						-0.6150	0.0300	7.88	41.17	30.42	-10.76	31.68	-9.49	
	-0.7230	-0.7356	-0.6400	20.76	23.92									50
						-0.5700	0.0050	1.31	46.29	40.19	-6.10	43.50	-2.79	
8/7/96	-0.7633	-0.7356	-0.6831	20.06	13.13									55
8/9/96						-0.5255	0.0020	0.53	51.41	62.46	11.06	55.19	3.78	
initial	-0.5919	-0.5919	-0.5174	18.64	18.64									65
final		-0.9240												
8/12/96						-0.7200	0.0050	1.31	61.64	33.65	95.29	53.59	-8.06	
	-0.9459	-0.9240	-0.8615	21.11	15.64									75
8/16/96						-0.6450	0.0100	2.63	71.88	79.04	7.16	73.29	1.41	75
						-0.6600			71.88	75.10	3.22	69.35	-2.53	
	-0.9217	-0.9240	-0.8376	21.04	21.61									85
8/19/96						-0.5880	0.0200	5.25	82.11	87.65	5.54	88.26	6.14	
	-0.9022	-0.9240	-0.8281	18.54	23.99									95
8/24/96						-0.5750	0.0080	2.10	92.35	85.95	-6.40	91.67	-0.68	
	-0.9274	-0.9240	-0.8583	17.29	16.44									105
8/27/96						-0.5250	0.0250	6.57	102.59	105.70	3.11	104.81	2.22	
	-0.9226	-0.9240	-0.8374	21.31	21.66									115
8/30/96						-0.4670		0.00	112.82	119.67	6.85	120.04	7.22	
AVE:				19.47	19.18						1.52		-0.28	
S.D.				1.81	3.82						7.45		5.58	

* "Measured" refers to values obtained using the measured zero.

"Selected" refers to values obtained using the average selected zero.

** ΔU_{equil} refers to the deviation of the value from the equilibrium pore pressure determined by the piezometers.


 Note: Shaded values not included in average and standard deviation calculations.

Table 4.5 Summary of Selection of Zero Voltage Values for Piezocone 790.

Piezocone 881														
Pen. Date	Measured U_o (volts)	Selected U_o (volts)	U_{20} (volts)	Meas. U_{20} (feet)	Selected U_{20} (feet)	U_{diss} (volts)	+/- U_{diss} (volts)	+/- U_{diss} (feet)	U_{equil} (feet)	Measured		Selected		Nom. Depth
										U_{diss} (feet)	ΔU_{equil} (feet)	U_{diss} (feet)	ΔU_{equil} (feet)	
8/2/96	-0.3263	-0.3277	-0.2230	27.36	27.73									45
8/5/96						-0.1910	0.0030	0.83	41.17	37.63	-3.55	38.01	-3.16	
8/9/96														
initial	-0.1291	-0.1291												65
final		-0.5465												
8/12/96						-0.2960	0.0040	1.11	61.64	46.41	108.06	69.66	8.02	
	-0.5090	-0.5465	-0.4485	16.02	25.95									75
8/16/96						-0.2500	-0.1000	-27.81	71.88	72.02	0.15	82.45	10.57	
	-0.5654	-0.5465	-0.4406	33.05	28.05									85
8/19/96						-0.2050	0.0400	11.12	82.11	100.22	18.11	94.97	12.85	
	-0.5395	-0.5465	-0.4314	28.63	30.48									95
8/24/96						-0.2000	0.0550	15.29	92.35	94.41	2.06	96.36	4.01	
	-0.5095	-0.5465	-0.4280	21.58	31.38									105
8/27/96						-0.1530	0.0700	19.47	102.59	99.14	-3.45	109.43	6.84	
	-0.6091	-0.5465	-0.4946	30.33	13.75									115
8/30/96						-0.0830	0.0850	23.64	112.82	146.31	33.49	128.89	16.07	
AVE:				26.16	26.22						7.80		7.89	
S.D.				6.26	6.42						14.92		5.64	

* "Measured" refers to values obtained using the measured zero.

"Selected" refers to values obtained using the average selected zero.

** ΔU_{equil} refers to the deviation of the value from the equilibrium pore pressure determined by the piezometers.


 Note: Shaded values not included in average and standard deviation calculations.

Table 4.6 Summary of Selection of Zero Voltage Values for Piezocone 881.

MIT Piezocone														
Pen. Date	Measured U_o (volts)	Selected U_o (volts)	U_{20} (volts)	Meas. U_{20} (feet)	Selected U_{20} (feet)	U_{diss} (volts)	+/- U_{diss} (volts)	+/- U_{diss} (feet)	U_{equil} (feet)	Measured		Selected		Nom. Depth
										U_{diss} (feet)	ΔU_{equil} (feet)	U_{diss} (feet)	ΔU_{equil} (feet)	
8/9/96	0.0790	0.0790	0.0273	20.59	20.59									65
final		-0.1983												
8/12/96						-0.3490	0.0030	1.26	61.64	179.17	117.52	63.09	1.45	
	-0.1980	-0.1983	-0.2470	19.54	19.42									75
8/16/96						-0.3720	0.0040	1.67	71.88	72.84	0.97	72.72	0.84	
	-0.1886	-0.1983	-0.2417	21.17	17.30									85
8/19/96						-0.3860	0.0040	1.67	82.11	82.64	0.53	78.58	-3.53	
	-0.2090	-0.1983	-0.2640	21.93	26.20									95
8/24/96						-0.4130	0.0250	10.47	92.35	85.40	-6.95	89.88	-2.47	
	-0.2061	-0.1983	-0.2557	19.78	22.89									105
8/27/96						-0.4430	0.0150	6.28	102.59	99.18	-3.40	102.44	-0.14	
	-0.1926	-0.1983	-0.2437	20.39	18.12									115
8/30/96						-0.4700	0.0050	2.09	112.82	116.13	3.31	113.75	0.92	
AVE:				20.57	20.75						18.66		-0.49	
S.D.				0.89	3.31						48.57		2.04	

* "Measured" refers to values obtained using the measured zero.

"Selected" refers to values obtained using the average selected zero.

** ΔU_{equil} refers to the deviation of the value from the equilibrium pore pressure determined by the piezometers.


 Note: Shaded values not included in average and standard deviation calculations.

Table 4.7 Summary of Selection of Zero Voltage Values for the MIT Piezocone.

CH #	Device Specifications				Transducer Calibration				System Calibration		
	Device **	Measurement	Make	Range	Factor	Units	R ²	Ave. Error (ksc,kg,cm)	Factor	R ²	Gain
5	P62	Pore Pressure	Kulite	35 ksc	-4640	ksc/v/v	0.999997	0.0169	-47.51	0.999987	98
11	P63	Pore Pressure	Kulite	35 ksc	-4579	ksc/v/v	0.999995	0.0159	-46.53	0.999995	98
7	P790	Pore Pressure	Keller	35 ksc	75930	ksc/v/v	0.999907	0.0216	80.08	0.999986	948
8	P790	Tip Load	Fugro	5000 kg	4056480	kg/v/v	0.999996	0.9743	4275.98	0.999891	949
9	P790	Friction Sleeve	Fugro	5000 kg	4087000	kg/v/v	0.999976	0.9710	4258.92	0.999991	960
1	P881	Pore Pressure	Keller	35 ksc	82820	ksc/v/v	0.999968	0.0135	84.78	0.999818	977
2	P881	Tip Load	Fugro	5000 kg	4227420	kg/v/v	0.999998	0.2754	4427.90	0.999987	955
3	P881	Friction Sleeve	Fugro	5000 kg	4186420	kg/v/v	0.999980	0.8341	4400.66	0.999988	951
13	MITC	Pore Pressure	DI	14 ksc	702.0	ksc/v/v	0.999938	0.0193	-70.20		10
14	MITC	Tip Load	MIT	450 kg	-1145730	kg/v/v	0.999984	0.1919	1187.31	0.999991	965
15	MITC	Friction Sleeve	MIT	450 kg	803520	kg/v/v	0.999941	0.3301	833.63	0.999979	964
16	MITC	Sleeve PP1	Cooper	14 ksc	6866.2	ksc/v/v	0.999994	0.0066	N/A		
17	MITC	Sleeve PP2	Cooper	14 ksc	5975.4	ksc/v/v	0.999892	0.0117	N/A		
19	Depth			150 cm	174.7	cm/v/v	0.999660		176.8	0.999964	1
19	Water			1 ksc	-93586	cm/v/v	0.999792	0.8772	-94531		1
21	Witness		DI	14 ksc	-699.4	ksc/v/v	0.999992	0.0102	-70.42	0.999993	10

* Calibration Factors at the conclusion of the Field Program, through the junction box

** P62 Piezoprobe with Kulite Pressure Transducer Serial # X2862; on 8/9/96 changed - Serial# D3289
P63 Piezoprobe with Kulite Pressure Transducer Serial # X2863
P790 Standard Piezocone #790
P881 Standard Piezocone, #881
MIT MIT Piezocone

Table 4.8 Summary of Device Calibration Factors.

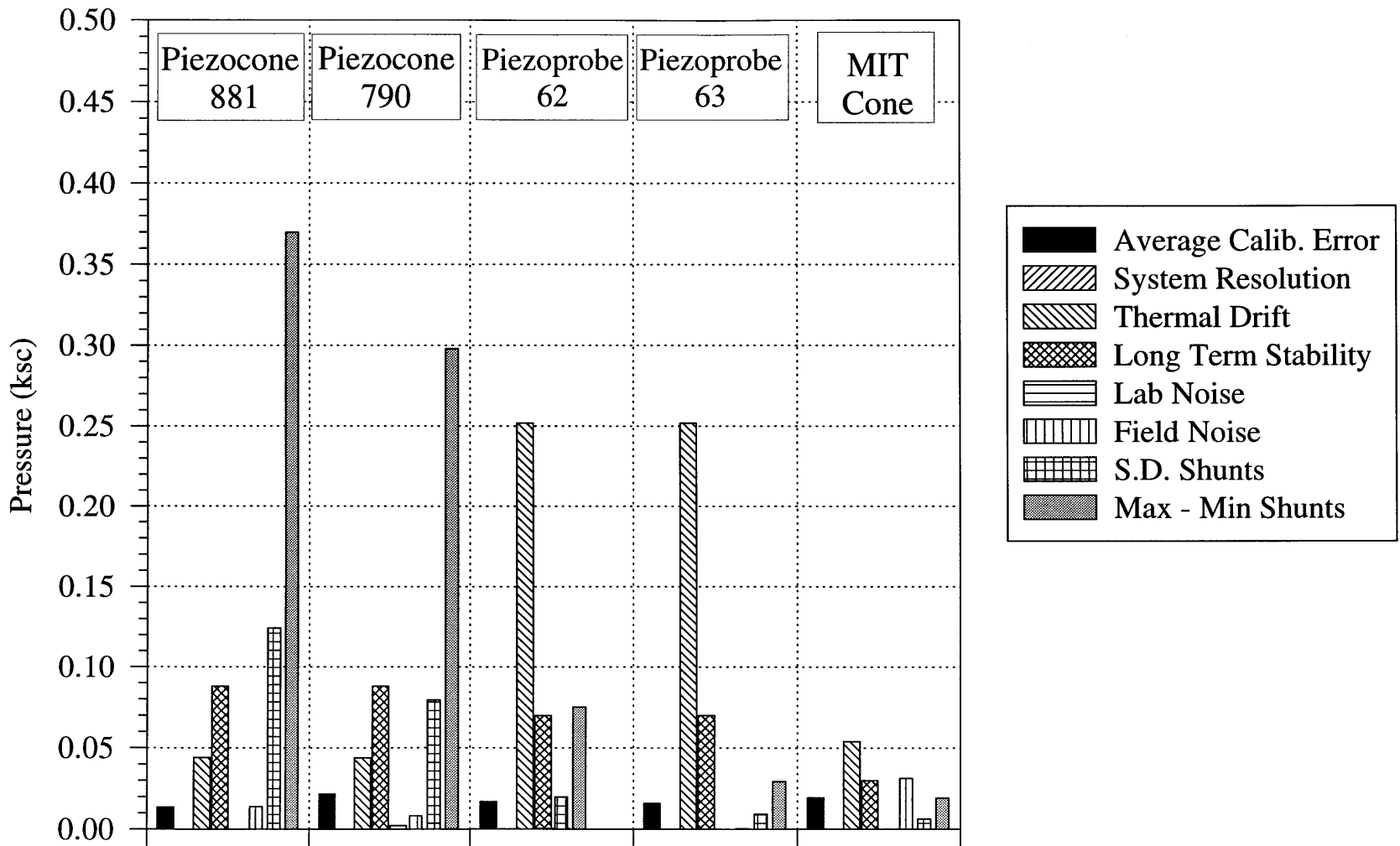


Figure 4.1 Summary of Electrical Noise Components for Pore Pressure Measurements of Each Device (After Varney et al., 1997).

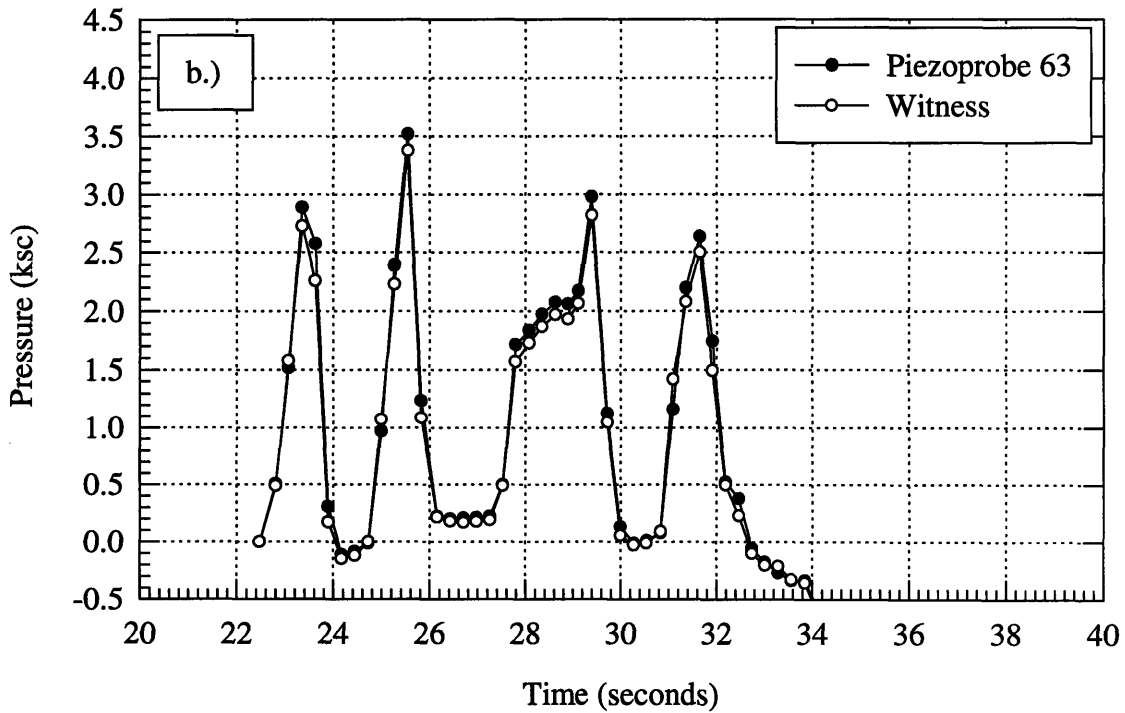
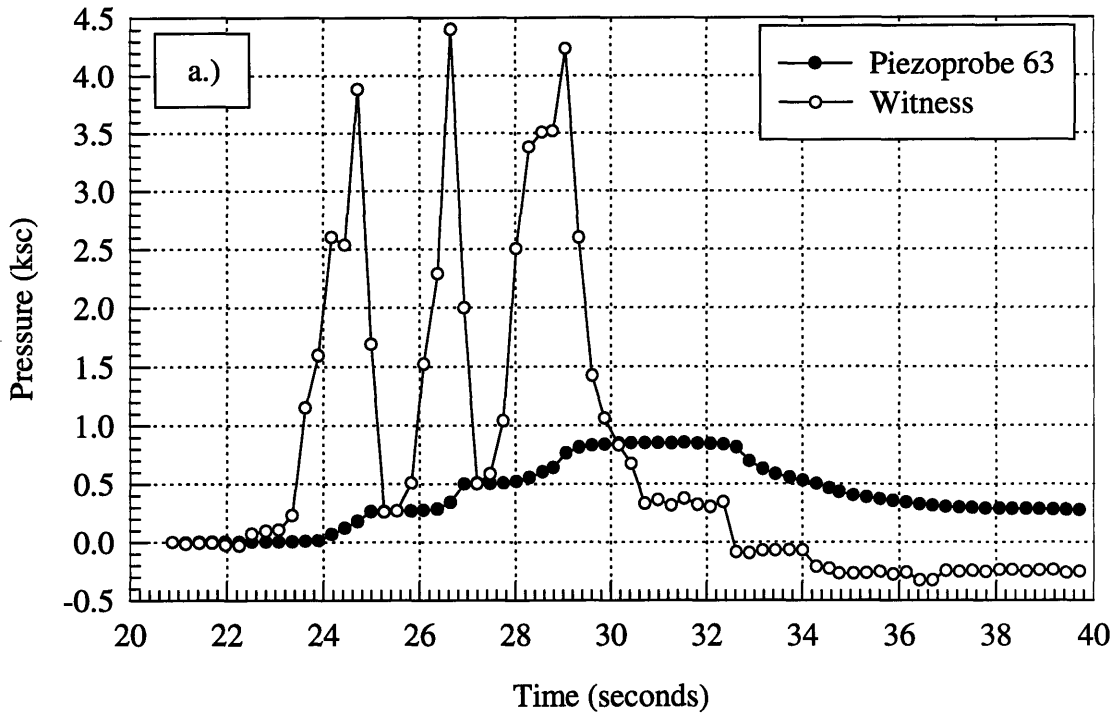


Figure 4.2 Example of a.) a Poor Response after Cavitation of the Porous Element and b.) of a Satisfactory Response with a Porous Element Saturated with Water (After

5. FIELD DATA

This chapter presents the field data and is divided into three main sections: 1) piezometer measurements of in situ pore pressures; 2) penetration measurements; and 3) dissipation records for each of the five penetrometers. Further interpretation of these data is given in Chapter 7.

5.1 Piezometers

Three piezometers were used to measure the in situ pore pressures. (cf. Section 4.1). All three devices were monitored at intervals of 1 to 2 days throughout the test program. Continuous records were obtained for each device for selected time periods, typically one to two weeks, by connecting a pressure transducer to the piezometer.

5.1.1 Determination of Equilibrium Pore Pressures

Figure 5.1 and Table 5.1 summarize the manual readings of piezometric head (relative to the National Geodetic Vertical Datum (NGVD))¹ for the three piezometers. These results demonstrate the time required for equilibration and also determine the value of in situ pore pressure.

M206A, installed in the sand layer at a depth of 5.33 meters (El. -3.55 m), measures an average piezometric head (H) = 0.52 meters, indicating an hydraulic head (H_p) = 4.07 meters (0.41 ksc). The piezometer was equilibrated by the first reading (elapsed time of 2 days).

M206B, installed in the middle of the clay at a depth of 25.91 (El. -24.1 m) measured H = 0.94 meters, indicating H_p = 25.04 meters (2.50 ksc). M206B required an elapsed time of 8 days to reach equilibrium.

M206C, installed at the clay/till interface at a depth of 42.52 (El. -40.68 m) measured H = 1.50 meters, indicating H_p = 42.18 meters (4.22 ksc). M206C also required an elapsed time of 8 days to reach equilibrium.

¹ All elevations are quoted with respect to the NGVD.
NGVD(m) = [Mean Lower Low Water, MLLW] - 1.49

These results can be interpreted by assuming a linear variation of the pressure head:

$$H_p = \frac{u_0}{\gamma_w} = 0.3938 - 1.0262y \quad \text{Equation 5.1}$$

where H_p is hydraulic head in meters, u_0 is the in situ pore pressure, and y is elevation (NGVD) in meters [$-41.0 \text{ m} \leq y \leq 0.4 \text{ m}$]. The goodness of fit coefficient, R^2 , is 0.99999.

Continuous electronic readings of pore pressure were obtained by inserting a 1/4" open ended tube saturated with water and attached to a pressure transducer into the piezometer standpipe. The transducer readings were used to determine the response time and tidal pressure fluctuations on the piezometers. Figure 5.2a through c show the response curves for the three piezometers.

Data obtained for M206A confirmed that the piezometer had nearly instantaneous response. Measurements of the piezometric head made over a period of several days showed that there was a definite variation in pore pressures which correlated with tidal cycles. However, the difference between average high and low tides during the monitoring period was 2.92 m. while the fluctuation measured by M206A in the sand layer was only 0.63 (Figure 5.2a). Apart from the magnitude of the pressure changes, the shape of the pressure cycle in the sand also differs from a typical tidal curve. The high tide portion of the curve in sand follows a parabolic pattern similar to the height versus time curve for open sea tides, but is lower than the tidal elevation. The low tide portion, however, is truncated at approximately $H = 0.46 \text{ m}$. This may reflect partial drainage of the peat into the ditch. (The bottom of the ditch is at El. 0.30 m)

The average water level within the sand layer was determined by extrapolating the electronic continuous readings to determine the water level fluctuation that would occur if the truncated portion of the curve did not exist. This would indicate a total fluctuation of $\Delta H = 0.91 \text{ meters}$ as opposed to the measured range $\Delta H = 0.63 \text{ m}$. By doing this and taking half the fluctuation, a time averaged water level of 0.52 m is estimated. It should be noted that this value is equal to the average from the manual readings. However, this

result is purely coincidental and caused by taking the manual readings at various times during the tidal cycle.

It is possible that the mean sea level over the duration of the field program is different from that occurring during the continuous measurement period. Therefore, the tide charts were used to determine the average high tide elevation (1.63 m) and the average low tide elevation (-1.49 m) on the test days from July 22nd to August 31st. The mean sea level during the field program was effectively the same as the mean sea level during the continuous monitoring period (El. 0.10 m). Therefore, the average water elevation for the M206A measuring point is accurately 0.52 meters.

In the upper clay layer, the response time of M206B (El. -24.1 m) was very slow. Figure 5.2b shows a response test in which the transducer required more than 4 days to recover from a 1.2 m imposed head difference. Therefore, the equilibrium value was taken from the long term manual readings and is assumed to be uninfluenced by the tide.

The deepest piezometer (M206C; El. -40.68 m) was located at the clay/till interface. As shown by Figure 5.2c, the response time is approximately the same as for the upper clay layer. However, the response time is still much slower than the tide cycle and again the pressure is assumed to be constant. The final profile of equilibrium pore pressure is plotted in Figure 5.3 using the above equation.

5.2 Penetration Results

Piezocones are typically used to determine both lateral and vertical spatial variability in soil deposits. Two types of penetration measurement were performed as part of this field program. A continuous profile was performed with Piezocone 790 at the beginning of the field program. The continuous profile provides a comparison point to the continuous profile obtained by Morrison (1984). In addition, each of the five devices recorded penetration measurements when installing the device at each depth. These data, referred to as “piecewise” data, are used to compare to the continuous profile.

5.2.1 Continuous Piezocone Profile

Piezocone P790 was pushed in 1.5 meter increments from a depth of 7.6 to 42.7 m. in the initial portion of the program in order to provide a continuous profile of pore pressure, cone resistance, and skin friction versus depth. Figure 5.4 presents the pore

pressure (u), corrected tip resistance (q_t) and sleeve friction (f_s), measured by piezocone 790, along with the piezometer measurement of the equilibrium pore pressure (u_o), and the total vertical stress (σ_{vo}). The soil profile as determined by Morrison (1984) is included on the right hand side of the figure.

Data from one 1.5 meter interval were lost due to a computer problem. The tip resistance has been corrected for the pore pressure using a correction factor of 0.286 determined during laboratory calibrations. The corrected tip resistance (q_t) is:

$$q_t = q_c + 0.286 \cdot u \quad \text{Equation 5.2}$$

where q_c is the measured tip (cone) resistance and u is the penetration pore pressure measured at the base of the cone.

Both the pore pressure and tip resistance increase with depth. The tip resistance follows the same trend as the pore pressure profile but with an offset of about 4 ksc above El. -19.24 m and 3 ksc below El. -19.24 m. The skin friction is generally in the range of 0.25 to 0.5 ksc with no trend with depth.

Above El. -8.27 m, both the pore pressure and tip resistance are highly variable, indicating layers of sand and clay. From El -8.27 to -11.32 m, u increases linearly with minor variability while q_t is constant with moderate variability. From El. -11.32 to -17.72 m, the pore pressure and tip resistance are shifted to higher values and increase with depth. Unfortunately, continuous profile data from El. -17.11 to -18.63 m were lost due to a computer problem. However, the profile shows less variation from El. -17.72 to -20.77 m and the soil is believed to be much softer than the surrounding layers, as judged by the fact that this portion of the hole collapsed during installations of the devices. The interval from El. -19.24 to -22.29 m shows a decrease in tip resistance with generally constant pore pressure. Below El. -22.29 m, the pore pressure and tip resistance increase linearly with depth. The pore pressure profile shows that the tip resistance increases more over this depth range than the pore pressure. Both extrapolate to 0 at the ground surface, suggesting a constant ratio between pore pressure and tip resistance. Within this lower layer, there are two major sand layers (El. -29.30 and -31.13 m) as well as a few layers in which both pore pressure and tip resistance decrease.

Figure 5.5 presents the continuous piezocone profile of tip resistance (q_c) determined by Morrison (1984). These values are uncorrected for the pore pressure factor and therefore present numbers less than the corrected values presented above. For comparison purposes, the uncorrected tip resistance values determined with Piezocone 790 for the 1996 piezocone profile are presented in Figure 5.6². The trends in the q_c profiles are identical. However, the values of q_c for the continuous penetration data obtained during the 1996 field program are higher by 1 ksc throughout the profile. This difference may be the result of a zero voltage offset in one of the devices since the difference is throughout the profile and the magnitude represents a small fraction of the 5 ton capacity of the device.

Figure 5.7 presents the penetration pore pressure profile obtained by Morrison for comparison with the pore pressure profile determined from the 1996 field program. The values of u are equivalent from El. -16 to -22 m. However, in the 1996 profile, values of u at elevations below and above this range are less than Morrison's profile by a value linearly increasing to 2 ksc at El. -40.5 m. The equilibrium pore pressure distributions determined by piezometers are identical for the two field programs. The pore pressure measurement location for the piezocone used to determine Morrison's profile is at the tip, while the profile for the 1996 field program was determined with a piezocone measuring the pore pressure at the base of the shaft. The pore pressure measured at the base of the shaft has been shown to measure lower pore pressures than the pore pressure measured at the tip location. (e.g. Aubeny, 1992; Nyirenda, 1989) Therefore, the values for the penetration pore pressure for the 1996 program are expected to be less than those measured for the 1984 field program due to the different pore pressure measurement locations. The reason for equivalent pore pressures in the range of El. -16 to -22 m is assumed to be a result of the soft clay layer.

5.2.2 Piecewise Penetration

Figure 5.8 through Figure 5.10 compare the continuous pressures with piecewise data obtained during installation of each device for dissipation measurements. These data

² Morrison's profile is determined with a 60° piezocone with pore pressure measured at the tip. The 1996 field program used Piezocone 790, a 60° piezocone with pore pressure measured at the base of the shaft.

are presented in Figure 5.8 for the piezocones, Figure 5.9 for the piezoprobes; and the in Figure 5.10 for the MIT Piezocone. Piecewise pore pressures for all three piezocones are equal to or slightly greater than those developed for continuous penetration. It should be noted that piecewise penetration generates consistently higher pore pressure in the lower clay. The cause of this is unknown. The piezoprobes consistently develop less pore pressure than continuous and piecewise penetration of the piezocones. This behavior is expected due to the tapered geometry and smaller diameter. The probes generate approximately 80 to 85 % of the pore pressures generated by the piezocones.

The MIT cone typically develops penetration pore pressures of the same magnitude as the standard piezocones and shows the same trend as the previous piezocone profile (Morrison, 1984) which was also measured with tip pore pressure. However, the MIT cone measures a relatively large decrease in pressure when penetration stops. This dynamic effect is a result of the MIT piezocone measuring pore pressure at the tip of the cone, making it more sensitive to changes in axial load.

5.3 Dissipation Results

Appendix A includes the individual dissipation plots as pore pressure versus dissipation time. These data are utilized for the subsequent interpretation in Chapter 7. The dissipation data for the five penetrometers are presented at each test depth in Figure 5.11 through Figure 5.20. Data are available for elevations between -12 and -33 meters (depths ranging from 45 ft to 115 ft). The top figure (a) presents the results in terms of pore pressure vs. time on a logarithmic scale. Zero time was determined from the end of penetration as indicated by the depth locator box measurements. The bottom figure (b) presents the normalized pore pressure during dissipation versus time on a log scale for the same measurements. The normalized pore pressure is calculated as the increment in excess pore pressure above the equilibrium pore pressure (taken from the piezometer data) divided by the increment between the installation excess pore pressure and the equilibrium value (i.e. $(u-u_o)/(u_i-u_o)$). The installation pore pressure is selected as the value at the end of continuous penetration, as determined by the depth locator box measurements. A minor amount of filtering has been used to eliminate jumps in the data

that are obviously not reflective of the behavior of the soil, but a result of electrical interference.

The dissipation plots of normalized pore pressure versus time on a logarithmic scale display certain characteristics specific to the type of device used to make the measurement. These characteristics change slightly with the soil characteristics, as described in Chapter 2. The piezocones are characterized by a continuously decreasing normalized pore pressure with time. The piezoprobe dissipation plots are characterized by a steeper slope than the piezocone, and display a “brake point” in which the rate of change of the dissipated pore pressure ratio decreases dramatically, approaching the rate of the piezocone. The “brake point” occurs at dissipated pore pressure ratios ranging between 10 and 20%. The dissipation plot for the MIT Piezocone displays a slope between that of the piezoprobes and the piezocones.

The first four figures (Figure 5.11, Figure 5.12, Figure 5.13, and Figure 5.14) present data for the Upper Clay Layer C. The rate of change of the dissipated pore pressure ratio for the piezocones varies in this layer. The only duplicate measurement at the same installation elevation in Upper Clay Layer C is at El. -12 m with Piezocone 790 and Piezocone 881. The piezocone installation pore pressure ranges from 5 to 6.5 ksc for the tests at El. -12 to -16 m. For the two successful tests using the piezoprobe (Piezoprobe 63) in this range, the installation pore pressure changes from 4 to approximately 6 ksc. The “brake point” occurs at a dissipated pore pressure ratio of 10% in the test at El. -13 m and at 15% for the test at El. -15 m.

The remaining figures (Figure 5.15 through Figure 5.20) present data in the Lower Clay Layers D and E. Layer D (El. -18 to -21 m, 60 to 75 ft) is somewhat more layered according to the continuous penetration measurements. In general, the value of the installation pore pressure increases with depth for all five devices.

The piezocone measurements are consistent and independent of depth for both Layers D and E. All of the curves decrease monotonically from the end of penetration and display similar rates of change of the dissipated pore pressure ratio.

The tapered probes are consistent between each other in the lower clay but show considerable variability in the shape of the curves between successive tests. For

Piezoprobe 63, the “brake point” occurs at 13 to 15%, while for Piezoprobe 62, this occurs at 17 to 20%. At large times the two sets of curves tend to converge showing that the probes do not reach equilibrium conditions any faster than the cones. Three of the four normalized dissipation plots for the piezoprobe tests in the softer Layer D show an increase in pressure after the “brake point” in the curve.

The MIT Piezocone cone is less consistent than the piezocones and the shapes of the curves do change in the early portions of dissipation.

Figure 5.21 through Figure 5.25 present the normalized dissipation curves for all measurements made with a device. The plots generally include measurements at 10 foot increments from El. -11.5 m to -33.0 m. This perspective provides evaluation of the individual devices and on the variation throughout the deposit.

The Piezocones (Figure 5.21 and Figure 5.22) yield similar results with the exception that P881 is definitely more noisy, seen mostly at large times. The results show that there is a decrease in the rate of dissipation between the upper and lower soils. The layering in Zone C is described by Morrison (1984) as having continuous and discontinuous silt seams and occasional large stones. The rates of dissipation are more variable in this layer and do not follow a consistent pattern with depth. The shapes of the curves, especially P881 at El. -11.8 m and El. -13.4 m (depth 45 and 50 ft), have unusual shapes which may be the layering effect. At El. -11.8 m, the normalized dissipation curve for Piezocone 881 lies beneath the curves for the lower deposit, but is parallel to these curves. The normalized dissipation curve at El. -13.4 m is initially slower to dissipate than the dissipation curves for the lower deposit, but crosses the set of curves within an elapsed time of 800 seconds. At El. -17.9 m and below, the data all plot within a very narrow band showing that the clay is uniform and the piezocones perform very consistently.

The tapered probes (Figure 5.23 and Figure 5.24) also produced similar results. In all cases below El. -17.9 m (depth 65 ft), the curves show a well defined “brake point” at 80 to 85 % dissipation. However, there is a small but definite difference at large times between the two devices. P62 has a less pronounced “brake point” which occurs at a higher normalized pressure and the pore pressures do not dissipate as completely. As

discussed in Chapter 4, this may be due to a zero offset. The level of noise is noticeably less than the piezocones. As with the piezocones, the results are inconsistent in the upper clay, Zone C. However, for the piezoprobes the variation in Upper Clay Layer C is much larger and the rate of dissipation is slower (not faster) than in the lower clay. The lower clay measurements are consistent between the two piezoprobes but have considerably more variation than the piezocones. This is assumed to be due to the smaller zone of influence around the probe which makes the results susceptible to smaller changes in soil layering. In this format, it is noticeable that the test at El. -27 m for Piezoprobe 62 is uncharacteristic in that the normalized dissipation ratio dips far below zero and then rises again. Therefore, this curve is not used as a comparison point for typical behavior, and is not included in subsequent calculations in Chapter 7.

The MIT Piezocone (Figure 5.25) shows the same basic trends as the piezoprobes. There are no measurements included for the MIT Piezocone in the Upper Clay Layer. The lower clay is very consistent and all plot in a narrow band with approximately the same level of noise as Piezocone 790.

5.3.1 Time for 50% Dissipation (t_{50})

The time to 50% dissipation (t_{50}) is defined as the time required to dissipate 50% of the increment from the installation pore pressure to the equilibrium pore pressure. This value varies between the 3 different geometries and between the measurements of a single cone. The first three measurements taken, (at El. -11.5, -13, and -14.5 m; depth 45, 50, and 55 ft) are within the upper region of the profile, which is a desiccated sandy clay, characterized by a higher value of preconsolidation pressure. The remaining measurements, from El. -18 to -33 m (65 to 115 ft depth) are within middle and lower clay zone. These results yield a tighter band of dissipation curves which can be used to characterize the differences between the three devices.

Table 5.2 presents the calculated times to 50% dissipation (t_{50}) for each device for each test. These are summarized in Figure 5.26a through e³. Piezoprobe 62 results are presented for El. -18.45 m and below. The measurement at El. -26.98 m is considered to

³ Note that the t_{50} scale for the piezoprobes is 0 to 200 seconds, while the range for the piezocones and the MIT Piezocone is 0 to 2000 seconds.

be atypical behavior and is therefore not included in the average and standard deviation of t_{50} values. The t_{50} value is 110 ± 41 seconds for Piezoprobe 62. In general, t_{50} tends to decrease with depth, or with decreasing OCR. The t_{50} value for Piezoprobe 63 over this range of measurements is 90 ± 10 seconds, and does not display a trend with depth. Therefore, the t_{50} value measured for Piezoprobe 63 has a lower average and a lower standard deviation over the same measurements. Piezoprobe 63 was also used at El. -13.3 and -14.82 m. Including the t_{50} values for these two tests increases the average and standard deviation to 102 ± 39 seconds.

The t_{50} values are much larger for the piezocones. For tests performed at El. -17 m and below the average and standard deviation for Piezocone 790 and Piezocone 881 is 1587 ± 215 and 1538 ± 159 seconds, respectively. Including the tests performed in the upper clay changes these values to 1426 ± 438 and 1451 ± 274 , respectively. In general, the t_{50} values tend to increase with decreasing OCR. The values between the two piezocones are more consistent with each other, relative to the range and difference between the piezoprobes.

The values of t_{50} for MIT Piezocone are available for tests elevations -17.79 m and below. The value is 646 ± 218 seconds, with a tendency to decrease slightly with depth.

The variation in t_{50} for the MIT Piezocone is similar in percent to that of the Piezoprobe 62, as the MIT Cone varies by 34% while the Piezoprobe 62 varies by 37%. Piezoprobe 63 varies by 10%, while Piezocone 790 and Piezocone 881 vary by 14% and 10% respectively. The piezocones were installed at opposite sides of the sand mat (approximately 30 feet apart) while the piezoprobes were installed in boreholes next to each other (approximate 10 feet apart). Piezoprobe 63 and Piezocone 790 vary by the same percentage across depth. This is significant as the 10% variation for the Piezoprobe involves a much smaller absolute difference in time (i.e. 41 versus 159 seconds).

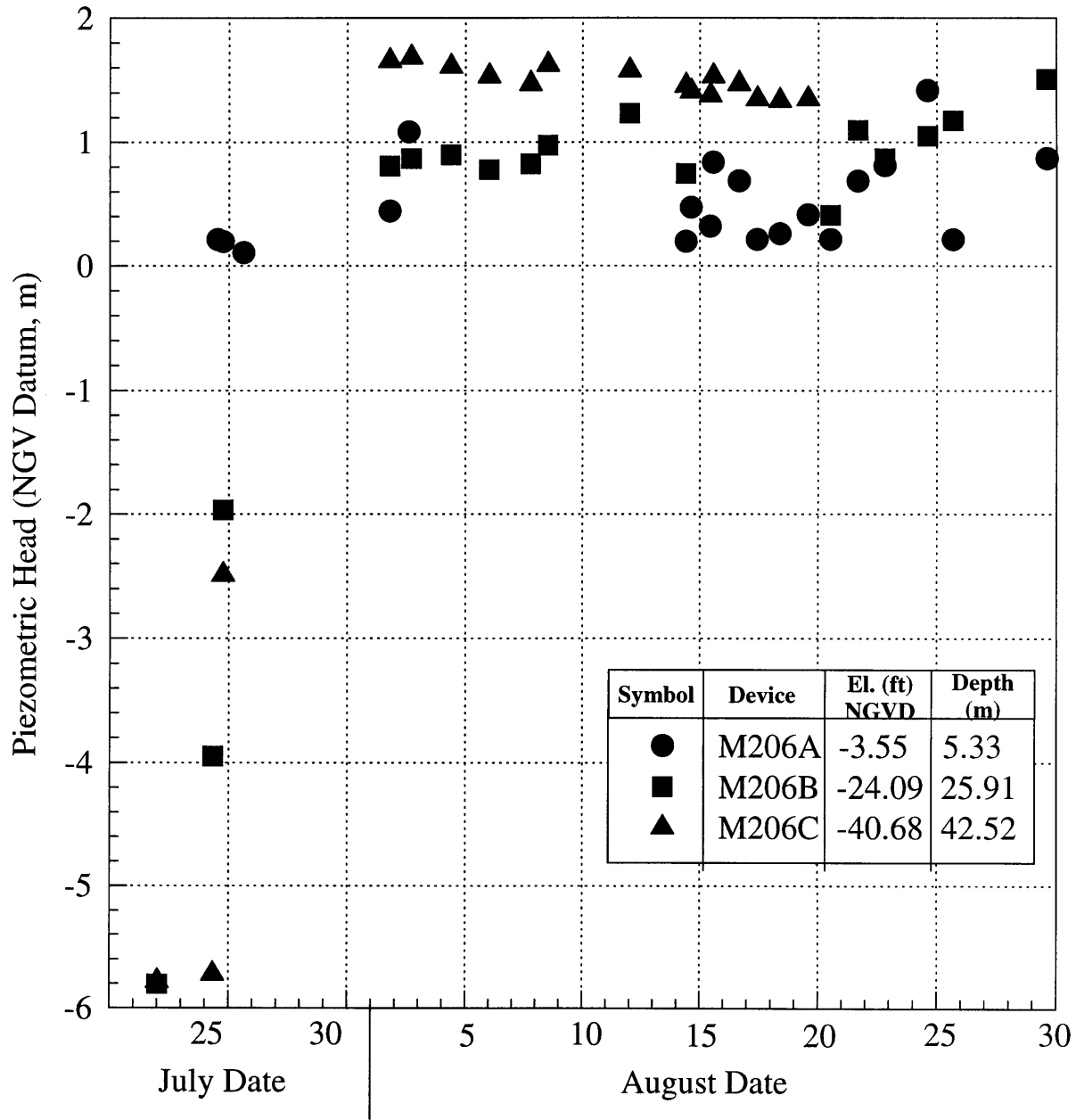
M206 Manual Readings			Depth in Meters			Elevation in Meters		
Date	Day	Time	M206A 5.33	M206B 25.91	M206C 42.52	M206A 1.78	M206B 1.81	M206C 1.84
7/22/96	1	pm		install	install			
7/23/96	2	am	install	>25	>25		-5.81	-5.78
7/25/96	4	8:00		5.76	7.56		-3.95	-5.72
7/25/96	4	12:40	1.57			0.21		
7/25/96	4	?	1.58	3.78	4.33	0.20	-1.97	-2.49
7/26/96	5	14:40	1.68			0.11		
8/1/96	11	19:00	1.34	1.01	0.18	0.44	0.81	1.66
8/2/96	12	14:15	0.70			1.08		
8/2/96	12	16:45		0.94	0.15		0.87	1.69
8/4/96	14	9:00		0.91	0.23		0.90	1.61
8/6/96	16	??		1.04	0.30		0.78	1.53
8/7/96	17	18:30		0.99	0.37		0.82	1.47
8/8/96	18	12:25		0.84	0.21		0.98	1.62
8/12/96	22	??		0.58	0.26		1.23	1.58
8/14/96	24	9:40	1.58	1.07	0.38	0.20	0.75	1.46
8/14/96	24	15:00	1.31		0.43	0.47		1.41
8/15/96	25	10:35	1.46		0.46	0.32		1.38
8/15/96	25	13:30	0.94		0.30	0.84		1.53
8/16/96	26	15:45	1.10		0.37	0.69		1.47
8/17/96	27	10:25	1.57		0.49	0.21		1.35
8/18/96	28	9:00	1.52		0.50	0.26		1.34
8/19/96	29	13:45	1.37		0.49	0.41		1.35
8/20/96	30	12:15	1.57	1.40		0.21	0.41	
8/21/96	31	16:05	1.10	0.72		0.69	1.10	
8/22/96	32	19:05	0.98	0.94		0.81	0.87	
8/24/96	34	14:35	0.37	0.76		1.42	1.05	
8/25/96	35	16:10	1.57	0.64		0.21	1.17	
8/29/96	39	14:30	0.91	0.30		0.87	1.51	

* Shaded values were not used to calculate average elevations due to the time required to equilibrate and the likely case that there was an error in determining the water level.

Table 5.1 Manual Piezometer Readings for M206A, M206B, and M206C.

Calculated t_{50} , Time for 50% Dissipation									
Piezoprobe 62		Piezoprobe 63		Piezocone 790		Piezocone 881		MIT Piezocone	
El. (m)	t_{50} (seconds)	El. (m)	t_{50} (seconds)	El. (m)	t_{50} (seconds)	El. (m)	t_{50} (seconds)	El. (m)	t_{50} (seconds)
				-11.62	593	-11.83	924		
		-13.30	85	-13.15	1835				
		-14.82	197	-14.67	891				
-18.45	178	-18.48	96	-17.72	1907	-17.93	1434	-17.79	866
-20.89	103	-20.92	98	-20.77	1607	-20.98	1470	-20.84	353
-23.94	114	-23.97	84	-23.81	1530	-24.02	1822	-23.89	885
-26.98	27	-27.02	94	-26.86	1513	-27.07	1606	-26.94	739
-30.03	80	-30.07	71	-29.91	1701	-30.12	1377	-29.99	561
-33.08	76	-33.11	94	-32.96	1261	-33.17	1521	-33.03	469

Table 5.2 Calculated Time for 50% Dissipation (t_{50}).



Notes:
 MLLW = Mean Lower Low Water
 NGVD = MLLW - 4.9 feet
 MLLW - 1.49 meters

Figure 5.1 Manual Piezometer Readings for M206A, M206B, and M206C over the Duration of the 1996 Field Program at Saugus (Station 246).

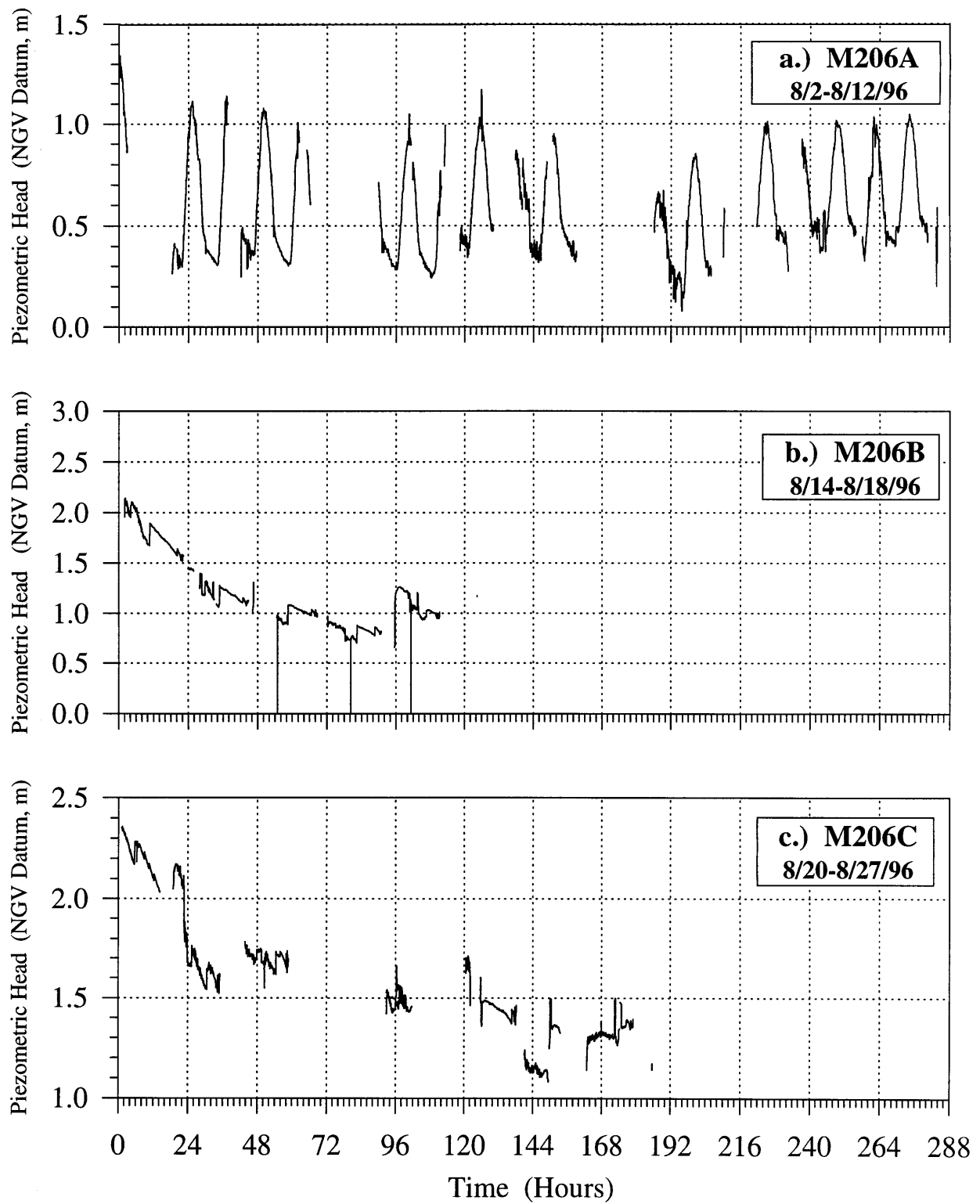


Figure 5.2 Response Curve for Piezometers: a.) M206A; b.) M206B; and c.) M206C.

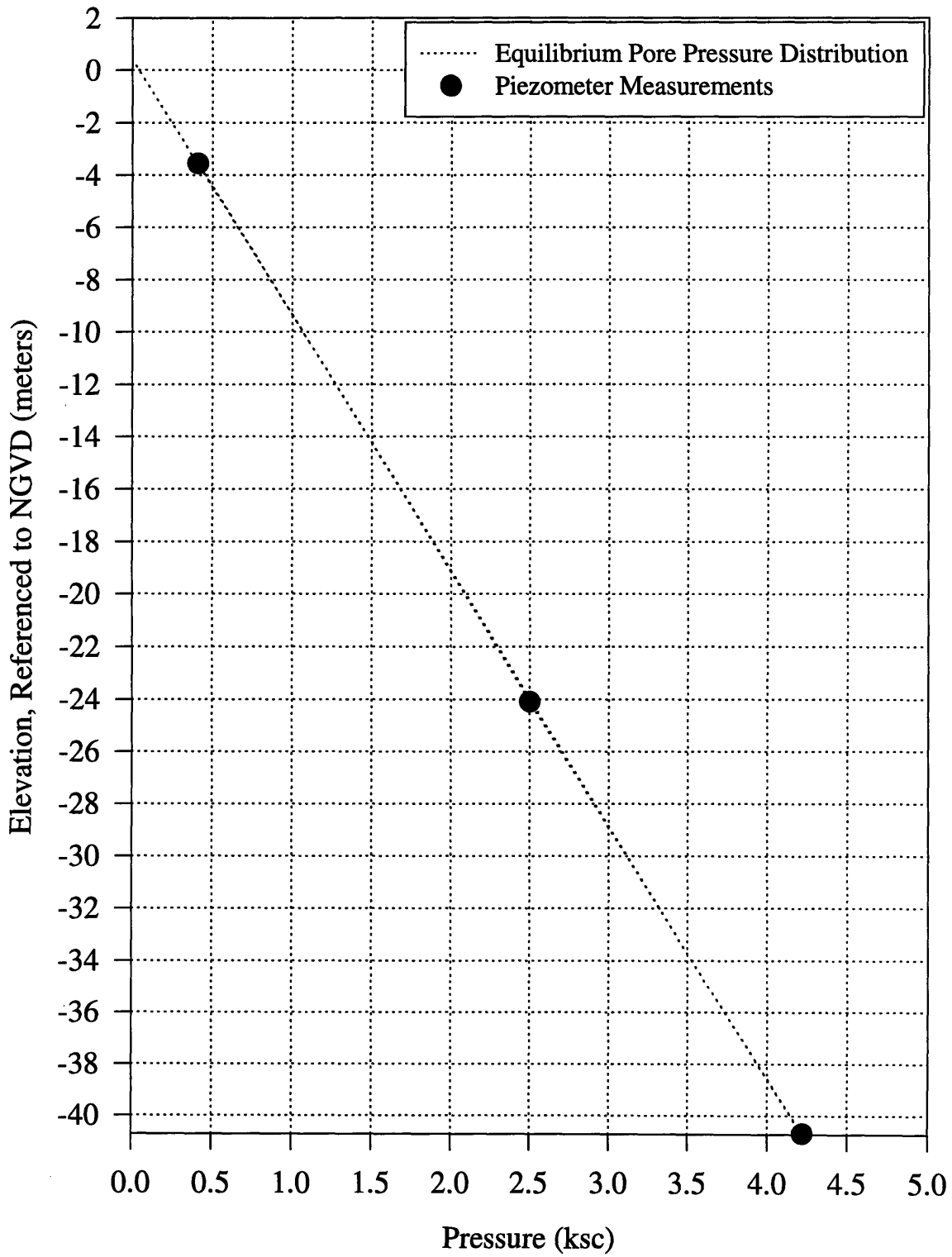


Figure 5.3 Equilibrium Pore Pressure Profile at Saugus (Station 246) Determined from Piezometers.

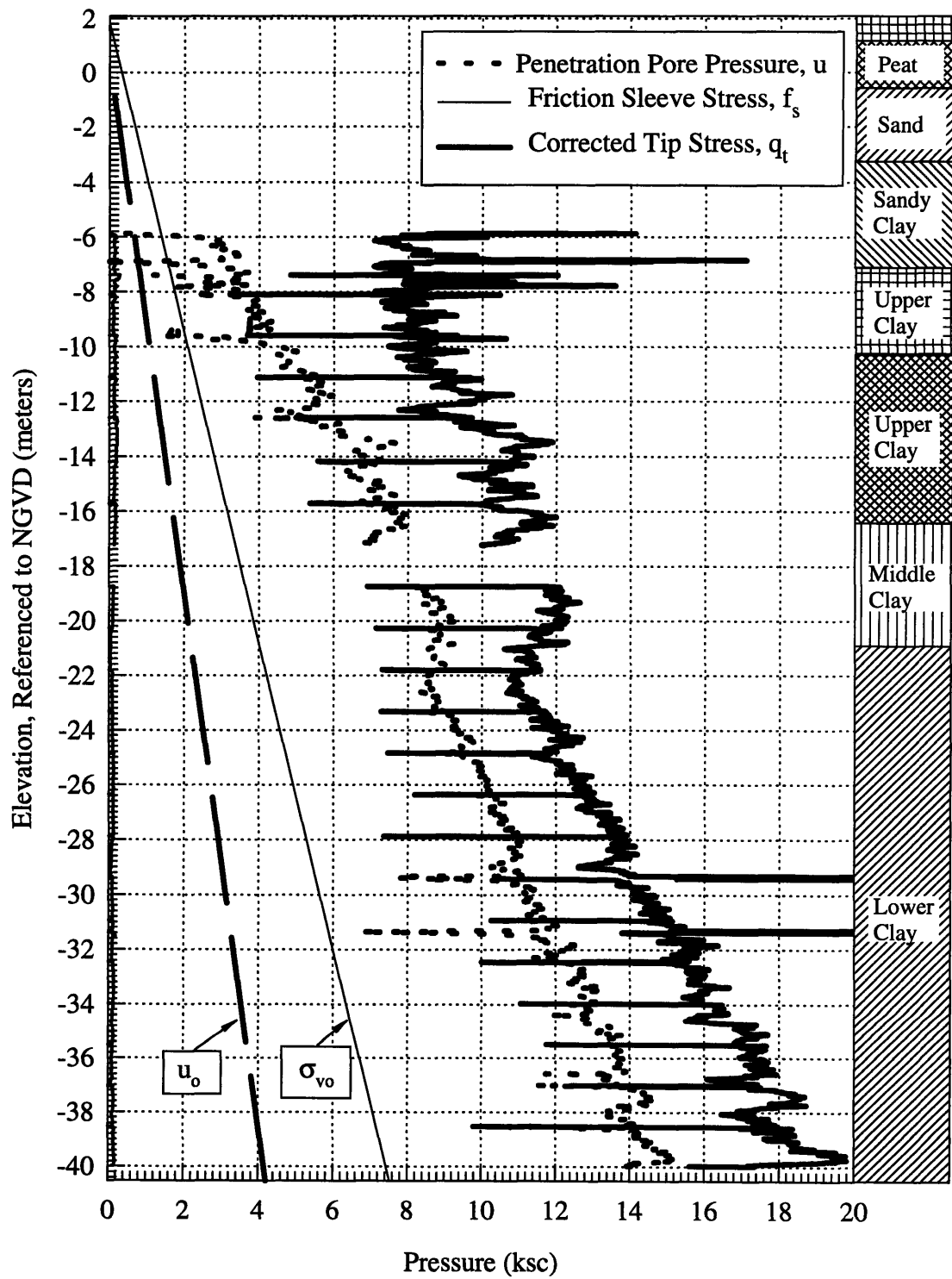


Figure 5.4 Pore Pressure, Corrected Tip Resistance and Sleeve Friction during Continuous Penetration with Piezocone 790 at Saugus (Station 246).

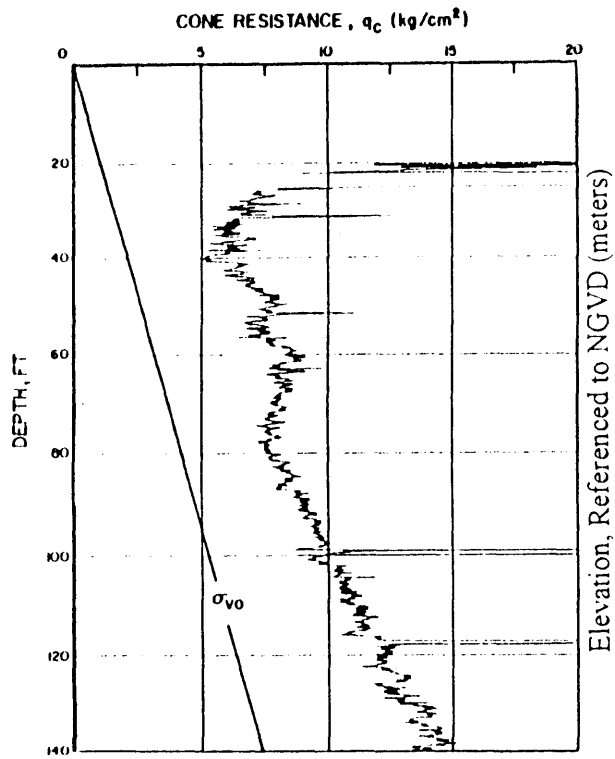


Figure 5.5 Uncorrected Tip Resistance Profile Using 60° Piezocone with Pore Pressure Measured At The Tip During 1982 Field Program. (After Morrison, 1984)

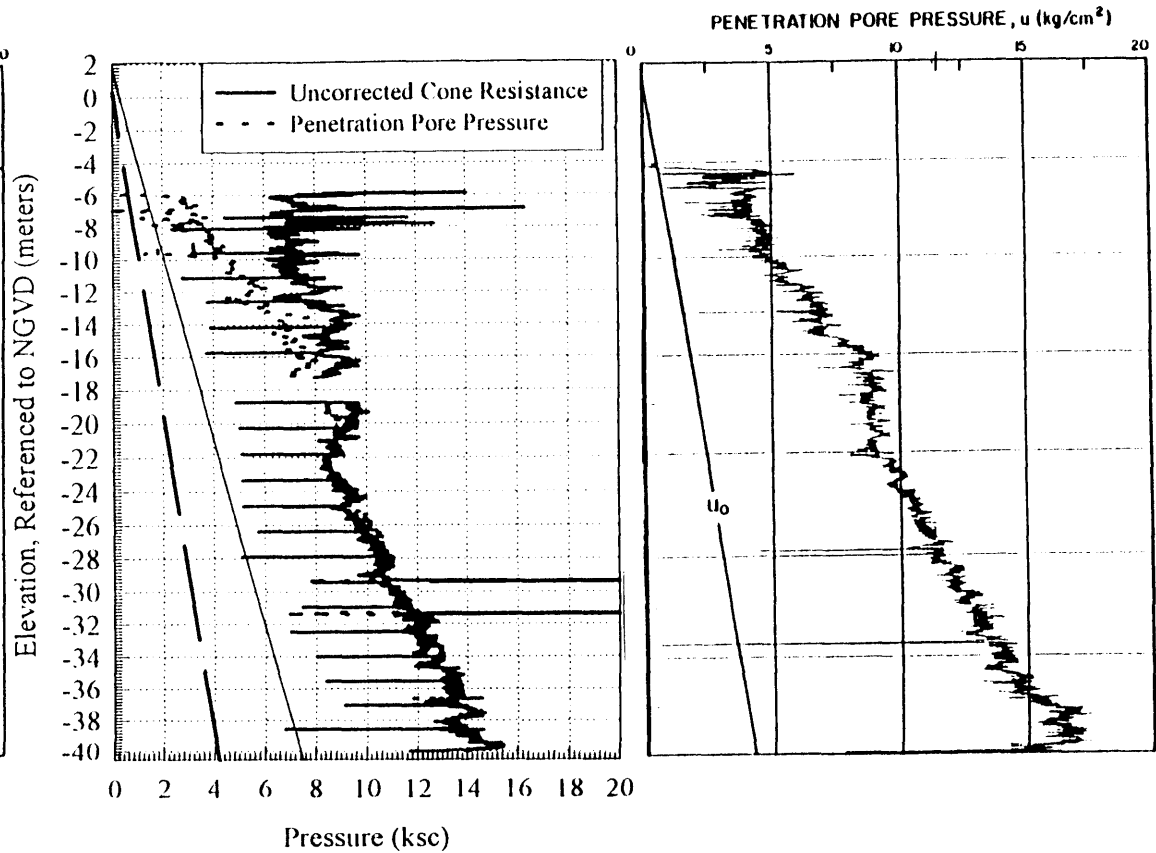


Figure 5.6 Pore Pressure and Uncorrected Tip Resistance Profile Using 60° Piezocone With Pore Pressure Measured At The Base Of The Shaft During 1996 Field Program.

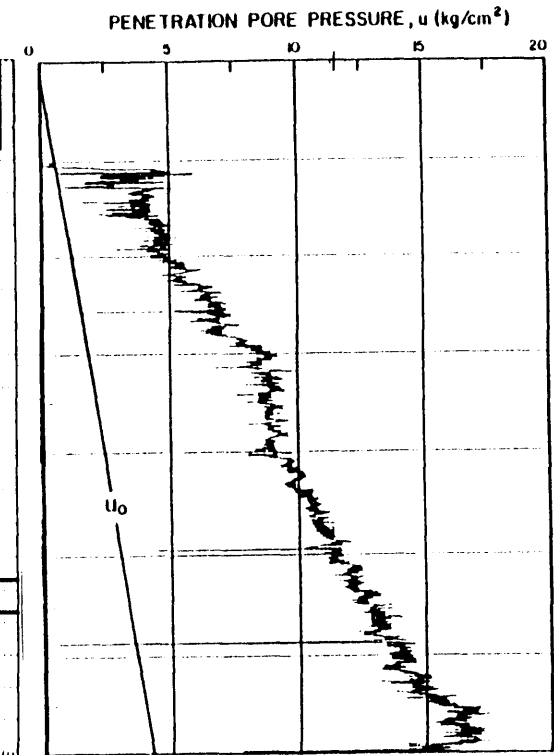


Figure 5.7 Pore Pressure Profile Using 60° Piezocone With Pore Pressure Measured At The Tip During 1982 Field Program. (After Morrison, 1984)

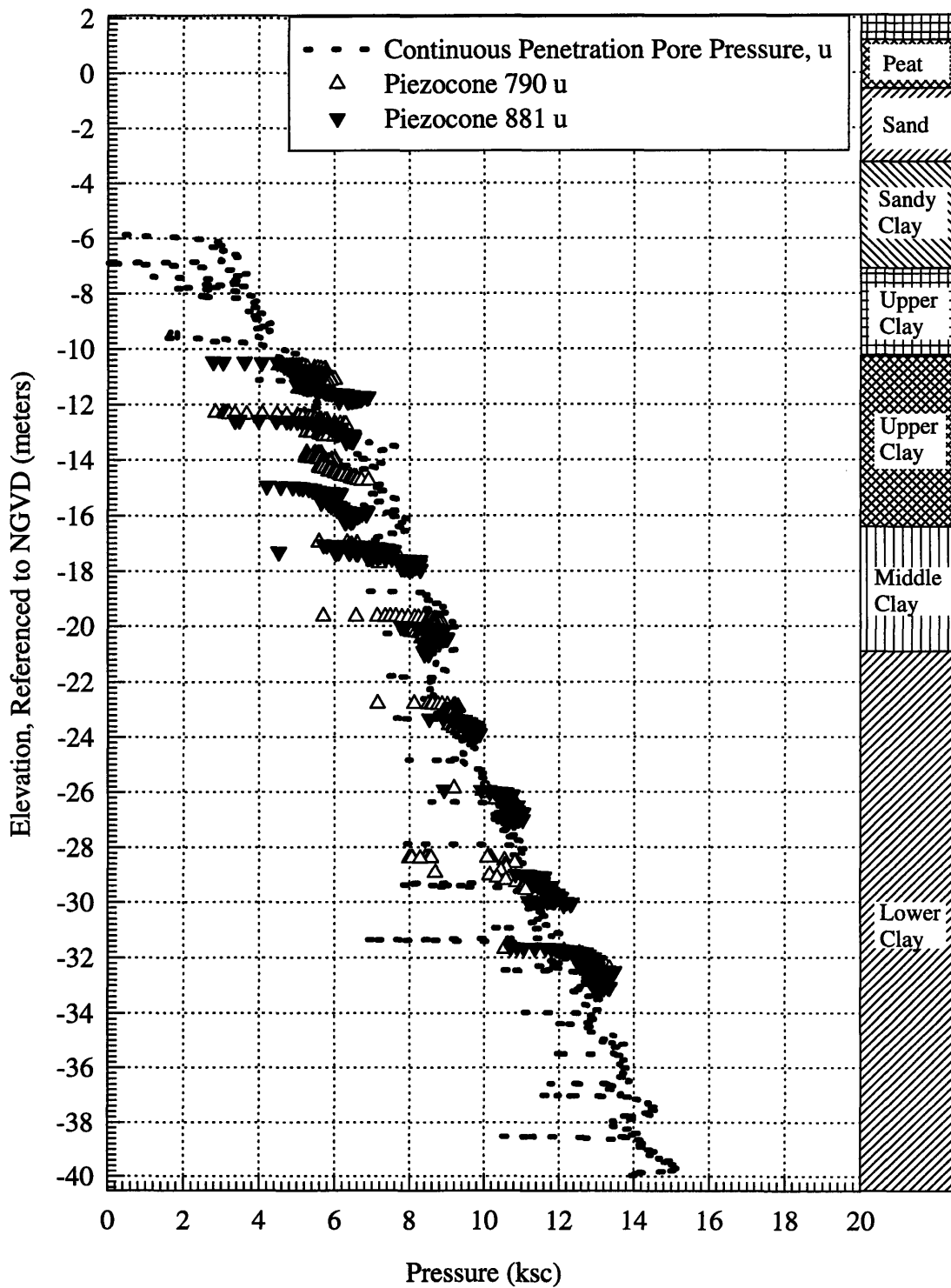


Figure 5.8 Comparison of Piecwise Penetration Pore Pressure with Standard Piezocones to Continuous Penetration Pore Pressure with Piezocone 790.

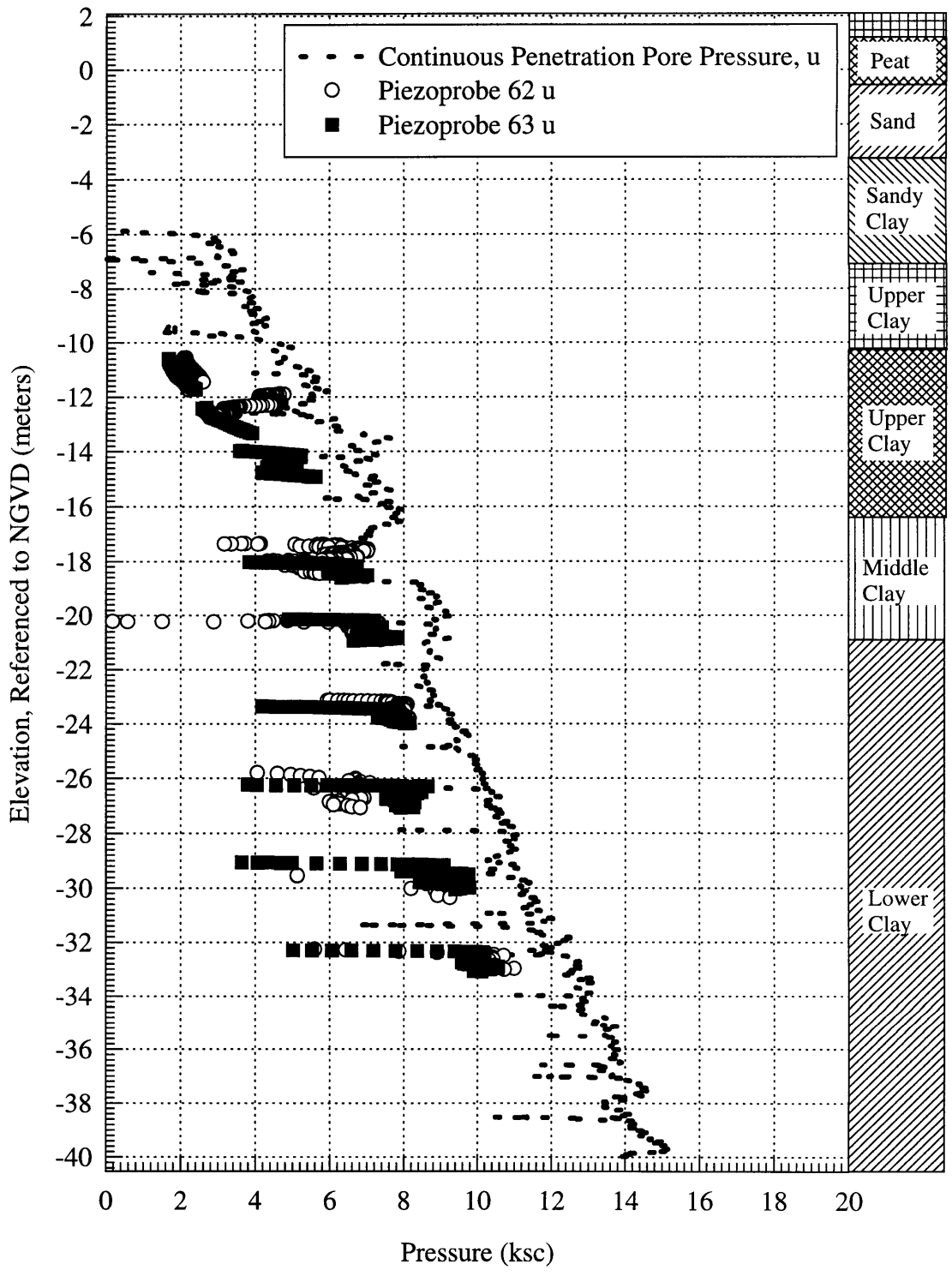


Figure 5.9 Comparison of Piecewise Penetration Pore Pressure with Tapered Piezoprobes to Continuous Penetration Pore Pressure with Piezocone 790.

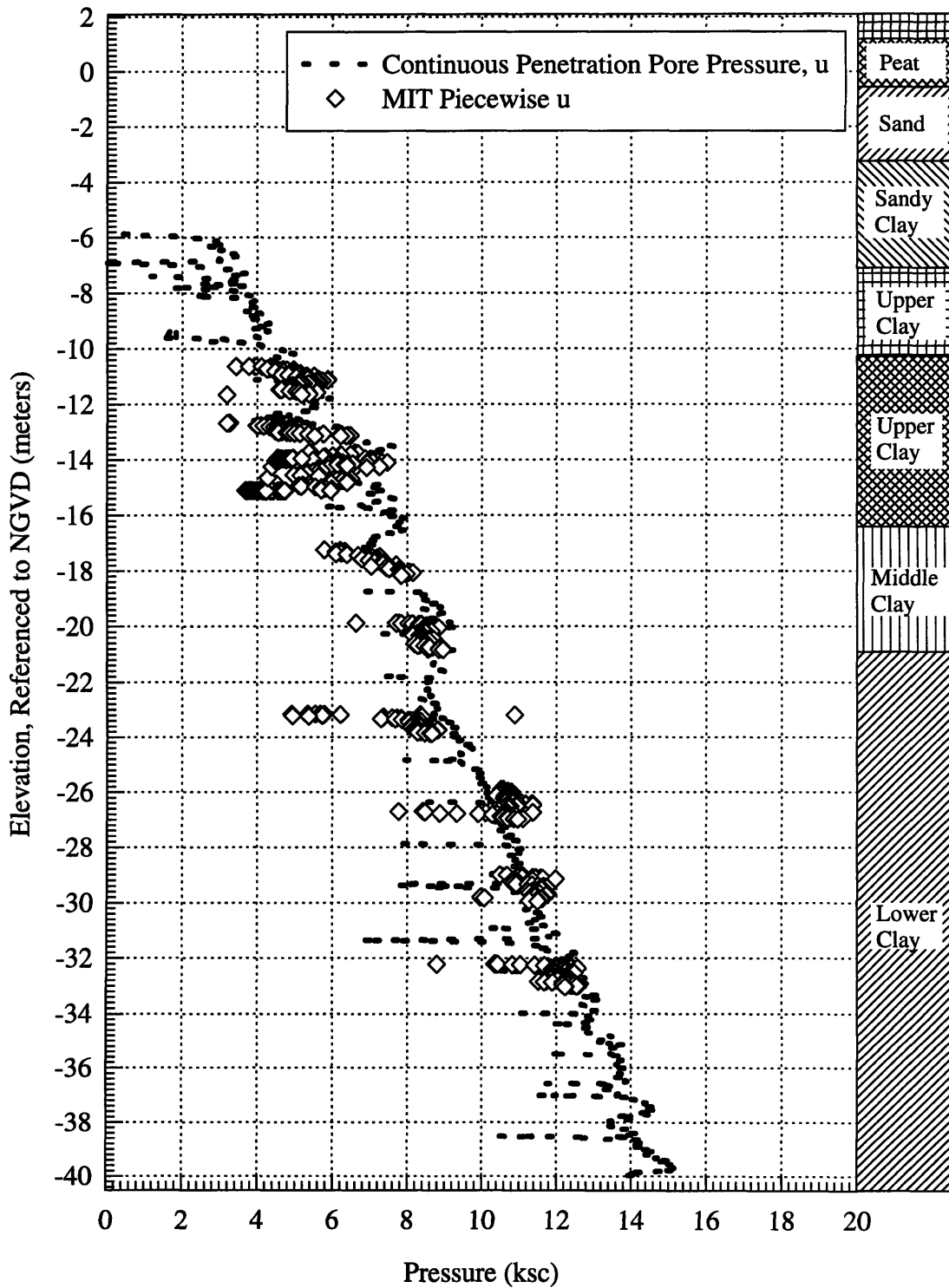


Figure 5.10 Comparison of Piecewise Penetration Pore Pressure with the MIT Piezocone to Continuous Penetration Pore Pressure with Piezocone 790.

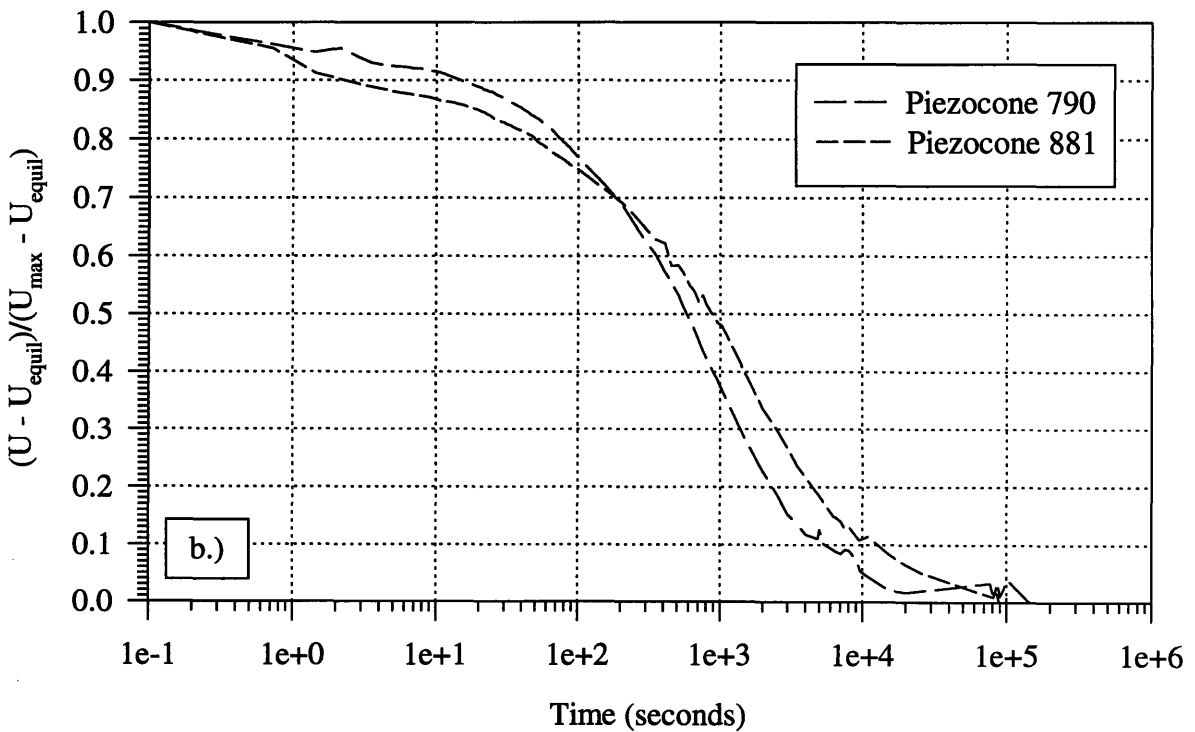
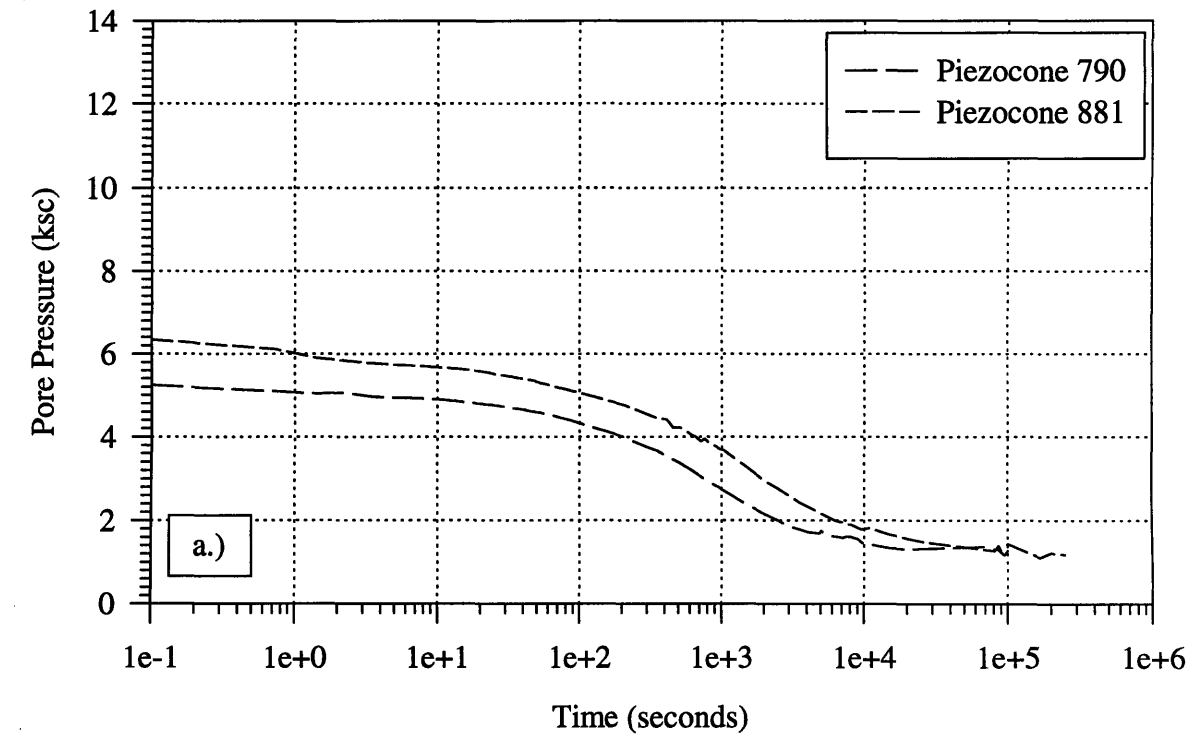


Figure 5.11 Dissipation Results for Piezocone 790 and Piezocone 881 at El. -12 m (45 ft. Depth).

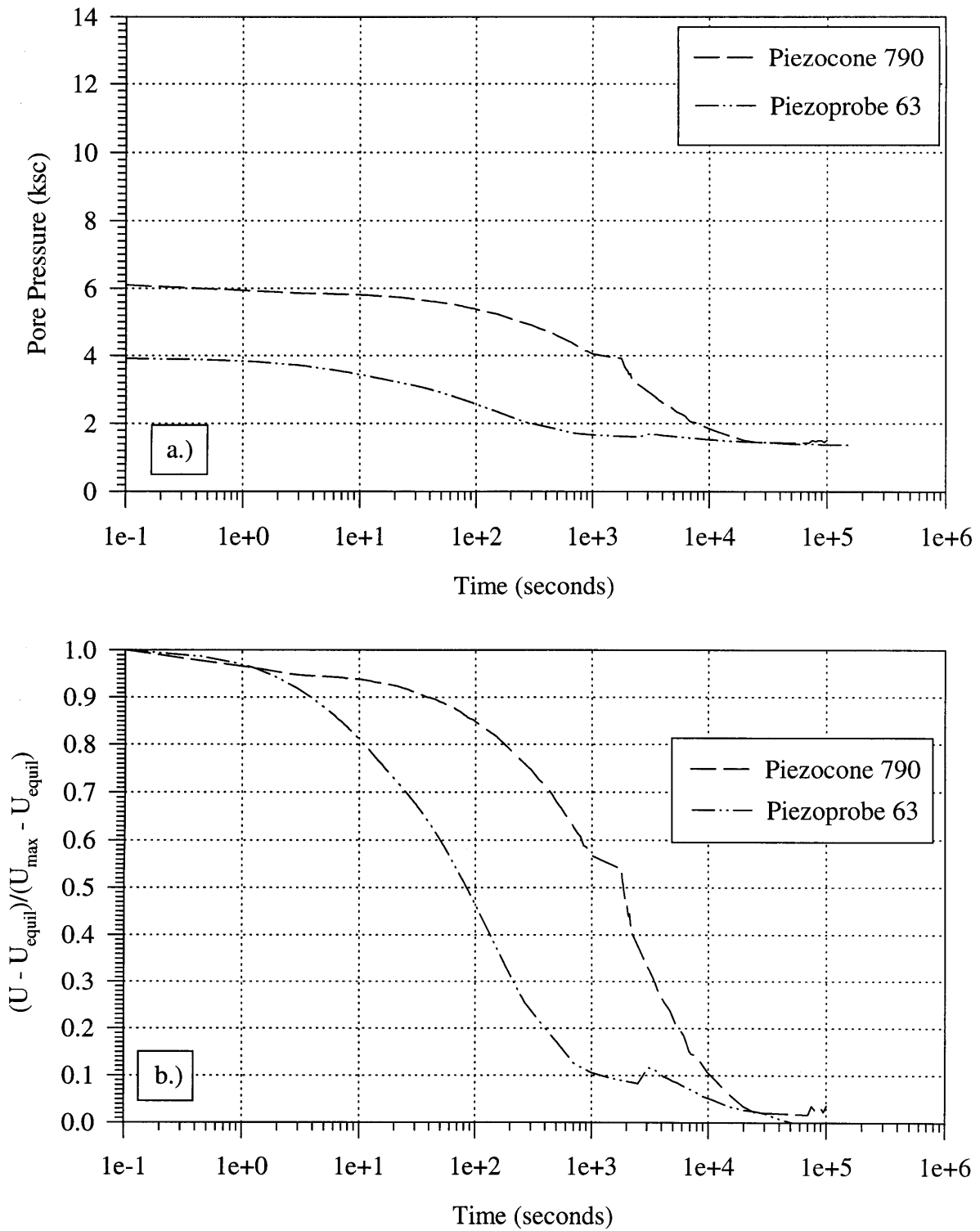


Figure 5.12 Dissipation Results for Piezocone 790 and Piezoprobe 63 at El. -13 m (50 ft. Depth).

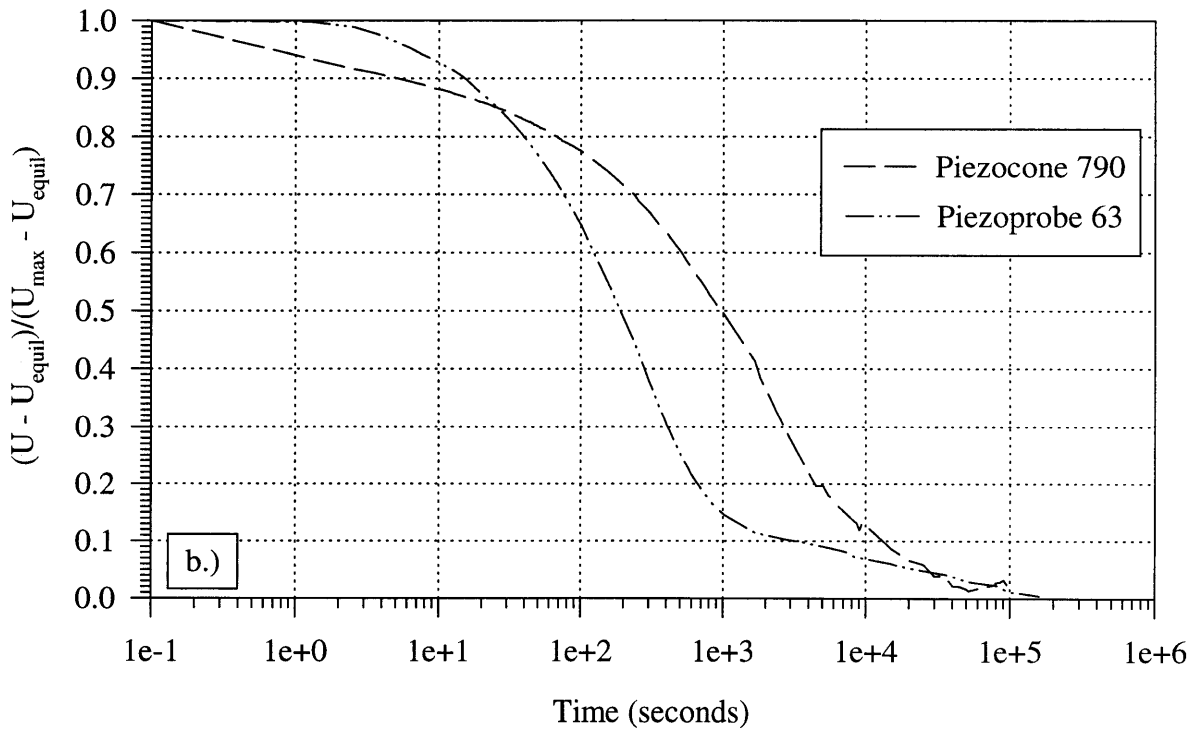
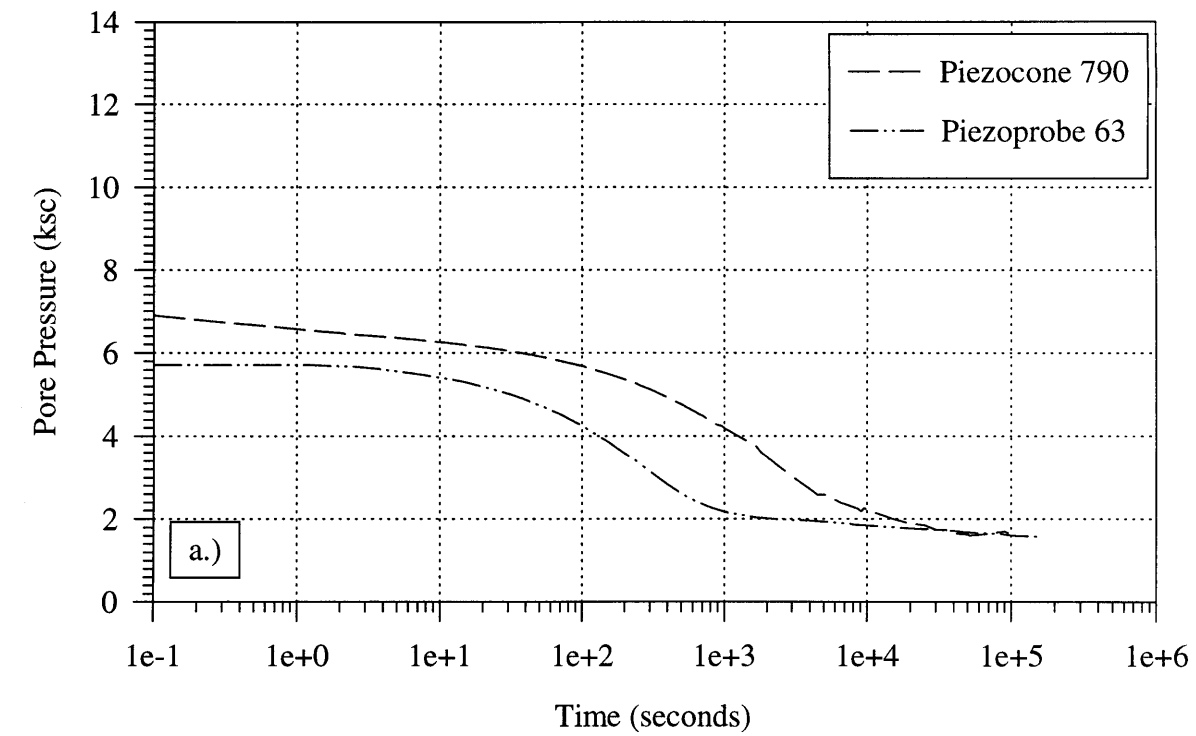


Figure 5.13 Dissipation Results for Piezocone 790 and Piezoprobe 63 at El. -15 m (55 ft. Depth).

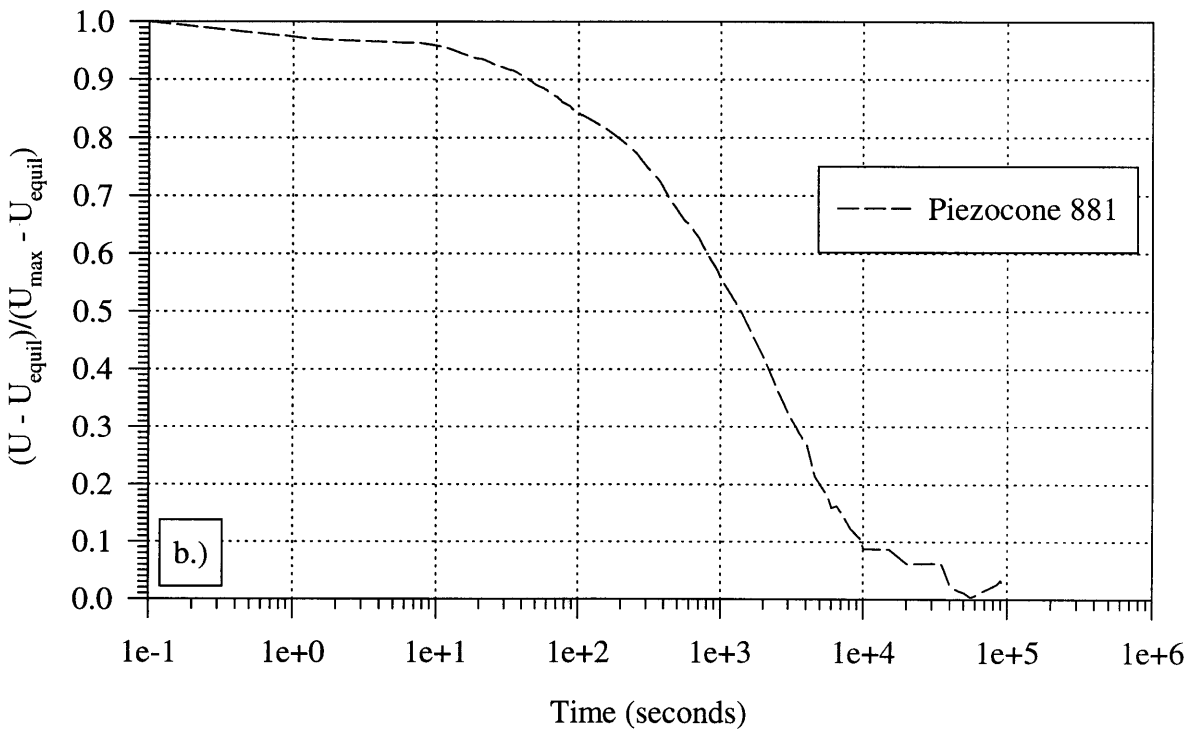
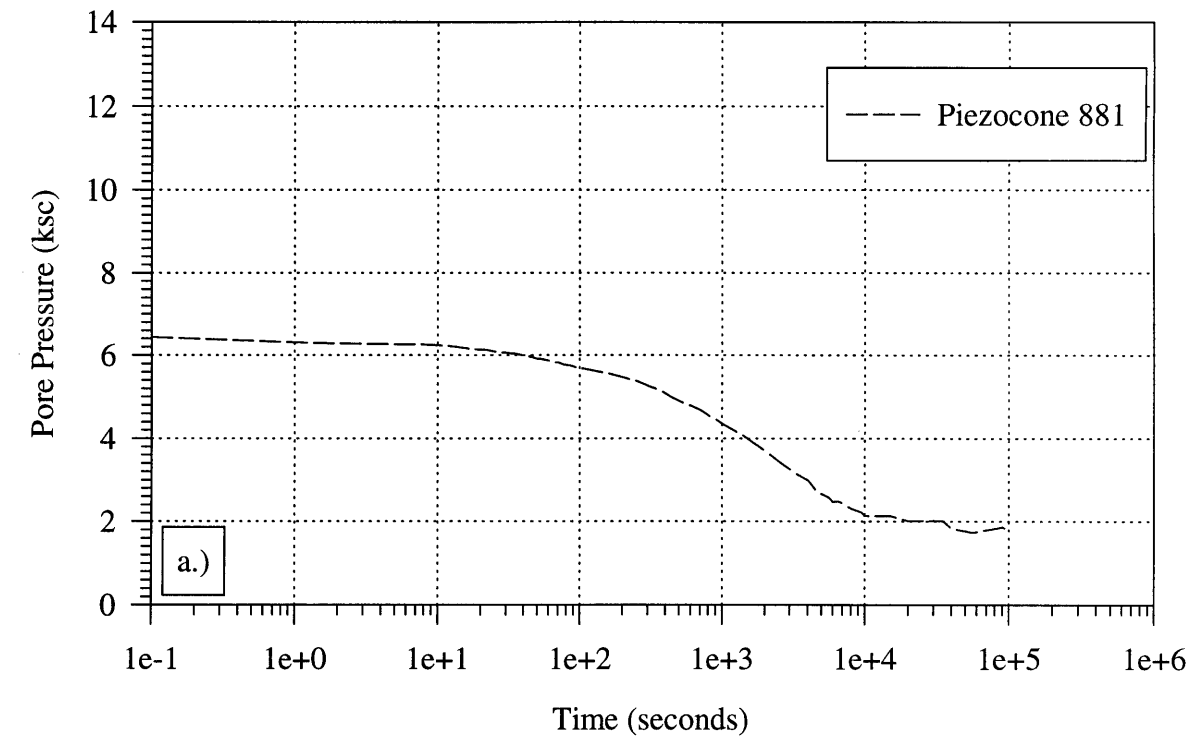


Figure 5.14 Dissipation Results for Piezocone 881 at El. -16 m (60 ft. Depth).

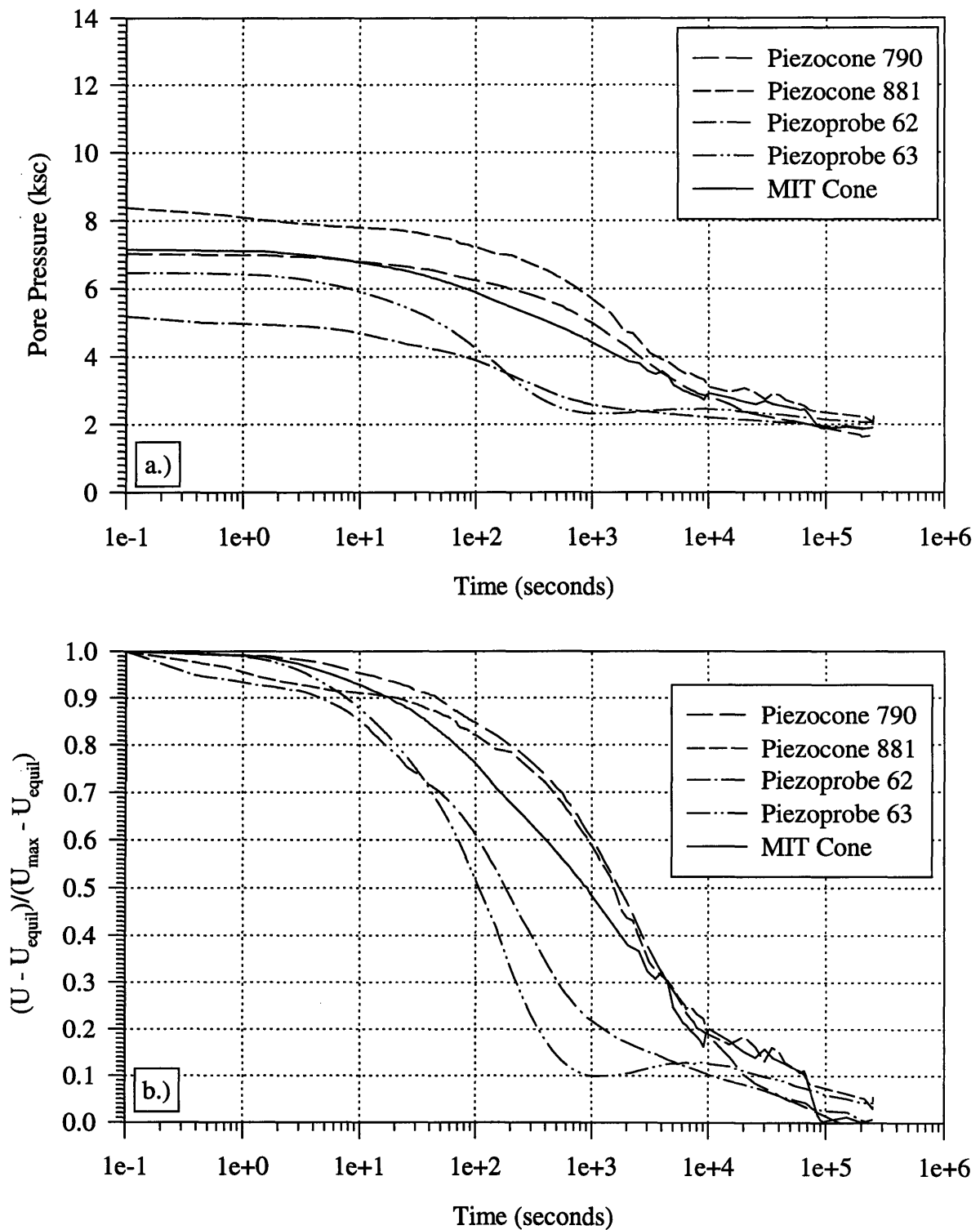


Figure 5.15 Dissipation Results for Piezocone 790, Piezocone 881, Piezoprobe 62, Piezoprobe 63, and the MIT Piezocone at El. -18 m (65 ft. Depth).

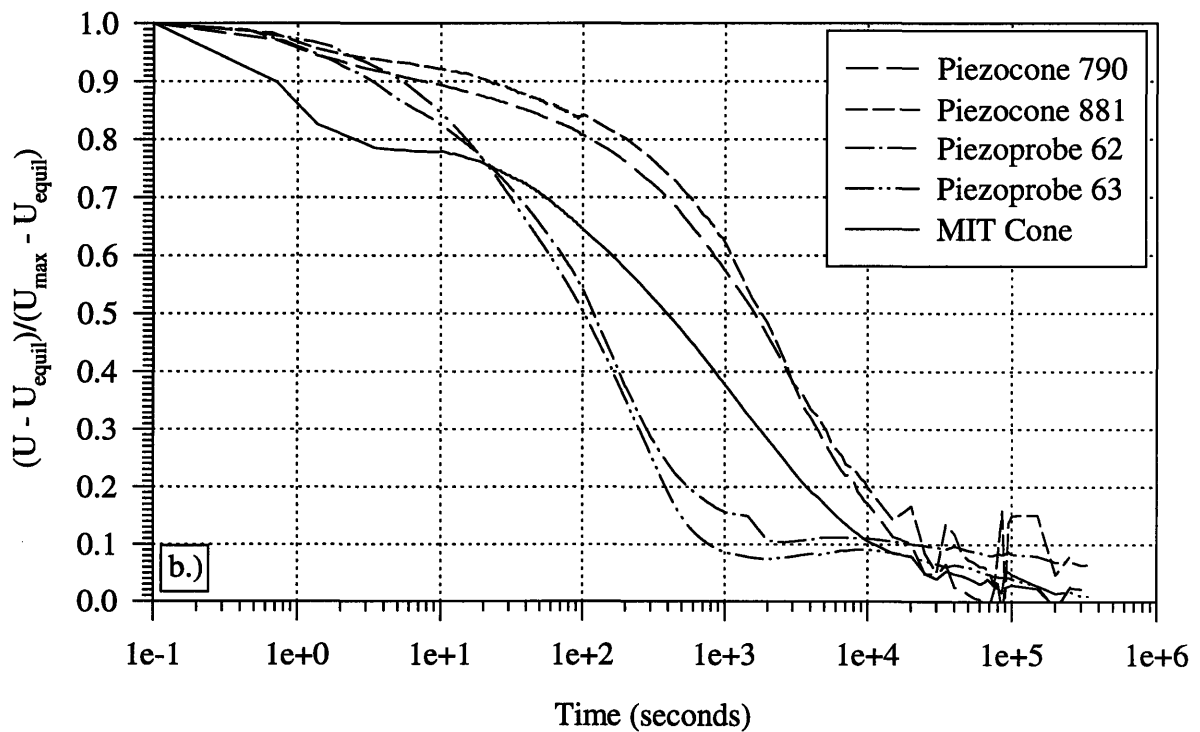
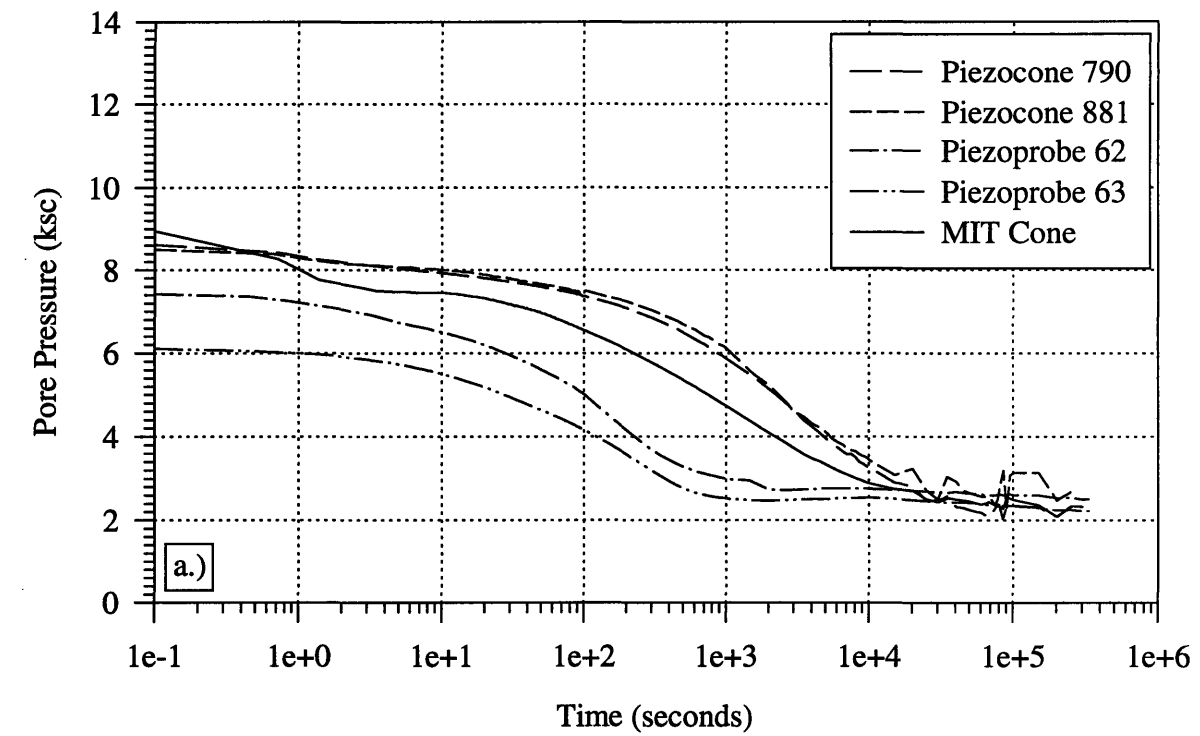


Figure 5.16 Dissipation Results for Piezocone 790, Piezocone 881, Piezoprobe 62, Piezoprobe 63, and the MIT Piezocone at El. -21 m (75 ft. Depth).

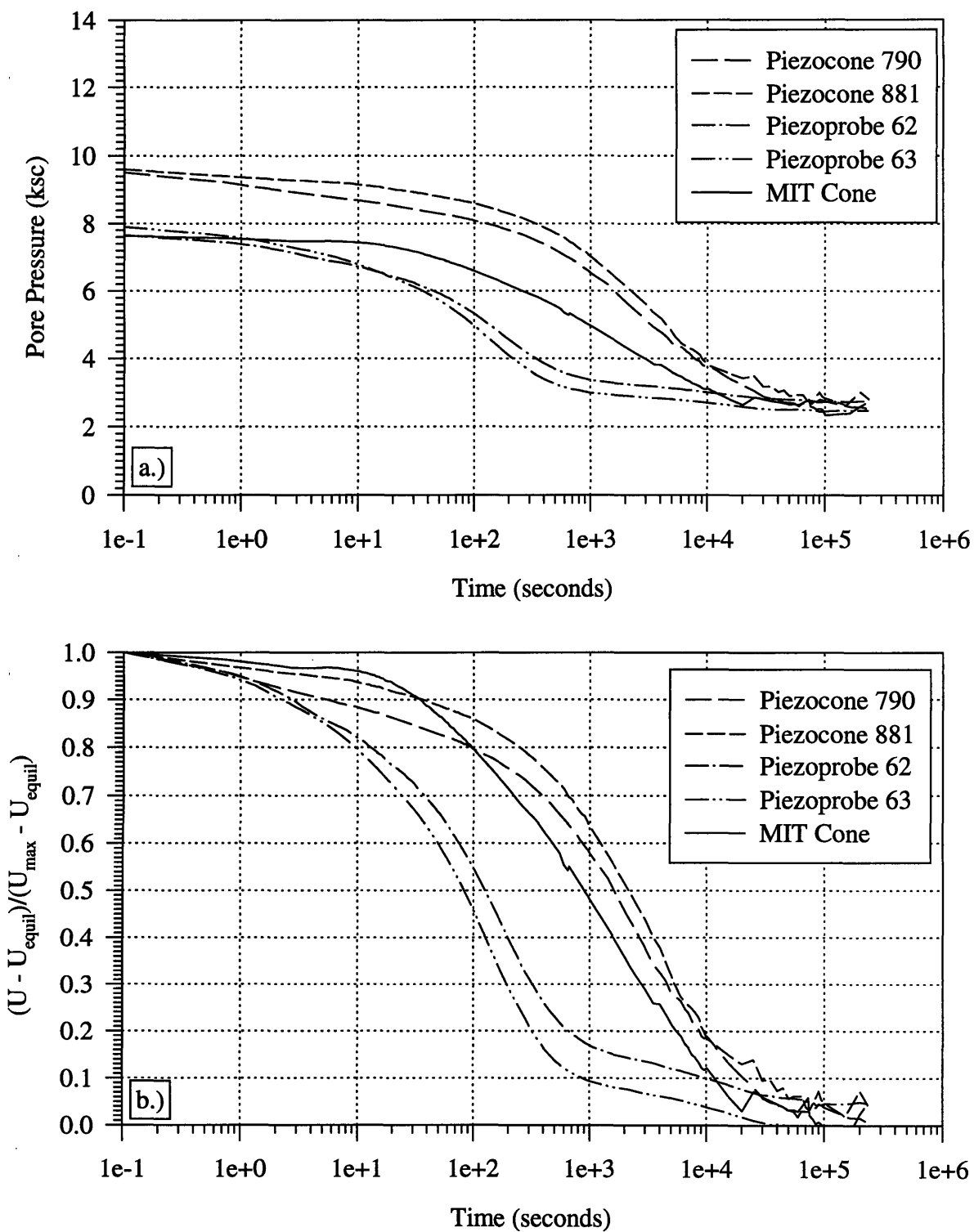


Figure 5.17 Dissipation Results for Piezocone 790, Piezocone 881, Piezoprobe 62, Piezoprobe 63, and the MIT Piezocone at El. -24 m (85 ft. Depth).

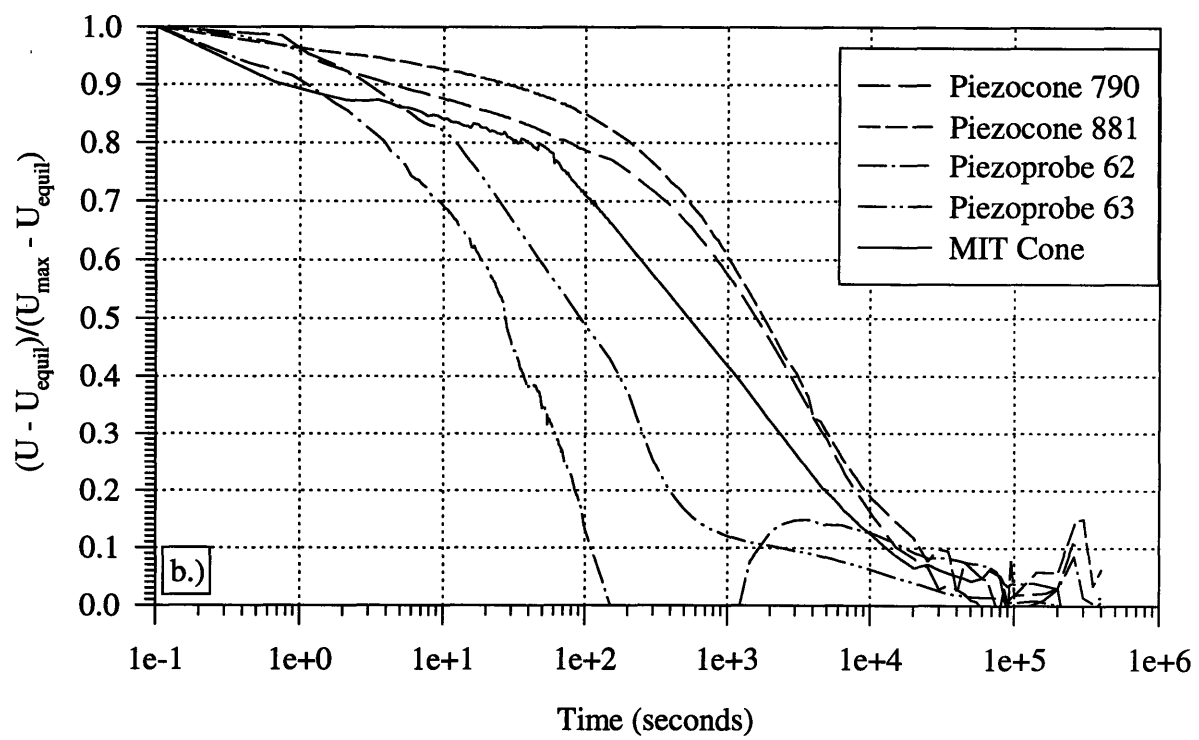
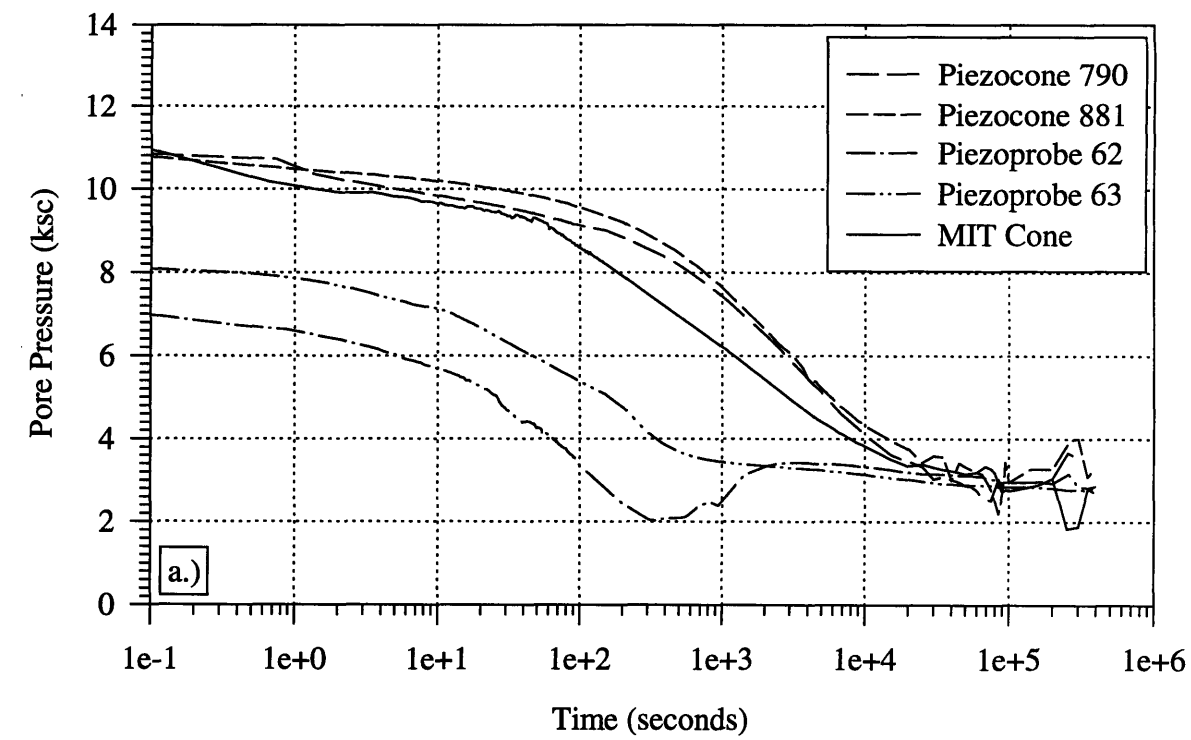


Figure 5.18 Dissipation Results for Piezocone 790, Piezocone 881, Piezoprobe 62, Piezoprobe 63, and the MIT Piezocone at El. -27 m (95 ft. Depth).

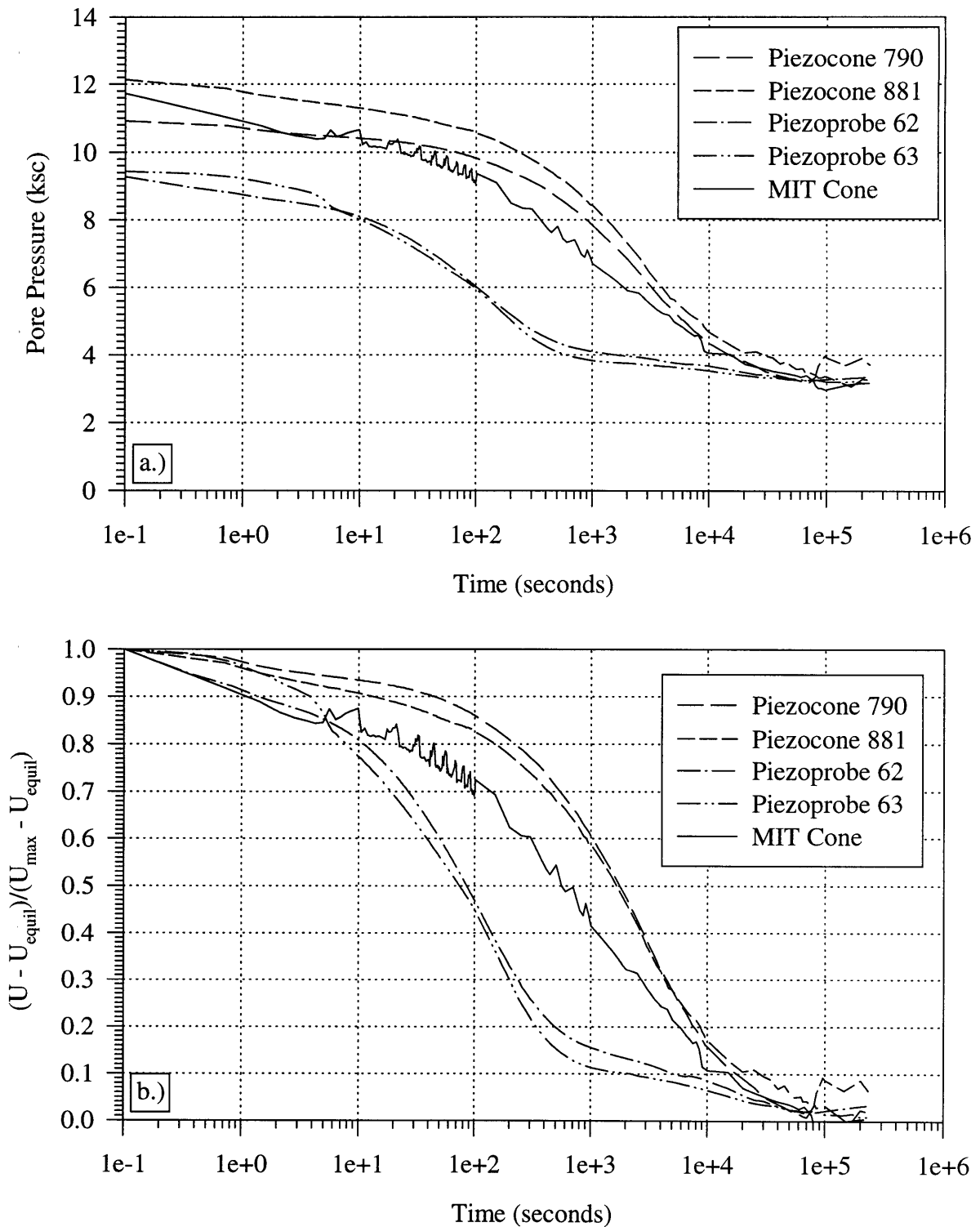


Figure 5.19 Dissipation Results for Piezocone 790, Piezocone 881, Piezoprobe 62, Piezoprobe 63, and the MIT Piezocone at El. -30 m (105 ft. Depth).

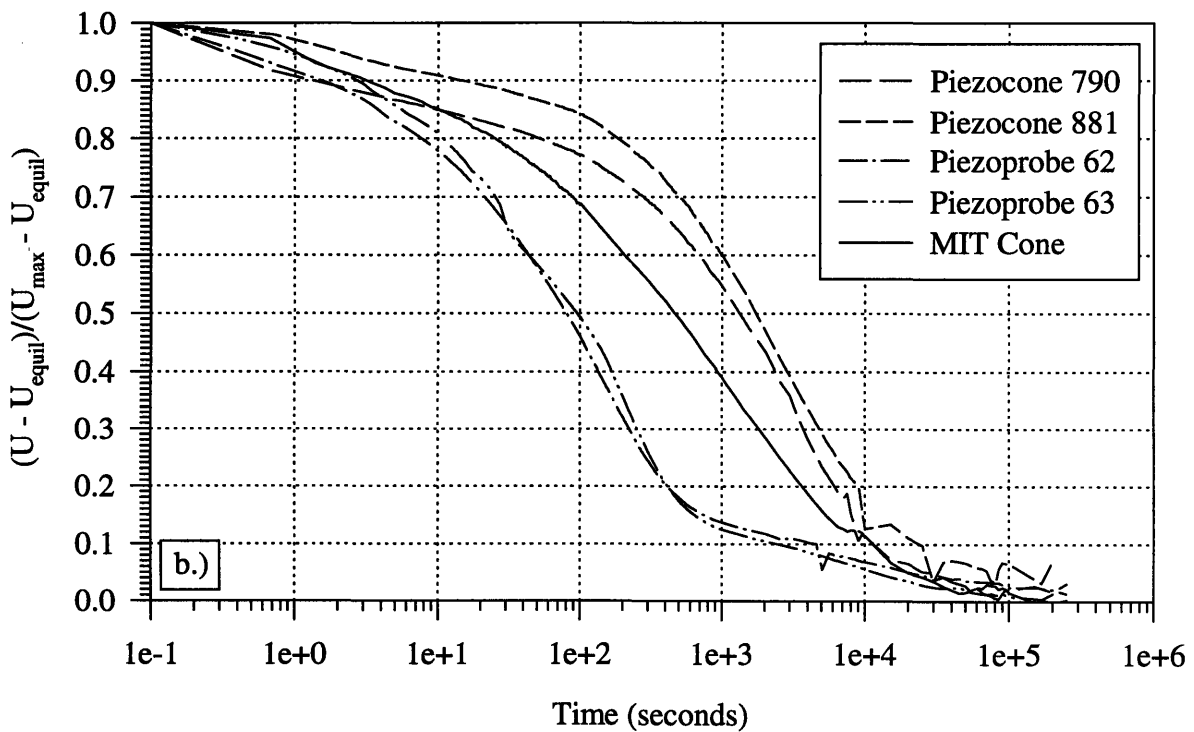
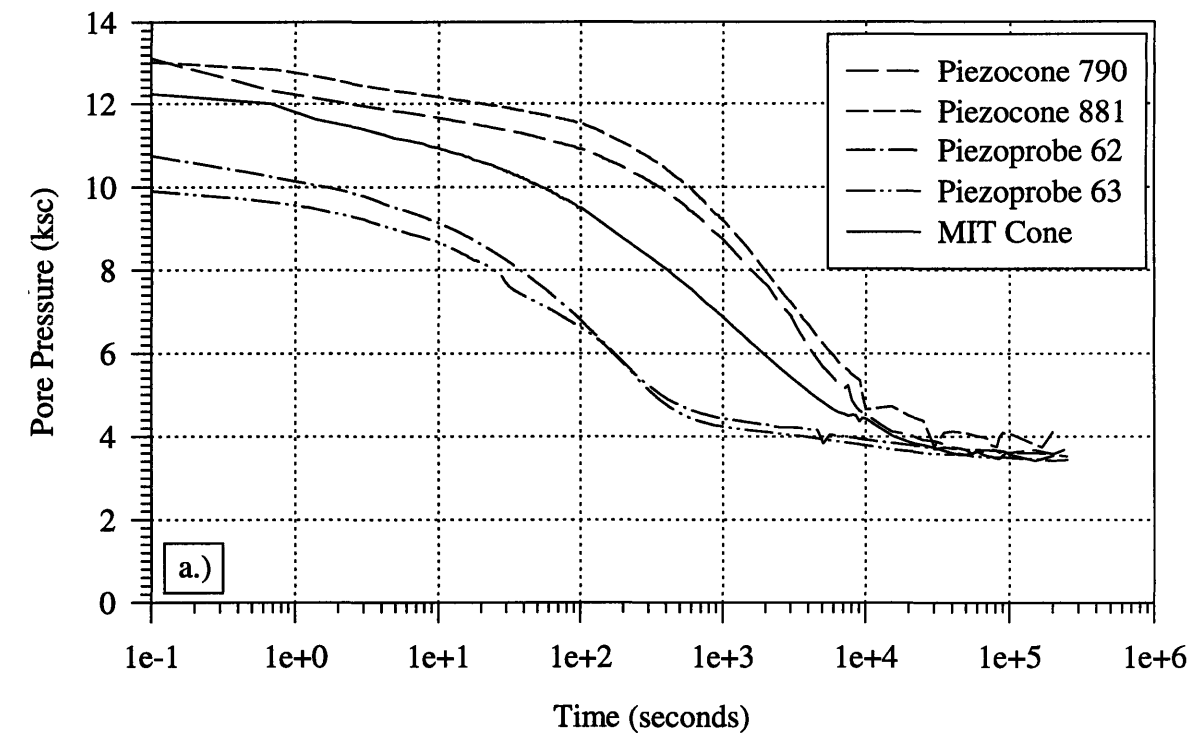


Figure 5.20 Dissipation Results for Piezocone 790, Piezocone 881, Piezoprobe 62, Piezoprobe 63, and the MIT Piezocone at El. -33 m (115 ft Depth).

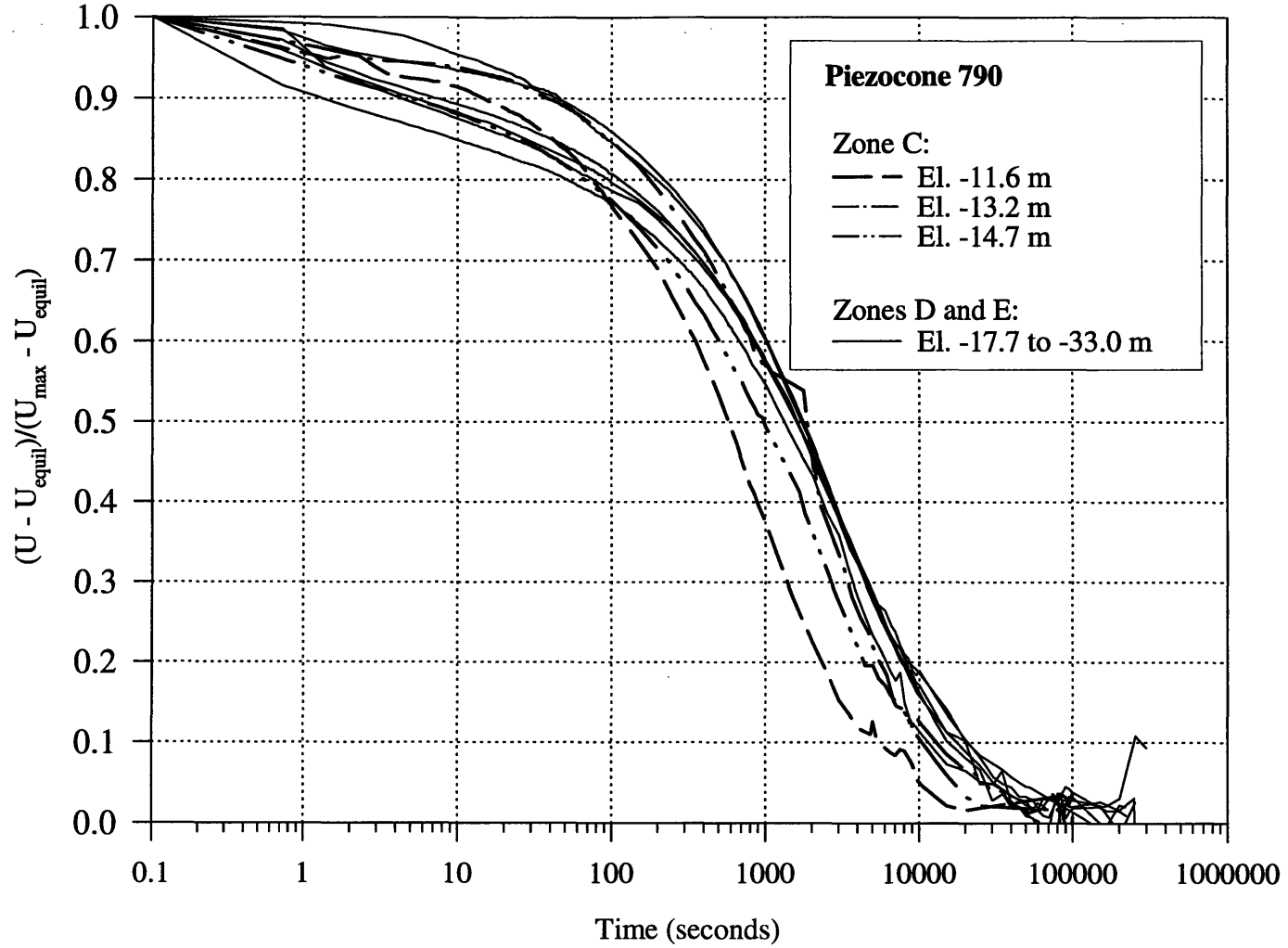


Figure 5.21 Normalized Pore Pressure vs. Time for Piezocone 790 Dissipations.

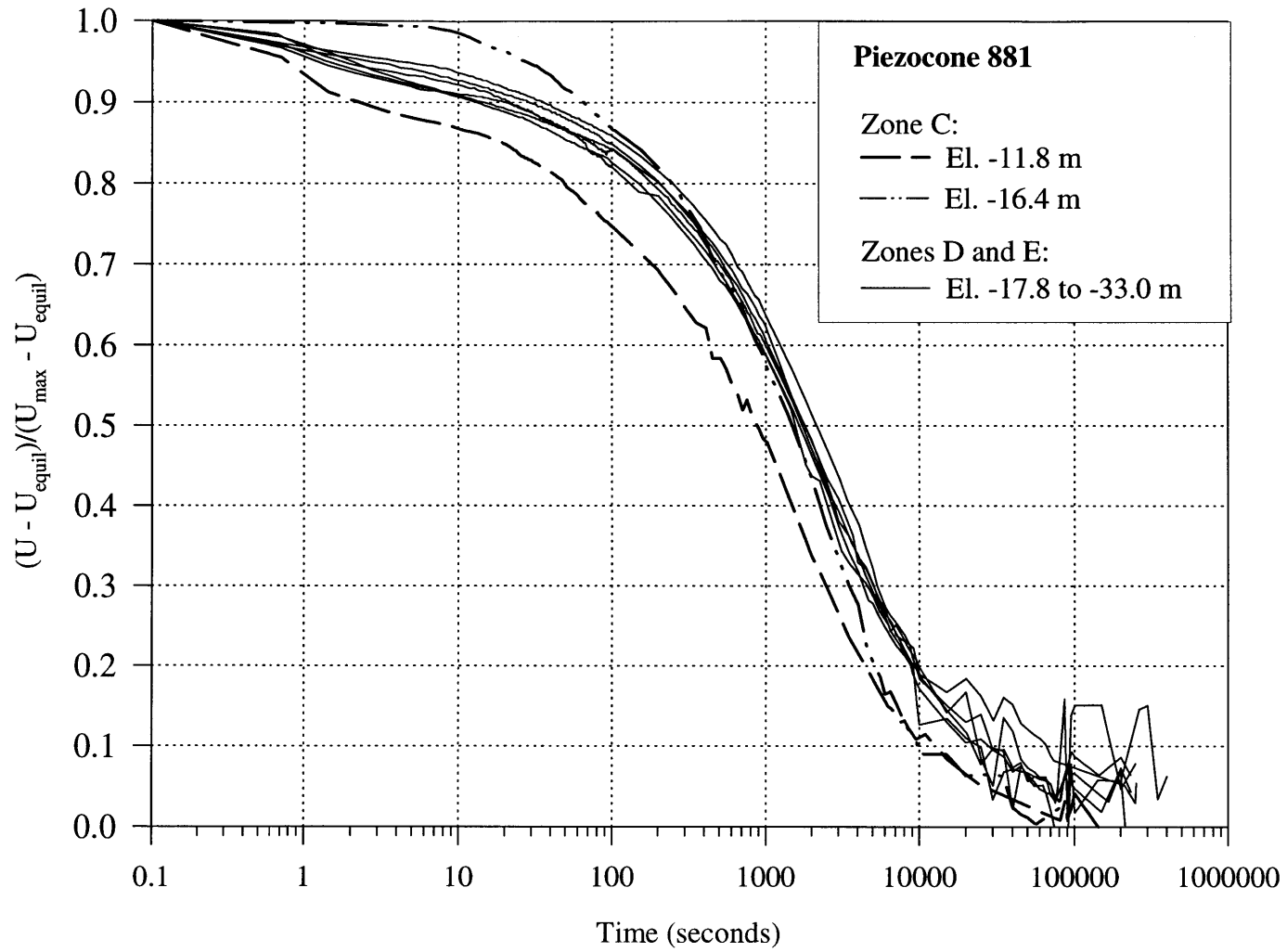


Figure 5.22 Normalized Pore Pressure vs. Time for Piezocone 881 Dissipations.

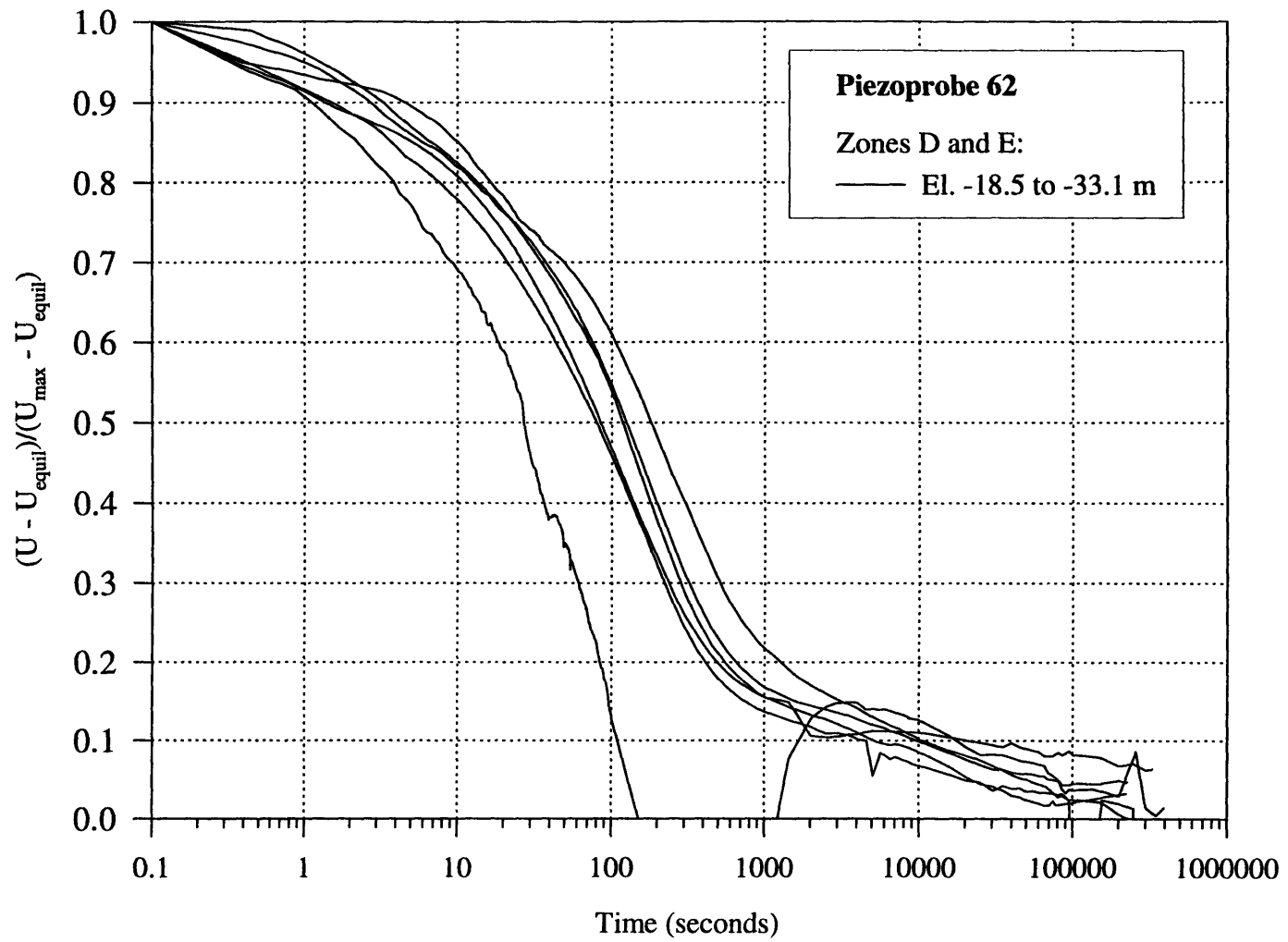


Figure 5.23 Normalized Pore Pressure vs. Time for Piezoprobe 62 Dissipations.

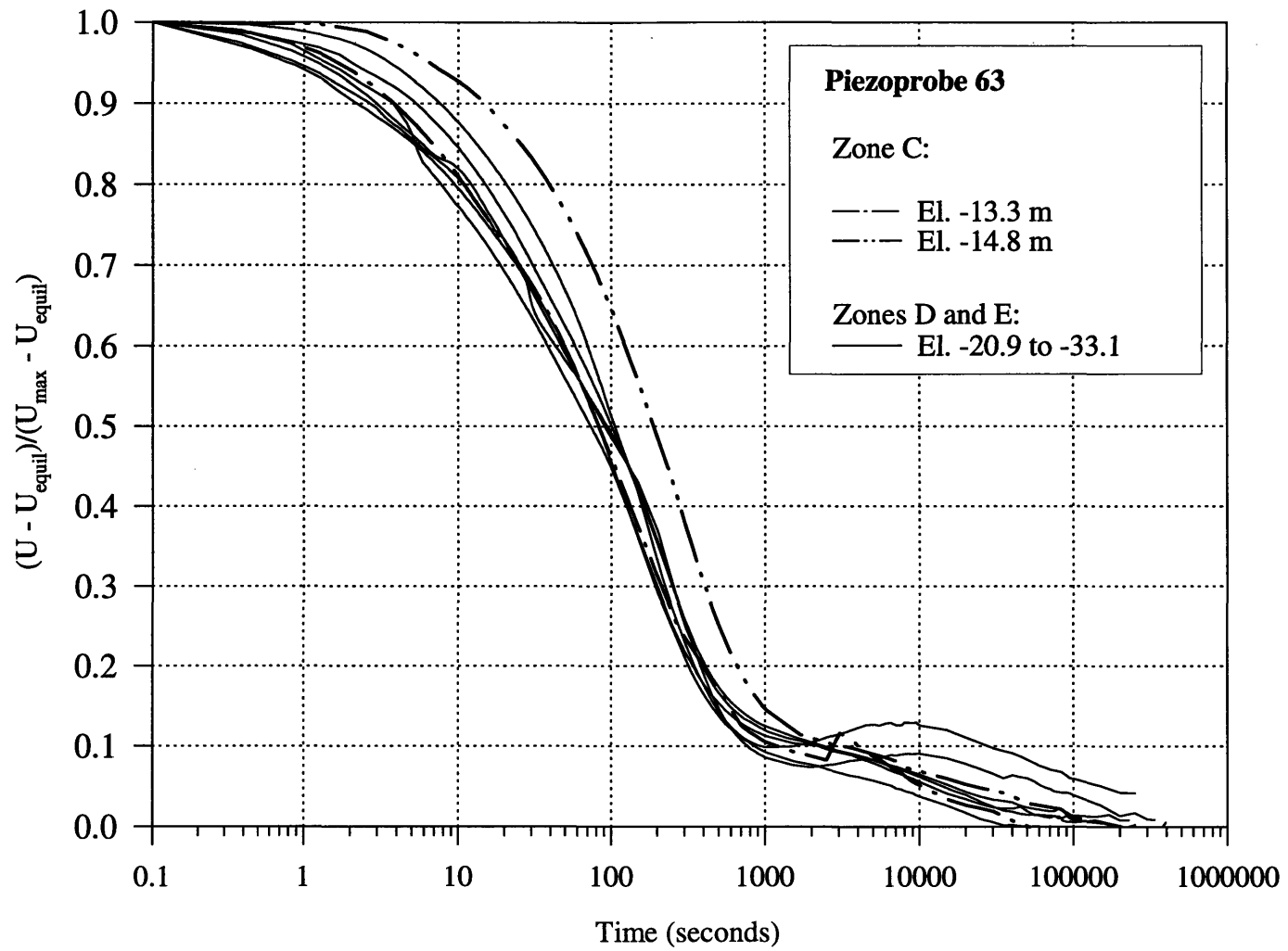


Figure 5.24 Normalized Pore Pressure vs. Time for Piezoprobe 63 Dissipations.

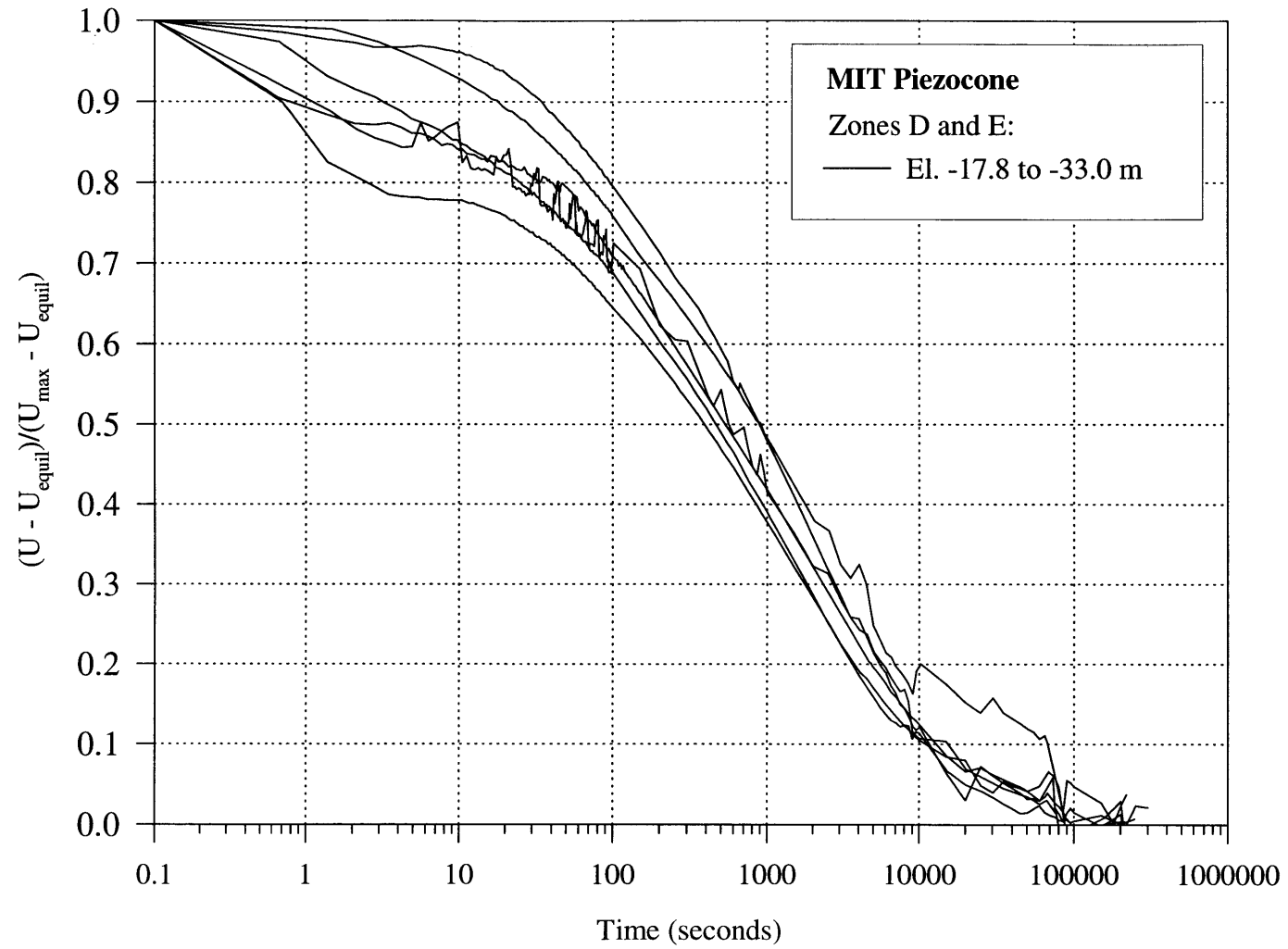


Figure 5.25 Normalized Pore Pressure vs. Time for the MIT Piezocone Dissipations.

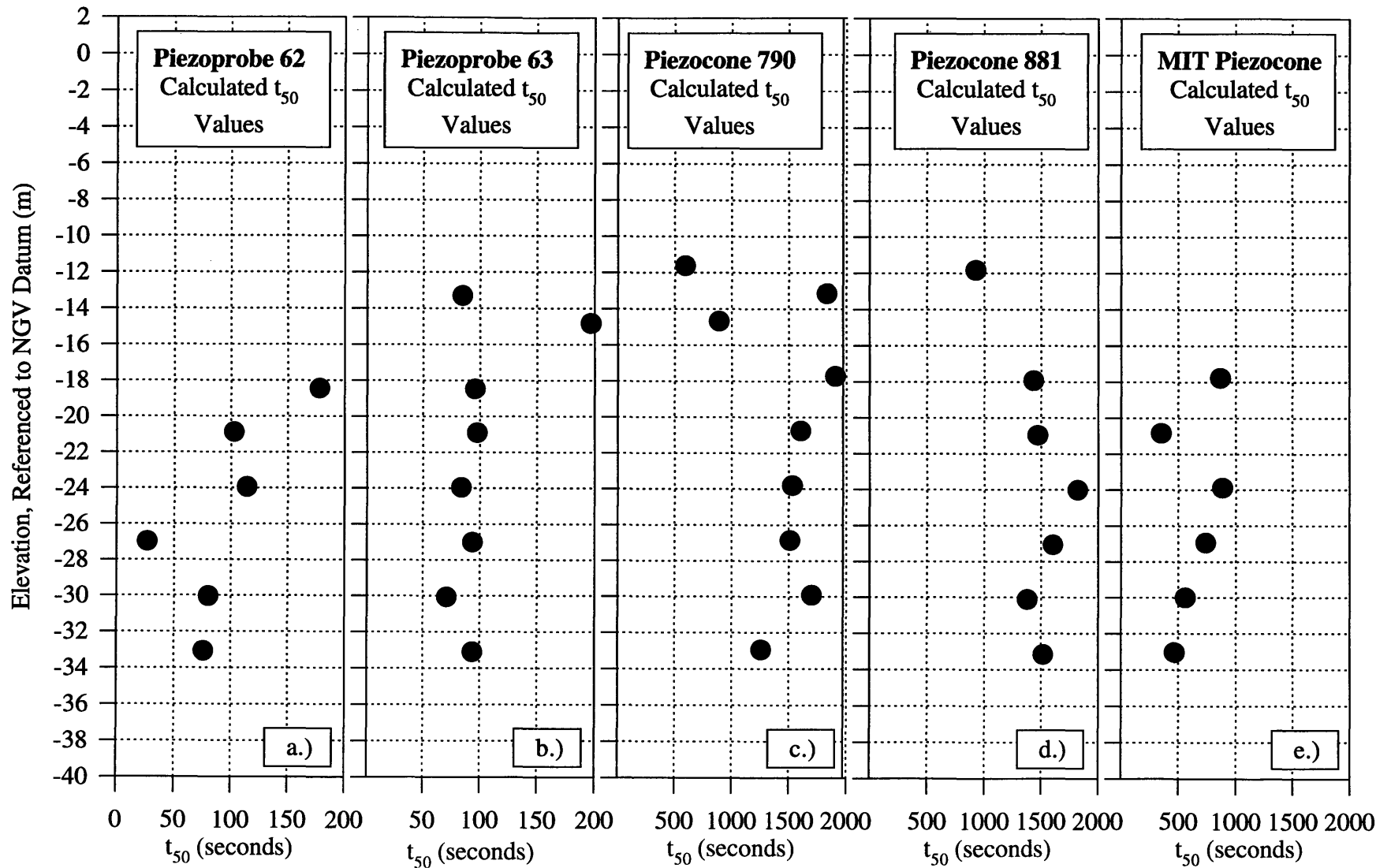


Figure 5.26 Calculated Time for 50% Dissipation (t_{50}) for: a.) Piezoprobe 62; b.) Piezoprobe 63; c.) Piezocone 790; d.) Piezocone 881; and e.) MIT Piezocone.

6. SUPPORTING LABORATORY INVESTIGATION DATA

A supporting laboratory investigation has been carried out in order to update previous information on the character and physical properties of the soil profile, and provide more extensive data on hydraulic conductivity properties of the Boston Blue Clay. The laboratory test program uses undisturbed samples obtained during the field program.¹ Figure 6.1 shows the locations of the 23 undisturbed samples² obtained during this program. This chapter gives a brief overview of the scope of the laboratory test program and methods, and summarizes the main results. More detailed information can be obtained in a forthcoming research report (Varney, Germaine, & Ladd, 1998).

6.1 Radiography

Radiography was performed on each of the 23 undisturbed samples. The x-rays for each tube were summarized logged on a sample log, indicating the relative quality, disturbance, layering, presence of rocks, shells, etc., and the location of the soil within the tube. The sample logs were used to select locations for index tests (Atterberg limits, grain size analysis, etc.) and engineering strength and consolidation test specimens.

Figure 6.2 presents a schematic of the setup used to perform radiography of the undisturbed sample tubes. The 30" long sample tubes are supported vertically in a stand in front of the x-ray beam. Since the tubes are cylindrical, x-rays that strike the center of the tube must travel through 0.2" of steel and 2.8" of soil, while those hitting the outer diameter of the tube penetrate much less soil. Therefore, aluminum plates of varying thickness are positioned in front of the specimen such that all x-rays penetrate an approximately equal mass of material. Vertical lines in the photograph are caused by abrupt changes in the thickness at the edges of these aluminum plates and the black background results from the lead shielding placed around the tube to reduce scattered radiation. Lead numbers and letters are attached to a yardstick at 1" intervals and aligned

¹ See sections 3.4 and 4.2 for sampling equipment and procedures, respectively.

² The 23 samples consist of 19 3" diameter samples and 4 3.5" diameter samples.

along the tube to provide distance reference marks. The tubes are x-rayed in three 10” segments, each exposed for 5 minutes to radiation from a Philips 3.8 ma, MG151-160kv constant potential high voltage generator which excites a metal ceramic double focus beryllium x-ray tube.

The radiographic image corresponds to an integration of all the material along the line from the x-ray source to the film. Changes in darkness depend on the relative absorption capacity of the materials being penetrated (i.e., soil, air, shells, etc.). As a result, features can only be seen if there is sufficient contrast in their absorption capacity. For example, an inclined crack within the sample will not be seen unless the x-ray path is parallel to the crack orientation. In general, changes in absorption capacity, and therefore changes in mass density, as small as 5% can be observed.

The sample quality is excellent as determined by the quality apparent in the radiographs. There are very few cracks in the samples, typically caused by the stress relief during sampling procedure. However, there are gravel sized particles in the tops of two of the tubes, presumably caused by debris falling from the sides of the borehole into the top of the tube. Layering can be seen in the radiographs by the shading contrast due to changes in soil density. Typically, bending of layers at the edges of the tubes occurs due to the sampling disturbance. However, spraying the tubes with lacquer before sampling, in combination with the careful sampling procedures appears to have resulted in high quality samples³.

6.2 Bedding Layer Thickness

Figure 6.3 shows the layer thicknesses for all sample tubes obtained as part of this field program. The layer thicknesses were determined by counting interfaces that appear on radiographs of the tubes. The layering does not change dramatically from the upper portion of the deposit to the lower portion of the deposit. This is an unexpected finding in that the upper layer was believed to be more layered than the lower deposit. This issue will be investigated further in Varney et al. (1998).

³ Treating the inside of the sampling tube with lacquer provides an interface with less skin friction than the untreated tube.

6.3 Atterberg Limits

A 3" to 3½" section of each sample tube was used for index tests. Disturbed sections are acceptable for Atterberg Limits and other index tests since the soil is remolded during testing. Each index test section was cut with a band saw. Laboratory torvanes and water content specimens were obtained from the ends of the section above the Atterberg Limit location, and the tube was resealed with wax. The cut section of the tube was extruded, a vertical wedge taken for a natural water content determination, and the rest of the soil in that section remolded. The soil was partitioned for the index tests to be performed, including Atterberg Limits, specific gravity, grain size analysis and organic content.

The Atterberg Limits were performed following the general procedure specified by ASTM method D4318 (ASTM, 1995), with the exception of progressively decreasing rather than increasing the water content for each successive liquid limit determination. The method currently suggested by ASTM consists of increasing the water content for each successive liquid limit test, which may lead to non-uniform water distribution in the sample and therefore is not followed.

Figure 6.4 and Table 6.1 summarize the liquid limit and plastic limit data, along with the natural water content determined from the vertical wedge of the sample. These results are consistent with previous studies such as Morrison (1984). The measured natural water content increases from 30% at El. -6 meters to 45% at El. -16 meters, then remains constant at $45 \pm 2\%$ with depth. The plasticity index increases from 14% at El. -6 meters to 26% at -12 meters, then remains constant at $26 \pm 2\%$ with depth. A plasticity chart is presented as Figure 6.5 which includes the undisturbed samples of Boston Blue Clay. Boston Blue Clay lies above the A-Line and is a low to medium plasticity clay.

6.4 Stress Profile

Total unit weights were determined from the water content measurements of the CRS, DSS, and natural water content wedge samples. A plot of these water contents versus depth is included as Figure 6.6. The following relation was used to determine the total unit weight from the water contents:

$$\gamma_t = \frac{(1 + \omega_n) \cdot G_s \cdot \gamma_w}{(1 + \omega_n \cdot G_s)} \quad \text{Equation 6.1}$$

where γ_t is the total unit weight (g/cm^3), ω_n is the natural water content, G_s is the specific gravity of the soil⁴, and γ_w is the unit weight of fresh water (g/cm^3). This equation assumes that the value of saturation is 100%. The values of measured and interpreted total unit weights are plotted as Figure 6.7. For elevations -10.20 to -16.45 meters, an average total weight of 1.85 g/cm^3 was used, for elevation -16.45 to -22.57 meters 1.81 g/cm^3 was used, for elevation -22.57 to -31.72 meters 1.77 g/cm^3 was used, and for elevations below -31.72 a total unit weight of 1.82 g/cm^3 was used.

The interpreted total unit weights are used to calculate the total vertical stress in the deposit⁵. The equilibrium pore pressure distribution was calculated from the piezometer data and calculations which is described in Section 5.1.1. The vertical effective stress is calculated by subtracting the equilibrium pore pressure from the total vertical stress. The in situ stress profile is presented in Figure 6.8.

6.5 Constant Rate of Strain Consolidation (CRSC) Testing

The CRSC tests were performed with the constant rate of strain device developed by Wissa et al. (1971), shown in Figure 6.9. In recent years, the device was modified to combine the cell pressure with the back pressure and eliminate the inner rolling diaphragm. The test is performed by trimming a 2.5 cm tall with a 6.35 cm diameter soil specimen into a solid ring. The ring is placed on the base of the CRS device on top of a fine porous ceramic stone⁶ hydraulically connected to a pressure transducer in a port saturated with water.

The device is pressurized using steps of 0.5 ksc in cell pressure to provide a confining cell pressure of 3.5 to 4.0 ksc while maintaining a constant sample height and

⁴ The specific gravity is assumed to be a nominal value of $G_s = 2.75$ as typical for a low plasticity index clay.

⁵ The interpreted total unit weights from this program were used for El. -10.20 m and below. Morrison's (1984) soil profile was used above this elevation, assuming $\sigma_{v0} = 2.07 \text{ ksc}$ at El. -10.20m

⁶ The porous element is a 1 bar, high air entry, ceramic porous stone.

then allowed to equilibrate for 12 hours. The sampling effective stress (σ_i) is determined after 12 hours of equilibrium. The base is then controlled by a gear and motor to apply a nominal constant rate of axial strain of 0.8% per hour. During the constant rate of strain process, the axial displacement, axial load, pore pressure, and cell pressure are recorded using the central data acquisition system. A CRSC test was performed on each tube obtained from boring B96 to develop a full stress history profile and measure the in situ vertical hydraulic conductivity. Summary tables of these CRSC tests are included as Table 6.2.

6.5.1 Preconsolidation Pressure

The preconsolidation values were determined from the CRSC test data, using both the Casagrande construction (Casagrande, 1936) and the Strain Energy technique (Becker et al., 1987) for interpretation of the consolidation curve. Sample constructions for determining the preconsolidation pressure from the Casagrande technique and from the Strain Energy technique are included as Figure 6.10 and Figure 6.11, respectively. The determined values of preconsolidation pressures are included in Table 6.2 and are summarized in Figure 6.12.

The overconsolidation ratio, OCR, which is calculated by dividing the preconsolidation pressure by the in situ vertical effective stress at the same elevation, is plotted in Figure 6.13. For this deposit, the OCR decreases from 3.6 at El. -6 meters to 1.2 at El. -22 meters, where it remains constant at 1.2 ± 0.1 with depth.

6.5.2 Hydraulic Conductivity

Values of hydraulic conductivity (k) were obtained from the CRSC tests and are included in Table 6.2. The calculation for hydraulic conductivity is derived directly from D'Arcy's Law which is:

$$k = \frac{Q}{iA} \quad \text{Equation 6.2}$$

where Q is the flow of the pore water out of the specimen, i is the hydraulic gradient, and A is the cross sectional area of the specimen. The resulting equation to calculate k from the CRSC test data is:

$$k = \frac{\varepsilon \cdot H_d^2 \cdot \gamma_w}{2 \cdot u_e}$$

Equation 6.3

where ε is the vertical strain rate, H_d is the drainage height, γ_w is the unit weight of water, and u_e is the excess pore pressure at the base of the specimen.

Values of in situ vertical hydraulic conductivity were obtained through interpretation of the measured trend of void ratio versus the log of hydraulic conductivity. The in situ hydraulic conductivity is determined at the point of intersection between a straight line through the normally consolidated region of a plot of void ratio (e) versus $\log k$ and the in situ void ratio of the CRSC specimen. This was performed to mitigate the effects of the initial variations in the determined k due to low excess pore pressure and disturbance caused by sampling (i.e. microcracks, leakage between the sample ring and the specimen due to imperfect seal, etc.). An example construction is provided as Figure 6.14. The values of hydraulic conductivity versus elevation plot is presented in Figure 6.15 along with the values presented by Morrison (1984). The hydraulic conductivity decreases from 3×10^{-7} cm/s at elevation -6 meters to 8×10^{-8} cm/s at elevation -15 meters, then remains essentially constant with depth. As shown, the hydraulic conductivity values for the soil deposit determined during this program are in a tighter band and at the upper bound of those presented by Morrison.

Figure 6.16 presents the void ratio versus hydraulic conductivity determined from the CRSC tests. As shown, there is no indicated trend of hydraulic conductivity with depth. Therefore, in Chapter 7, the values of hydraulic conductivity used to compare to the predicted values are determined from an average of the hydraulic conductivity values determined during CRSC tests conducted nearest the measurement point for the test depth.

Atterberg Limits						
Sample Tube	Depth (ft)	Elev (m)	ω_p (%)	ω_l (%)	ω_n (%)	PI (%)
1	25.19	-5.68	16.74	31.19	31.02	14.45
2	29.13	-6.88	19.45	41.16	34.02	21.71
3	34.13	-8.40	19.60	43.13	36.34	23.53
4	39.14	-9.93	18.03	38.04	32.60	20.01
5	42.11	-10.84	21.19	48.80	38.28	27.61
6	45.14	-11.76	20.14	40.42	36.96	20.28
7	49.16	-12.99	21.47	47.28	39.59	25.81
8	54.13	-14.50	22.01	50.10	40.33	28.09
9	59.26	-16.06	21.01	44.40	43.19	23.39
10	62.19	-16.96	23.69	53.16	48.18	29.47
11	65.13	-17.85	22.94	48.17	44.15	25.23
12	69.15	-19.08	23.86	49.10	43.99	25.24
13	74.16	-20.61	21.92	45.59	43.95	23.67
14	79.19	-22.14	22.70	46.85	46.09	24.15
15	84.21	-23.67	20.74	47.83	42.55	27.09
16	89.26	-25.21	22.71	51.09	45.42	28.38
17	94.13	-26.69	23.63	49.72	46.58	26.09
18	99.67	-28.38	21.98	43.87	41.59	21.89
19	104.14	-29.74	23.32	46.67	43.16	23.35
20	109.15	-31.27	24.02	47.38	45.43	23.36
21	114.18	-32.80	25.26	51.29	47.21	26.03
22	119.15	-34.32	22.68	47.83	43.04	25.15
23	124.13	-35.84	22.41	51.09	41.56	28.68

Table 6.1 Summary of Atterberg Limits.

		Index Tests			Specimen Data			Test Results						Remarks
Test #	Elev (m)	TV	W _i	W _n	W _n	e _i	W _f	σ' _s	u _b	ε	σ' _p C	σ' _{vo}	c _v (cm ² /s)	
Boring	Depth (ft)	SD	W _p	SD	W _n	e _i	W _f	σ' _s	u _b	ε	σ' _p C	σ' _{vo}	c _v (cm ² /s)	
Sample	Markers	# obs	I _p	# obs	S _i (%)	G _s	S _f (%)	(ksc)	(ksc)	(%/hr)	σ' _p SE	OCR C	k (cm/s)	
											OCR SE			
CRS184 B96 U16	-25.68 90.79 2.0 - 4.0	0.36 0.06 3		47.8 1.3 3	51.73 101.4	1.403 2.750		0.11	3.49	0.80	2.70 2.72	2.17 1.24 1.25	8.80E-08	Uniform Boston Blue Clay (BBC)
CRS185 B96 U15	-24.16 85.81 2.0 - 3.0	0.33 0.03 3		50.7	47.15 100.0	1.297 2.750		0.06	3.72	0.84	2.27 2.33	2.06 1.10 1.13	8.40E-08	Uniform BBC
CRS186 B96 U17	-27.20 95.79 2.5-3.5	0.39 0.04 3		44.0 1.9 3	54.00 99.9	1.462 2.750								No Consolidation data Blue-Grey, Slightly Sensitive, Mottled BBC
CRS187 B96 U19	-30.25 105.81 2.0 - 3.0	0.38 0.02 3		46.6 0.2 3	48.94 99.3	1.356 2.750		0.33	3.88	0.82	3.38 3.37	2.53 1.34 1.33	5.50E-08	
CRS189 B96 U20	-31.77 110.79 2.5 - 3.5	0.37 0.04 3		44.6 5.5 4	42.95 98.3	1.201 2.750		0.14	3.91	0.79	2.74 2.76	2.64 1.04 1.04	8.90E-08	
CRS190 B96 U21	-33.30 115.79 2.0 - 3.5	0.41 0.06 3		45.9 3.4 3	47.61 99.7	1.314 2.750		0.17	3.89	0.83	3.10 3.18	2.76 1.12 1.15	6.00E-08	Tension Crack Through Center of Sample
CRS191 B96 U13	-21.10 75.77 2.5 - 3.5	0.35 0.05 3		45.4 2.1 3	48.23 101.0	1.313 2.750		0.15	3.92	0.84	2.69 2.66	1.82 1.48 1.46	6.60E-08	Blue Grey, Moist, Soft to Medium Slightly Sensitive, Uniform BBC
CRS192 B96 U12	-19.60 70.85 1.5 - 3.0	0.45 0.01 3		40.1 3.7 3	41.24 101.5	1.118 2.750		0.29	3.90	0.83	2.79 2.79	1.70 1.64 1.64	7.40E-08	

a) Markers - Location within tube

b) Stresses in kg/cm²c) 1 kg/cm² = 98.6 kpa

d) Water Contents, Limits in %

e) c_v in normally consolidated range

f) k extrapolated to the in situ void ratio

Table 6.2 Summary Table of CRSC Tests.

		Index Tests			Specimen Data			Test Results						Remarks
Test #	Elev (m)	TV	W _i	W _n	W _n	e _i	W _f	σ' _s	u _b	ε	σ' _p C	σ' _{vo}	c _v (cm ² /s)	
Boring	Depth (ft)	SD	W _p	SD	W _n	e _i	W _f	σ' _s	u _b	ε	σ' _p C	σ' _{vo}	c _v (cm ² /s)	
Sample	Markers	# obs	I _p	# obs	S ₁ (%)	G _s	S _r (%)	(ksc)	(ksc)	(%/hr)	σ' _p SE	OCR C	k (cm/s)	
											OCR SE			
CRS193	-17.91	0.38		51.4								1.57		Moist, Grey, Slightly Sensitive, Uniform BBC
B96	65.31	0.03			49.04	1.338		0.15	3.92	0.87	2.73	1.73	5.60E-08	
U11	K - L5	3			100.8	2.750					2.75	1.75		
CRS195	-16.46	0.46		47.0								1.46		
B96	60.56	0.01		4.4	40.43	1.121		0.12	3.90	0.82	2.88	1.97	5.10E-08	
U9	4.5 - 6.0	3		4	99.2	2.750					2.89	1.98		
CRS197	-36.31	0.40		37.0								2.99		
B96	125.69	0.01		1.3	40.97	1.148		0.25	3.90	0.84	3.72	1.24	6.70E-08	
U23	3.5 - 5.0	3		2	98.2	2.750					3.64	1.22		
CRS198	-15.00	0.46		37.6								1.35		
B96	55.75	0.06		1.1	39.84	1.104		0.07	3.92	0.84	1.91	1.42	1.10E-07	
U8	2.5 - 3.5	3		4	99.2	2.750					1.99	1.47		
CRS199	-13.45	0.51		34.6								1.23		
B96	50.69	0.02		3.1	41.33	1.139		0.12	3.88	0.82	3.54	2.88	3.80E-08	
U7	2.0 - 3.0	3		4	99.8	2.750					3.43	2.79		
CRS201	-12.26	0.46		38.7								1.14		
B96	46.77	0.04		2.1	41.62	1.153		0.11	3.93	0.82	2.54	2.23	3.90E-08	
U6	2.0 - 3.0	3		4	99.3	2.750					2.56	2.25		
CRS202	-10.45	0.31		35.1								1.00		
B96	40.83	0.13		3.4	34.31	0.967		0.11	3.92	0.81	2.43	2.43	1.20E-07	
U4	2.0 - 3.0	3		4	97.6	2.750					2.36	2.36		
CRS205	-8.89	0.49		31.9								0.88		
B96	35.71	0.08		2.4	37.09	1.015		0.05	3.91	0.74	2.66	3.03	6.60E-08	
U3	3.0-4.0	3		4.0	100.6	2.750					2.54	2.89		

a) Markers - Location within tube

b) Stresses in kg/cm²c) 1 kg/cm² = 98.6 kpa

d) Water Contents, Limits in %

e) c_v in normally consolidated range

f) k extrapolated to the in situ void ratio

Table 6.2 (cont.) Summary Table of CRSC Tests.

Test # Boring Sample	Elev (m) Depth (ft) Markers	Index Tests			Specimen Data			Test Results						Remarks
		TV SD # obs	W _i W _p I _p	W _n SD # obs	W _n S _i (%)	e _i G _s	W _f S _r (%)	σ' _s (ksc)	u _b (ksc)	ε (%/hr)	σ' _p C σ' _p SE (ksc)	σ' _{vo} C OCR SE	c _v (cm ² /s) k (cm/s)	
CRS206 B96 U2	-7.26 30.37 1.5-3.5	0.46 0.01 3		32.8 3.8 4	30.66* 100.0*	0.843 2.750	28.22 112.09	0.14	3.88	0.83	2.17 2.18	0.75 2.88 2.89	N/A	Layers of Clay and Silt. Silt Crumbles. Top: Extensive Patching. Bottom: Some Patching
CRS210 B96 U14	-22.63 80.79 2.0-3.0	0.34 0.02 3		39.7 2.5 4.0	45.66 100.3	1.252 2.750	34.22 117.93	0.12	3.92	0.87	2.25 2.27	1.94 1.16 1.17	1.00E-07	Uniform, Moist, Slightly Sensitive BBC
CRS211 B96 U18	-28.72 100.77 1.5-2.5	0.38 0.02 3		41.0 2.9 3	44.15 100.0	1.214 2.750	32.52 103.36	0.15	3.92	0.84	2.62 2.63	2.41 1.09 1.09	1.10E-07	Slightly Sensitive BBC with Shells on Sealing Surface. Patched
CRS215 B96 U5	-11.36 43.83 2.0-3.0	0.43 0.02 3		37.2 1.8 4	44.32 100.8	1.209 2.750		0.13	3.91	0.84	2.75 2.70	1.07 2.57 2.52	1.40E-07	
CRS219 B96 U10	-17.46 63.83 2.0-3.0	0.42 0.03 4		46.5 2.8 4	44.24 100.2	1.214 2.750		0.19	3.90	0.87	3.38 3.37	1.54 2.20 2.19	7.00E-08	Resealed Vertical Cracks in Sample. Soft, Moist, Slightly Sensitive BBC
CRS220 B96 U22	-34.86 120.91 1.5-2.5	0.38 0.03 3		43.4 5.0 3	42.36 99.94	1.166 2.750	34.38 103.0	0.22	3.91	0.86	3.38 3.43	2.88 1.17 1.19	6.70E-08	Vertical Crack at Edge of Sample. Small Rocks. Silty Clay.
CRS221 B96 U1	-6.13 26.67 2.0-3.0	0.38 0.13 3		28.5 1.1 4	31.75 97.2	0.898 2.750	27.33 102.0	0.07	3.88	0.80	3.07 2.43	0.67 4.61 3.65	3.20E-07	Gray Silty Clay with Thin Layers of Silt, Small Vertical Cracks
CRS223 B96 U17	-27.15 95.62 4.5-6.5	0.34 0.04 3		45.5 1.9 4	51.01 100.4	1.399 2.750	33.17 104.36	0.22	3.89	0.88	2.90 2.89	2.29 1.27 1.26	8.00E-08	Slightly Sensitive Uniform BBC

a) Markers - Location within tube
 b) Stresses in kg/cm²
 *100% Saturation Assumed

c) 1 kg/cm² = 98.6 kpa
 d) Water Contents, Limits in %

e) cv in normally consolidated range
 f) k extrapolated to the in situ void ratio

Table 6.2 (cont.) Summary Table of CRSC Tests.

Test # Boring Sample	Elev (m) Depth (ft) Markers	Index Tests			Specimen Data			Test Results					Remarks	
		TV SD # obs	W _i W _p I _p	W _n SD # obs	W _n S _i (%)	e _i G _s	W _f S _f (%)	σ' _s (ksc)	u _b (ksc)	ε (%/hr)	σ' _p C σ' _p SE (ksc)	σ' _{vo} OCR C OCR SE		c _v (cm ² /s) k (cm/s)
CRS232 B96 U2	-7.44 30.96 4 - 5	0.30 0.05 3		32.2 4.9 4	35.59 98.7	0.991 2.750	33.3 103.57	0.09	3.92	0.79	3.30 3.23	0.77 4.30 4.21	9.40E-08	Below: Fine sand/silt layer, patch Above: BBC w/silt & sand lenses, slightly sensitive.
CRS233 B96 U5	-11.31 43.67 4 - 5	0.37 0.08 9		34.7 3.2 4.0	38.20 100.1	1.049 2.750	31.09 103.8	0.13	3.90	0.77	2.57 2.58	1.07 2.41 2.42	1.10E-07	Below: Silty sensitive BBC, moist. Above: Uniform, moist, sensitive BBC.

a) Markers - Location within tube
b) Stresses in kg/cm²

c) 1 kg/cm² = 98.6 kpa
d) Water Contents, Limits in %

e) cv in normally consolidated range
f) k extrapolated to the in situ void ratio

Table 6.2 (cont.) Summary Table of CRSC Tests.

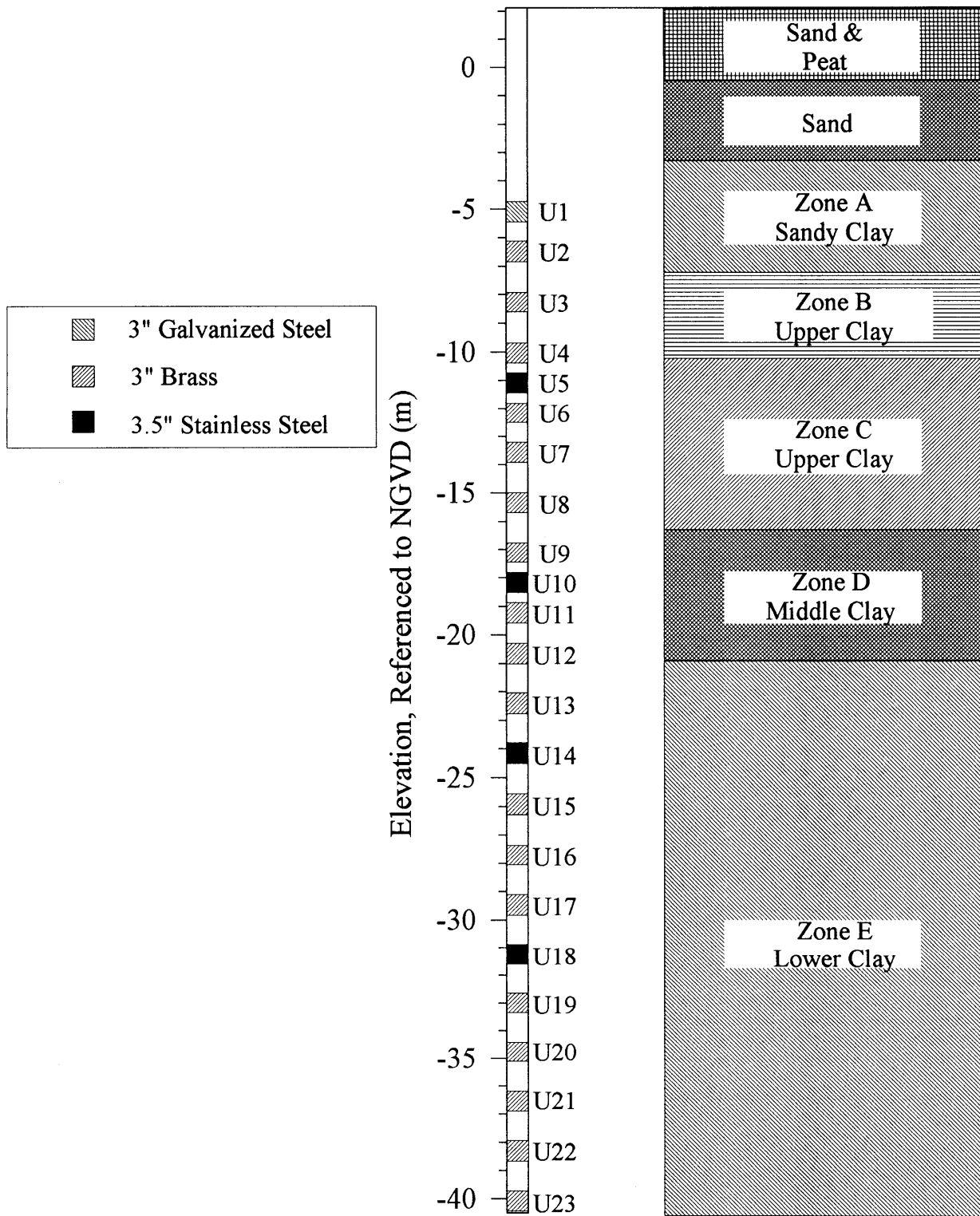


Figure 6.1 Location of Undisturbed Soil Samples obtained at Saugus (Station 246) during the 1996 Field Program.

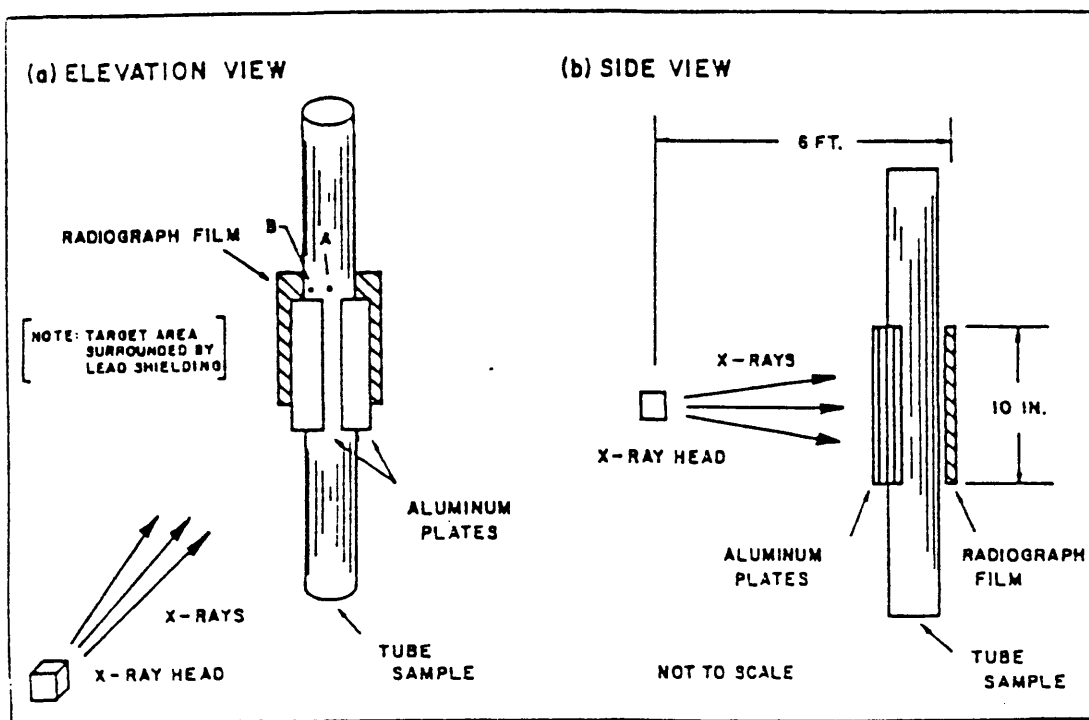


Figure 6.2 Schematic of Setup used to Perform Radiography on Undisturbed Soil Samples (After Ladd et al., 1980).

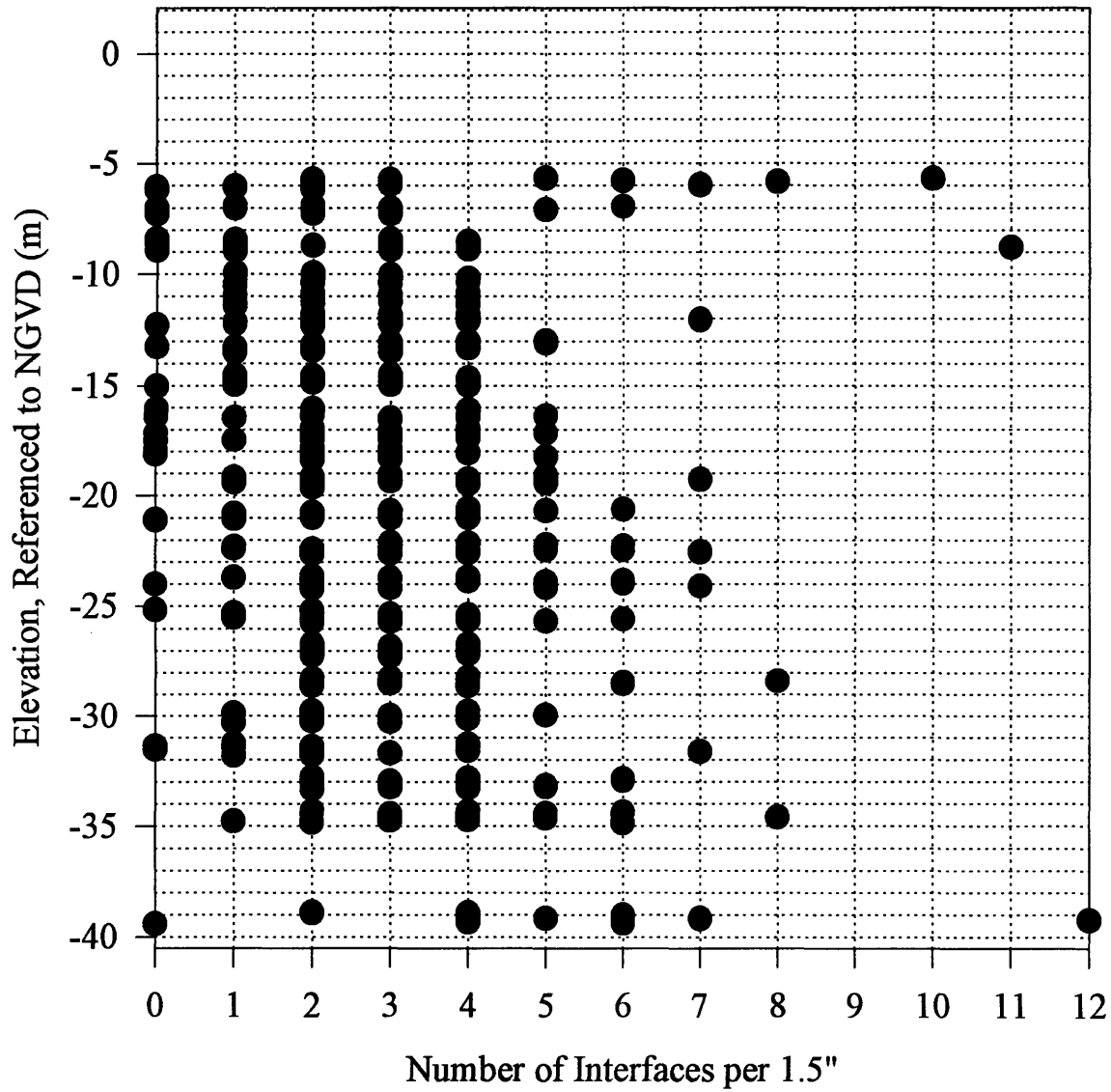


Figure 6.3 Layer Interface Distribution over the Deposit of Boston Blue Clay at Station 246, as Determined by the Number of Interfaces (per 1.5 Inches) seen on the Radiographs.

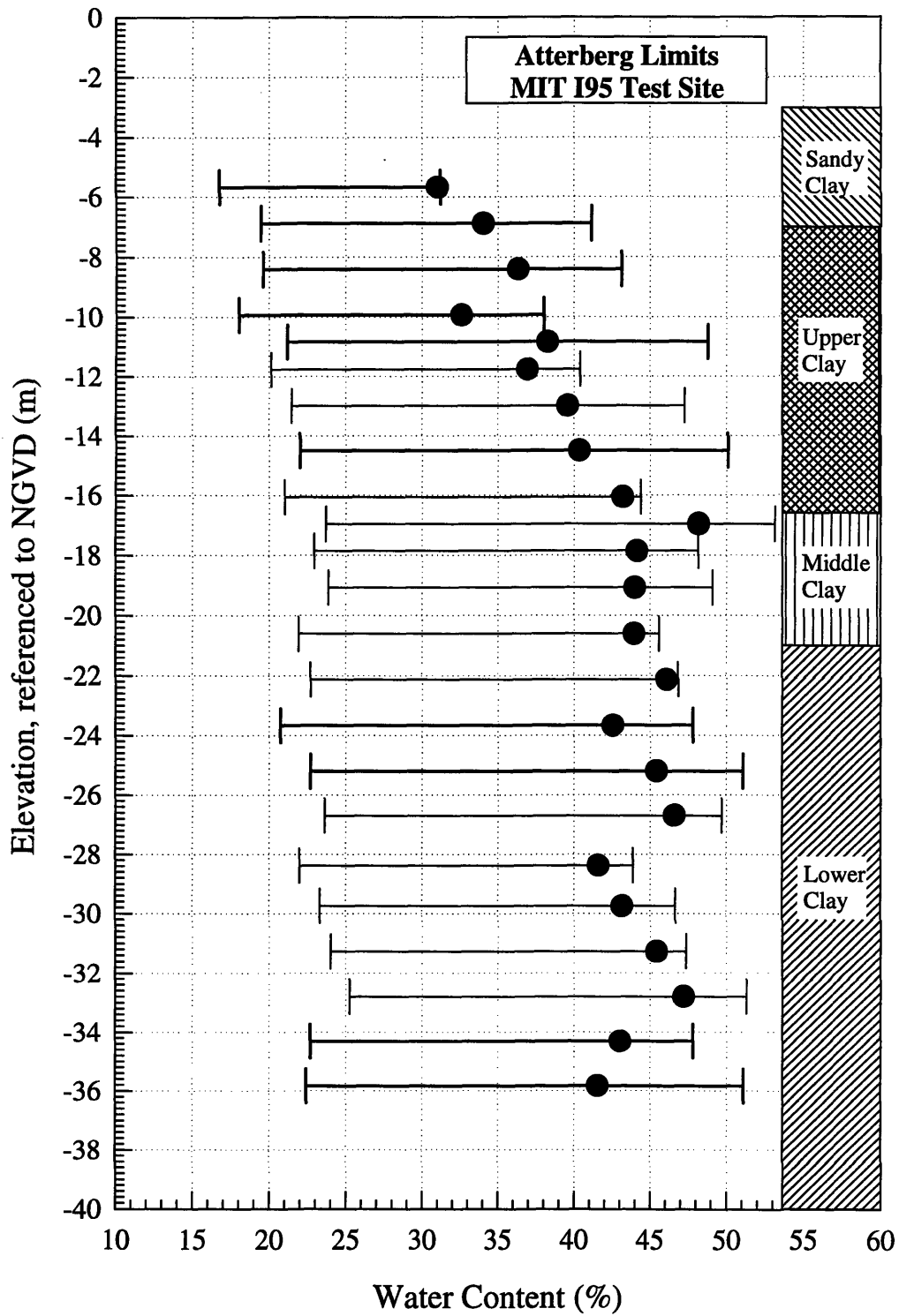


Figure 6.4 Plastic Limit, Liquid Limit, and Natural Water Content of Undisturbed Soil Samples obtained during the 1996 Field Program.

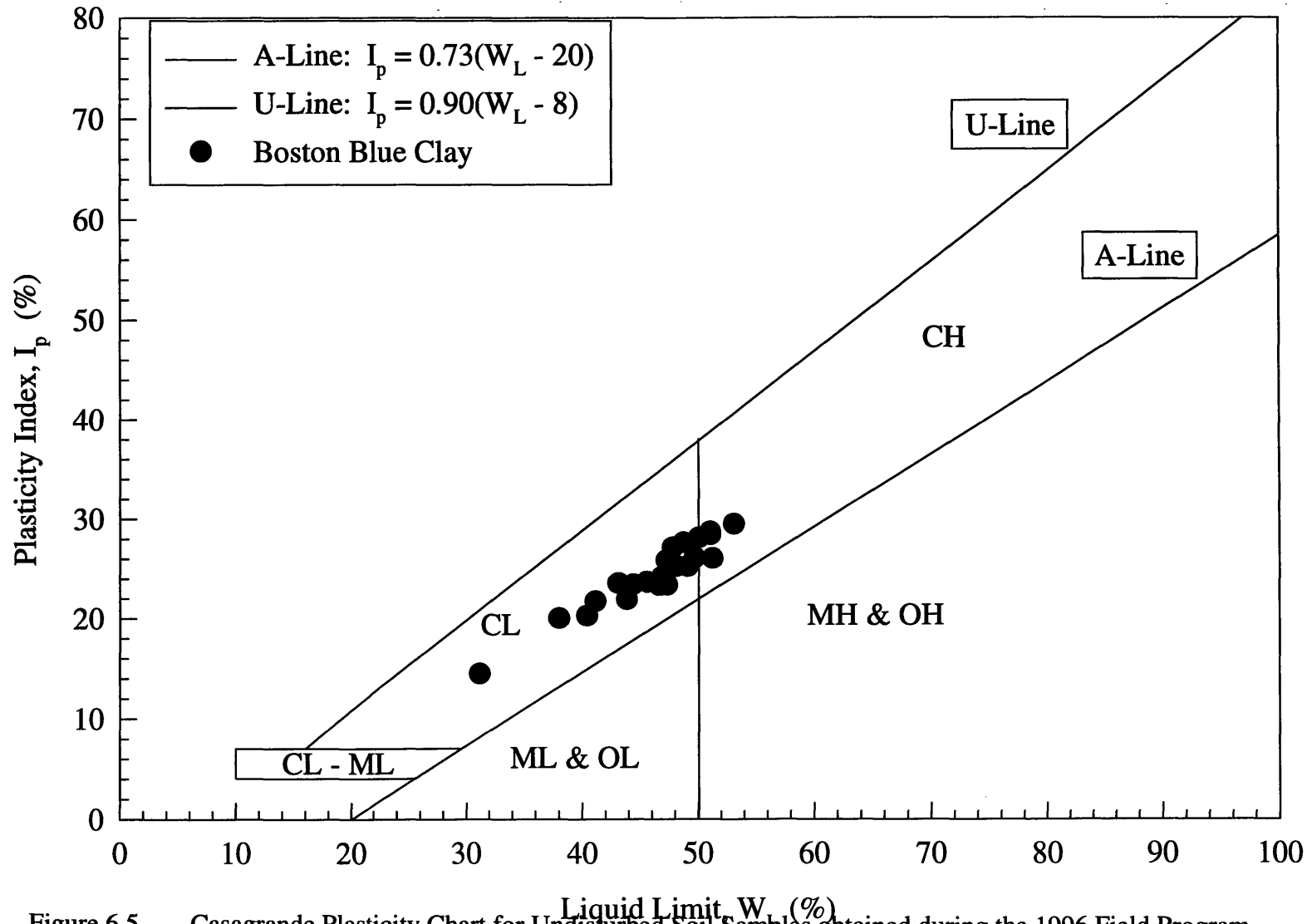


Figure 6.5 Casagrande Plasticity Chart for Undisturbed Soil Samples obtained during the 1996 Field Program.

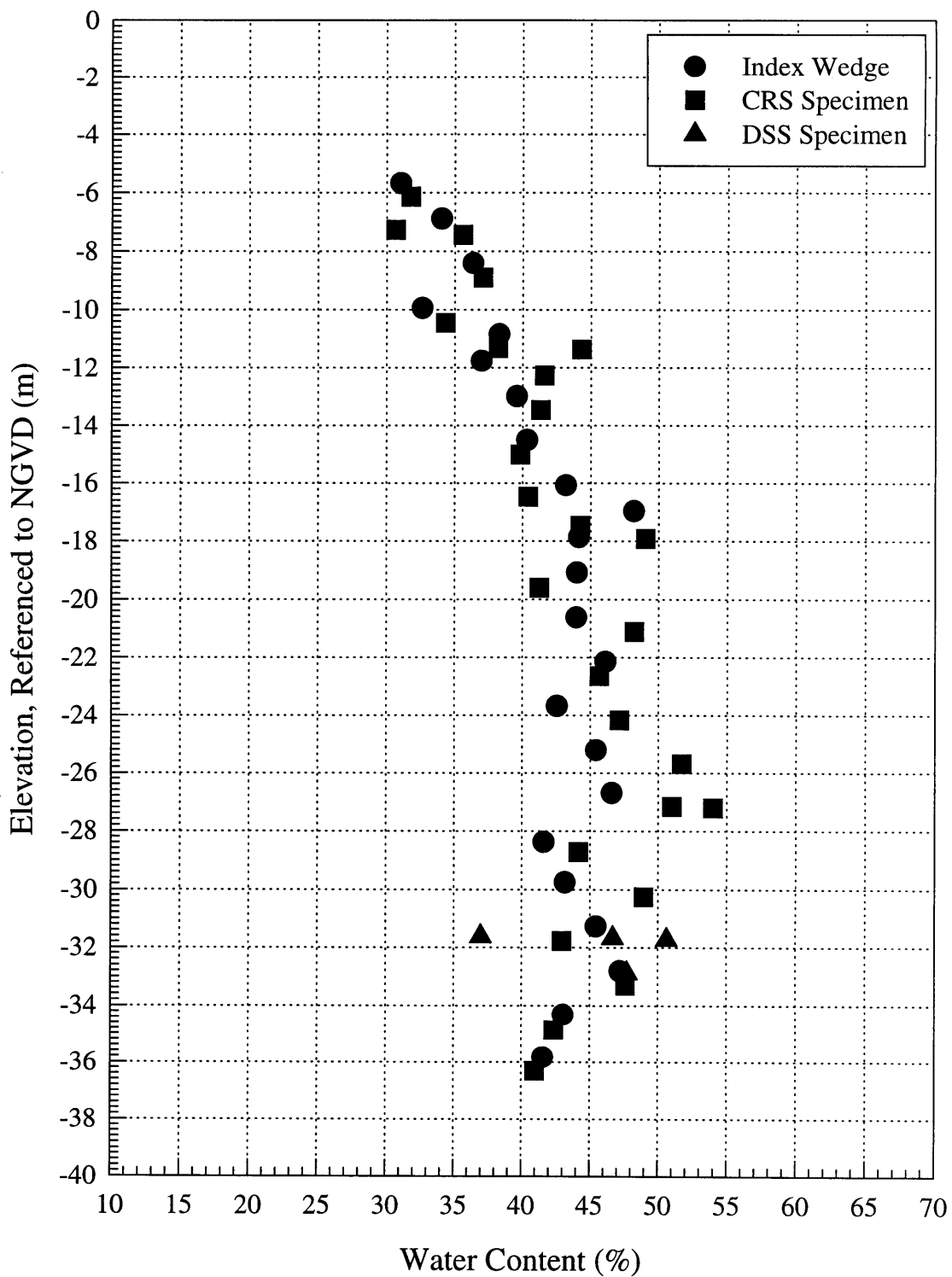


Figure 6.6 Water Content Profile for Undisturbed Soil Samples obtained during the 1996 Field Program at Saugus (Station 246).

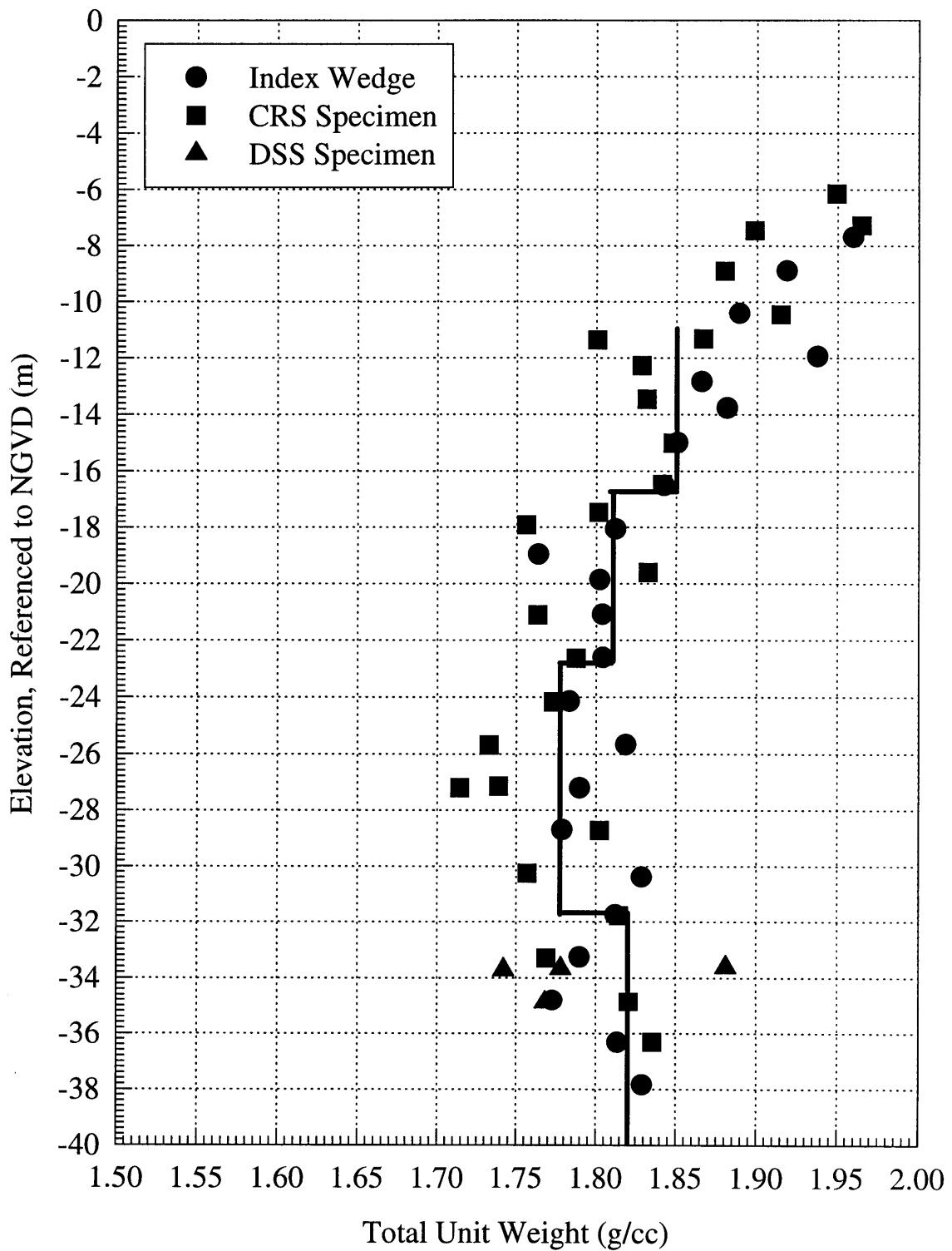


Figure 6.7 Total Unit Weight Profile and Interpreted Values of Total Unit Weight from Undisturbed Soil Samples obtained during the 1996 Field Program at Saugus (Station 246).

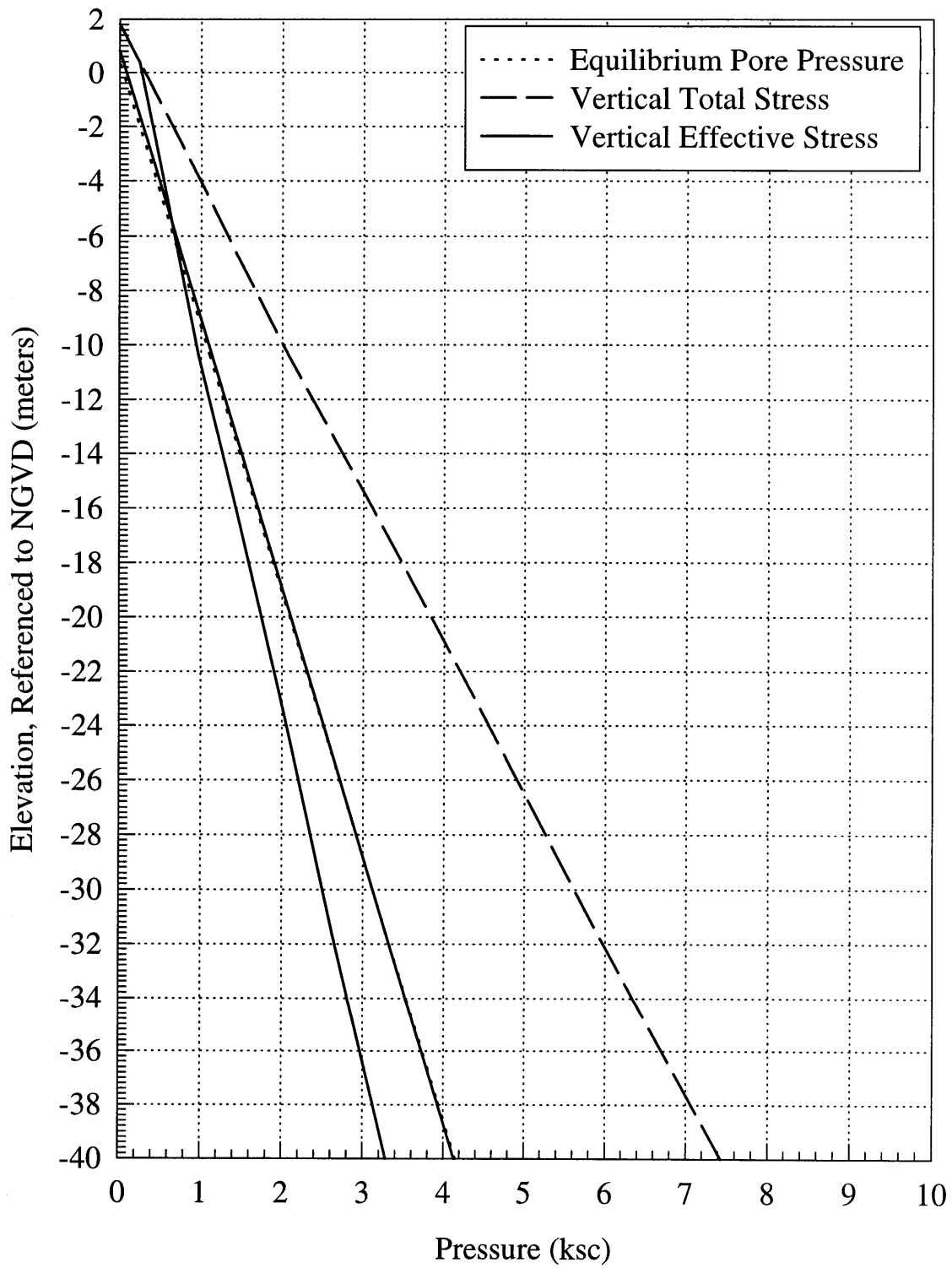


Figure 6.8 In Situ Stress Profile.

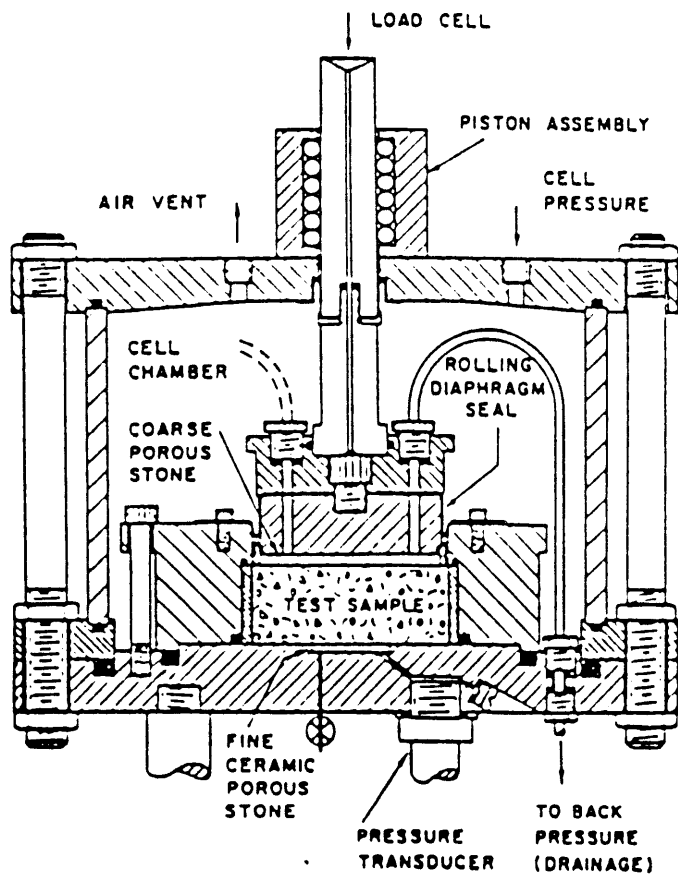


Figure 6.9 Schematic of Constant Rate of Strain Consolidation (CRSC) Device (After Wissa, 1971).

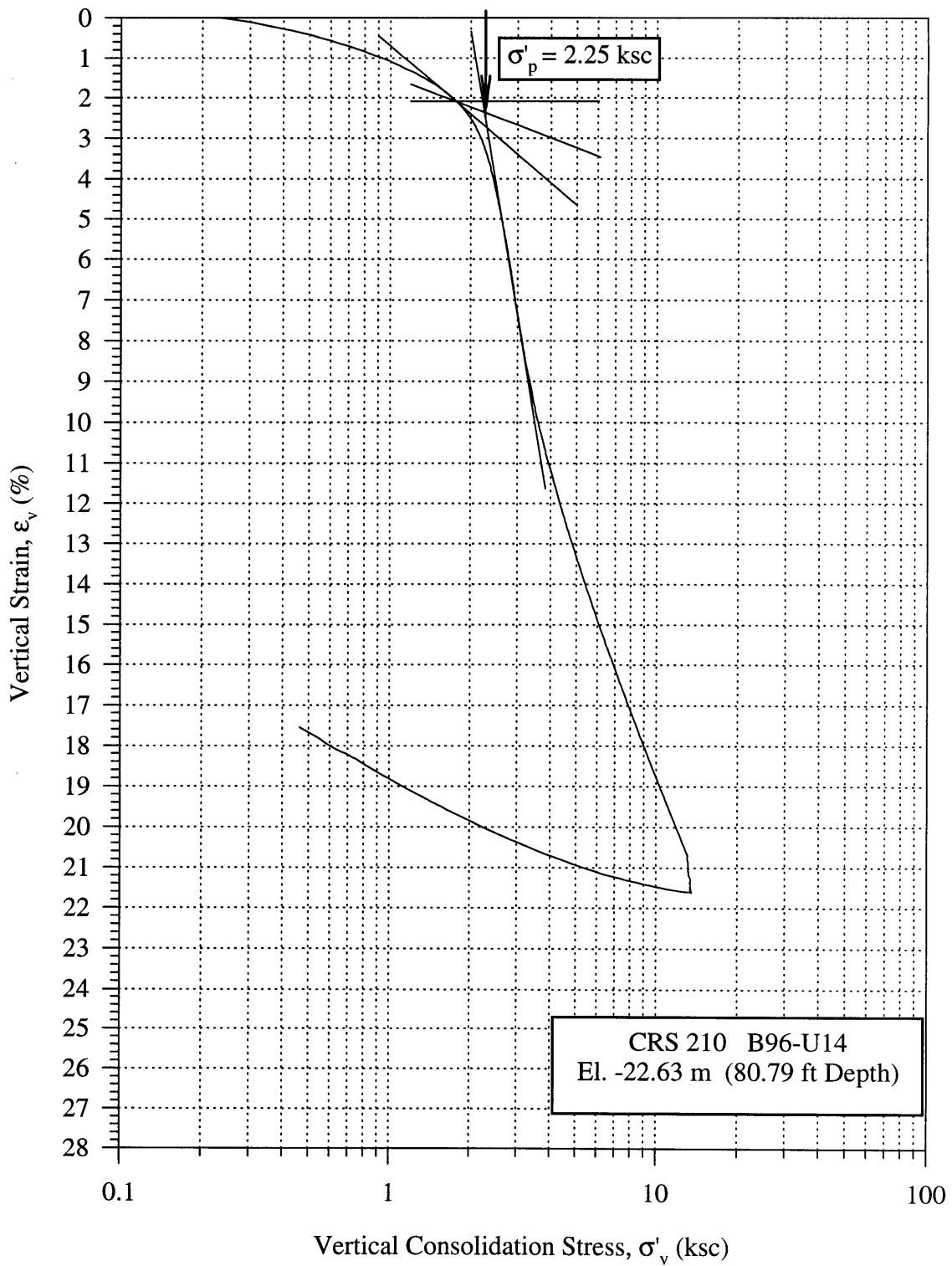


Figure 6.10 Example Construction of Casagrande Technique for Preconsolidation Pressure Performed on Data from Test Number CRS210.

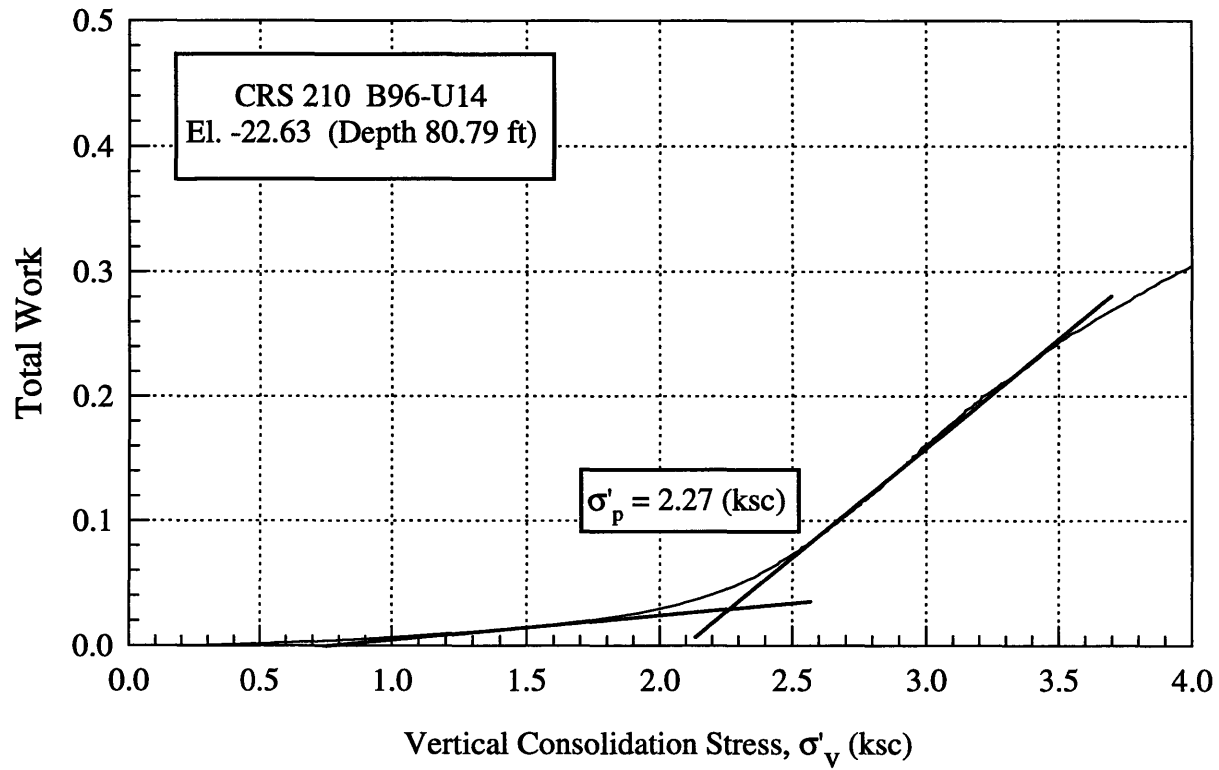


Figure 6.11 Example Construction of Strain Energy Technique for Preconsolidation Pressure Performed on Data from Test Number CRS210.

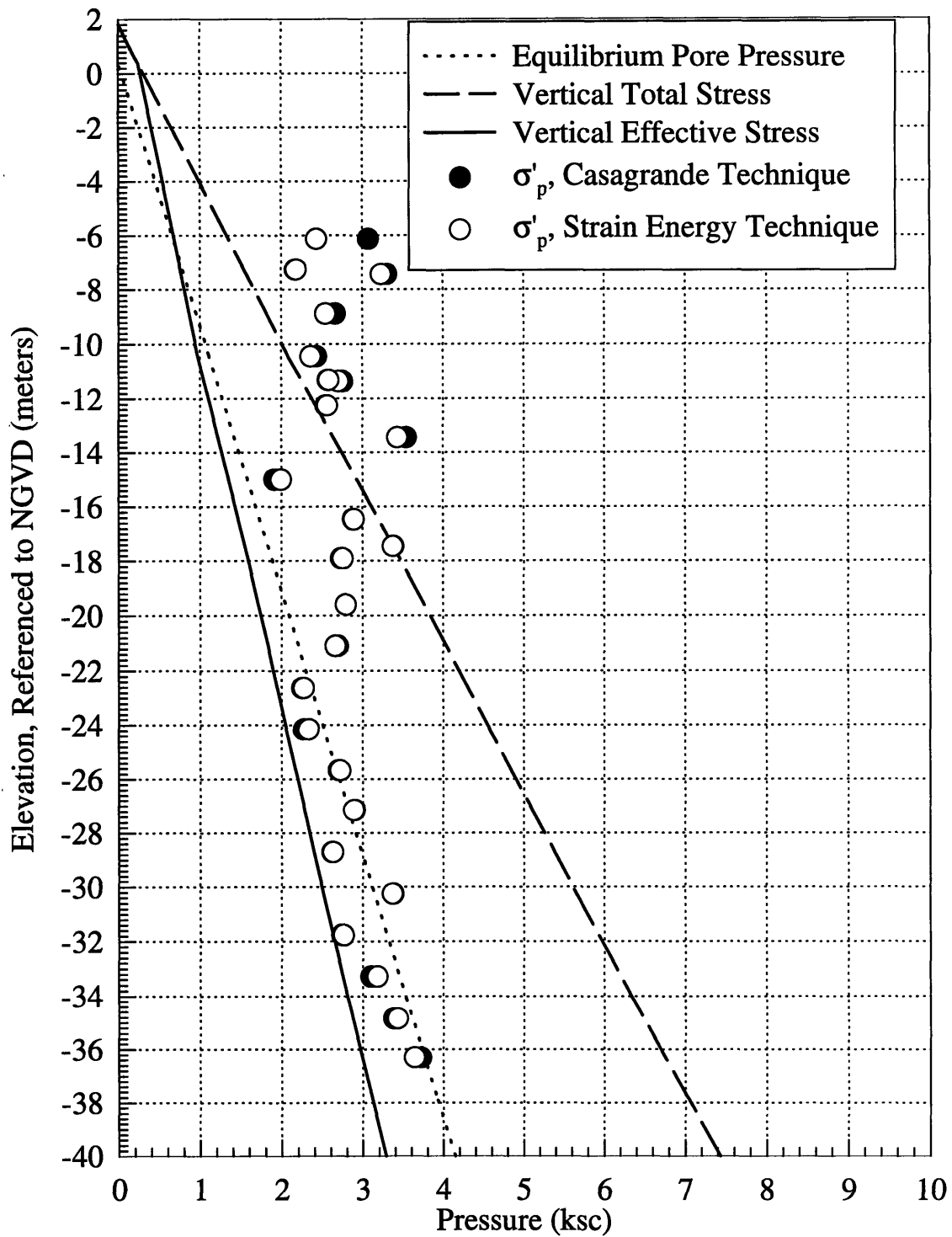


Figure 6.12 Preconsolidation Profile Determined from CRSC Tests Performed on Undisturbed Soil Samples obtained during the 1996 Field Program.

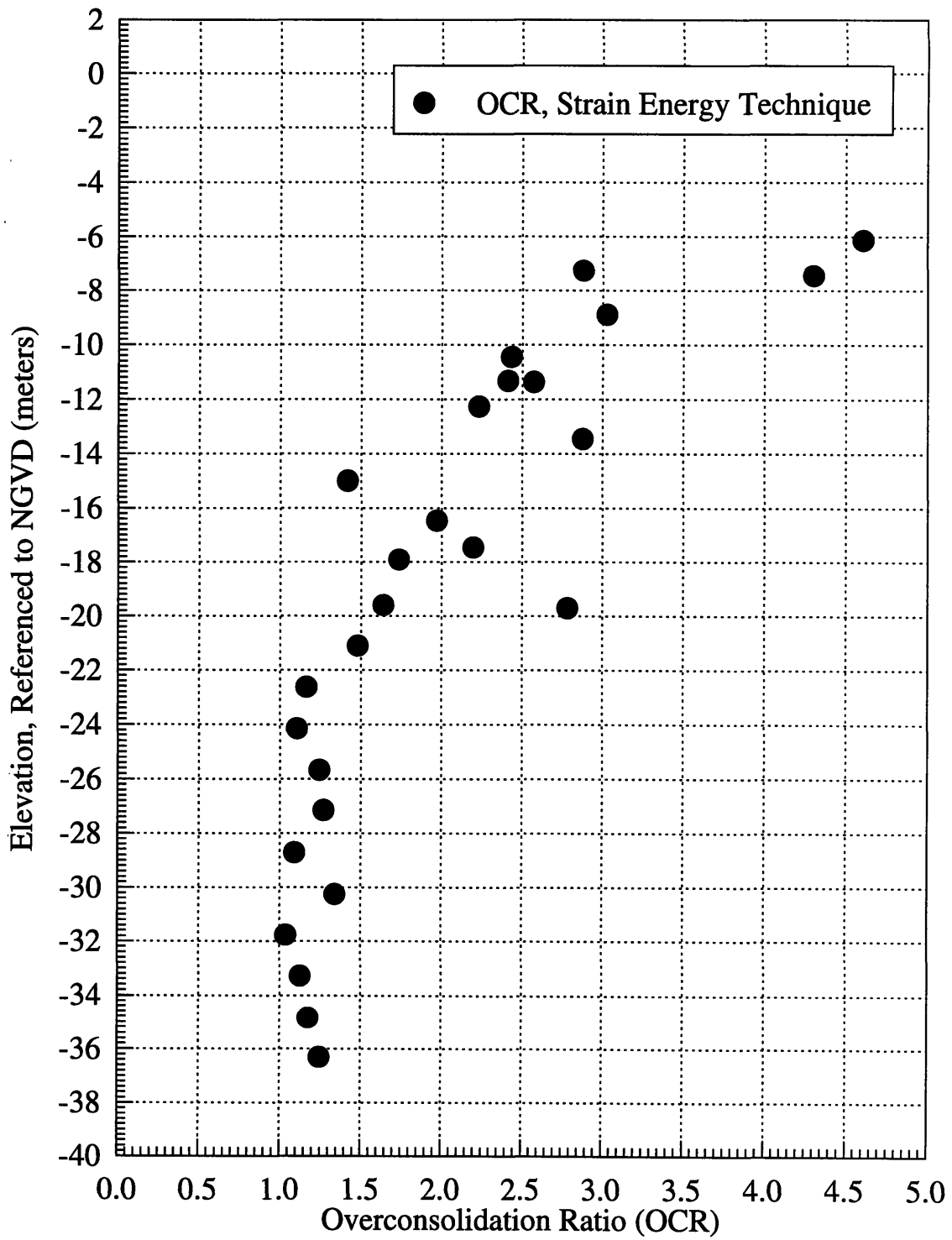


Figure 6.13 Overconsolidation Ratio (OCR) Profile.

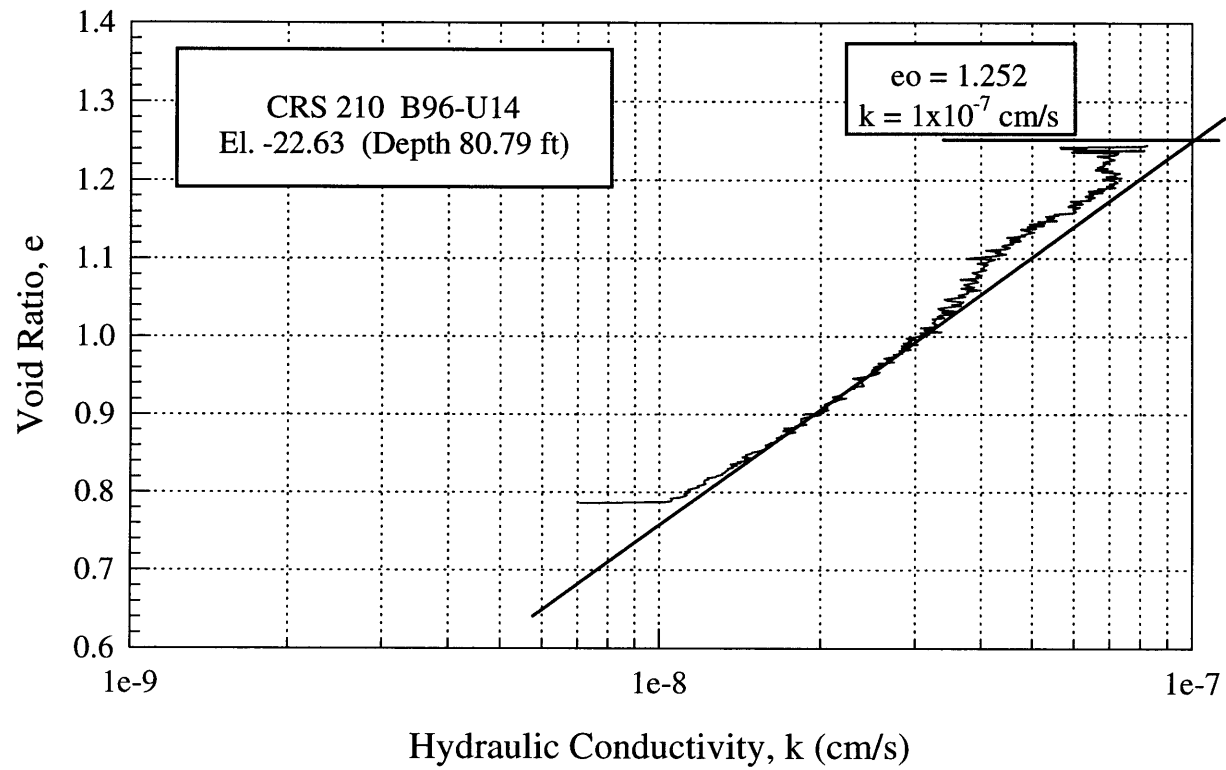


Figure 6.14 Example Construction of Determination of In Situ Hydraulic Conductivity Performed on Data from Test Number CRS210.

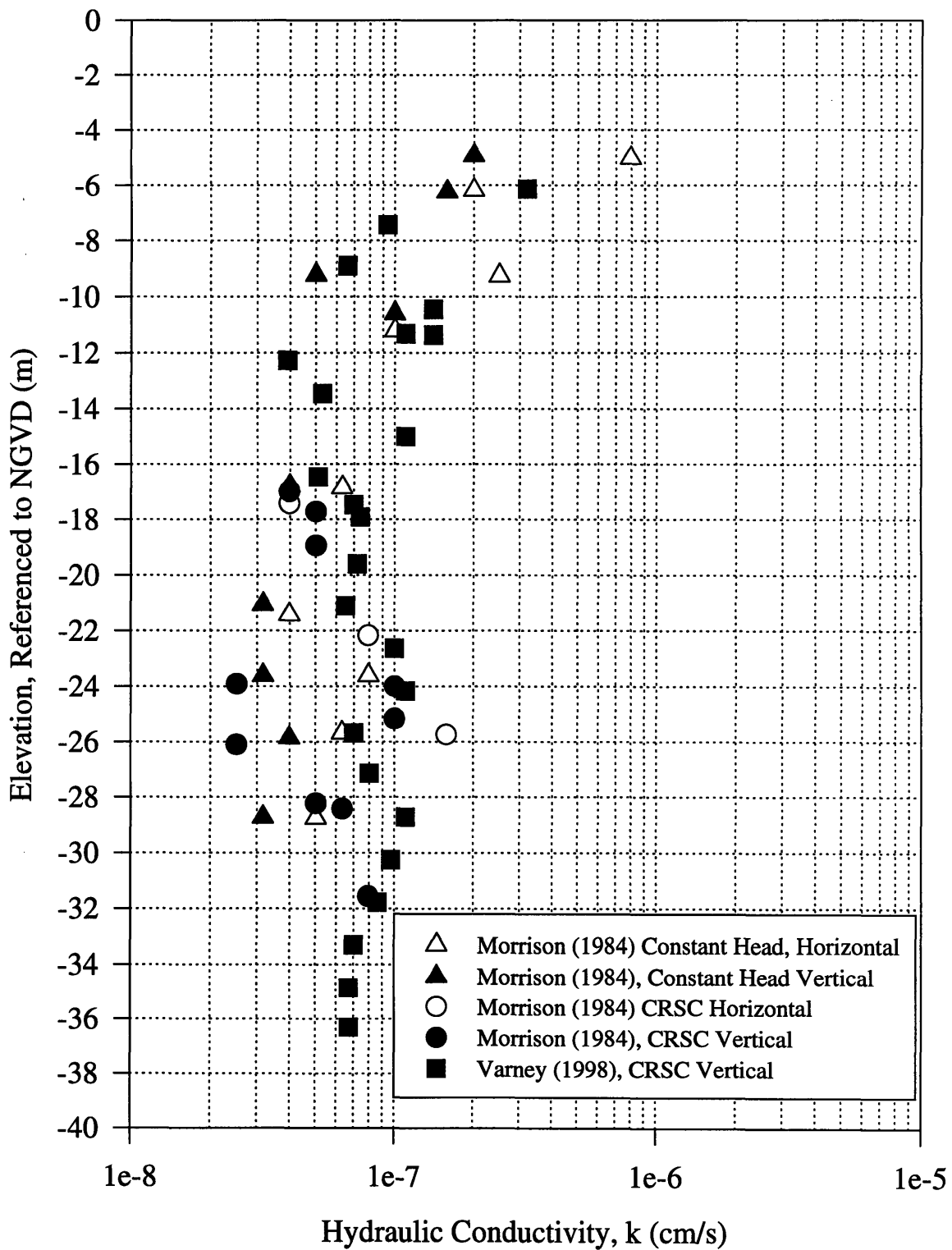


Figure 6.15 Summary of In Situ Hydraulic Conductivity Values for Undisturbed Samples at Saugus (Station 246) from the 1984 and the 1986 Field Programs.

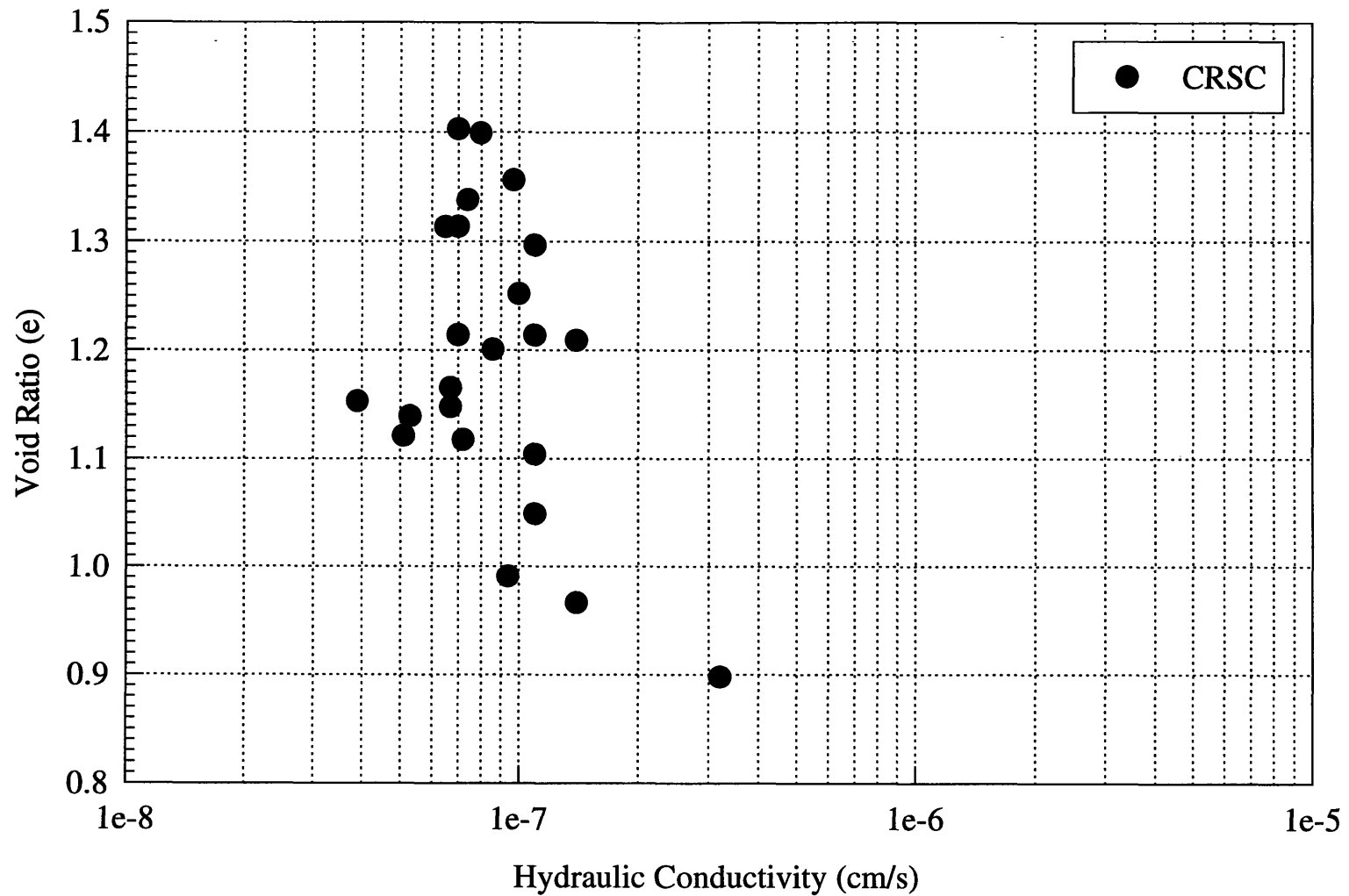


Figure 6.16 Void Ratio Versus Hydraulic Conductivity Measured from CRSC Tests Performed on Undisturbed Soil Samples at Station 246 (Varney, Germaine, & Ladd, 1998).

7. INTERPRETATION

The two main parameters to be determined from dissipation measurements are the in situ pore pressure (u_0) from partial dissipation records and the hydraulic conductivity (k). Section 7.1 provides the notation used in this chapter. Sections 7.2 and 7.3 evaluate u_0 and k , respectively from the test data obtained at Saugus and compare results from different devices and interpretation methods. Sections 7.4 through 7.7 consider the effects of other factors such as installation rate and installation pore pressure on the interpretation of k .

7.1 Notation

A number of symbols are used in this chapter in order to interpret and compare values of in situ hydraulic conductivity and equilibrium pore pressure by a number of methods. For ease of the reader, these symbols are presented here, along with a short description of their meaning:

k	hydraulic conductivity.
k_{conc}	hydraulic conductivity determined by the Concurrent Matching Method.
k_{conc-}	upper bound value of hydraulic conductivity determined by the Concurrent Matching Method.
k_{conc+}	lower bound value of hydraulic conductivity determined by the Concurrent Matching Method.
k_{lab}	hydraulic conductivity measured in the laboratory.
k_{R2}	hydraulic conductivity determined by the Goodness Of Fit method.
k_{t50}	hydraulic conductivity determined by the T ₅₀ Matching Method.
k_{t50ui-}	hydraulic conductivity determined by the T ₅₀ Matching Method using the installation pore pressure minus a standard deviation of the pore pressure measured during penetration.
k_{t50ui+}	hydraulic conductivity determined by the T ₅₀ Matching Method using the installation pore pressure plus a standard deviation of the pore pressure measured during penetration.
k_{t50uo-}	hydraulic conductivity determined by the T ₅₀ Matching Method using the dissipated pore pressure minus a standard deviation of the pore pressure measured during full dissipation.
k_{t50uo+}	hydraulic conductivity determined by the T ₅₀ Matching Method using the dissipated pore pressure minus a standard deviation of the pore pressure measured during full dissipation.

$k_{t50uipt}$	hydraulic conductivity determined by the T_{50} Matching Method and varying the initial dissipation point.
u	pore pressure.
u_{diss}	dissipated pore pressure measured from full dissipation tests.
u_{diss-}	dissipated pore pressure minus one standard deviation measured during full dissipation tests.
u_{diss+}	dissipated pore pressure plus one standard deviation measured during full dissipation tests.
u_i	installation pore pressure, measured at the end of penetration/start of dissipation.
u_{i-}	installation pore pressure minus one standard deviation in the value of pore pressure measured during penetration.
u_{i+}	installation pore pressure plus one standard deviation in the value of pore pressure measured during penetration.
u_o	in situ pore pressure measured by the piezometers.
u_{pen}	average pore pressure measured during penetration.

7.2 Determination of In Situ Pore Pressure (u_o)

The in situ pore pressure can be determined in a number of ways using dissipation data. This section evaluates u_o by three methods: 1) complete dissipation records, 2) Inverse Time ($1/t$) Extrapolation method, and 3) cross-correlation of dissipation records (Two Point Intersection Method) at different porous element locations as proposed by Sutabutr (1998) and Whittle et al. (1997).

7.2.1 Full Dissipation

Figure 7.1 illustrates the calculation of the fully dissipated pore pressure, u_{diss} , (± 1 SD) from one of the complete dissipation experiments performed at Saugus (Piezocone 790 at El. -29.91 m). Results of similar calculations for each of the devices and test depths is shown in Table 7.1¹. The standard deviation in u_{diss} for each dissipation curve reflects the amount of long term noise in the measurements. In general, the piezocones have considerable more noise.

The ratio of measured to estimated in situ pore pressure from the various devices follows:

¹ These measured pore pressures are also compared with reference values of u_o , determined from piezometers.

u_{diss}/u_o :

Piezoprobe 62	1.06±0.06
Piezoprobe 63	1.02±0.03
Piezocone 790	1.03±0.07
Piezocone 881	1.17±0.04
MIT Piezocone	1.00±0.05

Figure 7.2a compares the normalized dissipated pore pressures for Piezoprobes 62 and 63. Piezoprobe 62 consistently measures slightly higher values of u_{diss} than Piezoprobe 63 at the same tip elevation, while Piezoprobe 63 consistently has a smaller error band associated with the measurement of u_{diss} . This behavior is believed to be due to the integrity of the individual measurements². Both of the piezoprobes were obviously less influenced by electrical interference than the piezocone or the MIT Cone. The time required for full dissipation ranges from 1×10^5 to 3×10^5 seconds (i.e. 28 to 83 hrs).

Figure 7.2b shows the same data for the two standard piezocones. Piezocone 790 had fewer electrical connection problems than Piezocone 881. However, if the value at El. -17.8 m (Depth 65 ft) is ignored, the device performance is comparable to the piezoprobes with a higher average value. In contrast, the measurements from Piezocone 881 are significantly higher than the estimated range of u_o , indicating a zero offset problem. Piezocone 881 and Piezoprobe 62 consistently equilibrate at values which are higher than the in situ equilibrium pore pressure. Piezocone 881 is also noticeably affected by electrical noise at the longer dissipation times. Piezocone 790 required fewer electrical repairs and exhibited a smaller variation indicated by the standard deviation in the dissipated pore pressures and measures in situ pore pressures comparable to those measured by the piezoprobes. The time required for full dissipation ranges from 1×10^5 to 3×10^5 seconds.

Figure 7.2c shows the ratio of measured to estimated in situ pore pressures for the MIT Piezocone. The MIT Cone was less influenced by electrical noise than the piezocones, with the one exception of the installation at El -30 meters (105 ft depth) where there was a repeating jump in the MIT Piezocone data occurring throughout the

² The transducer in Piezoprobe 62 had frequent electrical problems that required repair.

entire dissipation record. The time required to achieve full dissipation is 1×10^5 to 3×10^5 seconds.

The time required for full dissipation does not vary significantly between the devices, the geometry types, or the elevation. Piezoprobe 63, Piezocone 790, and the MIT Piezocone measure dissipated pore pressures within 3% of the equilibrium pore pressures determined by the piezometers.

With the notable exception of Piezocone 881, the ratios of measured to estimated in situ pore pressures for all devices (u_{diss}/u_o) are in the range 1.00 to 1.06. The standard deviation indicates that the uncertainty in the measured dissipated pore pressure is due to electrical noise which is thoroughly discussed in Section 4.5.1.

7.2.2 Inverse Time (1/t) Extrapolation

The inverse time (1/t) method has been used to estimate the in situ pore pressure from incomplete dissipation records. The method involves plotting the measured pore pressure as a function of inverse time (on a natural scale). The equilibrium pore pressure ($u_{1/t}$) is estimated by extending a tangent line from the end of the dissipation record and finding the intersection pore pressure at $1/t = 0$. Figure 7.3a through c show an example of the 1/t construction, using the data from Piezoprobe 63 at El. -30 m (105 ft depth) as an example. Clearly, as the length of the dissipation record increases, the estimate of u_o becomes more reliable. Figure 7.3 a, b, and c show that the inverse time dissipation curve is non-linear at enlarged inverse time scales (1/t) and hence the 1/t extrapolation always overestimates u_{diss} . This particular dissipation curve yields a rise in the interpreted pore pressure during the range of 1/t equal to 0.002 to 0.

Figure 7.4 shows the plot of pore pressure versus 1/t generated from model predictions data for Piezoprobe 63 at -33.11 meters (115 ft depth). This curve also has a rise in pressure in the same range discussed above, but is less pronounced than the measured curve. This difference changes the ratio of t/t_{50} determined to predict the installation pore pressure within a 10% error and is the reason both a theoretical and measured t/t_{50} ratio are given below.

The error is defined in terms of the increment of pore pressure determined by the 1/t method ($u_{1/t}$) from the dissipated pore pressures normalized by the increment of the

installation pore pressure from the fully dissipated value, i.e. $(u_{1/t}-u_{diss})/(u_i-u_{diss})$. This error is defined relative to the dissipated pore pressure value rather than the equilibrium pore pressure determined by piezometers in order to evaluate the ability of the in situ pore pressure interpretation method rather than the ability of the individual device³. Appendix D presents tabulated values of predicted dissipated pore pressures using the 1/t method for the devices at various points in the dissipation curve. Figure 7.5 through Figure 7.7 present these values as a plot of the error versus the ratio of the time of the elapsed time in the dissipation record normalized by the time at 50% consolidation determined for the dissipation record for the particular device (t/t_{50}).

Figure 7.5 shows the theoretical and measured dissipated pore pressure ratios versus normalized time (t/t_{50}) for the piezoprobes. The theoretical curve lies above the measured data, indicating that the measured dissipation rate is quicker than the theoretical predictions. The measured data also plateaus and rises again, indicating that the plateau and rise in the measured data are more significant than predicted by the theoretical model. The theoretical data always predicts pore pressures higher than the in situ pore pressure, while the measured data occasionally underpredict in situ pore pressures between t/t_{50} ratios of 3 and 8. The error approaches 10% at a normalized time of 3 for the measured data and 6 for the model data at El. -33 m. The average t_{50} for the piezoprobes is 95 seconds, indicating that the piezoprobes require 285 seconds as determined by the measured data and 570 seconds as indicated by the theoretical data to estimate the in situ pore pressure to within 10 percent of the dissipated value.

Figure 7.6 shows the results for the piezocone dissipated pore pressure ratio. The theoretical curve lies above the measured data, with the exception of one set of data for each of the piezocones. Both sets are performed on the dissipation test at El. -17.8 m, while the theoretical prediction is performed for El. -33 m. Comparing the theoretical data to the measured data at El. -33 m indicates that the predicted dissipation rate is slower than the measured, as indicated for the piezoprobes. The measured and theoretical data predict pore pressures less than the in situ pore pressure. The piezocones predict the

³ The device ability is demonstrated by the equilibrium pore pressure determined from full dissipation records compared to the in situ pore pressure value determined from piezometers.

in situ pore pressure to within 10 percent at a time ratio of 3.5 for the measured data and 5.5 for the theoretical data. The average t_{50} for the piezocones is 1677 seconds, requiring a time of 5870 seconds as indicated by the measured data and 9224 seconds as indicated by the theoretical data to predict the pore pressure within the acceptable 10 percent band.

Figure 7.7 presents the $1/t$ results for the MIT Cone. The theoretical curve lies within the measured data, indicating that the predictions provide an average result. The measured data also frequently underpredicts the in situ pore pressure. The pore pressure can be predicted within a 10% error at a t/t_{50} ratio of 7 as determined by the measured data and theoretical data. The average t_{50} for the MIT Cone is 590 seconds, indicating an average requirement of 4,130 seconds to predict the dissipated pore pressure within 10%.

7.2.3 Two Point Intersection Method

Whittle et al. (1997) propose a method for cross-correlating the dissipation records measured at two (or more) locations on the surface of the tapered probe. Figure 7.8 shows that the dissipation behavior predicted for the tapered probe is separated into 3 stages. Stage I follows the dissipation of a simple pile having an equivalent radius. At the start of Stage II, the rate of dissipation slows down as the pressure from the upper shaft moves towards the measurement point. Finally, Stage II occurs when the dissipation is governed by the dissipation of the larger diameter section. Referring to Figure 7.9, the equilibrium pore pressure is estimated by comparing data measured at the tip (A) in Stage II with the response at a point above the taper, point C or point P. During undrained penetration, the initial excess pore pressure at C (or P) are significantly higher than at A, while dissipation at C (or P) is controlled by the radius of the drill rod (R_2). The rate of pore pressure dissipation in Stage I is always larger at the tip location than at point C (or P), due to the smaller radius rod. In contrast, the rates of pore pressure change in Stage III are always higher at point C (or P) (i.e., as the response at A is no longer linked to the tip geometry).

Based on these general observations, one method of comparing the response at A and C (or P) is through the magnitudes of the normalized dissipated pore pressure, $(u_i - u)/\sigma'_{vo}$ at the two points. Figure 7.9 shows that as a result of the variation in dissipation rates, a characteristic intersection point is created where the dissipated pore pressures, $(u_i -$

u) are identical for points A and C. This intersection point occurs within Stage II for the probe, and corresponds to a reference point on the predicted dissipation curve for $U_C = 0.11$ (for BBC(R), OCR = 2). The value of the excess pore pressure ratio is dependent on the soil type, stress level, and geometry of the device. The equilibrium pore pressure can then be estimated from incomplete dissipation records at A and C (or P) providing the intersection point is reached. Ideally, the intersection point can be found by measuring pore pressures at two points on the same device (i.e. points A and C). However, similar principles apply when comparing dissipation results from the tapered piezoprobe and standard piezocone devices (points A and P). Figure 7.10 through Figure 7.15 illustrate the estimation of u_o from the two point intersection method from measurements at El. -18 m to -33 meters (65 ft to 115 ft depth)⁴. The dissipation pore pressure increment ($u_i - u$) is plotted rather than the normalized values as illustrated in the two figures. Each figure contains the results of two piezoprobe and two piezocone tests. Hence, the data generate four intersection points, from which the minimum and maximum values of t_p and $(u_i - u)_p$ are reported in Table 7.2.

In all cases, the theoretical degree of dissipation (U_p) at the intersection point was used to interpret equilibrium pore pressure, u_{2pt} . This value is then compared to the dissipation pore pressure to eliminate errors associated with the electrical connections and calibrations. The Two Point Intersection Method predicts the following average ratios:

$$(u_{2pt} - u_{diss}) / (u_i - u_{diss}):$$

Piezoprobe 62	-0.01 ± 0.07
Piezoprobe 63	-0.02 ± 0.02

The overall average ratio is -0.01 with a standard deviation of 0.04. The measured time required to achieve the intersection condition ranges from $t_p = 517$ sec to 7225 sec (0.05 to 2 hrs) with an average of 3543 seconds (0.98 hrs).

7.2.4 Comparison of Methods For Estimating u_o

The field testing program measured the full dissipation of penetration induced pore pressures, requiring monitoring periods of up to 28 to 83 hrs. At full dissipation, the measured data (u_{diss}) are on average within 6% of the estimated values from piezometer

⁴ The measurement for Piezoprobe 62 at El. -27 m was excluded from this calculation.

monitoring data (at three depths). The full dissipation requires the longest measurement time of a minimum of 28 hours, as discussed in 7.2.1. However, this value varied with device due to uncertainty in calibration zeroes and electrical noise. The dissipated pore pressure was within 15% of the determined equilibrium pore pressure for the piezocones, within 10% for the piezoprobes, and generally within 5% for the MIT Piezocone.

The Two Point Intersection Method compares pore pressure dissipation measured at the tip of the tapered piezoprobe and at the base of the standard piezocone. Table 7.3 shows that times required to achieve the intersection condition are $t_p = 3600 \pm 2100$ seconds. The Two Point Intersection method predicts an average ratio $(u_{2pt} - u_{diss}) / (u_i - u_{diss}) = -0.01 \pm 0.04$. Hence, the Two Point Intersection Method can determine u_{diss} very precisely but requires a model prediction using the device geometry and the specific soil conditions. This may be a disadvantage in practice.

The $1/t$ method can be compared to the Two Point Intersection method by using the inverse time predictions at comparable dissipation times. This was done by using the range in match point times (t_p) for each elevation and computing an equilibrium pore pressure ($u_{1/t}$) for each device. Since the match point limits are established by intersection of both probes and cones, the predictions for these devices are associated with particular times. The MIT Piezocone was not used for the Two Point Intersection Method and therefore was interpreted using both time values. These predictions are presented in Table 7.3 along with the corresponding values of t_p/t_{50} for comparison to Figure 7.5, 7.6, and 7.7. The average values of the ratio $(u_{1/t} - u_{diss}) / (u_i - u_{diss})$ at comparable times to the Two Point Intersection Method are given below.

$(u_{1/t} - u_{diss}) / (u_i - u_{diss})$ at the Two Point Intersection Method Time:

Piezoprobes	0.10 ± 0.01
Piezocones	0.24 ± 0.12
MIT Piezocone	0.14 ± 0.08

Therefore, the Two Point Intersection Method provides a precise estimation of the equilibrium pore pressure in shorter times than the Inverse Time Method.

7.3 Determination of Hydraulic Conductivity

Field determinations of hydraulic conductivity (k) are based on model dissipation predictions presented in Chapter 2. Three methods are used here to determine hydraulic conductivity from the field data: i) the T_{50} Matching Method, ii) the R^2 , Goodness Of Fit Method; and iii) the Concurrent Matching Method. The hydraulic conductivity results for the Goodness Of Fit Method and the Concurrent Matching Method are described in Whittle et al. (1997) and Sutabutr (1998) and will be summarized here. All three methods for determining the hydraulic conductivity are then compared with the measurements of hydraulic conductivity from laboratory tests.

7.3.1 T_{50} Matching Method

The T_{50} matching method is the conventional procedure which matches the measured and model normalized pore pressure ratios [i.e., $(u-u_o)/(u_i-u_o)$] at 50% dissipation. Determination of the time for the measured data to reach 50% dissipation (t_{50}) requires a measurement of the installation pore pressure and an estimation of the dissipated pore pressure. The hydraulic conductivity is computed by matching the model time factor for 50% dissipation (T_{50}) to t_{50} . The equation for hydraulic conductivity (k) is:

$$k = \frac{T_{50} \gamma_w R_2^2}{\sigma' t_{50}} \quad \text{Equation 7.1}$$

where T_{50} is the model time factor, which is a function of probe geometry, in situ stress history, and soil properties, γ_w is the unit weight of water, R_2 is the radius of the shaft of the penetrometer, σ' is the in situ mean effective stress, and t_{50} is the elapsed time at 50% dissipation. This approach eliminates errors associated with prediction of the installation pore pressures $[(u_i-u_o)/\sigma'_{vo}]$ (Baligh, 1986b), and mitigates problems associated with uncertainties in measurements of u_i and u_o (after Levadoux & Baligh, 1986).

Two stress history profiles are used at this site. (Figure 7.16, Ladd et al., 1994). The values of T_{50} for each device for each test location were determined for each stress profile by Sutabutr (Whittle et al, 1998) and are included in Table 7.4

Table 7.4 presents the values of hydraulic conductivity determined by the T_{50} method for the two selected stress history profiles. Figure 7.17 presents a plot of elevation versus hydraulic conductivity predicted from the T_{50} method for the piezoprobes. Profile 1 consistently predicts a lower hydraulic conductivity than profile 2. This difference increases with OCR. In general, the values above El. -22 m suggest larger variability in the deposit. Below El. -22 m, the hydraulic conductivity predicted by the piezoprobes is constant with depth. For Profile 1, the average hydraulic conductivity below -22 m is $(3.65 \pm 0.44) \times 10^{-8}$ cm/s.⁵ Above this elevation, the hydraulic conductivity is lower with more variability.

Figure 7.18 presents the hydraulic conductivity for the piezocones interpreted from the T_{50} Matching Method. There is a small difference between the hydraulic conductivity predicted by this method using the two stress history profiles. Below El. -22 m, this difference is larger than the probes. The two predictions at El. -18 m and -21 m are nearly identical. As with the piezoprobes, the largest difference between the two predictions occurs in the upper layers (above El. -17 m). Below El. -22 m, the piezocone predicts a constant hydraulic conductivity $(2.68 \pm 0.28) \times 10^{-8}$ cm/s which is 75% of the probe value.

Figure 7.19 presents the hydraulic conductivity interpreted from the T_{50} Matching Method for the MIT Piezocone. Below El. -22 m, the difference between hydraulic conductivity values predicted by the two stress profiles is identical to the difference predicted using the piezocones. The MIT Cone also predicts a clear trend of increasing hydraulic conductivity (by 60%) with depth below El. -22 m. At El. -24 m, the predicted hydraulic conductivity is equivalent to that predicted by the piezocones, while the test at El. -33 m predicts a hydraulic conductivity slightly larger than the piezoprobe. Above El. -22 m, the values of hydraulic conductivity predicted with the MIT Cone are scattered and larger than the those predicted for the lower deposit.

The average interpreted hydraulic conductivity from the T_{50} method for the 5 devices is $(3.1 \pm 0.7) \times 10^{-8}$ cm/s based on Profile 1. Figure 7.20 shows the T_{50} interpreted hydraulic conductivity for all 3 devices. The lowest predictions of the value of the

⁵ This neglects the measurement of Piezoprobe 62 at El. 27 m, as was explained previously.

hydraulic conductivity are obtained with the piezocones, while the MIT Piezocone and the piezoprobes yield higher values. This perspective clearly illustrates the consistency below El. -22 m and the variability above.

7.3.2 R² Goodness of Fit Matching Method

An alternative to the single-time fitting method (T_{50}) is to use a more formal goodness-of-fit calculation. In this case, the calculations seek the hydraulic conductivity which maximizes the correlation coefficient between the predicted and measured pore pressure dissipation ratios. Although this technique is rational and uses the entire dissipation data set (over a specified time interval), it biases the curve fit towards Stages II and III. As a result, k is more prone to errors associated with uncertainties in u_0 .

The hydraulic conductivity interpreted from the R² goodness of fit method was determined in Whittle et al (1997) using Profile 1 stress history parameters and simultaneously performing a goodness of fit calculations on the two curves.

Figure 7.21 illustrates the prediction of hydraulic conductivity using the Goodness Of Fit method for Piezoprobe 63 at El. -33 m (115 ft depth). Values are presented in Table 7.5 for the dissipation measurements using the Goodness Of Fit determination on individual curves⁶.

Figure 7.22 presents the hydraulic conductivity predicted by the Goodness of Fit method versus elevation for the piezoprobes. Piezoprobe 63 predicts a value of 3.2×10^{-8} cm/s at El. -13.30 m (depth 50 ft) and shows a trend of slight increasing with depth. Piezoprobe 62 also determines a trend of increasing hydraulic conductivity with depth with a value of hydraulic conductivity of 2.8×10^{-8} cm/s at El. -18.45 m (depth 65 ft) increasing to 4.2×10^{-8} cm/s at El. -33.08 m (depth 115 ft). The average hydraulic conductivity predicted below El. -22 m with the tapered piezoprobes is $(4.3 \pm 0.7) \times 10^{-8}$ cm/s. This is 18% higher and 60% more variable than the T_{50} Matching Method. Piezoprobe 63 was available for measurements in clay Layer C (at El. -13.2 and -14.8 m). The average value of hydraulic conductivity above El. -22 m is $(2.87 \pm 0.85) \times 10^{-8}$ cm/s,

⁶ Analysis performed by Mr. John Sutabutr (1/98).

indicating that the piezoprobe predicts a lower value of hydraulic conductivity in soil with higher OCR.

Figure 7.23 presents the predicted hydraulic conductivity using the goodness of fit method for the piezocones. Using this method, the piezocones consistently yield lower values of hydraulic conductivity with less overall variability as compared to the piezoprobes. The average and standard deviation for the piezocones below El. -22 m is $(3.70 \pm 1.04) \times 10^{-8}$ cm/s. This is 23% larger than the hydraulic conductivity by the T₅₀ Method and 14% less than the piezoprobe values using the Goodness of Fit Method. In the upper layers, the average and standard deviation increase to $(5.98 \pm 3.00) \times 10^{-8}$ cm/s, indicating that the predicted hydraulic conductivity with the piezocones increases with increasing OCR.

Figure 7.24 presents the predicted hydraulic conductivity using the goodness of fit method for the MIT Cone. The goodness of fit method for the MIT Cones predicts an average hydraulic conductivity of $(4.9 \pm 2.5) \times 10^{-8}$ cm/s. The results have no particular trend with depth which is contrary to the results using the T₅₀ Method. This seems to suggest that the shape of the curves do not match well with the model predictions.

Figure 7.25 shows the complete data set of hydraulic conductivity values using the Goodness Of Fit method for the three types of devices. The piezocones predict the tightest band of value for hydraulic conductivity for El. below -17.8 m, predicts the lowest value of hydraulic conductivity, and shows no trend with depth. The Piezoprobes predict an average hydraulic conductivity higher than the piezocones with a higher standard deviation. The MIT Piezocone predicts the highest values but with the largest standard deviation. The piezoprobes determine an increasing value of hydraulic conductivity with depth while the piezocone predicts a slightly decreasing value of hydraulic conductivity with depth.

7.3.3 Concurrent Matching Method

A third approach for estimating hydraulic conductivity is to make a simultaneous interpretation of dissipation data at two (or more) monitoring points on the probe such as A and C in Figure 7.9. This approach evaluates the consistency of the analytical

predictions, but tends to put more weight on the Stage I dissipation as the measured data will inevitably include only partial dissipation at the second monitoring point.

The concurrent matching method (Whittle et al., 1997) determines an upper and lower bound on the predicted hydraulic conductivity value by determining a hydraulic conductivity that provides the best fit for the piezocones, then determining a second hydraulic conductivity value that provides a fit for the piezoprobes. The concurrent matching method is performed using dissipation data up to the intersection point as determined by the Two Point Intersection Method, (t_p , Section 7.2.3).

Table 7.6 lists the determined values of the hydraulic conductivity⁷ using the concurrent matching method and the four dissipation curves at each depth for the two piezoprobes and two piezocones. Figure 7.26 plots these values versus elevation of the measurement point. The elevation is taken as the average elevation for the devices for the nominal depth installment. Each value in the table and figure represents the average for the two sets of cone and probe curves.

The Concurrent Matching Method predicts a wide range between the lower and upper bound (a factor of 1.8 to 2.5) values of hydraulic conductivity. This band does not encompass the values obtained by the Goodness of Fit Method on the piezocones and piezoprobes. It is also shifted to lower values. Below El. -22 m, the lower bound is $(2.15 \pm 0.11) \times 10^{-8}$ cm/s and the upper bound is $(5.29 \pm 0.39) \times 10^{-8}$ cm/s. The Concurrent Matching Method shows a slight increase in values with depth.

7.3.4 Comparison of Field Hydraulic Conductivity Interpretation Methods

Table 7.7 compares the ratio of the hydraulic conductivity determined by each method to the lower bound from the Concurrent Matching Method (k_{conc-}). These values are listed below.

k_{conc+}/k_{conc-}	2.4±0.3	
k_{R2}/k_{conc-}	2.1±1.0	(neglecting the MIT Piezocone)
k_{T50}/k_{conc-}	1.7±0.9	

Therefore, the highest ratio is determined by the upper bound values of the concurrent matching method. This method also has the lowest standard deviation, indicating the

⁷ Analysis performed by Mr. John Sutabutr (Whittle et al., 1998).

most consistent over depth for the various devices. The T_{50} method predicts the lowest ratio of determined hydraulic conductivity to that predicted by the lower bound of the concurrent matching method. The T_{50} method also predicts a standard deviation closer to the standard deviation of the upper bound method than that of the goodness of fit method. The average ratio predicted from the goodness of fit method is between the T_{50} predicted value and the upper bound of the concurrent matching method. The standard deviation is also highest, indicating that the Goodness of Fit method is more device specific in its predictions.

This point can be determined by looking at the average values per device per a method. The piezocones predict ratios of 2.1 ± 1.0 and 1.5 ± 0.7 for the Goodness Of Fit method and the T_{50} method, respectively. The piezoprobes predict ratios of 3.2 ± 5.2 and 1.6 ± 0.3 , respectively, for the Goodness of Fit and the T_{50} method. The MIT Piezocone predicts extremely high ratios using the Goodness Of Fit Method ($k_{r2}/k_{conc} = 15.7 \pm 18.8$) which is believed to be due to the greater weight on Stages II and III for this interpretation. However, for the T_{50} Matching Method, the ratio for the MIT Piezocone is 2.0 ± 0.9 . These ratios demonstrate that the piezocones consistently predict the lowest values of hydraulic conductivity, the MIT Piezocone predicts the highest values, and the piezoprobes predict intermediate values. In addition, the T_{50} method is less sensitive to whether the Piezoprobes or the Piezocones are used to predict the hydraulic conductivity, as both devices predict lower values of hydraulic conductivity than predicted by the MIT Piezocone with the same method. However, the goodness of fit method predicts a higher hydraulic conductivity than the T_{50} Matching Method.

In summary, the piezocones predict the smallest ratio of hydraulic conductivity to that predicted by the lower bound of the concurrent matching method, whether interpreting from the T_{50} method or the goodness of fit method. The piezoprobes predict the highest ratio when used in conjunction with the Goodness of Fit method.

7.3.5 Comparison Of Laboratory and Field Determined Hydraulic Conductivity

The field predicted values of hydraulic conductivity can be compared to values measured in the laboratory. These will be discussed in terms of ratios of the hydraulic

conductivity determined from the laboratory investigation divided by the value predicted by a hydraulic conductivity interpretation method (i.e. k_{lab}/k_{T50} ; k_{lab}/k_{R2} ; and k_{lab}/k_{conc}).

Table 7.8 presents the values of hydraulic conductivity determined by the three interpretation methods presented here and the laboratory data presented in Chapter 6. The values of laboratory hydraulic conductivity used to compare to the predicted values are determined from an average of values determined from CRSC tests conducted nearest the field test depth.

Figure 7.27 presents the hydraulic conductivity ratio ($k_{lab}/k_{interpreted}$) versus elevation for a comparison between the laboratory and the T_{50} piezocone, T_{50} piezoprobe, and Concurrent Matching values. These were selected for presentation because they represent the typical trends and the T_{50} method has less scatter than the Goodness of Fit Method. Two outlying points (at El. -13 m and -27 m) were eliminated from the plot. In general, all the ratios are substantially greater than one, indicating that the field predictions are always less than the laboratory values. This comparison does not account for the difference between horizontal (field) and vertical (lab) hydraulic conductivity which would make the ratio even higher.

Below El. -22 m (the low OCR, soft clay) the ratio decreases constantly with increasing depth for all three comparisons. The piezoprobes give the lowest ratios which ranges from 2.5 down to 1.4. Above El. -22 m, the ratio decreases for all three comparisons. The results indicate that the offset between the field and laboratory determined hydraulic conductivities is not the result of a constant factor. By examining the value of the hydraulic conductivity used to calculate the ratio, it is obvious that the laboratory determined values of hydraulic conductivity are more variable than the predicted field values. The ratio for the piezocones changes more than the piezoprobes (T_{50} Method) across the profile, indicating the piezoprobes are more sensitive to changes in the hydraulic conductivity as determined in the laboratory.

Using the T_{50} matching method and stress history Profile 1, the ratio of the laboratory determined hydraulic conductivity to the value determined by the T_{50} matching

(k_{lab}/k_{T50}) method is presented below for all devices

k_{lab}/k_{T50} :

Piezoprobe 62	2.3±0.8
Piezoprobe 63	1.9±0.4
Piezocone 790	2.5±0.4
Piezocone 881	2.5±0.6
MIT Piezocone	1.9±0.8

As calculated in Table 7.8, the hydraulic conductivity is slightly and consistently lower for Profile 2, with an average ratio $k_{lab}/k_{T50} = 2.0 \pm 0.5$ while for Profile 1 this average is 2.3 ± 1.1 . The piezoprobes predict the highest value of the hydraulic conductivity, and the piezocones predict the lowest value using the T_{50} Matching Method.

The ratio using the Goodness of Fit Method produces the values listed below.

k_{lab}/k_{R2} :

Piezoprobe 62	1.7±0.7
Piezoprobe 63	1.4±0.7
Piezocone 790	1.6±0.3
Piezocone 881	2.5±0.6
MIT Piezocone	1.1±1.3

Therefore, the MIT Piezocone predicts an average value of hydraulic conductivity closest to the laboratory determined values as predicted by the Goodness Of Fit Method. The MIT Piezocone also measures the highest standard deviation.

The upper and lower bound values determined from the concurrent matching method also provide the upper and lower bounds on the predictions of k . The ratios are presented below.

k_{lab}/k_{conc+}	1.4±0.3
k_{lab}/k_{conc-}	3.3±0.5

The upper bound of the Concurrent Matching Method predicts values of hydraulic conductivity closest to the values predicted in the laboratory, while the lower bound predicts the lowest values. The T_{50} Method predicts the lower values of hydraulic conductivity than the Goodness of Fit Method.

7.4 Rate Sensitivity

The installation pore pressure is believed to be sensitive to the rate of installation of the device (e.g. Aubeny, 1992). Installations in the upper layers were performed with as little variation in penetration rate as possible, targeting the standard rate of 2 cm/s. Installations at El. -27 to -33 meters (depth 95 to 115 feet) were performed increasing the penetration rate at a location where the other identical device was installed at the standard rate. Table 7.9 through Table 7.11 present the installation rates and subsequent installation pore pressures at the end of penetration for the piezoprobes, piezocones, and the MIT Cone.

Aubeny (1992) presents the ratio of $(u_i - u_o) / \sigma'_{vo}$ for the piezocone for each measuring point. In this field program, the average ratio for Piezoprobe 62 and 63 is 2.39 ± 0.40 , and 2.47 ± 0.23 , respectively. The overall average ratio for the piezoprobes is 2.43. For Piezocone 790 and 881, the ratio $(u_i - u_o) / \sigma'_{vo}$ is 3.43 ± 0.18 and 3.60 ± 0.26 , respectively. The overall average ratio for the piezocones is 3.52. The ratio for the MIT Piezocone is 3.32 ± 0.43 . These ratios are averaged over the deposit with varying OCR's and penetration rates. However, the ratios are only slightly different for only the normally consolidated portions, (the lower four measurements) and for the lightly overconsolidated portions (OCR 1.5 and 1.8, top two measurements).

Figure 7.28 shows the ratio of $(u_i - u_o) / \sigma'_{vo}$ versus penetration rate for the piezocones and piezoprobes. Here it is clear that the installation pore pressure is higher for the piezocones than for the piezoprobes but that this ratio does not increase with penetration rate. There is even a slight decrease with increasing penetration pore pressure. These measured values are greater than Aubeny's predicted values for the simple pile (1.6 for OCR=1; 2.1 for OCR=2) predicted with the MIT-E3 model parameters. However, Aubeny reports piezocone data for South Boston (Ladd et al., 1980) with values of 3 to 3.5 for OCR's from 1 to 2, indicating that the measured ratios at Saugus are in the range reported for Boston Blue Clay.

7.5 Uncertainty in Installation Pore Pressure Value

The value which is selected for the installation pore pressure (u_i), has an effect on the determined hydraulic conductivity. The magnitude of this effect is examined using the T_{50} matching method and the hydraulic conductivity ratio. The hydraulic conductivity ratio is defined as the ratio of hydraulic conductivity determined with the variation in the installation pore pressure to the correct hydraulic conductivity (i.e. k_{t50u_i+}/k_{t50} or k_{t50u_i-}/k_{t50}). The range of the installation pore pressure is determined by the average \pm the standard deviation of the pore pressure during penetration of the device, listed in Table 7.12. These values are used to compute a new pore pressure at 50% dissipation. The t_{50} value is then obtained from the dissipation curve. The average variation in the installation pore pressures for all devices at all installation depths is 0.32 ± 0.17 ksc and does not vary significantly by device. The sensitivity of hydraulic conductivity to varying the value of installation pore pressure is presented in Table 7.13 for measurements below El. -18m.

Using the upper bound penetration pore pressure (u_{i+}) for the installation pore pressure results in a higher predicted hydraulic conductivity ratio. These values are:

$$k_{t50u_i+}/k_{t50}$$

Overall	1.09 \pm 0.22
Piezoprobe 62	1.18 \pm 0.43
Piezoprobe 63	1.06 \pm 0.11
Piezocone 790	1.07 \pm 0.10
Piezocone 881	1.03 \pm 0.07
MIT Piezocone	1.09 \pm 0.23

The piezocones are less sensitive and more consistent than either the piezoprobes or the MIT Piezocone.

Under predicting the installation pore pressure (using the lower bound of the penetration pore pressure) results in a lower determined hydraulic conductivity, as

follows.

k_{t50ui}/k_{t50} :

Overall	0.82±0.11
Piezoprobe 62	0.80±0.09
Piezoprobe 63	0.82±0.13
Piezocone 790	0.86±0.06
Piezocone 881	0.85±0.16
MIT Piezocone	0.74±0.08

Again, the piezocones are less affected but the scatter is about the same for all devices.

The MIT Cone is most sensitive to the value of the installation pore pressure when using the T_{50} matching method to determine hydraulic conductivity. The piezoprobes and piezocones are comparably influenced by the determination of installation pore pressure. On average, the variation of the installation pore pressure by ± 0.32 ksc causes an error in the determined hydraulic conductivity ratio k_{t50ui}/k_{t50} ranging from 0.80 to 1.18⁸.

7.6 Uncertainty in Dissipated Pore Pressure Value

The value which is selected for the dissipated pore pressure (u_{diss}) also affects the computed hydraulic conductivity. The variation in dissipated pore pressure was determined in Section 7.2.1 for determination of the equilibrium pore pressure. The range in values for the dissipated pore pressure is taken as the standard deviation of this determination, as shown in Table 7.1. A value of pore pressure at 50% dissipation is calculated using the new dissipated pore pressure value and a new t_{50} is extracted from the dissipation curve. The new t_{50} is used to recalculate the hydraulic conductivity. The overall variation in dissipated pore pressures is 0.13 ksc. The variation in the dissipated pore pressure is: 0.03 ksc for the piezoprobes, 0.18 ksc for the piezocones, and 0.27 ksc for the MIT Piezocone.

⁸ These ratios are also influenced by the choice of the stopping point for the installation of the device. As described in Chapter 4, the adopted procedure for the installations were to watch the pore pressure output on screen to insure the pore pressure had not undergone partial drainage. Therefore, the correct installation pore pressure is biased towards the upper bound of the penetration pore pressure.

The results showing the sensitivity of the hydraulic conductivity to the value of the dissipated pore pressure are presented in Table 7.14 and the averages are included here.

k_{t50u0+}/k_{t50} :

Overall	1.05±0.05
Piezoprobe 62	1.02±0.01
Piezoprobe 63	1.01±0.01
Piezocone 790	1.06±0.04
Piezocone 881	1.08±0.07
MIT Piezocone	1.08±0.06

The lower bound values for the dissipated pore pressure show similar results as is expected. The dissipated pore pressure for the upper and lower bound are different from the dissipated pore pressure used in the T_{50} analysis by the standard deviation.

k_{t50u0-}/k_{t50} :

Overall	0.96±0.04
Piezoprobe 62	0.99±0.01
Piezoprobe 63	0.99±0.00
Piezocone 790	0.95±0.04
Piezocone 881	0.93±0.05
MIT Piezocone	0.93±0.05

In examining the effects of the uncertainty in the dissipated equilibrium pore pressures, it is apparent that the dissipated pore pressure values measured by the piezoprobes are much more consistent than the piezocones. The variation in the measured dissipated pore pressure is directly related to the amount of electrical noise in the long term measurement of the pore pressure transducer in the respective devices. The piezocones have the most variation in dissipated pore pressure (± 0.18 ksc) resulting in a ratio of k_{t50u0-}/k_{t50} ranging from 0.93 to 1.08.

7.7 Initial Dissipation Point Sensitivity

In this field program, the end of penetration/start of dissipation is known very well due to the measurements of displacement during penetration and controlled installation procedure made from the ground surface. In offshore applications, penetration displacement is not typically measured and hence the start of dissipation is poorly

defined. An analysis was performed on the results of the field program to determine the sensitivity of the determined hydraulic conductivity to the choice of the initial dissipation point.

In this analysis, each of five data points (spanning an total of 2.1 to 3.5 seconds) previous to and subsequent to the established start of dissipation were used as the assumed start of dissipation. Measurements were processed using the assumed starting point for both the installation pore pressure and starting time, and the T_{50} method was used to interpret the value of hydraulic conductivity.

There is a time bias in choosing the 5 point span between the piezocones and the piezoprobes. The piezocone and MIT Cone dissipations required reading two additional channels for tip stress and for friction sleeve stress, and therefore caused a longer time interval between successive readings through the data acquisition. The typical time span for the piezoprobes is 2.1 seconds, while the piezocones and the MIT Piezocone typical time span was 3.5 seconds.

Figure 7.29a to c shows the effect of changing the initial point on the subsequent dissipation curve for one set of measurements. Figure 7.29a shows the penetration pore pressure versus time, along with 5 points into dissipation. The 10 solid circles indicate the points used as assumed initial points in this analysis. Figure 7.29b presents pressure during dissipation versus time on a logarithmic scale for the eleven dissipation plots. The curve with the correct initial dissipation point is plotted with a solid line. The curves with initial points chosen prior to the correct start of dissipation are plotted in dots, while those with initial points chosen after the start of dissipation are plotted in dashes.

Figure 7.30 presents a plot of pore pressure versus time on a natural scale for one of the dissipation measurements obtained with Piezoprobe 62 at El. -33 (115 ft). The figure clearly shows that the initial points comprise the steepest slope of the curve and therefore the fastest dissipation rate for both the piezocone and the piezoprobe is immediately following dissipation. The initial points comprise the steepest slope of the curve and therefore determine the fastest dissipation rate for both the piezocone and the piezoprobe.

Figure 7.29c presents the normalized excess pore pressure $((u-u_o)/(u_i-u_o))$ where u_o is the equilibrium pore pressure determined by piezometers) versus log time for the 11 curves. This trend is confirmed by the model prediction. Figure 7.31 a through c present the same analysis using a model prediction for a piezoprobe at 115 foot depth in Boston Blue Clay with a hydraulic conductivity of 3.3×10^{-8} cm/s. Here the initial point is varied by ± 2 seconds. This change in assumed starting time causes t_{50} to increase to 101 seconds from 90 seconds, resulting in a decrease of the hydraulic conductivity to 2.9×10^{-8} cm/s.

Varying the assumed initial point in either direction causes a decrease in the rate of dissipation during the initial portion of the normalized dissipation curve. When initial points are chosen too early (actually during the penetration of the device), the curves shift to longer times and must lie above the correct plot with the initial portion showing changes in pore pressure characteristic of the fluctuations during penetration. When initial points are chosen too late (actually during dissipation), the decreased dissipation rate causes the curves to lie above the correct plot. As the assumed initial point is set further into dissipation, the resulting dissipation curves moves further above the correct curve. As a result, the curve based on the start of dissipation always lies lowest on the normalized scale, indicating the highest hydraulic conductivity.

Table 7.15 summarizes the findings of this analysis. The table presents values of hydraulic conductivity determined using the correct initial dissipation point, the minimum value of hydraulic conductivity calculated for the 11 plots, and the corresponding time shift. The ratio between the computed hydraulic conductivity and the correctly interpreted hydraulic conductivity is used as a measure of the error.

For Boston Blue Clay, the effect of a few second error in the chosen start of dissipation is as important as the uncertainty in the value of the installation pore pressure.

The hydraulic conductivity ratios are as follows.

$k_{t_{50uip}}/k_{t_{50}}$:

Overall	0.81±0.11
Piezoprobe 62	0.82±0.06
Piezoprobe 63	0.85±0.07
Piezocone 790	0.81±0.08
Piezocone 881	0.87±0.03
MIT Piezocone	0.66±0.16

This analysis shows that the MIT Piezocone is most sensitive to the starting point due to a 3.5 second shift in the starting time. Therefore, the influence of a time shift of 2.1 seconds for the piezoprobes has the same effects as a time shift of 3.5 seconds for the piezocones. This is mainly due to the convergence on a lower bound value of hydraulic conductivity as later and later times are chosen for the initial dissipation point.

Plotting the normalized curves while altering the initial dissipation point provides a method to determine the correct start of dissipation in the absence of penetration displacement measurements. The correct interpretation will be associated with the lowest normalized curve.

Dissipated Pore Pressures Determined from Dissipation Tests																									
Nom.	Piezoprobe 62					Piezoprobe 63					Piezocone 790					Piezocone 881					MIT Cone				
Depth (ft)	Elev. (m)	u_{diss} (ksc)	SD (ksc)	u_o (ksc)	$\frac{u_{diss}}{u_o}$	Elev. (m)	u_{diss} (ksc)	SD (ksc)	u_o (ksc)	$\frac{u_{diss}}{u_o}$	Elev. (m)	u_{diss} (ksc)	SD (ksc)	u_o (ksc)	$\frac{u_{diss}}{u_o}$	Elev. (m)	u_{diss} (ksc)	SD (ksc)	u_o (ksc)	$\frac{u_{diss}}{u_o}$	Elev. (m)	u_{diss} (ksc)	SD (ksc)	u_o (ksc)	$\frac{u_{diss}}{u_o}$
65	-18.4	1.90	0.04	1.93	0.98	-18.5	2.08	0.02	1.94	1.07	-17.7	1.66	0.03	1.86	0.89	-17.9	2.18	0.09	1.88	1.16	-17.8	1.89	0.02	1.87	1.01
75	-20.9	2.52	0.02	2.18	1.15	-20.9	2.23	0.02	2.19	1.02	-20.8	2.20	0.17	2.17	1.01	-21.0	2.72	0.37	2.19	1.24	-20.8	2.36	0.15	2.18	1.08
85	-23.9	2.74	0.01	2.50	1.10	-24.0	2.47	0.02	2.50	0.99	-23.8	2.68	0.09	2.48	1.08	-24.0	2.86	0.15	2.50	1.14	-23.9	2.51	0.14	2.49	1.01
95	-27.0	2.93	0.05	2.81	1.04	-27.0	2.81	0.03	2.81	1.00	-26.9	2.96	0.33	2.80	1.06	-27.1	3.19	0.53	2.82	1.13	-26.9	2.60	0.43	2.80	0.93
105	-30.3	3.30	0.05	3.15	1.05	-30.1	3.19	0.02	3.12	1.02	-29.9	3.28	0.11	3.11	1.06	-30.1	3.81	0.13	3.13	1.22	-30.0	3.10	0.09	3.12	0.99
115	-33.1	3.57	0.04	3.43	1.04	-33.1	3.44	0.02	3.44	1.00	-33.0	3.64	0.06	3.42	1.06	-33.2	3.96	0.14	3.44	1.15	-33.0	3.40	0.34	3.43	0.99
			Average		1.06			Average		1.02			Average		1.03			Average		1.17			Average		1.00
			S.D.		0.06			S.D.		0.03			S.D.		0.07			S.D.		0.04			S.D.		0.05

Table 7.1 Summary of Dissipated Pore Pressures.

Determination of \bar{U}_o Two Point Method										
Depth (ft)	Probe	u_i (ksc)	\bar{U}_p	$(u_i - u)_p$ (ksc)	t_p (s)	$\frac{u_i - \Delta u_i = (u_i - u)_p}{(1 - \bar{U}_p)}$	$u_{2pt} = u_i - \Delta u_i$ (ksc)	u_{diss} (ksc)	$\frac{(u_{2pt} - u_{diss})}{(u_i - u_{diss})}$	
65	62	5.18	0.078	2.7	1085	2.93	2.25	1.90	0.11	
	63	6.47	0.078	4.0	7225	4.34	2.13	2.08	0.01	
75	62	7.42	0.078	4.7	517	5.11	2.31	2.52	-0.04	
	63	6.11	0.078	3.6	2445	3.93	2.18	2.23	-0.01	
85	62	7.65	0.106	4.6	3477	5.11	2.54	2.74	-0.04	
	63	7.89	0.106	5.1	5817	5.70	2.19	2.47	-0.05	
95	63	8.08	0.106	4.8	2799	5.37	2.71	2.81	-0.02	
105	62	9.27	0.106	5.4	4684	6.04	3.23	3.30	-0.01	
	63	9.44	0.106	5.8	2379	6.49	2.95	3.19	-0.04	
115	62	10.75	0.110	6.7	2725	7.53	3.22	3.57	-0.05	
	63	9.91	0.110	5.8	5817	6.52	3.39	3.44	-0.01	
					Maximum t_p	7225			Average	-0.01
					Minimum t_p	517			S.D.	0.04
					Average t_p	3543				
					S.D.	2102				

Table 7.2 Values of In Situ Pore Pressure Determined by the Two Point Intersection Method.

Nominal El. (m)	Two Point Intersection		Inverse Time (1/t) Method					
	Method		Piezoprobes		Piezocones		MIT Cone	
	$\frac{(U_{2pt}-U_{diss})}{(U_1-U_{diss})}$	t_p (s)	t_p t_{50}	$\frac{(U_{1/t}-U_{diss})}{(U_1-U_{diss})}$	t_p t_{50}	$\frac{(U_{1/t}-U_{diss})}{(U_1-U_{diss})}$	t_p t_{50}	$\frac{(U_{1/t}-U_{diss})}{(U_1-U_{diss})}$
-18	0.11	1085	6.1	0.12	0.6	0.42	1.3	0.27
	0.01	7225	0.6	0.09	5.0	0.11	8.4	0.09
-21	-0.04	517	5.0	0.13	0.3	0.5	1.5	0.32
	-0.01	2445	24.9	0.09	1.7	0.25	6.9	0.1
-24	-0.04	3477	30.5	0.09	1.9	0.21	3.9	0.14
	-0.05	5817	69.3	0.09	3.8	0.14	6.6	0.1
-27	-0.02	2799	29.8	0.10	1.9	0.21	3.8	0.14
					1.7	0.25		
-30	-0.01	4684	58.5	0.10	3.4	0.15	8.3	0.09
	-0.04	2379	33.5	0.10	1.4	0.27	4.2	0.13
-33	-0.05	2725	35.8	0.10	1.8	0.23	5.8	0.11
	-0.01	5817	61.9	0.10	4.6	0.12	12.4	0.07

Table 7.3 Comparison of u_0 Methods.

Summary of T ₅₀ Matching Method							
Nom. Depth (ft)	Device	Elev (m)	u _i (ksc)	u _{diss} (ksc)	t ₅₀ (s)	Profile1 k (x10 ⁻⁸ cm/s)	Profile2 k (x10 ⁻⁸ cm/s)
45	Piezococone 790	-11.62	5.24	1.23	593	13.00	16.65
	Piezococone 881	-11.83	6.35	1.18	924	8.30	10.69
50	Piezoprobe 63	-13.30	3.92	1.37	85	2.73	3.33
	Piezococone 790	-13.15	6.10	1.49	1835	2.12	2.73
55	Piezoprobe 63	-14.82	5.72	1.58	197	1.06	1.31
	Piezococone 790	-14.67	6.89	1.66	891	3.97	5.11
65	Piezoprobe 62	-18.45	5.18	1.90	178	1.86	2.24
	Piezoprobe 63	-18.48	6.47	2.08	96	3.43	4.13
	Piezococone 790	-17.72	7.03	1.66	1907	2.46	2.56
	Piezococone 881	-17.93	8.38	2.18	1434	3.26	3.40
	MIT Cone	-17.79	7.16	1.89	866	3.34	3.40
75	Piezoprobe 62	-20.89	7.42	2.52	103	2.80	3.37
	Piezoprobe 63	-20.92	6.11	2.23	98	2.95	3.54
	Piezococone 790	-20.77	8.61	2.20	1607	2.55	2.66
	Piezococone 881	-20.98	8.49	2.72	1470	2.78	2.91
	MIT Cone	-20.84	8.95	2.36	353	7.16	7.29
85	Piezoprobe 62	-23.94	7.65	2.72	114	3.11	3.33
	Piezoprobe 63	-23.97	7.89	2.47	84	4.24	4.53
	Piezococone 790	-23.81	9.51	2.68	1530	2.99	3.44
	Piezococone 881	-24.02	9.60	2.86	1822	2.51	2.89
	MIT Cone	-23.89	7.64	2.51	885	2.84	3.25
95	Piezoprobe 62	-26.98	6.98	2.93	27	12.00	12.80
	Piezoprobe 63	-27.02	8.08	2.81	94	3.42	3.65
	Piezococone 790	-26.86	10.83	2.96	1513	2.74	3.14
	Piezococone 881	-27.07	10.76	3.19	1606	2.58	2.96
	MIT Cone	-26.94	10.94	2.60	739	3.06	3.53
105	Piezoprobe 62	-30.03	9.27	3.30	80	3.64	3.89
	Piezoprobe 63	-30.07	9.44	3.19	71	4.09	4.38
	Piezococone 790	-29.91	10.92	3.28	1701	2.22	2.55
	Piezococone 881	-30.12	12.14	3.81	1377	2.74	3.15
	MIT Cone	-29.99	11.73	3.10	561	3.68	4.22
115	Piezoprobe 62	-33.08	10.75	3.57	76	3.93	4.26
	Piezoprobe 63	-33.11	9.91	3.44	94	3.16	3.43
	Piezococone 790	-32.96	13.12	3.64	1261	3.09	3.55
	Piezococone 881	-33.17	13.03	3.96	1521	2.56	2.94
	MIT Cone	-33.03	12.24	3.40	469	4.55	5.23

Table 7.4 Hydraulic Conductivity (k) Determined by the T₅₀ Matching Method.

Goodness of Fit Predictions															
Nom.	Piezoprobe 62			Piezoprobe 63			Piezocone 790			Piezocone 881			MIT Piezocone		
Depth (ft)	Elev. (m)	Predicted k (cm/s)	R ²	Elev. (m)	Predicted k (cm/s)	R ²	Elev. (m)	Predicted k (cm/s)	R ²	Elev. (m)	Predicted k (cm/s)	R ²	Elev. (m)	Predicted k (cm/s)	R ²
45							-11.62	1.00E-07	0.991	-11.83	1.08E-07	0.932			
50				-13.30	3.20E-08	0.983	-13.15	3.80E-08	0.904						
55				-14.82	1.20E-08	0.998	-14.67	7.20E-08	0.950						
65	-18.45	2.80E-08	0.980	-18.48	3.40E-08	0.993	-17.72	3.40E-08	0.994	-17.93	4.40E-08	0.962	-17.79	3.40E-08	0.993
75	-20.89	3.20E-08	0.984	-20.92	3.40E-08	0.991	-20.77	4.80E-08	0.965	-20.98	3.40E-08	0.969	-20.84	9.60E-07	0.964
85	-23.94	3.40E-08	0.990	-23.97	5.20E-08	0.989	-23.81	4.20E-08	0.971	-24.02	2.80E-08	0.988	-23.89	2.60E-08	0.988
95	-26.98	1.36E-07	0.961	-27.02	4.60E-07	0.997	-26.86	5.20E-08	0.945	-27.07	3.20E-08	0.984	-26.94	4.40E-07	0.991
105	-30.03	4.00E-08	0.993	-30.07	5.00E-08	0.990	-29.91	2.80E-08	0.994	-30.12	3.40E-08	0.976	-29.99	4.20E-07	0.986
115	-33.08	4.20E-08	0.851	-33.11	3.80E-08	0.981	-32.96	5.20E-08	0.882	-33.17	2.80E-08	0.802	-33.03	5.20E-08	0.987

Table 7.5 Hydraulic Conductivity (k) Determined by the Goodness of Fit Method and Profile 1 (from Sutabutr, 1998).

Concurrent Matching Method					
Depth (ft)	Elevation (m)	Match Point (T/t)	Upper Bound Predicted k (cm/s)	Match Point (T/t)	Lower Bound Predicted k (cm/s)
50	-13.30	1.6×10^{-5}	4.82E-08	9.0×10^{-6}	2.71E-08
55	-14.82	1.7×10^{-5}	3.29E-08	5.0×10^{-6}	1.37E-08
65	-18.14	1.3×10^{-5}	3.35E-08	7.0×10^{-6}	1.81E-08
75	-20.89	2.2×10^{-5}	4.97E-08	8.5×10^{-6}	1.92E-08
85	-23.94	2.7×10^{-5}	5.61E-08	1.0×10^{-5}	2.08E-08
95	-26.99	2.6×10^{-5}	4.89E-08	1.2×10^{-5}	2.26E-08
105	-30.04	3.3×10^{-5}	5.64E-08	1.3×10^{-5}	2.22E-08
115	-33.08	3.2×10^{-5}	5.02E-08	1.3×10^{-5}	2.04E-08

Table 7.6 Hydraulic Conductivity (k) Determined by the Concurrent Matching Method (from Sutabutr, 1998).

Ratio of Hydraulic Conductivity						
Determined by Method and Device to Lower Bound Concurrent Matching						
	k_{conc-}/k_{conc-}		k_{R2}/k_{conc-}		k_{T50}/k_{conc-}	
	Average	S.D.	Average	S.D.	Average	S.D.
All Devices	2.4	0.3	5.4	10.0	1.7	0.9
Piezoprobe 62			2.5	1.8	2.1	1.6
Piezoprobe 63			4.1	6.6	1.6	0.4
Piezoprobes			3.2	5.2	1.6	0.3
Piezocone 790			2.4	1.3	1.6	0.9
Piezocone 881			1.6	0.4	1.4	0.2
Piezocones			2.1	1.0	1.5	0.7
MIT Cone			15.7	18.8	2.0	0.9

Table 7.7 Ratio of Hydraulic Conductivity from a Method to the Value Determined by the Lower Bound of the Concurrent Matching Method.

Device	Lab.	Nom. Depth (ft)	t_{50} Matching Method					Goodness of Fit Predictions			Concurrent Matching				
	k_{lab} ($\times 10^{-8}$ cm/s)		Elev. (m)	Profile1 k ($\times 10^{-8}$ cm/s)	k_{lab}/k_{prof1}	Profile2 k ($\times 10^{-8}$ cm/s)	k_{lab}/k_{prof2}	Elev. (m)	Predicted k ($\times 10^{-8}$ cm/s)	k_{lab}/k_{gof}	Elev. (m)	Predicted Upper k ($\times 10^{-8}$ cm/s)	k_{lab}/k_{conc-u}	Predicted Lower k ($\times 10^{-8}$ cm/s)	k_{lab}/k_{conc-l}
790	14.00	45	-11.62	13.00	1.08	16.70	0.84	-11.62	10.00	1.40					
881	14.00		-11.83	8.30	1.69	10.70	1.31	-11.83	10.80	1.30					
63	4.60	50	-13.30	2.73	1.68	3.33	1.38	-13.30	3.20	1.44	-13.22	4.82	0.95	2.71	1.70
790	4.60		-13.15	2.12	2.17	2.73	1.68	-13.15	3.80	1.21					
63	8.00	55	-14.82	1.06	7.55	1.31	6.11	-14.82	1.20	6.67	-14.75	3.29	2.43	1.37	5.84
790	8.00		-14.67	3.97	2.02	5.11	1.57	-14.67	7.20	1.11					

Table 7.8 Hydraulic Conductivity Comparison between Interpretation Methods and Laboratory Data.

Device	Lab.	Nom. Depth (ft)	t_{50} Matching Method					Goodness of Fit Predictions			Concurrent Matching				
	k_{lab} ($\times 10^{-8}$ cm/s)		Elev. (m)	Profile1 k ($\times 10^{-8}$ cm/s)	k_{lab}/k_{T50}	Profile2 k ($\times 10^{-8}$ cm/s)	k_{lab}/k_{T50}	Elev. (m)	Predicted k ($\times 10^{-8}$ cm/s)	k_{lab}/k_{R2}	Elev. (m)	Predicted Upper k ($\times 10^{-8}$ cm/s)	k_{lab}/k_{conc+}	Predicted Lower k ($\times 10^{-8}$ cm/s)	k_{lab}/k_{conc-}
62	6.00	65	-18.45	1.86	3.23	2.24	2.68	-18.45	2.80	2.14	-18.14	3.35	1.79	1.81	3.31
63	6.00		-18.48	3.43	1.75	4.13	1.45	-18.48	3.40	1.76					
790	6.00		-17.72	2.46	2.44	2.56	2.34	-17.72	3.40	1.76					
881	6.00		-17.93	3.26	1.84	3.40	1.76	-17.93	4.40	1.36					
MIT	6.00		-17.79	3.34	1.80	3.40	1.76	-17.79	3.40	1.76					
62	6.60	75	-20.89	2.80	2.36	3.37	1.96	-20.89	3.20	2.06	-20.89	4.97	1.33	1.92	3.44
63	6.60		-20.92	2.95	2.24	3.54	1.86	-20.92	3.40	1.94					
790	6.60		-20.77	2.55	2.59	2.66	2.48	-20.77	4.80	1.38					
881	6.60		-20.98	2.78	2.37	2.91	2.27	-20.98	3.40	1.94					
MIT	6.60		-20.84	7.16	0.92	7.29	0.91	-20.84	96.00	0.07					
62	8.40	85	-23.94	3.11	2.70	3.33	2.52	-23.94	3.40	2.47	-23.94	5.61	1.50	2.08	4.04
63	8.40		-23.97	4.24	1.98	4.53	1.85	-23.97	5.20	1.62					
790	8.40		-23.81	2.99	2.81	3.44	2.44	-23.81	4.20	2.00					
881	8.40		-24.02	2.51	3.35	2.89	2.91	-24.02	2.80	3.00					
MIT	8.40		-23.89	2.84	2.96	3.25	2.58	-23.89	2.60	3.23					
62	8.10	95	-26.98	12.00	0.68	12.80	0.63	-26.98	13.60	0.60	-26.99	4.89	1.66	2.26	3.58
63	8.10		-27.02	3.42	2.37	3.65	2.22	-27.02	46.00	0.18					
790	8.10		-26.86	2.74	2.96	3.14	2.58	-26.86	5.20	1.56					
881	8.10		-27.07	2.58	3.14	2.96	2.74	-27.07	3.20	2.53					
MIT	8.10		-26.94	3.06	2.65	3.53	2.29	-26.94	44.00	0.18					
62	5.50	105	-30.03	3.64	1.51	3.89	1.41	-30.03	4.00	1.38	-30.04	5.64	0.98	2.22	2.48
63	5.50		-30.07	4.09	1.34	4.38	1.26	-30.07	5.00	1.10					
790	5.50		-29.91	2.22	2.48	2.55	2.16	-29.91	2.80	1.96					
881	5.50		-30.12	2.74	2.01	3.15	1.75	-30.12	3.40	1.62					
MIT	5.50		-29.99	3.68	1.49	4.22	1.30	-29.99	42.00	0.13					
62	6.00	115	-33.08	3.93	1.53	4.26	1.41	-33.08	4.20	1.43	-33.08	5.02	1.20	2.04	2.94
63	6.00		-33.11	3.16	1.90	3.43	1.75	-33.11	3.80	1.58					
790	6.00		-32.96	3.09	1.94	3.55	1.69	-32.96	5.20	1.15					
881	6.00		-33.17	2.56	2.34	2.94	2.04	-33.17	2.80	2.14					
MIT	6.00		-33.03	4.55	1.32	5.23	1.15	-33.03	5.20	1.15					

Table 7.8 (cont.) Hydraulic Conductivity Comparison between Interpretation Methods and Laboratory Data.

Nominal Depth (ft)	Piezoprobe 62							Piezoprobe 63							
	Elev (m)	Pen. Rate (cm/s)	u_i (ksc)	u_o (ksc)	σ'_{vo} (ksc)	OCR	$\frac{(u_i-u_o)}{\sigma'_{vo}}$	Elev (m)	Pen. Rate (cm/s)	u_i (ksc)	u_o (ksc)	σ'_{vo} (ksc)	OCR	$\frac{(u_i-u_o)}{\sigma'_{vo}}$	
65	-18.45	1.8	5.18	1.93	1.62	1.7	2.01	-18.48	1.1	6.47	1.94	1.62	1.7	2.80	
75	-20.89	1.5	7.42	2.18	1.80	1.5	2.90	-20.92	1.3	6.11	2.19	1.81	1.4	2.17	
85	-23.94	1.3	7.65	2.50	2.04	1.2	2.53	-23.97	1.7	7.89	2.50	2.04	1.2	2.64	
95	-26.98	8.6	6.98	2.81	2.27	1.2	1.84	-27.02	2.0	8.08	2.81	2.28	1.2	2.31	
105	-30.34	16.0	9.27	3.15	2.53	1.2	2.42	-30.07	1.6/3.2/5.2	9.44	3.12	2.51	1.2	2.52	
115	-33.08	9.9	10.75	3.43	2.74	1.2	2.67	-33.11	2.3	9.91	3.44	2.75	1.2	2.36	
							Average	2.39						Average	2.47
							S.D.	0.40						S.D.	0.23

Table 7.9 Summary of Installation Rate and Subsequent Value of $(u_i-u_o)/\sigma'_{vo}$ for the Piezoprobes.

Nominal Depth (ft)	Piezocone 790							Piezocone 881							
	Elev (m)	Pen. Rate (cm/s)	u_i (ksc)	u_o (ksc)	σ'_{vo} (ksc)	OCR	$\frac{(u_i-u_o)}{\sigma'_{vo}}$	Elev (m)	Pen. Rate (cm/s)	u_i (ksc)	u_o (ksc)	σ'_{vo} (ksc)	OCR	$\frac{(u_i-u_o)}{\sigma'_{vo}}$	
65	-17.72	1.7	7.03	1.86	1.56	1.8	3.32	-17.93	1.4	8.38	1.88	1.58	1.8	4.13	
75	-20.77	1.4	8.61	2.17	1.79	1.5	3.59	-20.98	1.6	8.49	2.19	1.81	1.4	3.48	
85	-23.81	1.7	9.51	2.48	2.03	1.2	3.46	-24.02	1.2	9.60	2.50	2.05	1.2	3.47	
95	-26.86	8.8	10.83	2.80	2.26	1.2	3.55	-27.07	1.6	10.76	2.82	2.28	1.2	3.48	
105	-29.91	11.8	10.92	3.11	2.50	1.2	3.13	-30.12	1.3	12.14	3.13	2.51	1.2	3.58	
115	-32.96	13	13.12	3.42	2.73	1.2	3.55	-33.17	2	13.03	3.44	2.75	1.2	3.49	
Average							3.43	Average							3.60
S.D.							0.18	S.D.							0.26

Table 7.10 Summary of Installation Rate and Subsequent Value of $(u_i-u_o)/s'_{vo}$ for the Piezocones.

Rate Sensitivity							
Nominal	MIT Cone						
Depth (ft)	Elev (m)	Pen. Rate (cm/s)	u_i (ksc)	u_o (ksc)	σ'_{vo} (ksc)	OCR	$\frac{(u_i-u_o)}{\sigma'_{vo}}$
65	-17.79	1.4	7.16	1.87	1.57	1.8	3.38
75	-20.84	1.6	8.95	2.18	1.80	1.5	3.76
85	-23.89	1.8	7.64	2.49	2.03	1.2	2.53
95	-26.94	1.5	10.94	2.80	2.27	1.2	3.58
105	-29.99	2.9	11.73	3.12	2.50	1.2	3.44
115	-33.03	1.7	12.24	3.43	2.74	1.2	3.22
Average							3.32
S.D.							0.43

Table 7.11 Summary of Installation Rate and Subsequent Value of $(u_i-u_o)/s'_{vo}$ for the MIT Piezocone.

Penetration Pore Pressures Determined from Installations															
Nom.	Piezoprobe 62			Piezoprobe 63			Piezocone 790			Piezocone 881			MIT Cone		
Depth (ft)	Elev. (m)	U _{pen} (ksc)	S.D. (ksc)	Elev. (m)	U _{pen} (ksc)	S.D. (ksc)	Elev. (m)	U _{pen} (ksc)	S.D. (ksc)	Elev. (m)	U _{pen} (ksc)	S.D. (ksc)	Elev. (m)	U _{pen} (ksc)	S.D. (ksc)
65	-18.45	5.42	0.60	-18.48	6.39	0.25	-17.72	6.98	0.38	-17.93	7.56	0.81	-17.79	7.14	0.56
75	-20.89	6.91	0.24	-20.92	7.11	0.31	-20.77	8.55	0.15	-20.98	8.63	0.17	-20.84	8.50	0.20
85	-23.94	7.80	0.17	-23.97	7.77	0.19	-23.81	9.19	0.13	-24.02	9.64	0.16	-23.89	8.32	0.22
95	-26.98	6.54	0.33	-27.02	8.03	0.26	-26.86	10.53	0.29	-27.07	10.65	0.19	-26.94	10.59	0.56
105	-30.34	8.93	0.35	-30.07	8.81	0.44	-29.91	10.76	0.67	-30.12	11.61	0.25	-29.99	11.30	0.39
115	-33.08	10.42	0.28	-33.11	10.02	0.24	-32.96	13.08	0.20	-33.17	12.91	0.24	-33.03	12.14	0.25

Table 7.12 Summary of Penetration Pore Pressures.

Sensitivity of Hydraulic Conductivity to Installation Pore Pressure in T_{50} Matching Method													
Device	Nominal Depth	Elev. (m)	Results from T_{50} Matching			Upper Bound Uncertainty in u_i				Lower Bound Uncertainty in u_i			
			u_i (ksc)	t_{50} (s)	k_{t50} ($\times 10^{-8}$ cm/s)	u_{i+} (ksc)	t_{50i+} (s)	k_{t50i+} ($\times 10^{-8}$ cm/s)	$\frac{k_{t50i+}}{k_{t50}}$	u_{i-} (ksc)	t_{50i-} (s)	k_{t50i-} ($\times 10^{-8}$ cm/s)	$\frac{k_{t50i-}}{k_{t50}}$
62	65	-18.45	5.18	178	1.86	6.02	87	3.80	2.04	4.82	232	1.42	0.77
63		-18.48	6.47	96	3.43	6.64	89	3.72	1.08	6.14	110	3.01	0.88
790		-17.72	7.03	1907	2.46	7.36	1612	2.90	1.18	6.60	2302	2.03	0.83
881		-17.93	8.38	1434	3.26	8.37	1446	3.24	0.99	6.75	2594	1.81	0.55
MIT		-17.79	7.16	866	3.34	7.70	589	4.91	1.47	6.58	1279	2.26	0.68
62	75	-20.89	7.42	103	2.80	7.15	116	2.49	0.89	6.67	140	2.06	0.74
63		-20.92	6.11	98	2.95	7.42	37	7.80	2.65	6.80	55	5.25	1.78
790		-20.77	8.61	1607	2.55	8.70	1534	2.67	1.05	8.40	1789	2.29	0.90
881		-20.98	8.49	1470	2.78	8.80	1331	3.07	1.10	8.46	1479	2.77	0.99
MIT		-20.84	8.95	353	7.16	8.70	406	6.23	0.87	8.30	509	4.97	0.69
62	85	-23.94	7.65	114	3.11	7.97	97	2.65	1.17	7.63	115	3.08	0.99
63		-23.97	7.89	84	4.24	7.96	82	4.32	1.02	7.58	95	3.73	0.88
790		-23.81	9.51	1530	2.99	9.32	1647	2.78	0.93	9.06	1805	2.54	0.85
881		-24.02	9.60	1822	2.51	9.80	1651	2.77	1.10	9.48	1932	2.37	0.94
MIT		-23.89	7.64	885	2.84	8.54	513	4.89	1.73	8.10	678	3.70	1.31
62	95	-26.98	6.98	27	12.00	6.87	27	11.80	0.99	6.21	34	9.40	0.79
63		-27.02	8.08	94	3.42	8.29	87	3.67	1.07	7.77	112	2.85	0.83
790		-26.86	10.83	1513	2.74	10.82	1517	2.73	1.00	10.24	1846	2.24	0.82
881		-27.07	10.76	1606	2.58	10.84	1560	2.65	1.03	10.46	1779	2.33	0.90
MIT		-26.94	10.94	739	3.06	11.07	712	3.18	1.04	9.95	943	2.40	0.78
62	105	-30.03	9.27	80	3.64	9.29	79	3.68	1.01	8.58	106	2.74	0.75
63		-30.07	9.44	71	4.09	9.25	78	3.72	0.91	8.37	117	2.48	0.61
790		-29.91	10.92	1701	2.22	11.43	1430	2.64	1.19	10.09	2140	1.76	0.79
881		-30.12	12.14	1377	2.74	11.86	1487	2.54	0.93	11.36	1727	2.19	0.80
MIT		-29.99	11.73	561	3.68	11.69	565	3.66	0.99	10.91	813	2.54	0.69
62	115	-33.08	10.75	76	3.93	10.70	77	3.86	0.98	10.14	95	3.13	0.80
63		-33.11	9.91	94	3.16	10.26	78	3.81	1.21	9.78	102	2.91	0.92
790		-32.96	13.12	1261	3.09	13.28	1194	3.26	1.06	12.88	1316	2.96	0.96
881		-33.17	13.03	1521	2.56	13.15	1475	2.64	1.03	12.67	1687	2.31	0.90
MIT		-33.03	12.24	469	4.55	12.39	442	4.82	1.06	11.89	543	3.92	0.86

Table 7.13 Summary of Sensitivity of Hydraulic Conductivity to Variation in the Installation Pore Pressure Value.

Sensitivity of Hydraulic Conductivity to Dissipation Pore Pressure in T ₅₀ Matching Method													
Device	Nominal Depth	Elev. (m)	Results from T ₅₀ Matching			Upper Bound Uncertainty in u _{diss}				Lower Bound Uncertainty in u _{diss}			
			u _{diss} (ksc)	t ₅₀ (s)	k _{t50} (x10 ⁻⁸ cm/s)	u _{diss+} (ksc)	t _{50diss+} (s)	k _{t50diss+} (x10 ⁻⁸ cm/s)	k _{t50diss+} k _{t50}	u _{diss-} (ksc)	t _{50diss-} (s)	k _{t50diss-} (x10 ⁻⁸ cm/s)	k _{t50diss-} k _{t50}
62	65	-18.45	1.90	178	1.86	1.94	173	1.91	1.03	1.86	183	1.81	0.97
63		-18.48	2.08	96	3.43	2.10	95	3.48	1.01	2.06	97	3.41	0.99
790		-17.72	1.66	1907	2.46	1.69	1860	2.52	1.03	1.63	1938	2.42	0.98
881		-17.93	2.18	1434	3.26	2.27	1367	3.43	1.05	2.09	1484	3.16	0.97
MIT		-17.79	1.89	866	3.34	1.91	853	3.39	1.02	1.87	879	3.29	0.99
62	75	-20.89	2.52	103	2.80	2.55	103	2.80	1.00	2.51	104	2.78	0.99
63		-20.92	2.23	98	2.95	2.25	98	2.95	1.00	2.21	100	2.89	0.98
790		-20.77	2.20	1607	2.55	2.37	1477	2.77	1.09	2.03	1761	2.32	0.91
881		-20.98	2.72	1470	2.78	3.09	1305	3.14	1.13	2.35	1669	2.45	0.88
MIT		-20.84	2.36	353	7.16	2.51	319	7.92	1.11	2.21	384	6.58	0.92
62	85	-23.94	2.72	114	3.11	2.75	112	3.16	1.02	2.73	113	3.13	1.01
63		-23.97	2.47	84	4.24	2.49	83	4.27	1.01	2.45	84	4.22	1.00
790		-23.81	2.68	1530	2.99	2.77	1476	3.10	1.04	2.59	1586	2.89	0.96
881		-24.02	2.86	1822	2.51	2.99	1719	2.66	1.06	2.73	1942	2.36	0.94
MIT		-23.89	2.51	885	2.84	2.65	815	3.08	1.09	2.37	953	2.63	0.93
62	95	-26.98	2.93	27	12.00	2.98	26	12.29	1.03	2.88	27	11.83	0.99
63		-27.02	2.81	94	3.42	2.84	93	3.44	1.01	2.78	94	3.40	0.99
790		-26.86	2.96	1513	2.74	3.29	1338	3.09	1.13	2.63	1699	2.44	0.89
881		-27.07	3.19	1606	2.58	3.72	1335	3.10	1.20	2.66	1882	2.20	0.85
MIT		-26.94	2.60	739	3.06	3.03	651	3.48	1.13	2.17	827	2.74	0.89
62	105	-30.03	3.30	80	3.64	3.35	78	3.72	1.02	3.25	82	3.54	0.97
63		-30.07	3.19	71	4.09	3.21	71	4.09	1.00	3.17	72	4.04	0.99
790		-29.91	3.28	1701	2.22	3.39	1643	2.30	1.04	3.17	1765	2.14	0.96
881		-30.12	3.81	1377	2.74	3.94	1335	2.83	1.03	3.68	1418	2.66	0.97
MIT		-29.99	3.10	561	3.68	3.19	554	3.73	1.01	3.01	579	3.57	0.97
62	115	-33.08	3.57	76	3.93	3.61	75	3.96	1.01	3.53	77	3.86	0.98
63		-33.11	3.44	94	3.16	3.46	93	3.19	1.01	3.42	95	3.13	0.99
790		-32.96	3.64	1261	3.09	3.70	1238	3.15	1.02	3.58	1275	3.06	0.99
881		-33.17	3.96	1521	2.56	4.10	1470	2.65	1.03	3.82	1572	2.48	0.97
MIT		-33.03	3.40	469	4.55	3.74	410	5.20	1.14	3.06	542	3.93	0.86

Table 7.14 Summary of Sensitivity of Hydraulic Conductivity to Variation in the Dissipated Pore Pressure Value.

Sensitivity of Hydraulic Conductivity to Initial Dissipation Point in T ₅₀ Matching Method									
Device	Nominal Depth	Elev. (m)	Results from T ₅₀ Matching			Upper Bound Uncertainty in Initial Point			
			u ₁ (ksc)	t ₅₀ (s)	k _{t50} (x10 ⁻⁸ cm/s)	Δ _{time} (s)	t _{50upt} (s)	k _{t50upt} (x10 ⁻⁸ cm/s)	$\frac{k_{t50upt}}{k_{t50}}$
62	65	-18.45	5.18	184	1.80	2.09	219	1.51	0.84
63		-18.48	6.47	107	3.09	2.09	112	2.95	0.96
790		-17.72	7.03	1739	2.69	7.41	1899	2.47	0.92
881		-17.93	8.38	1568	2.99	3.50	1756	2.67	0.89
MIT		-17.79	7.16	912	3.17	7.41	1105	2.62	0.83
62	75	-20.89	7.42	121	2.39	2.08	138	2.09	0.88
63		-20.92	6.11	102	2.83	2.09	115	2.51	0.89
790		-20.77	8.61	1625	2.52	3.52	2017	2.03	0.81
881		-20.98	8.49	1821	2.25	3.36	2130	1.92	0.85
MIT		-20.84	8.95	391	6.46	3.46	891	2.84	0.44
62	85	-23.94	7.65	128	2.77	2.09	151	2.35	0.85
63		-23.97	7.89	82	4.32	2.14	100	3.54	0.82
790		-23.81	9.51	1647	2.78	3.46	2010	2.28	0.82
881		-24.02	9.60	2175	2.10	3.40	2449	1.87	0.89
MIT		-23.89	7.64	891	2.82	3.46	977	2.57	0.91
62	95	-26.98	6.98	27	11.83	2.14	31	10.31	0.87
63		-27.02	8.08	91	3.51	2.08	103	3.10	0.88
790		-26.86	10.83	1604	2.58	3.52	2091	1.98	0.77
881		-27.07	10.76	1826	2.27	3.53	2069	2.00	0.88
MIT		-26.94	10.94	696	3.25	3.46	902	2.51	0.77
62	105	-30.03	9.27	85	3.42	2.07	114	2.55	0.75
63		-30.07	9.44	74	3.93	2.08	89	3.26	0.83
790		-29.91	10.92	1794	2.11	3.52	2005	1.88	0.89
881		-30.12	12.14	1710	2.21	3.51	2046	1.85	0.84
MIT		-29.99	11.73	560	3.69	3.52	982	2.10	0.57
62	115	-33.08	10.75	80	3.71	2.09	109	2.72	0.73
63		-33.11	9.91	95	3.13	2.10	124	2.40	0.77
790		-32.96	13.12	1361	2.86	3.52	1982	1.97	0.69
881		-33.17	13.03	1740	2.24	3.52	2079	1.87	0.84
MIT		-33.03	12.24	463	4.60	3.47	670	3.18	0.69

Table 7.15 Summary of Sensitivity of Hydraulic Conductivity to Variation of the Initial Dissipation Point.

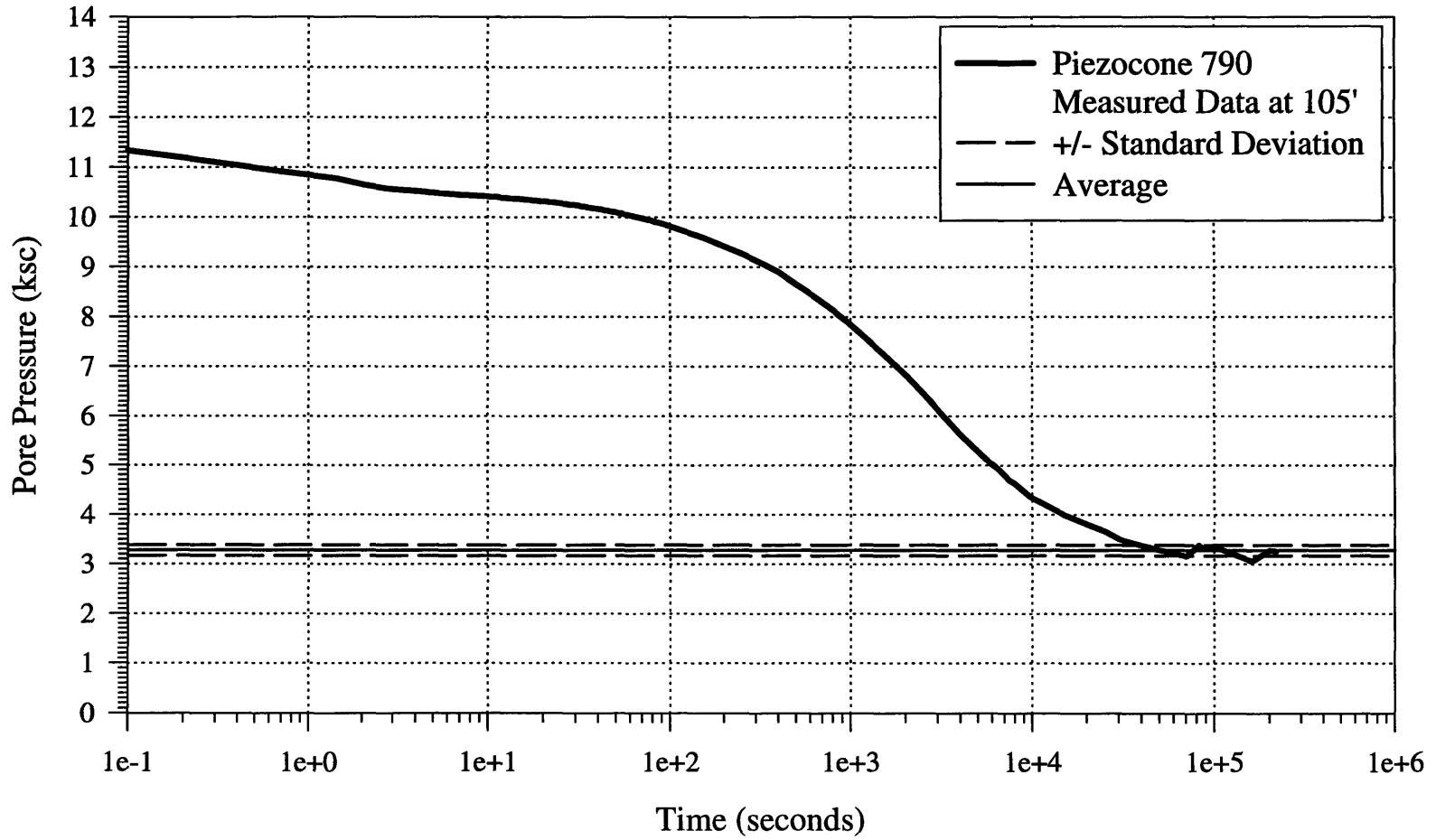


Figure 7.1 Example of Dissipated Pore Pressure Value Determination.

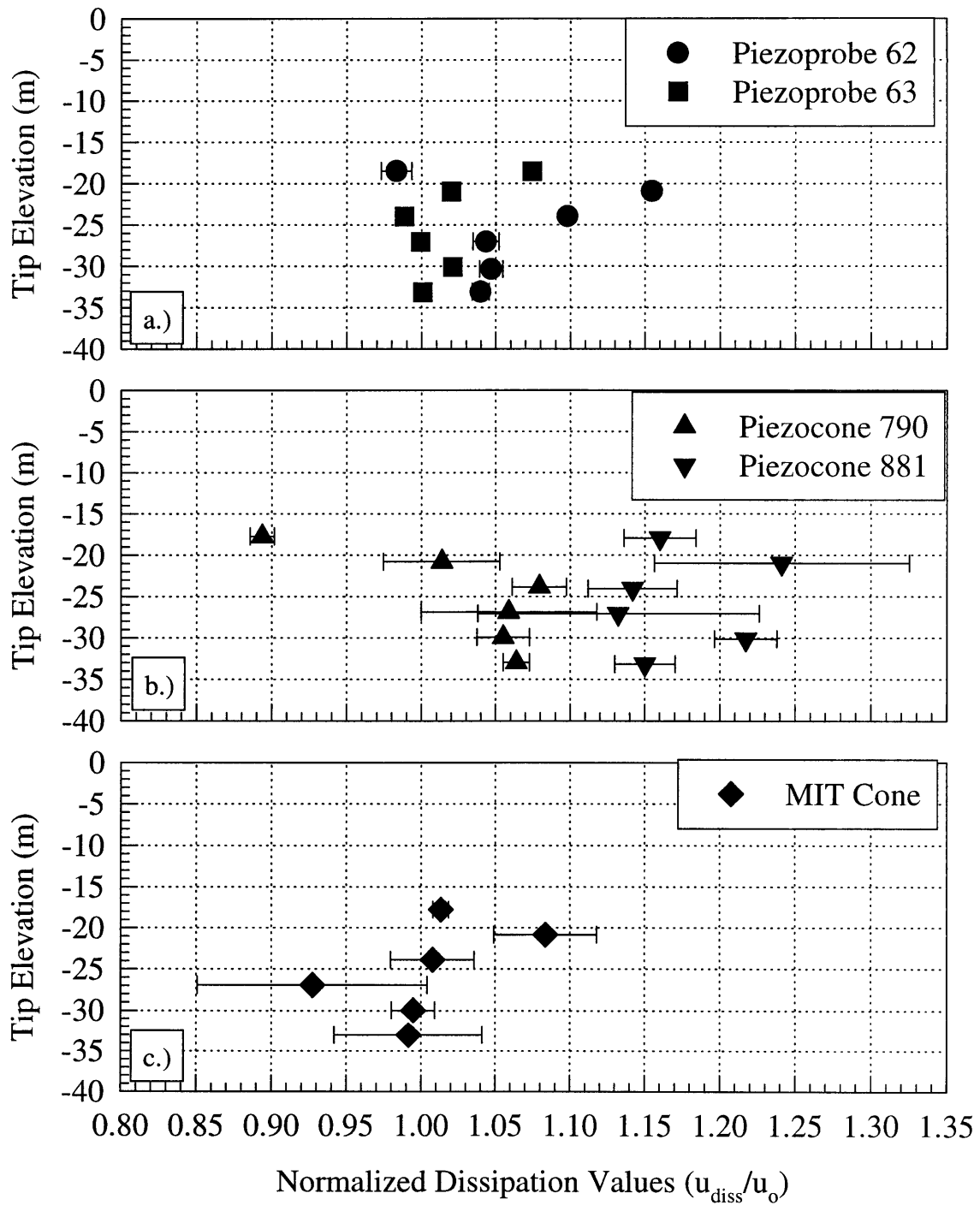


Figure 7.2 Dissipated Pore Pressure Ratio (u_{diss}/u_o) for: a.) Piezoprobe 62 and Piezoprobe 63; b.) Piezocone 790 and Piezocone 881; and c.) the MIT Piezocone.

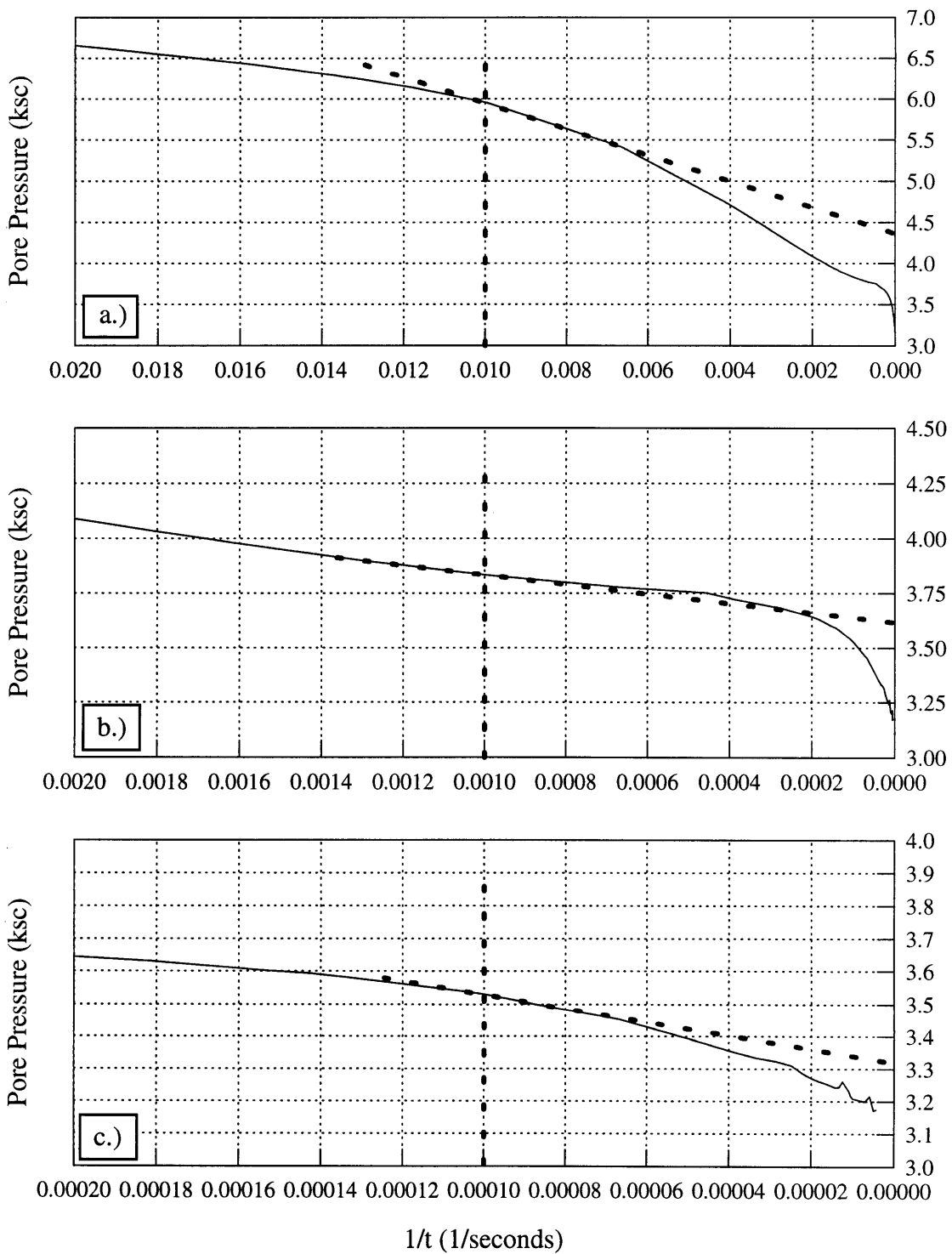


Figure 7.3 Example of Inverse Time Construction on Measured Data: Piezoprobe 63 at El. - 30 m (105 ft Depth).

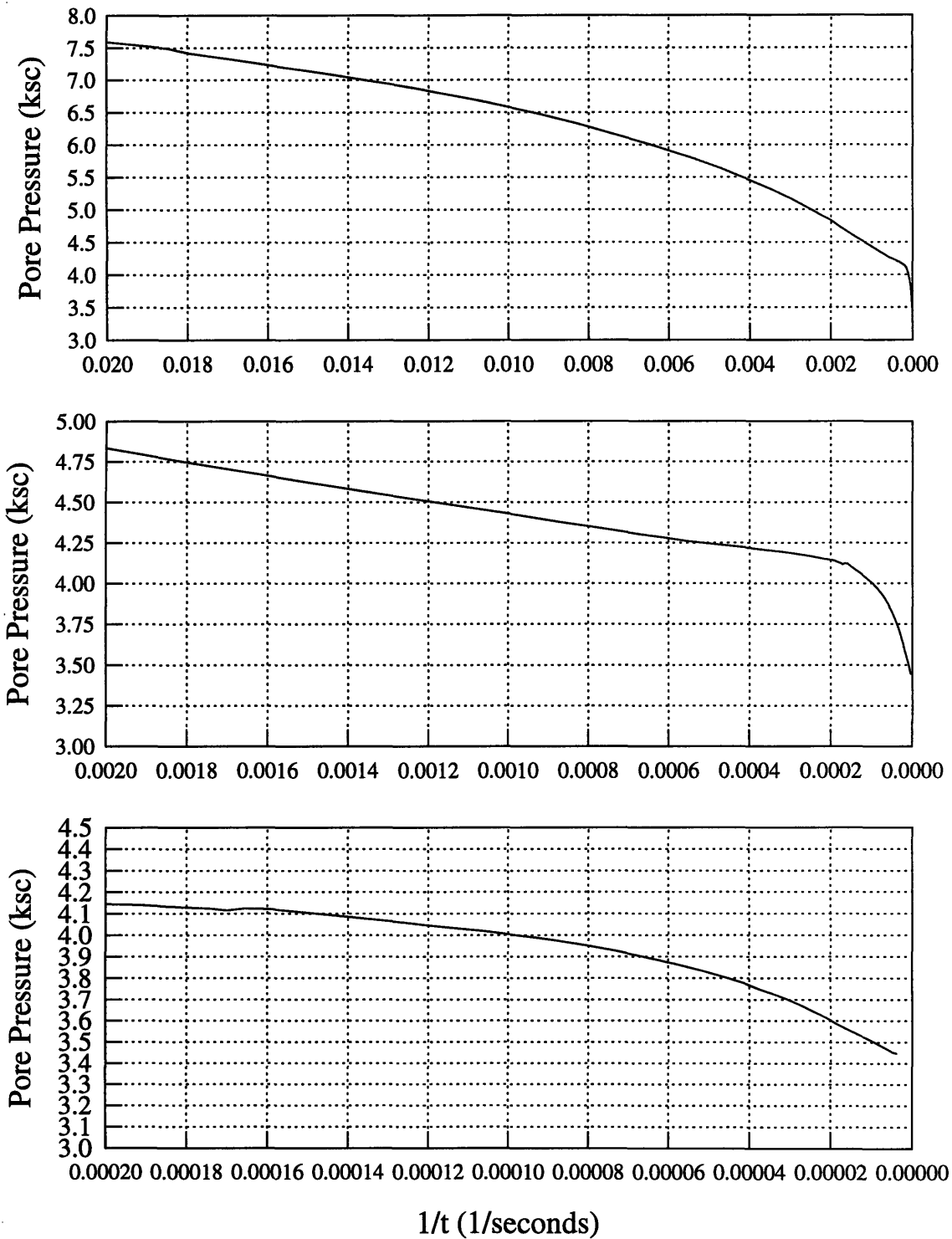


Figure 7.4 Example of Inverse Time Plot for Model Prediction: Piezoprobe at El. -33 m (Depth 115 ft).

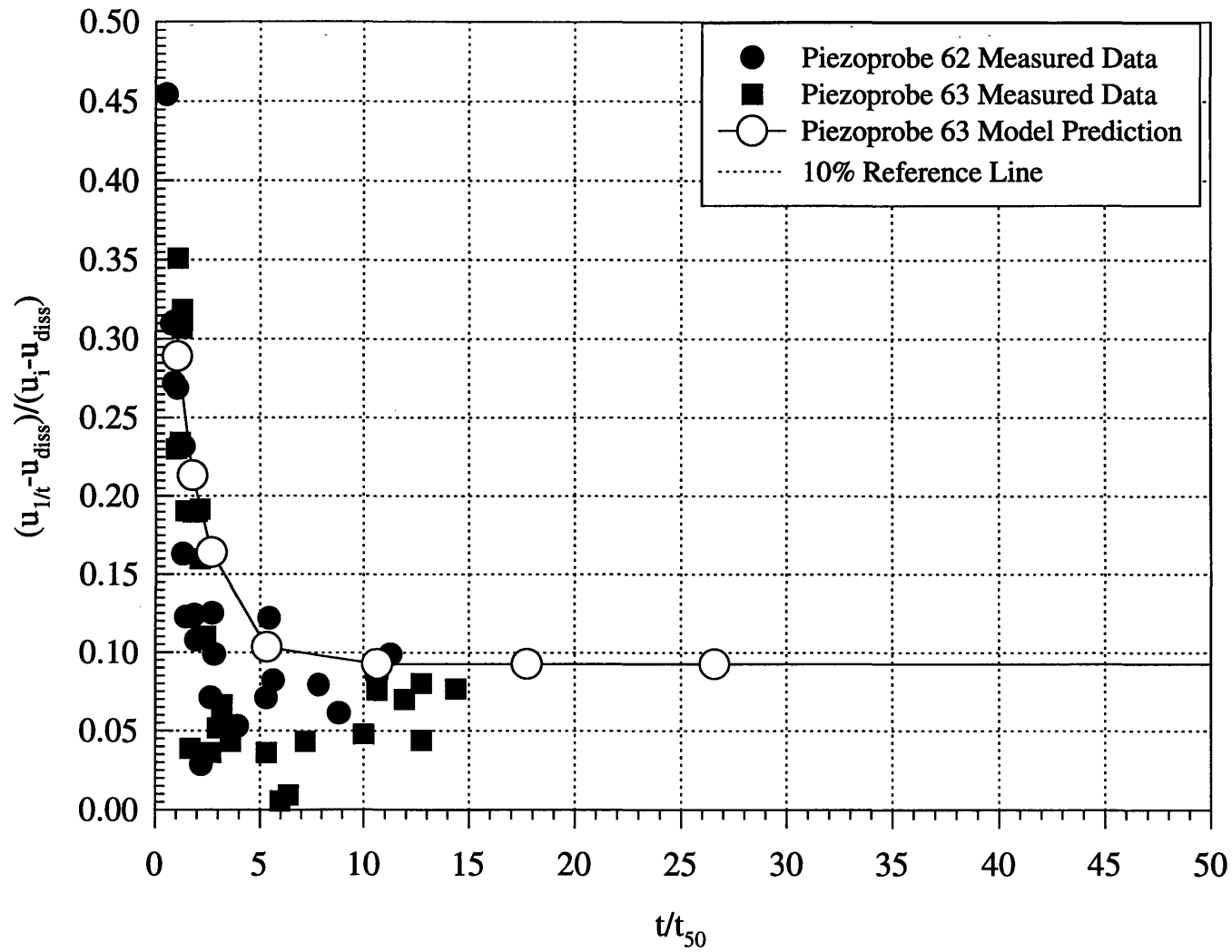


Figure 7.5 Convergence of the Pore Pressure Predicted by the Inverse Time Extrapolation Method to the Equilibrium Pore Pressure for the Piezoprobes.

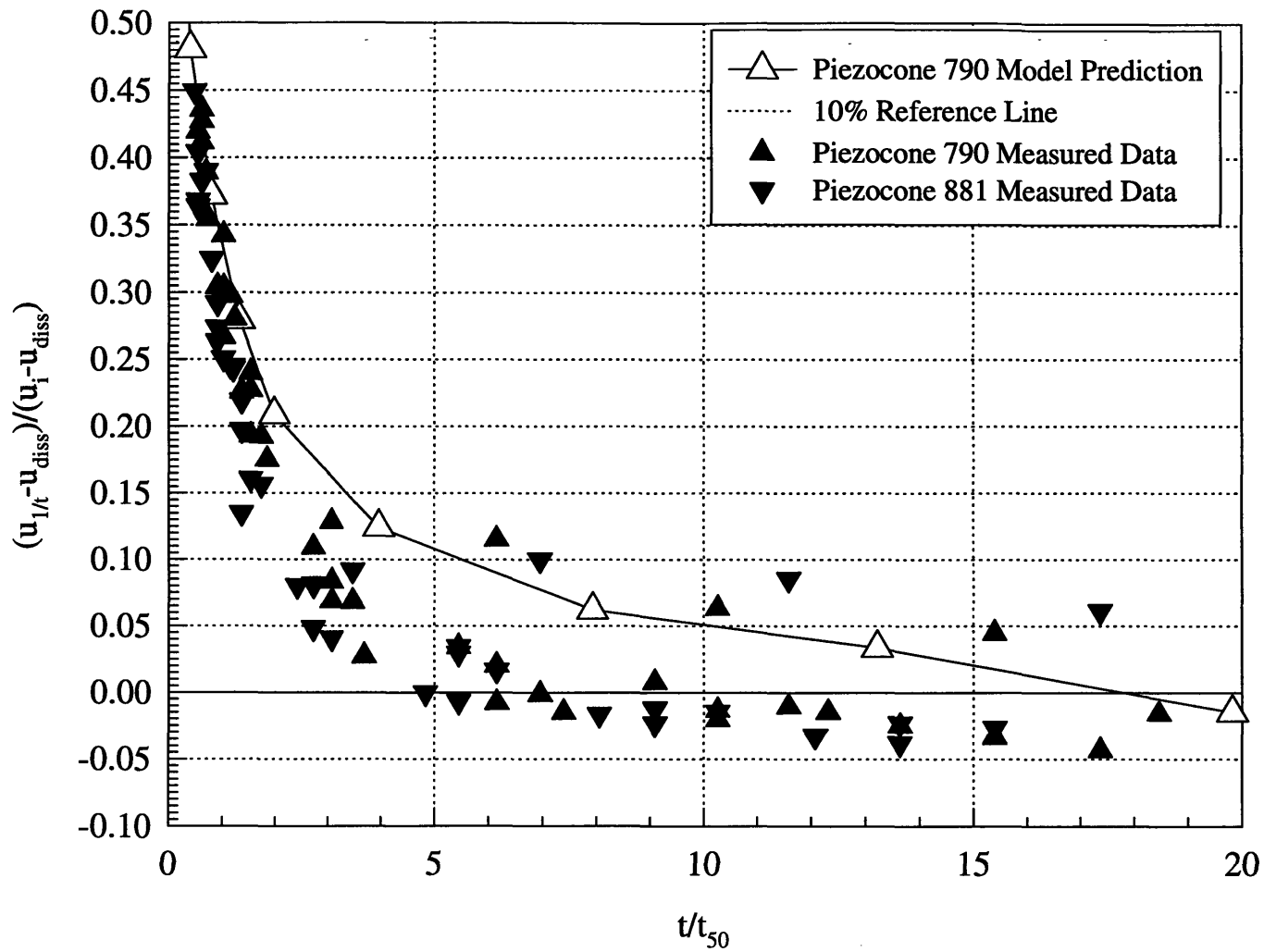


Figure 7.6 Convergence of the Pore Pressure Predicted by the Inverse Time Extrapolation Method to the Equilibrium Pore Pressure for the Piezocones.

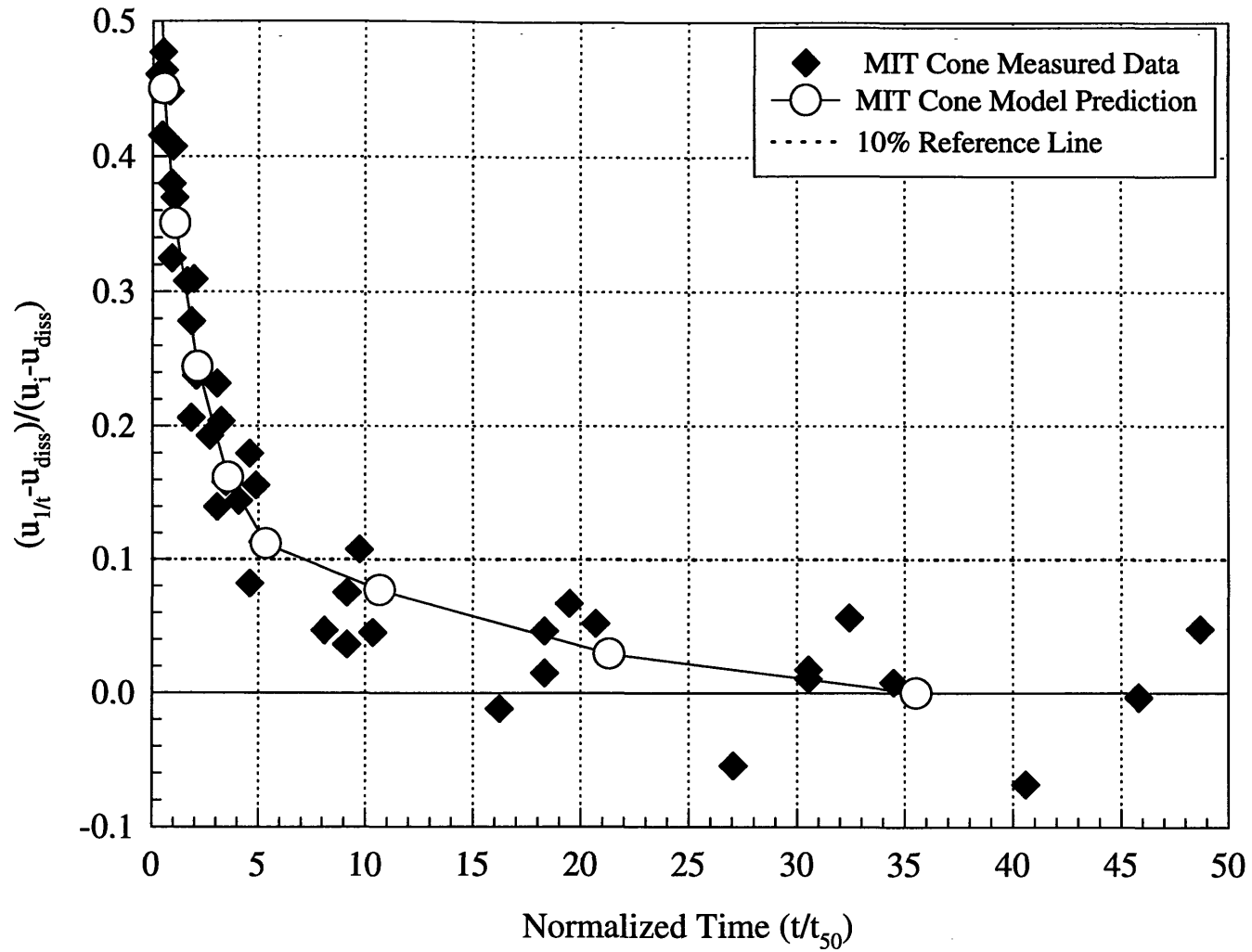


Figure 7.7 Convergence of the Pore Pressure Predicted by the Inverse Time Extrapolation Method to the Equilibrium Pore Pressure for the MIT Piezocone.

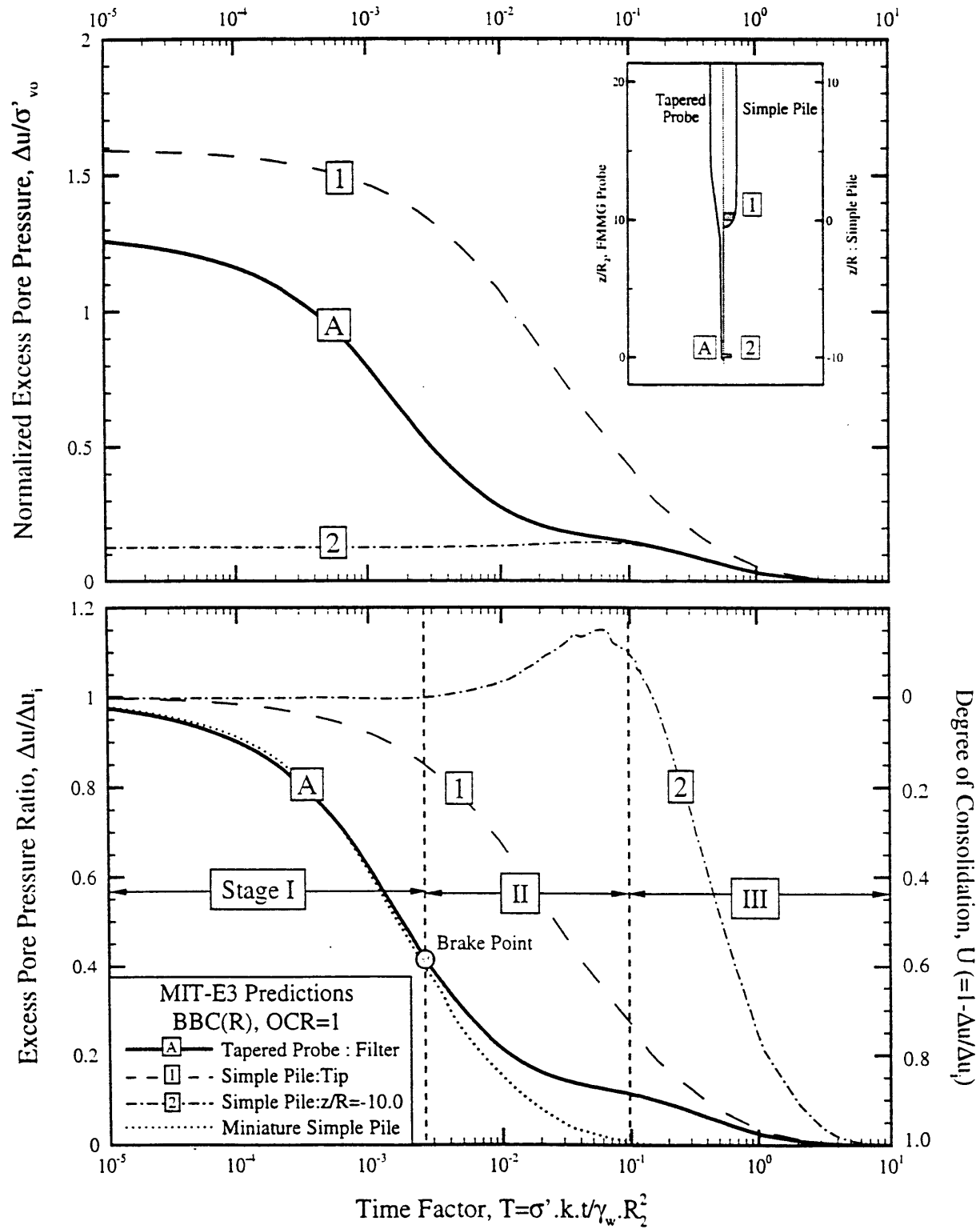


Figure 7.8 Probe Geometry and Brake Point (After Whittle et al., 1997).

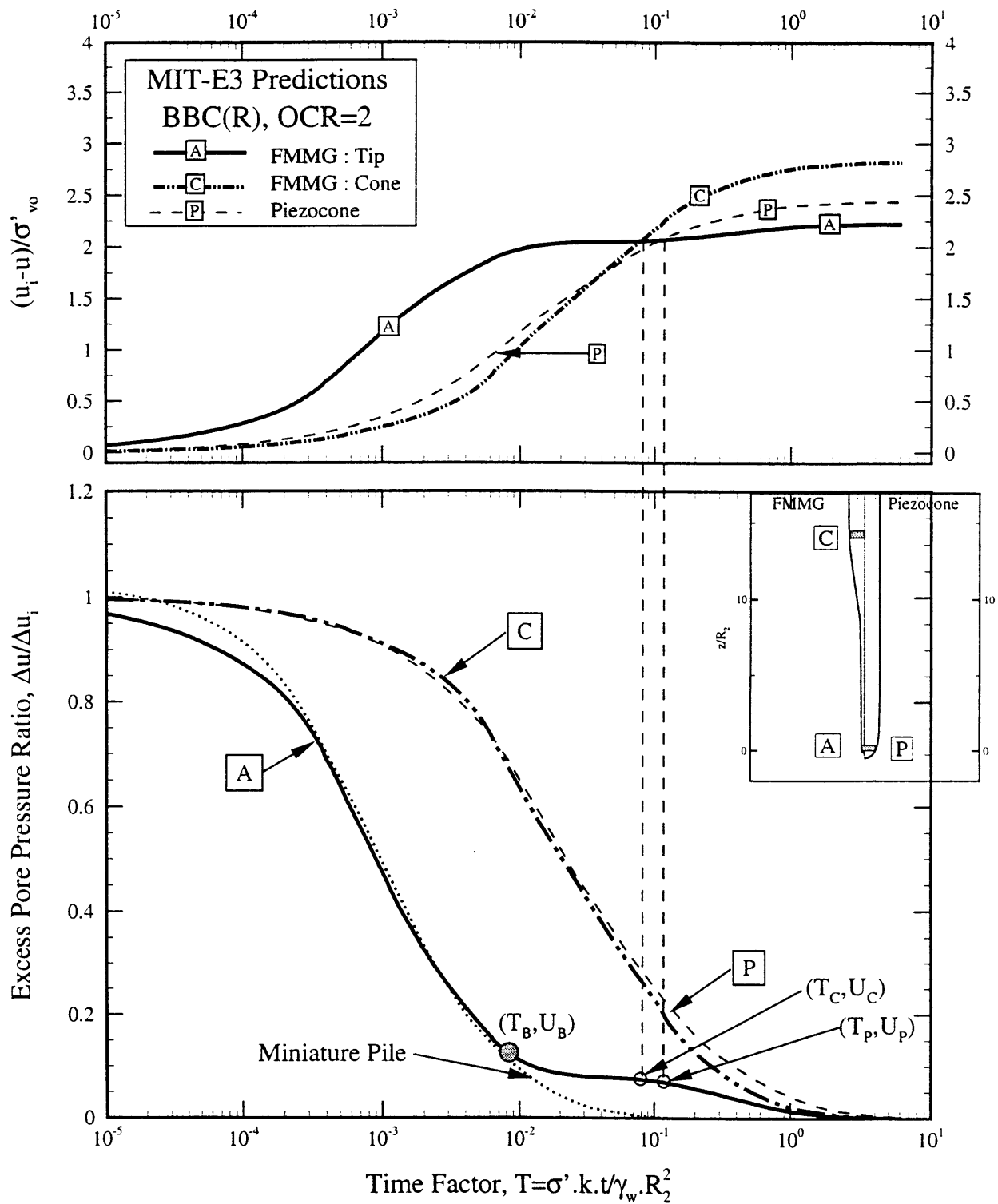


Figure 7.9 Two Point Intersection Method for u_0 (After Whittle et al., 1997).

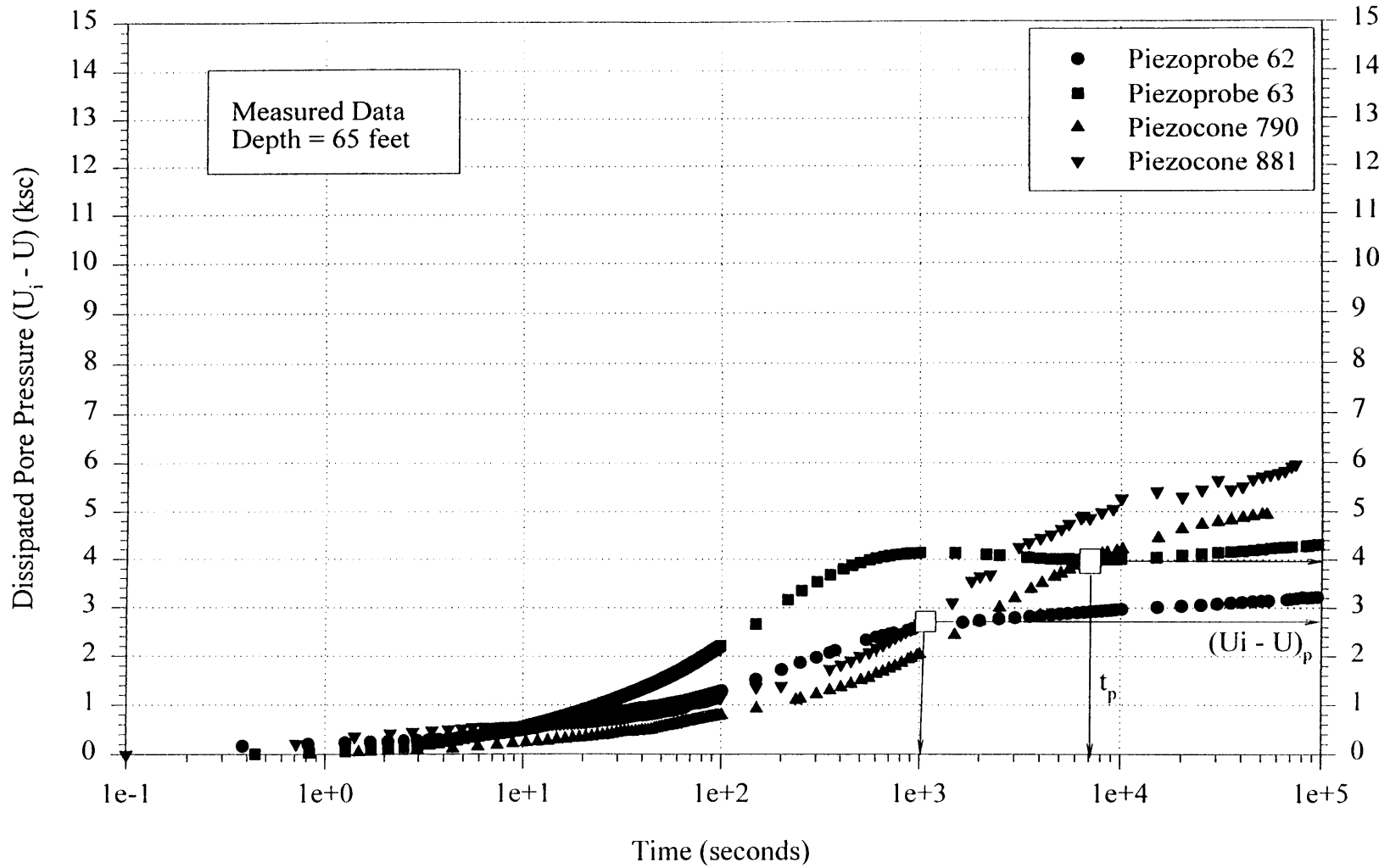


Figure 7.10 Two Point Intersection Construction for Determining u_0 ; El. -18 m (Depth 65 ft).

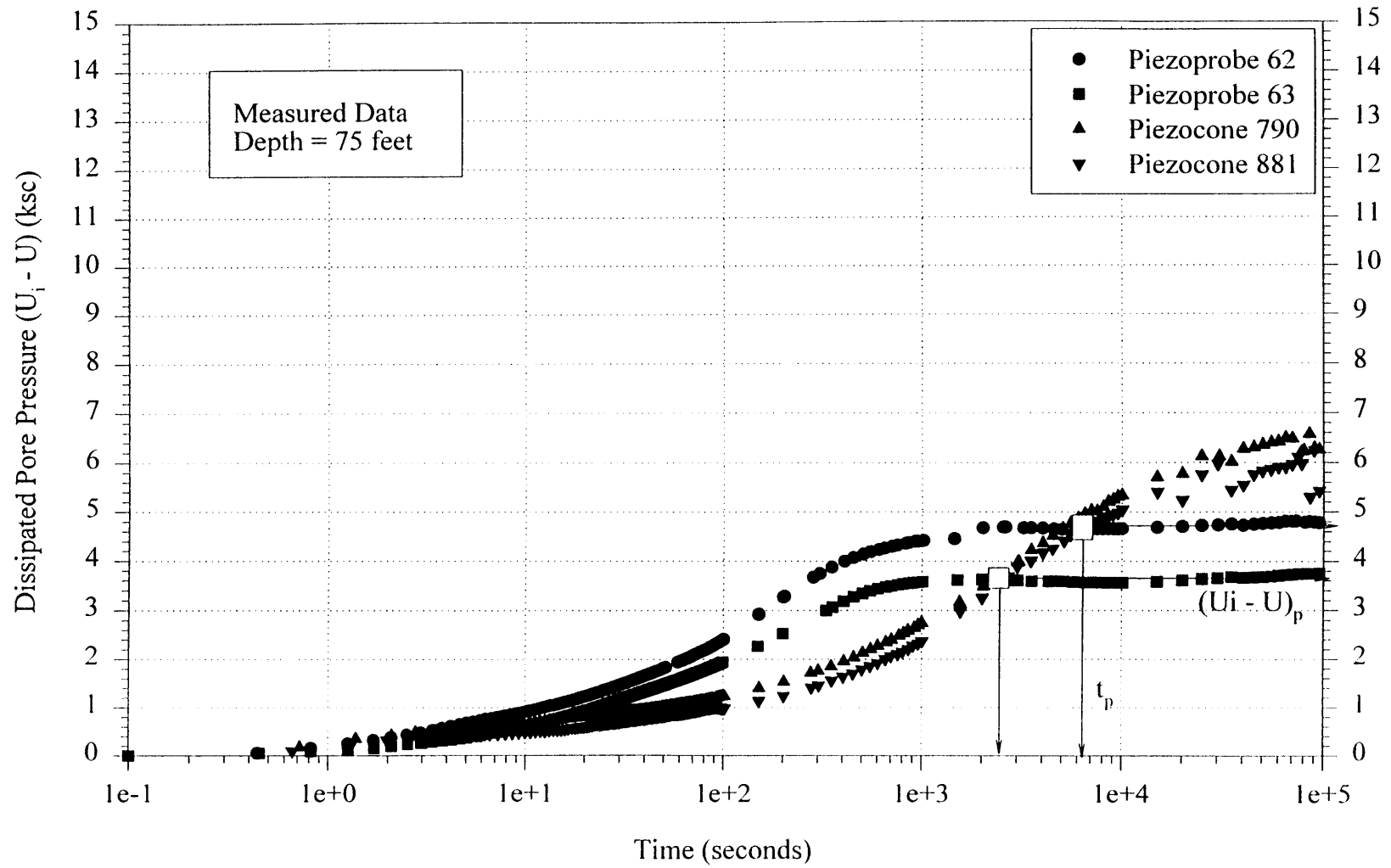


Figure 7.11 Two Point Intersection Construction for Determining u_0 ; El. -21 m (Depth 75 ft).

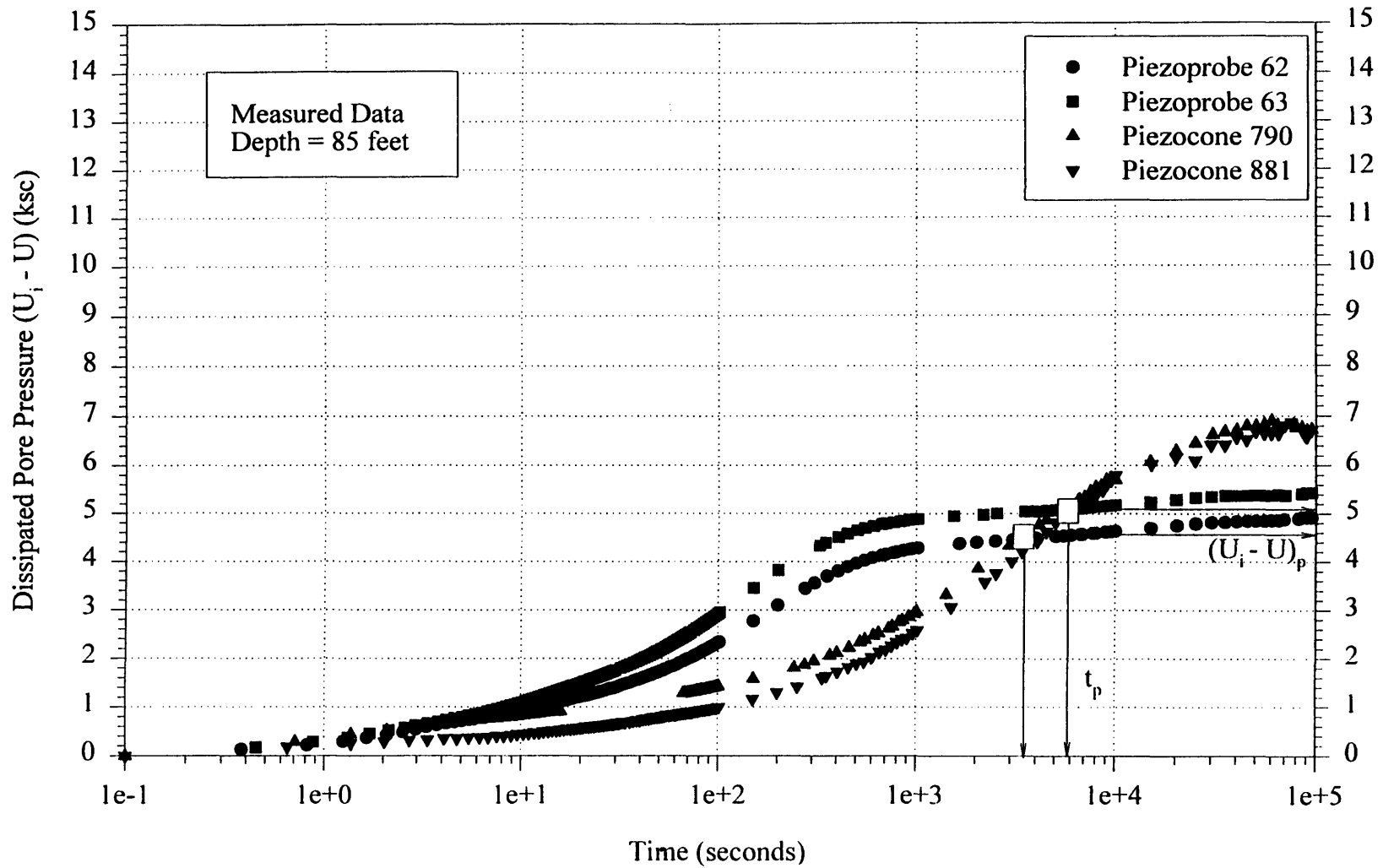


Figure 7.12 Two Point Intersection Construction for Determining u_0 : El. -24 m (Depth 85 ft).

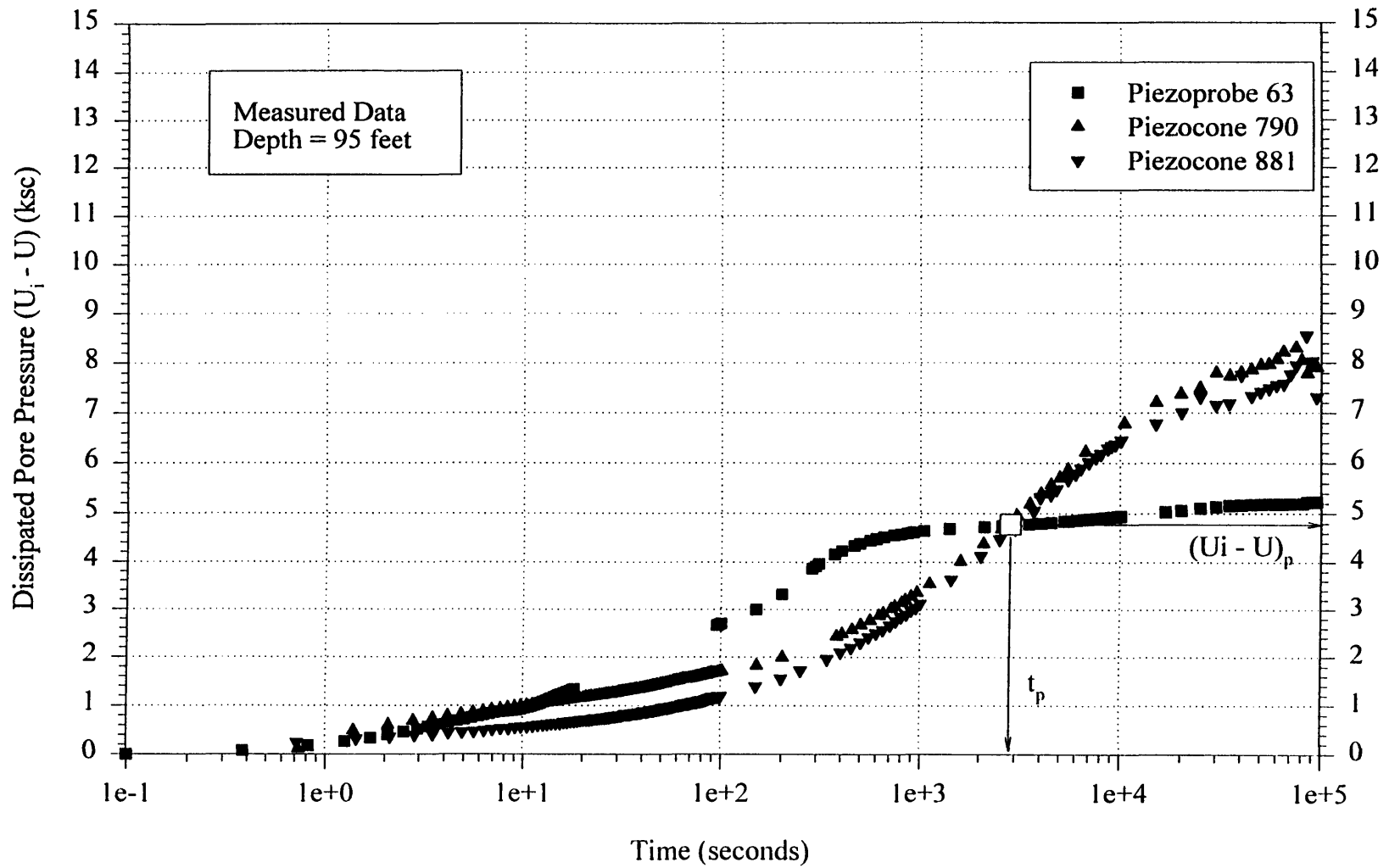


Figure 7.13 Two Point Intersection Construction for Determining u_0 : El. -27 m (Depth 95 ft).

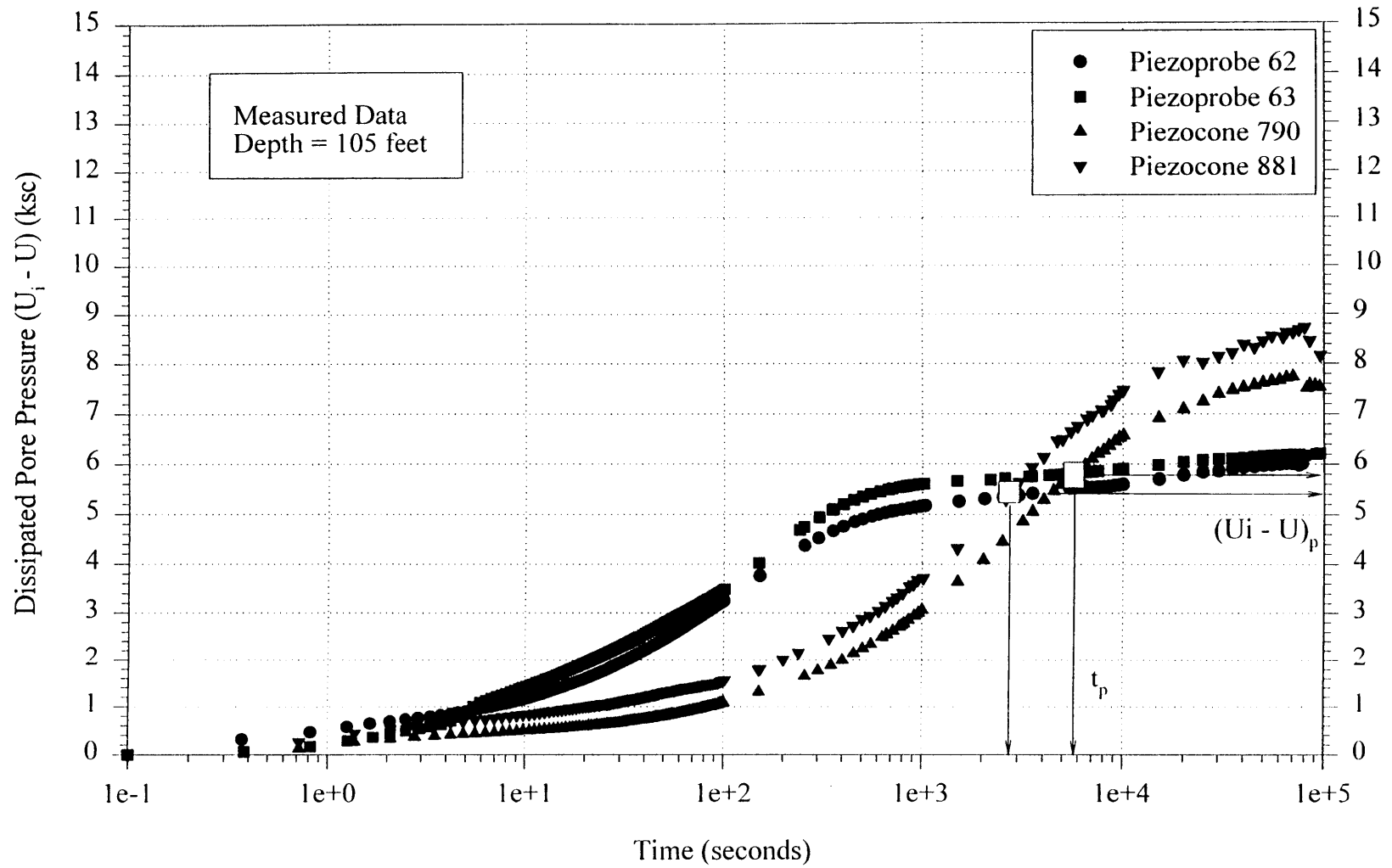


Figure 7.14 Two Point Intersection Construction for Determining u_0 ; El. -30 m (Depth 105 ft).

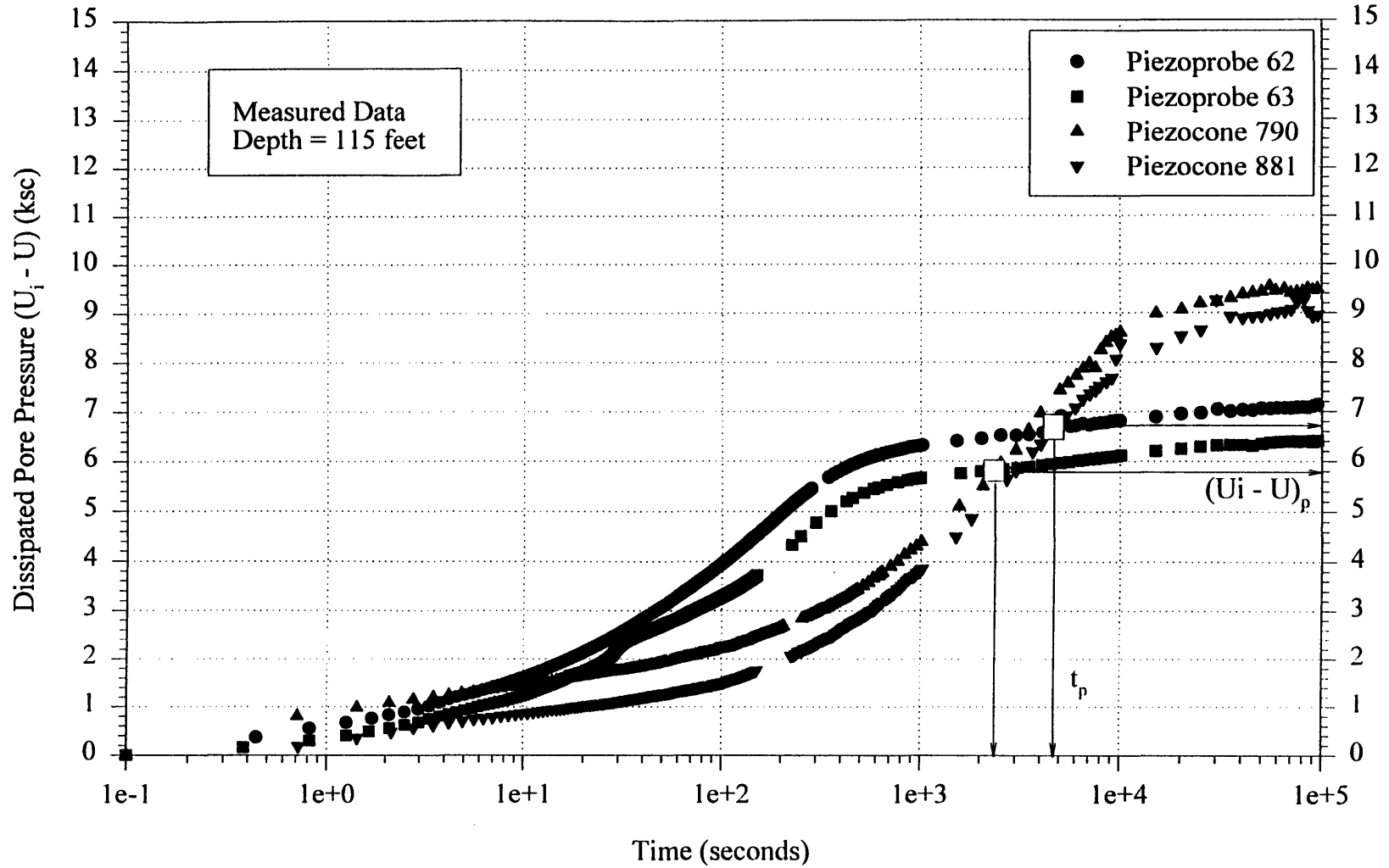


Figure 7.15 Two Point Intersection Construction for Determining u_0 : El. -33 m (Depth 115 ft).

Vertical Stresses; σ'_{v0} , σ'_p and σ_v (EOC) (kPa)

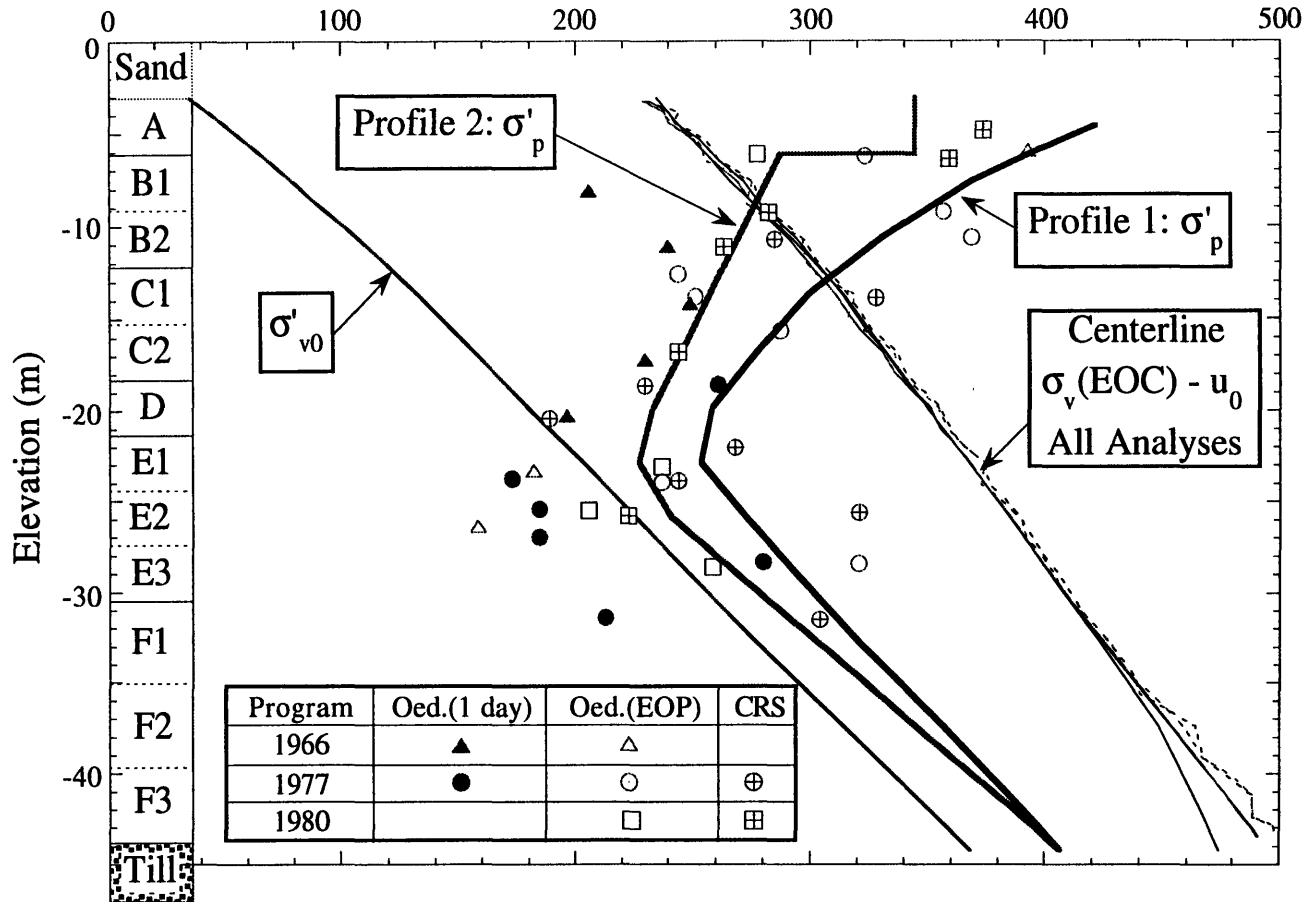


Figure 7.16 Stress History Profiles 1 & 2 (After Ladd et al., 1994).

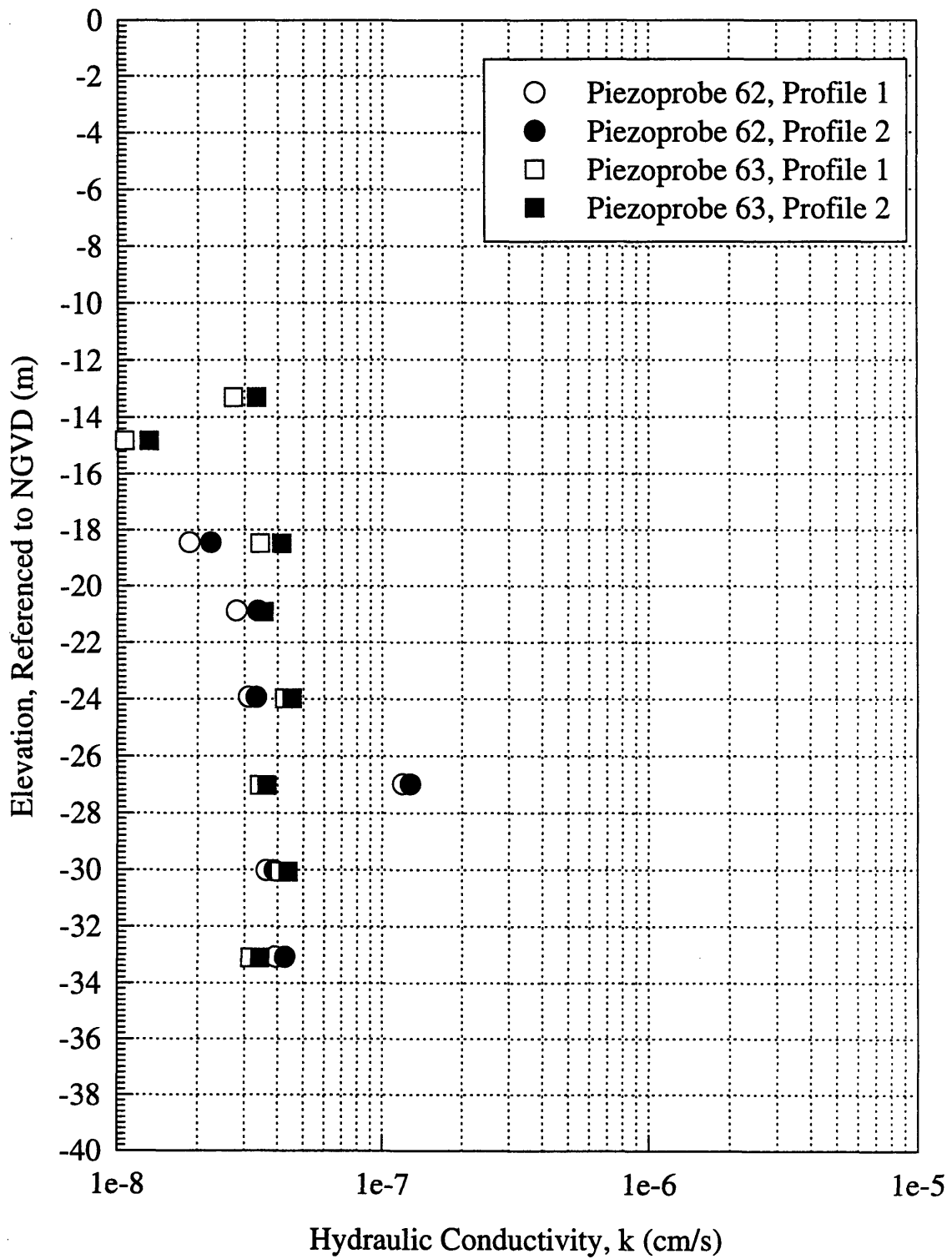


Figure 7.17 Summary of Interpretation of Hydraulic Conductivity from the T_{50} Interpretation Method with Data Measured by the Piezoprobes.

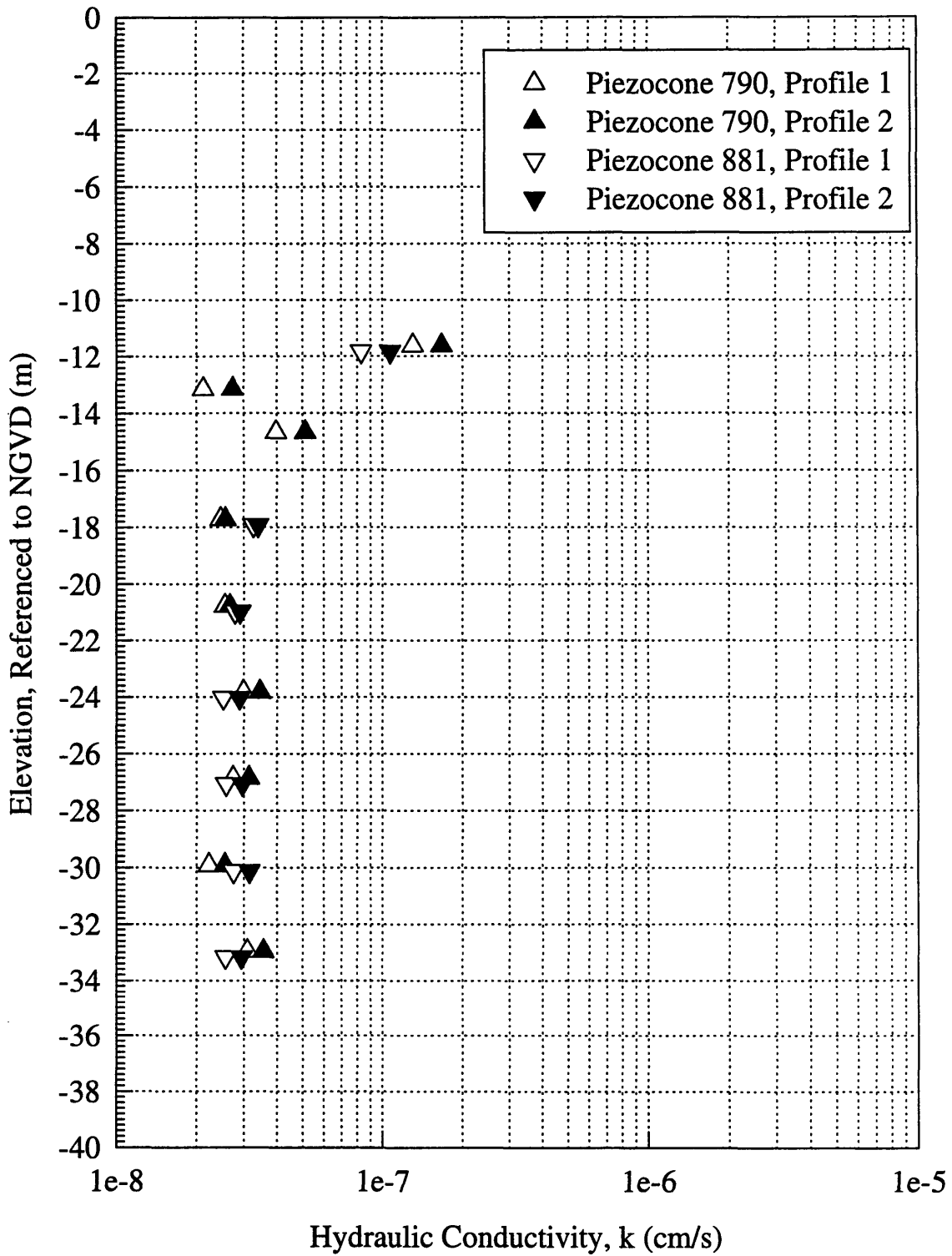


Figure 7.18 Summary of Interpretation of Hydraulic Conductivity from the T_{50} Interpretation Method with Data Measured by the Piezocones.

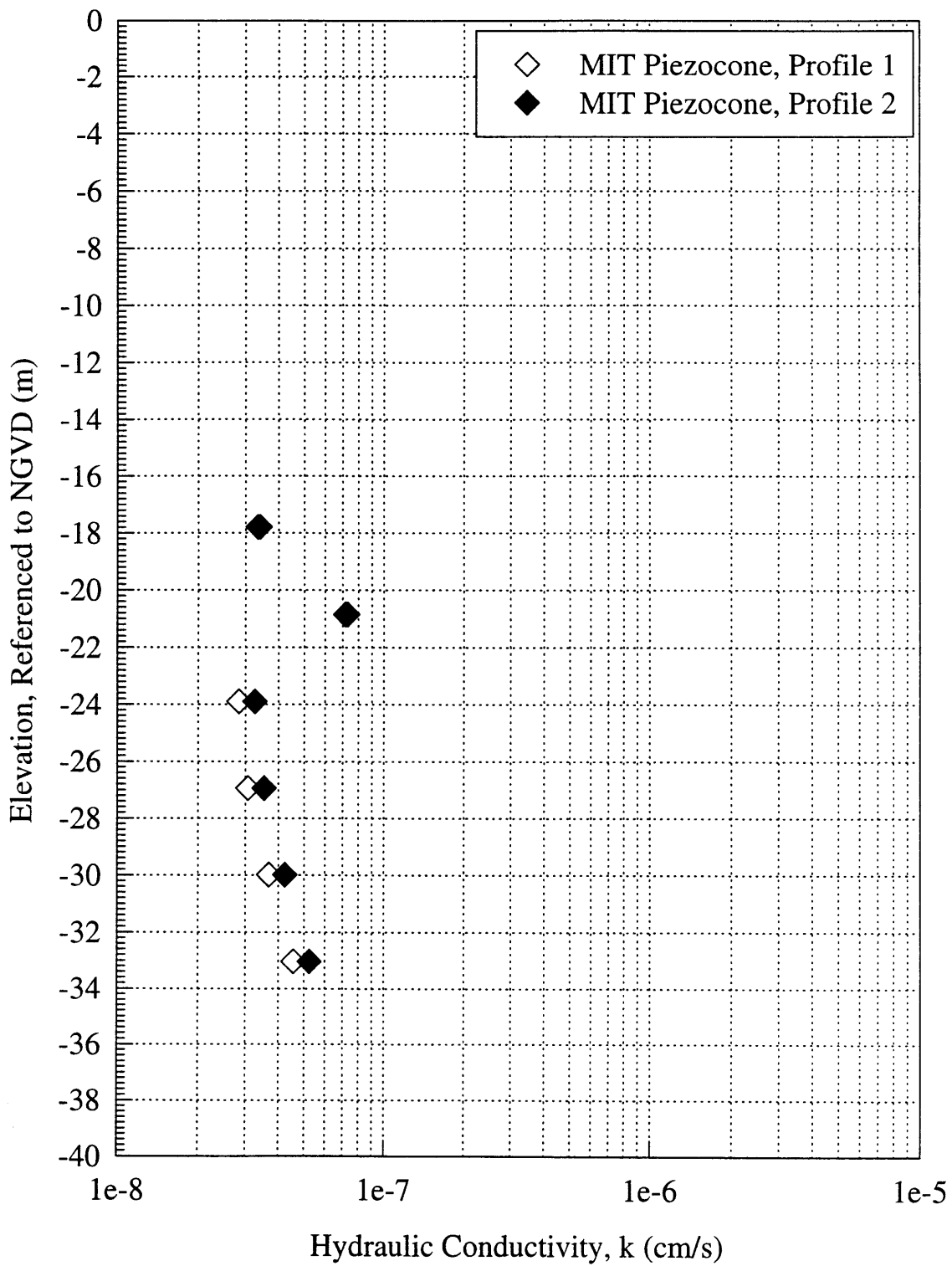


Figure 7.19 Summary of Interpretation of Hydraulic Conductivity from the T_{50} Interpretation Method with Data Measured by the MIT Piezocone.

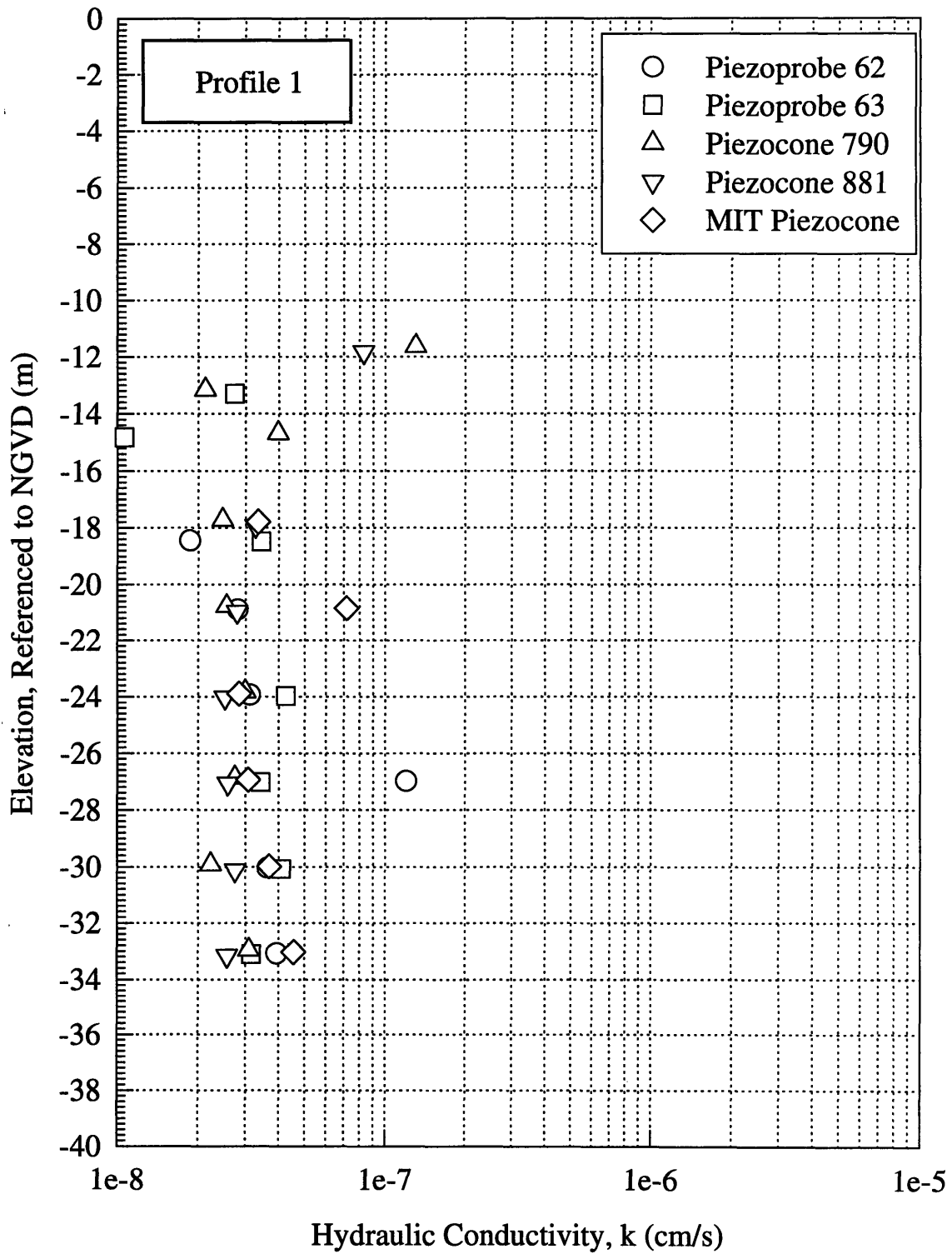


Figure 7.20 Summary of Interpretation of Hydraulic Conductivity from the T_{50} Interpretation Method with Data Measured by the Piezoprobes, Piezocones, and MIT Piezocone.

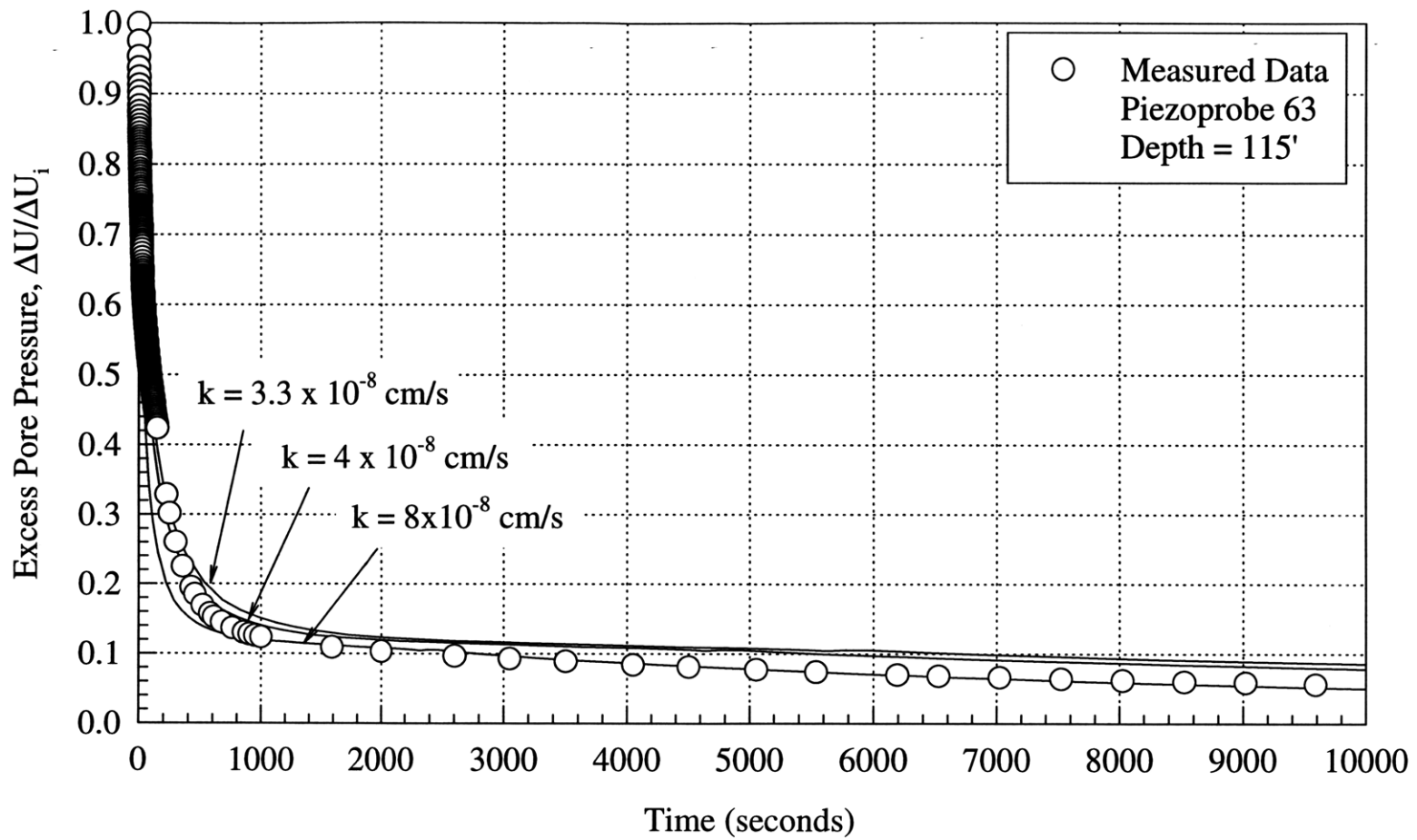


Figure 7.21 Example of the Goodness of Fit Matching Method.

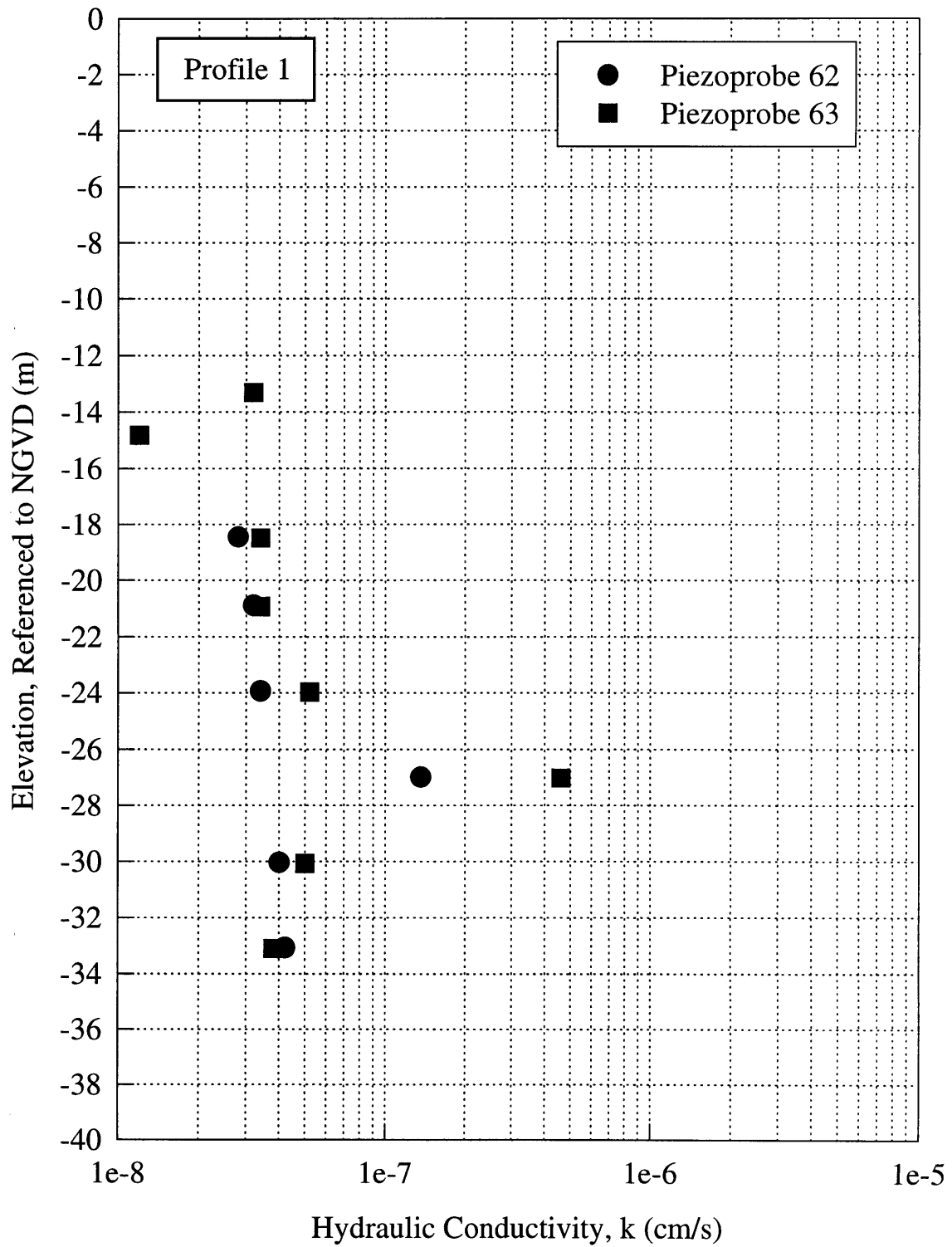


Figure 7.22 Summary of Interpretation of Hydraulic Conductivity from the Goodness of Fit Matching Method with Data Measured by the Piezoprobes (After Sutabutr, 1998).

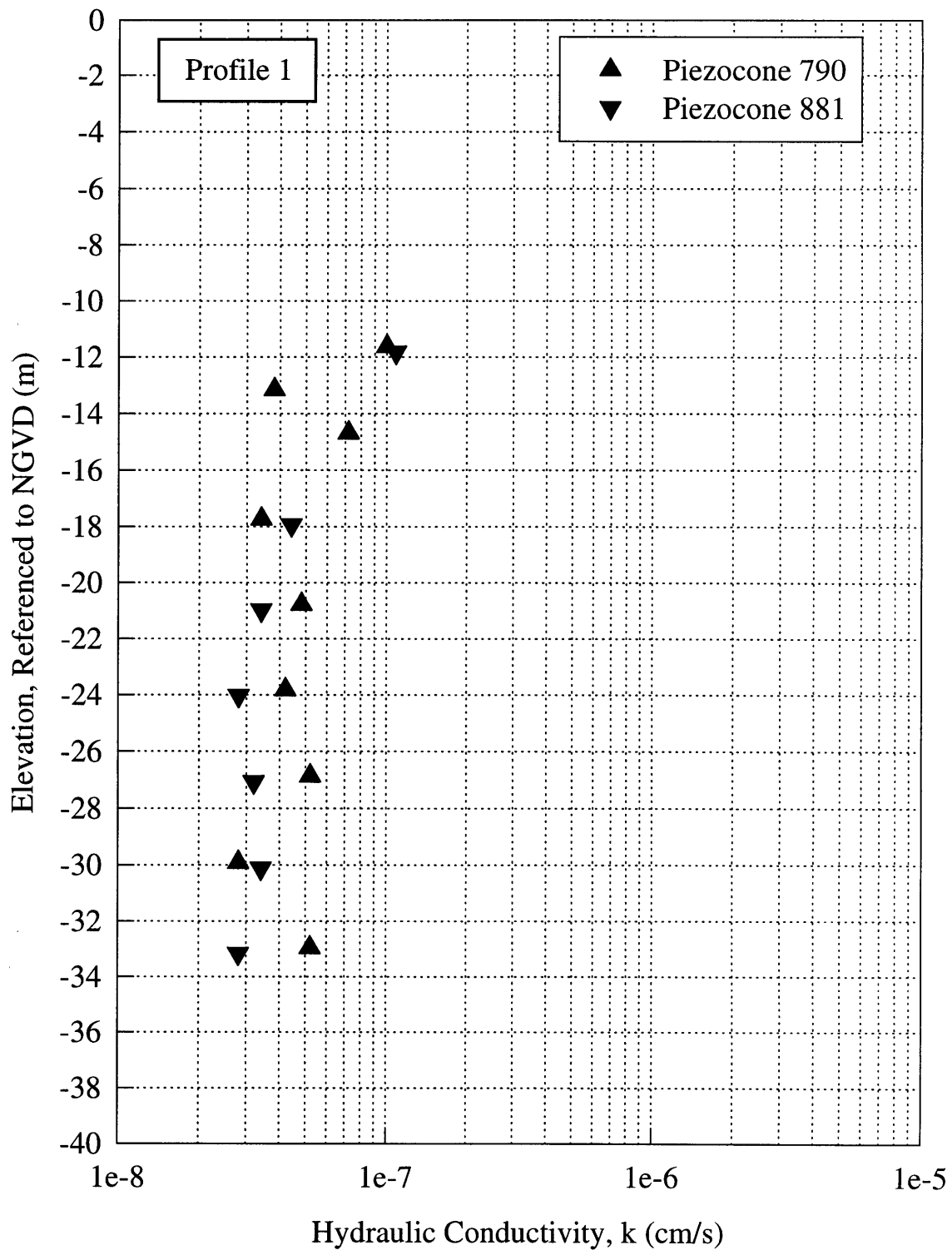


Figure 7.23 Summary of Interpretation of Hydraulic Conductivity from the Goodness of Fit Matching Method with Data Measured by the Piezocones (After Sutabutr, 1998).

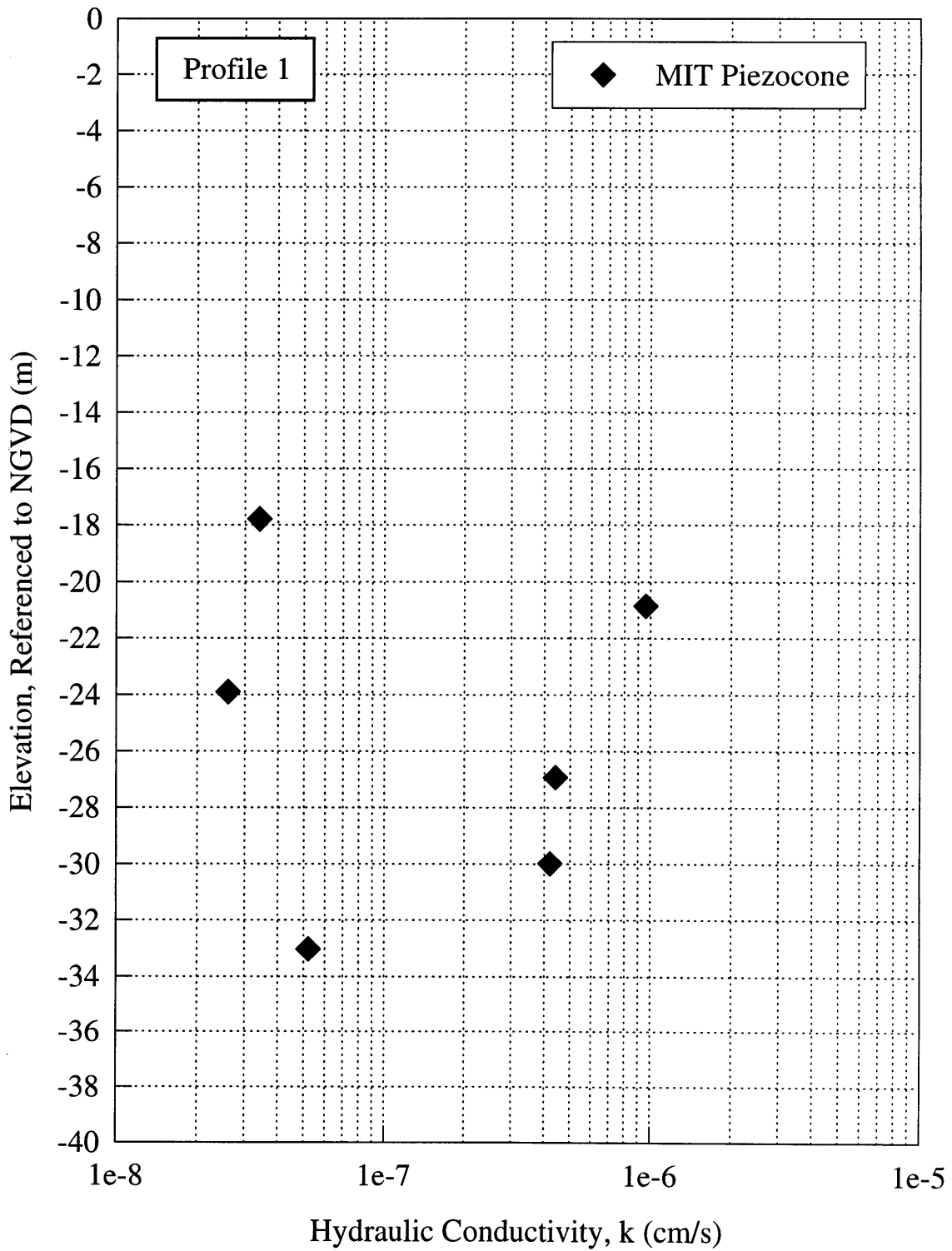


Figure 7.24 Summary of Interpretation of Hydraulic Conductivity from the Goodness of Fit Matching Method with Data Measured by the MIT Piezocone (After Sutabutr, 1998).

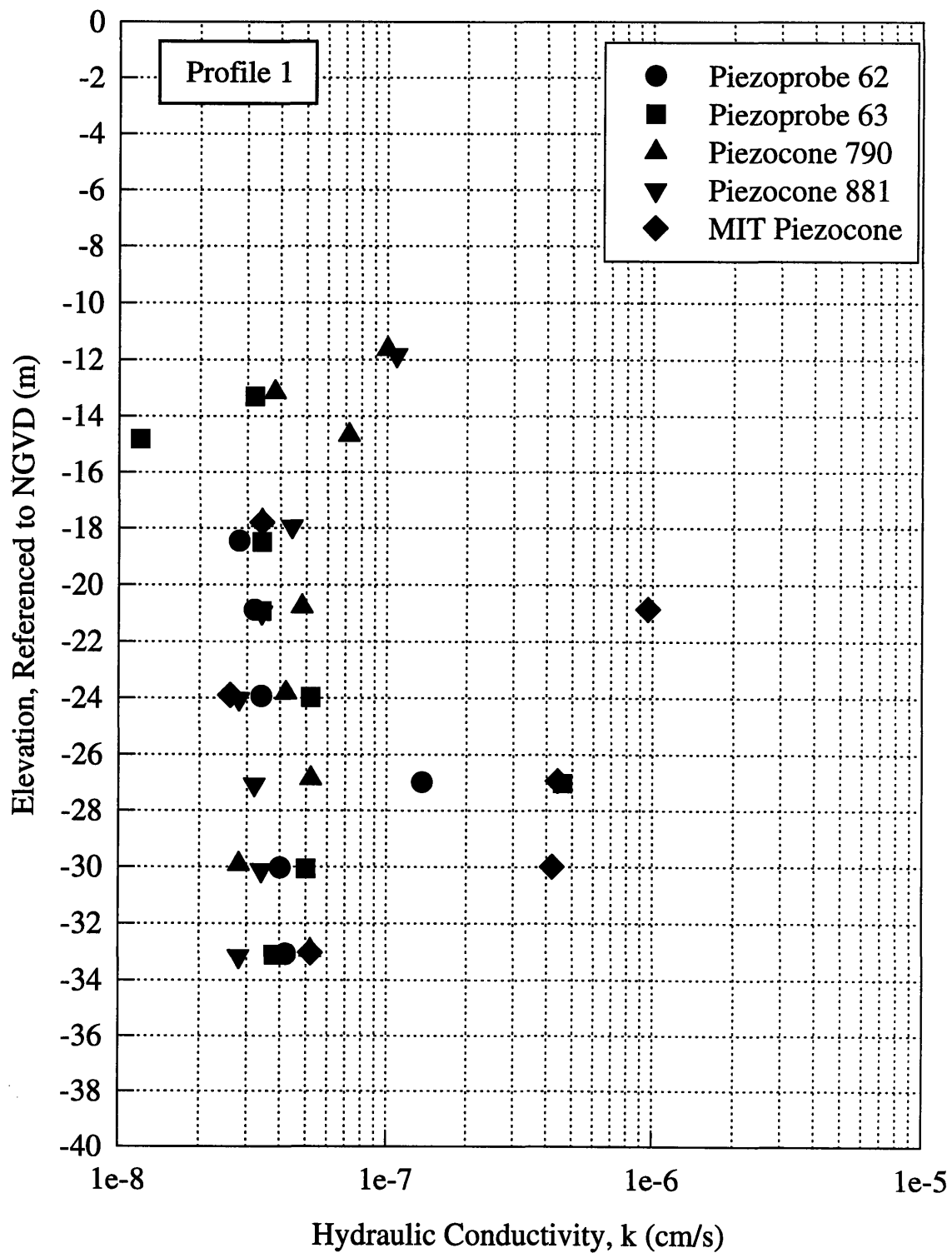


Figure 7.25 Summary of Interpretation of Hydraulic Conductivity from the Goodness of Fit Matching Method with Data Measured by the Piezoprobes, Piezocones, and the MIT Piezocone (After Sutabutr, 1998).

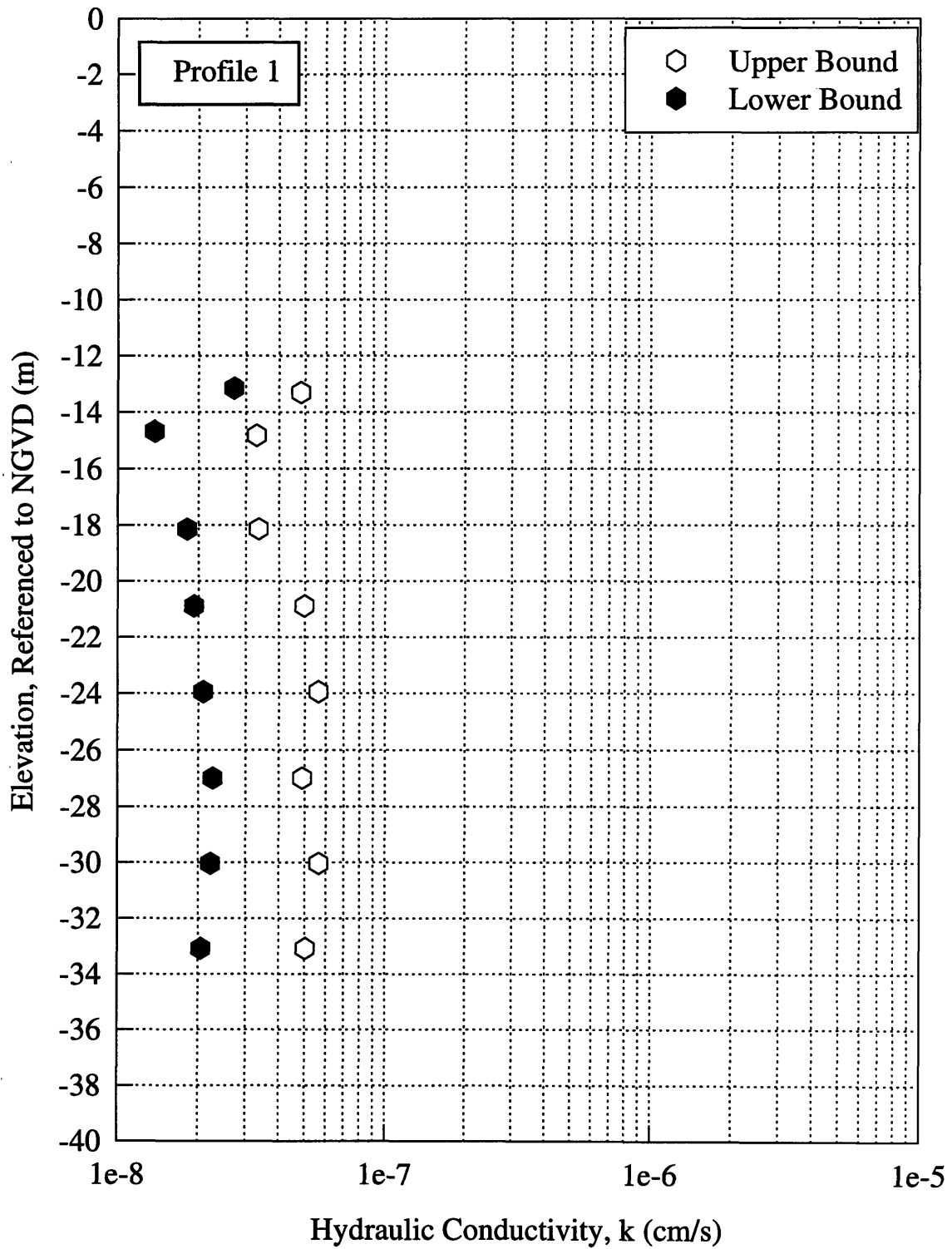


Figure 7.26 Summary of Interpretation of Hydraulic Conductivity from the Concurrent Matching Method with Data Measured by the Piezoprobes and Piezocones (After Sutabutr, 1998).

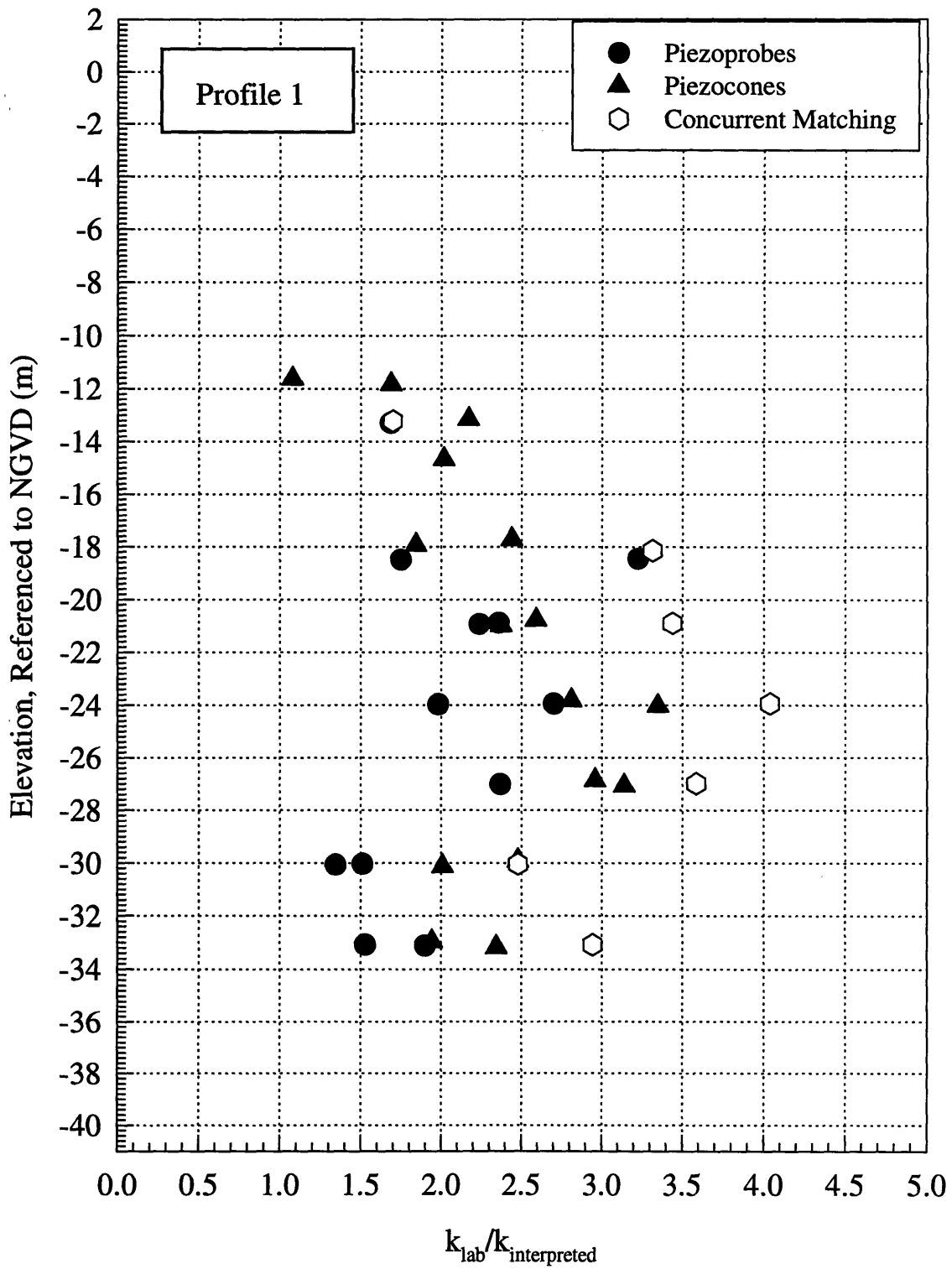


Figure 7.27 Summary of the Ratio $k_{lab}/k_{interpreted}$ for the Piezoprobes and the Piezocones.

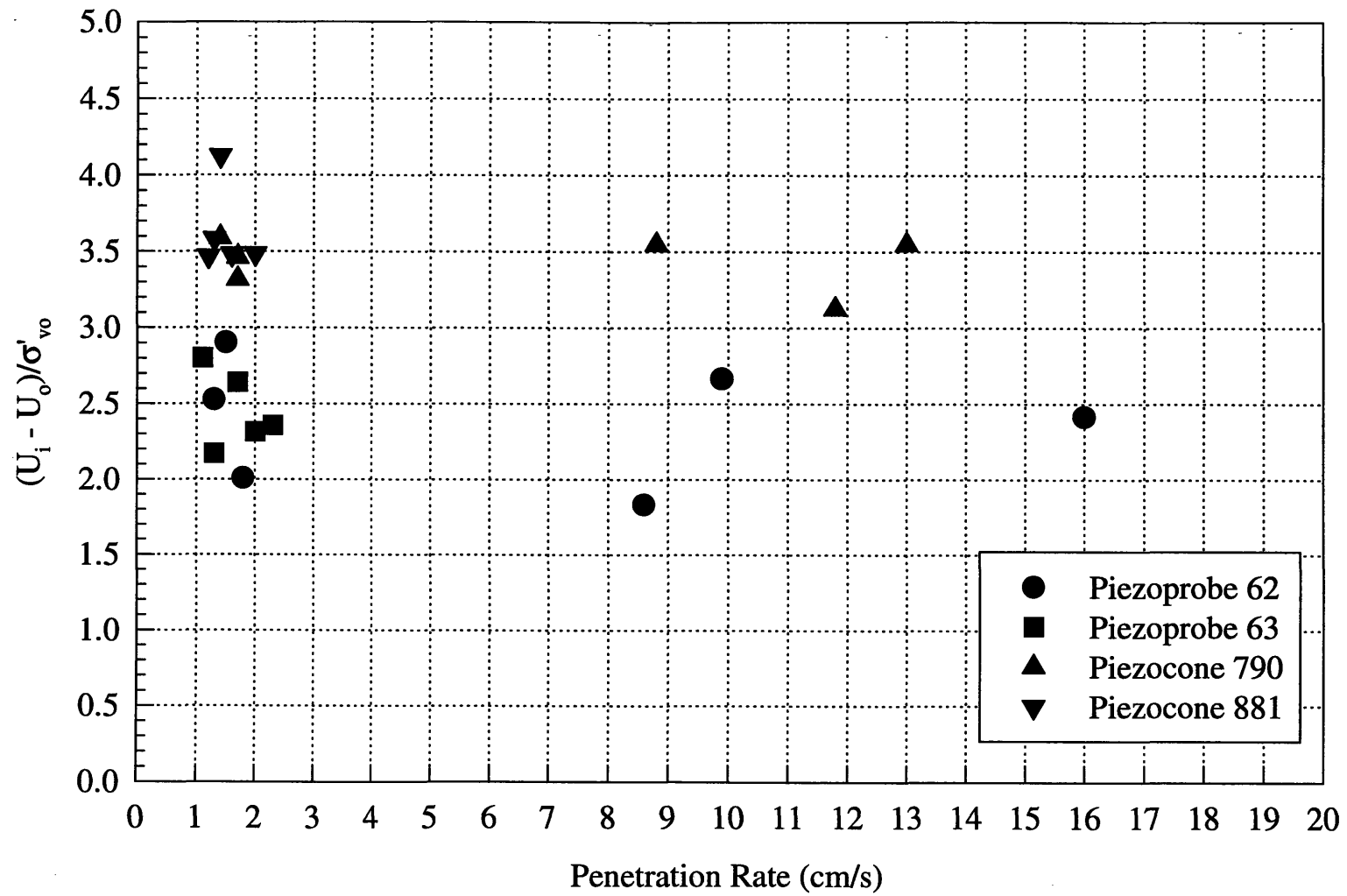


Figure 7.28 Penetration Pore Pressure Ratio $[(u_i - u_o)/\sigma'_{vo}]$ versus Penetration Rate for the Piezoprobes and the Piezocones.

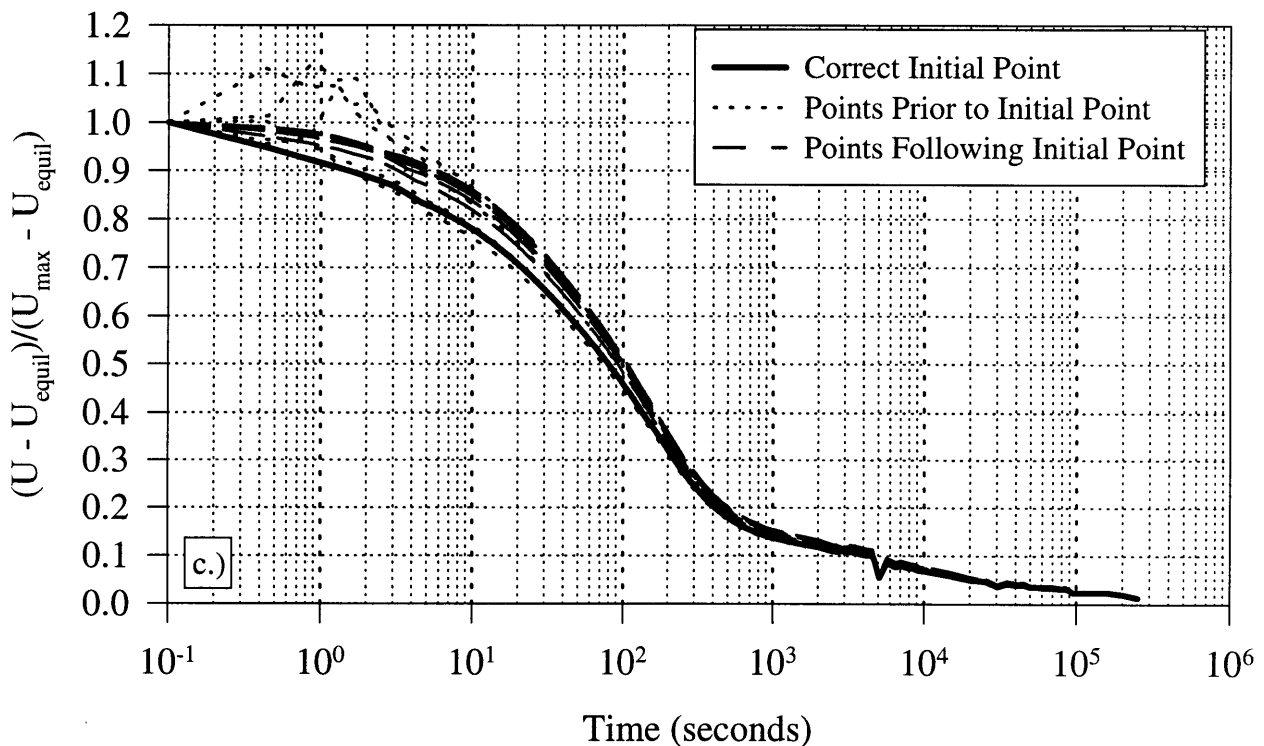
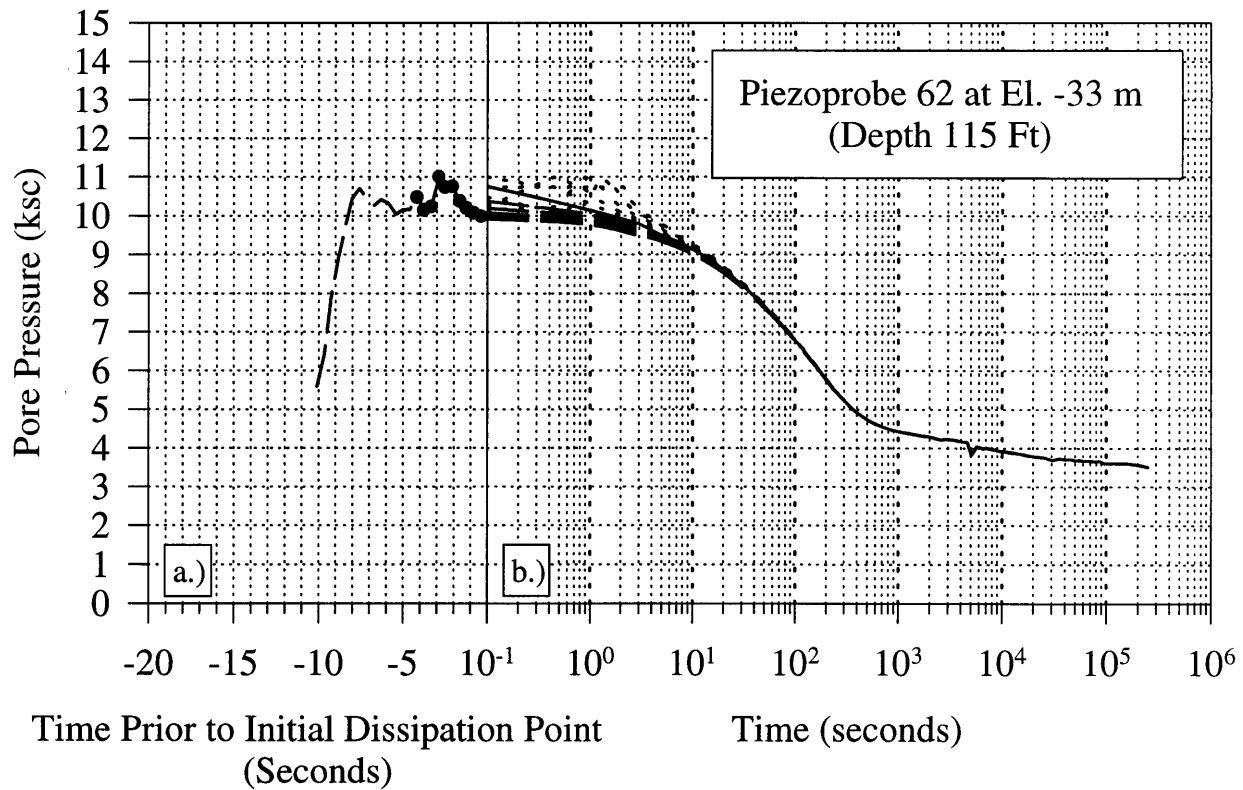


Figure 7.29 Initial Dissipation Point Variation on Measured Data for Piezoprobe 62 at El. -33 m (Depth 115 ft.): a.) Penetration; b.) Dissipation, Absolute Pore Pressure; c.) Dissipation, Normalized Pore Pressure.

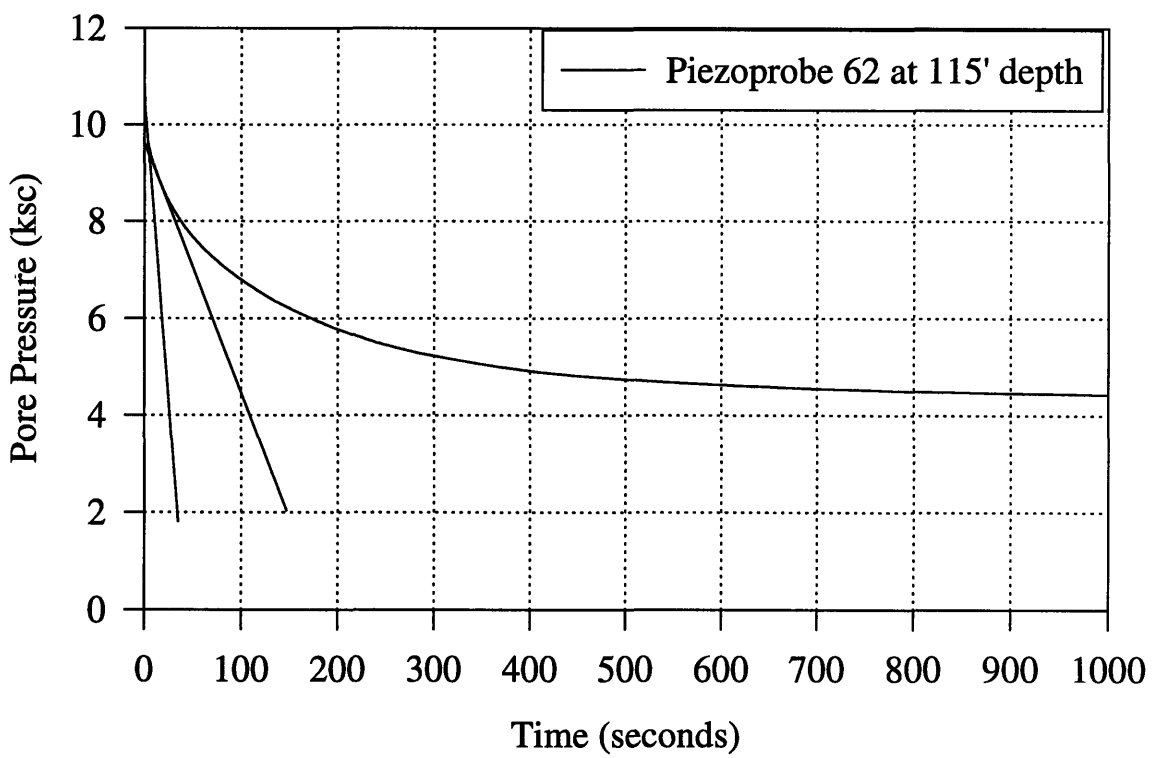


Figure 7.30 Slope of the Dissipation Curve of Absolute Pressure Versus Time using Measured Data for Piezoprobe 62 at El. -33 m (Depth 115 ft).

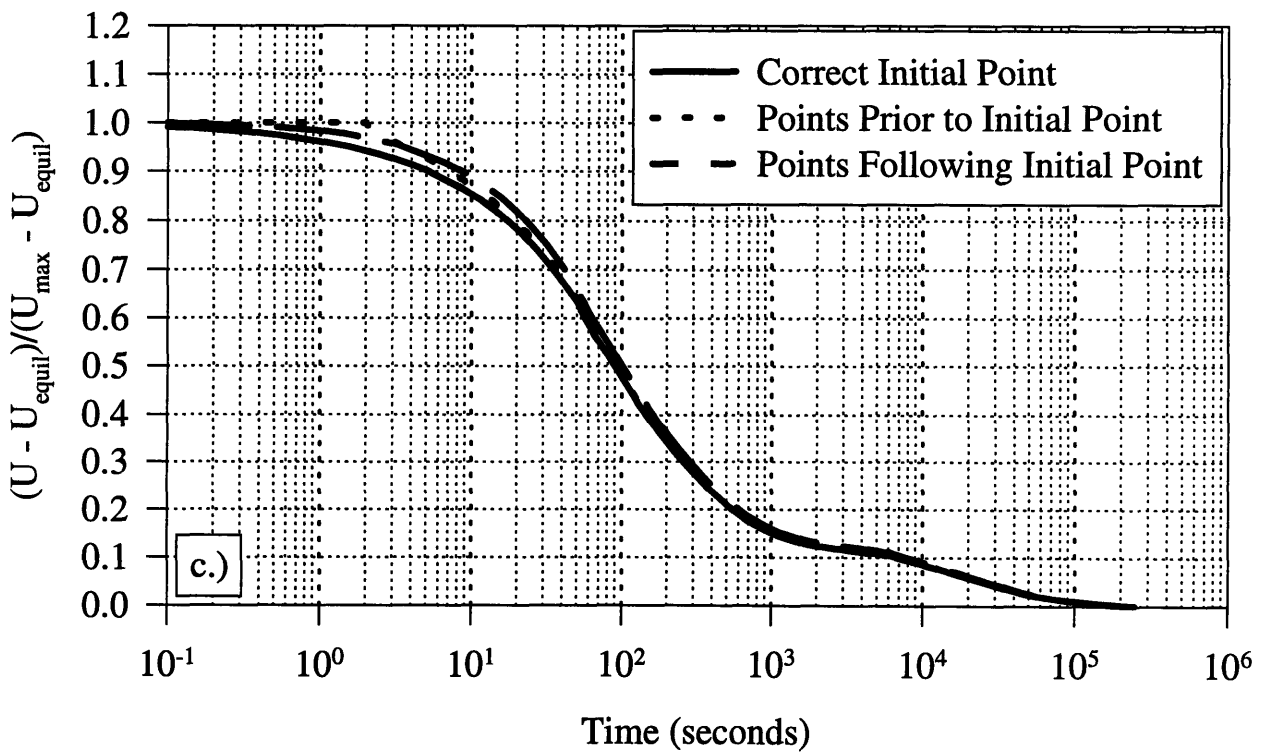
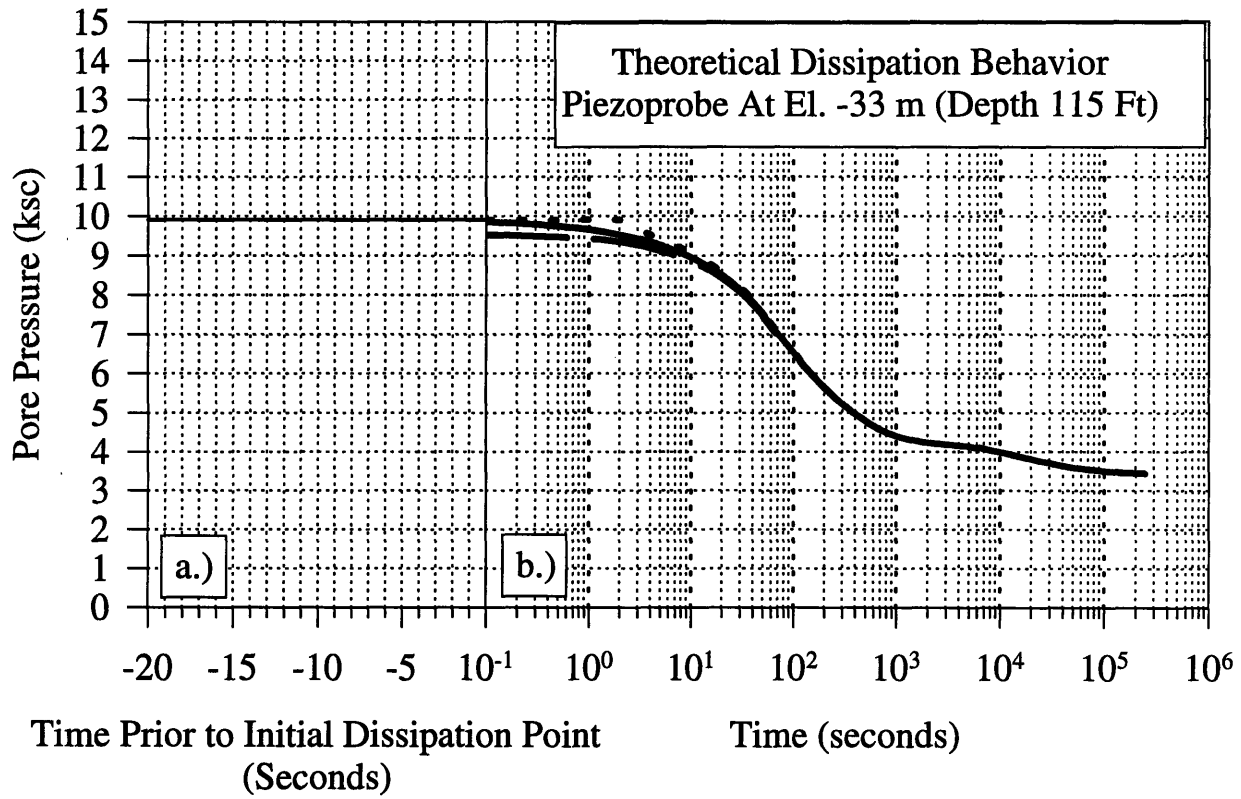


Figure 7.31 Initial Dissipation Point Variation on Theoretical Data for the Piezoprobe at El. -33 m (Depth 115 ft.): a.) Penetration; b.) Dissipation, Absolute Pore Pressure; c.) Dissipation, Normalized Pore Pressure Ratio.

8. SUMMARY, CONCLUSIONS, AND RECOMMENDATIONS

This chapter summarizes the findings of the thesis, draws conclusions from the results, and provides recommendations concerning the efficient performance of field programs and for further studies in the area.

8.1 Summary and Conclusions

The Saugus test site is extremely well documented as a result of past MIT research projects. The site stratigraphy consists of a glacial till overlain by a 37 m (120 ft) deposit of soft and slightly overconsolidated low plasticity marine illitic clay (Boston Blue Clay), and 6 m (20 ft) of surficial top layers of sand and peat. The piezocone profile obtained for this field program is similar to that obtained from a previous study performed at Station 246 (Morrison, 1984). Piezometers were used to determine the equilibrium pore pressure at the site, and support previous investigations indicating that there is a slight artesian pressure (0.15 ksc) in the till.

This thesis presents the results of a research program conducted at the site to perform complete dissipation tests with the piezoprobe and compare to that of the standard piezocone. An MIT research piezocone was also used in this study. In this program, full dissipation was allowed in order to characterize the complete dissipation curve and compare the performance of the three devices.

The stress profile determined by this program is comparable to that presented in Morrison (1984). The profile defines the deposit has having variability in the upper layers, while the lower deposit is soft and uniform. The stress history profile determined by CRS consolidation tests indicates that the OCR decreases from 4.6 to 1.2 above El. -22 m (depth 80 Ft.) and remains constant at 1.18 ± 0.09 below this elevation. The CRSC determined values of vertical hydraulic conductivity indicate a more permeable upper crust above El. -22 m, decreasing from 3×10^{-7} cm/s at El. -13 m to 8×10^{-8} cm/s. Below El. -22 m, the hydraulic conductivity essentially remains constant at $8.6 \pm 1.7 \times 10^{-8}$ cm/s. These values are in the range of Morrison's reported values, but have a smaller variability.

Pore pressure dissipation measurements were performed with two tapered piezoprobes, two standard piezocones, and an MIT research piezocone at various elevations throughout the clay deposit. The dissipation curves for all devices are more variable in the upper zones of the deposit as compared to the lower zones in terms of the shape of the dissipation curve and the slope of the normalized dissipation curve. Below El. -18 m (65 ft), the normalized curves have similar slopes for a particular type of device across the test measurements. However, the piezoprobes vary more than the piezocones, which is believed to be a result of higher sensitivity to local soil conditions. The MIT Piezocone (with pore pressure measured at the tip) is more sensitive to axial load and therefore is affected procedures such as post penetration unloading of the drill string.

The measured pore pressure dissipation records are consistent with model predictions for the various device geometries. The dissipation response of the tapered piezoprobe is affected by pore pressures generated by the larger diameter drill rods above the probe. As a result, the dissipation curve exhibits an accelerated rate of dissipation followed by a characteristic “brake point”. Subsequently, full dissipation is not improved by the geometry. However, the piezoprobe reaches 50% dissipation 17 times faster than the conventional piezocone. The location of the “brake point” depends on soil properties but is in the range of 80-90% dissipation.

Full dissipation requires on the order of 10^5 seconds (28 hours) for all five penetrometers and all elevations in Boston Blue Clay. Final measured dissipation is within 6% of the measured equilibrium values. Partial dissipation records can be used to extrapolate in situ pore pressures from partial dissipation records. Of the two methods used, the Two Point Matching Method (Sutabutr, 1998) predicts the pore pressures within 5% within 1 hours. This method is also more accurate than the Inverse Time Method for the same elapsed dissipation time. The Inverse Time Method at this time predicts the pore pressures within 10% for the piezoprobes, 24% for the piezocones, and 14% for the MIT Piezocone.

The prediction of hydraulic conductivity from dissipation curves is dependent on the type of device and the interpretation method used. In this thesis, the Two Point Intersection, T_{50} Matching, and Concurrent Matching Methods were used to predict

hydraulic conductivities from the measured dissipation data. All devices and all methods underpredict the laboratory determined values of hydraulic conductivity generally by a factor of 2 to 2.5. The piezoprobes and the MIT Research Piezocone predict values of hydraulic conductivity closest to the laboratory determined values. The piezocones predict lower values of hydraulic conductivity with a smaller standard deviation. Overall, for all devices and all methods, the theoretical predictions determine a hydraulic conductivity of 0.5 of the laboratory determined value.

The hydraulic conductivity determined by the T_{50} matching method is performed by determining the installation pore pressure (u_i) and the dissipated pore pressure (u_{diss}). Sensitivity to the estimation of u_i and u_{diss} is evaluated by varying the values by rational methods and determining the resulting hydraulic conductivity range. For an error in estimating one of these values by ± 0.33 ksc, the average determined k ranges from 1.1 to 0.8 times the correct value, indicating an overestimation of the hydraulic conductivity by 10% or under predicting k by 20% in Boston Blue Clay.

The sensitivity of the hydraulic conductivity value to the initial dissipation time and pressure value is determined by an initial point sensitivity analysis. This analysis indicates that the hydraulic conductivity value is always greatest at the correct initial point. Choosing a starting point after dissipation has already started by 3.5 seconds, causes the determined hydraulic conductivity of Boston Blue Clay to be 80% of the correct value. Therefore, the effect of this point has the same significance as an error in estimating the installation or dissipated pore pressure by 0.33 ksc. The correct initial point can be determined by plotting the normalized dissipation curves on a normalized scale and determining the lowest lying plot.

8.1.1 Relative Performance Between the Three Types of Devices

The tapered piezoprobe does accelerate significantly the initial phase of dissipation compared to piezocone devices. Hence, extrapolation of the u_0 values and extraction of hydraulic conductivity can be attempted after a much shorter monitoring period. At present, the tapered probe includes only one porous element and hence, the proposed Two Point Intersection Method and the Concurrent Matching Method can only be used in conjunction with piezocone data. However, by minor re-design of the tapered

piezoprobe with two measurement points, it may be possible to achieve reliable estimates of u_0 and k from incomplete dissipation records.

At present, the established method of determining the in situ pore pressure by the T_{50} method where the dissipation measurements must be conducted until 50% dissipation takes advantage of the piezoprobe decreased dissipation time up until this point. The tapered piezoprobe was able to reach 50% dissipation faster than the piezocones by a factor of 17. The Kulite transducer used in the tapered piezoprobe also has the advantage of being easily accessible and within the range required for this particular program. The Kulite transducer is tailored to higher pressure applications offshore by easily replacing the 35 ksc (500 p.s.i.) capacity transducer with a higher capacity interchangeable transducer.

8.2 Recommendations

The consistency of procedures is extremely important in being able to evaluate the obtained data effectively. The following recommendations provide the author's opinion of the most useful actions performed to insure high quality field data.

8.2.1 Procedures

- The calibration with individually shielded cables should be performed before the start of the field program. The resistances of all transducers should be measured while still in the lab to determine if moisture is a cause for some of the odd measurements.
- The saturation procedures were extremely effective and provided high quality data. In addition, substituting the 45 minute ultrasound saturation technique for the 24 hour bell jar evacuation and saturation technique saved an entire cycle of time. With the system used for this program, an ultrasound bath and a supply of distilled water could provide the saturation system required for saturated porous elements required for the accuracy of the pore pressure measurements.
- During penetration and subsequent dissipation tests, the instances where the device was stopped in a more plastic layer (indicated by a rise in pore pressure) was helpful in preventing partial drainage of the soil. This made the interpretation of data simple for determining the start of dissipation and the effects of partial drainage did not have

to be considered in the interpretation of hydraulic conductivity. On this same note, maintaining the axial load on the drill rods for the initial portion of dissipation also helped in the interpretation of the dissipation. Otherwise, the tapered piezoprobes and the piezocones would be subject to the effects of axial load as the tip pore pressure measurement on the MIT Piezocone is.

8.2.2 Equipment

- The data acquisition system used for this field program provides accurate and frequent recording of data. However, the ability of the program to record simultaneous tasks is essential, not only for the conductance of the program, but for efficiency in interpreting the data. In addition to not being able to record some of the early portions of dissipation as another device was being installed, the present system required time rectifying and combining data files as simultaneous tasks were not possible. The data acquisition system required for this type of program must have the capabilities of simultaneous tasking, with interactive abilities of changing the reading interval and graphically displaying real time data, in addition to being able to record this many channels with the minimum required reading interval for performing response evaluations.
- The data was infiltrated with electrical influences most notable during long term dissipation. Upon recent discoveries in the MIT geotechnical laboratories, it is believed that including capacitors on the Sheahan card will prevent these influences on the data. In addition, the electrical connections must not have stray soldering paste or flux as these also attract outside electrical influences.
- The daytime power system was extremely effective and essentially only required maintenance of the gas supply. However, the overnight power system was only sufficient for short periods of time. The required battery power was miscalculated and in reality the system utilized would require 10 12 volt marine batteries. With sufficient power supply, the data acquisition system would be operable overnight providing continuous data acquisition. Another advantage of continuous data acquisition is that the transducers would not be experiencing warm-up cycles during which the transducer output drifts due to thermal effects. When power had turned off

by the arrival in the morning, a twenty minute warm-up period was imposed to prevent erroneous drifting readings from the transducers.

- The couplings used to connect the penetrometers to the drill rod were designed with effective seals. However, the number of threads on this connection were far too numerous to provide efficient operation in the case of repairing electrical problems. Drill rods are designed for easy and efficient connection with the box threads and only 3 turns to complete the connection. Drill rods do not require a watertight seal in general, but the design of the couplings could be modified with efficiency in mind. The threads could be reduced and still provide the watertight seal required to protect the electrical connections for on shore use.
- The upper shaft on the piezoprobes required altering for this field program. The Kulite transducers bottomed out on the internal threads. This transducer is sealed by an o-ring face seal and therefore bottoming out would cause a leak into the saturated shaft. This point should be noted for other programs using this device.
- One simple device that proved extremely effective was the “depth locator box” used to measure displacement. This made interpretation of the penetration rate simple and provided an exact measurement of total displacement, along with coordinating the pore pressure, axial load, and skin friction measurements with a depth to compare across devices.

8.2.3 Further Investigations

- Further applications of the tapered piezoprobe would benefit from a redesign to include two pore pressure measurement locations on the piezoprobe. In this manner, the Two Point Intersection Method for determining the in situ pore pressure and the Concurrent Matching Method for determining the in situ hydraulic conductivity could be used more effectively than is presently done in this thesis. This device would both mitigate the effects encountered here of cross hole and device variability for the pore pressure measurement location were on two separate devices, but would also reduce the time required for the intersection point.

- Finally, further investigations are required to determine the discrepancy between the field determined and the laboratory determined hydraulic conductivity. This should be evaluated both by refinement of the soil model parameters for natural Boston Blue Clay and by performing other types of laboratory hydraulic conductivity tests (i.e. constant head).

REFERENCES

- American Society for Testing and Materials (ASTM). (1995). *Annual Book of ASTM Standards*, Volume 04.08, Ed. Philadelphia, PA.
- Aubeny, C.P. (1992) "Rational interpretation of in situ tests in cohesive soils," Ph.D Thesis, MIT, Cambridge, MA., pg. 433.
- Baligh, M.M. (1985) "Strain path method," *Journal of Geotechnical Engineering*, ASCE, 111(9), 1108-1136.
- Baligh, M.M. (1986a) "Undrained deep penetration: 1. Shear stresses," *Geotechnique*, 36(4), pg. 487-501.
- Baligh, M.M. (1986b) "Undrained deep penetration: II. Pore pressures," *Geotechnique*, 36(4), pg. 487-501.
- Baligh, M.M., Azzouz, A.S., Chin, C.T. (1987) "Disturbances due to 'ideal' tube sampling," *ASCE Journal of Geotechnical Engineering*, 113(7), pg. 739-757.
- Baligh, M.M., Azzouz, A.S., Wissa, A.Z., Martin, R.T., Morrison, M.J., "The Piezocone Penetrometer," *Proceedings of ASCE Convention on Cone Penetration Testing and Experience*, St. Louis, Missouri, Oct. 1981, pp. 247-263.
- Baligh, M.M., Levadoux, J-N. (1980) "Pore pressure dissipation after cone penetration," MIT Report No. 80-11, Order No. 662, Department of Civil Engineering., MIT, Cambridge, MA.
- Baligh, M.M., Vivatrat, V., Ladd, C.C. (1980) "Cone penetration in soil profiling," *Journal of Geotechnical Engineering* ASCE, 106(4), pg. 447-461.
- Becker, D.E., Crooks, J.H.A., Been, K., and Jeffries, M.G. (1987). "Work as a criterion for determining in situ and yield stresses in clays," *Canadian Geotech. J.* 24(4), 549-564.
- Campanella, R.G., Robertson, P.K. (1988) "Current status of the piezocone test," *Proc. ISOPT-1*, Orlando, CA, Vol. 1, pp 93-116.
- Casagrande, A. (1936). "The determination of the pre-consolidation load and its practical significance," *Proc. 1st ICSMFE*, Cambridge, 3, 60-64.
- Chin, C.T. (1986), "Open-ended pile penetration in saturated clays," PhD Thesis, MIT, Cambridge, MA, pg. 296.

- de Ruiter, J., (1971) "Electric penetrometer for site investigation", *ASCE Journal of the Soil Mech. and Fdn. Engrg. Division*, Vol. 97, SM2, pp 457-472.
- Elghaib, M.K. (1989) "Prediction and interpretation of piezocone data during undrained, drained and partially drained penetration," PhD Thesis, MIT, Cambridge, MA.
- Germaine, J.T. (1982) "Evaluation of Self-Boring Pressuremeter Tests in Soft Cohesive Soils," SM Thesis, MIT, Cambridge, MA.
- Ghantous, I.M. (1982) "Stability and settlement analyses on an embankment clay," SM Thesis, MIT, Cambridge, MA.
- Janbu, N., Senneset, K. (1974) "Effective stress interpretation of in situ static penetration tests," *Proceedings of the European Symposium on Penetration Test I*, Stockholm, Vol. 2.2, pp. 181-193.
- Jones, G.A., Rust, E. (1983) "Piezometer probe (CUPT) for subsoil identification", *Int. Symp. Soil and Rock Investigation by in situ Testing*, Paris, pp1-19.
- Jordan, W.S. (1979). "Determination of negative pore pressure for embankment design," MS Thesis, Department of Civil & Environmental Engineering, MIT, Cambridge, MA.
- Ladd, C.C., Azzouz, A.S., Martin, R.T., Day, R.W., and Malek, A.M. (1980). "Evaluation of compositional and engineering properties of offshore venezuelan soils," Research Report R80-14. Department of Civil Engineering, MIT Cambridge, and Instituto Tecnologico Venezolano Del Petroleo, MA.
- Ladd, C.C., Germaine, J.T. Baligh, M.M., Lacasse, S.M. (1980) "Evaluation of self-boring pressuremeter tests in Boston Blue Clay," Research Report R 79-4. Department of Civil Engineering, MIT Cambridge, MA, and FHWA/RD-80/52.
- Levadoux, J.-N. (1980) "Pore pressures in clays due to cone penetration," PhD Thesis, MIT, Cambridge, MA.
- Levadoux, J-N., Baligh, M.M. (1986) "Consolidation after undrained piezocone penetration. I prediction," *Journal of Geotechnical Engineering*, ASCE, 112(7), pg 707-726.
- Marr, W.A. (1974). "In situ measurement of stress in soils," MS Thesis, MIT, Cambridge MA.
- MIT (1975). "Proceedings of the foundation deformation prediction symposium," Report No. GHWA-RD-75-515, FHWA, Washington, D. C., 2 Volumes.

- Morrison, M.J. (1984) "In situ measurements on a model pile in clay," PhD Thesis, MIT, Cambridge, MA.
- Rouse, H. (1959) *Advanced Mechanics of Fluids*, Wiley & Sons, New York.
- Schmertmann, J.H. (1974) "Pore pressures that produce nonconservative qc data," discussion. *Proceedings of the European Symposium on Penetration Test I*, Stockholm, Vol. 2.2, pp. 245.
- Senneset, K. (1974), "Penetration testing in Norway", *Proceedings 1st European Symposium on Penetration Testing*, Stockholm, Vol. 1, pp. 85-89.
- Senneset, K., Janbu, N., Srafi, O.G. (1982) "Strength and deformations parameters from cone penetration tests," *Proc. ESOPT-II*, Amsterdam, Vol 2, pp. 863-870.
- Sheahan, T.C., (1992). "An experimental study of the time-dependent undrained shear behavior of resedimented clay using automated stress path triaxial equipment," Sc.D. Thesis, Department of Civil & Environmental Engineering, MIT, Cambridge, MA.
- Sutabutr, T. (1998) PhD Thesis in progress, MIT Cambridge, MA.
- Tortensson, B.A. (1975) "Pore pressure sounding instrument," *Proceedings of the ASCE Specialty Conference on In Situ Measurement of Soil Properties*, Raleigh, Vol. 2, pp. 48-54.
- Varney, A.J., Germaine, J.T. (1997) "Laboratory characterization of soil properties at MIT test site Saugus, MA," Research Report No. R97-01, Department of Civil & Environmental Engineering, Cambridge, MA.
- Varney, A.J., Germaine, J.T., Ladd, C.C. (1998) "Forthcoming MIT research report on laboratory investigation of undisturbed soil samples at Saugus (Station 246).
- Vivatrat, V. (1978) "Cone penetration in clays," PhD Thesis, MIT, Cambridge, MIT, MA.
- Weinstein, A. (1948) "On axially symmetric flows," *Quarterly of Applied Mathematics*, 5(4), pg. 429-434.
- Whittle, A.J. (1987) "A constitutive model for overconsolidated clays with application the cyclic loading of friction piles," ScD Thesis, MIT, Cambridge, MA.
- Whittle, A.J. (1992) "Assessment of an effective stress analysis for predicting the performance of driven piles in clays," *Advances in Underwater Technology, Ocean Science and Offshore Engineering Volume 28, Offshore Site Investigation*

and Foundation Behavior, Society for Underwater Technology, London, pp607-643.

- Whittle, A.J. (1995) "Strain path analyses of pore pressure dissipation for Fugro-McClelland tapered piezoprobe," Unpublished report submitted to Fugro-McClelland Marine Geosciences, Inc. Houston.
- Whittle, A.J., Aubeny, C.P., Rafalovich, A., Ladd, C.C, Baligh, M.M. (1991) "Interpretation of in situ tests in cohesive soils using rational methods," Research Report R91-01, MIT Department of Civil Engineering, pg. 228
- Whittle, A.J., Degroot, D.J., Ladd, C.C., Seah, T-H. (1994) "Model prediction of the anisotropic behavior of Boston Blue Clay," Journal of Geotechnical Engineering, ASCE, 120(1), 199-255.
- Whittle, A.J., Kavvas, M.J. (1994) "Formulation of the MIT-E3 constitutive model for overconsolidated clays," Journal of Geotechnical Engineering, ASCE, 120(1), pg. 173-199.
- Whittle, J.A., Sutabutr, T, Germaine, J.T., Varney, A.J. (1997) "Validation of Piezoprobe Dissipation Data and Application to Pile Design," MIT Report R97-03, Department of Civil & Environmental Engineering, Cambridge, MA.
- Wissa, A.E., Martin, R.T. Garlanger, J.E. (1975), "The piezometer probe," Proceedings of the ASCE Specialty Conference on In Situ Measurement of Soil Properties, Raleigh, Vol. 1, pp. 536-545.
- Wissa, A.E.Z., Christian, J.G., Davis, E.H., & Hedburge, S. (1971). "Consolidation at Constant Rate of Strain" *JSMFD*, ASCE, Vol. 97, No SM10, pp. 1393-1413.
- Zeeb, P.J. (1996) "Piezocone Mapping, Groundwater Monitoring, and Flow Modeling in a Riverine Peatland: Implications for the Transport of Arsenic," PhD Thesis, Department of Civil & Environmental Engineering, Cambridge, MA.

Appendix A

Appendix A consists of examples of BASIC codes written and altered by Dr. John T. Germaine for performing the field program data acquisition tasks. Twelve programs were written:

Response (5)

Device specific *Response* programs were written to record the pore pressure output for a device and the witness pressure transducer. The programs are named with an “R” indicating *Response* program, and the number of the device (i.e. “R62”, “R63”, “R790”, “R881”, “RMIT”).

Penetration (5)

Device specific *Penetration* programs were written to record the outputs of the transducers (pore pressure in all cases and axial load cell and friction sleeve if the device had them) along with the depth locator box. The programs are named with a “P” indicated *Penetration* program, and the number of the device (i.e. “P62”, “P63”, “P790”, “P881”, “PMIT”).

Dissipation (1)

One *Dissipation* program was written to record all transducers on all five devices in addition to the water level transducer (for piezometer continuous readings). The program is named “Diss”.

Night (1)

One *Night* program was written to record dissipation data overnight. This program was written with the feature of saving every ten readings to a new file name. This was necessary in order to avoid losing data due to the loss of battery power. The program is named “Night”.

The following pages include copies of the code for “R62”, “P62”, “P790”, “Diss”, and “Night” in order to prevent unnecessary repetition, but to indicate the data acquisition sequencing for all cases.

“R62”

RSP62.bas

```
10 REM DATA ACQUISITION PROGRAM 2/7/93*****
20 REM LAST REVISED 12/20/94 JTG
30 REM
40 SCREEN 0
50 CLS
60 GOSUB 5120
70 REM
80 PROGRAMS="RESPONSE FOR PIEZOPROBE 62"
90 FLAG=0
100 FLAG1=0
110 FLAG2=0 'used for data storage
120 FLAG3=0 'used to control storage in array
130 FLAG4=0 'used to indicate data file specified
140 FLAGA=0 'change delt
150 FLAGB=0 'change frame
160 FLAGC=0 'change plot channels
170 FLAGE=0
180 FLAGF=0
190 REM
200 PRINT TAB(26) " THIS PROGRAM IS":PRINT
210 PRINT TAB(26) " PART":PRINT
220 PRINT TAB(26) " OF THE":PRINT:PRINT
230 PRINT TAB(26) " DATA ACQUISITION SYSTEM":PRINT
240 PRINT TAB(26) " FOR THE":PRINT
250 PRINT TAB(26) " GEOTECHNICAL LABORATORY":PRINT:PRINT
260 PRINT TAB(26) " DEPARTMENT OF":PRINT:PRINT
270 PRINT TAB(26) " CIVIL AND ENVIRONMENTAL ENGINEERING":PRINT
280 PRINT TAB(26) "MASSACHUSETTS INSTITUTE OF TECHNOLOGY":PRINT
290 PRINT:PRINT
300 INPUT "PRESS 'return' TO CONTINUE".ZS
310 CLS
320 PRINT TAB(1) "THIS PROGRAM COLLECTS DATA AT A RELATIVELY SLOW RATE"
330 PRINT TAB(1) "THE PROGRAM REQUIRES AN AD1170 DATA ACQUISITION CARD"
340 PRINT TAB(1) "THE USER CAN INTERACTIVELY CHANGE THE READING RATE"
350 PRINT TAB(1) " AND CHOOSE TO SAVE OR IGNORE THE DATA AS IT IS RECORDED":PRINT
360 PRINT TAB(1) "THIS IS PROGRAM REVISION 1.1 PROGRAMED 12/20/94":PRINT:PRINT
370 REM
380 INPUT "PRESS 'return' TO CONTINUE".ZS
390 REM
400 REM INPUT INTTIME AND INTBIT*****
410 CLS
420 PRINT TAB(1) "THE DATA ACQUISITION CARD HAS SOFTWARE SELECTABLE
PARAMETERS WHICH YOU MUST NOW SELECT FROM THE FOLLOWING LIST": PRINT:PRINT
430 PRINT TAB(1) "THE INTEGRATION TIME (N): "
440 PRINT TAB(1) " where N=0 1 msec N=4 100 msec"
450 PRINT TAB(1) " N=1 10 msec N=5 166.7 msec"
460 PRINT TAB(1) " N=2 16.7 msec N=6 300 msec"
470 PRINT TAB(1) " N=3 20 msec"
480 INPUT INTTIME
490 INTTIME=2
500 INTTIME=INTTIME+16
510 PRINT:PRINT:PRINT "THE BIT PRECISION: "
520 PRINT TAB(1) " options 8,10,12,14,16,18,20,22"
530 INPUT INTBIT
```

```

540     INTBIT=18
550     INTBIT=INTBIT-7
560     REM
570     REM
580     REM
590     REM SET PARAMETERS FOR SLOW READINGS*****
600     REM
610     INPUT "PRESS 'return' TO CONTINUE",Z$
620     CLS
630     PRINT TAB(1) "PROVIDE THE FOLLOWING INFORMATION FOR THE
READINGS":PRINT:PRINT
640     INPUT "ENTER THE NUMBER OF CHANNELS TO BE RECORDED OR INPUT FROM DISC:
",N:PRINT:PRINT
650     N=2
660     GOTO 780
670     FOR I=0 TO (N-1)
680         CLS
690         PRINT "ENTER CARD ADDRESS"
700         INPUT AD1170(I)
710         PRINT "ENTER THE CHANNEL NUMBER FOR CHANNEL position NO.",(I+1);": "
720         PRINT "   for the AD1170 card the first channel is 0"
730         INPUT CH(I)
740         PRINT "ENTER THE TRANSDUCER NO. FOR CHANNEL NO. ";CH(I);": "
750         INPUT TR(I)
760         PRINT:PRINT
770     NEXT I
780     AD1170(0)=896: AD1170(1)=992
790     CH(0)=1:CH(1)=6
800     REM SET UP AD-1170*****
810     REM
820     CLS
825     PRINT "THIS IS THE PROGRAM FOR ";PROGRAM$"
830     PRINT:PRINT "   THE A/D CONVERTER IS BEING INITIALIZED"
840     FOR I=0 TO N-1
850         OUT AD1170(I),60:WAIT AD1170(I),1,1
860         OUT AD1170(I)+1,INTBIT:WAIT AD1170(I),1,1
870         OUT AD1170(I),48:WAIT AD1170(I),1,1
880         OUT AD1170(I),176:WAIT AD1170(I),1,1
890         OUT AD1170(I),184:WAIT AD1170(I),1,1
900         MUX!(I)=AD1170(I)+8
910     NEXT I
920     GNDCHANNEL=15
930     REFCHANNEL=14
940     CHANNEL=0
950     REM
960     REM
970     REM MAIN PROGRAM*****
980     REM
990     GOSUB 3940
1000    GOTO 1190
1010    REM
1020    REM
1030    REM DRAW FRAME AND SET SCALES*****
1040    REM
1050    SCREEN 0
1060    KEY OFF

```

```

1070     CLS
1080     INPUT "ENTER MIN X VALUE (sec): ",MINX
1090     INPUT "ENTER MAX X VALUE (sec): ",MAXX
1100     INPUT "ENTER MIN Y VALUE (volts): ",MINY
1110     INPUT "ENTER MAX Y VALUE (volts): ",MAXY
1120     REM
1130     CLS
1140     IF FLAG=1 THEN GOSUB 1890
1150     IF FLAG=1 THEN GOSUB 3560
1160     RETURN
1170     REM
1180     REM SET FUNCTION KEYS*****
1190     REM
1200     IF FLAG=1 THEN SCREEN 0
1210     CLS
1220     PRINT "PRESS F1' TO START OR F6' TO READ FROM DISC."
1230     KEY 1,"START"
1240     KEY 6,"DISC"
1250     ON KEY (1) GOSUB 1330
1260     ON KEY (6) GOSUB 4790
1270     KEY (1) ON
1280     KEY (6) ON
1290     KEY ON
1300     REM   FLAG=1
1310     GOTO 1310
1320     REM
1330     REM SLOW READING ROUTINE ACTIVATED WITH START KEY*****
1340     REM
1350     FLAG5=0
1360     FLAGF=0
1370     FLAG6=0
1380     GOSUB 5120
1390     KEY 1,"BYPASS"
1400     KEY 2,"  "
1410     KEY 3,"  "
1420     KEY 4,"DELT"
1430     KEY 5,"SCALE"
1440     KEY 6,"CHANEL"
1450     KEY 7,"END"
1460     KEY 8,"  "
1470     KEY 9,"  "
1480     KEY 10,"  "
1490     KEY (1) ON
1500     KEY (2) OFF
1510     KEY (3) OFF
1520     KEY (4) ON
1530     KEY (5) ON
1540     KEY (6) ON
1550     KEY (7) ON
1560     KEY (8) OFF
1570     KEY (9) OFF
1580     KEY (10) OFF
1590     ON KEY (1) GOSUB 3630
1600     ON KEY (4) GOSUB 4110
1610     ON KEY (5) GOSUB 4140
1620     ON KEY (6) GOSUB 4170

```

```

1630     ON KEY (7) GOSUB 3080
1640 REM
1650 REM
1660 REM TAKE SET OF READINGS ON KEYBOARDS CUE*****
1670 REM
1680     CLS
1690     SCREEN 0
1710     IF FLAG2=1 THEN ERASE VOLTS,TIME
1720     INPUT "ENTER NUMBER OF READINGS: ",J
1730     DIM VOLTS(J,N), TIME(J)
1740     FLAG2=1
1741     TM = TIMER
1742     T0=TM
1743     DIAZ=0
1744     SDATE$=DATES
1745     STIME$=TIMES
1750     PRINT
1760     INPUT "ENTER THE TIME INTERVAL (sec): ",DELT:PRINT:PRINT
1770     INPUT "DO YOU WANT TO STORE THE DATA (Y/N)? ",AS
1780     IF AS="Y" THEN GOTO 1810
1790     GOTO 1840
1800     PRINT
1810     PRINT "ENTER DATA FILE NAME: "
1820     INPUT " eight characters and no extension: ",FILE1$
1830     FLAG4=1
1840     GOSUB 1030
1850     PRINT "PRESS `return` WHEN READY, START TEST AT BEEP"
1860     AS=INKEY$
1870     IF AS<>CHR$(13) THEN GOTO 1860
1880 REM
1890 REM SETUP WINDOW*****
1900 REM
1910     SCREEN 9
1920     KEY ON
1930 REM
1940     LOCATE 21,30
1950     PRINT "TIME (SEC)"
1960 REM
1970     LOCATE 7,1
1980     PRINT "V"
1990     LOCATE 8,1
2000     PRINT "O"
2010     LOCATE 9,1
2020     PRINT "L"
2030     LOCATE 10,1
2040     PRINT "T"
2050     LOCATE 11,1
2060     PRINT "A"
2070     LOCATE 12,1
2080     PRINT "G"
2090     LOCATE 13,1
2100     PRINT "E"
2110 REM
2120     LOCATE 1,2
2130     PRINT MAXY
2140     LOCATE 19,2

```

```

2150     PRINT MINY
2160 REM
2170     LOCATE 20.5
2180     PRINT MINX
2190     LOCATE 20.74
2200     PRINT MAXX
2210 REM
2220     LOCATE 23.1
2230     VIEW (50,3)-(600,260),,1
2240 REM
2250     WINDOW (MINX,MINY)-(MAXX,MAXY)
2260 REM
2270     CLS
2280     DX=MAXX-MINX
2290     DY=MAXY-MINY
2300 REM
2310     FOR I=MINX+(DX/10) TO MAXX-(DX/10) STEP DX/10
2320         LINE (I,MINY)-(I,MAXY),,,&H1F11
2330     NEXT I
2340 REM
2350     FOR I=MINY+(DY/5) TO MAXY-(DY/5) STEP DY/5
2360         LINE (MINX,I)-(MAXX,I),,,&H1F11
2370     NEXT I
2380     IF FLAG5=1 THEN GOTO 3570 ELSE IF FLAGF=1 THEN GOTO 3540
2390     IF FLAG1=1 THEN RETURN
2400 REM
2410 REM MAIN DATA READING LOOP*****
2420 REM
2430     FLAG1=1
2440     COUNTER = 0
2480     BEEP
2490     FLAG=1
2500 REM
2510     FOR K=0 TO 1
2520         OUT MUX!(K),CH(K)
2530         OUT AD1170(K),INTTIME
2540     NEXT K
2550     FOR K=0 TO 1
2560         WAIT AD1170(K),1,1
2570         OUT MUX!(K), GNDCHANNEL
2580         LBYTE = INP(AD1170(K)+1)
2590         MBYTE = INP(AD1170(K)+2)
2600         HBYTE = INP(AD1170(K)+3)
2610         VOLTS(COUNTER,K) = (LBYTE+256*MBYTE+65536!*HBYTE)*10/2^(INTBIT+7)-5
2620     NEXT K
2720     T=TIMER
2730     IF T<TM THEN DIAZ=DIAZ+86400!
2740     TM=T :DS=DATES
2750     TIME(COUNTER)=T-T0+DIAZ
2760     FOR K=1 TO IC
2770         IF COUNTER<>0 THEN LINE (TIME(COUNTER-1),VOLTS(COUNTER-1,K-1))-
(TIME(COUNTER),VOLTS(COUNTER,K-1))
2780     NEXT K
2790     LOCATE 23.1
2800     PRINT "
2810     LOCATE 23,1

```



```

2820     PRINT INT(TIME(COUNTER)), COUNTER;"/":J
2830     FOR K=1 TO N
2840         LOCATE 23.20+K*10
2850         PRINT USING "##.####";VOLTS(COUNTER.K-1)
2860     NEXT K
2870     IF COUNTER=J THEN GOTO 3040
2880     TD=0
2890     IF TM+DELT<86400! THEN GOTO 2960
2900     TD=86400!
2910     WHILE DATE$=D$
2920         IF FLAGA=1 THEN FLAGA=0 : GOSUB 3790
2930         IF FLAGB=1 THEN FLAGB=0 : GOSUB 1050
2940         IF FLAGC=1 THEN FLAGC=0 : GOSUB 3910
2950     WEND
2960     IF FLAGA=1 THEN FLAGA=0 : GOSUB 3790
2970     WHILE TIMER < TM + DELT - TD
2980         IF FLAGA=1 THEN FLAGA=0 : GOSUB 3790
2990         IF FLAGB=1 THEN FLAGB=0 : GOSUB 1050
3000         IF FLAGC=1 THEN FLAGC=0 : GOSUB 3910
3010     WEND
3020     IF FLAG3=0 THEN COUNTER=COUNTER+1
3030     GOTO 2500
3040     REM DATA ARRAY FULL
3050     GOSUB 4210
3060     GOTO 3280
3070     REM
3080     REM DATA PROCESSING ROUTINES AFTER READINGS COMPLETE*****
3090     REM
3100     REM
3110     LOCATE 23.1
3120     PRINT " "
3130     LOCATE 23.1
3140     INPUT "DO YOU WANT TO CONTINUE COLLECTION MODE (Y/N)";ANS$
3150     LOCATE 23.1
3160     PRINT " "
3170     IF ANS$="N" THEN :GOSUB 4210 : RETURN 3280
3180     LOCATE 23.1
3190     INPUT "DO YOU WANT TO START A NEW DATA FILE (Y/N)";ANS$
3200     IF ANS$="Y" THEN GOTO 3240
3210     LOCATE 23.1
3220     PRINT " "
3230     RETURN
3240     GOSUB 4210
3250     FLAG=0 :FLAG1=0
3260     SCREEN 0 : CLS
3270     RETURN 1660
3280     REM
3290     KEY 1," "
3300     KEY 2,"SCALE"
3310     KEY 3,"CHANEL"
3320     KEY 4," "
3330     KEY 5,"END"
3340     KEY 6," "
3350     KEY 7," "
3360     KEY 8," "
3370     KEY 9," "

```

```

3380     KEY 10."      "
3390     KEY (1) OFF
3400     KEY (2) ON
3410     KEY (3) ON
3420     KEY (4) OFF
3430     KEY (5) ON
3440     KEY (6) OFF
3450     KEY (7) OFF
3460     KEY (8) OFF
3470     KEY (9) OFF
3480     KEY (10) OFF
3490     ON KEY (2) GOSUB 1050
3500     ON KEY (3) GOSUB 3910
3510     ON KEY (5) GOSUB 5010
3520     FLAGF=1
3530     GOTO 3530
3540     GOSUB 3550
3550     REM PLOT DATA IN MEMORY*****
3560     IF FLAG1=0 THEN RETURN
3570     FOR I=1 TO COUNTER
3580         FOR K=1 TO IC
3590             LINE(TIME(I-1),VOLTS(I-1,NCP(K-1)))-(TIME(I),VOLTS(I,NCP(K-1)))
3600         NEXT K
3610     NEXT I
3620     RETURN
3630     REM BYPASS READINGS*****
3640     REM
3650         KEY 1, "SAVE"
3660         KEY (1) ON
3670         ON KEY (1) GOSUB 3710
3680         FLAG3=1
3690         RETURN
3700     REM
3710     REM KEEP DATA*****
3720     REM
3730         KEY 1, "BYPASS"
3740         KEY (1) ON
3750         ON KEY (1) GOSUB 3630
3760         FLAG3=0
3770         RETURN
3780     REM
3790     REM CHANGE TIME INTERVAL FOR SLOW READINGS*****
3800     REM
3810         LOCATE 23,1
3820         PRINT "                "
3830         LOCATE 23,1
3840         INPUT "ENTER NEW TIME INTERVAL (sec): ",DELT
3850         LOCATE 23,1
3860         PRINT "                "
3870         RETURN 2880
3880     REM
3890     REM REDEFINE CHANNEL POSITIONS TO BE PLOTTED*****
3900     REM
3910         LOCATE 23,1
3920         PRINT "                "
3930         LOCATE 23,1

```

```

3940     INPUT "ENTER NUMBER OF CHANNELS TO BE PLOTTED: ".IC
3950     FOR I=0 TO (IC-1)
3960         LOCATE 23.1
3970         PRINT "                "
3980         LOCATE 22.1
3990         PRINT "                "
4000         LOCATE 22.1
4010         PRINT "ENTER";(I+1);"TH CHANNEL TO BE PLOTTED:"
4020         INPUT NCP(I)
4030         NCP(I)=NCP(I)-1
4040     NEXT I
4050     LOCATE 22.1
4060     PRINT "                "
4070     LOCATE 23.1
4080     PRINT "                "
4090     GOSUB 3550
4100     RETURN
4110     REM CHANGE DELT FLAG*****
4120     FLAGA=1
4130     RETURN
4140     REM CHANGE FRAME FLAG*****
4150     FLAGB=1
4160     RETURN
4170     REM CHANGE PLOT CHANNELS FLAG*****
4180     FLAGC=1
4190     RETURN
4200     REM
4210     REM DATA STORAGE SECTION*****
4220     REM
4230     IF FLAG4=0 THEN RETURN
4240     FILE2$=FILE1$+".DAT"
4250     OPEN "O", #2, FILE2$
4260     GOSUB 4380
4270     FOR I=0 TO COUNTER
4280         PRINT #2, INT(100*TIME(I))/100,
4290         FOR K=0 TO N-1
4300             PRINT #2, INT(1000000!*VOLTS(I,K))/1000000!,
4310             NEXT K
4320         PRINT #2, " "
4330     NEXT I
4340     CLOSE #2
4350     RETURN
4360     REM SETUP OUTPUT FILE (HEADINGS ETC.)*****
4370     REM
4380     WRITE #2, PROGRAM$
4390     C$=CHR$(34)
4400     WRITE #2, FILE2$,N,STIMES:WRITE #2, SDATES$
4420     PRINT #2, C$;"CRD NBR";C$;
4430     FOR I=0 TO N-1
4440         PRINT #2, C$;AD1170(I);C$;
4450     NEXT I
4460     PRINT #2, ""
4461     PRINT #2, C$;"CH NBR";C$;
4462     FOR I=0 TO N-1
4463         PRINT #2, C$;CH(I);C$;
4464     NEXT I

```

```

4465 PRINT #2. ""
4470 PRINT #2. CS;"SECONDS";CS:
4480 FOR I=0 TO N-1
4490     PRINT #2. CS;"VOLTS";CS:
4500 NEXT I
4510 PRINT #2. ""
4511 PRINT #2. CS;"CLOCK";CS:
4520 FOR I=0 TO N-1
4530     PRINT #2, CS;I;CS:
4540 NEXT I
4550 PRINT #2. " "
4750 RETURN
4760 REM
4770 REM INPUT DATA DIRECTLY FROM DISC*****
4780 REM
4790 INPUT "ENTER DATA FILE TO READ FROM: ",FILE3$
4800 PRINT "ENTER THE NUMBER OF DATA READINGS "
4810 INPUT " (must be at least as large as actual file)";J
4820 FILE3$=FILE3$+".DAT"
4830 OPEN "I", #3, FILE3$
4840 GOSUB 5170
4850 IF FLAG1=1 THEN ERASE VOLTS,TIME
4860 DIM VOLTS(J,N), TIME(J)
4870 COUNTER=0
4880 INPUT #3, TIME(COUNTER)
4890     FOR I=0 TO N-1
4900         INPUT #3, VOLTS(COUNTER,I)
4910     NEXT I
4920 IF EOF(3)=-1 THEN GOTO 4950
4930 COUNTER=COUNTER+1
4940 GOTO 4880
4950 FLAG1=0 : CLS
4960 GOSUB 3940
4970 FLAG=1 : FLAG1=1
4980 GOSUB 1030
4990 GOTO 3280
5000 REM END OF PROGRAM*****
5010 INPUT "ARE YOU FINISHED (Y/N)";ANS$
5020 IF ANS$="Y" THEN GOTO 5080
5030 GOSUB 5110
5040 SCREEN 0
5050 FLAG=0
5060 FLAG1=0
5070 GOTO 620
5080 SCREEN 0
5090 STOP
5100 END
5110 REM*****RESET FUNCTION KEYS*****
5120 FOR I=1 TO 10
5130     KEY I. " "
5140 NEXT I
5150 KEY OFF
5160 RETURN
5170 REM SETUP OUTPUT FILE (HEADINGS ETC.)*****
5180 REM
5190 INPUT #3. PROGRAM

```

```
5200 INPUT #3, FILE3$
5210 INPUT #3, N
5220 INPUT #3, TTIMES
5230 INPUT #3, DDATES
5240 INPUT #3, A
5250 INPUT #3, PROGRAM
5260 INPUT #3, XS
5270 INPUT #3, XS
5280 FOR I=0 TO N-1
5290     INPUT #3, TR$(I)
5300 NEXT I
5310 INPUT #3, XS
5320 FOR I=0 TO N-1
5330     INPUT #3, XS
5340 NEXT I
5350 FOR I=0 TO N
5360     INPUT #3, X
5370 NEXT I
5380 FOR I=0 TO N
5390     INPUT #3, X
5400 NEXT I
5410 FOR I=0 TO N
5420     INPUT #3, X
5430 NEXT I
5440 INPUT #3, XS
5450 INPUT #3, TTIMES
5460 FOR I=0 TO N-1
5470     INPUT #3, CH(I)
5480 NEXT I
5490 INPUT #3, XS
5500 FOR I=0 TO N-1
5510     INPUT #3, XS
5520 NEXT I
5530 RETURN
```

“P62”

P62.bas

```
10 REM DATA ACQUISITION PROGRAM 2/7/93*****
20 REM LAST REVISED 12/20/94 JTG
30 REM
40 SCREEN 0
50 CLS
60 GOSUB 5120
70 REM
80 PROGRAMS="PIEZOPROBE 28-62"
90 FLAG=0
100 FLAG1=0
110 FLAG2=0 'used for data storage
120 FLAG3=0 'used to control storage in array
130 FLAG4=0 'used to indicate data file specified
140 FLAGA=0 'change delt
150 FLAGB=0 'change frame
160 FLAGC=0 'change plot channels
170 FLAGE=0
180 FLAGF=0
190 REM
200 PRINT TAB(26) " THIS PROGRAM IS":PRINT
210 PRINT TAB(26) " PART":PRINT
220 PRINT TAB(26) " OF THE":PRINT:PRINT
230 PRINT TAB(26) " DATA ACQUISITION SYSTEM":PRINT
240 PRINT TAB(26) " FOR THE":PRINT
250 PRINT TAB(26) " GEOTECHNICAL LABORATORY":PRINT:PRINT
260 PRINT TAB(26) " DEPARTMENT OF":PRINT:PRINT
270 PRINT TAB(26) " CIVIL AND ENVIRONMENTAL ENGINEERING":PRINT
280 PRINT TAB(26) " MASSACHUSETTS INSTITUTE OF TECHNOLOGY":PRINT
290 PRINT:PRINT
300 INPUT "PRESS 'return' TO CONTINUE".ZS
310 CLS
320 PRINT TAB(1) "THIS PROGRAM COLLECTS DATA AT A RELATIVELY SLOW RATE"
330 PRINT TAB(1) "THE PROGRAM REQUIRES AN AD1170 DATA ACQUISITION CARD"
340 PRINT TAB(1) "THE USER CAN INTERACTIVELY CHANGE THE READING RATE"
350 PRINT TAB(1) " AND CHOOSE TO SAVE OR IGNORE THE DATA AS IT IS RECORDED":PRINT
360 PRINT TAB(1) "THIS IS PROGRAM REVISION 1.1 PROGRAMED 12/20/94":PRINT:PRINT
370 REM
380 INPUT "PRESS 'return' TO CONTINUE",ZS
390 REM
400 REM INPUT INTTIME AND INTBIT*****
410 CLS
420 PRINT TAB(1) "THE DATA ACQUISITION CARD HAS SOFTWARE SELECTABLE
PARAMETERS WHICH YOU MUST NOW SELECT FROM THE FOLLOWING LIST": PRINT:PRINT
430 PRINT TAB(1) "THE INTEGRATION TIME (N): "
440 PRINT TAB(1) " where N=0 1 msec N=4 100 msec"
450 PRINT TAB(1) " N=1 10 msec N=5 166.7 msec"
460 PRINT TAB(1) " N=2 16.7 msec N=6 300 msec"
470 PRINT TAB(1) " N=3 20 msec"
480 INPUT INTTIME
490 INTTIME=5
500 INTTIME=INTTIME+16
510 PRINT:PRINT:PRINT "THE BIT PRECISION: "
520 PRINT TAB(1) " options 8,10,12,14,16,18,20,22"
530 INPUT INTBIT
```

```

540     INTBIT=22
550     INTBIT=INTBIT-7
560     REM
570     REM
580     REM
590     REM SET PARAMETERS FOR SLOW READINGS*****
600     REM
610 '     INPUT "PRESS 'return' TO CONTINUE",Z$
620     CLS
630     PRINT TAB(1) "PROVIDE THE FOLLOWING INFORMATION FOR THE
READINGS":PRINT:PRINT
640 '     INPUT "ENTER THE NUMBER OF CHANNELS TO BE RECORDED OR INPUT FROM DISC:
",N:PRINT:PRINT
650     N=2
660     GOTO 780
670     FOR I=0 TO (N-1)
680         CLS
690         PRINT "ENTER CARD ADDRESS"
700         INPUT AD1170(I)
710         PRINT "ENTER THE CHANNEL NUMBER FOR CHANNEL position NO.",(I+1);": "
720         PRINT "   for the AD1170 card the first channel is 0"
730         INPUT CH(I)
740         PRINT "ENTER THE TRANSDUCER NO. FOR CHANNEL NO.":CH(I);": "
750         INPUT TR(I)
760         PRINT:PRINT
770     NEXT I
780     AD1170(0)=896: AD1170(1)=768
790     CH(0)=1:CH(1)=6
800     REM SET UP AD-1170*****
810     REM
820     CLS
825     PRINT "THIS IS THE PROGRAM FOR ";PROGRAM$"
830     PRINT:PRINT "       THE A/D CONVERTER IS BEING INITIALIZED"
840     FOR I=0 TO N-1
850         OUT AD1170(I),60:WAIT AD1170(I),1,1
860         OUT AD1170(I)+1,INTBIT:WAIT AD1170(I),1,1
870         OUT AD1170(I),48:WAIT AD1170(I),1,1
880         OUT AD1170(I),176:WAIT AD1170(I),1,1
890         OUT AD1170(I),184:WAIT AD1170(I),1,1
900         MUX!(I)=AD1170(I)+8
910     NEXT I
920     GNDCHANNEL=15
930     REFCHANNEL=14
940     CHANNEL=0
950     REM
960     REM
970     REM MAIN PROGRAM*****
980     REM
990         GOSUB 3940
1000        GOTO 1190
1010     REM
1020     REM
1030     REM DRAW FRAME AND SET SCALES*****
1040     REM
1050         SCREEN 0
1060         KEY OFF

```



```

1070     CLS
1080     INPUT "ENTER MIN X VALUE (sec): ",MINX
1090     INPUT "ENTER MAX X VALUE (sec): ",MAXX
1100     INPUT "ENTER MIN Y VALUE (volts): ",MINY
1110     INPUT "ENTER MAX Y VALUE (volts): ",MAXY
1120     REM
1130     CLS
1140     IF FLAG=1 THEN GOSUB 1890
1150     IF FLAG=1 THEN GOSUB 3560
1160     RETURN
1170     REM
1180     REM SET FUNCTION KEYS*****
1190     REM
1200     IF FLAG=1 THEN SCREEN 0
1210     CLS
1220     PRINT "PRESS F1' TO START OR F6' TO READ FROM DISC."
1230     KEY 1,"START"
1240     KEY 6,"DISC"
1250     ON KEY (1) GOSUB 1330
1260     ON KEY (6) GOSUB 4790
1270     KEY (1) ON
1280     KEY (6) ON
1290     KEY ON
1300     REM   FLAG=1
1310     GOTO 1310
1320     REM
1330     REM SLOW READING ROUTINE ACTIVATED WITH START KEY*****
1340     REM
1350     FLAG5=0
1360     FLAGF=0
1370     FLAG6=0
1380     GOSUB 5120
1390     KEY 1,"BYPASS"
1400     KEY 2,"  "
1410     KEY 3,"  "
1420     KEY 4,"DELT"
1430     KEY 5,"SCALE"
1440     KEY 6,"CHANEL"
1450     KEY 7,"END"
1460     KEY 8,"  "
1470     KEY 9,"  "
1480     KEY 10,"  "
1490     KEY (1) ON
1500     KEY (2) OFF
1510     KEY (3) OFF
1520     KEY (4) ON
1530     KEY (5) ON
1540     KEY (6) ON
1550     KEY (7) ON
1560     KEY (8) OFF
1570     KEY (9) OFF
1580     KEY (10) OFF
1590     ON KEY (1) GOSUB 3630
1600     ON KEY (4) GOSUB 4110
1610     ON KEY (5) GOSUB 4140
1620     ON KEY (6) GOSUB 4170

```

```

1630     ON KEY (7) GOSUB 3080
1640 REM
1650 REM
1660 REM TAKE SET OF READINGS ON KEYBOARDS CUE*****
1670 REM
1680     CLS
1690     SCREEN 0
1710     IF FLAG2=1 THEN ERASE VOLTS,TIME
1720     INPUT "ENTER NUMBER OF READINGS: ",J
1730     DIM VOLTS(J,N), TIME(J)
1740     FLAG2=1
1741     TM = TIMER
1742     T0=TM
1743     DIAZ=0
1744     SDATES=DATES$
1745     STIMES=TIMES$
1750     PRINT
1760     INPUT "ENTER THE TIME INTERVAL (sec): ",DELT:PRINT:PRINT
1770     INPUT "DO YOU WANT TO STORE THE DATA (Y/N)? ",AS$
1780     IF AS="Y" THEN GOTO 1810
1790     GOTO 1840
1800     PRINT
1810     PRINT "ENTER DATA FILE NAME: "
1820     INPUT " eight characters and no extension: ".FILE1$
1830     FLAG4=1
1840     GOSUB 1030
1850     PRINT "PRESS 'return' WHEN READY. START TEST AT BEEP"
1860     AS=INKEY$
1870     IF AS<>CHR$(13) THEN GOTO 1860
1880 REM
1890 REM SETUP WINDOW*****
1900 REM
1910     SCREEN 9
1920     KEY ON
1930 REM
1940     LOCATE 21,30
1950     PRINT "TIME (SEC)"
1960 REM
1970     LOCATE 7,1
1980     PRINT "V"
1990     LOCATE 8,1
2000     PRINT "O"
2010     LOCATE 9,1
2020     PRINT "L"
2030     LOCATE 10,1
2040     PRINT "T"
2050     LOCATE 11,1
2060     PRINT "A"
2070     LOCATE 12,1
2080     PRINT "G"
2090     LOCATE 13,1
2100     PRINT "E"
2110 REM
2120     LOCATE 1,2
2130     PRINT MAXY
2140     LOCATE 19,2

```

```

2150     PRINT MINY
2160  REM
2170     LOCATE 20,5
2180     PRINT MINX
2190     LOCATE 20,74
2200     PRINT MAXX
2210  REM
2220     LOCATE 23,1
2230     VIEW (50,3)-(600,260),,1
2240  REM
2250     WINDOW (MINX.MINY)-(MAXX,MAXY)
2260  REM
2270     CLS
2280     DX=MAXX-MINX
2290     DY=MAXY-MINY
2300  REM
2310     FOR I=MINX+(DX/10) TO MAXX-(DX/10) STEP DX/10
2320         LINE (I.MINY)-(I.MAXY),,,&H1F11
2330     NEXT I
2340  REM
2350     FOR I=MINY+(DY/5) TO MAXY-(DY/5) STEP DY/5
2360         LINE (MINX.I)-(MAXX.I),,,&H1F11
2370     NEXT I
2380     IF FLAG5=1 THEN GOTO 3570 ELSE IF FLAGF=1 THEN GOTO 3540
2390     IF FLAG1=1 THEN RETURN
2400  REM
2410  REM MAIN DATA READING LOOP*****
2420  REM
2430     FLAG1=1
2440     COUNTER = 0
2480     BEEP
2490     FLAG=1
2500  REM
2510     FOR K=0 TO 1
2520         OUT MUX!(K),CH(K)
2530         OUT AD1170(K),INTTIME
2540     NEXT K
2550     FOR K=0 TO 1
2560         WAIT AD1170(K),1,1
2570         OUT MUX!(K), GNDCHANNEL
2580         LBYTE = INP(AD1170(K)+1)
2590         MBYTE = INP(AD1170(K)+2)
2600         HBYTE = INP(AD1170(K)+3)
2610         VOLTS(COUNTER.K) = (LBYTE+256*MBYTE+65536!*HBYTE)*10/2^(INTBIT+7)-5
2620     NEXT K
2720     T=TIMER
2730     IF T<TM THEN DIAZ=DIAZ+86400!
2740     TM=T :D$=DATES
2750     TIME(COUNTER)=T-T0+DIAZ
2760     FOR K=1 TO IC
2770         IF COUNTER<>0 THEN LINE (TIME(COUNTER-1),VOLTS(COUNTER-1,K-1))-
(TIME(COUNTER),VOLTS(COUNTER.K-1))
2780     NEXT K
2790     LOCATE 23,1
2800     PRINT "
2810     LOCATE 23,1

```

```

2820     PRINT INT(TIME(COUNTER)), COUNTER:""/":J
2830     FOR K=1 TO N
2840         LOCATE 23.20+K*10
2850         PRINT USING "##.#####":VOLTS(COUNTER,K-1)
2860     NEXT K
2870     IF COUNTER=J THEN GOTO 3040
2880     TD=0
2890     IF TM+DELT<86400! THEN GOTO 2960
2900     TD=86400!
2910     WHILE DATE$=D$
2920         IF FLAGA=1 THEN FLAGA=0 : GOSUB 3790
2930         IF FLAGB=1 THEN FLAGB=0 : GOSUB 1050
2940         IF FLAGC=1 THEN FLAGC=0 : GOSUB 3910
2950     WEND
2960     IF FLAGA=1 THEN FLAGA=0 : GOSUB 3790
2970     WHILE TIMER < TM + DELT - TD
2980         IF FLAGA=1 THEN FLAGA=0 : GOSUB 3790
2990         IF FLAGB=1 THEN FLAGB=0 : GOSUB 1050
3000         IF FLAGC=1 THEN FLAGC=0 : GOSUB 3910
3010     WEND
3020     IF FLAG3=0 THEN COUNTER=COUNTER+1
3030     GOTO 2500
3040     REM DATA ARRAY FULL
3050     GOSUB 4210
3060     GOTO 3280
3070     REM
3080     REM DATA PROCESSING ROUTINES AFTER READINGS COMPLETE*****
3090     REM
3100     REM
3110     LOCATE 23.1
3120     PRINT " "
3130     LOCATE 23.1
3140     INPUT "DO YOU WANT TO CONTINUE COLLECTION MODE (Y/N)";ANS$
3150     LOCATE 23.1
3160     PRINT " "
3170     IF ANS$="N" THEN :GOSUB 4210 : RETURN 3280
3180     LOCATE 23.1
3190     INPUT "DO YOU WANT TO START A NEW DATA FILE (Y/N)";ANS$
3200     IF ANS$="Y" THEN GOTO 3240
3210     LOCATE 23.1
3220     PRINT " "
3230     RETURN
3240     GOSUB 4210
3250     FLAG=0 :FLAG1=0
3260     SCREEN 0 : CLS
3270     RETURN 1660
3280     REM
3290     KEY 1," "
3300     KEY 2,"SCALE"
3310     KEY 3,"CHANEL"
3320     KEY 4," "
3330     KEY 5,"END"
3340     KEY 6," "
3350     KEY 7," "
3360     KEY 8," "
3370     KEY 9," "

```

```

3380     KEY 10," "
3390     KEY (1) OFF
3400     KEY (2) ON
3410     KEY (3) ON
3420     KEY (4) OFF
3430     KEY (5) ON
3440     KEY (6) OFF
3450     KEY (7) OFF
3460     KEY (8) OFF
3470     KEY (9) OFF
3480     KEY (10) OFF
3490     ON KEY (2) GOSUB 1050
3500     ON KEY (3) GOSUB 3910
3510     ON KEY (5) GOSUB 5010
3520     FLAGF=1
3530     GOTO 3530
3540     GOSUB 3550
3550     REM PLOT DATA IN MEMORY*****
3560     IF FLAG1=0 THEN RETURN
3570     FOR I=1 TO COUNTER
3580         FOR K=1 TO IC
3590             LINE(TIME(I-1),VOLTS(I-1,NCP(K-1)))-(TIME(I),VOLTS(I,NCP(K-1)))
3600         NEXT K
3610     NEXT I
3620     RETURN
3630     REM BYPASS READINGS*****
3640     REM
3650     KEY 1,"SAVE"
3660     KEY (1) ON
3670     ON KEY (1) GOSUB 3710
3680     FLAG3=1
3690     RETURN
3700     REM
3710     REM KEEP DATA*****
3720     REM
3730     KEY 1,"BYPASS"
3740     KEY (1) ON
3750     ON KEY (1) GOSUB 3630
3760     FLAG3=0
3770     RETURN
3780     REM
3790     REM CHANGE TIME INTERVAL FOR SLOW READINGS*****
3800     REM
3810     LOCATE 23,1
3820     PRINT " "
3830     LOCATE 23,1
3840     INPUT "ENTER NEW TIME INTERVAL (sec): ",DELT
3850     LOCATE 23,1
3860     PRINT " "
3870     RETURN 2880
3880     REM
3890     REM REDEFINE CHANNEL POSITIONS TO BE PLOTTED*****
3900     REM
3910     LOCATE 23,1
3920     PRINT " "
3930     LOCATE 23,1

```

```

3940 INPUT "ENTER NUMBER OF CHANNELS TO BE PLOTTED: ",IC
3950 FOR I=0 TO (IC-1)
3960 LOCATE 23,1
3970 PRINT " "
3980 LOCATE 22,1
3990 PRINT " "
4000 LOCATE 22,1
4010 PRINT "ENTER";(I+1);"TH CHANNEL TO BE PLOTTED:"
4020 INPUT NCP(I)
4030 NCP(I)=NCP(I)-1
4040 NEXT I
4050 LOCATE 22,1
4060 PRINT " "
4070 LOCATE 23,1
4080 PRINT " "
4090 GOSUB 3550
4100 RETURN
4110 REM CHANGE DELT FLAG*****
4120 FLAGA=1
4130 RETURN
4140 REM CHANGE FRAME FLAG*****
4150 FLAGB=1
4160 RETURN
4170 REM CHANGE PLOT CHANNELS FLAG*****
4180 FLAGC=1
4190 RETURN
4200 REM
4210 REM DATA STORAGE SECTION*****
4220 REM
4230 IF FLAG4=0 THEN RETURN
4240 FILE2$=FILE1$+".DAT"
4250 OPEN "O", #2, FILE2$
4260 GOSUB 4380
4270 FOR I=0 TO COUNTER
4280 PRINT #2, INT(100*TIME(I))/100,
4290 FOR K=0 TO N-1
4300 PRINT #2, INT(1000000!*VOLTS(I,K))/1000000!.
4310 NEXT K
4320 PRINT #2, " "
4330 NEXT I
4340 CLOSE #2
4350 RETURN
4360 REM SETUP OUTPUT FILE (HEADINGS ETC.)*****
4370 REM
4380 WRITE #2, PROGRAM$
4390 CS=CHR$(34)
4400 WRITE #2, FILE2$,N,STIMES:WRITE #2, SDATES$
4420 PRINT #2, CS;"CRD NBR";CS;
4430 FOR I=0 TO N-1
4440 PRINT #2, CS:AD1170(I);CS;
4450 NEXT I
4460 PRINT #2, ""
4461 PRINT #2, CS;"CH NBR";CS;
4462 FOR I=0 TO N-1
4463 PRINT #2, CS;CH(I);CS;
4464 NEXT I

```

```

4465     PRINT #2, ""
4470     PRINT #2, CS;"SECONDS":CS;
4480     FOR I=0 TO N-1
4490         PRINT #2, CS;"VOLTS":CS;
4500     NEXT I
4510     PRINT #2, ""
4511     PRINT #2, CS;"CLOCK":CS;
4520     FOR I=0 TO N-1
4530         PRINT #2, CS:I;CS;
4540     NEXT I
4550     PRINT #2, " "
4750     RETURN
4760     REM
4770     REM INPUT DATA DIRECTLY FROM DISC*****
4780     REM
4790     INPUT "ENTER DATA FILE TO READ FROM: ",FILE3$
4800     PRINT "ENTER THE NUMBER OF DATA READINGS "
4810     INPUT " (must be at least as large as actual file)":J
4820     FILE3$=FILE3$+".DAT"
4830     OPEN "I", #3, FILE3$
4840     GOSUB 5170
4850     IF FLAG1=1 THEN ERASE VOLTS,TIME
4860     DIM VOLTS(J,N), TIME(J)
4870     COUNTER=0
4880     INPUT #3, TIME(COUNTER)
4890     FOR I=0 TO N-1
4900         INPUT #3, VOLTS(COUNTER,I)
4910     NEXT I
4920     IF EOF(3)=-1 THEN GOTO 4950
4930     COUNTER=COUNTER+1
4940     GOTO 4880
4950     FLAG1=0 : CLS
4960     GOSUB 3940
4970     FLAG=1 : FLAG1=1
4980     GOSUB 1030
4990     GOTO 3280
5000     REM END OF PROGRAM*****
5010     INPUT "ARE YOU FINISHED (Y/N)":ANSS
5020     IF ANSS="Y" THEN GOTO 5080
5030     GOSUB 5110
5040     SCREEN 0
5050     FLAG=0
5060     FLAG1=0
5070     GOTO 620
5080     SCREEN 0
5090     STOP
5100     END
5110     REM*****RESET FUNCTION KEYS*****
5120     FOR I=1 TO 10
5130         KEY I, " "
5140     NEXT I
5150     KEY OFF
5160     RETURN
5170     REM SETUP OUTPUT FILE (HEADINGS ETC.)*****
5180     REM
5190     INPUT #3, PROGRAM

```

```
5200 INPUT #3, FILE3$
5210 INPUT #3, N
5220 INPUT #3, TTIMES
5230 INPUT #3, DDATES
5240 INPUT #3, A
5250 INPUT #3, PROGRAM
5260 INPUT #3, XS
5270 INPUT #3, XS
5280 FOR I=0 TO N-1
5290     INPUT #3, TR$(I)
5300 NEXT I
5310 INPUT #3, XS
5320 FOR I=0 TO N-1
5330     INPUT #3, XS
5340 NEXT I
5350 FOR I=0 TO N
5360     INPUT #3, X
5370 NEXT I
5380 FOR I=0 TO N
5390     INPUT #3, X
5400 NEXT I
5410 FOR I=0 TO N
5420     INPUT #3, X
5430 NEXT I
5440 INPUT #3, XS
5450 INPUT #3, TTIMES
5460 FOR I=0 TO N-1
5470     INPUT #3, CH(I)
5480 NEXT I
5490 INPUT #3, XS
5500 FOR I=0 TO N-1
5510     INPUT #3, XS
5520 NEXT I
5530 RETURN
```


“P790”

P790.bas

```
10 REM DATA ACQUISITION PROGRAM 2/7/93*****
20 REM LAST REVISED 12/20/94 JTG
30 REM
40 SCREEN 0
50 CLS
60 GOSUB 5120
70 REM
80 PROGRAM$="PIEZOCONE 790"
90 FLAG=0
100 FLAG1=0
110 FLAG2=0 'used for data storage
120 FLAG3=0 'used to control storage in array
130 FLAG4=0 'used to indicate data file specified
140 FLAGA=0 'change delt
150 FLAGB=0 'change frame
160 FLAGC=0 'change plot channels
170 FLAGE=0
180 FLAGF=0
190 REM
200 PRINT TAB(26) " THIS PROGRAM IS":PRINT
210 PRINT TAB(26) " PART":PRINT
220 PRINT TAB(26) " OF THE":PRINT:PRINT
230 PRINT TAB(26) " DATA ACQUISITION SYSTEM":PRINT
240 PRINT TAB(26) " FOR THE":PRINT
250 PRINT TAB(26) " GEOTECHNICAL LABORATORY":PRINT:PRINT
260 PRINT TAB(26) " DEPARTMENT OF":PRINT:PRINT
270 PRINT TAB(26) " CIVIL AND ENVIRONMENTAL ENGINEERING":PRINT
280 PRINT TAB(26) "MASSACHUSETTS INSTITUTE OF TECHNOLOGY":PRINT
290 PRINT:PRINT
300 INPUT "PRESS 'return' TO CONTINUE".Z$
310 CLS
320 PRINT TAB(1) "THIS PROGRAM COLLECTS DATA AT A RELATIVELY SLOW RATE"
330 PRINT TAB(1) "THE PROGRAM REQUIRES AN AD1170 DATA ACQUISITION CARD"
340 PRINT TAB(1) "THE USER CAN INTERACTIVELY CHANGE THE READING RATE"
350 PRINT TAB(1) " AND CHOOSE TO SAVE OR IGNORE THE DATA AS IT IS RECORDED":PRINT
360 PRINT TAB(1) "THIS IS PROGRAM REVISION 1.1 PROGRAMED 12/20/94":PRINT:PRINT
370 REM
380 INPUT "PRESS 'return' TO CONTINUE".Z$
390 REM
400 REM INPUT INTTIME AND INTBIT*****
410 CLS
420 PRINT TAB(1) "THE DATA ACQUISITION CARD HAS SOFTWARE SELECTABLE
PARAMETERS WHICH YOU MUST NOW SELECT FROM THE FOLLOWING LIST": PRINT:PRINT
430 PRINT TAB(1) "THE INTEGRATION TIME (N): "
440 PRINT TAB(1) " where N=0 1 msec N=4 100 msec"
450 PRINT TAB(1) " N=1 10 msec N=5 166.7 msec"
460 PRINT TAB(1) " N=2 16.7 msec N=6 300 msec"
470 PRINT TAB(1) " N=3 20 msec"
480 INPUT INTTIME
490 INTTIME=5
500 INTTIME=INTTIME+16
510 PRINT:PRINT:PRINT "THE BIT PRECISION: "
520 PRINT TAB(1) " options 8,10,12,14,16,18,20,22"
530 INPUT INTBIT
```

```

540     INTBIT=22
550     INTBIT=INTBIT-7
560 REM
570 REM
580 REM
590 REM SET PARAMETERS FOR SLOW READINGS*****
600 REM
610     INPUT "PRESS 'return' TO CONTINUE",ZS
620     CLS
630     PRINT TAB(1) "PROVIDE THE FOLLOWING INFORMATION FOR THE
READINGS":PRINT:PRINT
640     INPUT "ENTER THE NUMBER OF CHANNELS TO BE RECORDED OR INPUT FROM DISC:
",N:PRINT:PRINT
650 N=4
660 GOTO 780
670     FOR I=0 TO (N-1)
680         CLS
690         PRINT "ENTER CARD ADDRESS"
700         INPUT AD1170(I)
710         PRINT "ENTER THE CHANNEL NUMBER FOR CHANNEL position NO.",(I+1);": "
720         PRINT "    for the AD1170 card the first channel is 0"
730         INPUT CH(I)
740         PRINT "ENTER THE TRANSDUCER NO. FOR CHANNEL NO. ";CH(I);": "
750         INPUT TR(I)
760         PRINT:PRINT
770     NEXT I
780 AD1170(0)=768:AD1170(1)=896:AD1170(2)=992:AD1170(3)=768
790 CH(0)=2:CH(1)=2:CH(2)=2:CH(3)=6
800 REM SET UP AD-1170*****
810 REM
820     CLS
825     PRINT "THIS IS THE PROGRAM FOR ";PROGRAMS
830     PRINT:PRINT "    THE A/D CONVERTER IS BEING INITIALIZED"
840     FOR I=0 TO N-1
850         OUT AD1170(I),60:WAIT AD1170(I),1.1
860         OUT AD1170(I)+1,INTBIT:WAIT AD1170(I),1.1
870         OUT AD1170(I),48:WAIT AD1170(I),1.1
880         OUT AD1170(I),176:WAIT AD1170(I),1.1
890         OUT AD1170(I),184:WAIT AD1170(I),1.1
900         MUX!(I)=AD1170(I)+8
910     NEXT I
920     GNDCHANNEL=15
930     REFCHANNEL=14
940     CHANNEL=0
950 REM
960 REM
970 REM MAIN PROGRAM*****
980 REM
990     GOSUB 3940
1000    GOTO 1190
1010 REM
1020 REM
1030 REM DRAW FRAME AND SET SCALES*****
1040 REM
1050     SCREEN 0
1060     KEY OFF

```

```

1070     CLS
1080     INPUT "ENTER MIN X VALUE (sec): ",MINX
1090     INPUT "ENTER MAX X VALUE (sec): ",MAXX
1100     INPUT "ENTER MIN Y VALUE (volts): ",MINY
1110     INPUT "ENTER MAX Y VALUE (volts): ",MAXY
1120     REM
1130     CLS
1140     IF FLAG=1 THEN GOSUB 1890
1150     IF FLAG=1 THEN GOSUB 3560
1160     RETURN
1170     REM
1180     REM SET FUNCTION KEYS*****
1190     REM
1200     IF FLAG=1 THEN SCREEN 0
1210     CLS
1220     PRINT "PRESS F1' TO START OR F6' TO READ FROM DISC."
1230     KEY 1,"START"
1240     KEY 6,"DISC"
1250     ON KEY (1) GOSUB 1330
1260     ON KEY (6) GOSUB 4790
1270     KEY (1) ON
1280     KEY (6) ON
1290     KEY ON
1300     REM     FLAG=1
1310     GOTO 1310
1320     REM
1330     REM SLOW READING ROUTINE ACTIVATED WITH START KEY*****
1340     REM
1350     FLAG5=0
1360     FLAGF=0
1370     FLAG6=0
1380     GOSUB 5120
1390     KEY 1,"BYPASS"
1400     KEY 2,"  "
1410     KEY 3,"  "
1420     KEY 4,"DELT"
1430     KEY 5,"SCALE"
1440     KEY 6,"CHANEL"
1450     KEY 7,"END"
1460     KEY 8,"  "
1470     KEY 9,"  "
1480     KEY 10,"  "
1490     KEY (1) ON
1500     KEY (2) OFF
1510     KEY (3) OFF
1520     KEY (4) ON
1530     KEY (5) ON
1540     KEY (6) ON
1550     KEY (7) ON
1560     KEY (8) OFF
1570     KEY (9) OFF
1580     KEY (10) OFF
1590     ON KEY (1) GOSUB 3630
1600     ON KEY (4) GOSUB 4110
1610     ON KEY (5) GOSUB 4140
1620     ON KEY (6) GOSUB 4170

```

```

1630     ON KEY (7) GOSUB 3080
1640 REM
1650 REM
1660 REM TAKE SET OF READINGS ON KEYBOARDS CUE*****
1670 REM
1680     CLS
1690     SCREEN 0
1710     IF FLAG2=1 THEN ERASE VOLTS,TIME
1720     INPUT "ENTER NUMBER OF READINGS: ",J
1730     DIM VOLTS(J,N), TIME(J)
1740     FLAG2=1
1741     TM = TIMER
1742     T0=TM
1743     DIAZ=0
1744     SDATES=DATES
1745     STIMES=TIMES
1750     PRINT
1760     INPUT "ENTER THE TIME INTERVAL (sec): ",DELT:PRINT:PRINT
1770     INPUT "DO YOU WANT TO STORE THE DATA (Y/N)? ",AS
1780     IF AS="Y" THEN GOTO 1810
1790     GOTO 1840
1800     PRINT
1810     PRINT "ENTER DATA FILE NAME: "
1820     INPUT " eight characters and no extension: ",FILE1$
1830     FLAG4=1
1840     GOSUB 1030
1850     PRINT "PRESS 'return' WHEN READY, START TEST AT BEEP"
1860     AS=INKEYS
1870     IF AS<>CHR$(13) THEN GOTO 1860
1880 REM
1890 REM SETUP WINDOW*****
1900 REM
1910     SCREEN 9
1920     KEY ON
1930 REM
1940     LOCATE 21,30
1950     PRINT "TIME (SEC)"
1960 REM
1970     LOCATE 7,1
1980     PRINT "V"
1990     LOCATE 8,1
2000     PRINT "O"
2010     LOCATE 9,1
2020     PRINT "L"
2030     LOCATE 10,1
2040     PRINT "T"
2050     LOCATE 11,1
2060     PRINT "A"
2070     LOCATE 12,1
2080     PRINT "G"
2090     LOCATE 13,1
2100     PRINT "E"
2110 REM
2120     LOCATE 1,2
2130     PRINT MAXY
2140     LOCATE 19,2

```

```

2150     PRINT MINY
2160 REM
2170     LOCATE 20.5
2180     PRINT MINX
2190     LOCATE 20.74
2200     PRINT MAXX
2210 REM
2220     LOCATE 23,1
2230     VIEW (50,3)-(600,260),,1
2240 REM
2250     WINDOW (MINX,MINY)-(MAXX.MAXY)
2260 REM
2270     CLS
2280     DX=MAXX-MINX
2290     DY=MAXY-MINY
2300 REM
2310     FOR I=MINX+(DX/10) TO MAXX-(DX/10) STEP DX/10
2320         LINE (I,MINY)-(I,MAXY),,,&H1F11
2330     NEXT I
2340 REM
2350     FOR I=MINY+(DY/5) TO MAXY-(DY/5) STEP DY/5
2360         LINE (MINX,I)-(MAXX,I),,,&H1F11
2370     NEXT I
2380     IF FLAG5=1 THEN GOTO 3570 ELSE IF FLAGF=1 THEN GOTO 3540
2390     IF FLAG1=1 THEN RETURN
2400 REM
2410 REM MAIN DATA READING LOOP*****
2420 REM
2430     FLAG1=1
2440     COUNTER = 0
2480     BEEP
2490     FLAG=1
2500 REM
2510     FOR K=0 TO 2
2520         OUT MUX!(K),CH(K)
2530         OUT AD1170(K).INTTIME
2540     NEXT K
2550     FOR K=0 TO 2
2560         WAIT AD1170(K),1,1
2570         OUT MUX!(K), GNDCHANNEL
2580         LBYTE = INP(AD1170(K)+1)
2590         MBYTE = INP(AD1170(K)+2)
2600         HBYTE = INP(AD1170(K)+3)
2610         VOLTS(COUNTER,K) = (LBYTE+256*MBYTE+65536!*HBYTE)*10/2^(INTBIT+7)-5
2620     NEXT K
2630     K=3
2640     OUT MUX!(K),CH(K)
2650     OUT AD1170(K).INTTIME
2660     WAIT AD1170(K),1,1
2670     OUT MUX!(K), GNDCHANNEL
2680     LBYTE = INP(AD1170(K)+1)
2690     MBYTE = INP(AD1170(K)+2)
2700     HBYTE = INP(AD1170(K)+3)
2710     VOLTS(COUNTER,K) = (LBYTE+256*MBYTE+65536!*HBYTE)*10/2^(INTBIT+7)-5
2720     T=TIMER
2730     IF T<TM THEN DIAZ=DIAZ+86400!

```

```

2740     TM=T :DS=DATES
2750     TIME(COUNTER)=T-T0+DIAZ
2760     FOR K=1 TO IC
2770         IF COUNTER<>0 THEN LINE (TIME(COUNTER-1),VOLTS(COUNTER-1,K-1))-
(TIME(COUNTER),VOLTS(COUNTER,K-1))
2780     NEXT K
2790         LOCATE 23,1
2800         PRINT "
2810         LOCATE 23,1
2820         PRINT INT(TIME(COUNTER)), COUNTER;" / ";J
2830     FOR K=1 TO N
2840         LOCATE 23,20+K*10
2850         PRINT USING "##.#####";VOLTS(COUNTER,K-1)
2860     NEXT K
2870     IF COUNTER=J THEN GOTO 3040
2880     TD=0
2890     IF TM+DELT<86400! THEN GOTO 2960
2900     TD=86400!
2910     WHILE DATES=DS
2920         IF FLAGA=1 THEN FLAGA=0 : GOSUB 3790
2930         IF FLAGB=1 THEN FLAGB=0 : GOSUB 1050
2940         IF FLAGC=1 THEN FLAGC=0 : GOSUB 3910
2950     WEND
2960     IF FLAGA=1 THEN FLAGA=0 : GOSUB 3790
2970     WHILE TIMER < TM + DELT - TD
2980         IF FLAGA=1 THEN FLAGA=0 : GOSUB 3790
2990         IF FLAGB=1 THEN FLAGB=0 : GOSUB 1050
3000         IF FLAGC=1 THEN FLAGC=0 : GOSUB 3910
3010     WEND
3020     IF FLAG3=0 THEN COUNTER=COUNTER+1
3030     GOTO 2500
3040     REM DATA ARRAY FULL
3050     GOSUB 4210
3060     GOTO 3280
3070     REM
3080     REM DATA PROCESSING ROUTINES AFTER READINGS COMPLETE*****
3090     REM
3100     REM
3110     LOCATE 23,1
3120     PRINT "
3130     LOCATE 23,1
3140     INPUT "DO YOU WANT TO CONTINUE COLLECTION MODE (Y/N)";ANS$
3150     LOCATE 23,1
3160     PRINT "
3170     IF ANS$="N" THEN :GOSUB 4210 : RETURN 3280
3180     LOCATE 23,1
3190     INPUT "DO YOU WANT TO START A NEW DATA FILE (Y/N)";ANS$
3200     IF ANS$="Y" THEN GOTO 3240
3210     LOCATE 23,1
3220     PRINT "
3230     RETURN
3240     GOSUB 4210
3250     FLAG=0 :FLAG1=0
3260     SCREEN 0 : CLS
3270     RETURN 1660
3280     REM

```

```

3290     KEY 1."  "
3300     KEY 2."SCALE"
3310     KEY 3."CHANEL"
3320     KEY 4."  "
3330     KEY 5."END"
3340     KEY 6."  "
3350     KEY 7."  "
3360     KEY 8."  "
3370     KEY 9."  "
3380     KEY 10."  "
3390     KEY (1) OFF
3400     KEY (2) ON
3410     KEY (3) ON
3420     KEY (4) OFF
3430     KEY (5) ON
3440     KEY (6) OFF
3450     KEY (7) OFF
3460     KEY (8) OFF
3470     KEY (9) OFF
3480     KEY (10) OFF
3490     ON KEY (2) GOSUB 1050
3500     ON KEY (3) GOSUB 3910
3510     ON KEY (5) GOSUB 5010
3520     FLAGF=1
3530     GOTO 3530
3540     GOSUB 3550
3550     REM PLOT DATA IN MEMORY*****
3560     IF FLAG1=0 THEN RETURN
3570     FOR I=1 TO COUNTER
3580         FOR K=1 TO IC
3590             LINE(TIME(I-1),VOLTS(I-1,NCP(K-1)))-(TIME(I),VOLTS(I,NCP(K-1)))
3600         NEXT K
3610     NEXT I
3620     RETURN
3630     REM BYPASS READINGS*****
3640     REM
3650     KEY 1. "SAVE"
3660     KEY (1) ON
3670     ON KEY (1) GOSUB 3710
3680     FLAG3=1
3690     RETURN
3700     REM
3710     REM KEEP DATA*****
3720     REM
3730     KEY 1. "BYPASS"
3740     KEY (1) ON
3750     ON KEY (1) GOSUB 3630
3760     FLAG3=0
3770     RETURN
3780     REM
3790     REM CHANGE TIME INTERVAL FOR SLOW READINGS*****
3800     REM
3810     LOCATE 23,1
3820     PRINT "
3830     LOCATE 23,1
3840     INPUT "ENTER NEW TIME INTERVAL (sec): ",DELT

```



```

3850     LOCATE 23,1
3860     PRINT "
3870     RETURN 2880
3880 REM
3890 REM REDEFINE CHANNEL POSITIONS TO BE PLOTTED*****
3900 REM
3910     LOCATE 23,1
3920     PRINT "
3930     LOCATE 23,1
3940     INPUT "ENTER NUMBER OF CHANNELS TO BE PLOTTED: ",IC
3950     FOR I=0 TO (IC-1)
3960         LOCATE 23,1
3970         PRINT "
3980         LOCATE 22,1
3990         PRINT "
4000         LOCATE 22,1
4010         PRINT "ENTER";(I+1);"TH CHANNEL TO BE PLOTTED:"
4020         INPUT NCP(I)
4030         NCP(I)=NCP(I)-1
4040     NEXT I
4050     LOCATE 22,1
4060     PRINT "
4070     LOCATE 23,1
4080     PRINT "
4090     GOSUB 3550
4100     RETURN
4110 REM CHANGE DELT FLAG*****
4120     FLAGA=1
4130     RETURN
4140 REM CHANGE FRAME FLAG*****
4150     FLAGB=1
4160     RETURN
4170 REM CHANGE PLOT CHANNELS FLAG*****
4180     FLAGC=1
4190     RETURN
4200 REM
4210 REM DATA STORAGE SECTION*****
4220 REM
4230     IF FLAG4=0 THEN RETURN
4240     FILE2$=FILE1$+".DAT"
4250     OPEN "O", #2, FILE2$
4260     GOSUB 4380
4270     FOR I=0 TO COUNTER
4280         PRINT #2, INT(100*TIME(I))/100,
4290         FOR K=0 TO N-1
4300             PRINT #2, INT(1000000!*VOLTS(I,K))/1000000!,
4310             NEXT K
4320         PRINT #2, " "
4330     NEXT I
4340     CLOSE #2
4350     RETURN
4360 REM SETUP OUTPUT FILE (HEADINGS ETC.)*****
4370 REM
4380     WRITE #2, PROGRAMS
4390     C$=CHR$(34)
4400     WRITE #2, FILE2$,N,STIMES:WRITE #2, SDATES$

```

```

4420 PRINT #2, CS:"CRD NBR":CS:
4430 FOR I=0 TO N-1
4440 PRINT #2, CS:AD1170(I);CS:
4450 NEXT I
4460 PRINT #2, ""
4461 PRINT #2, CS:"CH NBR":CS:
4462 FOR I=0 TO N-1
4463 PRINT #2, CS;CH(I);CS:
4464 NEXT I
4465 PRINT #2, ""
4470 PRINT #2, CS:"SECONDS":CS:
4480 FOR I=0 TO N-1
4490 PRINT #2, CS;"VOLTS":CS:
4500 NEXT I
4510 PRINT #2, ""
4511 PRINT #2, CS:"CLOCK":CS
4520 FOR I=0 TO N-1
4530 PRINT #2, CS:I;CS:
4540 NEXT I
4550 PRINT #2, " "
4750 RETURN
4760 REM
4770 REM INPUT DATA DIRECTLY FROM DISC*****
4780 REM
4790 INPUT "ENTER DATA FILE TO READ FROM: ",FILE3$
4800 PRINT "ENTER THE NUMBER OF DATA READINGS "
4810 INPUT " (must be at least as large as actual file)";J
4820 FILE3$=FILE3$+".DAT"
4830 OPEN "I", #3, FILE3$
4840 GOSUB 5170
4850 IF FLAG1=1 THEN ERASE VOLTS,TIME
4860 DIM VOLTS(J.N), TIME(J)
4870 COUNTER=0
4880 INPUT #3, TIME(COUNTER)
4890 FOR I=0 TO N-1
4900 INPUT #3, VOLTS(COUNTER.I)
4910 NEXT I
4920 IF EOF(3)=-1 THEN GOTO 4950
4930 COUNTER=COUNTER+1
4940 GOTO 4880
4950 FLAG1=0 : CLS
4960 GOSUB 3940
4970 FLAG=1 : FLAG1=1
4980 GOSUB 1030
4990 GOTO 3280
5000 REM END OF PROGRAM*****
5010 INPUT "ARE YOU FINISHED (Y/N)";ANSS
5020 IF ANSS="Y" THEN GOTO 5080
5030 GOSUB 5110
5040 SCREEN 0
5050 FLAG=0
5060 FLAG1=0
5070 GOTO 620
5080 SCREEN 0
5090 STOP
5100 END

```

```

5110 REM*****RESET FUNCTION KEYS*****
5120   FOR I=1 TO 10
5130   KEY I. "    "
5140   NEXT I
5150   KEY OFF
5160   RETURN
5170 REM SETUP OUTPUT FILE (HEADINGS ETC.)*****
5180 REM
5190   INPUT #3, PROGRAM
5200   INPUT #3. FILE3$
5210   INPUT #3, N
5220   INPUT #3, TTIMES$
5230   INPUT #3. DDATE$
5240   INPUT #3. A
5250   INPUT #3. PROGRAM
5260   INPUT #3. XS
5270   INPUT #3, XS
5280   FOR I=0 TO N-1
5290     INPUT #3, TR$(I)
5300   NEXT I
5310   INPUT #3, XS
5320   FOR I=0 TO N-1
5330     INPUT #3, XS
5340   NEXT I
5350   FOR I=0 TO N
5360     INPUT #3, X
5370   NEXT I
5380   FOR I=0 TO N
5390     INPUT #3, X
5400   NEXT I
5410   FOR I=0 TO N
5420     INPUT #3, X
5430   NEXT I
5440   INPUT #3. XS
5450   INPUT #3, TTIMES$
5460   FOR I=0 TO N-1
5470     INPUT #3, CH(I)
5480   NEXT I
5490   INPUT #3, XS
5500   FOR I=0 TO N-1
5510     INPUT #3, XS
5520   NEXT I
5530   RETURN

```

“NIGHT”

NIGHT.bas

```
10 REM DATA ACQUISITION PROGRAM 2/7/93*****
20 REM LAST REVISED 12/20/94 JTG
30 REM
40 SCREEN 0
50 CLS
60 GOSUB 5520
70 REM
80 PROGRAMS="OVER NIGHT DISSIPATION PROGRAM"
90 FLAG=0
100 FLAG1=0
110 FLAG2=0 'used for data storage
120 FLAG3=0 'used to control storage in array
130 FLAG4=0 'used to indicate data file specified
140 FLAGA=0 'change delt
150 FLAGB=0 'change frame
160 FLAGC=0 'change plot channels
170 FLAGE=0
180 FLAGF=0
190 REM
200 PRINT TAB(26) " THIS PROGRAM IS":PRINT
210 PRINT TAB(26) " PART":PRINT
220 PRINT TAB(26) " OF THE":PRINT:PRINT
230 PRINT TAB(26) " DATA ACQUISITION SYSTEM":PRINT
240 PRINT TAB(26) " FOR THE":PRINT
250 PRINT TAB(26) " GEOTECHNICAL LABORATORY":PRINT:PRINT
260 PRINT TAB(26) " DEPARTMENT OF":PRINT:PRINT
270 PRINT TAB(26) " CIVIL AND ENVIRONMENTAL ENGINEERING":PRINT
280 PRINT TAB(26) "MASSACHUSETTS INSTITUTE OF TECHNOLOGY":PRINT
290 PRINT:PRINT
300 INPUT "PRESS 'return' TO CONTINUE".Z$
310 CLS
320 PRINT TAB(1) "THIS PROGRAM COLLECTS DATA AT A RELATIVELY SLOW RATE"
330 PRINT TAB(1) "THE PROGRAM REQUIRES AN AD1170 DATA ACQUISITION CARD"
340 PRINT TAB(1) "THE USER CAN INTERACTIVELY CHANGE THE READING RATE"
350 PRINT TAB(1) " AND CHOOSE TO SAVE OR IGNORE THE DATA AS IT IS RECORDED":PRINT
360 PRINT TAB(1) "THIS IS PROGRAM REVISION 1.1 PROGRAMED 12/20/94":PRINT:PRINT
370 REM
380 INPUT "PRESS 'return' TO CONTINUE".Z$
390 REM
400 REM INPUT INTTIME AND INTBIT*****
410 CLS
420 PRINT TAB(1) "THE DATA ACQUISITION CARD HAS SOFTWARE SELECTABLE
PARAMETERS WHICH YOU MUST NOW SELECT FROM THE FOLLOWING LIST": PRINT:PRINT
430 PRINT TAB(1) "THE INTEGRATION TIME (N): "
440 PRINT TAB(1) " where N=0 1 msec N=4 100 msec"
450 PRINT TAB(1) " N=1 10 msec N=5 166.7 msec"
460 PRINT TAB(1) " N=2 16.7 msec N=6 300 msec"
470 PRINT TAB(1) " N=3 20 msec"
480 INPUT INTTIME
490 INTTIME=5
500 INTTIME=INTTIME+16
510 PRINT:PRINT:PRINT "THE BIT PRECISION: "
520 PRINT TAB(1) " options 8,10,12,14,16,18,20,22"
```

```

530 INPUT INTBIT
540 INTBIT=22
550 INTBIT=INTBIT-7
560 REM
570 REM
580 REM
590 REM SET PARAMETERS FOR SLOW READINGS*****
600 REM
610 INPUT "PRESS 'return' TO CONTINUE",Z$
620 CLS
630 PRINT TAB(1) "PROVIDE THE FOLLOWING INFORMATION FOR THE
READINGS":PRINT:PRINT
640 INPUT "ENTER THE NUMBER OF CHANNELS TO BE RECORDED OR INPUT FROM DISC:
",N:PRINT:PRINT
650 N=13
660 GOTO 790
670 FOR I=0 TO (N-1)
680 CLS
690 PRINT "ENTER CARD ADDRESS"
700 INPUT AD1170(I)
710 PRINT "ENTER THE CHANNEL NUMBER FOR CHANNEL position NO.":(I+1);": "
720 PRINT " for the AD1170 card the first channel is 0"
730 INPUT CH(I)
740 PRINT "ENTER THE TRANSDUCER NO. FOR CHANNEL NO.":CH(I);": "
750 INPUT TR(I)
760 PRINT:PRINT
770 NEXT I
780 DIM AD1170(13),CH(13),TR(13)
790 DIM AD1170(12),CH(12),TR(12),MUX!(12)
800 AD1170(0)=768:AD1170(1)=896:AD1170(2)=992:AD1170(3)=896
810 AD1170(4)=768:AD1170(5)=896:AD1170(6)=992:AD1170(7)=896
820 AD1170(8)=768:AD1170(9)=896:AD1170(10)=992:AD1170(11)=768
830 AD1170(12)=992
840 CH(0)=0:CH(1)=0:CH(2)=0:CH(3)=1
850 CH(4)=2:CH(5)=2:CH(6)=2:CH(7)=3
860 CH(8)=4:CH(9)=4:CH(10)=4:CH(11)=6:CH(12)=6
870 REM SET UP AD-1170*****
880 REM
890 CLS
900 PRINT:PRINT PROGRAMS
910 PRINT:PRINT " THE A/D CONVERTER IS BEING INITIALIZED"
920 FOR I=0 TO N-1
930 OUT AD1170(I),60:WAIT AD1170(I),1,1
940 OUT AD1170(I)+1,INTBIT:WAIT AD1170(I),1,1
950 OUT AD1170(I),48:WAIT AD1170(I),1,1
960 OUT AD1170(I),176:WAIT AD1170(I),1,1
970 OUT AD1170(I),184:WAIT AD1170(I),1,1
980 MUX!(I)=AD1170(I)+8
990 NEXT I
1000 GNDCHANNEL=15
1010 REFCHANNEL=14
1020 CHANNEL=0
1030 REM
1040 REM
1050 REM MAIN PROGRAM*****
1060 REM

```

```

1070     GOSUB 4440
1080     GOTO 1270
1090     REM
1100     REM
1110     REM DRAW FRAME AND SET SCALES*****
1120     REM
1130     SCREEN 0
1140     KEY OFF
1150     CLS
1160     INPUT "ENTER MIN X VALUE (sec): ",MINX
1170     INPUT "ENTER MAX X VALUE (sec): ",MAXX
1180     INPUT "ENTER MIN Y VALUE (volts): ",MINY
1190     INPUT "ENTER MAX Y VALUE (volts): ",MAXY
1200     REM
1210     CLS
1220     IF FLAG=1 THEN GOSUB 2020
1230     IF FLAG=1 THEN GOSUB 4060
1240     RETURN
1250     REM
1260     REM SET FUNCTION KEYS*****
1270     REM
1280     IF FLAG=1 THEN SCREEN 0
1290     CLS
1300     PRINT "PRESS F1' TO START OR F6' TO READ FROM DISC."
1310     KEY 1,"START"
1320     KEY 6,"DISC"
1330     ON KEY (1) GOSUB 1410
1340     ON KEY (6) GOSUB 5190
1350     KEY (1) ON
1360     KEY (6) ON
1370     KEY ON
1380     REM   FLAG=1
1390     GOTO 1390
1400     REM
1410     REM SLOW READING ROUTINE ACTIVATED WITH START KEY*****
1420     REM
1430     FLAG5=0
1440     FLAGF=0
1450     FLAG6=0
1460     GOSUB 5520
1470     KEY 1,"BYPASS"
1480     KEY 2,"  "
1490     KEY 3,"  "
1500     KEY 4,"DELT"
1510     KEY 5,"SCALE"
1520     KEY 6,"CHANEL"
1530     KEY 7,"END"
1540     KEY 8,"  "
1550     KEY 9,"  "
1560     KEY 10,"  "
1570     KEY (1) ON
1580     KEY (2) OFF
1590     KEY (3) OFF
1600     KEY (4) ON
1610     KEY (5) ON
1620     KEY (6) ON

```

```

1630     KEY (7) ON
1640     KEY (8) OFF
1650     KEY (9) OFF
1660     KEY (10) OFF
1670     ON KEY (1) GOSUB 4130
1680     ON KEY (4) GOSUB 4610
1690     ON KEY (5) GOSUB 4640
1700     ON KEY (6) GOSUB 4670
1710     ON KEY (7) GOSUB 3580
1720 REM
1730 REM
1740 REM TAKE SET OF READINGS ON KEYBOARDS CUE*****
1750 REM
1760     CLS
1770     SCREEN 0
1780     IF FLAG2=1 THEN ERASE VOLTS.TIME
1790     INPUT "ENTER NUMBER OF READINGS: ",J
1800     DIM VOLTS(J.N), TIME(J)
1810     FLAG2=1
1820     PRINT
1830     TM = TIMER
1840     STIMES=TIMES
1850     SDATES=DATES
1860     T0=TM
1870     DIAZ=0
1880     INPUT "ENTER THE TIME INTERVAL (sec): ".DELT:PRINT:PRINT
1890     INPUT "DO YOU WANT TO STORE THE DATA (Y/N)? ",A$
1900     IF A$="Y" THEN GOTO 1930
1910     GOTO 1970
1920     PRINT
1930     PRINT "ENTER DATA FILE NAME: "
1935     PRINT "This is the overnight version of the program"
1936     PRINT " the file name will be changed every 12 readings"
1937     PRINT " by incrementing the eighth character in the name"
1940     INPUT " SEVEN characters and no extension: ",FILE1$
1942     NF=65 USED TO SELECT THE CHARACTER OF THE FILE NAME
1950     FLAG4=1
1960     GOSUB 4710 ' SAVE HEADER AND OPEN FILE
1970     GOSUB 1110
1980     PRINT "PRESS 'return' WHEN READY, START TEST AT BEEP"
1990     A$=INKEY$
2000     IF A$<>CHR$(13) THEN GOTO 1990
2010 REM
2020 REM SETUP WINDOW*****
2030 REM
2040     SCREEN 9
2050     KEY ON
2060 REM
2070     LOCATE 21,30
2080     PRINT "TIME (SEC)"
2090 REM
2100     LOCATE 7,1
2110     PRINT "V"
2120     LOCATE 8,1
2130     PRINT "O"
2140     LOCATE 9,1

```



```

2150 PRINT "L"
2160 LOCATE 10,1
2170 PRINT "T"
2180 LOCATE 11,1
2190 PRINT "A"
2200 LOCATE 12,1
2210 PRINT "G"
2220 LOCATE 13,1
2230 PRINT "E"
2240 REM
2250 LOCATE 1,2
2260 PRINT MAXY
2270 LOCATE 19,2
2280 PRINT MINY
2290 REM
2300 LOCATE 20,5
2310 PRINT MINX
2320 LOCATE 20,74
2330 PRINT MAXX
2340 REM
2350 LOCATE 23,1
2360 VIEW (50,3)-(600,260),,1
2370 REM
2380 WINDOW (MINX,MINY)-(MAXX,MAXY)
2390 REM
2400 CLS
2410 DX=MAXX-MINX
2420 DY=MAXY-MINY
2430 REM
2440 FOR I=MINX+(DX/10) TO MAXX-(DX/10) STEP DX/10
2450 LINE (I,MINY)-(I,MAXY),,,&H1F11
2460 NEXT I
2470 REM
2480 FOR I=MINY+(DY/5) TO MAXY-(DY/5) STEP DY/5
2490 LINE (MINX,I)-(MAXX,I),,,&H1F11
2500 NEXT I
2510 IF FLAG5=1 THEN GOTO 4070 ELSE IF FLAGF=1 THEN GOTO 4040
2520 IF FLAG1=1 THEN RETURN
2530 REM
2540 REM MAIN DATA READING LOOP*****
2550 REM
2560 FLAG1=1
2570 COUNTER = 0
2580 BEEP
2590 FLAG=1
2600 REM
2610 FOR K=0 TO 2
2620 OUT MUX!(K),CH(K)
2630 OUT AD1170(K),INTTIME
2640 NEXT K
2650 FOR K=0 TO 2
2660 WAIT AD1170(K),1.1
2670 OUT MUX!(K), GNDCHANNEL
2680 LBYTE = INP(AD1170(K)+1)
2690 MBYTE = INP(AD1170(K)+2)
2700 HBYTE = INP(AD1170(K)+3)

```

```

2710     VOLTS(COUNTER.K) = (LBYTE+256*MBYTE+65536!*HBYTE)*10/2^(INTBIT+7)-5
2720 NEXT K
2730 FOR K=4 TO 6
2740     OUT MUX!(K),CH(K)
2750     OUT AD1170(K),INTTIME
2760 NEXT K
2770 FOR K=4 TO 6
2780     WAIT AD1170(K),1.1
2790     OUT MUX!(K), GNDCHANNEL
2800     LBYTE = INP(AD1170(K)+1)
2810     MBYTE = INP(AD1170(K)+2)
2820     HBYTE = INP(AD1170(K)+3)
2830     VOLTS(COUNTER.K) = (LBYTE+256*MBYTE+65536!*HBYTE)*10/2^(INTBIT+7)-5
2840 NEXT K
2850 FOR K=8 TO 10
2860     OUT MUX!(K),CH(K)
2870     OUT AD1170(K),INTTIME
2880 NEXT K
2890 FOR K=8 TO 10
2900     WAIT AD1170(K),1.1
2910     OUT MUX!(K), GNDCHANNEL
2920     LBYTE = INP(AD1170(K)+1)
2930     MBYTE = INP(AD1170(K)+2)
2940     HBYTE = INP(AD1170(K)+3)
2950     VOLTS(COUNTER.K) = (LBYTE+256*MBYTE+65536!*HBYTE)*10/2^(INTBIT+7)-5
2960 NEXT K
2970 K=3
2980     OUT MUX!(K),CH(K)
2990     OUT AD1170(K),INTTIME
3000     WAIT AD1170(K),1.1
3010     OUT MUX!(K), GNDCHANNEL
3020     LBYTE = INP(AD1170(K)+1)
3030     MBYTE = INP(AD1170(K)+2)
3040     HBYTE = INP(AD1170(K)+3)
3050     VOLTS(COUNTER.K) = (LBYTE+256*MBYTE+65536!*HBYTE)*10/2^(INTBIT+7)-5
3055 D(0)=7 : D(1)=11 : D(2)=12
3060 FOR K=0 TO 2
3061     OUT MUX!(D(K)),CH(D(K))
3062     OUT AD1170(D(K)),INTTIME
3063 NEXT K
3064 FOR K=0 TO 2
3065     WAIT AD1170(D(K)),1.1
3066     OUT MUX!(D(K)), GNDCHANNEL
3067     LBYTE = INP(AD1170(D(K))+1)
3068     MBYTE = INP(AD1170(D(K))+2)
3069     HBYTE = INP(AD1170(D(K))+3)
3070     VOLTS(COUNTER.D(K)) = (LBYTE+256*MBYTE+65536!*HBYTE)*10/2^(INTBIT+7)-5
3071 NEXT K
3150 T=TIMER
3160 IF T<TM THEN DIAZ=DIAZ+86400!
3170 TM=T :D$=DATES
3180 TIME(COUNTER)=T-T0+DIAZ
3190 IF FLAG4=1 THEN GOSUB 5030     'SAVE DATA
3200 FOR K=1 TO IC
3210     IF COUNTER<>0 THEN LINE (TIME(COUNTER-1),VOLTS(COUNTER-1,K-1))-
(TIME(COUNTER),VOLTS(COUNTER.K-1))

```

```

3220     NEXT K
3230         LOCATE 22,1
3240         PRINT " "
3250         LOCATE 23,1
3260         PRINT " "
3270         LOCATE 22,1
3280         PRINT INT(TIME(COUNTER)), COUNTER:"/";J
3290     FOR K=1 TO 6
3300         LOCATE 22,20+K*9
3310         PRINT USING "#.####";VOLTS(COUNTER,K-1)
3320     NEXT K
3330     FOR K=7 TO 13
3340         LOCATE 23,11+(K-6)*9
3350         PRINT USING "#.####";VOLTS(COUNTER,K-1)
3360     NEXT K
3370     IF COUNTER=J THEN GOTO 3540
3380     TD=0
3390     IF TM+DELT<86400! THEN GOTO 3460
3400     TD=86400!
3410     WHILE DATES=DS
3420         IF FLAGA=1 THEN FLAGA=0 : GOSUB 4290
3430         IF FLAGB=1 THEN FLAGB=0 : GOSUB 1130
3440         IF FLAGC=1 THEN FLAGC=0 : GOSUB 4410
3450     WEND
3460         IF FLAGA=1 THEN FLAGA=0 : GOSUB 4290
3470     WHILE TIMER < TM + DELT - TD
3480         IF FLAGA=1 THEN FLAGA=0 : GOSUB 4290
3490         IF FLAGB=1 THEN FLAGB=0 : GOSUB 1130
3500         IF FLAGC=1 THEN FLAGC=0 : GOSUB 4410
3510     WEND
3520     IF FLAG3=0 THEN COUNTER=COUNTER+1
3530     GOTO 2600
3540     REM DATA ARRAY FULL
3550     IF FLAG4=1 THEN GOSUB 5120 'CLOSE ARRAY
3560     GOTO 3780
3570     REM
3580     REM DATA PROCESSING ROUTINES AFTER READINGS COMPLETE*****
3590     REM
3600     REM
3610     LOCATE 23,1
3620     PRINT " "
3630     LOCATE 23,1
3640     INPUT "DO YOU WANT TO CONTINUE COLLECTION MODE (Y/N)";ANSS
3650     LOCATE 23,1
3660     PRINT " "
3670     IF ANSS="N" THEN :GOSUB 5120 : RETURN 3780
3680     LOCATE 23,1
3690     INPUT "DO YOU WANT TO START A NEW DATA FILE (Y/N)";ANSS
3700     IF ANSS="Y" THEN GOTO 3740
3710     LOCATE 23,1
3720     PRINT " "
3730     RETURN
3740     GOSUB 4710
3750     FLAG=0 : FLAG1=0
3760     SCREEN 0 : CLS
3770     RETURN 1740

```

```

3780 REM
3790 KEY 1." "
3800 KEY 2."SCALE"
3810 KEY 3."CHANEL"
3820 KEY 4." "
3830 KEY 5."END"
3840 KEY 6." "
3850 KEY 7." "
3860 KEY 8." "
3870 KEY 9." "
3880 KEY 10." "
3890 KEY (1) OFF
3900 KEY (2) ON
3910 KEY (3) ON
3920 KEY (4) OFF
3930 KEY (5) ON
3940 KEY (6) OFF
3950 KEY (7) OFF
3960 KEY (8) OFF
3970 KEY (9) OFF
3980 KEY (10) OFF
3990 ON KEY (2) GOSUB 1130
4000 ON KEY (3) GOSUB 4410
4010 ON KEY (5) GOSUB 5410
4020 FLAGF=1
4030 GOTO 4030
4040 GOSUB 4050
4050 REM PLOT DATA IN MEMORY*****
4060 IF FLAG1=0 THEN RETURN
4070 FOR I=1 TO COUNTER
4080 FOR K=1 TO IC
4090 LINE(TIME(I-1),VOLTS(I-1,NCP(K-1)))-(TIME(I),VOLTS(I,NCP(K-1)))
4100 NEXT K
4110 NEXT I
4120 RETURN
4130 REM BYPASS READINGS*****
4140 REM
4150 KEY 1."SAVE"
4160 KEY (1) ON
4170 ON KEY (1) GOSUB 4210
4180 FLAG3=1
4190 RETURN
4200 REM
4210 REM KEEP DATA*****
4220 REM
4230 KEY 1."BYPASS"
4240 KEY (1) ON
4250 ON KEY (1) GOSUB 4130
4260 FLAG3=0
4270 RETURN
4280 REM
4290 REM CHANGE TIME INTERVAL FOR SLOW READINGS*****
4300 REM
4310 LOCATE 23,1
4320 PRINT " "
4330 LOCATE 23,1

```

```

4340     INPUT "ENTER NEW TIME INTERVAL (sec): ",DELT
4350     LOCATE 23,1
4360     PRINT "                "
4370     RETURN 3380
4380     REM
4390     REM REDEFINE CHANNEL POSITIONS TO BE PLOTTED*****
4400     REM
4410     LOCATE 23,1
4420     PRINT "                "
4430     LOCATE 23,1
4440     INPUT "ENTER NUMBER OF CHANNELS TO BE PLOTTED: ",IC
4450     FOR I=0 TO (IC-1)
4460         LOCATE 23,1
4470         PRINT "                "
4480         LOCATE 22,1
4490         PRINT "                "
4500         LOCATE 22,1
4510         PRINT "ENTER";(I+1);"TH CHANNEL TO BE PLOTTED:"
4520         INPUT NCP(I)
4530         NCP(I)=NCP(I)-1
4540     NEXT I
4550     LOCATE 22,1
4560     PRINT "                "
4570     LOCATE 23,1
4580     PRINT "                "
4590     GOSUB 4050
4600     RETURN
4610     REM CHANGE DELT FLAG*****
4620     FLAGA=1
4630     RETURN
4640     REM CHANGE FRAME FLAG*****
4650     FLAGB=1
4660     RETURN
4670     REM CHANGE PLOT CHANNELS FLAG*****
4680     FLAGC=1
4690     RETURN
4700     REM
4710     REM DATA STORAGE SECTION*****
4720     REM
4730     REM set up header and open file
4740     IF FLAG4=0 THEN RETURN
4750     FILE2$=FILE1$+".DAT"
4760     OPEN "O", #2, FILE2$
4770     WRITE #2, PROGRAMS
4780     CS=CHR$(34)
4790     WRITE #2, FILE2$,N,STIMES:WRITE #2, SDATES
4800     PRINT #2, CS;"CRD NUM";CS;
4810     FOR I=0 TO N-1
4820         PRINT #2, CS;AD1170(I);CS;
4830     NEXT I
4840     PRINT #2, ""
4850     PRINT #2, CS;"CH NUM";CS;
4860     FOR I=0 TO N-1
4870         PRINT #2, CS;CH(I);CS;
4880     NEXT I
4890     PRINT #2, ""

```

```

4900 PRINT #2, C$;"SECONDS";C$;
4910 FOR I=0 TO N-1
4920     PRINT #2, C$;"VOLTS";C$;
4930 NEXT I
4940 PRINT #2, ""
4950 WRITE #2, "****"
4960 PRINT #2, C$;"CLOCK";C$;
4970 FOR I=0 TO N-1
4980     PRINT #2,C$;I;C$;
4990 NEXT I
5000 PRINT #2, " "
5005 CLOSE #2
5010 RETURN
5020 REM
5030 REM STORE EACH DATA POINT
5040 REM
5043 IF COUNTER= 0 THEN GOTO 5045
5044 IF COUNTER/12=INT(COUNTER/12) THEN NF=NF+1
5045 OPEN "A", #2, FILE1$+CHR$(NF)+".DAT"
5050 PRINT #2, INT(100*TIME(COUNTER))/100,
5060     FOR K=0 TO N-1
5070         PRINT #2, INT(1000000!*VOLTS(COUNTER,K))/1000000!,
5080     NEXT K
5090 PRINT #2, " "
5095 CLOSE #2
5100 RETURN
5110 REM
5120 REM CLOSE DATA ARRAY*****
5130 REM
5140 CLOSE #2
5150 RETURN
5160 REM
5170 REM INPUT DATA DIRECTLY FROM DISC*****
5180 REM
5190 INPUT "ENTER DATA FILE TO READ FROM: ",FILE3$
5200 PRINT "ENTER THE NUMBER OF DATA READINGS "
5210 INPUT " (must be at least as large as actual file)";J
5220 FILE3$=FILE3$+".DAT"
5230 OPEN "I", #3, FILE3$
5240 GOSUB 5570
5250 IF FLAG1=1 THEN ERASE VOLTS,TIME
5260 DIM VOLTS(J,N), TIME(J)
5270 COUNTER=0
5280 INPUT #3, TIME(COUNTER)
5290     FOR I=0 TO N-1
5300         INPUT #3, VOLTS(COUNTER,I)
5310     NEXT I
5320 IF EOF(3)=-1 THEN GOTO 5350
5330 COUNTER=COUNTER+1
5340 GOTO 5280
5350 FLAG1=0 : CLS
5360 GOSUB 4440
5370 FLAG=1 : FLAG1=1
5380 GOSUB 1110
5390 GOTO 3780
5400 REM END OF PROGRAM*****

```

```

5410 INPUT "ARE YOU FINISHED (Y/N)":ANS$
5420 IF ANS$="Y" THEN GOTO 5480
5430 GOSUB 5510
5440 SCREEN 0
5450 FLAG=0
5460 FLAG1=0
5470 GOTO 620
5480 SCREEN 0
5490 STOP
5500 END
5510 REM*****RESET FUNCTION KEYS*****
5520 FOR I=1 TO 10
5530 KEY I, " "
5540 NEXT I
5550 KEY OFF
5560 RETURN
5570 REM SETUP OUTPUT FILE (HEADINGS ETC.)*****
5580 REM
5590 INPUT #3, PROGRAM
5600 INPUT #3, FILE3$
5610 INPUT #3, N
5620 INPUT #3, TTIMES
5630 INPUT #3, DDATES
5640 INPUT #3, A
5650 INPUT #3, PROGRAM
5660 INPUT #3, XS
5670 INPUT #3, XS
5680 FOR I=0 TO N-1
5690 INPUT #3, TRS(I)
5700 NEXT I
5710 INPUT #3, XS
5720 FOR I=0 TO N-1
5730 INPUT #3, XS
5740 NEXT I
5750 FOR I=0 TO N
5760 INPUT #3, X
5770 NEXT I
5780 FOR I=0 TO N
5790 INPUT #3, X
5800 NEXT I
5810 FOR I=0 TO N
5820 INPUT #3, X
5830 NEXT I
5840 INPUT #3, XS
5850 INPUT #3, TTIMES
5860 FOR I=0 TO N-1
5870 INPUT #3, CH(I)
5880 NEXT I
5890 INPUT #3, XS
5900 FOR I=0 TO N-1
5910 INPUT #3, XS
5920 NEXT I
5930 RETURN

```

“DISS”

DISS.bas

```
10 REM DATA ACQUISITION PROGRAM 2/7/93*****
20 REM LAST REVISED 12/20/94 JTG
30 REM
40 SCREEN 0
50 CLS
60 GOSUB 5520
70 REM
80 PROGRAMS="DISSIPATION PROGRAM"
90 FLAG=0
100 FLAG1=0
110 FLAG2=0 'used for data storage
120 FLAG3=0 'used to control storage in array
130 FLAG4=0 'used to indicate data file specified
140 FLAGA=0 'change delt
150 FLAGB=0 'change frame
160 FLAGC=0 'change plot channels
170 FLAGE=0
180 FLAGF=0
190 REM
200 PRINT TAB(26) " THIS PROGRAM IS":PRINT
210 PRINT TAB(26) " PART":PRINT
220 PRINT TAB(26) " OF THE":PRINT:PRINT
230 PRINT TAB(26) " DATA ACQUISITION SYSTEM":PRINT
240 PRINT TAB(26) " FOR THE":PRINT
250 PRINT TAB(26) " GEOTECHNICAL LABORATORY":PRINT:PRINT
260 PRINT TAB(26) " DEPARTMENT OF":PRINT:PRINT
270 PRINT TAB(26) " CIVIL AND ENVIRONMENTAL ENGINEERING":PRINT
280 PRINT TAB(26) "MASSACHUSETTS INSTITUTE OF TECHNOLOGY":PRINT
290 PRINT:PRINT
300 INPUT "PRESS 'return' TO CONTINUE".ZS
310 CLS
320 PRINT TAB(1) "THIS PROGRAM COLLECTS DATA AT A RELATIVELY SLOW RATE"
330 PRINT TAB(1) "THE PROGRAM REQUIRES AN AD1170 DATA ACQUISITION CARD"
340 PRINT TAB(1) "THE USER CAN INTERACTIVELY CHANGE THE READING RATE"
350 PRINT TAB(1) " AND CHOOSE TO SAVE OR IGNORE THE DATA AS IT IS RECORDED":PRINT
360 PRINT TAB(1) "THIS IS PROGRAM REVISION 1.1 PROGRAMED 12/20/94":PRINT:PRINT
370 REM
380 INPUT "PRESS 'return' TO CONTINUE".ZS
390 REM
400 REM INPUT INTTIME AND INTBIT*****
410 CLS
420 PRINT TAB(1) "THE DATA ACQUISITION CARD HAS SOFTWARE SELECTABLE
PARAMETERS WHICH YOU MUST NOW SELECT FROM THE FOLLOWING LIST": PRINT:PRINT
430 PRINT TAB(1) "THE INTEGRATION TIME (N): "
440 PRINT TAB(1) " where N=0 1 msec N=4 100 msec"
450 PRINT TAB(1) " N=1 10 msec N=5 166.7 msec"
460 PRINT TAB(1) " N=2 16.7 msec N=6 300 msec"
470 PRINT TAB(1) " N=3 20 msec"
480 INPUT INTTIME
490 INTTIME=5
500 INTTIME=INTTIME+16
510 PRINT:PRINT:PRINT "THE BIT PRECISION: "
520 PRINT TAB(1) " options 8,10,12,14,16,18,20,22"
530 INPUT INTBIT
```

```

540     INTBIT=22
550     INTBIT=INTBIT-7
560 REM
570 REM
580 REM
590 REM SET PARAMETERS FOR SLOW READINGS*****
600 REM
610 `   INPUT "PRESS 'return' TO CONTINUE",Z$
620     CLS
630     PRINT TAB(1) "PROVIDE THE FOLLOWING INFORMATION FOR THE
READINGS":PRINT:PRINT
640 `   INPUT "ENTER THE NUMBER OF CHANNELS TO BE RECORDED OR INPUT FROM DISC:
",N:PRINT:PRINT
650 N=13
660 GOTO 790
670     FOR I=0 TO (N-1)
680         CLS
690         PRINT "ENTER CARD ADDRESS"
700         INPUT AD1170(I)
710         PRINT "ENTER THE CHANNEL NUMBER FOR CHANNEL position NO. ";(I+1);": "
720         PRINT "   for the AD1170 card the first channel is 0"
730         INPUT CH(I)
740         PRINT "ENTER THE TRANSDUCER NO. FOR CHANNEL NO. ";CH(I);": "
750         INPUT TR(I)
760         PRINT:PRINT
770     NEXT I
780 DIM AD1170(13),CH(13),TR(13)
790 DIM AD1170(12),CH(12),TR(12),MUX!(12)
800 AD1170(0)=768: AD1170(1)=896 :AD1170(2)=992 :AD1170(3)=896
810 AD1170(4)=768: AD1170(5)=896 :AD1170(6)=992 :AD1170(7)=896
820 AD1170(8)=768: AD1170(9)=896 :AD1170(10)=992 :AD1170(11)=768
830 AD1170(12)=992
840 CH(0)=0:CH(1)=0:CH(2)=0:CH(3)=1
850 CH(4)=2:CH(5)=2:CH(6)=2:CH(7)=3
860 CH(8)=4:CH(9)=4:CH(10)=4:CH(11)=6:CH(12)=6
870 REM SET UP AD-1170*****
880 REM
890     CLS
900     PRINT : PRINT " DISSIPATION PROGRAM"
910     PRINT:PRINT "       THE A/D CONVERTER IS BEING INITIALIZED"
920     FOR I=0 TO N-1
930         OUT AD1170(I),60 :WAIT AD1170(I),1,1
940         OUT AD1170(I)+1,INTBIT:WAIT AD1170(I),1,1
950         OUT AD1170(I),48:WAIT AD1170(I),1,1
960         OUT AD1170(I),176:WAIT AD1170(I),1,1
970         OUT AD1170(I),184:WAIT AD1170(I),1,1
980         MUX!(I)=AD1170(I)+8
990     NEXT I
1000     GNDCHANNEL=15
1010     REFCHANNEL=14
1020     CHANNEL=0
1030 REM
1040 REM
1050 REM MAIN PROGRAM*****
1060 REM
1070     GOSUB 4440

```

```

1080     GOTO 1270
1090  REM
1100  REM
1110  REM DRAW FRAME AND SET SCALES*****
1120  REM
1130     SCREEN 0
1140     KEY OFF
1150     CLS
1160     INPUT "ENTER MIN X VALUE (sec): ",MINX
1170     INPUT "ENTER MAX X VALUE (sec): ",MAXX
1180     INPUT "ENTER MIN Y VALUE (volts): ",MINY
1190     INPUT "ENTER MAX Y VALUE (volts): ",MAXY
1200  REM
1210     CLS
1220     IF FLAG=1 THEN GOSUB 2020
1230     IF FLAG=1 THEN GOSUB 4060
1240     RETURN
1250  REM
1260  REM SET FUNCTION KEYS*****
1270  REM
1280     IF FLAG=1 THEN SCREEN 0
1290     CLS
1300     PRINT "PRESS F1` TO START OR F6` TO READ FROM DISC."
1310     KEY 1,"START"
1320     KEY 6,"DISC"
1330     ON KEY (1) GOSUB 1410
1340     ON KEY (6) GOSUB 5190
1350     KEY (1) ON
1360     KEY (6) ON
1370     KEY ON
1380  REM   FLAG=1
1390     GOTO 1390
1400  REM
1410  REM SLOW READING ROUTINE ACTIVATED WITH START KEY*****
1420  REM
1430     FLAG5=0
1440     FLAGF=0
1450     FLAG6=0
1460     GOSUB 5520
1470     KEY 1,"BYPASS"
1480     KEY 2,"  "
1490     KEY 3,"  "
1500     KEY 4,"DELT"
1510     KEY 5,"SCALE"
1520     KEY 6,"CHANEL"
1530     KEY 7,"END"
1540     KEY 8,"  "
1550     KEY 9,"  "
1560     KEY 10,"  "
1570     KEY (1) ON
1580     KEY (2) OFF
1590     KEY (3) OFF
1600     KEY (4) ON
1610     KEY (5) ON
1620     KEY (6) ON
1630     KEY (7) ON

```

```

1640     KEY (8) OFF
1650     KEY (9) OFF
1660     KEY (10) OFF
1670     ON KEY (1) GOSUB 4130
1680     ON KEY (4) GOSUB 4610
1690     ON KEY (5) GOSUB 4640
1700     ON KEY (6) GOSUB 4670
1710     ON KEY (7) GOSUB 3580
1720 REM
1730 REM
1740 REM TAKE SET OF READINGS ON KEYBOARDS CUE*****
1750 REM
1760     CLS
1770     SCREEN 0
1780     IF FLAG2=1 THEN ERASE VOLTS,TIME
1790     INPUT "ENTER NUMBER OF READINGS: ",J
1800     DIM VOLTS(J,N), TIME(J)
1810     FLAG2=1
1820     PRINT
1830     TM = TIMER
1840     STIMES=TIMES
1850     SDATES=DATES
1860     T0=TM
1870     DIAZ=0
1880     INPUT "ENTER THE TIME INTERVAL (sec): ",DELT:PRINT:PRINT
1890     INPUT "DO YOU WANT TO STORE THE DATA (Y/N)? ",AS
1900     IF AS="Y" THEN GOTO 1930
1910     GOTO 1970
1920     PRINT
1930     PRINT "ENTER DATA FILE NAME: "
1940     INPUT " eight characters and no extension: ",FILE1$
1950     FLAG4=1
1960     GOSUB 4710 ' SAVE HEADER AND OPEN FILE
1970     GOSUB 1110
1980     PRINT "PRESS 'return' WHEN READY, START TEST AT BEEP"
1990     AS=INKEY$
2000     IF AS<>CHR$(13) THEN GOTO 1990
2010 REM
2020 REM SETUP WINDOW*****
2030 REM
2040     SCREEN 9
2050     KEY ON
2060 REM
2070     LOCATE 21,30
2080     PRINT "TIME (SEC)"
2090 REM
2100     LOCATE 7,1
2110     PRINT "V"
2120     LOCATE 8,1
2130     PRINT "O"
2140     LOCATE 9,1
2150     PRINT "L"
2160     LOCATE 10,1
2170     PRINT "T"
2180     LOCATE 11,1
2190     PRINT "A"

```

```

2200     LOCATE 12.1
2210     PRINT "G"
2220     LOCATE 13.1
2230     PRINT "E"
2240     REM
2250     LOCATE 1,2
2260     PRINT MAXY
2270     LOCATE 19,2
2280     PRINT MINY
2290     REM
2300     LOCATE 20,5
2310     PRINT MINX
2320     LOCATE 20,74
2330     PRINT MAXX
2340     REM
2350     LOCATE 23,1
2360     VIEW (50,3)-(600,260),,1
2370     REM
2380     WINDOW (MINX,MINY)-(MAXX,MAXY)
2390     REM
2400     CLS
2410     DX=MAXX-MINX
2420     DY=MAXY-MINY
2430     REM
2440     FOR I=MINX+(DX/10) TO MAXX-(DX/10) STEP DX/10
2450         LINE (I,MINY)-(I,MAXY)...&H1F11
2460     NEXT I
2470     REM
2480     FOR I=MINY+(DY/5) TO MAXY-(DY/5) STEP DY/5
2490         LINE (MINX,I)-(MAXX,I)...&H1F11
2500     NEXT I
2510     IF FLAG5=1 THEN GOTO 4070 ELSE IF FLAGF=1 THEN GOTO 4040
2520     IF FLAG1=1 THEN RETURN
2530     REM
2540     REM MAIN DATA READING LOOP*****
2550     REM
2560     FLAG1=1
2570     COUNTER = 0
2580     BEEP
2590     FLAG=1
2600     REM
2610     FOR K=0 TO 2
2620         OUT MUX!(K),CH(K)
2630         OUT AD1170(K),INTTIME
2640     NEXT K
2650     FOR K=0 TO 2
2660         WAIT AD1170(K),1,1
2670         OUT MUX!(K), GNDCHANNEL
2680         LBYTE = INP(AD1170(K)+1)
2690         MBYTE = INP(AD1170(K)+2)
2700         HBYTE = INP(AD1170(K)+3)
2710         VOLTS(COUNTER,K) = (LBYTE+256*MBYTE+65536!*HBYTE)*10/2^(INTBIT+7)-5
2720     NEXT K
2730     FOR K=4 TO 6
2740         OUT MUX!(K),CH(K)
2750         OUT AD1170(K),INTTIME

```

```

2760     NEXT K
2770     FOR K=4 TO 6
2780         WAIT AD1170(K),1,1
2790         OUT MUX!(K), GNDCHANNEL
2800         LBYTE = INP(AD1170(K)+1)
2810         MBYTE = INP(AD1170(K)+2)
2820         HBYTE = INP(AD1170(K)+3)
2830         VOLTS(COUNTER,K) = (LBYTE+256*MBYTE+65536!*HBYTE)*10/2^(INTBIT+7)-5
2840     NEXT K
2850     FOR K=8 TO 10
2860         OUT MUX!(K),CH(K)
2870         OUT AD1170(K),INTTIME
2880     NEXT K
2890     FOR K=8 TO 10
2900         WAIT AD1170(K),1,1
2910         OUT MUX!(K), GNDCHANNEL
2920         LBYTE = INP(AD1170(K)+1)
2930         MBYTE = INP(AD1170(K)+2)
2940         HBYTE = INP(AD1170(K)+3)
2950         VOLTS(COUNTER,K) = (LBYTE+256*MBYTE+65536!*HBYTE)*10/2^(INTBIT+7)-5
2960     NEXT K
2970     K=3
2980         OUT MUX!(K),CH(K)
2990         OUT AD1170(K),INTTIME
3000         WAIT AD1170(K),1,1
3010         OUT MUX!(K), GNDCHANNEL
3020         LBYTE = INP(AD1170(K)+1)
3030         MBYTE = INP(AD1170(K)+2)
3040         HBYTE = INP(AD1170(K)+3)
3050         VOLTS(COUNTER,K) = (LBYTE+256*MBYTE+65536!*HBYTE)*10/2^(INTBIT+7)-5
3055     D(0)=7 : D(1)=11 : D(2)=12
3060     FOR K=0 TO 2
3061         OUT MUX!(D(K)),CH(D(K))
3062         OUT AD1170(D(K)),INTTIME
3063     NEXT K
3064     FOR K=0 TO 2
3065         WAIT AD1170(D(K)),1,1
3066         OUT MUX!(D(K)), GNDCHANNEL
3067         LBYTE = INP(AD1170(D(K))+1)
3068         MBYTE = INP(AD1170(D(K))+2)
3069         HBYTE = INP(AD1170(D(K))+3)
3070         VOLTS(COUNTER,D(K)) = (LBYTE+256*MBYTE+65536!*HBYTE)*10/2^(INTBIT+7)-5
3071     NEXT K
3150     T=TIMER
3160     IF T<TM THEN DIAZ=DIAZ+86400!
3170     TM=T : DS=DATES
3180     TIME(COUNTER)=T-T0+DIAZ
3190     IF FLAG4=1 THEN GOSUB 5030         'SAVE DATA
3200     FOR K=1 TO IC
3210         IF COUNTER<>0 THEN LINE (TIME(COUNTER-1),VOLTS(COUNTER-1,K-1))-
(TIME(COUNTER),VOLTS(COUNTER,K-1))
3220     NEXT K
3230         LOCATE 22,1
3240         PRINT "
3250         LOCATE 23,1
3260         PRINT "

```

```

3270     LOCATE 22,1
3280     PRINT INT(TIME(COUNTER)), COUNTER;"/";J
3290     FOR K=1 TO 6
3300         LOCATE 22,20+K*9
3310         PRINT USING "#.####";VOLTS(COUNTER,K-1)
3320     NEXT K
3330     FOR K=7 TO 13
3340         LOCATE 23,11+(K-6)*9
3350         PRINT USING "#.####";VOLTS(COUNTER,K-1)
3360     NEXT K
3370     IF COUNTER=J THEN GOTO 3540
3380     TD=0
3390     IF TM+DELT<86400! THEN GOTO 3460
3400     TD=86400!
3410     WHILE DATES=D$
3420         IF FLAGA=1 THEN FLAGA=0 : GOSUB 4290
3430         IF FLAGB=1 THEN FLAGB=0 : GOSUB 1130
3440         IF FLAGC=1 THEN FLAGC=0 : GOSUB 4410
3450     WEND
3460     IF FLAGA=1 THEN FLAGA=0 : GOSUB 4290
3470     WHILE TIMER < TM + DELT - TD
3480         IF FLAGA=1 THEN FLAGA=0 : GOSUB 4290
3490         IF FLAGB=1 THEN FLAGB=0 : GOSUB 1130
3500         IF FLAGC=1 THEN FLAGC=0 : GOSUB 4410
3510     WEND
3520     IF FLAG3=0 THEN COUNTER=COUNTER+1
3530     GOTO 2600
3540     REM DATA ARRAY FULL
3550     IF FLAG4=1 THEN GOSUB 5120 'CLOSE ARRAY
3560     GOTO 3780
3570     REM
3580     REM DATA PROCESSING ROUTINES AFTER READINGS COMPLETE*****
3590     REM
3600     REM
3610     LOCATE 23,1
3620     PRINT "
3630     LOCATE 23,1
3640     INPUT "DO YOU WANT TO CONTINUE COLLECTION MODE (Y/N)";ANSS
3650     LOCATE 23,1
3660     PRINT "
3670     IF ANSS="N" THEN :GOSUB 5120 : RETURN 3780
3680     LOCATE 23,1
3690     INPUT "DO YOU WANT TO START A NEW DATA FILE (Y/N)";ANSS
3700     IF ANSS="Y" THEN GOTO 3740
3710     LOCATE 23,1
3720     PRINT "
3730     RETURN
3740     GOSUB 4710
3750     FLAG=0 :FLAG1=0
3760     SCREEN 0 : CLS
3770     RETURN 1740
3780     REM
3790     KEY 1,"
3800     KEY 2,"SCALE"
3810     KEY 3,"CHANEL"
3820     KEY 4,"

```

```

3830     KEY 5."END"
3840     KEY 6."  "
3850     KEY 7."  "
3860     KEY 8."  "
3870     KEY 9."  "
3880     KEY 10." "
3890     KEY (1) OFF
3900     KEY (2) ON
3910     KEY (3) ON
3920     KEY (4) OFF
3930     KEY (5) ON
3940     KEY (6) OFF
3950     KEY (7) OFF
3960     KEY (8) OFF
3970     KEY (9) OFF
3980     KEY (10) OFF
3990     ON KEY (2) GOSUB 1130
4000     ON KEY (3) GOSUB 4410
4010     ON KEY (5) GOSUB 5410
4020     FLAGF=1
4030     GOTO 4030
4040     GOSUB 4050
4050     REM PLOT DATA IN MEMORY*****
4060     IF FLAG1=0 THEN RETURN
4070     FOR I=1 TO COUNTER
4080         FOR K=1 TO IC
4090             LINE(TIME(I-1),VOLTS(I-1,NCP(K-1)))-(TIME(I),VOLTS(I,NCP(K-1)))
4100         NEXT K
4110     NEXT I
4120     RETURN
4130     REM BYPASS READINGS*****
4140     REM
4150     KEY 1. "SAVE"
4160     KEY (1) ON
4170     ON KEY (1) GOSUB 4210
4180     FLAG3=1
4190     RETURN
4200     REM
4210     REM KEEP DATA *****
4220     REM
4230     KEY 1. "BYPASS"
4240     KEY (1) ON
4250     ON KEY (1) GOSUB 4130
4260     FLAG3=0
4270     RETURN
4280     REM
4290     REM CHANGE TIME INTERVAL FOR SLOW READINGS*****
4300     REM
4310     LOCATE 23,1
4320     PRINT "                "
4330     LOCATE 23,1
4340     INPUT "ENTER NEW TIME INTERVAL (sec): ",DELT
4350     LOCATE 23,1
4360     PRINT "                "
4370     RETURN 3380
4380     REM

```



```

4390 REM REDEFINE CHANNEL POSITIONS TO BE PLOTTED*****
4400 REM
4410 LOCATE 23,1
4420 PRINT " "
4430 LOCATE 23,1
4440 INPUT "ENTER NUMBER OF CHANNELS TO BE PLOTTED: ",IC
4450 FOR I=0 TO (IC-1)
4460 LOCATE 23,1
4470 PRINT " "
4480 LOCATE 22,1
4490 PRINT " "
4500 LOCATE 22,1
4510 PRINT "ENTER";(I+1);"TH CHANNEL TO BE PLOTTED:"
4520 INPUT NCP(I)
4530 NCP(I)=NCP(I)-1
4540 NEXT I
4550 LOCATE 22,1
4560 PRINT " "
4570 LOCATE 23,1
4580 PRINT " "
4590 GOSUB 4050
4600 RETURN
4610 REM CHANGE DELT FLAG*****
4620 FLAGA=1
4630 RETURN
4640 REM CHANGE FRAME FLAG*****
4650 FLAGB=1
4660 RETURN
4670 REM CHANGE PLOT CHANNELS FLAG*****
4680 FLAGC=1
4690 RETURN
4700 REM
4710 REM DATA STORAGE SECTION*****
4720 REM
4730 REM set up header and open file
4740 IF FLAG4=0 THEN RETURN
4750 FILE2$=FILE1$+".DAT"
4760 OPEN "O", #2, FILE2$
4770 WRITE #2, PROGRAMS
4780 CS=CHR$(34)
4790 WRITE #2, FILE2$,N,STIMES:WRITE #2, SDATES
4800 PRINT #2, CS;"CRD NBR";CS;
4810 FOR I=0 TO N-1
4820 PRINT #2, CS;AD1170(I);CS;
4830 NEXT I
4840 PRINT #2, ""
4850 PRINT #2, CS;"CH NBR";CS;
4860 FOR I=0 TO N-1
4870 PRINT #2, CS;CH(I);CS;
4880 NEXT I
4890 PRINT #2, ""
4900 PRINT #2, CS;"SECONDS";CS;
4910 FOR I=0 TO N-1
4920 PRINT #2, CS;"VOLTS";CS;
4930 NEXT I
4940 PRINT #2, ""

```

```

4950     WRITE #2, "****"
4960     PRINT #2, CS;"CLOCK";CS;
4970     FOR I=0 TO N-1
4980         PRINT #2, CS:I:CS;
4990     NEXT I
5000     PRINT #2, " "
5005     CLOSE #2
5010     RETURN
5020 REM
5030 REM STORE EACH DATA POINT
5040 REM
5045     OPEN "A", #2, FILE2$
5050         PRINT #2, INT(100*TIME(COUNTER))/100,
5060         FOR K=0 TO N-1
5070             PRINT #2, INT(1000000!*VOLTS(COUNTER,K))/1000000!,
5080             NEXT K
5090             PRINT #2, " "
5095     CLOSE #2
5100     RETURN
5110 REM
5120 REM CLOSE DATA ARRAY*****
5130 REM
5140     CLOSE #2
5150     RETURN
5160 REM
5170 REM INPUT DATA DIRECTLY FROM DISC*****
5180 REM
5190     INPUT "ENTER DATA FILE TO READ FROM: ".FILE3$
5200     PRINT "ENTER THE NUMBER OF DATA READINGS "
5210     INPUT " (must be at least as large as actual file)";J
5220     FILE3$=FILE3$+".DAT"
5230     OPEN "I", #3, FILE3$
5240     GOSUB 5570
5250     IF FLAG1=1 THEN ERASE VOLTS,TIME
5260     DIM VOLTS(J,N), TIME(J)
5270     COUNTER=0
5280     INPUT #3, TIME(COUNTER)
5290         FOR I=0 TO N-1
5300             INPUT #3, VOLTS(COUNTER,I)
5310         NEXT I
5320     IF EOF(3)=-1 THEN GOTO 5350
5330     COUNTER=COUNTER+1
5340     GOTO 5280
5350     FLAG1=0 : CLS
5360     GOSUB 4440
5370     FLAG=1 : FLAG1=1
5380     GOSUB 1110
5390     GOTO 3780
5400 REM END OF PROGRAM*****
5410     INPUT "ARE YOU FINISHED (Y/N)";ANSS
5420     IF ANSS="Y" THEN GOTO 5480
5430     GOSUB 5510
5440     SCREEN 0
5450     FLAG=0
5460     FLAG1=0
5470     GOTO 620

```

```

5480     SCREEN 0
5490     STOP
5500     END
5510     REM*****RESET FUNCTION KEYS*****
5520     FOR I=1 TO 10
5530     KEY I. "      "
5540     NEXT I
5550     KEY OFF
5560     RETURN
5570     REM SETUP OUTPUT FILE (HEADINGS ETC.)*****
5580     REM
5590     INPUT #3, PROGRAM
5600     INPUT #3, FILE3$
5610     INPUT #3, N
5620     INPUT #3, TTIMES
5630     INPUT #3, DDATE$
5640     INPUT #3, A
5650     INPUT #3, PROGRAM
5660     INPUT #3, XS
5670     INPUT #3, XS
5680     FOR I=0 TO N-1
5690     INPUT #3, TR$(I)
5700     NEXT I
5710     INPUT #3, XS
5720     FOR I=0 TO N-1
5730     INPUT #3, XS
5740     NEXT I
5750     FOR I=0 TO N
5760     INPUT #3, X
5770     NEXT I
5780     FOR I=0 TO N
5790     INPUT #3, X
5800     NEXT I
5810     FOR I=0 TO N
5820     INPUT #3, X
5830     NEXT I
5840     INPUT #3, XS
5850     INPUT #3, TTIMES
5860     FOR I=0 TO N-1
5870     INPUT #3, CH(I)
5880     NEXT I
5890     INPUT #3, XS
5900     FOR I=0 TO N-1
5910     INPUT #3, XS
5920     NEXT I
5930     RETURN

```

Appendix B

Appendix B consists of a table of “Shunt” values obtained to evaluate the effects of voltage reference shifts. A “shunt” value is obtained by reading the voltage value of a circuit that has been shorted out by connecting the high side of the output directly to the low side. The recorded value is the reference value for ground. Changes in the ground value of the voltage with result in an equivalent shift in the voltage output reading for the transducers.

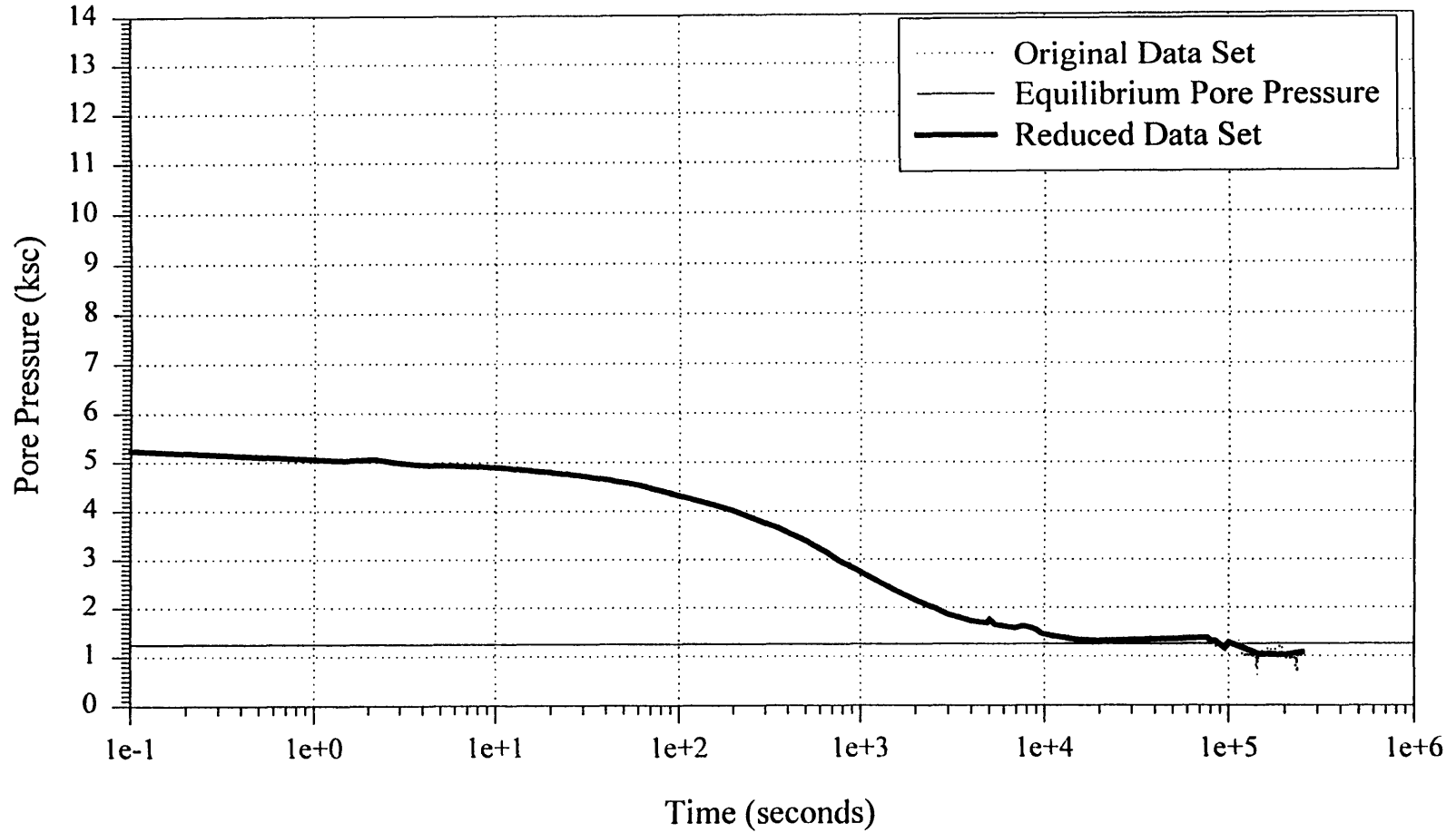
Date	Time	ch1	ch2	ch3	ch5	ch7	ch8	ch9	ch11	ch13	ch14	ch15	ch19	ch21
15-Aug	10:55	-0.1970	-0.3460	-0.1500	-0.0372	-0.2400	-0.3270	-0.3140	-0.0550	-0.0037	-0.2700	-0.1470	-0.0060	-0.0150
	13:10	-0.2170	-0.3470	-0.1630	-0.0335	-0.2650	-0.3320	-0.3310	-0.0570	-0.0035	-0.2425	-0.1380	-0.0060	-0.0150
	18:45	-0.1920	-0.3310	-0.1770	-0.0337	-0.2540	-0.3460	-0.3350	-0.0580	-0.0035	-0.2240	-0.1450	-0.0060	-0.0147
16-Aug	15:15	-0.1980	-0.2965	-0.1730	-0.0276	-0.2420	-0.3320	-0.3277	-0.0551	-0.0041	-0.2594	-0.1679	-0.0065	-0.0255
17-Aug	17:15	-0.1734	-0.3184	-0.1802	-0.0338	-0.2352	-0.3520	-0.3083	-0.0560	-0.0036	-0.2550	-0.1573	-0.0061	-0.0153
18-Aug	14:03	-0.1767	-0.3464	-0.1738	-0.0343	-0.2420	-0.3520	-0.3260	-0.0575	-0.0040	-0.2450	-0.1480	-0.0066	-0.0156
20-Aug	12:20	-0.1989	-0.3505	-0.1707	-0.0324	-0.2460	-0.3512	-0.3375	-0.0560	-0.0042	-0.2275	0.1395	-0.0067	-0.0161
21-Aug	15:50	-0.1830	-0.3245	-0.1642	-0.0276	-0.2478	-0.3045	-0.3215	-0.0530	-0.0046	-0.2345	-0.1343	-0.0072	-0.0170
22-Aug	10:30	-0.1100	-0.3390	-0.1780	-0.0282	-0.1604	-0.3268	-0.3188	-0.0526	0.0755	-0.2471	-0.1531	0.0729	-0.0163
22-Aug	6:20	-0.1200	-0.3470	-0.1731	-0.0333	-0.1663	-0.3296	-0.3381	-0.0544	0.0757	-0.4520	-0.1509	0.0731	-0.0156
22-Aug	*6:20	-0.1161	-0.3508	-0.1752	-0.0323	-0.1637	-0.3260	-0.3331	-0.0535	0.0756	-0.2540	-0.1520	0.0731	-0.0156
23-Aug	10:00	-0.2167	-0.3255	-0.1655	-0.0259	-0.2724	-0.3138	-0.3311	-0.0517	-0.0045	-0.2345	-0.1545	-0.0071	-0.0168
24-Aug	14:50	-0.1763	-0.3474	-0.1549	-0.0300	-0.2456	-0.3451	-0.3180	-0.0572	-0.0047	-0.2534	-0.1513	-0.0069	-0.0161
25-Aug	8:40	-0.1766	-0.3682	-0.1743	-0.0328	-0.2437	-0.3478	-0.3234	-0.0573	-0.0033	-0.2381	-0.1264	-0.0058	-0.0148
25-Aug	19:00	-0.2079	-0.3389	-0.1715	-0.0214	-0.2555	-0.3344	-0.3125	-0.0564	-0.0040	-0.2339	-0.1465	-0.0061	-0.0151
29-Aug	14:40	-0.1774	-0.3124	-0.1684	-0.0322	-0.2467	-0.3265	-0.3430	-0.0549	-0.0045	-0.2245	-0.1277	-0.0069	-0.0167
29-Aug	18:45	-0.1844	-0.3140	-0.1720	-0.0272	-0.2538	-0.2970	-0.3460	-0.0519	-0.0048	-0.2380	-0.2070	-0.0072	-0.0172
31-Aug	12:30	-0.1909	-0.3187	-0.1705	-0.0271	-0.2412	-0.3415	-0.3121	-0.0538	-0.0046	-0.2268	-0.1298	-0.0071	-0.0167
Card Number		1	2	3	2	1	2	3	2	1	2	3	1	3
Average (V)		-0.1785	-0.3346	-0.1697	-0.0306	-0.2345	-0.3325	-0.3265	-0.0551	0.0092	-0.2533	-0.1332	0.0067	-0.0164
Std Dev (V)		0.0146	0.0189	0.0080	0.0042	0.0099	0.0174	0.0116	0.0020	0.0005	0.0137	0.0770	0.0005	0.0026
Max (V)		-0.1100	-0.2965	-0.1500	-0.0214	-0.1604	-0.2970	-0.3083	-0.0517	0.0757	-0.2240	0.1395	0.0731	-0.0147
Min (V)		-0.2170	-0.3682	-0.1802	-0.0372	-0.2724	-0.3520	-0.3460	-0.0580	-0.0048	-0.4520	-0.2070	-0.0072	-0.0255
Max - Min (V)		-0.1070	-0.0717	-0.0302	-0.0158	-0.1120	-0.0550	-0.0377	-0.0063	-0.0805	-0.2280	-0.3465	-0.0803	-0.0108
Std Dev (ksc)		0.1241	0.8363	0.0236	0.0199	0.0795	0.7419	0.0329	0.0094	0.0064	0.2964	0.0777		0.0337
Max-Min (ksc)		-0.9071	-3.1748	-0.0886	-0.0751	-0.8969	-2.3518	-0.1070	-0.0293	-1.0275	-4.9207	-0.3499		-0.1383

*Asterisk indicates values are taken while system on batteries. Others taken while system on Generator
Standard Deviations do not include values in boldface

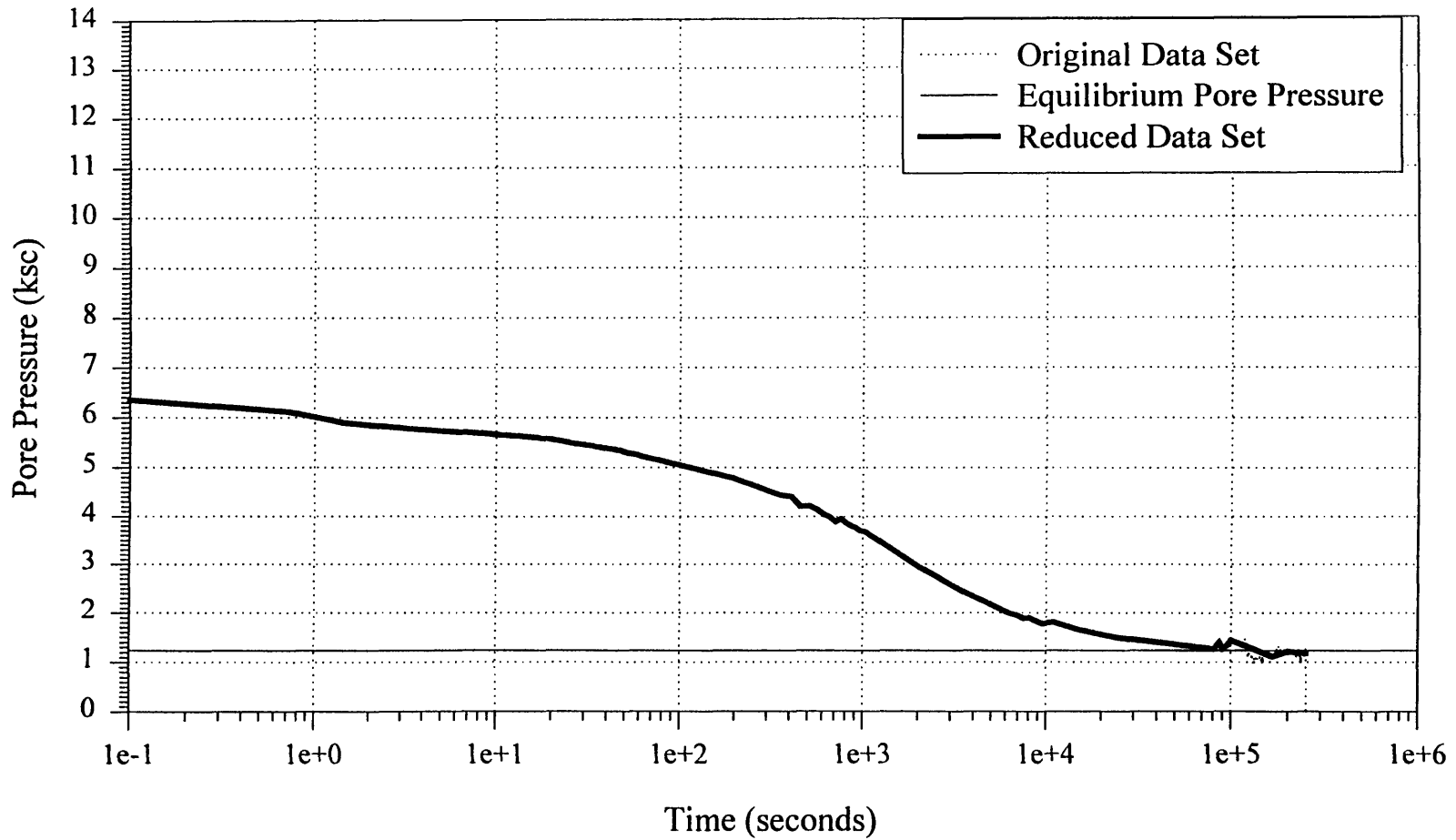
Appendix C

Appendix C consists of the individual dissipation plots for each of the satisfactory tests performed. They are plotted on an absolute pressure versus time on a logarithmic scale. The data has been reduced by taking 20 points per log cycle for elapsed dissipation times in excess of 1000 seconds. A minor amount of filtering has been performed to remove spikes in the data that are a result of electrical shorts while connecting and disconnecting instruments from the junction box, and from single point electrical influence anomalies. No other filtering has been performed.

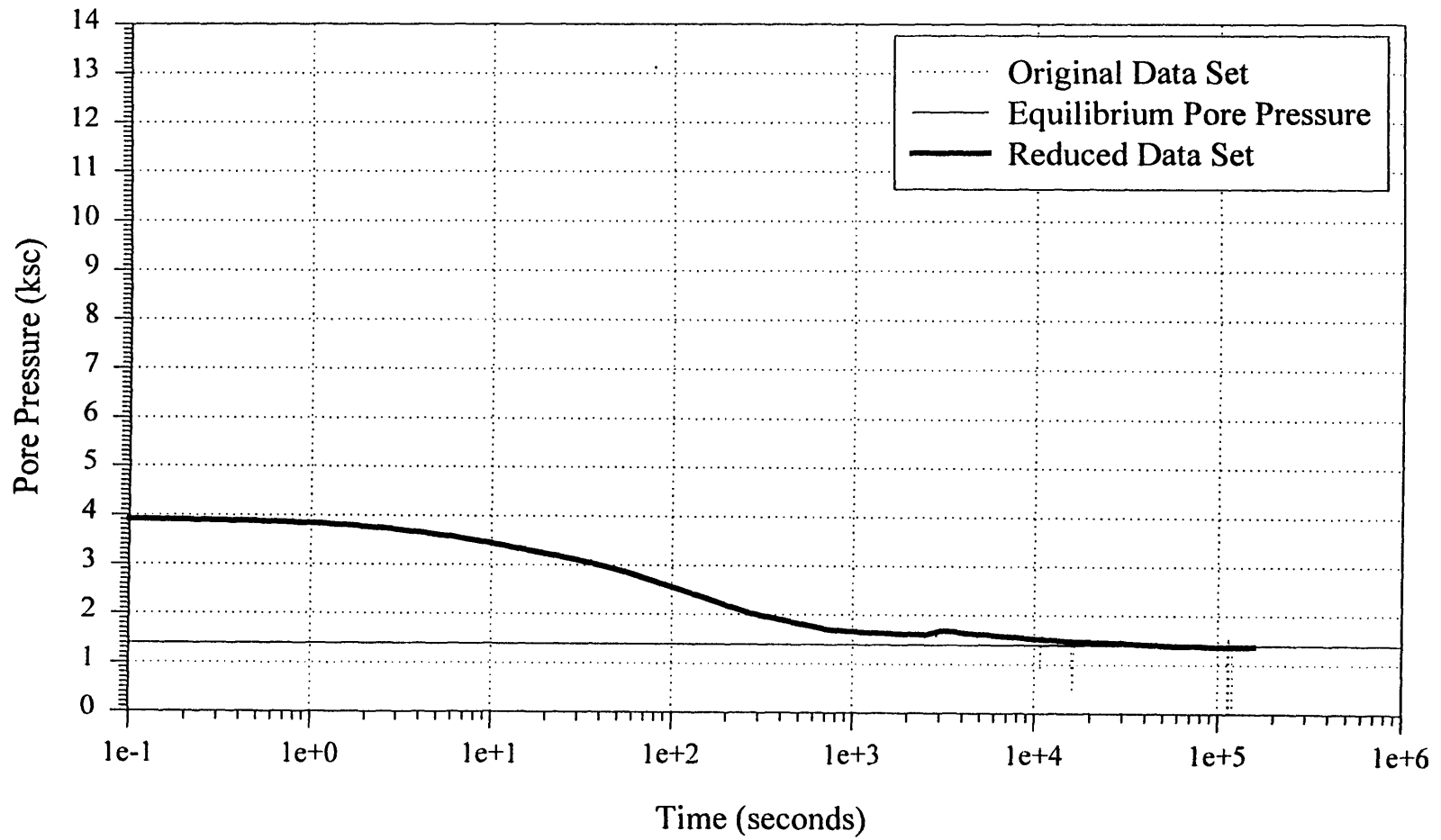
Piezocone 790 Dissipation at 45'
Elevation -11.62 m



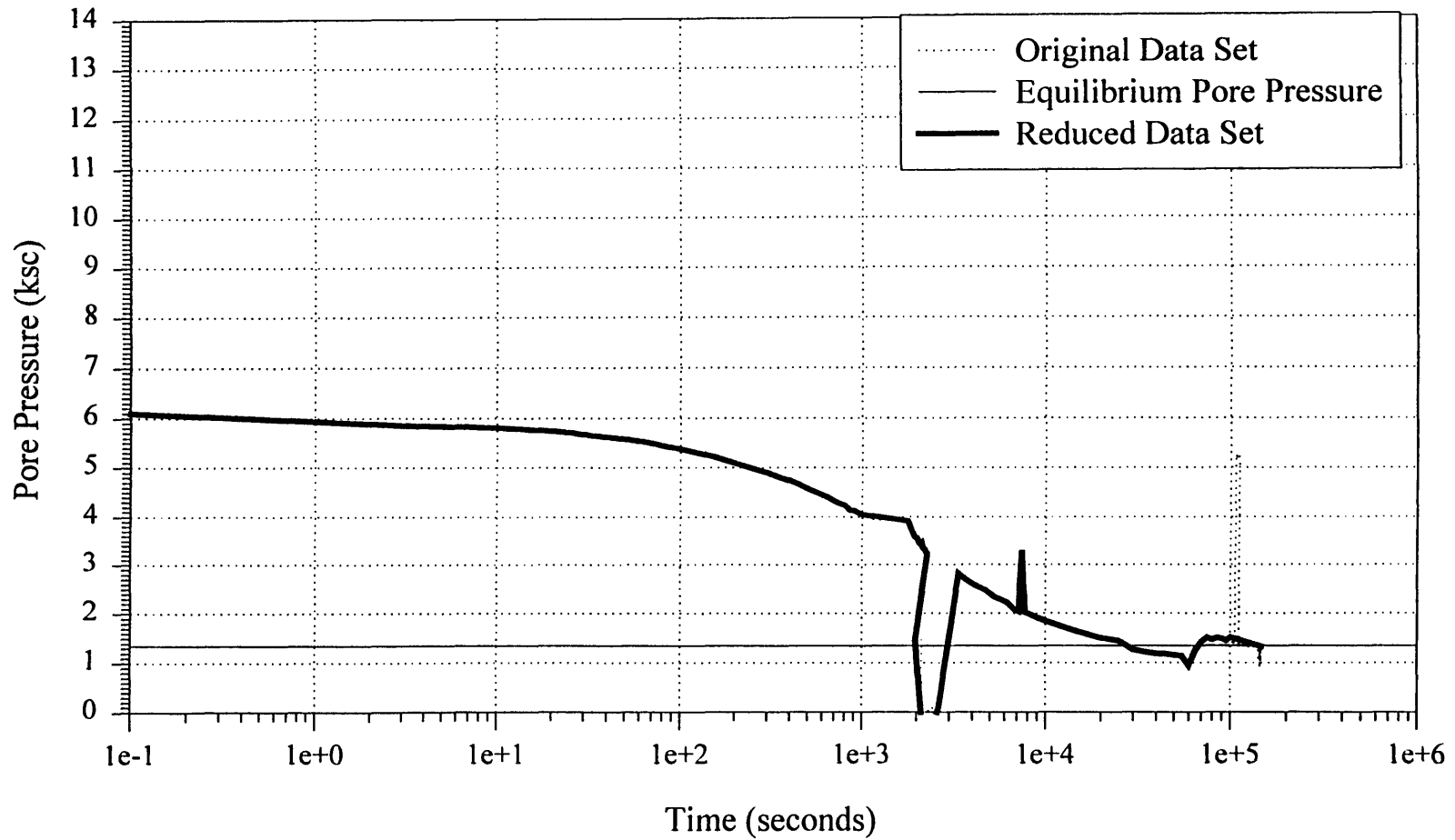
Piezocone 881 Dissipation at 45'
Elevation -11.83 m



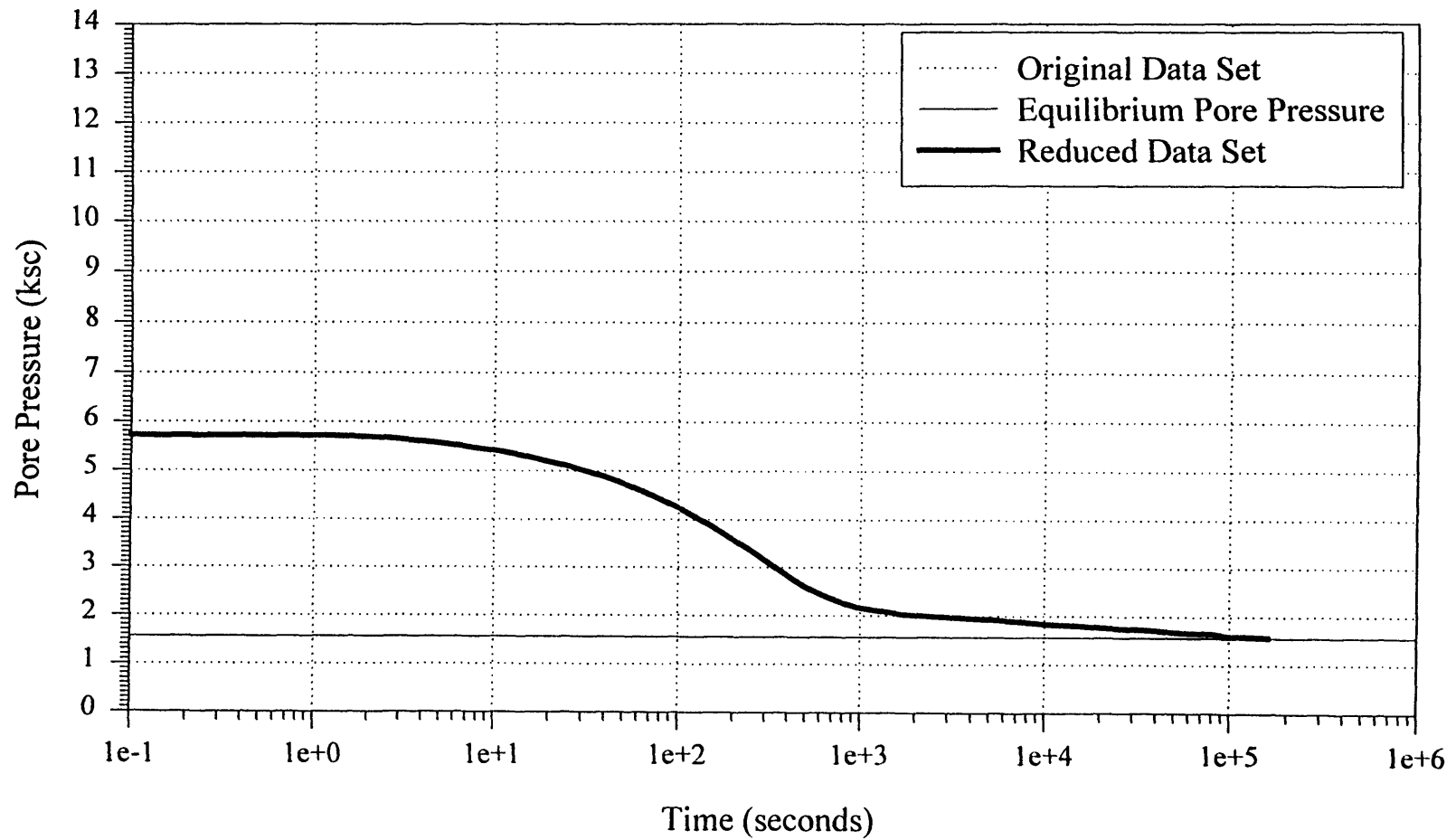
Piezoprobe 63 Dissipation at 50'
Elevation -13.30 m



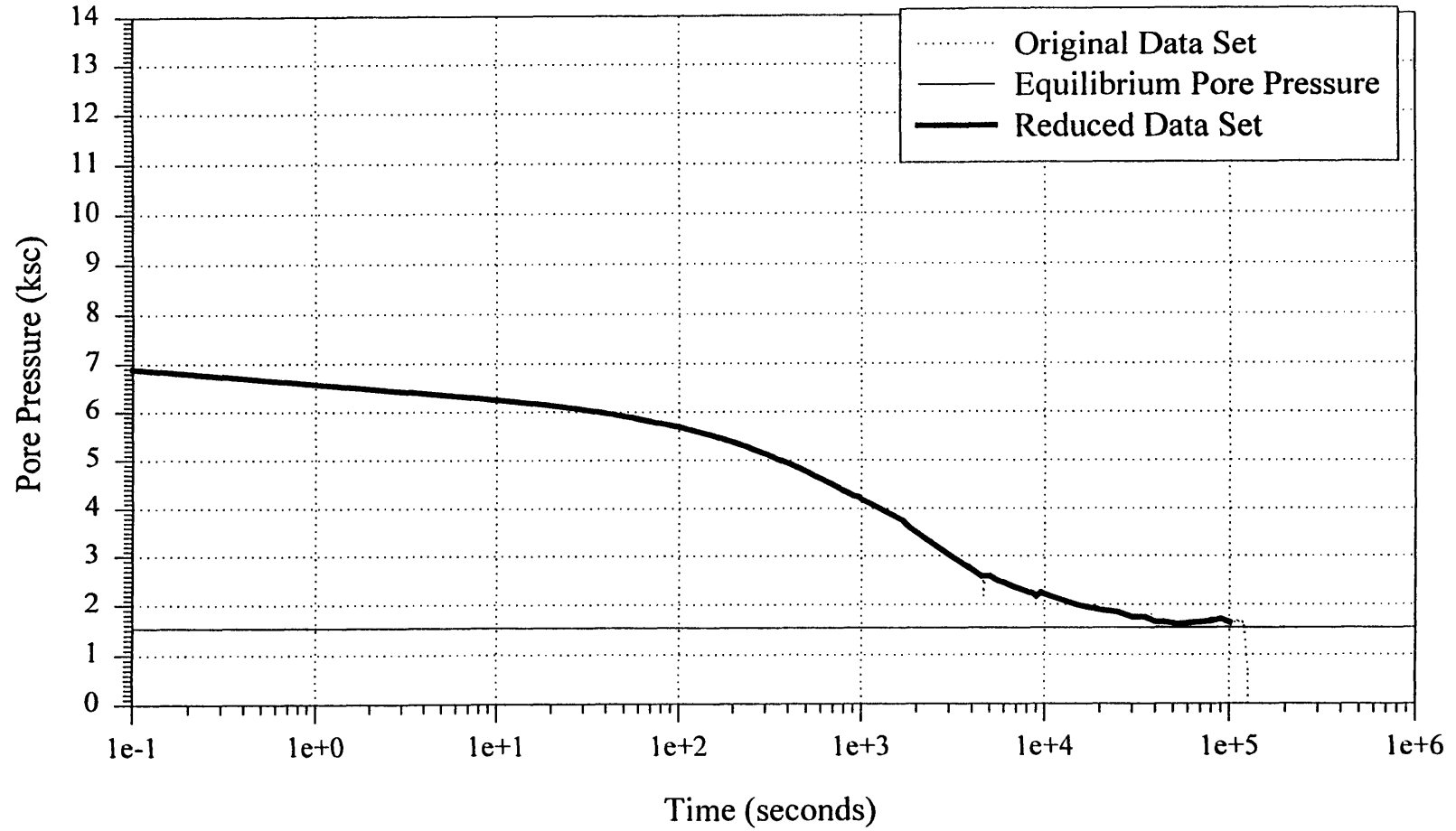
Piezocone 790 Dissipation at 50'
Elevation -13.15 m



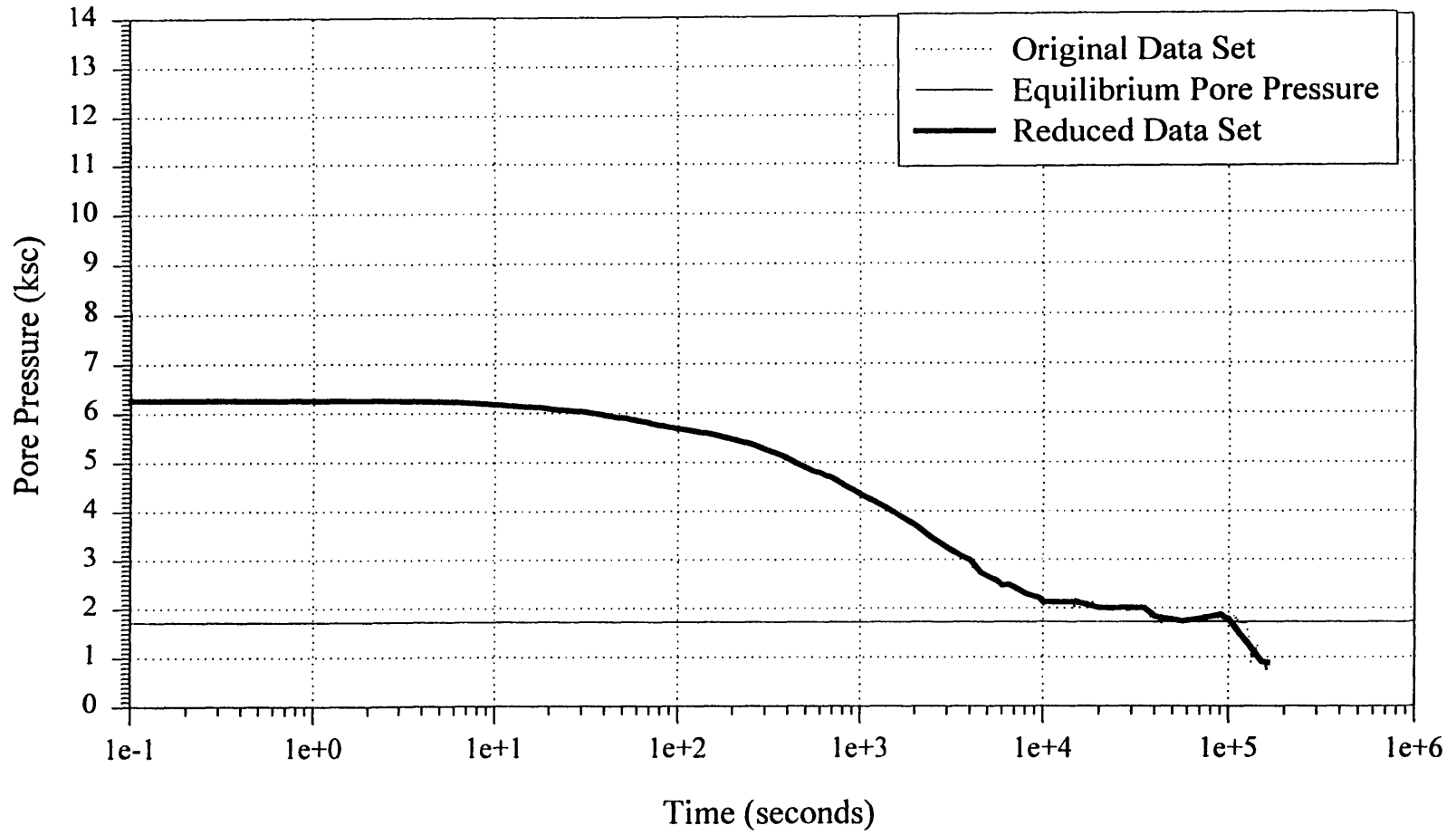
Piezoprobe 63 Dissipation at 55'
Elevation -14.82 m



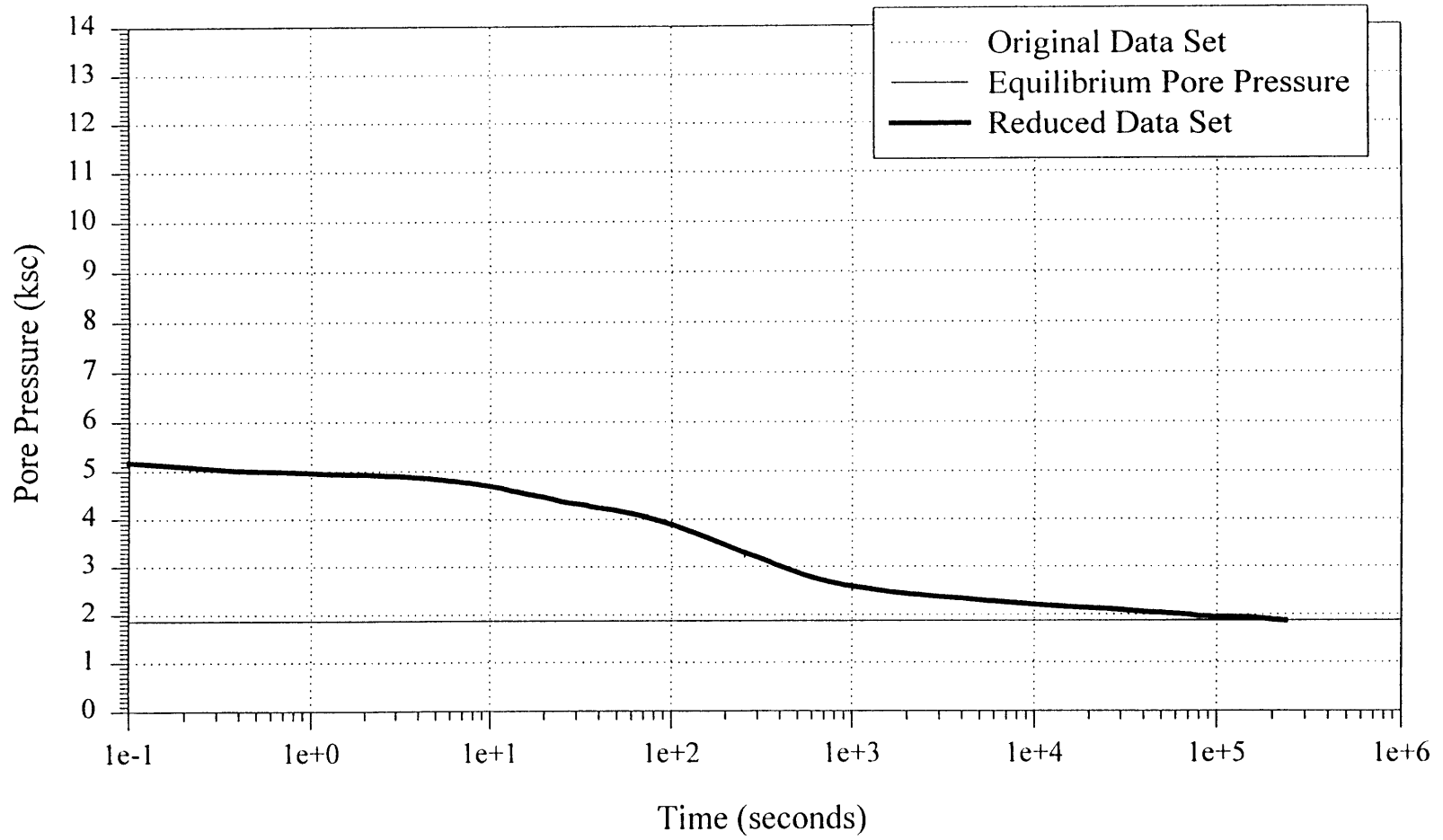
Piezocone 790 Dissipation at 55'
Elevation -14.67 m



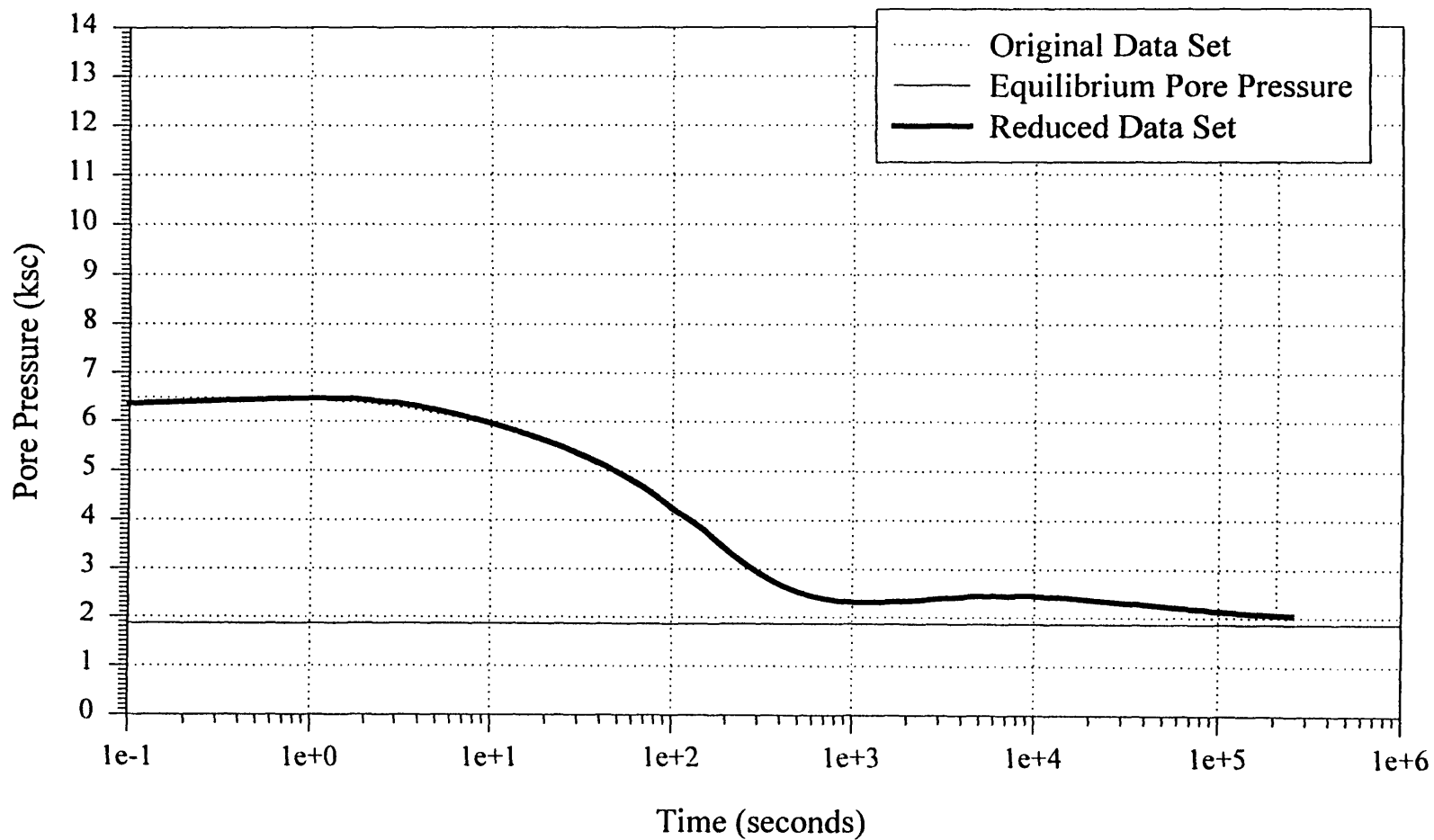
Piezocone 881 Dissipation at 60'
Elevation -16.40 m



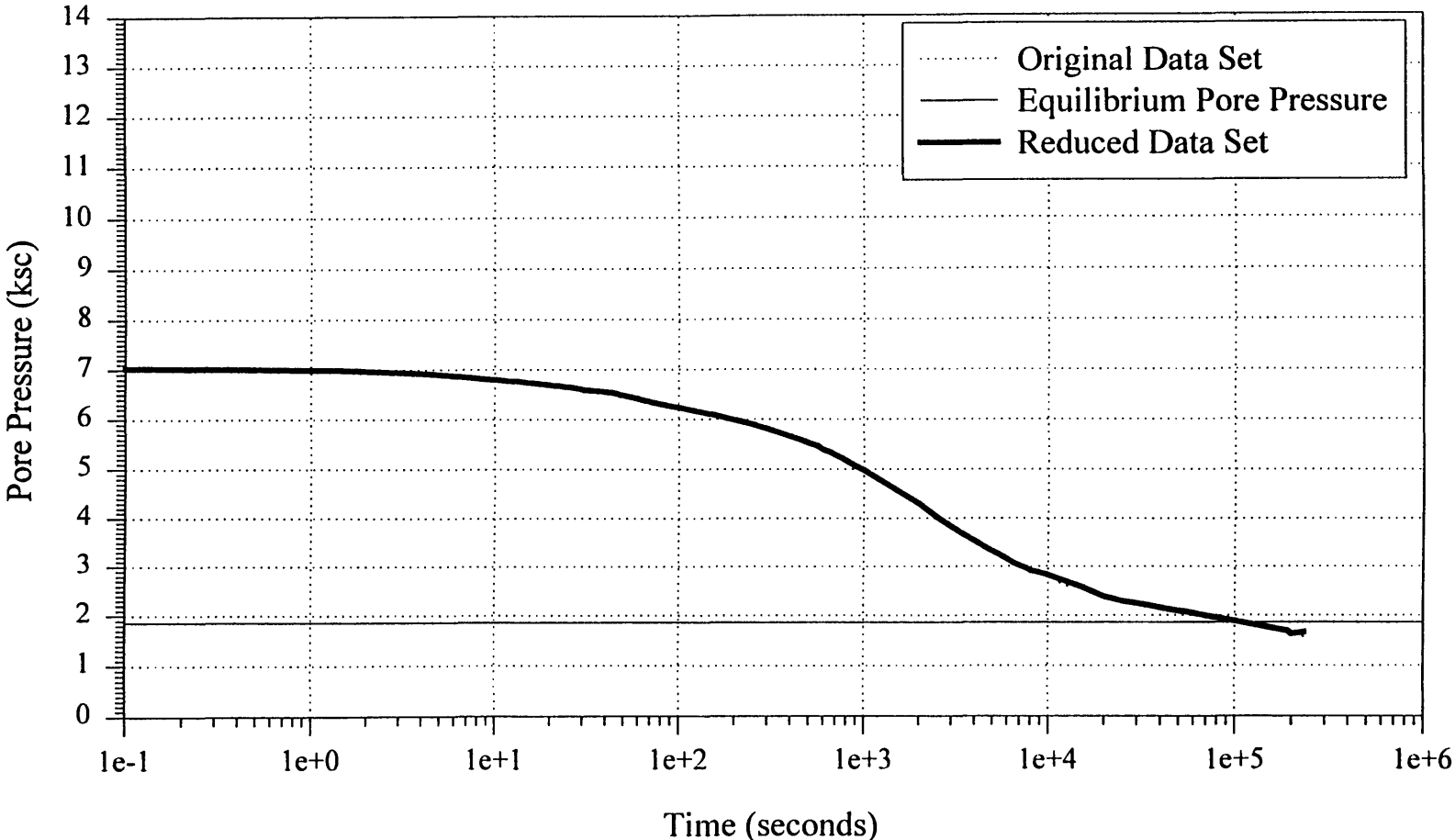
Piezoprobe 62 Dissipation at 67'
Elevation -18.45 m



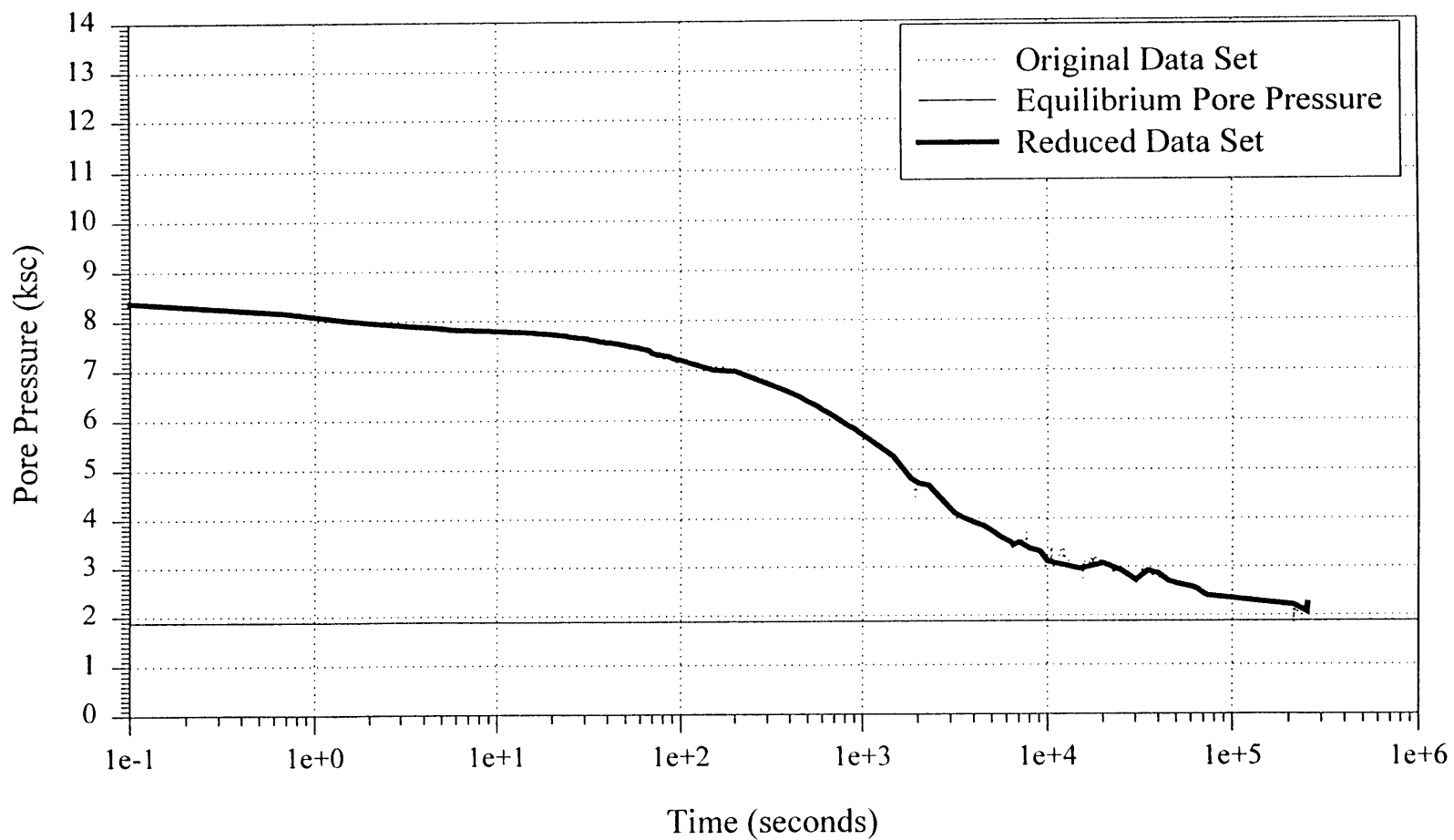
Piezoprobe 63 Dissipation at 67'
Elevation -18.48 m



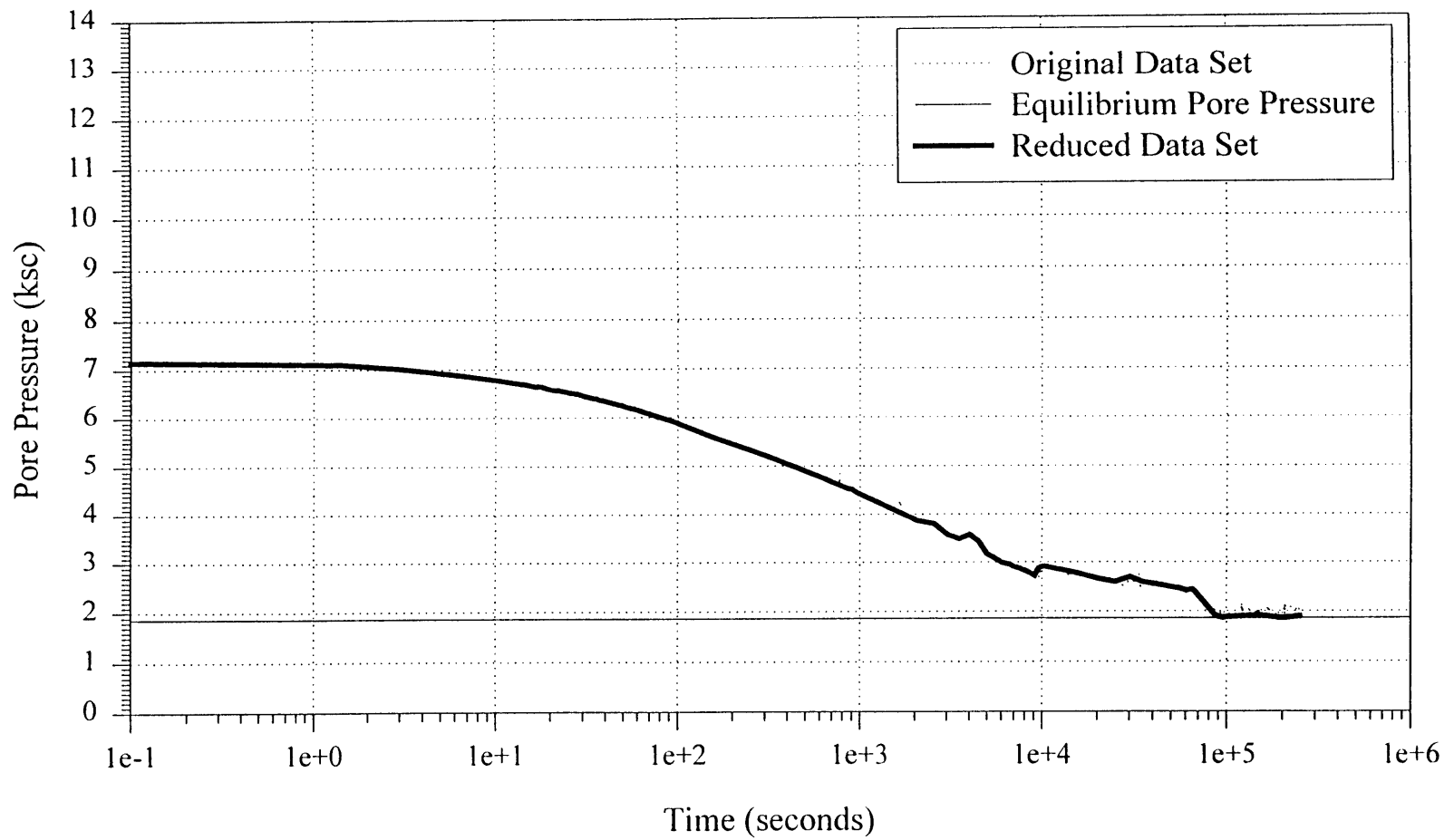
Piezocone 790 Dissipation at 65'
Elevation -17.72 m



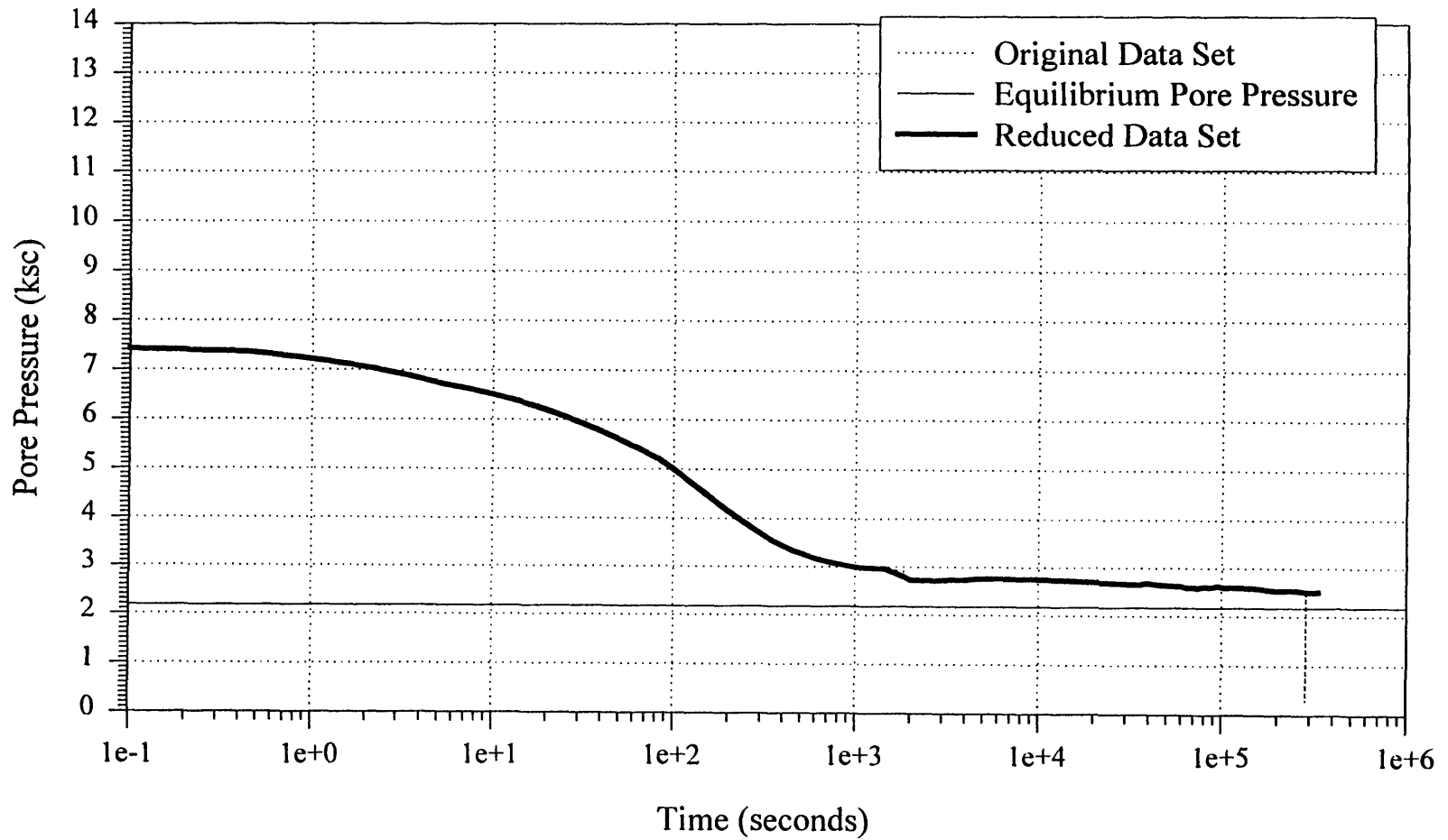
Piezocone 881 Dissipation at 65'
Elevation -17.93 m



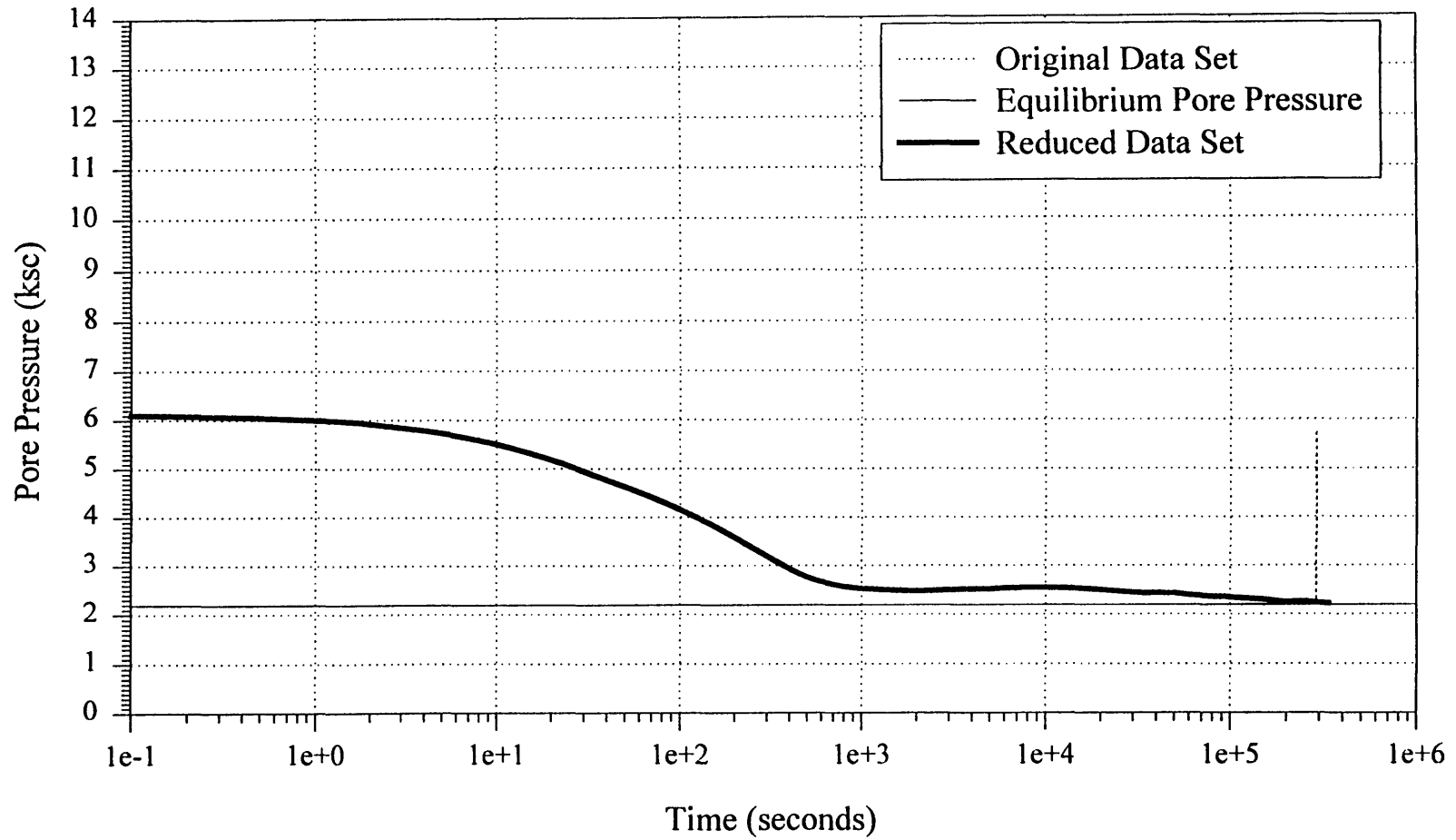
MIT Cone Dissipation at 65'
Elevation -17.79 m



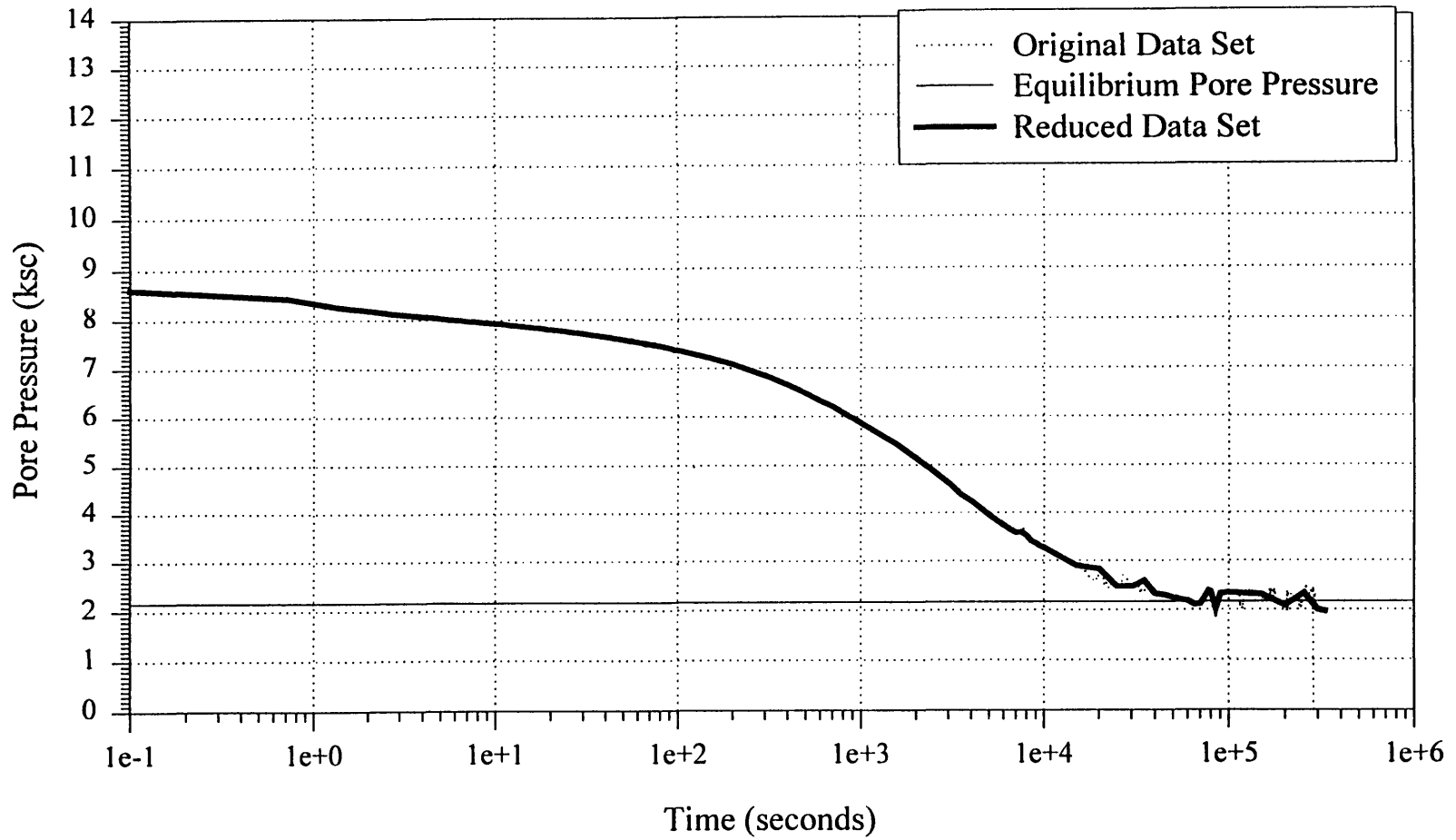
Piezoprobe 62 Dissipation at 75'
Elevation -20.89 m



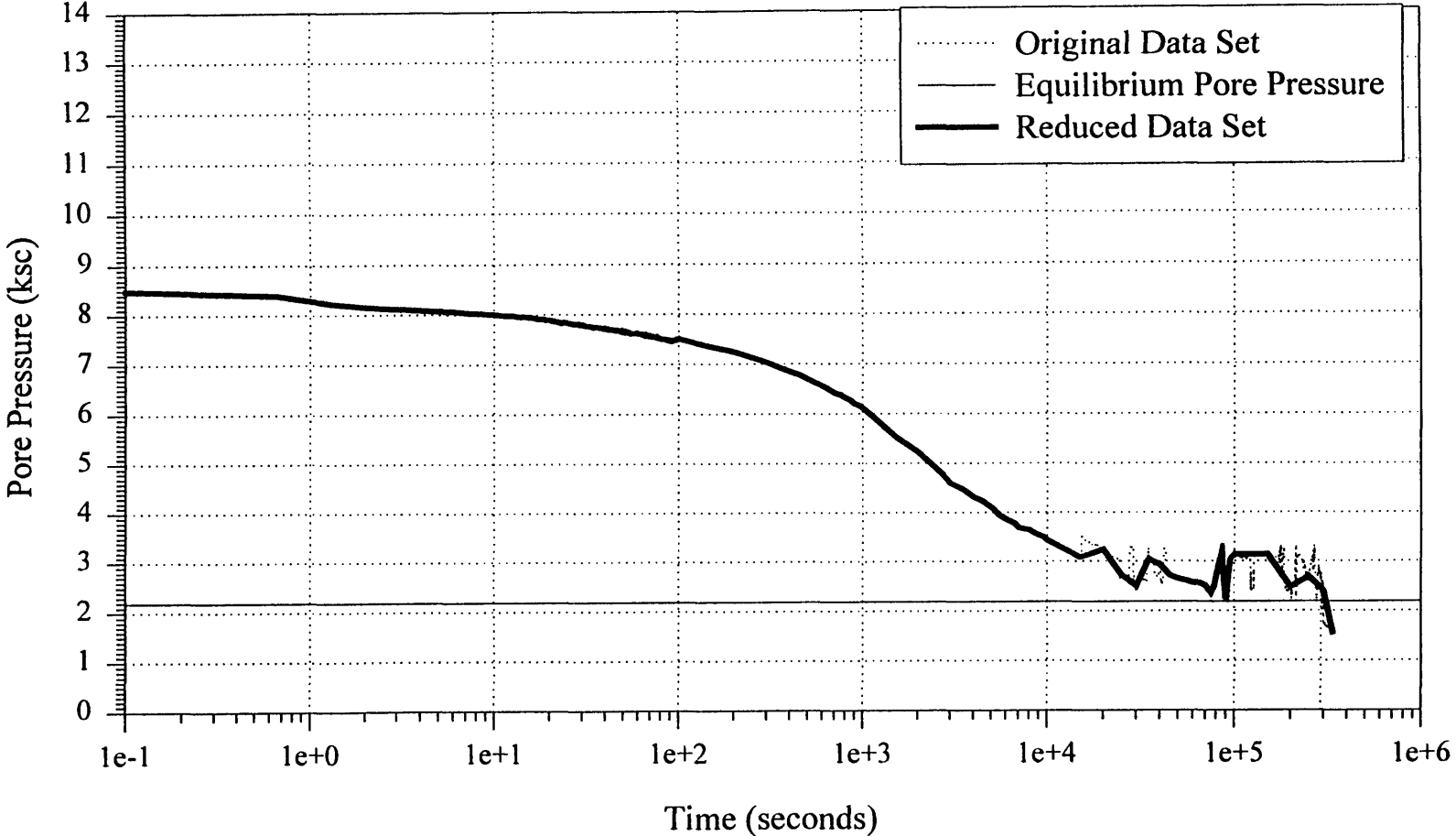
Piezoprobe 63 Dissipation at 75'
Elevation -20.92 m



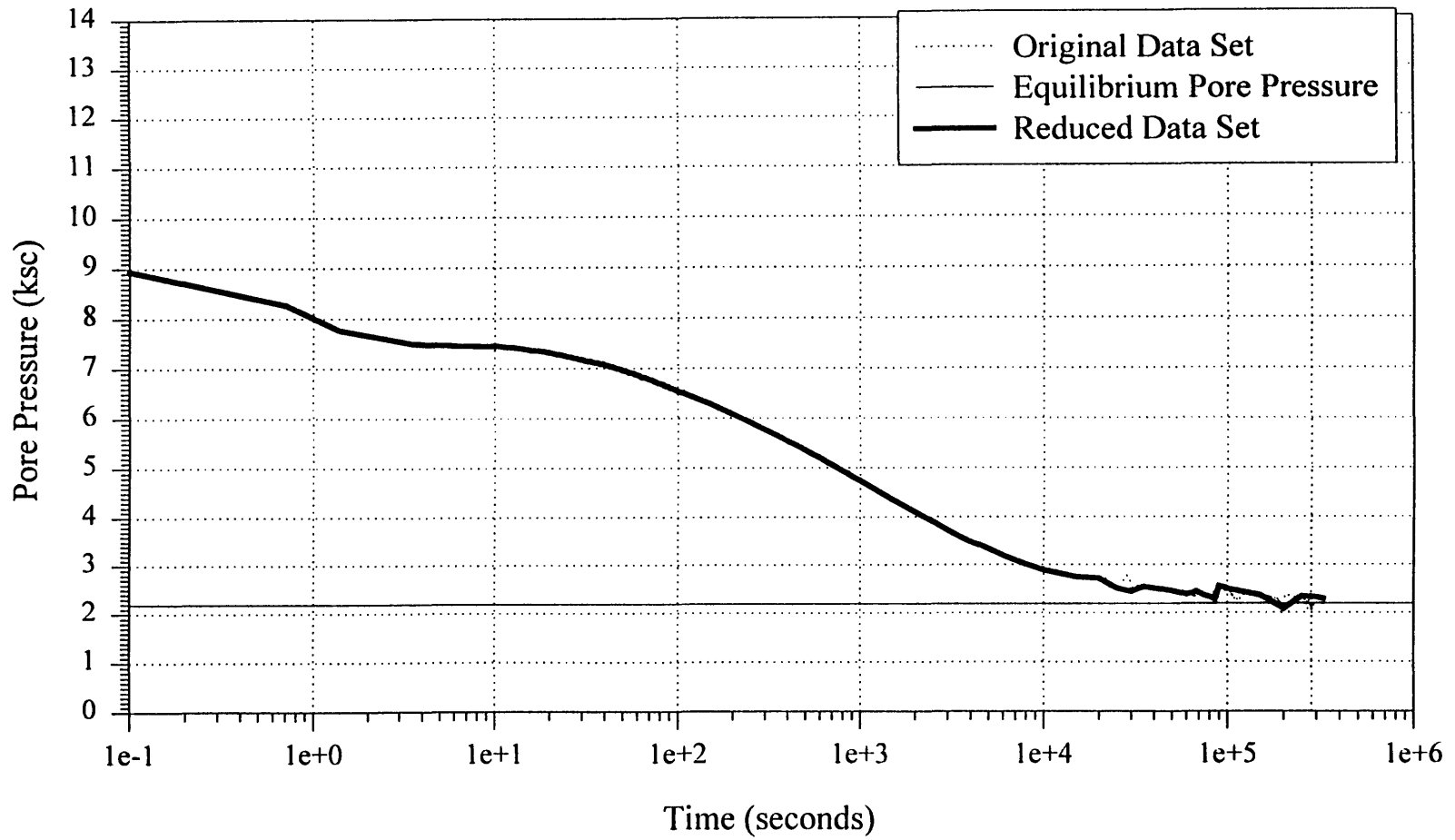
Piezocone 790 Dissipation at 75'
Elevation -20.77 m



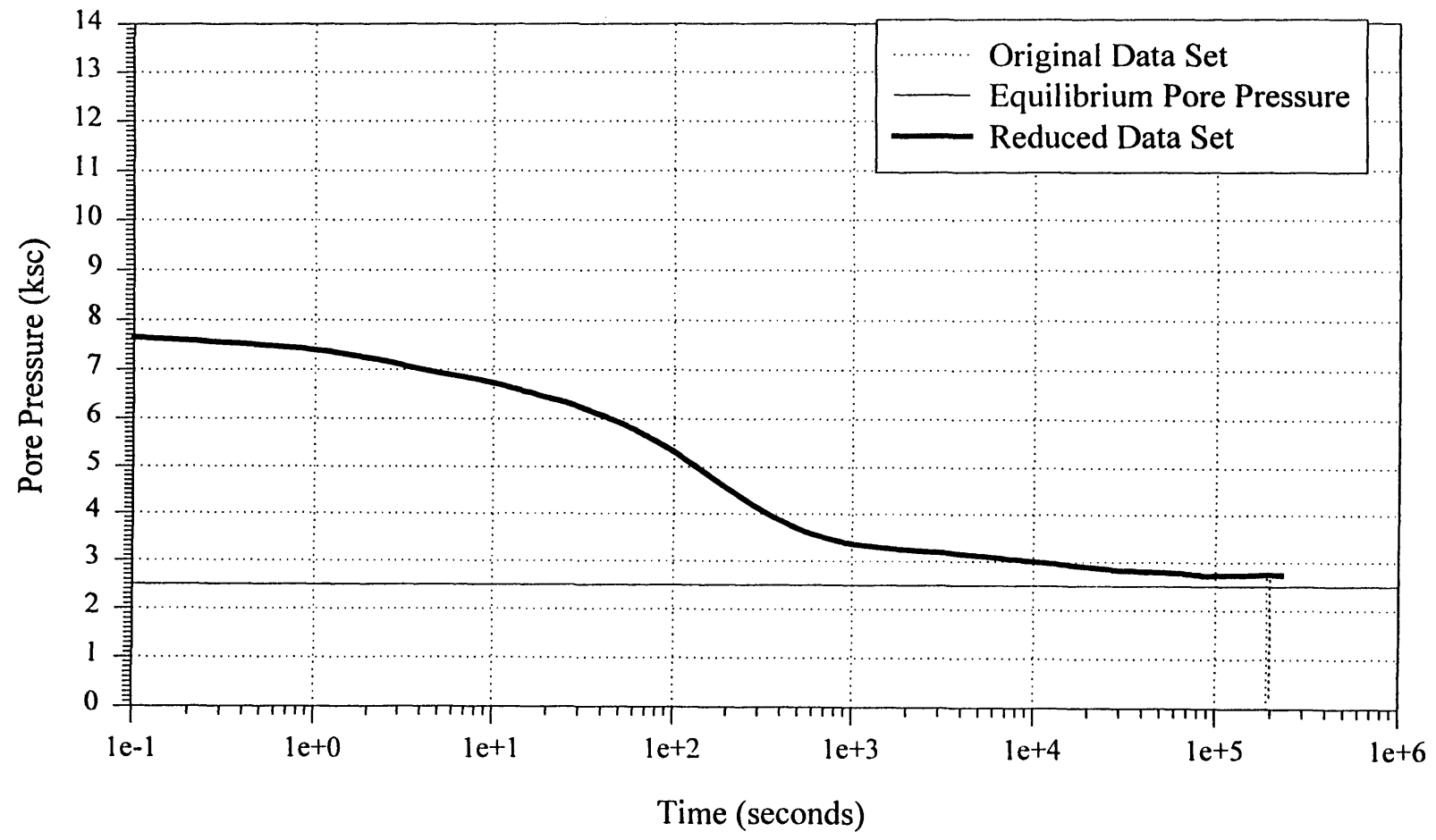
Piezocone 881 Dissipation at 75'
Elevation -20.98 m



MIT Cone Dissipation at 75'
Elevation -20.98 m

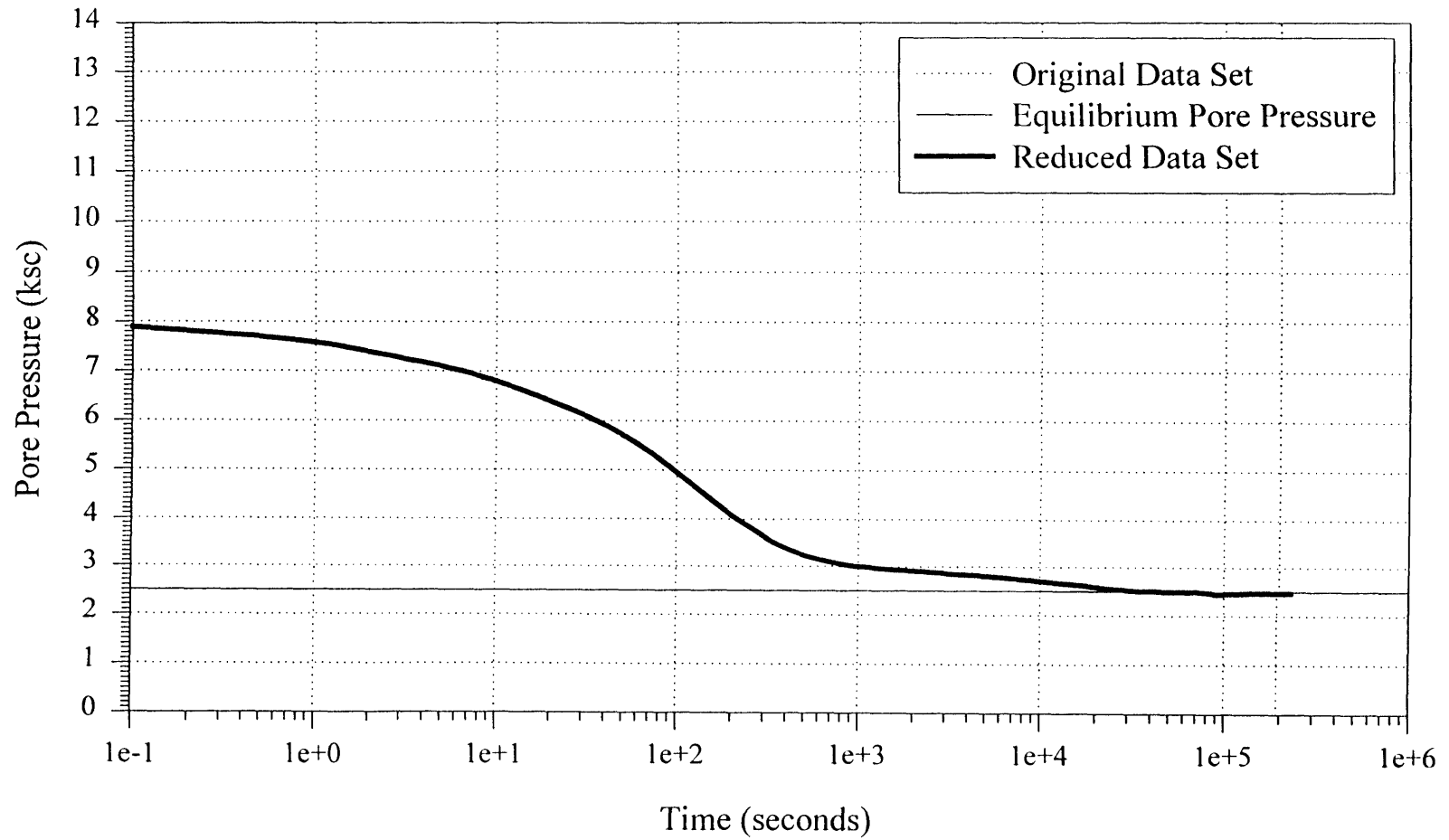


Piezoprobe 62 Dissipation at 85'
Elevation -23.94 m

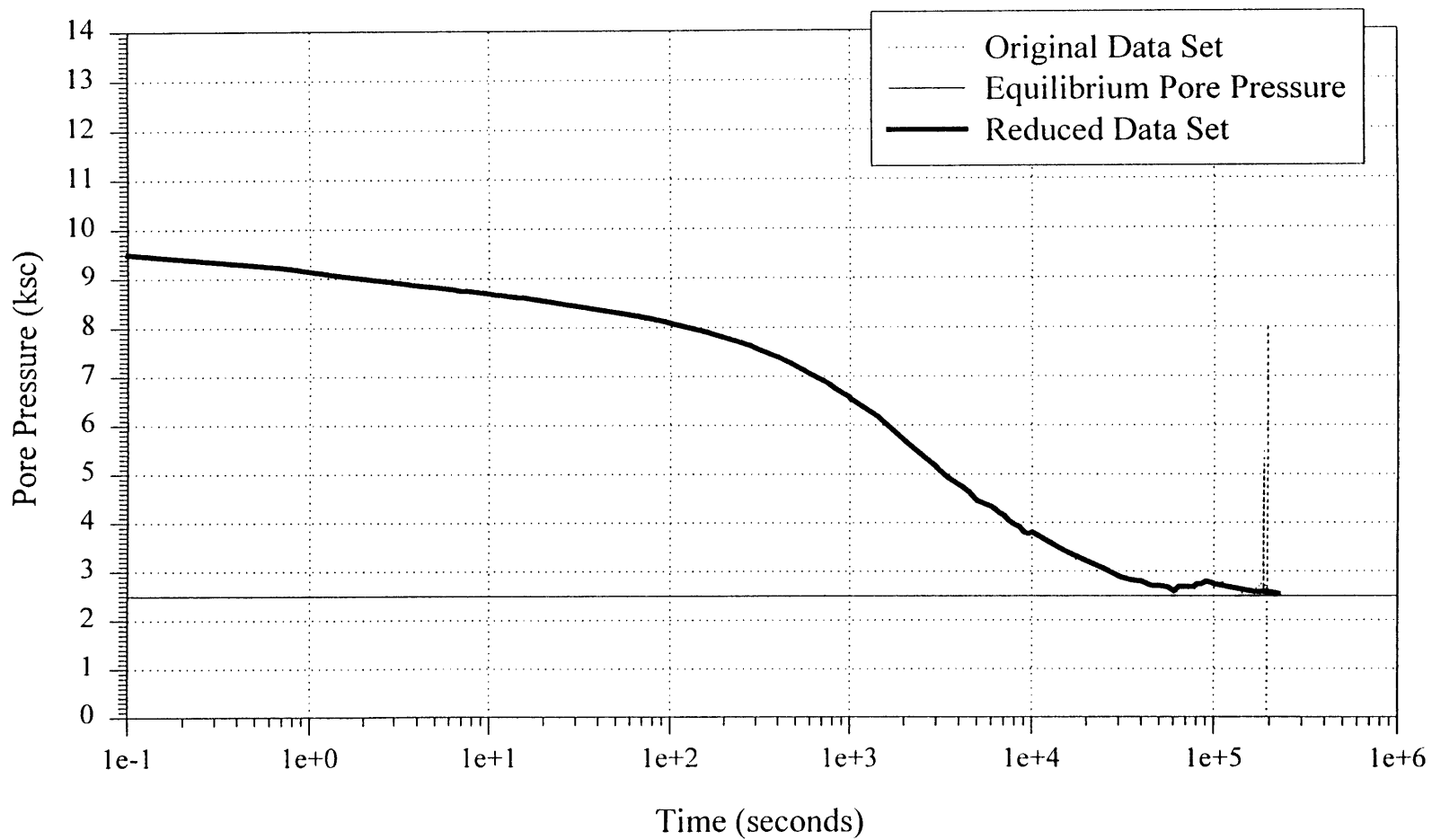


350

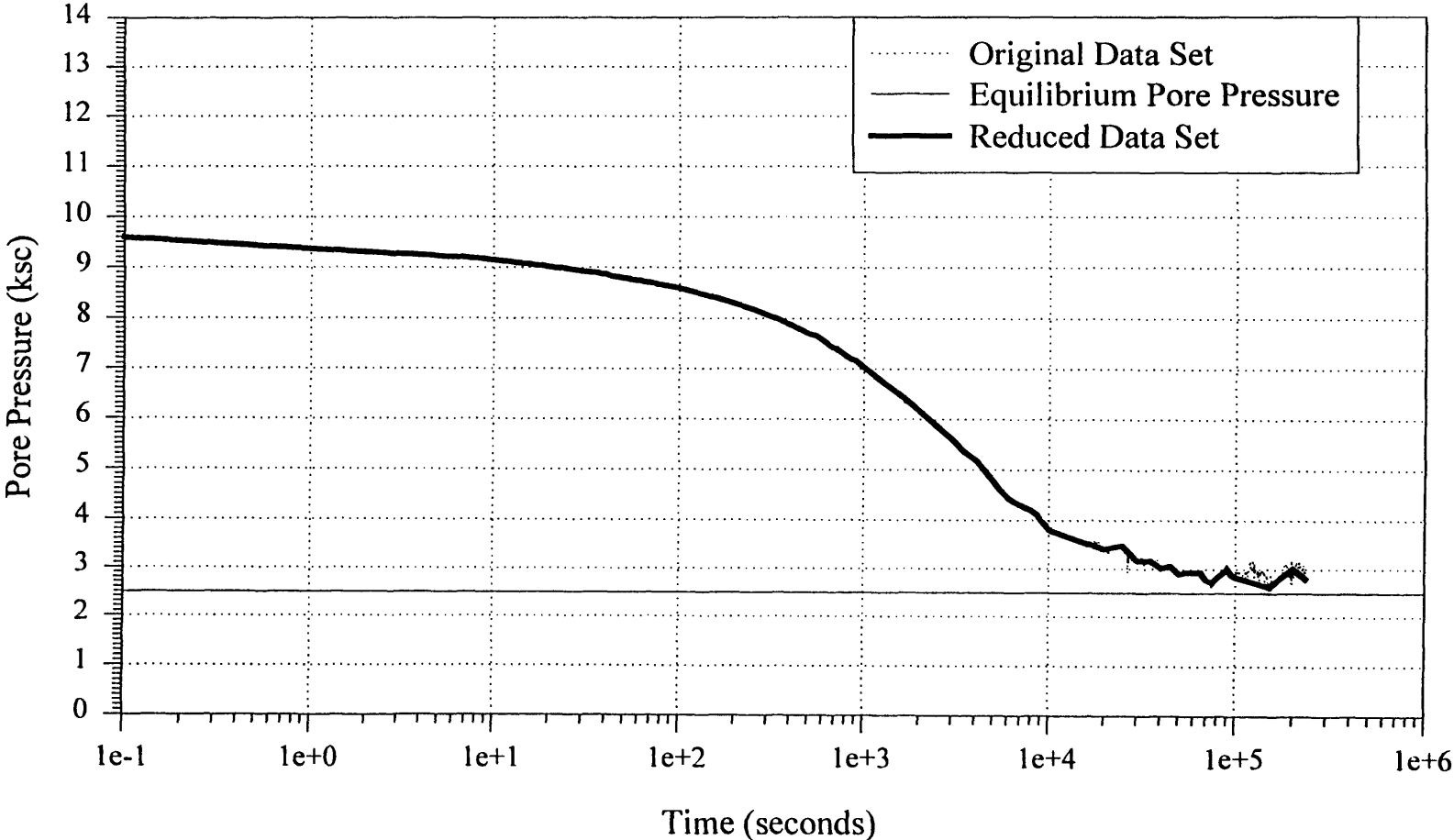
Piezoprobe 63 Dissipation at 85'
Elevation -23.97 m



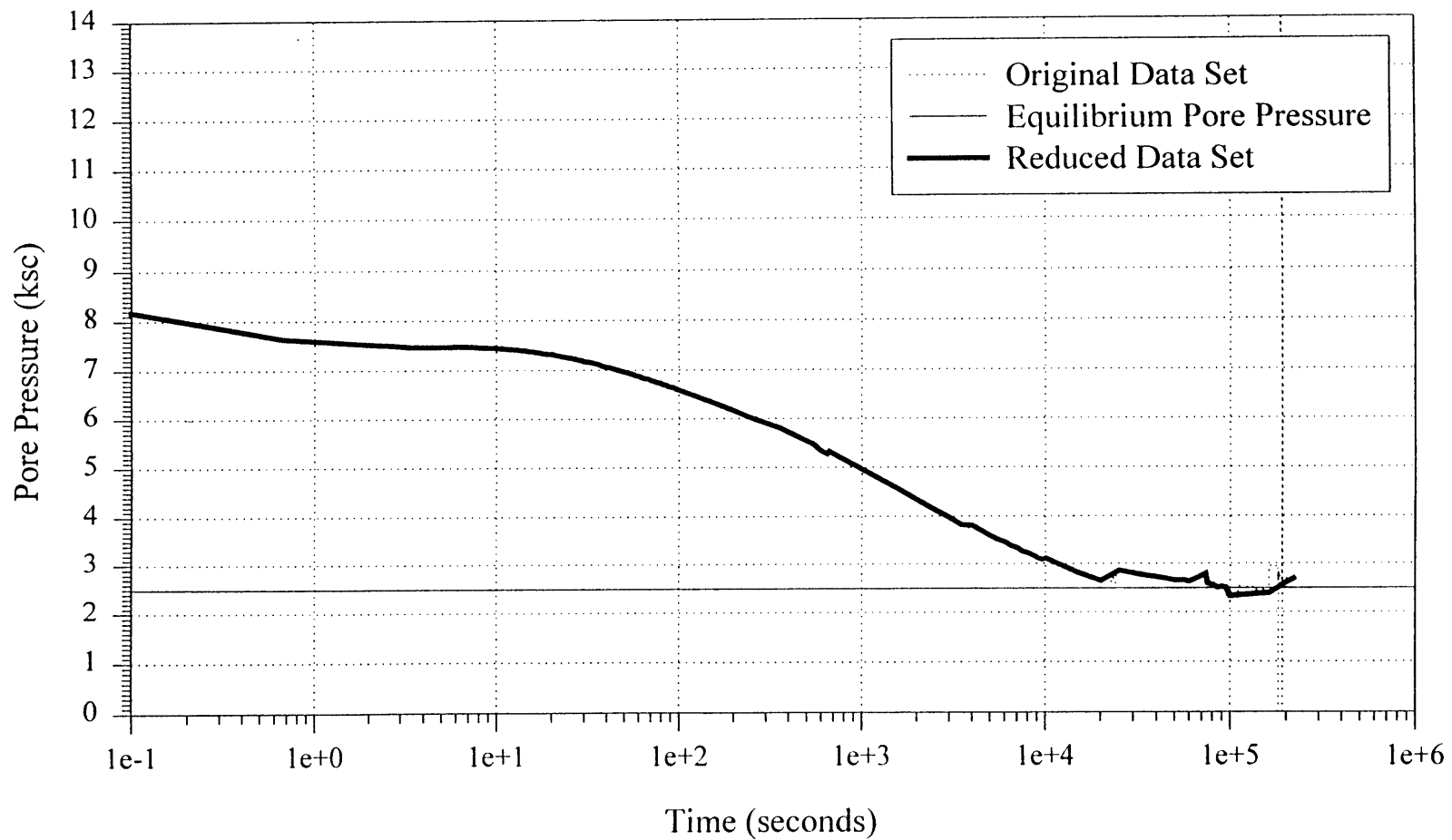
**Piezocone 790 Dissipation at 85'
Elevation -23.81 m**



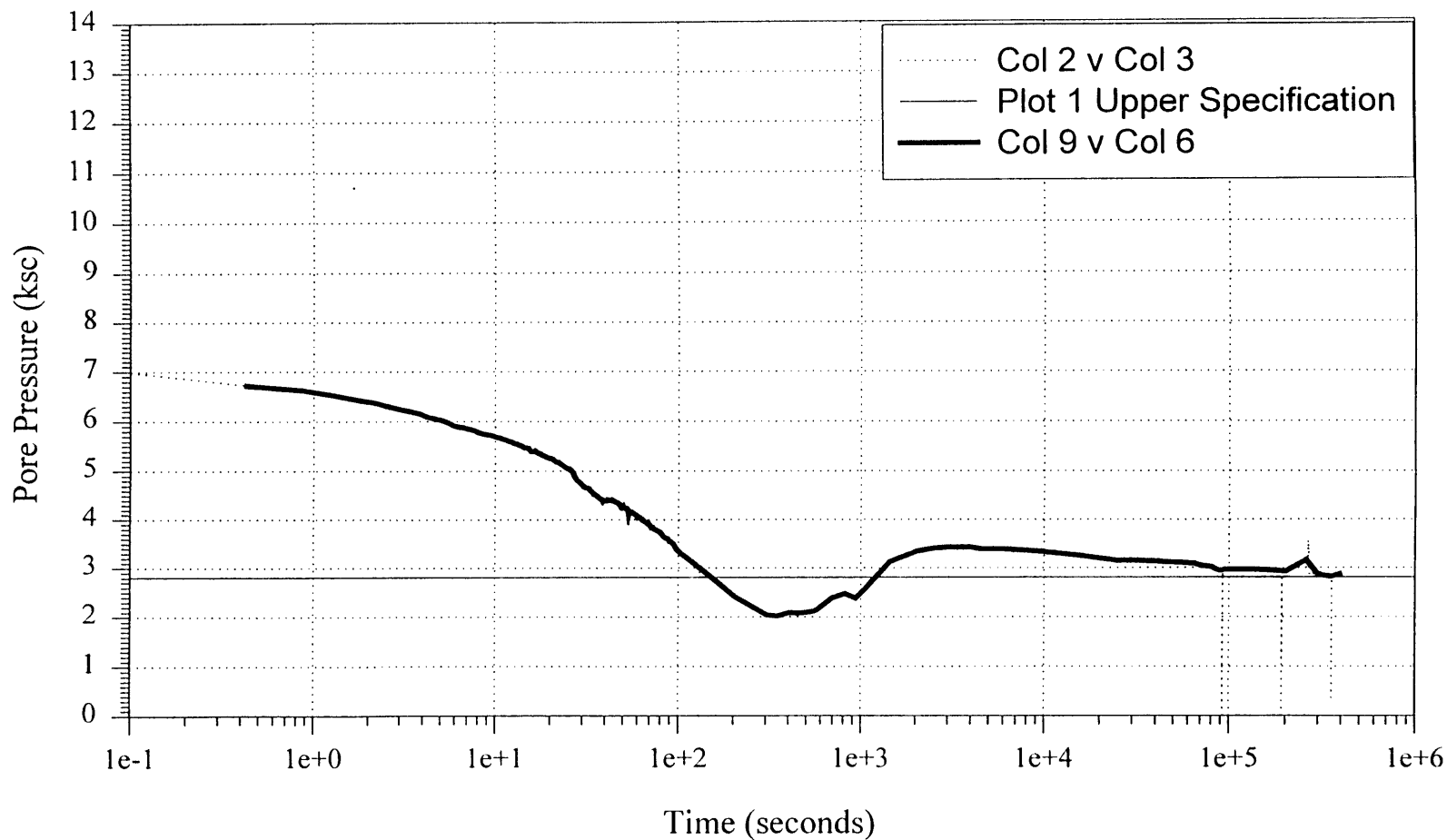
Piezocone 881 Dissipation at 85'
Elevation -24.02 m



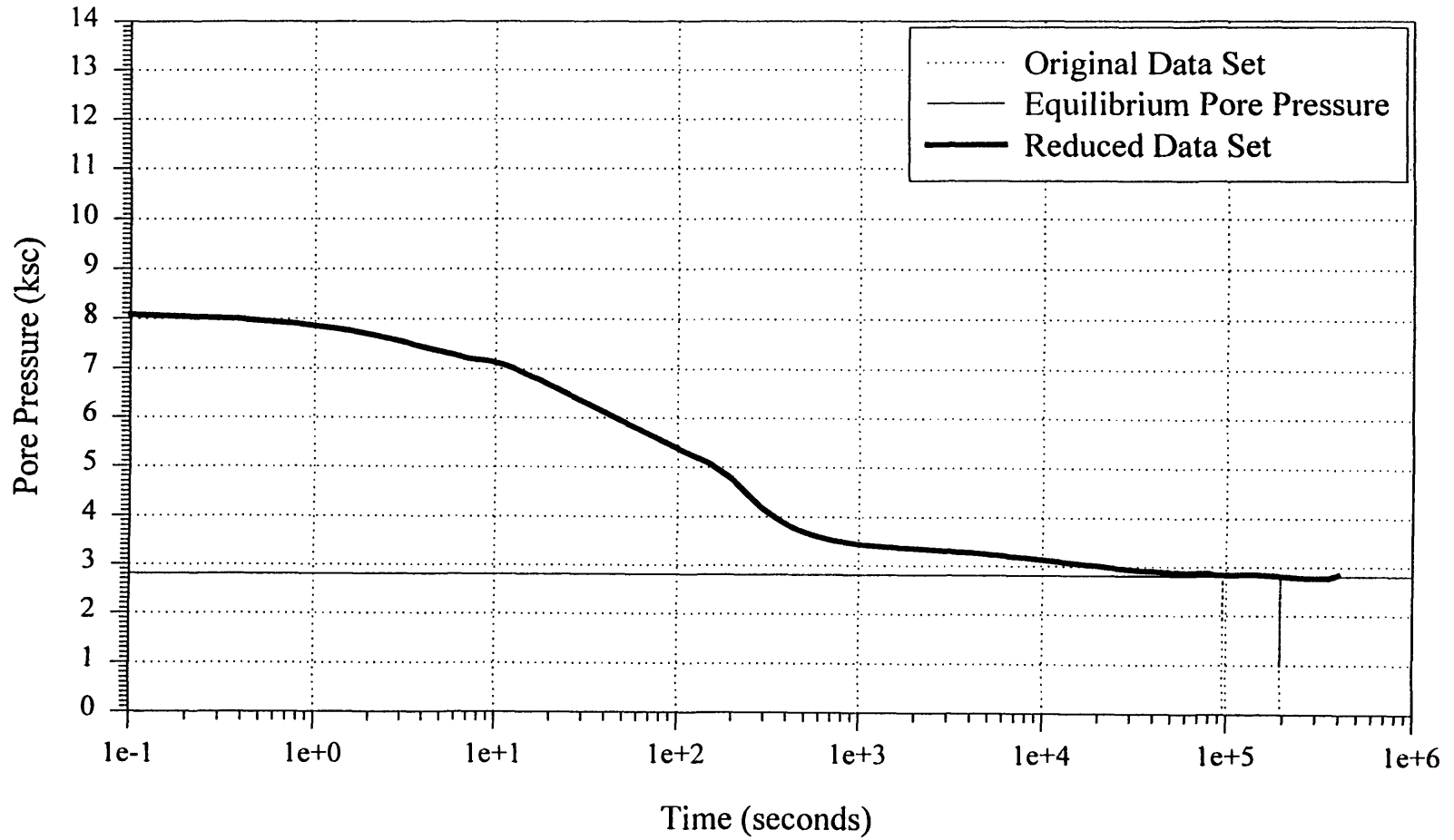
MIT Cone Dissipation at 85'
Elevation -23.89 m



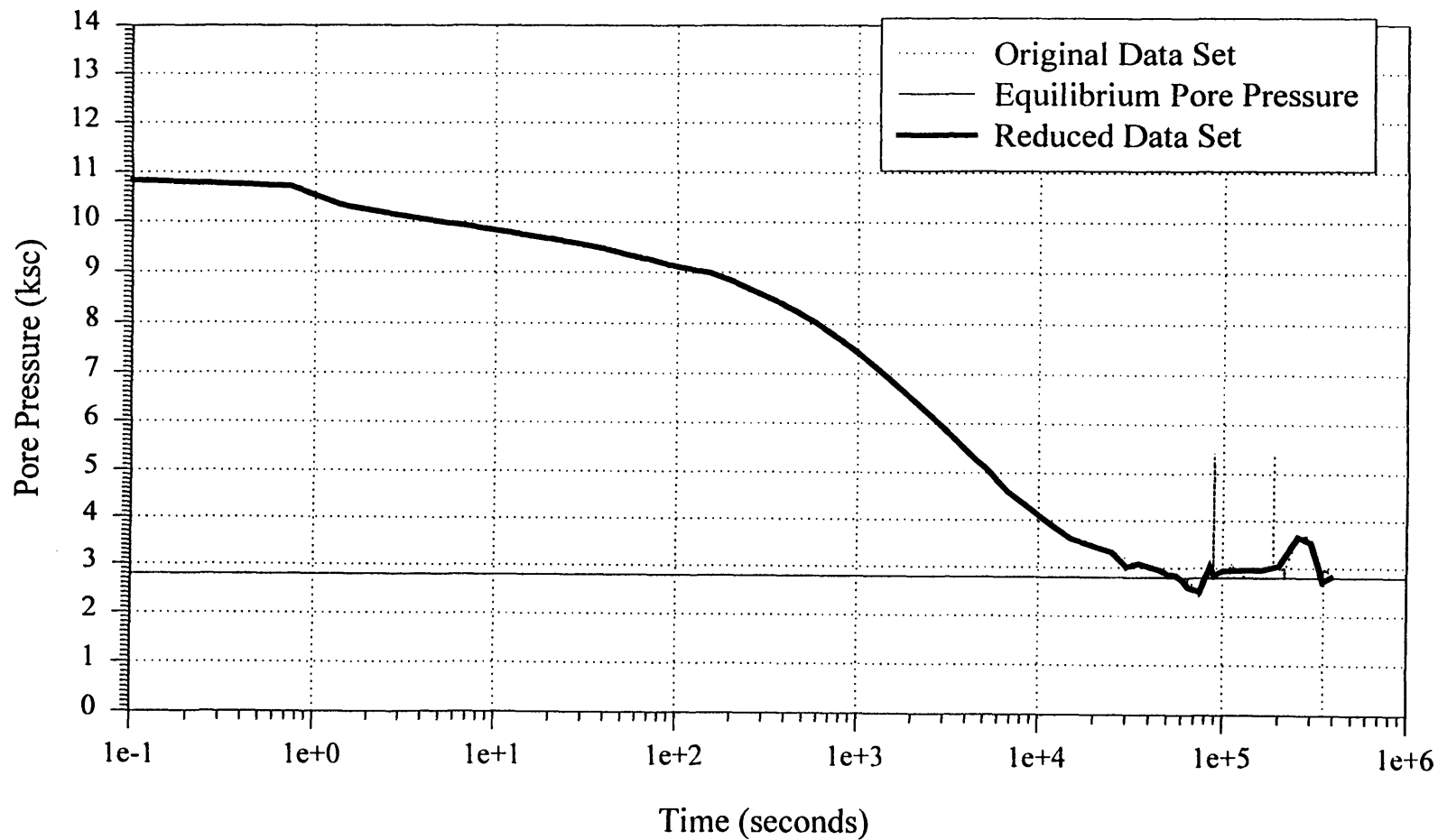
Piezoprobe 62 Dissipation at 95'
Elevation -26.98 m



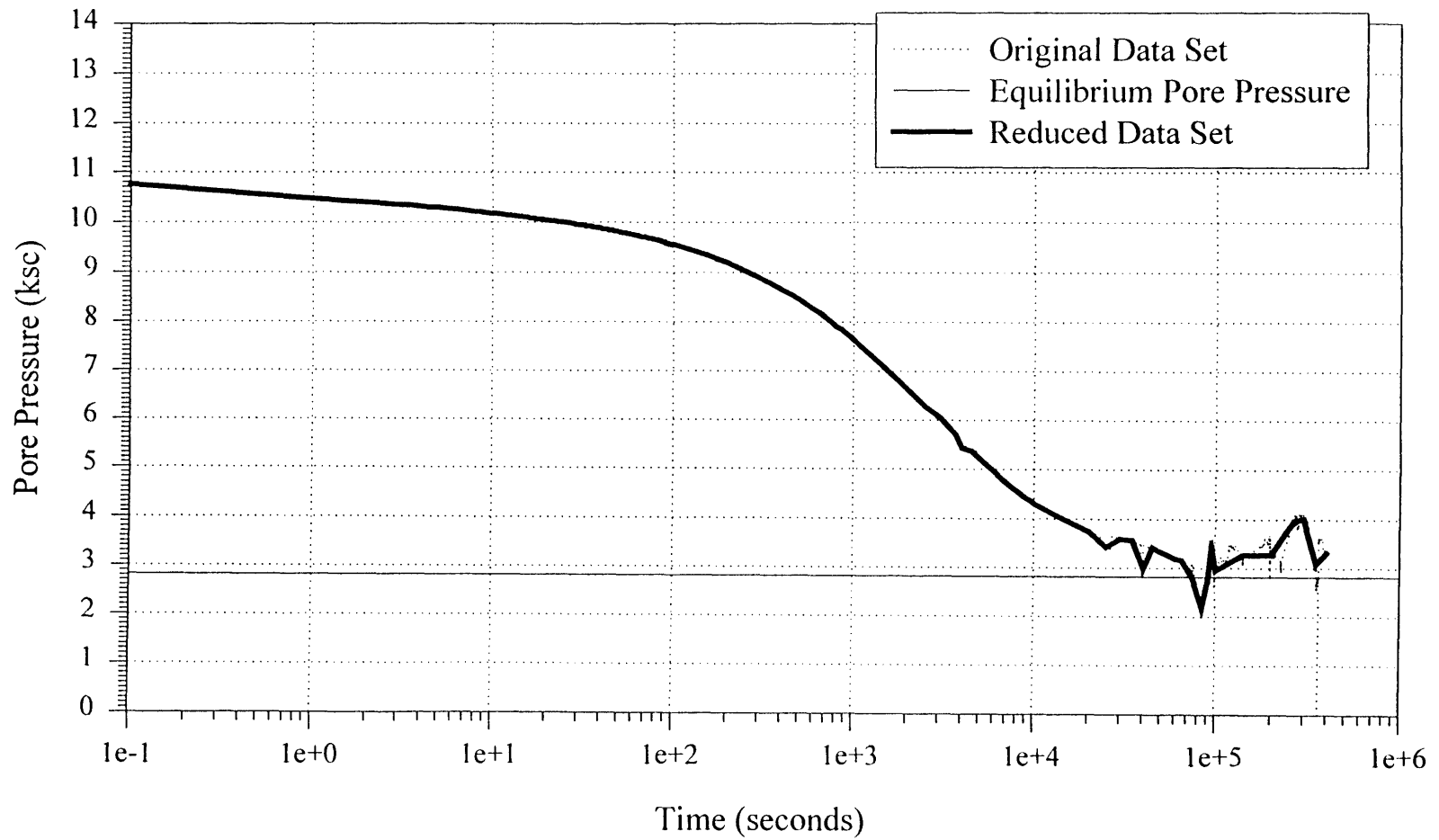
Piezoprobe 63 Dissipation at 95'
Elevation -27.02 m



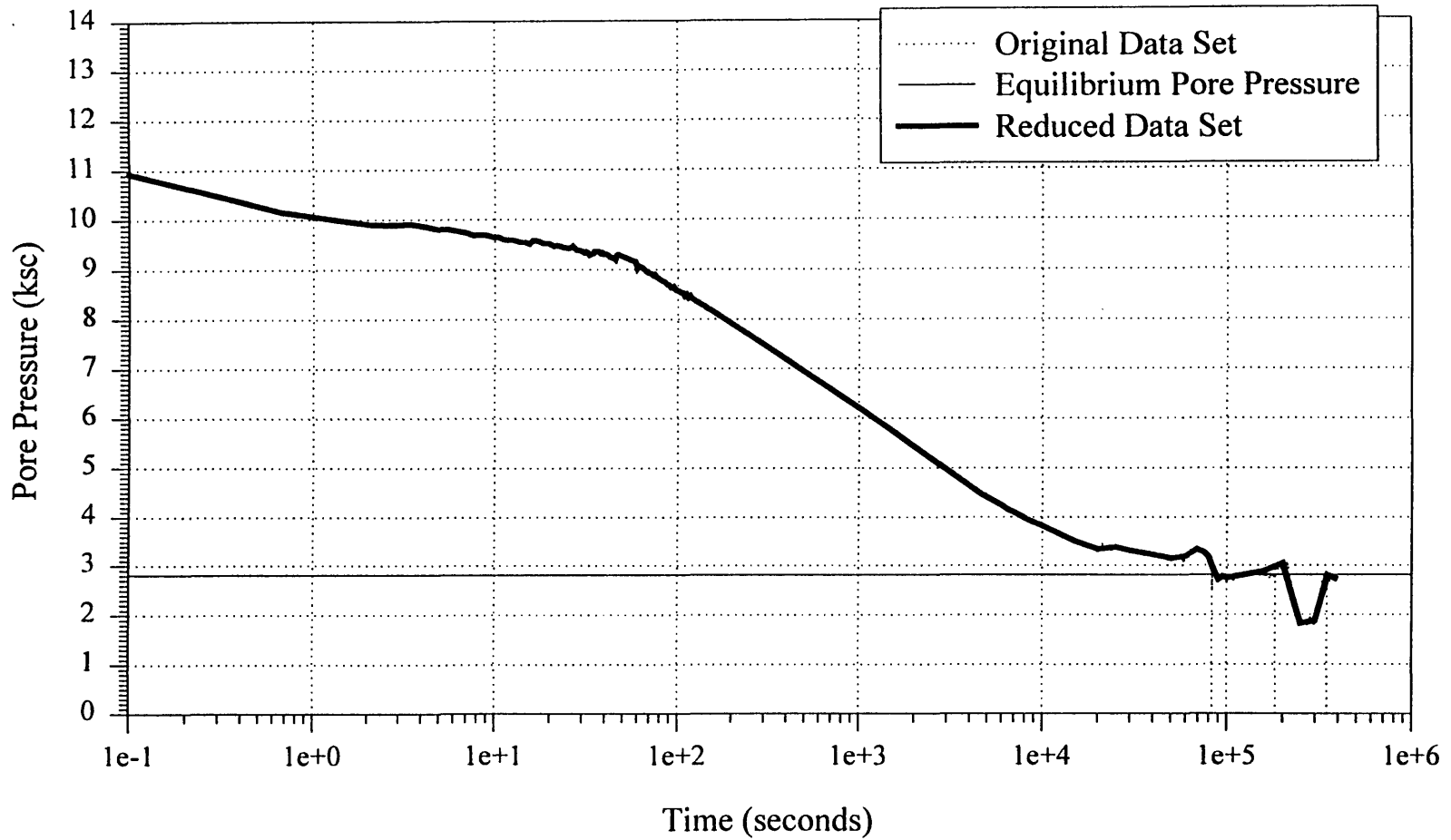
Piezocone 790 Dissipation at 95'
Elevation -26.86 m



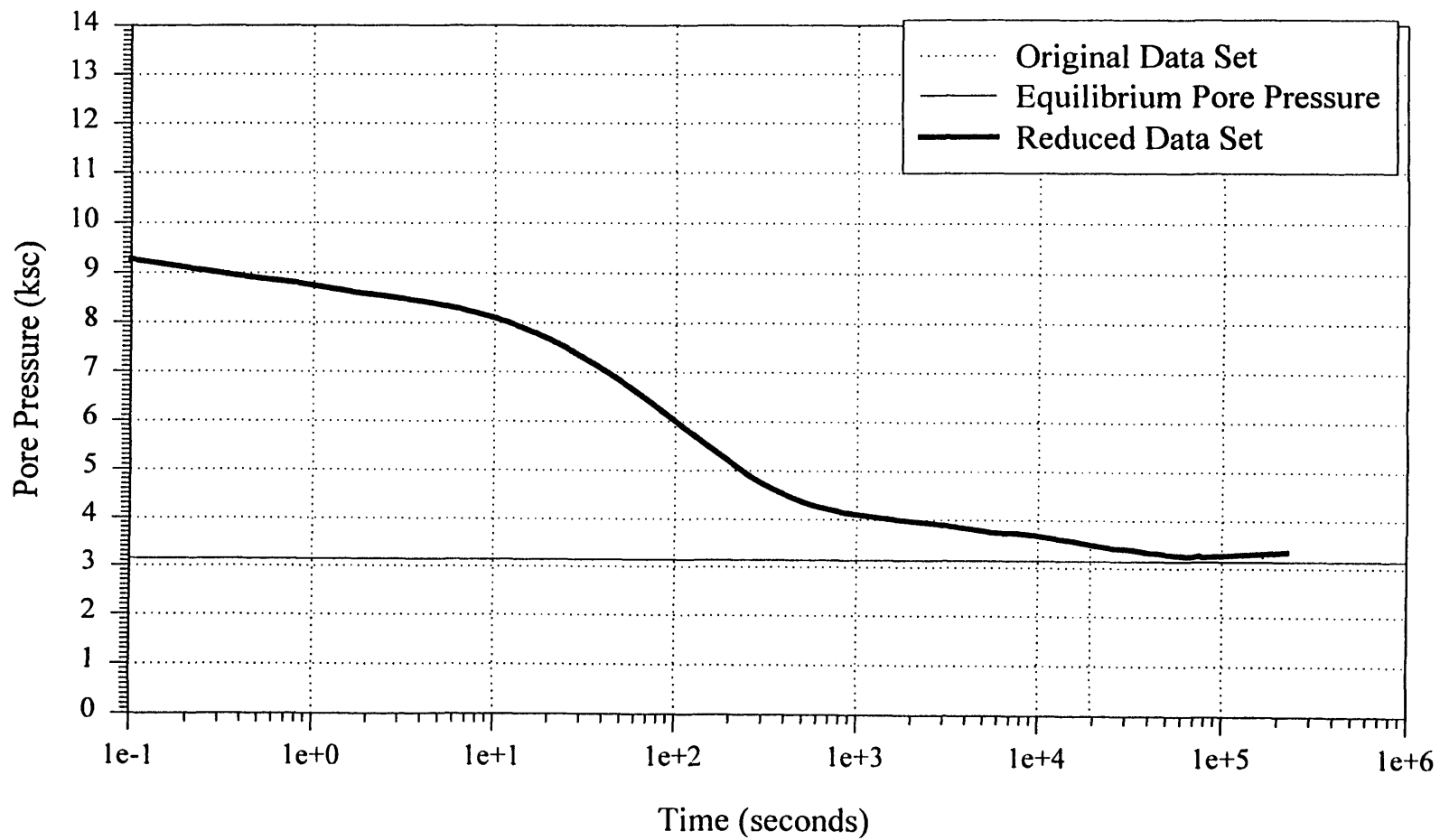
**Piezocone 881 Dissipation at 95'
Elevation -27.07 m**



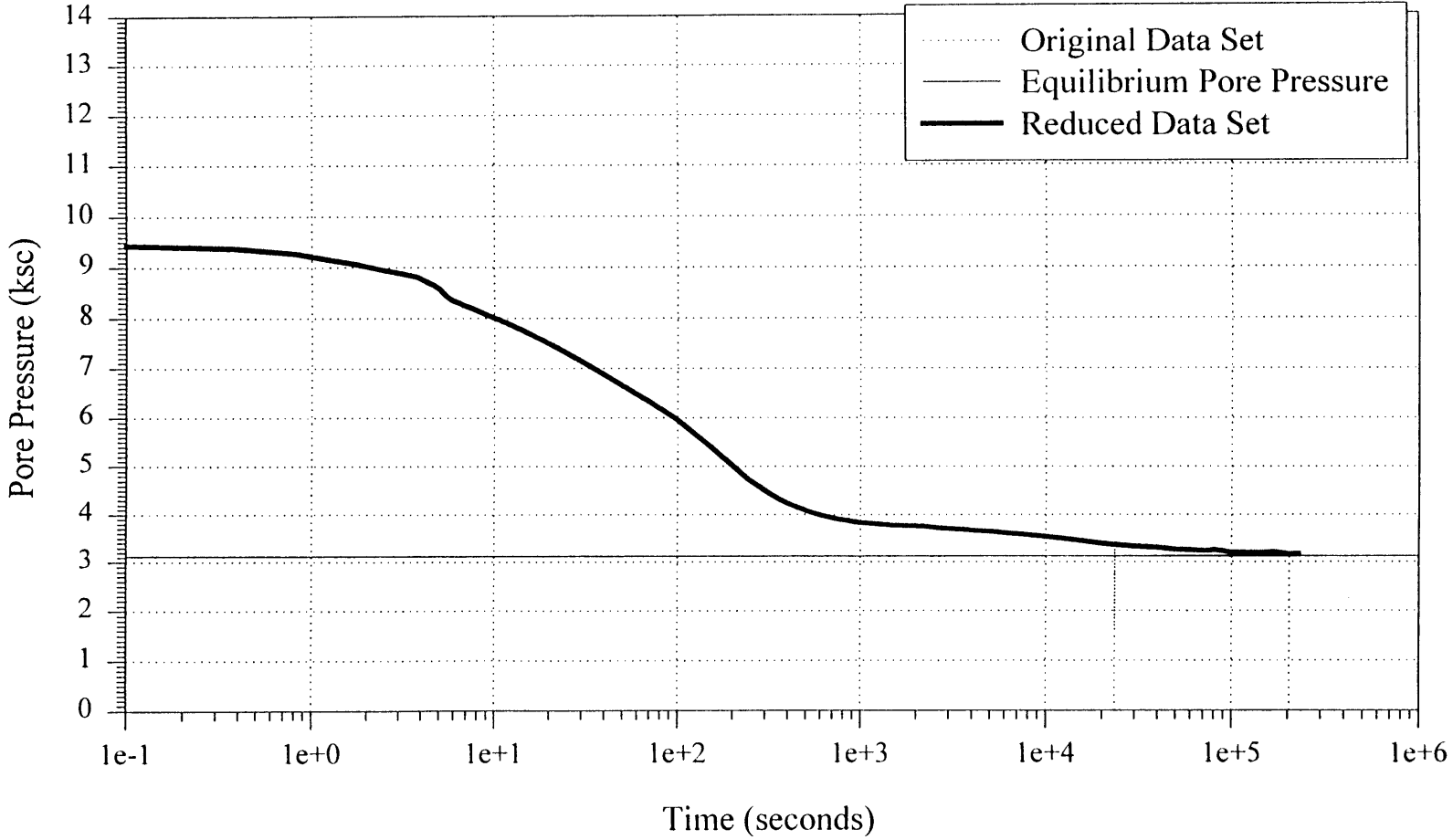
MIT Cone Dissipation at 95'
Elevation -26.94 m



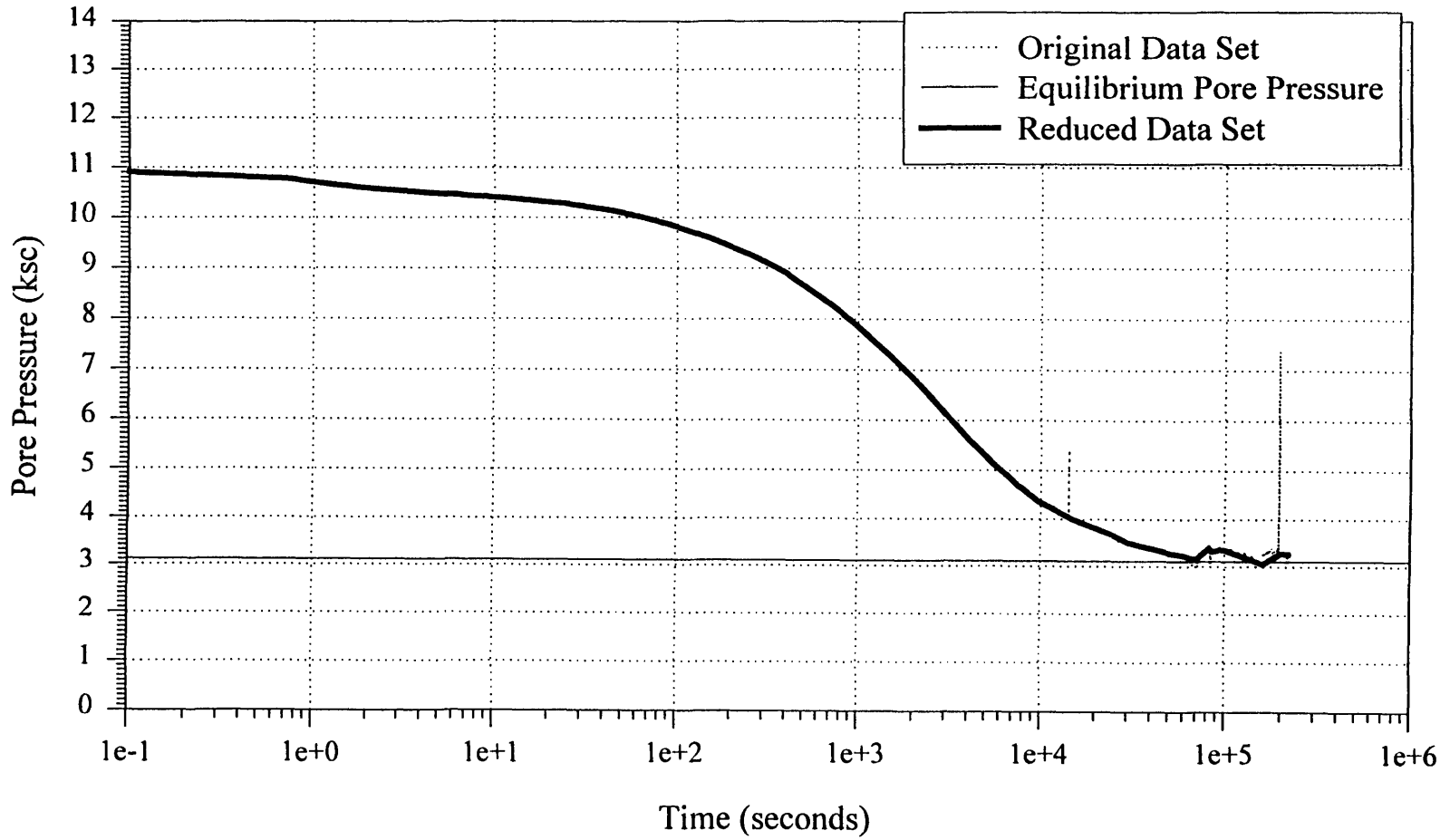
Piezoprobe 62 Dissipation at 106'
Elevation -30.34 m



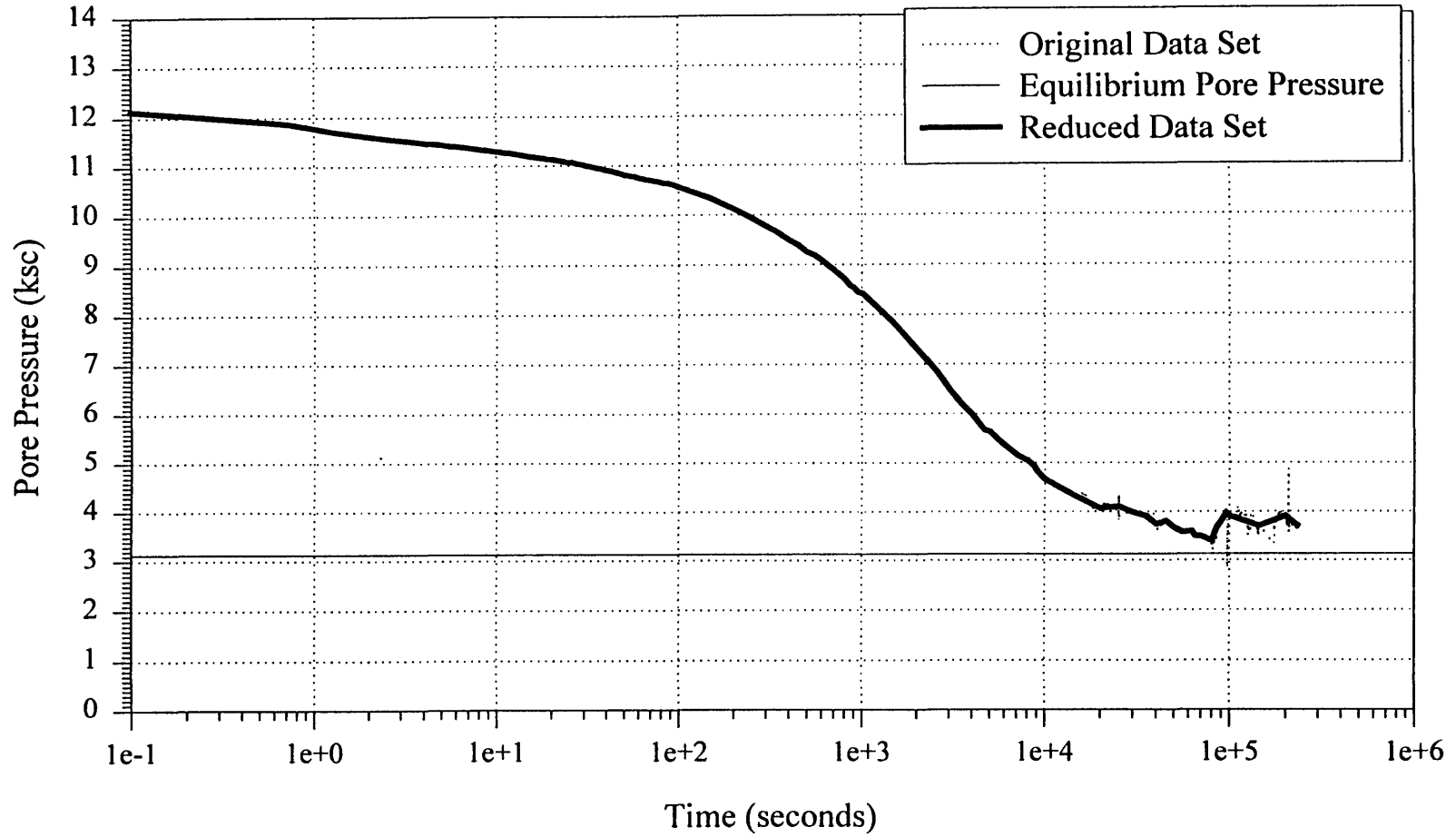
**Piezoprobe 63 Dissipation at 105'
Elevation -30.07 m**



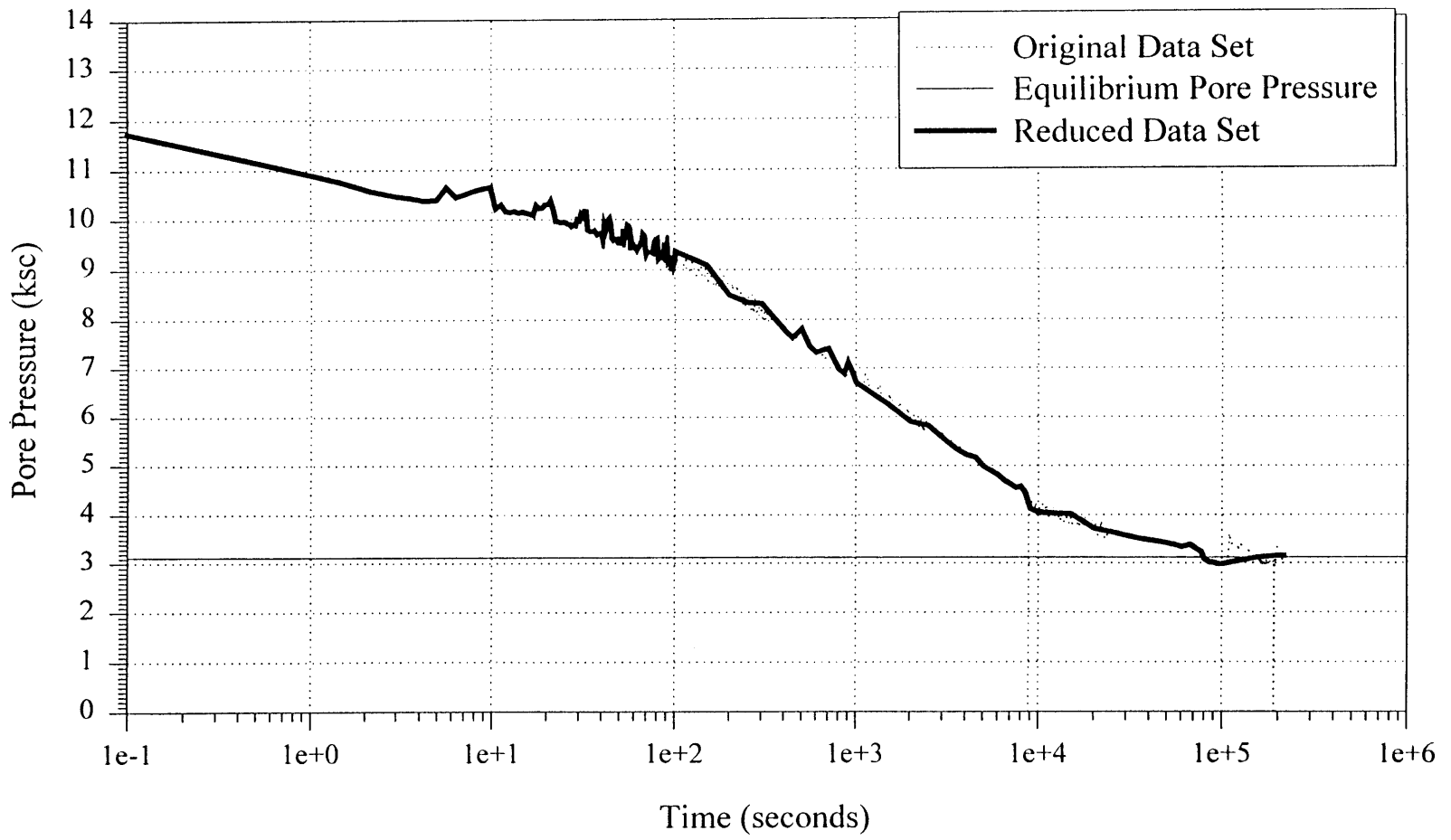
Piezocone 790 Dissipation at 105'
Elevation -29.91 m



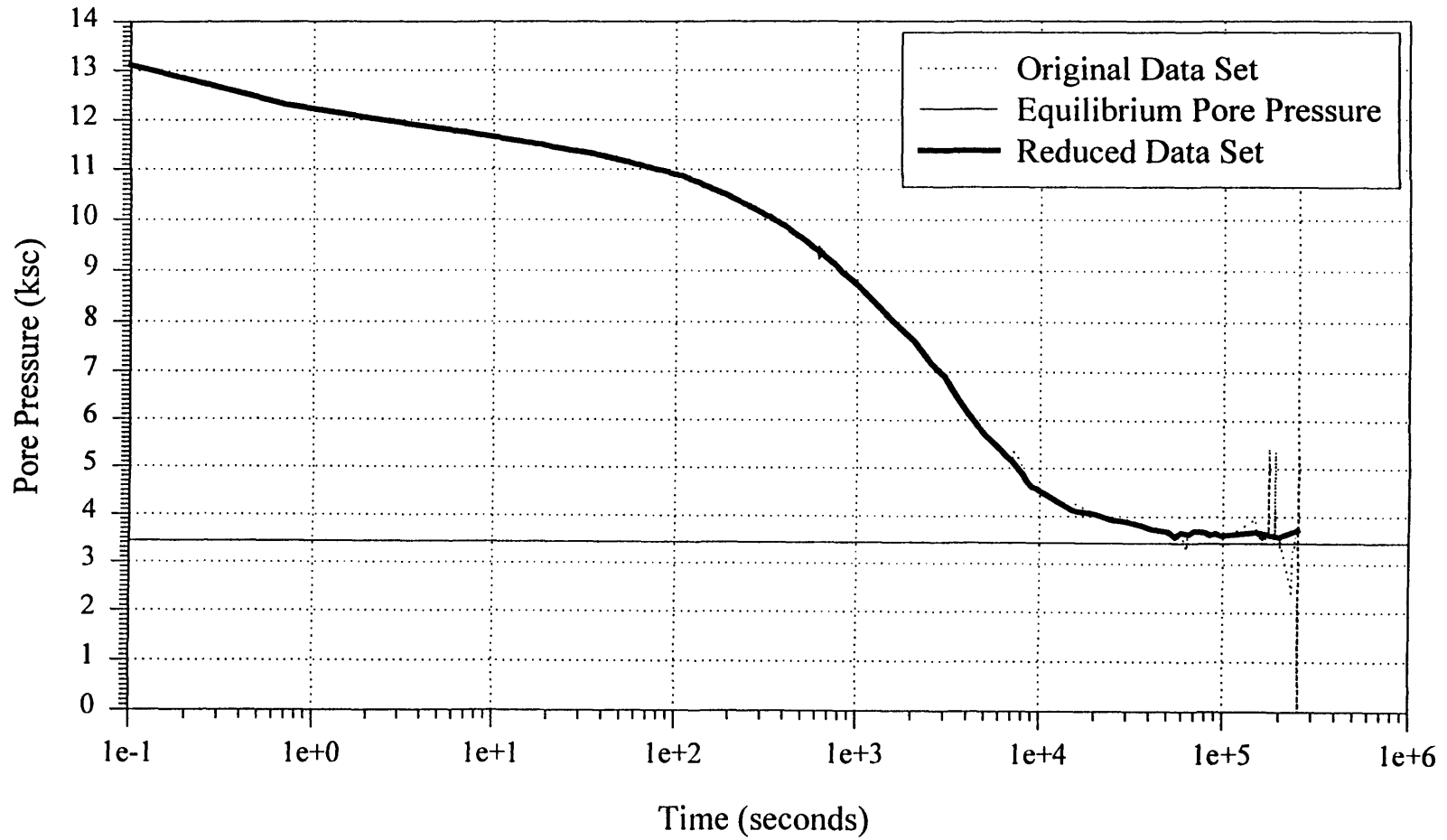
Piezocone 881 Dissipation at 105'
Elevation -30.12 m



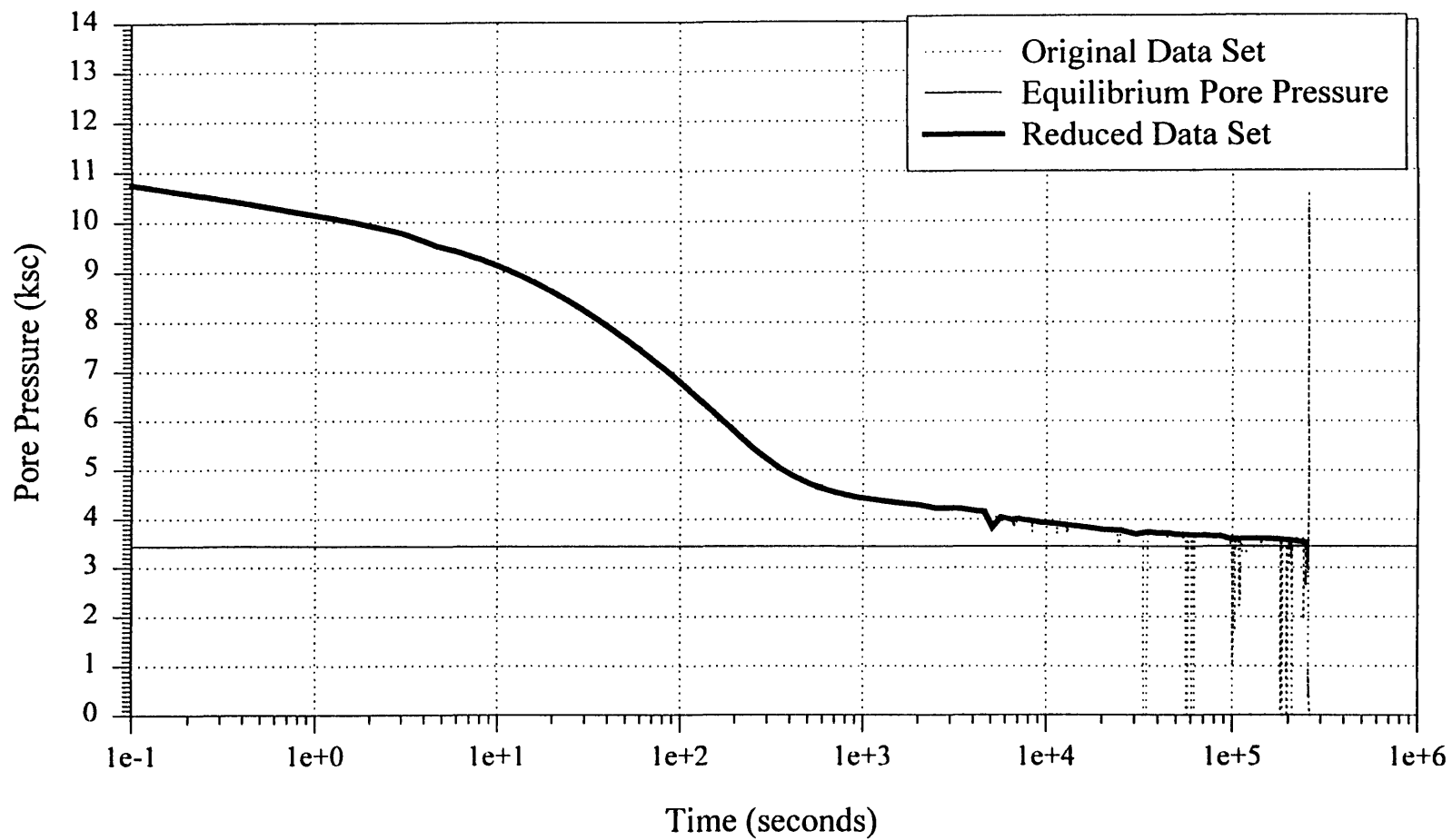
MIT Cone Dissipation at 105'
Elevation -29.99 m



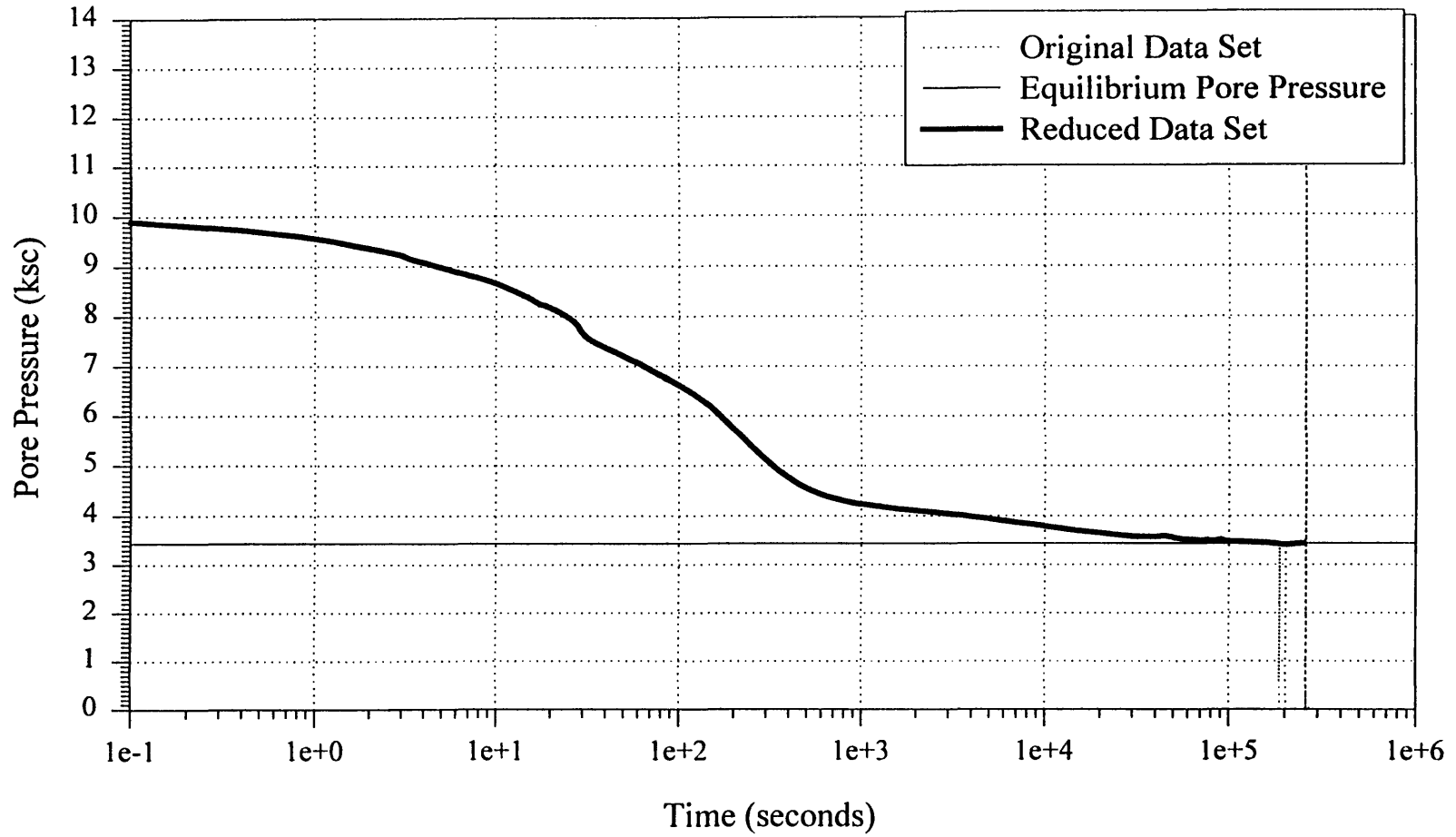
**Piezocone 790 Dissipation at 115'
Elevation -32.96 m**



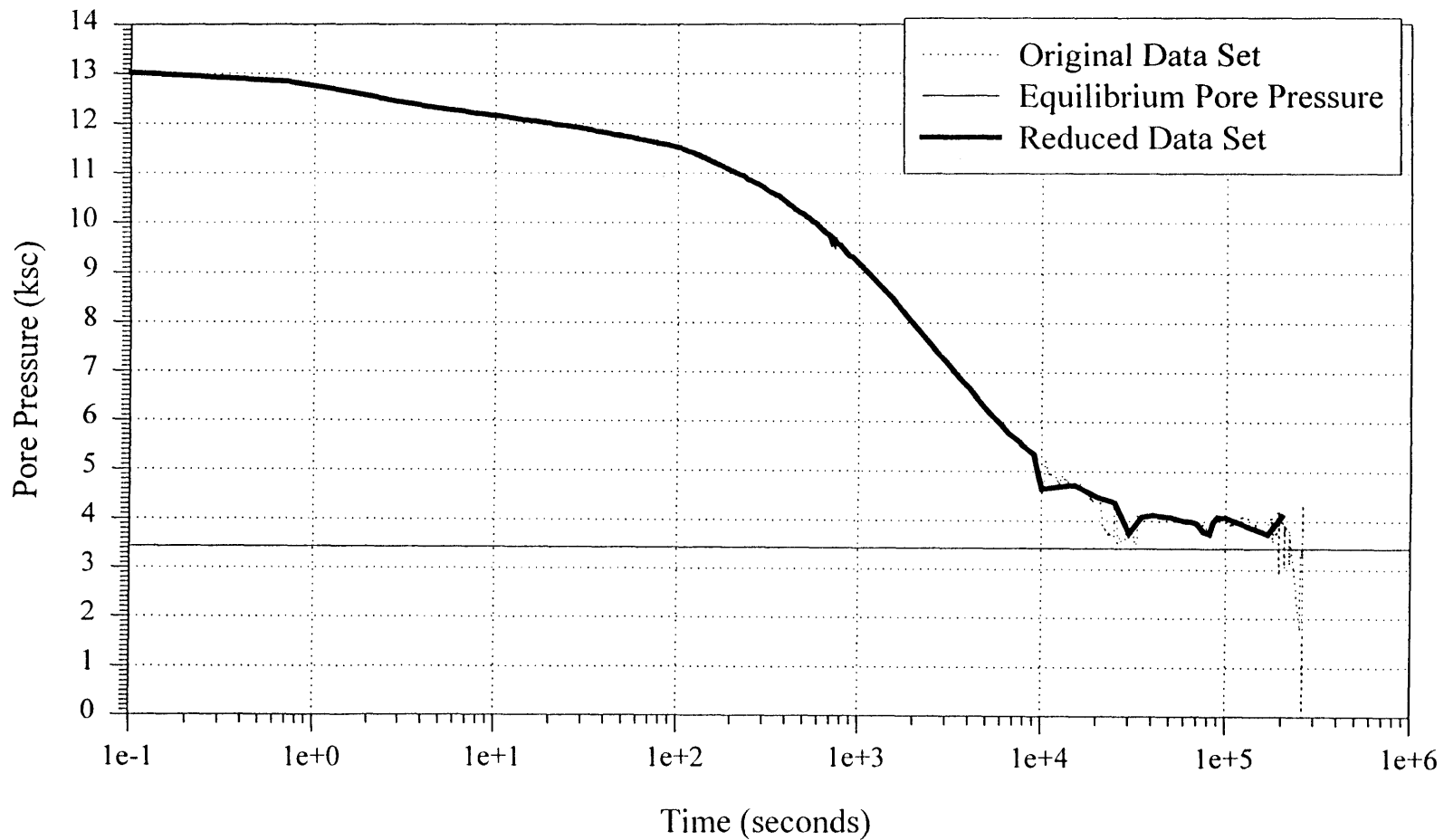
Piezoprobe 62 Dissipation at 115'
Elevation -33.08 m



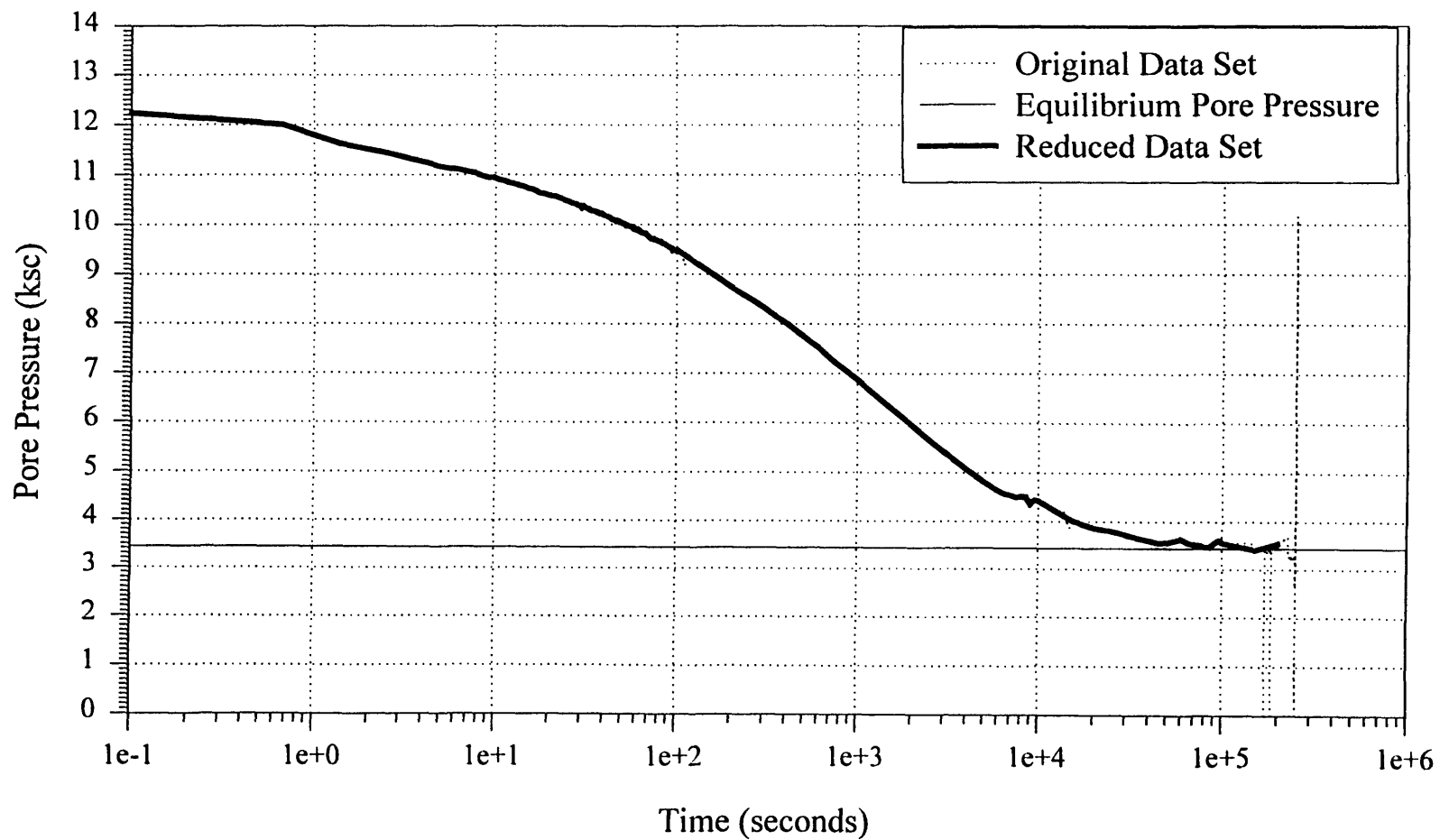
Piezoprobe 63 Dissipation at 115'
Elevation -33.11 m



Piezocone 881 Dissipation at 115'
Elevation -33.17 m



MIT Cone Dissipation at 115'
Elevation -33.03 m



Appendix D

Appendix D consists of a table of extrapolation values of in situ pore pressure determined from the Inverse Time Extrapolation Method at various times in the dissipation record.

Piezoprobe 62: 1/t Method for Determination of u_o								
Depth	Elev. (m)	t_{50} (seconds)	u_i (ksc)	u_{diss} (ksc)	t (seconds)	$u_{1/t}$ (ksc)	t/t_{50}	$\frac{(u_{1/t}-u_{diss})}{(u_i-u_{diss})}$
67	-18.45	183.3	5.18	1.90	100	3.39	0.55	0.45
					166.7	2.92	0.91	0.31
					250	2.66	1.36	0.23
					500	2.31	2.73	0.13
					1000	2.30	5.46	0.12
					10000	2.09	54.56	0.06
					16667	2.08	90.93	0.05
					25000	2.02	136.39	0.04
					75	-20.89	112.9	7.42
166.7	3.13	1.48	0.12					
250	2.67	2.21	0.03					
500	2.50	4.43	-0.01					
1000	2.83	8.86	0.06					
10000	2.72	88.57	0.04					
16667	2.65	147.63	0.02					
25000	2.62	221.43	0.02					
85	-23.94	127.4	7.65	2.74				
					166.7	3.54	1.31	0.16
					250	3.27	1.96	0.11
					500	3.00	3.92	0.05
					1000	3.13	7.85	0.08
					10000	2.86	78.49	0.02
					16667	2.76	130.82	0.00
					25000	2.71	196.23	-0.01
					95	-26.98	28	6.98
166.7	1.25	5.95	-0.41					
250	1.25	8.93	-0.41					
500	n/a	17.86	#VALUE!					
1000	n/a	35.71	#VALUE!					
10000	n/a	357.14	#VALUE!					
16667	3.08	595.25	0.04					
25000	3.06	892.86	0.03					
106	-30.34	88.6	9.27	3.3				
					166.7	4.04	1.88	0.12
					250	3.89	2.82	0.10
					500	3.79	5.64	0.08
					1000	3.89	11.29	0.10
					10000	3.45	112.87	0.03
					16667	3.24	188.12	-0.01
					25000	3.20	282.17	-0.02
					115	-33.08	94.1	10.75
166.7	4.45	1.77	0.12					
250	4.08	2.66	0.07					
500	4.08	5.31	0.07					
1000	4.18	10.63	0.08					
10000	3.76	106.27	0.03					
16667	3.65	177.12	0.01					
25000	3.60	265.67	0.00					

Piezoprobe 63: 1/t Method for Determination of u_o								
Depth	Elev. (m)	t_{50} (seconds)	u_i (ksc)	u_{diss} (ksc)	t (seconds)	$u_{1/t}$ (ksc)	t/t_{50}	$\frac{(u_{1/t}-u_{diss})}{(u_i-u_{diss})}$
67	-18.48	100	6.47	2.08	100	3.09	1.00	0.23
					166.7	2.25	1.67	0.04
					250	2.00	2.50	-0.02
					500	2.00	5.00	-0.02
					1000	2.29	10.00	0.05
					10000	2.41	100.00	0.08
					16667	2.26	166.67	0.04
					25000	2.21	250.00	0.03
75	-20.92	78.5	6.11	2.23	100	3.42	1.27	0.31
					166.7	2.85	2.12	0.16
					250	2.44	3.18	0.05
					500	2.17	6.37	-0.02
					1000	2.40	12.74	0.04
					10000	2.52	127.39	0.07
					16667	2.44	212.32	0.05
					25000	2.36	318.47	0.03
85	-23.97	83.8	7.89	2.47	100	3.74	1.19	0.23
					166.7	3.50	1.99	0.19
					250	2.75	2.98	0.05
					500	2.50	5.97	0.01
					1000	2.85	11.93	0.07
					10000	2.57	119.33	0.02
					16667	2.47	198.89	0.00
					25000	2.40	298.33	-0.01
95	-27.02	94.1	8.08	2.81	100	4.66	1.06	0.35
					166.7	3.81	1.77	0.19
					250	3.00	2.66	0.04
					500	3.00	5.31	0.04
					1000	3.21	10.63	0.08
					10000	2.95	106.27	0.03
					16667	2.89	177.12	0.02
					25000	2.80	265.67	0.00
105	-30.07	69.5	9.44	3.19	100	4.38	1.44	0.19
					166.7	3.88	2.40	0.11
					250	3.46	3.60	0.04
					500	3.46	7.19	0.04
					1000	3.67	14.39	0.08
					10000	3.32	143.88	0.02
					16667	3.22	239.81	0.00
					25000	3.20	359.71	0.00
115	-33.11	78.5	9.91	3.44	100	5.50	1.27	0.32
					166.7	4.68	2.12	0.19
					250	3.87	3.18	0.07
					500	3.50	6.37	0.01
					1000	3.96	12.74	0.08
					10000	3.54	127.39	0.02
					16667	3.51	212.32	0.01
					25000	3.45	318.47	0.00

Piezocone 790: 1/t Method for Determination of u_o								
Depth	Elev. (m)	t_{50} (seconds)	u_i (ksc)	u_{diss} (ksc)	t (seconds)	$u_{1/t}$ (ksc)	t/t_{50}	$\frac{(u_{1/t}-u_{diss})}{(u_i-u_{diss})}$
65	-17.72	1623.8	7.03	1.66	100	5.88	0.06	0.79
					166.7	5.60	0.10	0.73
					250	5.42	0.15	0.70
					500	4.92	0.31	0.61
					1000	4.00	0.62	0.44
					1666.7	3.50	1.03	0.34
					2500	2.95	1.54	0.24
					5000	2.35	3.08	0.13
					10000	2.28	6.16	0.12
					16667	2.00	10.26	0.06
					25000	1.90	15.40	0.04
					75	-20.77	1833	8.61
166.7	6.69	0.09	0.70					
250	6.38	0.14	0.65					
500	5.69	0.27	0.54					
1000	4.89	0.55	0.42					
1666.7	4.15	0.91	0.30					
2500	3.65	1.36	0.23					
5000	2.90	2.73	0.11					
10000	2.42	5.46	0.03					
16667	2.25	9.09	0.01					
25000	2.04	13.64	-0.02					
85	-23.81	1623.8	9.51	2.68				
					166.7	7.38	0.10	0.69
					250	7.13	0.15	0.65
					500	6.50	0.31	0.56
					1000	5.60	0.62	0.43
					1666.7	4.50	1.03	0.27
					2500	4.00	1.54	0.19
					5000	3.25	3.08	0.08
					10000	2.82	6.16	0.02
					16667	2.59	10.26	-0.01
					25000	2.45	15.40	-0.03
					95	-26.86	1623.8	10.83
166.7	8.93	0.10	0.76					
250	8.33	0.15	0.68					
500	7.83	0.31	0.62					
1000	6.20	0.62	0.41					
1666.7	5.35	1.03	0.30					
2500	4.75	1.54	0.23					
5000	3.50	3.08	0.07					
10000	2.90	6.16	-0.01					
16667	2.80	10.26	-0.02					
25000	2.70	15.40	-0.03					

Piezocone 790: 1/t Method for Determination of u_o								
Depth	Elev. (m)	t_{50} (seconds)	u_i (ksc)	u_{diss} (ksc)	t (seconds)	$u_{1/t}$ (ksc)	t/t_{50}	$\frac{(u_{1/t}-u_{diss})}{(u_i-u_{diss})}$
Piezocone 790: 1/t Method for Determination of u_o								
Depth	Elev. (m)	t_{50} (seconds)	u_i (ksc)	u_{diss} (ksc)	t (seconds)	$u_{1/t}$ (ksc)	t/t_{50}	$\frac{(u_{1/t}-u_{diss})}{(u_i-u_{diss})}$
105	-29.91	1438.4	10.91	3.28	100	9.25	0.07	0.55
					166.7	8.83	0.12	0.51
					250	8.63	0.17	0.49
					500	7.75	0.35	0.41
					1000	6.25	0.70	0.27
					1666.7	5.55	1.16	0.21
					2500	4.75	1.74	0.13
					5000	3.80	3.48	0.05
					10000	3.27	6.95	0.00
					16667	3.20	11.59	-0.01
25000	2.95	17.38	-0.03					
115	-32.96	1353.9	13.12	3.64	100	10.25	0.07	0.70
					166.7	9.75	0.12	0.64
					250	9.38	0.18	0.61
					500	8.50	0.37	0.51
					1000	7.00	0.74	0.35
					1666.7	6.30	1.23	0.28
					2500	5.30	1.85	0.18
					5000	3.90	3.69	0.03
					10000	3.50	7.39	-0.01
					16667	3.50	12.31	-0.01
25000	3.49	18.47	-0.02					

Piezocone 881: 1/t Method for Determination of u_o								
Depth	Elev. (m)	t_{50} (seconds)	u_i (ksc)	u_{diss} (ksc)	t (seconds)	$u_{1/t}$ (ksc)	t/t_{50}	$\frac{(u_{1/t}-u_{diss})}{(u_i-u_{diss})}$
65	-17.93	1438.4	8.38	2.18	100	6.67	0.07	0.72
					166.7	6.67	0.12	0.72
					250	6.20	0.17	0.65
					500	5.60	0.35	0.55
					1000	4.60	0.70	0.39
					1666.7	3.70	1.16	0.25
					2500	3.15	1.74	0.16
					5000	2.75	3.48	0.09
					10000	2.80	6.95	0.10
					16667	2.71	11.59	0.09
					25000	2.56	17.38	0.06
75	-20.98	1833	8.49	2.72	100	7.08	0.05	0.76
					166.7	6.97	0.09	0.74
					250	6.63	0.14	0.68
					500	6.13	0.27	0.59
					1000	4.82	0.55	0.36
					1666.7	4.30	0.91	0.27
					2500	3.50	1.36	0.14
					5000	3.00	2.73	0.05
					10000	2.89	5.46	0.03
					16667	2.65	9.09	-0.01
					25000	2.50	13.64	-0.04
85	-24.02	2069.1	9.6	2.86	100	8.00	0.05	0.76
					166.7	7.95	0.08	0.76
					250	7.68	0.12	0.72
					500	7.00	0.24	0.61
					1000	5.89	0.48	0.45
					1666.7	5.05	0.81	0.32
					2500	4.50	1.21	0.24
					5000	3.40	2.42	0.08
					10000	2.86	4.83	0.00
					16667	2.75	8.06	-0.02
					25000	2.64	12.08	-0.03
95	-26.98	1833	10.76	3.19	100	9.00	0.05	0.77
					166.7	8.67	0.09	0.72
					250	8.21	0.14	0.66
					500	7.42	0.27	0.56
					1000	6.25	0.55	0.40
					1666.7	5.40	0.91	0.29
					2500	4.85	1.36	0.22
					5000	3.80	2.73	0.08
					10000	3.45	5.46	0.03
					16667	3.10	9.09	-0.01
					25000	2.10	13.64	-0.14

Piezocone 881: 1/t Method for Determination of u_o								
Depth	Elev. (m)	t_{50} (seconds)	u_i (ksc)	u_{diss} (ksc)	t (seconds)	$u_{1/t}$ (ksc)	t/t_{50}	$\frac{(u_{1/t}-u_{diss})}{(u_i-u_{diss})}$
Piezocone 881: 1/t Method for Determination of u_o								
Depth	Elev. (m)	t_{50} (seconds)	u_i (ksc)	u_{diss} (ksc)	t (seconds)	$u_{1/t}$ (ksc)	t/t_{50}	$\frac{(u_{1/t}-u_{diss})}{(u_i-u_{diss})}$
105	-30.12	1623.8	12.14	3.81	100	9.83	0.06	0.50
					166.7	9.50	0.10	0.47
					250	9.04	0.15	0.43
					500	8.33	0.31	0.37
					1000	7.00	0.62	0.26
					1666.7	5.90	1.03	0.17
					2500	5.15	1.54	0.11
					5000	4.15	3.08	0.03
					10000	3.95	6.16	0.01
					16667	3.69	10.26	-0.01
25000	3.59	15.40	-0.02					
115	-33.17	1833	13.03	3.96	100	10.90	0.05	0.77
					166.7	10.41	0.09	0.71
					250	10.14	0.14	0.68
					500	9.00	0.27	0.56
					1000	7.30	0.55	0.37
					1666.7	6.35	0.91	0.26
					2500	5.75	1.36	0.20
					5000	4.70	2.73	0.08
					10000	3.90	5.46	-0.01
					16667	3.75	9.09	-0.02
25000	3.75	13.64	-0.02					

MIT Cone: 1/t Method for Determination of u_o								
Depth	Elev. (m)	t_{50} (seconds)	u_i (ksc)	u_{diss} (ksc)	t (seconds)	$u_{1/t}$ (ksc)	t/t_{50}	$\frac{(u_{1/t}-u_{diss})}{(u_i-u_{diss})}$
65	-17.79	833.8	7.16	1.89	100	5.30	0.12	0.65
					166.7	5.00	0.20	0.59
					250	4.68	0.30	0.53
					500	4.18	0.60	0.43
					1000	3.64	1.20	0.33
					1666.7	3.27	2.00	0.26
					2500	3.00	3.00	0.21
					5000	2.45	6.00	0.11
					10000	2.70	11.99	0.15
					16667	1.96	19.99	0.01
					25000	1.70	29.98	-0.04
75	-20.84	545.6	8.95	2.36	100	5.93	0.18	0.54
					166.7	5.40	0.31	0.46
					250	5.10	0.46	0.42
					500	4.50	0.92	0.32
					1000	3.72	1.83	0.21
					1666.7	3.28	3.05	0.14
					2500	2.90	4.58	0.08
					5000	2.60	9.16	0.04
					10000	2.46	18.33	0.02
					16667	2.43	30.55	0.01
					25000	2.34	45.82	0.00
85	-23.89	616	7.64	2.51	100	6.08	0.16	0.70
					166.7	5.63	0.27	0.61
					250	5.37	0.41	0.56
					500	4.81	0.81	0.45
					1000	4.09	1.62	0.31
					1666.7	3.50	2.71	0.19
					2500	3.25	4.06	0.14
					5000	2.75	8.12	0.05
					10000	2.45	16.23	-0.01
					16667	2.23	27.06	-0.05
					25000	2.16	40.58	-0.07
95	-26.94	513.4	10.94	2.6	100	7.50	0.19	0.59
					166.7	7.00	0.32	0.53
					250	6.58	0.49	0.48
					500	6.00	0.97	0.41
					1000	5.18	1.95	0.31
					1666.7	4.30	3.25	0.20
					2500	3.90	4.87	0.16
					5000	3.50	9.74	0.11
					10000	3.16	19.48	0.07
					16667	3.07	32.46	0.06
					25000	3.00	48.69	0.05

MIT Cone: 1/t Method for Determination of u_o								
Depth	Elev. (m)	t_{50} (seconds)	u_i (ksc)	u_{diss} (ksc)	t (seconds)	$u_{1/t}$ (ksc)	t/t_{50}	$\frac{(u_{1/t}-u_{diss})}{(u_i-u_{diss})}$
MIT Cone: 1/t Method for Determination of u_o								
Depth	Elev. (m)	t_{50} (seconds)	u_i (ksc)	u_{diss} (ksc)	t (seconds)	$u_{1/t}$ (ksc)	t/t_{50}	$\frac{(u_{1/t}-u_{diss})}{(u_i-u_{diss})}$
105	-29.99	545.6	11.73	3.1	100	8.88	0.18	0.49
					166.7	7.92	0.31	0.41
					250	7.42	0.46	0.37
					500	6.38	0.92	0.28
					1000	5.50	1.83	0.20
					1666.7	5.10	3.05	0.17
					2500	4.65	4.58	0.13
					5000	3.75	9.16	0.06
					10000	3.50	18.33	0.03
					16667	3.25	30.55	0.01
					25000	3.07	45.82	0.00
115	-33.03	483	12.24	3.4	100	8.17	0.21	0.54
					166.7	7.92	0.35	0.51
					250	7.50	0.52	0.46
					500	6.67	1.04	0.37
					1000	5.50	2.07	0.24
					1666.7	4.80	3.45	0.16
					2500	4.40	5.18	0.11
					5000	3.80	10.35	0.05
					10000	3.86	20.70	0.05
					16667	3.47	34.51	0.01
					25000	3.41	51.76	0.00